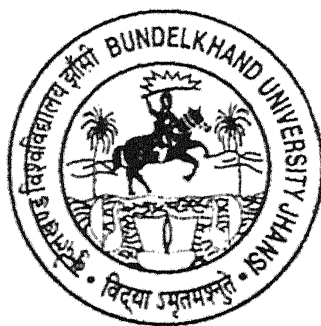


“ THERMAL CURRENT STUDIES IN ELECTRET STATE OF POLYMER FOILS”

**Thesis Submitted
To**



BUNDELKHAND UNIVERSITY, JHANSI

For the Award of the Degree of

**DOCTOR OF PHILOSOPHY
In
PHYSICS**

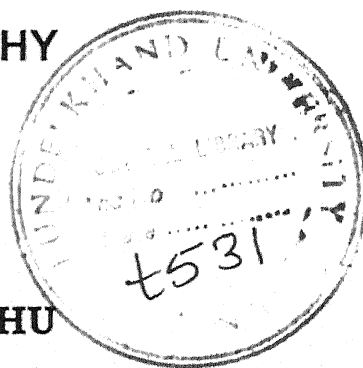
By

DEVENDRA KUMAR SAHU

Deptt. of Physics

Institute of Basic Sciences

Bundelkhand University, Jhansi (U.P.)



Under the Supervision of

Dr. Rudra Kant Srivastava

M.Sc. Ph.D.

**Reader, Department of Physics
Bipin Bihari Post Graduate College,
Jhansi (U.P.)**

Dr. Pawan Kumar Khare

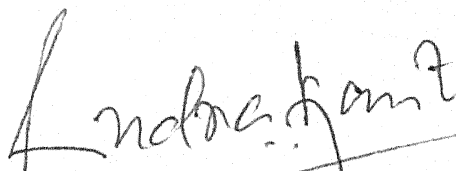
M.Sc. Ph.D.

**Reader, Department of P.G. Studies
and Research in Physics and Electronics
Rani Durgawati University, Jabalpur (M.P.)**

CERTIFICATE

This is to certify that :

- (i) The candidate, **Shri Devendra Kumar Sahu** has worked for his Ph.D. degree under the joint supervision and guidance of **Dr. Pawan Kumar Khare**, Department of Postgraduate Studies and Research in Physics and Electronics, Rani Durgavati University, Jabalpur (M.P.) and me in the Department of Physics, Bipin Bihari P. G. College, Jhansi for more than two academic years.
- (ii) He has put more than 200 days attendance in the department.
- (iii) The thesis entitled "**THERMAL CURRENT STUDIES IN ELECTRET STATE OF POLYMER FOILS**" embodies the original research work done by **Shri Devendra Kumar Sahu** on the approved topic.
- (iv) Such work has not been submitted to any other university.
- (v) He fulfills all the requirements laid under the clauses of Ph.D. ordinances, Bundelkhand University, Jhansi.



Dr. Rudra Kant Srivastava
Supervisor
Department of Physics
Bipin Bihari College, Jhansi
JHANSI (U.P.)

CERTIFICATE

This is to certify that :

- (vi) The candidate, **Shri Devendra Kumar Sahu** has worked for his Ph.D. degree under the joint supervision and guidance of **Dr. Rudra Kant Srivastava**, Department of Physics, Bipin Bihari P. G. College, Jhansi and me in the Department of Physics, Bipin Bihari P. G. College, Jhansi for more than two academic years.
- (vii) He has put more than 200 days attendance in the department.
- (viii) The thesis entitled "**THERMAL CURRENT STUDIES IN ELECTRET STATE OF POLYMER FOILS**" embodies the original research work done by **Shri Devendra Kumar Sahu** on the approved topic.
- (ix) Such work has not been submitted to any other university.
- (x) He fulfills all the requirements laid under the clauses of Ph.D. ordinances, Bundelkhand University, Jhansi.



Dr. Pawan Kumar Khare

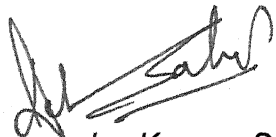
Co-Supervisor

Department of Postgraduate Studies &
Research in Physics & Electronics,
Rani Durgavati Vishwavidyalaya,
JABALPUR (M.P.)

DECLARATION

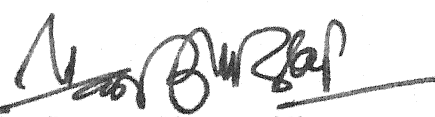
I hereby declare that with the exception of the guidance and suggestions received from my Supervisors **Dr. Rudra Kant Srivastava**, Reader, Department of Physics, Bipin Bihari P. G. College, Jhansi (U.P.) and **Dr. Pawan Kumar Khare**, Reader, Department of P. G. Studies and Research in Physics and Electronics, Rani Durgavati University, Jabalpur (M.P.), the work reported in this thesis is the outcome of my own unaided efforts.

JHANSI
Date : 19 NOV 2003

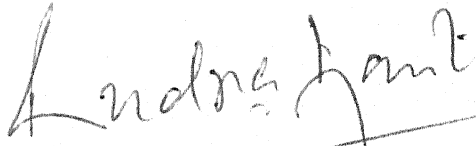


Devendra Kumar Sahu
Department of Physics,
Institute of Basic Sciences,
Bundelkhand University,
JHANSI - 284 001 (U.P.)

Forwarded



Dr. Pawan Kumar Khare
Co-Supervisor
Department of P. G. Studies and
Research in Physics & Electronics
Rani Durgavati University
JABALPUR - 482 004 (M.P.)



Dr. Rudra Kant Srivastava
Supervisor
Reader, Department of Physics,
Bipin Bihari P. G. College,
JHANSI - 284 001 (U.P.)

ACKNOWLEDGEMENTS

I wish to express my heartfelt gratitude and honours to my Supervisors **Dr. Rudra Kant Srivastava**, Reader, Department of Physics, Bipin Bihari (P.G.) College, Jhansi (U.P.) and **Dr. Pawan Kumar Khare**, Reader, Department of Postgraduate Studies and Research in Physics and Electronics, Rani Durgavati University, Jabalpur (M.P.) for their unflinching and excellent guidance and valuable suggestions at almost every stage in the progress of the present investigation. It is no exaggeration to say that without their inspiring and day to day affectionate gestures the work simply could not have been completed. Both of my Supervisors are not only in a formal sense but intrinsically devoted personalities in full capacity also. I have no words to depict their innumerable qualities of head and heart.

I am much indebted to **Professor Ramesh Chandra**, Honourable Vice-Chancellor, Bundelkhand University, Jhansi, **Shri V. K. Sinha**, Registrar and Professor, **Prof. S. P. Singh**, Dean, Faculty of Science and Director, Institute of Basic Sciences, Bundelkhand University, Jhansi for providing all types of assistance and facilities without which the present research work could not have been completed.

I am thankful to **Dr. U. P. Singh**, Principal, Bipin Bihari P.G. College, Jhansi for forwarding the application form for Registration to carry out the research work.

I am thankful to **Dr. Sunil Kumar Khare**, Asstt. Professor, Department of Chemistry, Indian Institute of Technology, New Delhi, for providing necessary knowledge in Polymer Sciences.

I am indebted to Dr. J. P. Srivastava, Asstt. Librarian, Central Library, D.D.C., New Delhi for enriching and updating my knowledge and helping in the collection of literature in the present research work.

I am also thankful to Dr. Gajala Rizvi, Dr. R. K. Agarwal, and my friends Mr. Akhilesh Rawat, Mr. Ashutosh Verma and Dr. Sanjeev Srivastava for their whole hearted co-operation during the research work.

I convey my sincere thanks to my respected uncle Shri J. P. Niranjana, Er. S. C. Vivek, my brothers, Suresh Sahu, Dharmesh Sahu and sisters Ujjala and Neetu for their unvaluable assistance. My special and sincere thanks goes to my wife Smt. Anju Sahu for her constant encouragement. At last, but not the least I express my most sincere gratitude and regards to my dear and respected Parents Shri R. G. Sahu and Smt. Kaushilya Devi and in-laws Shri Har Govind Sahu and Smt. Geeta Devi for their affection, assistance and constant encouragement.

Jhansi



Devendra Kumar Sahu

Dated : 19 NOV 2003

P R E F A C E

Materials exhibiting dielectric relaxation necessarily show charge storage and electret behaviour if an electric field is applied to them. The phenomenon has been associated with two types of effects. A frozen-in polarisation or trapped charge can either induce internal effects or create an external electric field. In the first case, the physical properties of the material can be modified leading, for instance, to piezoelectricity or to nonlinear effects. In the second case, an external electric field of large magnitude can be created.

As far as the internal effects are concerned, many attempts have been made to take advantage of the useful mechanical properties of the polymers, such as their low acoustical impedance, their flexibility and the possibility to have them in large lateral or long linear dimensions. Piezoelectric polymers have found many applications, but still at a very reduced level. New developments are now being made in electro-optics and the potential here seems to be quite large.

As far as electrets, which can create an external electric field, are concerned, large scale applications have already been developed, the main one being in the field of condenser microphones. Various types of sensors are also being studied out of the acoustical frequency range, for instance, to produce or detect ultrasonic waves.

Commodity as well as engineering plastics have found applications in various appliances in substantial quantities. The performance requirements of materials used in devices have, however, changed considerably in the recent past. These requirements may include higher temperature, high impact strength, mouldable components, improved resistivity and charge storage properties.

With the view to present a unified picture of the various findings, the various chapters of the present investigation are as follows :

Chapter I covers the general introduction to the relevant topics such as the electret state, polymer structure of material, mechanism of polarization and concept of electrical contacts. It further lays down the techniques for investigation of electrical properties and a review for material used for carrying out the present investigation.

Chapter II deals with the various methods for film formation and present experimental techniques, measurement of film thickness, types of electrodes, circuit configuration and principle equipment used in the investigation.

Chapter III is devoted to the theoretical background of various electrical properties proposed for present investigation, such as transient current in charging and discharging mode, steady state conduction current, thermally stimulated discharge current (TSDC) and dielectric measurement. Theory of transient charging and discharging currents, last decade's work,

various mechanism responsible for conduction and effect of various parameters on electrical conduction and different conduction parameters have been discussed. The chapter also covers the techniques and theories of TSDC, effect of different factors on TSDC spectra, evaluation of TSDC data and last decade's work on TSDC. The chapter has been concluded with the introduction of dielectric measurement, theoretical interpretation of dielectric constant and losses and various factors affecting dielectric behaviour of polymers.

Chapter IV covers the general introduction of Thermally stimulated depolarization currents (TSDC). The experimental observations for TSDC measurements of polyvinylidene fluoride samples in short circuit configuration, their results and interpretations are discussed in this chapter.

Chapter V consists of the general introduction of transient currents in charging and discharging modes, time dependence current models, experimental part and results obtained from polyvinylidene fluoride samples and their interpretation.

Chapter VI deals with the general introduction of steady state conduction current, experimental part and the results obtained during the experimental observation with detailed discussion.

Chapter VII exhibits the general introduction of dielectric behaviour of polymer, basic theory of dielectric constants, experimental part followed by the results and discussion.

The last **Chapter VIII** of the thesis reviews the results the obtained from the above mentioned studies and discusses the correlation between these results.

The references are given at the end of each chapter.

The author has communicated some original research papers for publication in various Journals as a subsidiary matter in support of candidature for the Ph.D. degree. Two of the papers are accepted in the Bulletin of Material Sciences, Indian Academy of Sciences, Bangalore and Indian Journal of Physics, Indian Association for Cultivation of Science, Kolkata. The entire work has been carried out during the period July 2001 to June 2003.

CONTENTS

Certificate	i
Certificate	ii
Declaration	iii
Acknowledgement	iv-v
Preface	vi-ix

CHAPTER 1 GENERAL INTRODUCTION 1-63

1.1	Introduction	1
1.2	Polymeric Materials	3
1.3	Charge Storage in Dielectric Materials	5
1.4	Polarization in Polymers	7
1.4-1	Dielectric Dispersion Phenomena in Polymers	7
1.4.2	Factors affecting Dielectric Relaxation Behaviour of Polymers	8
1.5	The Electret State in Polymers	9
1.5-1	Effect of Different Factors on Electret State	12
1.5-2	Investigation of Electret State	13
1.5-3	Types of Electrets	16
1.6	Mechanism of Charging	18
1.6-1	Microscopic Displacement of Charges	19
1.6-2	Dipole Polarisation	19
1.6-3	Macroscopic Space Charge Polarisation	19
1.6-4	Barrier Polarisation	20
1.6-5	External Polarisation	20
1.7	Charging Techniques	21
1.7-1	Thermal Method	21
1.7-2	Electron Beam Method	22
1.7-3	Photoelectric Method	22
1.8	Techniques for Investigation of Electrical Characteristics of Polymers	23
1.8(a)	Dark Conduction Current Measurements	24
1.8(b)	Transient Current Measurement	28
1.8(c)	Thermally Stimulated Discharge Current (TSDC) Measurement	33

1.8(d)	Dielectric Measurement	34
1.9	Aim and Scope of the Present Investigation	37
1.10	Polymer used - Poly(vinylidene fluoride)	38
1.10-1	Physical, Chemical and Morphological Properties of PVDF	40
Table 1.1	Characteristics of 5-crystalline forms of PVDF	45
	References	46

CHAPTER 2 EXPERIMENTAL DETAILS

64-90

2.1	Introduction	64
2.2	Different Methods of Film Formation	64
2.2(a)	Glow Discharge Polymerization	65
2.2(b)	Polymerization by Electron Bombardment	65
2.2(c)	Photolytic Polymerization using Ultraviolet Radiation	65
2.2(d)	Vacuum Evaporation	66
2.2(e)	Films from polymer solution	66
	(i) Isothermal Immersion Technique	67
	(ii) Casting from the Solution	67
2.3	Measurement of Thickness of the Film	69
2.3(a)	Optical	69
2.3(b)	Electrical	70
2.3(c)	Mechanical	70
2.4	Electrical Contacts	71
2.4(a)	Ohmic Contacts	72
2.4(b)	Neutral Contacts	73
2.4(c)	Blocking Contacts	73
2.5	Electrodes	74
2.5(a)	Painted Electrodes	75
2.5(b)	Liquid Contact Electrodes	75
2.5(c)	Pressed Metal Foil Electrodes	76
2.5(d)	Vacuum Deposited Electrodes	76
2.6	Vacuum Coating of Polymer Films	77
2.6-i	Vacuum Coating Unit	77
2.6-ii	Operation for Electrode Deposition	79
2.7	Circuitry and Instrumentation	81

2.8	Measurement Techniques	83
(a)	Transient and D.C. Conductivity Measurements	83
(b)	Dielectric Measurements	84
(c)	Thermally Stimulated Discharge Current (TSDC) Measurement	85
	References	89

CHAPTER 3 91-167

THEORETICAL BACKGROUND OF STUDIES

3.1	Thermally Stimulated Discharge Current (TSDC)	91
3.2	Factors governing the TSD Spectra	92
3.2-i	Effect of Poling Temperature	92
3.2-ii	Effect of Poling Field	93
3.2-iii	Effect of Poling Time	94
3.2-iv	Effect of Deliberately Added Impurities	94
3.2-v	Effect of Heating Rate	95
3.3	Theory of TSD	95
(a)	TSD of dipoles with one relaxation time	95
(b)	TSD for a distribution of relaxation time	99
3.4	Mechanism of TSD	101
3.5	TSD Parameters	104
3.5-i	Activation Energy	104
(a)	Initial Rise Method	105
(b)	Graphical Integration Method	106
(c)	Methods based on the variation of heating rates	107
(d)	Activation energy for distributed processes	108
3.5-ii	Relaxation Time (τ_0)	109
3.5-iii	Charge Released (Q)	110
3.6	Transient Currents in Charging and Discharging Modes	111
3.7	Theory of Transient Charging and Discharging Currents in Polymers	112
3.8	Theory of Electrical Conduction Mechanism in Polymer Films.	115
(i)	Ionic Conduction	116
(ii)	Tunnelling Mechanism	116
(iii)	Hopping Mechanism	117
(iv)	Richardson-Schottky Emission	118
(v)	Poole-Frenkel Effect	119
(vi)	Space Charge Limited Current	120

3.9	Conduction Parameters	122
(i)	Power 'm"	122
(ii)	Conductivity	123
(iii)	Activation Energy	123
3.10	Effect of Environment and other Factors on Electrical Conduction of Polymers	123
3.11	Models Explaining Steady State Conduction	128
(i)	Block Band Theory	128
(ii)	The Tunnelling Method	129
(iii)	The Hopping Model	130
(iv)	Richardson Schottky Effect	132
(v)	Poole Frenkel Effect	133
(vi)	Space Charge Limited Currents	134
3.12	Dielectric Behaviour	137
(i)	Dielectric relaxation in polymers	138
(ii)	Dielectric properties	139
	(a) Macroscopic description of static dielectric constant	
(iii)	Dielectric properties of insulators in alternating fields	141
3.13	The Complex Dielectric Constant and Dielectric Losses	141
3.14	Dielectric Losses and Relaxation Time	143
3.15	Different Types of Relaxation in Polymers	145
3.16	Factors Affecting Dielectric Behaviour of Polymers	146
(a)	Effect of polar groups	146
(b)	Effect of substituents	146
(c)	Effect of side group isomerism	146
(d)	Effect of stereoregularity	147
(e)	Effect of plasticizers	147
(f)	Effect of copolymerization	148
(g)	Effect of crosslinking	148
(h)	Effect of pressure	148
3.17	Factors Affecting Dielectric Constant	148
(a)	Temperature	148
(b)	Frequency	149
(c)	Field	150
(d)	Humidity	150
(e)	Impurity	151
(f)	Nature of the Polymer	151
	References	152

CHAPTER 4 **168-218**
THERMALLY STIMULATE DISCHARGE CURRENT STUDY

4.1	Introduction	168
4.2	Poling of the Film	179
4.3	Methods Used for Studying TSD	181
	(a) Measurement of TSDC with shorted electrodes.	181
	(b) Measurement of TSDC with open circuit (air gap) electrodes.	182
	(c) Measurement of TSD charge by transferring the induced charge to an electrometer.	182
	(d) Measurement of TSD charge by field cancellation method.	183
4.4	Detection Efficiency of Various TSD Methods	183
4.5	Thermally Stimulated Discharge Current (TSDC) Measurement	185
4.6	Results and Discussion	186
	Tables 4.1-4.7	200-206
	References	207

CHAPTER 5 **219-242**
**TRANSIENT CURRENTS IN CHARGING
AND DISCHARGING MODES**

5.1	Introduction	219
5.2	Time Dependence Current Models	221
	(a) Electrode polarization	221
	(b) Dipole orientation	221
	(c) Hopping mechanism	223
	(d) Tunnelling model	224
	(e) Charge injection leading to trapped space charge effects	225
5.3	Experimental	227
5.4	Results and Discussion	228
	References	240

CHAPTER 6 **243-268**
DARK CONDUCTION CURRENT MEASUREMENT

6.1	Introduction	243
6.2	Experimental	253

6.3	Results and Discussion	254
	Table 6.1	262
	References	263

CHAPTER 7 269-287

DIELECTRIC MEASUREMENT

7.1	Introduction - Dielectric Behaviour of Polymer	269
7.2	Basic Theory	274
7.3	Experimental	277
7.4	Results and Discussion	277
	References	285

CHAPTER 8 288-319

REVIEW OF THE RESULTS AND CORRELATION

(A)	Thermally Stimulated Discharge Current	293
(B)	Transient Currents in Charging and Discharging Modes	297
(C)	Steady State Conduction Currents	303
(D)	Dielectric Measurement	306
	References	317
	List of Research Papers Submitted	318

/ ***** /

CHAPTER I

GENERAL

INTRODUCTION

1.1 INTRODUCTION

Since the formation of the earth over 4 billion years ago, in its giant laboratory "Nature", elements like carbon, hydrogen, oxygen and nitrogen have been combining to form complex molecules. Such a combination triggered off the most intriguing and fascinating process called life, the material basis for whose origin was a polymer. Thus, the human life was associated with polymers in the form of food, clothing, wood etc.

In the laboratory, polymers have obviously not been discovered overnight. They came out of long and persevering studies by a host of motivated scientists whose work has enriched human life. Today, the overall insight into polymer science and technology is so deep that a material scientist can create an almost limitless range of new materials. Just as an architect, a polymer scientist can produce innumerable plastics, rubbers, foams, fibres, etc. by judiciously combining various chemicals to react under desired conditions.

In recent times studies in polymers in the form of thin films have gained attention, due to their fascinating properties, disordered structure, potential applications and growing need of solid state devices. Polymer thin films are being used in a number of exploratory electronic technologies such as thin film triodes, thin film memory circuits, cryotron logic and associating storage circuits etc., apart from their use as insulators. Also, these are finding many technological applications such as electret

microphones, electrostatic voltage generators, air filters [1], IR detectors and transducers.

The physical properties of all polymers are not alike. The polymer properties depend on average molecular weight and molecular weight distribution of the polymer. But even these two parameters do not fully characterise a polymer. Two polymer samples can have the same chemical structure and almost similar molecular weight distributions, but may have different properties due to the difference in structure. All properties depend on intermolecular and intramolecular interactions of polymer chains in the aggregated state. Such interactions are caused by forces, such as dispersion force, induction force, dipole interaction and hydrogen bonding, acting within various parts of the same molecule as well as between the neighbouring molecules. The nature and the magnitude of such interactions force depend apart from the chemical characteristics of the monomer on the manner in which these monomeric units are linked with each other in the polymer [2], whereas the number and chemical nature of monomeric units forming the macromolecule gives an overall picture of the polymer chain, the manner in which they are linked gives the finer aspects of the picture. The number of monomeric units depicts the macrostructure and the mode of their interlinking indicates the microstructure of the polymer molecule. The polymers can be classified basing on the chemical structure; organic or inorganic, depending on whether the chain backbone is made

essentially of carbon-carbon (C-C) links or not. Polygermane is an inorganic polymer.

1.2 POLYMERIC MATERIALS

A polymer is a chemical substance whose molecules are large and consists of many small repeating units covalently bonded together. For instance, polyethylene consisting of essentially long chains of $(-\text{CH}_2-\text{CH}_2-)$ repeating units. The length of the polymer chain is specified by the number of repeat units in the chain and is called degree of polymerization which may vary over a wide range from few units to several thousand units in a chain. Unlike other materials, polymers do not have a unique molecular weight but are described in terms of average molecular weights.

Polymers are generally classified into two groups, viz., the non-polar and the polar polymers. The non-polar polymers have no permanent dipole moment whereas the polar polymers possess permanent dipole moment.

Polymers can exist as amorphous materials, as crystalline materials or as mixture of crystalline amorphous materials. Even highly crystalline polymers contain considerable amount of amorphous material. The properties of the polymer are determined by its structure, molecular weight, degree of crystallinity and chemical composition. The most prominent change in the physical properties of the polymers takes place at their glass transition temperature which is the characteristic property of an individual polymer.

Vast use of organic polymers has attracted scientists, engineers and technologists, all over the world, for studying their various, properties and characteristics. Synthesis, mixing and blending of different polymers have given them to play around with the characteristics to suit their specific requirements. Polymers are inexpensive and hence affordable by all. These days polymers have become the most important commodity without which it is difficult to sustain the life.

In early days, polymers in the form of plastics were regarded electrically as simply good insulators. But now, observations as substitutes in electrical response have shed a great deal of light on their molecular and charge particle dynamics. Such studies have enabled the development of materials which meet exacting electrical engineering requirements. Research along these lines has demonstrated the feasibility of obtaining materials with entirely novel set of properties. Also, such a research has led to the discovery of 'electret' displaying an unusual electrostatic phenomenon. Electrets made of different polymers have a very important use as transducers in electret microphones [3,4]. Subsequent researches led to permanent electrification of electrets. Such electrets are utilised in xerographic reproduction techniques [5], gas filters [6], relay switches [7], medical appliances like radiation dosimeters [8], optoelectronic devices like video/TV cameras [9], maritime devices like hydrophones [10], electret motors [11], electret generators [12], tachometers [13], vibrational fans, thin film transistors and thin film memory circuits [14,15] and many other areas.

Such scientific, technological and commercial applications have led to an explosive activities of research in polymers for different phenomena like charging and discharging, charge transport in polymer and the formation behaviour of electrets.

The polymers have contributed a great deal in electrical insulation, but high fields yield these polymers causing electrical breakdown. Although the causes of breakdown have been attempted to be explained in a number of ways in terms of models, understanding of high field transport in polymers is far behind and needs to be studied in greater details. Of the many factors which cause the electrical breakdown, composition of polymers, electrical stress applied, charge transport in the bulk and temperature are some of the important factors. There are ways and means of improving the performance of a polymer by mixing or blending/doping of other suitable polymers.

1.3 CHARGE STORAGE IN DIELECTRIC MATERIALS

Polymers or in general dielectrics when placed in an electric field undergo polarization, which involves the appearance of electronic charges on the surface of the dielectrics. These charges, known as induced charge, are not free and they generate a field in the dielectric called depolarization field whose direction is opposite to the direction of the field causing polarization.

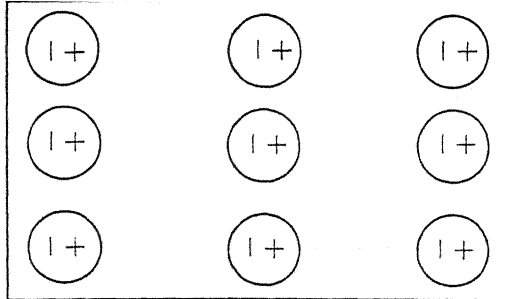
Any material is made up of atoms and is treated as an electronic system consisting of positively charged nuclei surrounded by negatively

charged electron clouds. By the application of external field, electron cloud experiences a displacement relative to the nucleus, causing induced dipole moments in the material. This is called "electronic polarization (P_e)".

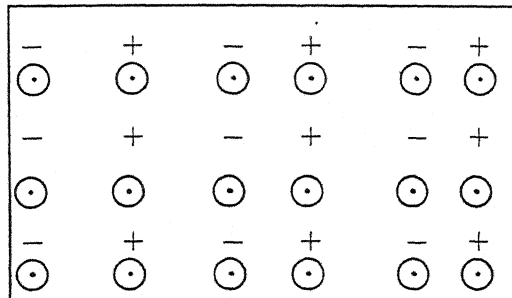
Molecules are made up of different atoms that contain charges with different signs. The external field acts upon them and causes their equilibrium position to change. This is an induced polarization known as "atomic polarization (P_1)".

If the centres of gravity of the positive and negative charges in a molecule, made up of different atom, do not overlap, then the molecule will have a permanent dipole moment. On application of external field, dipoles align themselves in the direction of the field which results in the appearance of "orientation" or "dipole polarization (P_o)".

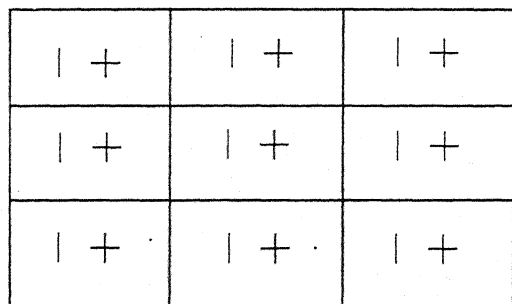
The above mechanisms of polarization are due to the charges that are locally bound in atoms or in molecules. But the free charge carriers which are present in the bulk of the material displace themselves in the dielectric on the application of the electric field, causing various types of polarization. In the dielectric the intrinsic charges during their motion may be trapped at some centres such as grain boundaries, defects, etc. and hence it may result in the "Maxwell-Wagner or interfacial polarization (P_i)". The excess charges deposited or injected from the electrode results in space-charge polarization (P_s). A complete picture of different types of polarization is shown in Figure 1.1



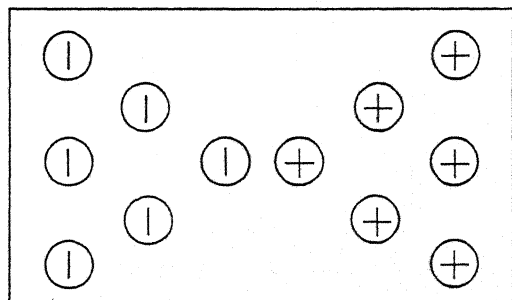
Atomic polarization



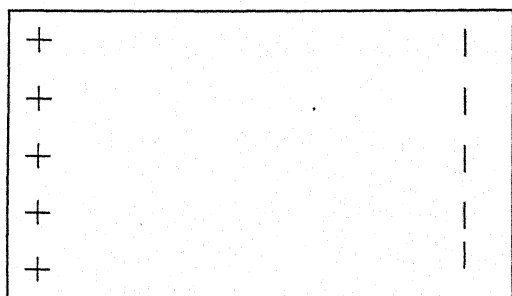
Dipolar polarization



Interfacial polarization



Space polarization



External polarization

Fig. 1.1 : Polarization mechanisms in dielectric materials

1.4 POLARIZATION IN POLYMERS

Application of electric field to a solid polymer material produces polarization phenomena which brings a net dipole moment over the bulk, in its direction. In case of non-polar materials, the dipole moment is due to the induced dipoles where as in a polar material it is due to the orientation of dipoles in the field direction.

1.4-1 DIELECTRIC DISPERSION PHENOMENA IN POLYMERS

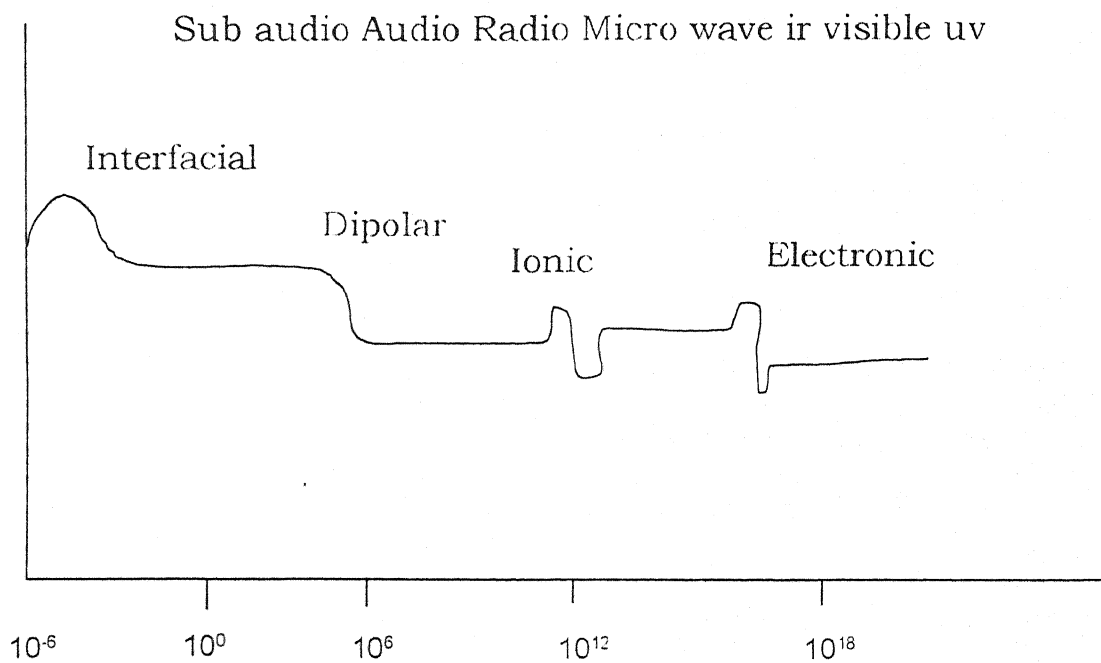
Dielectric A.C. Bridge measurements have been used as an effective tool in characterizing the molecular motion and the dielectric relaxation behaviour in polymers [16-28]. A lot of work has been done on various dielectrics by this technique.

When a solid dielectric material is subjected to an alternating electric field, polarization phenomena occur and the resulting dielectric constant is given by -

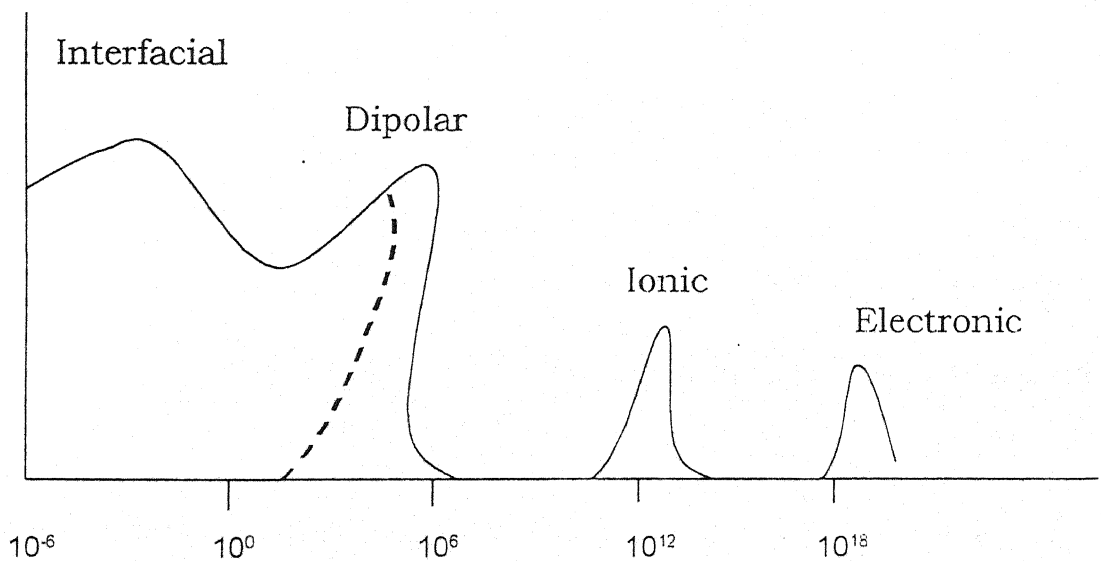
$$\varepsilon = \varepsilon' - i\varepsilon'' \quad \dots (1.1)$$

ε' and ε'' are real and imaginary part of dielectric constant. Interfacial polarization is observed at very low frequencies. Dipolar polarization generally occurs in the frequency range 10 to 10^6 Hz. Atomic and electronic polarizations are observed in the IR and optical frequency ranges (Fig. 1.2).

The displacement of polar groups of polymers require some time and is thus dependent on the frequency and temperature which lead to different dispersion phenomena according to the segmental motion of the



(a)



(b)

Fig. 1.2: (a) Variation of permittivity with frequency for simple dielectric

(b) Variation of loss tangent with frequency for simple dielectric.

polymer chain or orientation of the polar side groups. Actually at frequencies and temperatures where dispersion occurs, only a part of the electrical energy is stored while some of it is dissipated as heat. The electrical energy stored per cycle is proportional to the real part of the permittivity and the energy loss per cycle is proportional to the imaginary part of permittivity. The loss factor exhibits a maximum at frequencies at which dielectric permittivity ϵ' shows a dispersion (Fig. 1.3).

Technique employed for the characterization of relaxations in polymers influences the molecules of a polymer in a different way and thus the response of a system to different stimuli may be very different.

1.4-2 FACTORS AFFECTING DIELECTRIC RELAXATION BEHAVIOUR OF POLYMERS

(a) Effect of polar group

The α -relaxation is basically dependent on the intra and inter molecular interactions. The greater the inter molecular interaction, the less mobile are the molecules and the higher is the relaxation temperature at which maximum loss occurs and larger is the relaxation time. Exchange of non polar substitutes increases dipole-dipole interaction.

(b) Effect of substituents

Introduction of very bulky substituents into the side chains or increasing the side chains decreases the mobility sharply.

(c) Effect of side group isomerism

In case of isomers, magnitude of α and β relaxation are different.

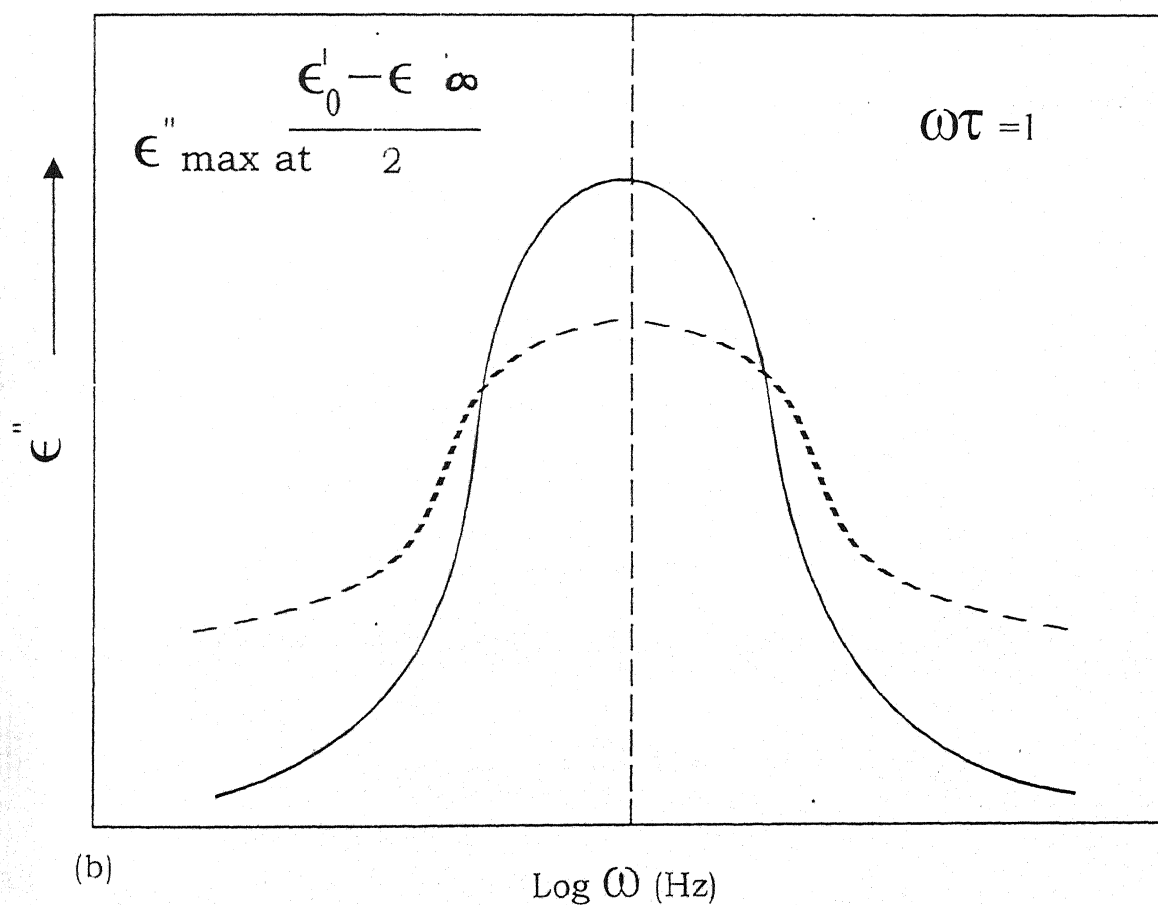
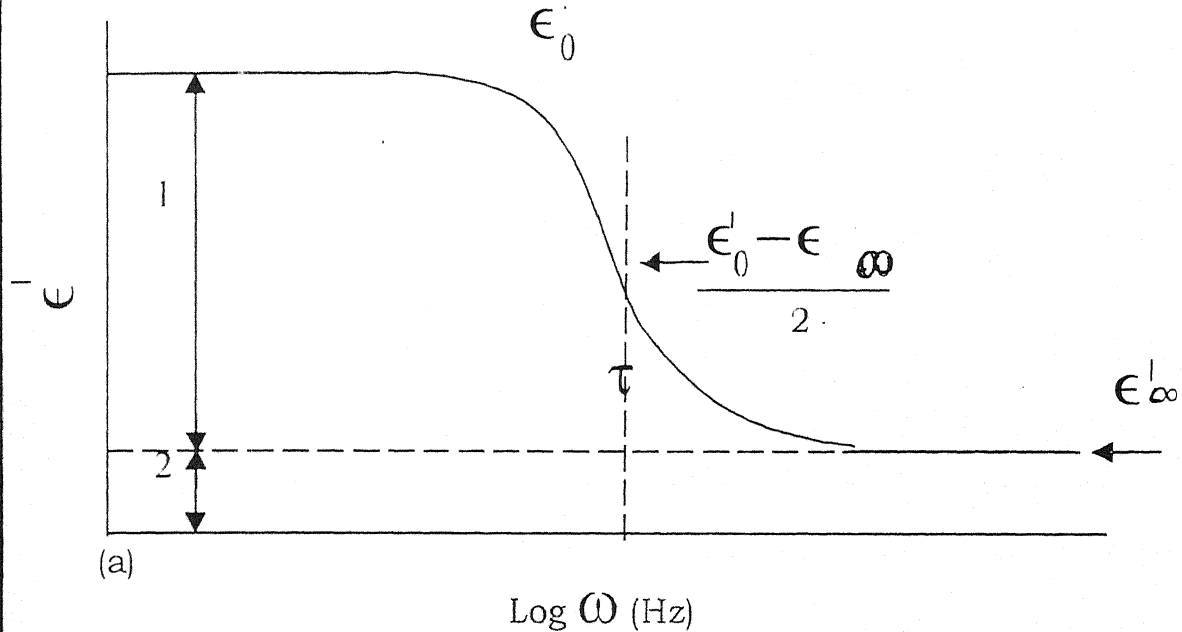


Fig. 1.3 Behavior of dielectric constant (ϵ') and loss factor (ϵ'') for polar polymers as a function of frequency (broadening of loss curve is caused by multiple relaxation times and is shown by the dotted line)

- ϵ_0 - Static dielectric constant
- ϵ_∞ - High frequency dielectric constant
- τ = Dielectric relaxation time.
- 1 - Dipole contribution
- 2 - Electronic contribution

(d) Effect of stereoregularity

The dielectric properties of polymers are substantially dependent on the stereoregular nature of the polymer, because the percentage, the length and quantitative proportion of syndiotactic and isotactic sections have a significant effect on the molecular mobility of polymers.

(e) Effect of plasticizers

Dielectric relaxation of polymers shift towards lower temperature side on the addition of plasticizers. This is because plasticizers (i) increase molecular mobility, (ii) increase free volume, (iii) decrease T_g of the polymers.

(f) Effect of crosslinking

Cross linking always decreases molecular mobility and increases temperature and relaxation time of α process.

(g) Effect of copolymerization

Dielectric properties of copolymers vary according to the composition and the ratio of monomeric units.

(h) Effect of pressure

Pressure influences the relaxation time of the process in which the intermolecular interaction plays an important role.

1.5 THE ELECTRET STATE IN POLYMERS

Here, we discuss some important aspects of electrets and types of electrets.

When a dielectric or polymer piece is subjected to an electric field, the polymer piece exhibits electrical charge storage even after the applied field is removed. This charge is temporary in nature and decays with respect to time. Such a dielectric piece is known as the electret.

The electret charge may consist of 'real' charge, such as surface-charge layer or space charge; it may be a 'true' polarisation; or it may be a combination of these. This is shown in Fig. 1.3a.

While a true polarisation is usually a frozen-in alignment of dipoles, the real charges comprise of layers of trapped positive and negative carriers, often positioned at or near the two surfaces of the dielectric respectively. On metallised electrets, a compensation charge may residue on the electrode, unable to cross the energy barrier between metal and dielectric. Mostly, the net charge on an electret is zero or close to zero and its fields are due to charge separation and not caused by a net charge [29].

An electret not covered by metal electrodes produce an external electrostatic field if its polarisation and real charges do not compensate each other everywhere in the dielectric. Such an electret, thus in a sense, is the electrostatic analogue of a permanent magnet, although electret properties may be caused by polar and monopolar charge while magnetic properties are only due to magnetic dipoles.

An electret can be simply defined as a dielectric material which possesses a semi-permanent polarization [30-31]. The term electret is an electric counterpart of a magnet since they carry opposite charge on either

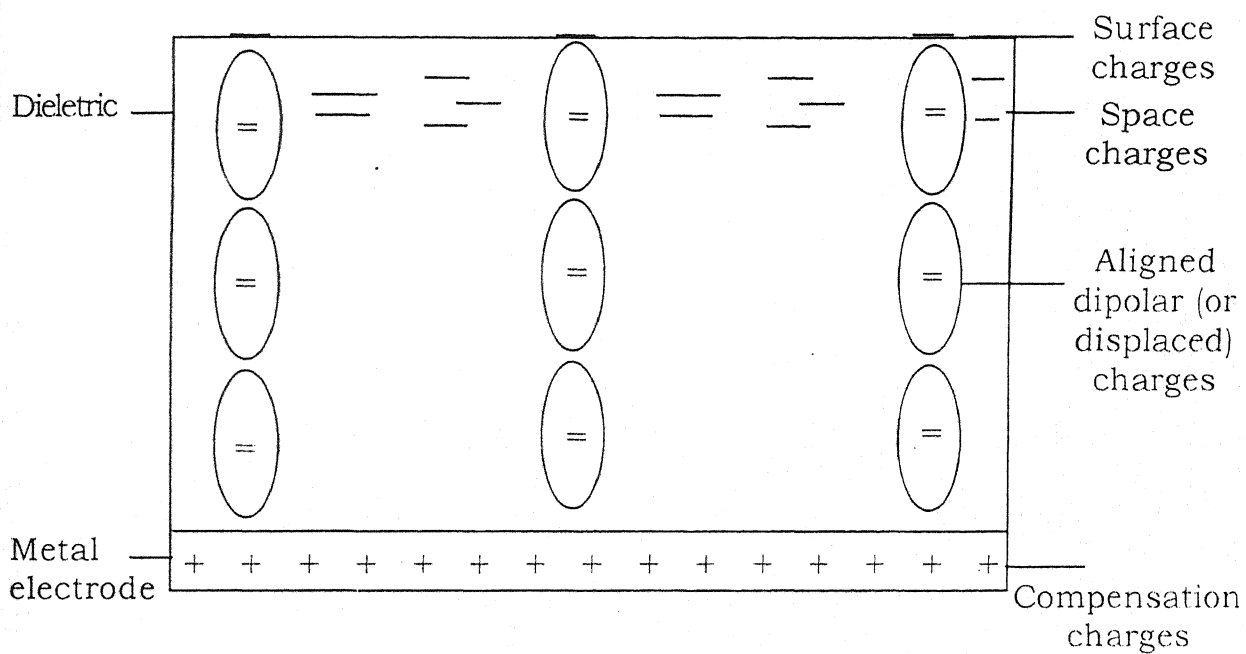


Fig. 1.30 A dielectric with various types of charges

side. Many types of electrets have been discovered and the names of these electrets are given on the basis of the method by which they are prepared. They are termoelectrets [32-35], photoelectrets [36-38], thermophotoelectrets [39-40], radioelectrets [41-42], magnetoelectrets [43-45], prepared under the simultaneous treatment of electric field and heat; electric field and light; electric field, heat and light; electric field and high energy radiations; magnetic field and heat respectively. The thesis deals only with termoelectrets.

Heaviside [46] was the first who got the idea of an electret. Eguchi [32-33] made the first termoelectret by using a mixture of carnauba wax, bees wax and resin. He melted equal parts of carnauba wax and resin, along with some bees wax, and permitted the substance to solidify in a strong electric field. He found that disks prepared in this way exhibited a strong negative charge on the face which had been in contact with the anode and vice-versa. Later Gemant [47] introduced the concepts of "heterocharge" and "homocharge". According to Gemant's terminology, a charge on the electret of the same sign is the polarity of the adjacent electrode is called a homocharge, and a charge of opposite sign to the polarity of the forming electrode is called a heterocharge.

Mikolo [48] classified electrets into two groups, viz., those comparatively high conductivity yielding heterocharges only and those of much lower conductivity capable of developing homocharge.

The first attempt towards the theory of the electret was made by Adams [49] and subsequently developed by Gemant [47], Gross [50-51] and Perlman and Meurier [52].

Electret research gradually moved to organic substances and polymers where fundamental solid state properties could be correlated with electret behaviour [30,53,54]. Recently, electret phenomena has received more attention because of their applications in electret microphones [55], electrophotography [56], electrostatic voltage generators [57], radiation dosimeters [58,59], etc.

A large number of workers have reported the electret effect in inorganic solids [60-62], organic solids [63-66], liquid crystals [67,68], polar polymers [69-76], non-polar polymers [77-79], copolymers [80-82] and biopolymers [83-85] etc. This literature on electret has been reviewed by Gutman [86] and Johnson [87].

1.5-1 EFFECT OF DIFFERENT FACTORS ON ELECTRET STATE

Electret state of polymeric materials is highly sensitive to the environmental conditions such as humidity, pressure, high energy radiations, etc. The charge of an electret also depends on the thickness of the dielectric and electrode materials used during the preparation of thermoelectret. Vander-schueren [88] and others [89-91] have shown that when an electret is exposed to high humid atmosphere, their charge decreases. Several workers [92-94] have found that thermoelectret charge

decreases with lowering the pressure. It is proposed that charge decrease is either due to desorption of charge sources from the surface of electret or due to spark breakdown at the electret surface [93,94].

Grass and DeMoraes [58] observed that on exposing a thermoelectret to Co^{60} γ -rays [89], its charge decreases. Linear relationship has been established between the loss of charge and dosage of high energy radiation [58,95] and this effect has been explained on the basis of degradation of cross linking of the polymer on irradiation.

Khanna [96] and Perlman [97] have found that the magnitude of charge of an electret increases with its thickness. There are number of observations to the fact that electrode material used in the formation of electret plays an important role in the electret [98-100]. A good correlation between the surface charge and the work-function of the metal used as electrode has been reported [97,98].

1.5-2 INVESTIGATION OF ELECTRET STATE

Measurement of charge has a special importance in the study of electret phenomena. Many techniques such as induction method [33,47,92], dissectible capacitor [70-101] generating voltmeter method [102], vibrating electrode method [103], electron beam method [104], etc. have been employed. However, none of these methods could provide a deeper insight into the electret phenomena. A significant breakthrough was achieved in the study of electret phenomena with the discovery of heat

accelerated decay of electret charges. It is known that a dielectret medium takes a long time to relax to the steady state at room temperature because at such low temperature the dipoles and charges remain virtually immobile.

Gray in 1732 [105] observed the "perpetual attractive power" in a number of dielectrics particularly in waxes, resins and sulphur. Much later in 1839, Faraday [106] theorised the electret properties due to application of an external electric field when he referred to a dielectric which retains all electric moment after externally applied field was switched off. Heaviside [107] in 1892 coined it as an 'electret'.

Systematic research into electric properties began in 1919 when Japanese Physicist Eguchi [108] formed electrets from the same materials used by Gray employing the thermal method consisting of the application of an electrical field to the cooling melt. He found that the dielectrics exhibited charges on their two surfaces which changed sign after a few days from a polarity opposite to one that of the adjacent forming electrode. The charges were later named 'heterocharge' and 'homocharge', respectively, indicating their relation to the forming electrode.

Subsequently, research on photoconductors image formation by Carlson [109] led to the development of xerography. Further studies in this field were carried out by Nadjakoff [110] and Fridkin and Zheludev [111]. Selenyi's work was related with the study of breakdown of thermal charge release. During the development of xerography, a simple charging method

related to Selenyi's ion-beam technique depending on the application of corona discharge was used [109,112] and later extended to thin films [113]. In 1937, Gross [114] used the Boltzmann-Hopkinson superposition principle valid for linear dielectrics to develop a mathematical formalism for the discharge of electrode charges over the internal resistance of dielectric and for the decay of polarisation in dielectric. Further insight into the nature of charge retention was achieved from the studies of Gerson and Rohrbaugh [115] which indicated that carrier trapping could play an important role in electrets.

It is interesting to note that the first ever electret device offered for commercial use was thick electret microphone under the name "No Voltage Veloton". Its large scale application came during World War II in Japanese field equipment.

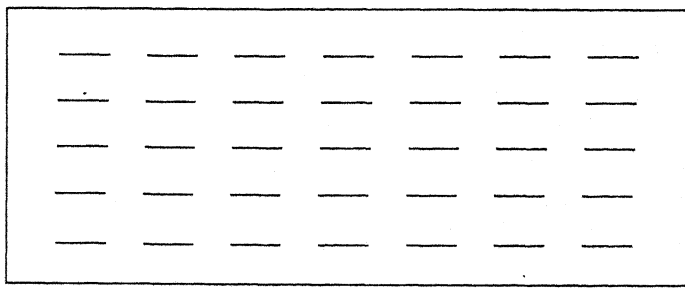
Randall and Wilkins [116] used the thermal depolarisation method for the first time for investigation of phosphorescence. In 1964, this method was applied to the case of dipole polarisation by Bucci and coworkers [117,118] who suggested the name Ionic Thermal Conductivity (ITC). It allows determination of activation energy and dipole relaxation time from the measurement of depolarisation currents obtained on linear heating of dielectric. A host of recent work has been devoted to the application of ITC methods or related thermally stimulated current techniques for investigating dipolar and space-charge respectively [119-123]. These studies have culminated in a very comprehensive treatise by van Turnhout [124]. The

early literature on electrets was reviewed by several authors notably by Fridkin and Zheludev [111] and Gross [125]. Lupu *et al.* [126] have carried out study of electret state on polyvinyl chloride (PVC). In the last decade phenomenal progress has been made in the field of electrets; more efficient charging techniques have been developed, new materials capable of storing more charge for considerably longer duration have been identified and synthesised, techniques with very good resolution for precise determination of charge centroid and its distribution in the material bulk have been devised, etc. [127,128].

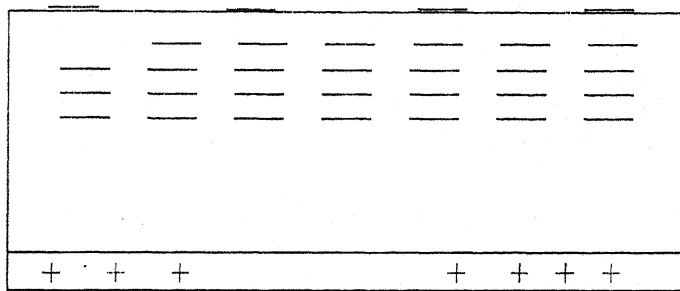
1.5-3 TYPES OF ELECTRETS

The classical electrets were made of thick plates of caruba wax. Presently, thin films made of polymers like teflon materials, polyfluoroethylene propylene (FEP), polyvinylidene fluoride (PVDF) and polytetrafluoroethylene (PTFE), polypropylene, polyethylene, etc. are utilised in making electrets [129-134]. Examples of different nonmetallised and metallised electrets are shown in Fig. 1.4. Various types of electrets are enumerated below :

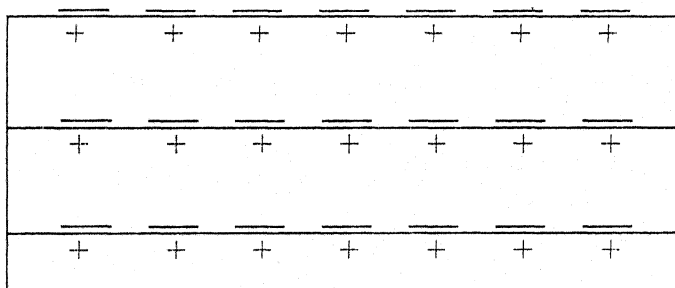
- (a) **Thermoelectret** : It is obtained by polarising a dielectric by simultaneous application of heat and electric field [135,136].
- (b) **Electroelectret** : An electret prepared at room temperature by applying high electric field is called an electroelectret [137-139].



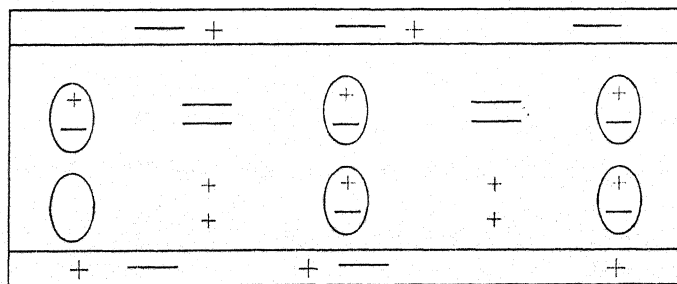
(a) A nonmetallised monocharge electret



(b) One-sided metallised electret with surface and space charges



(c) One-sided metallised electret with surface charges and charges displaced within domain



(d) Two-sided metallised electret with dipolar and space charges

Fig. 1.4: Example of electrets

- (c) **Radioelectret** : An electret prepared under the simultaneous action of high energy radiation such as X-rays, β -rays, γ -rays, monoenergetic electron beams, etc. and an electric field is called a radioelectret. These are less stable comparatively [140-142].
- (d) **Photoelectret** : An electret prepared by charging by an electric field under exposure to ultraviolet or visible radiation with enough energy to release carriers (either band to band transition or excitation out of deep traps). Such electret remains polarised for a much longer time when kept in dark. Photoelectrets were first prepared by Nadzhakov [143,144] and later studied extensively by Fridkin and Zheludev [145] and Kallmann *et al.* [146-147].
- (e) **Thermophotoelectret** : A photoconducting dielectric polarised at high temperature by light radiation of high energy under an applied electric field results into a thermophotoelectret. This was first prepared by Padgett [148].
- (f) **Magnetolectret** : It is obtained by cooling the softened or molten dielectric in a magnetic field. Bhatnagar developed this for the first time [149-151].
- (g) **Autophotoelectret** : Recently, Andreich [152] has observed voltage which increases exponentially with intensity of light and approaches nearly 1.0 V, when Al-As₂ S₃-Pt configuration is illuminated. This photo emf persists for a long time in dark. Persistence of photo-

induced voltage in dark was termed as an autophotoelectret, since this polarisation is achieved without applying any field.

- (h) **Mechanoelectret** : An electret prepared by charging a dielectric by a mechanical effect, i.e., deformation or friction is called mechanoelectret [153].
- (i) **Pseudoelectret** : These are prepared by polarising a dielectric under the action of an ionising irradiation such as γ -rays without the application of an electric field [154].
- (j) **Cathodoelectret** : These electrets are obtained by charging a dielectric under the simultaneous action of electric field and a beam of electrons [155-156].
- (k) **Bioelectret** : Electrets prepared from biological materials and biopolymers are called bioelectrets [157].
- (l) **Metal polymer electret** : Recently, a new type of electret has been formed by heat treatment of polymer layer sandwiched between two short-circuited electrodes in metal-1 polymer-metal-2 configuration. The new type of electret state has been called metal polymer electret and has been successfully used in bearings, seal corrosion durability systems, machine behaviour controls and so on [158,159].

1.6 MECHANISM OF CHARGING

Charging or polarisation of a dielectric for preparing an electret entails simultaneous occurrence of the following phenomena; namely,

microscopic displacement of charges, dipole orientation, macroscopic space charge polarisation, barrier polarisation, and external polarisation.

1.6-1 MICROSCOPIC DISPLACEMENT OF CHARGES

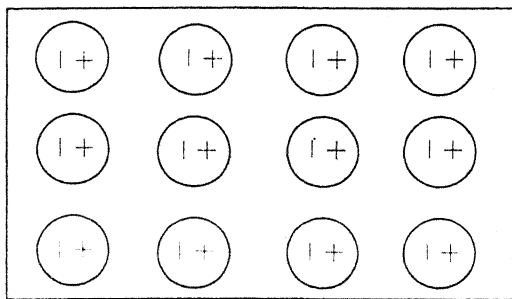
When an electric field is applied to the dielectric, it produces a small movement of charges within the atoms and molecules of a dielectric, displacing the negative electron cloud relative to the positive nucleus generating a small dipole moment. This type of polarisation is called microscopic or electronic polarisation or deformation [Fig. 1.5(a)] and its time scale cannot be changed from outside.

1.6-2 DIPOLE POLARISATION

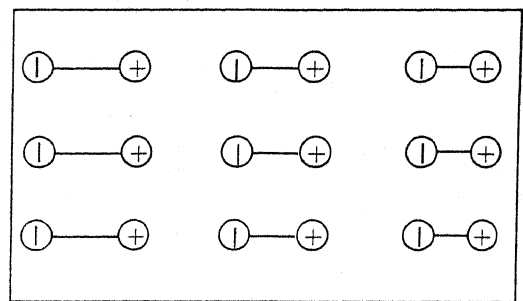
Many dielectric including polymers have a permanent dipole moment. This dipole moment may be a deliberate part of the structure (carboxylic group, chlorinated hydrocarbons, etc.) or may be accidental or unavoidable impurities (carbonyl group in polyethylene). Under normal temperatures, the dipoles are randomly arranged and the resultant dipole moment is zero. An external electric field when applied, tends to orient these elementary dipoles along its own direction producing an electric moment of the whole body. This is called dipolar polarisation and occurs in the entire volume [Fig. 1.5(b)].

1.6-3 MACROSCOPIC SPACE CHARGE POLARISATION

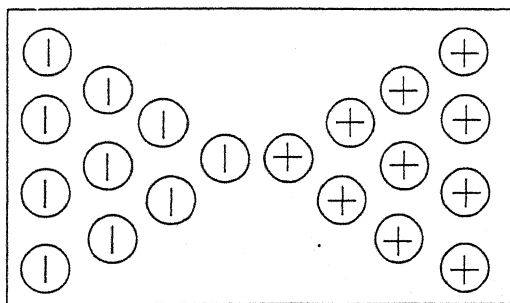
All dielectrics contain a small number of free charges, i.e. ions or electrons or both. These free charges are randomly distributed and there is



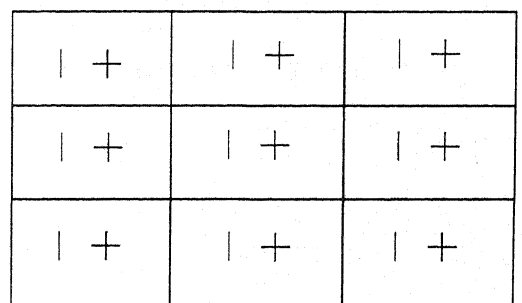
(a) Microscopic polarisation



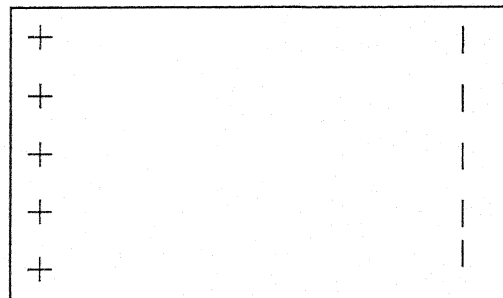
(b) Dipole polarisation



(c) Space charge polarisation



(d) Barrier polarisation



(e) External polarisation

Fig. 1.5 : Different types of polarisation

no net dipole moment when one arranges all the charges. In such materials, the applied electric field causes displacement of the positive and negative charges, resulting in accumulation of the cations near the cathode and of the anions near the anode. If a space charge of opposite sign develops in front of an electrode, the potential distribution deviates from the linear nature; in that case, the potential drop near the electrode is larger than in the centre. This effect results into a macroscopic space charge potential [Fig. 1.5(c)].

1.6-4 BARRIER POLARISATION

In a heterogeneous dielectric, often there exists some microscopic domains or grains separated by highly resistive interfaces. In such dielectrics, the free charge carriers can move relatively freely only within the grains. This results in piling up of free charges along the barriers causing in barrier polarisation [Fig. 1.5(d)].

1.6-5 EXTERNAL POLARISATION

A dielectric can also be charged by direct injection of charge carriers when a large electric field of the order of 10^5 V cm^{-1} is applied between the electrodes in intimate contact with it. Alternatively, charges may be sprayed or deposited upon the dielectric if a high voltage electrode is in contact with the dielectric and a corona discharge occurs either in the neighbouring air space at the edges of the arrangement or in the thin air space between the

electrodes and dielectric. The deposition or injection of charge on either surface produces an external polarisation [Fig. 1.5(e)].

1.7 CHARGING TECHNIQUES

There are various techniques for polarisation or charging of dielectrics, viz., thermal method, corona and other charging methods, liquid contact method, electron beam method, and photoelectric method.

1.7-1 THERMAL METHOD

In this method, an electric field is applied on a polymeric dielectric at a high temperature and thereafter it is cooled down while the field is still applied.

Eguchi [160,161] used this method for polarising a dielectric for preparing the thermoelectret. Dielectric relaxation is due to hindrances of the motions of the permanent dipoles and free charges by frictional forces. Therefore, a polar polymer is not immediately affected by the application or removal of an electric field. Only a part of its polarisation which originates from electron and ion displacement within the atoms or molecules responds almost instantaneously. Since friction is exponentially proportional to the temperature, the response time of permanent dipoles and free charges changes remarkably with temperature. By heating, the response time is accelerated and by cooling it is slowed down. In polymers, the response time changes sharply near the glass transition temperature (T_g), where the conformational motion of the main chain segments set in. Hence, polymers having their T_g above room temperature can be charged permanently by

subjecting them to a field-temperature treatment. A schematic arrangement of the method based on the above principle is depicted in Fig. 1.6.

The material is heated above the T_g , and is kept at this temperature for sometime (say 30-60 minutes) to reach the thermal equilibrium due to the motion of permanent dipoles and free charges. Thereafter, at the time t_0 , an electric field of the order of 10^4 V cm^{-4} or larger is applied which causes an alignment of permanent dipoles and drift of free charges to the electrodes. After some time (say approximately an hour), at the time t_f , the material is cooled to the room temperature T_r while the electric field is still there.

1.7-2 ELECTRON BEAM METHOD

The sample polymer is charged by injection of electron of proper energy into it. When the range of electron striking the dielectric (here a polymer piece), is less than the thickness of the polymer sample, the electrons are trapped inside and sample gets charged. If the range of the electrons is greater than the polymer sample thickness, charging occurs mainly due to the secondary emission of back scattering.

1.7-3 PHOTOELECTRIC METHOD

When inorganic photoconductors like PVK-TNF are irradiated with ultraviolet or visible light under an applied field, a permanent polarisation is achieved due to the generation of charge carriers in the sample. These carriers are then displaced by the applied field eventually trapped at the

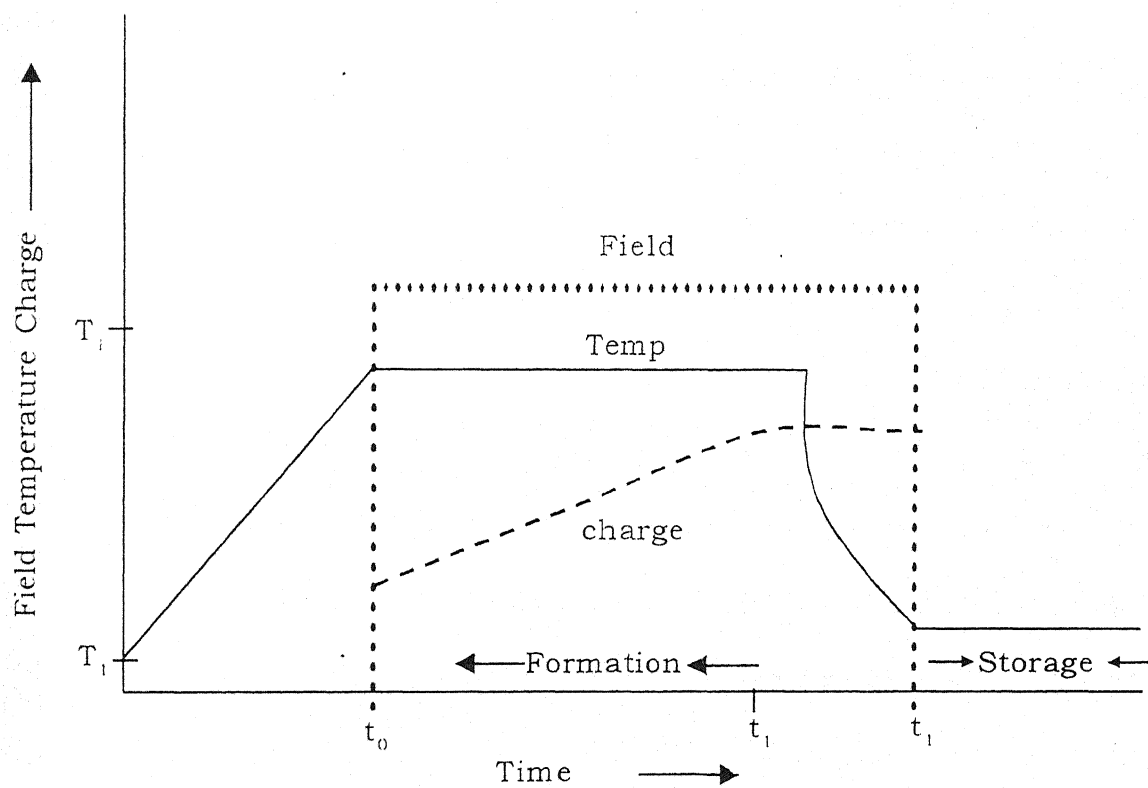


Fig. 1.6: Field temperature programme for the formation of a polymer electret

dielectric electrode interface or in the volume resulting in a two separate charge clouds of opposite sign or a single charge cloud.

1.8 TECHNIQUES FOR INVESTIGATION OF ELECTRICAL CHARACTERISTICS OF POLYMERS

The knowledge of electrical characteristics, such as type and origin of charge carriers, their storage and transport in polymer are extremely important for making stable and useful electrets. Studies of a number of methods have been carried out, viz. capacitive probe [162-165], dynamic capacitor [166,167], compensation method [168,169], split Faraday cup [170], sectioning and planning methods [171,172], light radiation release methods [173], indirect methods [174,175], thermally stimulated discharge [176], combined induction depolarisation method [177], etc. Some methods with very good resolution efficiency of determining the type and distribution of charge, such as thermal pulse method [178], pressure pulse method [179] etc. have also been devised in the last decade. However, accurate information about the electrical characteristics can be easily obtained by the following important experimental techniques :

- (a) Dark conduction current measurements,
- (b) Transient current measurements,
- (c) Thermally stimulated discharge current (TSDC) measurements, and
- (d) Dielectric measurements.

1.8(a) TRANSIENT CURRENT MEASUREMENTS

The transient current phenomena have been studied by many investigators like Spear [180], Kepler [181], Davies [182] etc. Spear carried out studies on selenium films where he measured the transient time of charge carriers and hole mobility. Kepler utilised a light pulse technique to measure the charge carrier mobility in anthracene crystals. Davies measured directly contacted electron transfer to polyethylene from a variety of metals.

Thielen, Vanderschueren *et al.* [183,184] carried out studies on several polymers like PMMA, PEMA, PVC, PS, etc. and came to the conclusion that at temperature lower than the glass transition temperature under low to moderate fields, the transient currents are essentially governed by dipolar mechanisms and as such are very much dependent on the temperature ranges of various molecular relaxation processes of the material under investigation.

Transient currents in dielectrics observed upon the application of a step voltage have been studied extensively to give an insight into the polarization processes in the materials undertaken for the study. It is generally accepted that the transient currents in an insulating material, on the application or removal of a step voltage, may be attributed to one or more of the following mechanisms : (i) electrode polarization, (ii) dipole orientation, (iii) charge storage leading to trapped space-charge effects, (iv) tunnelling of charge from the electrodes to empty traps, (v) hopping of charge carriers through localized states. The above processes have been reviewed by several scientists and it

has been established that the observed time dependence alone does not permit any discrimination to be made between various mechanisms. The argument for and against a particular mechanism is to be found by considering the variation of transient currents on various experimental parameters also, such as temperature, field and frequency. Polymers contain a large number of structural disorders and, therefore, contain discrete traps levels in their bulk. The role of various polarization processes and their relative contributions to the electret state of the polymer is not yet fully understood. Particularly, the space charge structure including the trap distribution of energy and also over the volume of the polymer, are still to be well understood. Such informations are also being obtained by carrying out the measurements of absorption and short circuit isothermal desorption (discharging) currents at various temperatures. The d.c. step response technique in which the current response is measured as a function of time after d.c. voltage is applied to, or removed from the sample, is the isothermal analogue of TSDC measurement, as it determines the discharging current at constant temperatures instead of varying temperatures.

Polyvinylidene fluoride (PVDF) is a polar polymer that exhibits excellent chemical resistance and good mechanical properties. In spite of its activeness for many applications, the conduction mechanism is presently not well understood. In the present thesis, we have attempted to identify the nature of the transient conduction and thermally stimulated discharge currents in pure polyvinyl films by comparing the observed dependence on

parameters such as electric field, electrode material, temperature, time and relation between the charge and discharge currents, in the light of characteristic features of various proposed mechanisms.

1.8(a)-1 TRANSIENT CURRENTS IN CHARGING AND DISCHARGING MODES

The charging or absorption current is obtained immediately after the application of a step voltage on a dielectric specimen, while the discharging or desorption current is obtained on removal of the step voltage provided the temperature is kept constant. Both the charging and discharging currents decay approximately as t^{-n} , where t is the time elapsed after the application or removal of the step voltage, and the exponent n is a constant depending upon the properties of the material and the experimental conditions. Charging current decays with time until a steady state current, usually known as conduction current, is reached. On the other hand, isothermal discharging current decays for a long time depending upon the internal phenomena taking place irrespective of the steady state current level.

The nature of transient charging and discharging currents differ from material to material depending upon the mechanisms involved. The origin of these transient currents is still a subject of much controversy and a large number of mechanisms have been proposed. The combined effect of one or more may be responsible for the observed decay pattern of the transient currents. The discharging current is usually mirror image of charging current, provided that a steady state current does not occur. Hence,

discharging currents can yield information about charging processes even when the corresponding charging current is masked by conduction current at charging. Quantitative as well as qualitative analysis can be made on comparing the experimental values of the decay exponent obtained under various experimental conditions.

This technique is time consuming hence it is not very popular, but results of this long time technique are most consistent than any other technique because the electrical disturbances and instantaneous variations in other experimental parameters affect these experiments much less as compared to those involved in the fast discharge processes.

The origin of isothermal charging and discharging currents has not been clearly accounted for in most of the dielectric materials because of lack of experimental data covering an adequate range of experimental parameters, i.e., field, temperature, electrode material, etc. However, the results are available for many materials although covering very few experimental conditions, which are insufficient to yield clear and firm conclusions.

In view of this it becomes worthwhile to undertake a detailed study of transient currents and to correlate the results obtained with those of other studies. This is expected to give a proper clarification of the transient response of charging and discharging in polymers, which is of prime importance for the analysis of the electret effect in polymer dielectrics.

1.8(b) DARK CONDUCTION CURRENTS - AN INTRODUCTION

It was not many years ago when the interest in the electrical properties of polymers was effectively limited to their electrical insulating ability. This situation has changed very markedly in recent years. The replacement of inorganic semiconductors and metals by organic macromolecules has recently been termed "Molecular Electronics". The large number of atoms per organic molecule makes a great variety of modifications possible and therefore subtle variation in electrical properties should be possible.

The conduction in polymers is a complex process and takes place due to intrinsic charge carrier generation and charge carrier injection from the electrode contacts at high electric field. The theoretical and experimental analysis have been thoroughly carried out by Kao and Hwang [185]. The band theory, mobility theory, carrier production and transport mechanisms have been dealt with by Wintle in his monograph [186]. The review article on electrical conduction by Adamec and Calderwood [187] takes up the time dependence of the conductivity of PVC, PMMA, PC and epoxynovalac resin and gives a theory for the origin of free charge carriers.

Recent work has been done by Molitan [188] who gave the theoretical model in terms of the SP_2 dangling-band states after carrying out conduction measurements on poly(paraphenylene). Chandra and Chandra [189] studied the mixed anion effect in polyethylene oxide-based sodium-ion-conducting polymer electrolytes. Ieda *et al.* [190] in their review

article have in detail takes up the high field conduction and breakdown of low density polyethylene, polystyrene, polyisobutylene, polyvinyl chloride, polymethyl methacrylate and elongated high density polyethylene.

The process of charge transport in polymeric semiconductors is a complex phenomena. The actual nature of conduction mechanism in a variety of polymeric films is still a matter of speculation. Although the body of experimental information on the study of electronic properties of polymeric materials is enormous, no comprehensive theoretical approach, which can adequately interpret all observations and measurements, so far has been proposed. The complexity and chemical structure of numerous long chain high mol. wt. polymers make it difficult to consider the transport behaviour in terms of generalised transport theory. In most cases models derived for conventional semiconductors are applied to polymeric systems.

The electrical conductivity (σ) of a solid is defined [191] as the ratio of current density (J) to the electric field (F). The conventional measuring technique consists of applying a known voltage across a sample of known dimensions and determining the current in the external circuit.

$$\text{Electrical conductivity} = \frac{\text{Current density (J)}}{\text{Electric Field (F)}} = \frac{(I / A)}{(V / d)} = \frac{Id}{VA}$$

where d and A are thickness and area of the sample, respectively.

The magnitude of conductivity depends on the number of charge carriers and their mobility. The mobility of the carriers is the measure of the ease with which the carrier can pass from one molecule to another. In view

of the relatively large intermolecular spacings common to polymeric systems, mobility values are several order below to those of conventional semiconductors.

The charge carriers may be generated intrinsically or from impurities, in which case, they may be electrons, holes or ions. Alternatively, holes and electrons may be injected from the electrodes. Therefore, conduction may be of two types - ionic or electronic, i.e., current carriers are free ions or electrons.

A semiconductor is p-type with n-type depending on whether it is having excess of holes or electrons. The charge carriers are called majority or minority carriers depending on which predominates.

In general, polymers are insulating materials having conductivities ranging from 10^{-10} S/cm for polyvinyl chloride to 10^{-18} S/cm for polytetrafluoroethylene, which are many orders of magnitude below the conductivities associated with metals (Fig. 1.7).

1.8(b)-1 ELECTRICAL CONDUCTION IN POLYMERS - A BRIEF SURVEY

Saegusa [192] in 1926 was the first to measure the conductivity in paraffin wax as a function of temperature. Clark and Williams [193] in 1933 published an excellent work on the conductivity of organic solids and they were the first to establish unequivocally the exponential relation between conductivity and temperature in these materials. Fuoss [194] did similar

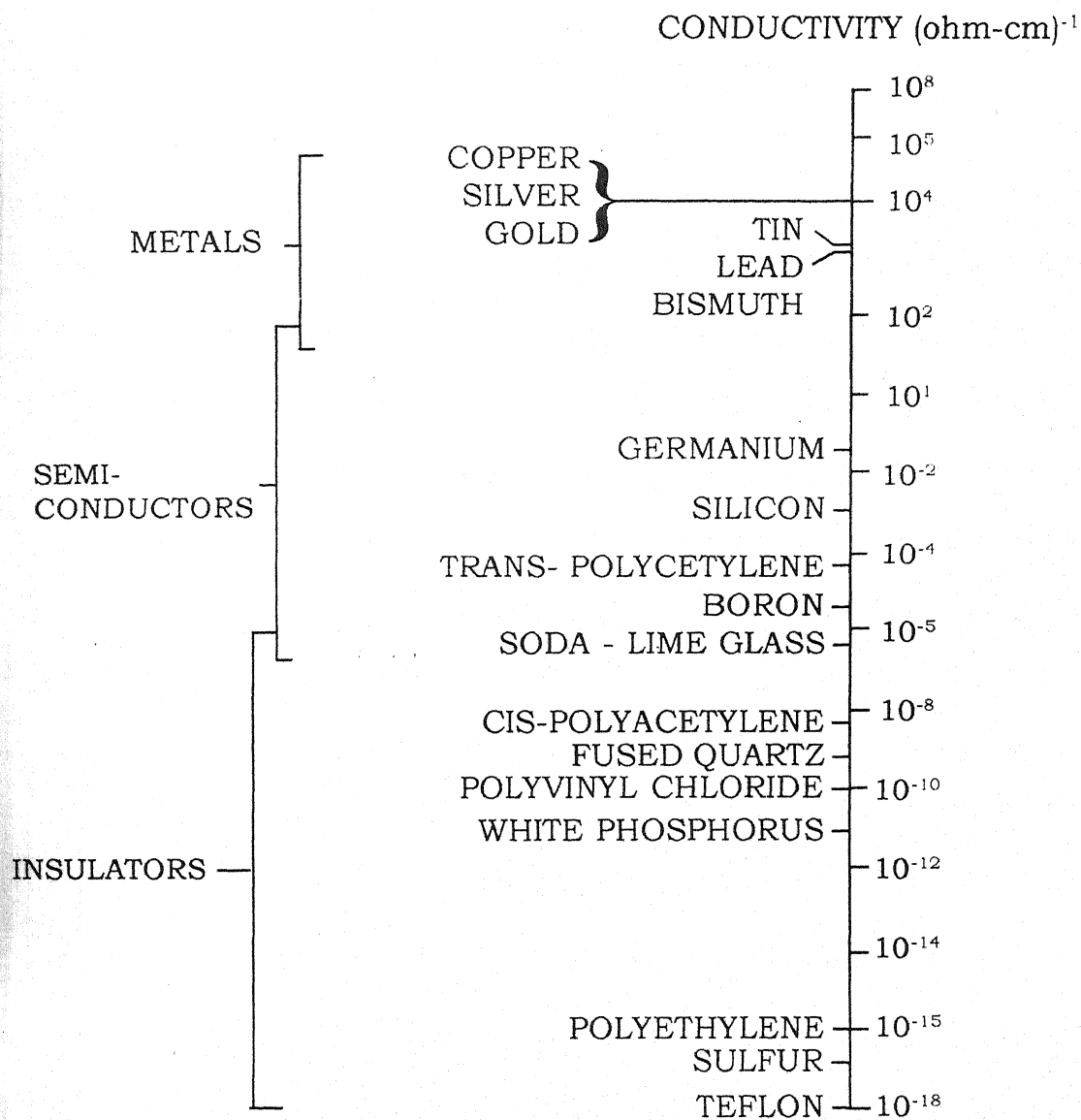


Fig. 1.7 : Conductivity of various metallic, semiconductor and insulating materials.

work on a number of polymers and supported the exponential relation of Clark and Williams [193]. In 1954, Akamatu *et al.* [194,195] observed for the first time that some solid organic charge transfer complexes display a surprisingly high conductivity. A significant breakthrough in the study of electrical properties of organic solids occurred with the discovery of tetracyanoquinodimethane (TCNQ) ion radical salts [196]. These salts have general stoichiometric formula $M^+ (TCNQ)_n^-$ and depending on M and n, the properties of these materials have been observed to vary from those of insulators to those of metals. Highly conducting polymers have been prepared by utilizing some of the knowledge gained from the studies of solid charge transfer complexes. In 1977, Shirakawa *et al.* [197] showed that highly conductive polymers could be prepared by adding small quantities of either electron donating or electron accepting species to conjugated polymers. The discovery [198] of poly(sulphur nitride) in 1973 as an intrinsically conducting polymer gave a tremendous boost for the search of other polymers.

The very exciting possibility for polymers has been discovered by Little [199]. He proposed that it might be possible to prepare polymers that are superconductors and these polymers could have superconducting transition temperature well above the room temperature.

All these results and speculations have led to an increasing tempo in research on electrical properties of polymers. A large number of excellent reviews of this work have been published. A particular mention should be

made about the works of Gutmann and Lyons [191], Meier [200], Kepler [201], Bogulsavskii and Vanikov [202], Seanor [203] and Skotheim [204].

A wealth of information on the process of charge transport in polymeric films can be obtained from the measurement of electrical properties as a function of temperature, electric field and frequency. There is ample evidence for ionic and electronic conduction in a variety of polymers. Von Roggen [205] and others [206-208] have reported that conduction in polymers is ionic in nature. The conduction in polyvinylchloride is reported to be ionic and is attributed to H^+ and Cl^- ions [208]. Few workers [209,210] have suggested protonic conduction in polyamides.

Electronic conduction in polymers has been extensively studied [211-213]. Myoshi and Chino proposed electronic conduction in polyethylene [213]. A number of authors [214-218] have studied the conductivity of biopolymers. A complication in the study of biopolymers is that they contain a large amount of water. If before the measurement, the biopolymer is dried, many of its properties become completely different from those which it had in the living organism. In the study of proteins containing water it is difficult to distinguish the electronic conductivity from ionic conductivity. Consequently, the results of experimental studies carried out with different proteins are extremely contradictory. Some authors state that ionic [216] or protonic [217] conduction exists in a protein, other have concluded that proteins are electronic semiconductors [218].

Several mechanisms such as tunnelling, hopping, Richardson-Schottky emission, Poole-Frenkel effect, space charge limited current, etc. have been proposed to explain the transport of charge carriers in polymeric films. The theoretical details of these mechanisms are given in Chapter III.

1.8(c) THERMALLY STIMULATED DISCHARGE CURRENT (TSDC) MEASUREMENTS

Polymers are generally good dielectrics which are capable of storing charge in them permanently, when subjected to field-temperature treatment and are known as thermoelectrets. When such thermoelectrets are subjected to a programmed heat treatment, they give rise to a current in the external circuit which is known as thermally stimulated discharge current (TSDC). TSDC is an accurate, sensitive and convenient method for studying the charging and discharging processes in dielectrics. These currents are due to the dielectric relaxation behaviour and motion of free charges in the polymers. Hence, TSDC technique can be used to understand the low frequency dielectric behaviour and relaxation processes on the atomic scale. Because of the high sensitivity of the technique, it is also used to investigate the low concentration of the dipolar impurities, formation and aggregation of impurity-vacancy complexes, phase transitions, photographic response of silver halide, etc.

Thermally stimulated discharge current (TSD) technique is a powerful method to gain an insight into the mechanisms of charge migration and dipolar motions. The process of TSD measurement involves

the poling of the polymer film for certain values of poling parameters such as poling field (E_p), poling temperature (T_p) and poling time (t_p) and its heating in a specially designed cell, with a constant heating rate. The details of each step involved in this measurement are discussed below.

1.8(d) DIELECTRIC MEASUREMENT

The dielectric behaviour of polymeric films is of direct interest to both the basic studies of electrical conduction through such films and their application in capacitors for microelectronics. To obtain high values of capacitance the dielectric constant should be high and the thickness be small. Due to the difficulty of obtaining structurally continuous and stable ultrathin films, capacitor applications are generally limited to thick films. The evaluation of the dielectric properties of insulator films is carried out by measuring simultaneously the capacitance and the dissipation factor over a wide range of frequencies and temperature [218-a].

The most important property of dielectrics is their ability to be polarised under the action of an external electric field. The basic parameter of a dielectric describing its properties from the view point of the process of its polarization or propagation of electromagnetic waves in it, or more generally from the view point of the processes of its interaction with an electric field is the permittivity. Permittivity (dielectric constant) is the number which shows by how many times the capacitance of a vacuum capacitor will increase if the capacitor is filled with the dielectric without

changing its dimensions and shape. It is a macroscopic parameter of a dielectric which reflects the properties of a given substance in a sufficiently large volume but not the properties of the separate atoms and molecules in the substance. As all the other electrical parameters of dielectrics, the permittivity depends on the changeable external factors such as the frequency of voltage applied to the dielectric, temperature, pressure, humidity, etc. In a number of cases these dependences are of paramount practical importance [218b-d].

When an electric field acts on matter, the latter dissipates a certain quantity of electric energy that transforms into heat energy. This phenomenon is known as 'the expense' or 'loss' of power, meaning an average electric power dissipated in matter during a certain interval of time. As distinct from conductors, most of the dielectrics display a characteristic feature : under a given voltage the dissipation of power in these dielectrics depends on the voltage frequency; the expense of power at an alternating voltage is markedly higher than at a direct voltage, and rapidly grows with increase in frequency, voltage and capacitance, and also depends on the material of the dielectric. The amount of power losses in a dielectric under the action of the voltage applied to it is commonly known as dielectric losses. This is the general term determining the loss of power in an electric insulation both at a direct and an alternating voltage. The dielectric loss angle is an important parameter both for the material of a dielectric and an insulated portion. All other conditions being equal, the dielectric losses

grow with the so called loss tangent ($\tan \delta$). Sometimes the quality factor of an insulation portion is determined, i.e. the value reciprocal of the loss tangent.

A number of reports [218e-h] on the dielectric properties of polymer films have been published. The value of $\tan \delta$ exhibits a maximum at a frequency at which dielectric permittivity (ϵ) shows dispersion. Some polymers show polarization when compressed or distorted. The general theory of dielectric dispersion has already been elaborated. It follows from general considerations that dielectric dispersion is analogous to mechanical dispersion and similar mathematical treatment may be used to describe both these phenomena.

The maxima in dielectric loss occurs at temperatures at which motion of large segments of the main chain or different polar side groups begins. Thus, these temperatures are related to the temperature at which the same transitions are observed in mechanical studies (at the same frequency). These are, however, cases in which transition temperature differ considerably. This may result from different fields acting in both these cases. Dielectric behaviour of high polymers is generally characterized by the distribution of relaxation times. These distributions may be obtained by the procedure applied to obtain distributions of mechanical relaxation times. In many cases they are similar but not identical.

Notable progress has been made in the understanding of the mechanism of dielectric dispersion. Several phenomenological models [218i,j] have been proposed relating the main relaxation to free volume. Petrosian [218k] deduced dielectric parameters for a polymer system using the general dielectric loss theory and found values consistent with those derived from experimental results. Dielectric behaviour of amorphous polymer systems in macroscopic and molecular terms was analysed by Cook *et al.* [218l]. Pollock [218m] developed a theory of dielectric constants arising from electron localized states which contribute to elucidation of conductivity. Ishida [218n] reviewed the effects of stereoregularity, pressure, crystallinity, plasticizers, and so electric field an absorption due to motions of molecular chain segments (α_c), micro-Brownian motion of main chain segments in amorphous region (α_a), and local relaxation (β).

1.9 AIM AND SCOPE OF THE PRESENT INVESTIGATION

Polymers are widely used in many areas of electrical and electronic devices in diverse applications because of their extremely small size, abundance, diversity, ease of processing and fabrication. These materials are unique because of the range of structural forms that can be synthesized and the way in which changes can be made in the structure in a local or a general way.

It can be observed from the review of the available literature that charge storage phenomena is rather sensitive to the structure of the electret forming material. It has been reported that even the electret state in

a polymer can be produced not only by conventional methods, but also by merely bringing about some structural changes in the electret forming material. During the past few years, therefore, main efforts have been directed towards understanding the relationship between the structure and properties of the electret forming materials.

1.10 POLYMER USED - POLY(VINYLIDENE FLUORIDE)

The molecular origin of the transition is not the same for all the polymers. A brief description of various relaxations of poly(vinylidene fluoride) (PVDF) is given below :

(A) Relaxations in PVDF :

Lovinger [218(i)] have investigated relaxation in PVDF by studying dielectric behaviour through mechanical, NMR and piezoelectric investigations [218(ii)]. Dielectric studies of PVDF in the frequency range (1 Hz - 1 MHz) shows three transitions corresponding to the α^- , β^- and γ^- relaxation.

α -relaxation : Peterlin *et al.* [218 ii,iii] have investigated α -relaxation and attributed it to amorphous regions. However, Yano [218iv], Sasabe *et al.* [218v] and Osaki [218vi] have attributed these α -relaxation to crystalline regions. Later Nakagawa *et al.* [218 vii] and Yano [218 viii] offered convincing evidence of a crystalline α -transition. This was confirmed by nuclear magnetic resonance studies by other workers [218ix].

β -relaxation : β -relaxation is attributed to micro-Brownian motion of amorphous segments [218vi,ix,x]. It is related to glass transition temperature and occurs around (-40°C).

β' -relaxation : The β' -relaxation has been reported to occur at 50°C . This occurs in amorphous region and has been attributed to chain fold motion [218ix].

γ -relaxation : The γ -relaxation has been observed at around -70°C . It is attributable to amorphous phase and is associated with chain relaxations in amorphous regions [218iii,ix].

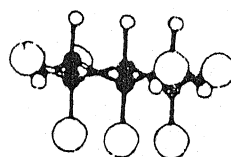
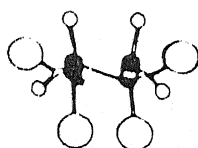
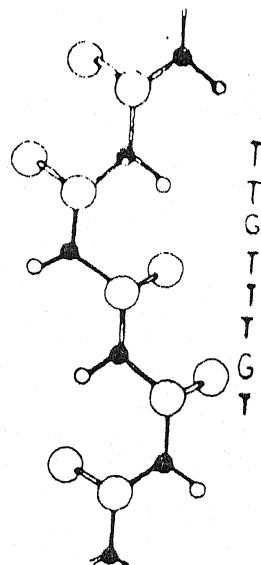
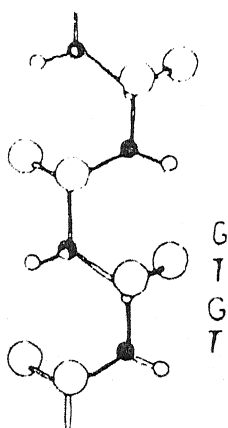
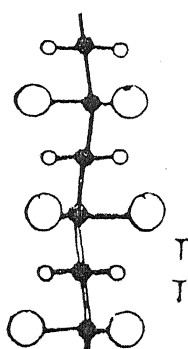
Orientation and poling of PVDF have been found to influence its relaxation behaviour. Application of pressure increases the α -relaxation temperature. The intensity of α -relaxation is found to decrease by the process of poling and orientation. Yamada *et al.* [218x] have reported that a crystalline α -relaxation (α_c) at about 58°C in PVDF is intensified after drawing and annealing. This has been attributed to molecular motion of crystalline regions of a well defined β -phase PVDF. A transition around 70°C has been reported for PVDF-TrFe copolymer [218xi-xvi]. In case of composites, a transition around 80°C has been observed which was absent in pure PVDF. This indicates that the relaxation and transitions in PVDF are much more complicated and depend not only on thermal history of the sample but also varies with other factors such as constituent phases, pressure, poling, orientation and the composition of the sample.

1.10-1 PHYSICAL, CHEMICAL AND MORPHOLOGICAL PROPERTIES OF PVDF

PVDF is of fundamental interest for its different crystalline phases and phase transitions. PVDF can present five distinct crystalline structures depending on the formation conditions of the polymer. Four of these phases designated as α , β , γ and δ are respectively by form II, I, III and IV (or IIp) are stable at room temperatures, a fifth form, ϵ , could exist just below the melting point [219] (Fig. 1.8, 1.9).

The α -phase of PVDF crystallizes directly from the melt [220]. The β -phase is normally obtained by mechanical deformation of α -form [221]. The β -form may also be grown from solution under special conditions [222]. Growth from solutions such as dimethyl sulfoxide or dimethyl acetamide usually leads to γ form [223].

PVDF is inherently polar. The hydrogen atoms are positively charged and the fluorine atoms negatively charged with respect to the carbon atom in the polymer. The net moment of a group of molecules in a liquid region of PVDF will be zero in the absence of an applied field because of the random orientation of individual dipoles. In the crystal, there are β and γ (Form I and III) phase where the molecules are reported to form a planer zig-zag (all trans) conformation [224] with the dipole moments parallel in the unit cell. β and γ crystal forms of PVDF are, therefore, inherently polar. The γ phase is a polar form. This is an intermediate phase between α and β phase, and can be viewed as a



β -FORM
(TT)

α -AND δ -FORMS
(TG, TG)

γ -FORM
(T₃G, T₃G)

(a)

(b)

(c)

Fig: 1.8

SCHEMATIC MODELS OF MOLECULAR CONFORMATIONS IN
PUDF MOLECULES PROJECTED FROM NORMAL (TOP) AND
PARALLEL (BOTTOM) TO THE CHAIN AXIS

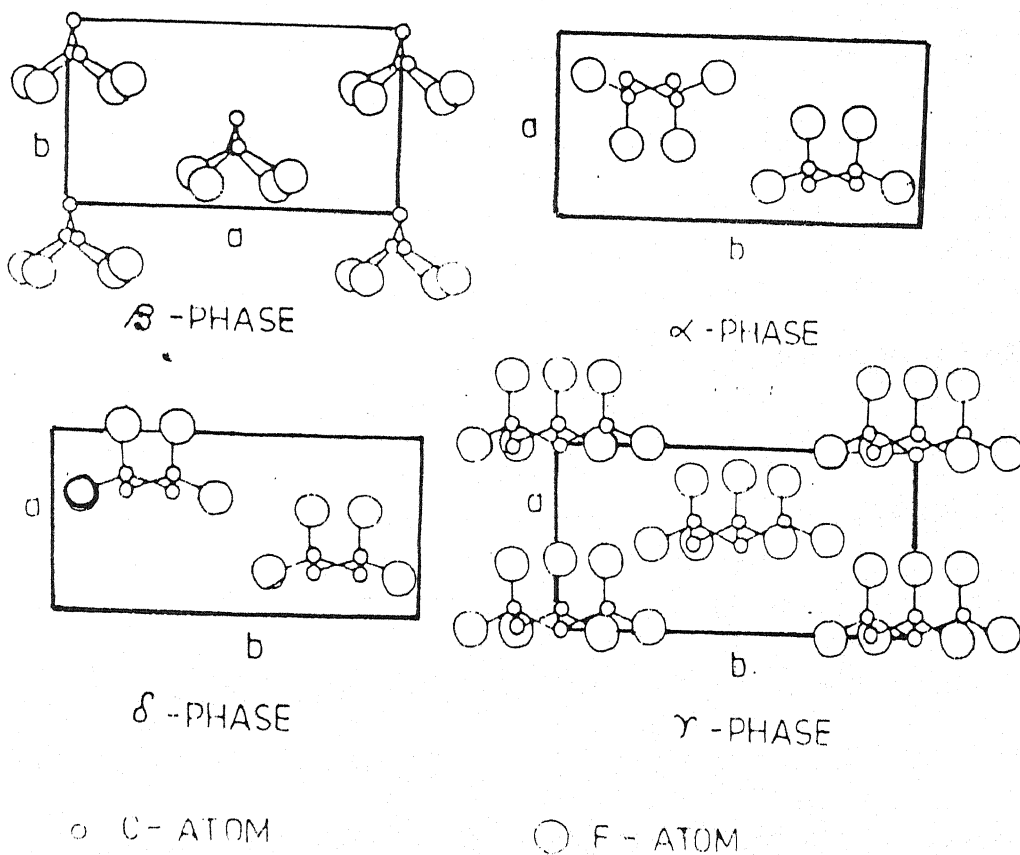


FIG 1-9 CRYSTAL STRUCTURES OF PVDF.

kinked all trans conformation. Mechanical orientation of γ phase yields β phase. The crystals of β PVDF are orthorhombic and have two CH_2CF_2 monomers per primitive cell with lattice spacings $a = 0.858$ nm, $b = 0.491$ nm, $c = 0.256$ nm. The magnitude of the dipole moment for each monomer unit is 7.0×10^{-13} cm. Phase II (α form) has trans-gauch-trans-gauch (TGTG') conformation. It has a net dipole moment with a component normal to the molecular axis but the chains pack to form an antipolar unit cell [224]. However, phase II is not non polar under all circumstances but can have unit cell dipole moments of 5×10^{-30} cm after orientation of poled films (Fig. 1.10 to 1.11). The fraction of crystal amorphous interface in the PVDF homopolymer is 0.35. Crystallinity of PVDF homopolymer is 0.63 [225].

X-rays [226] and infrared [227] results (data) indicate that poling changes morphology in PVDF [228]. Other technique for controlling the morphology include crystallization from solution [229] and high temperature annealing [230].

Depolarization studies were carried out on PVDF electrets by Takamatsu and Fukada [231]. Depolarization studies of roll drawn PVDF films show that it can retain a large polarization and show a fairly large piezoelectric effect without being polarized electrically [232]. The depolarization current of a PVDF film prepared by solvent casting is

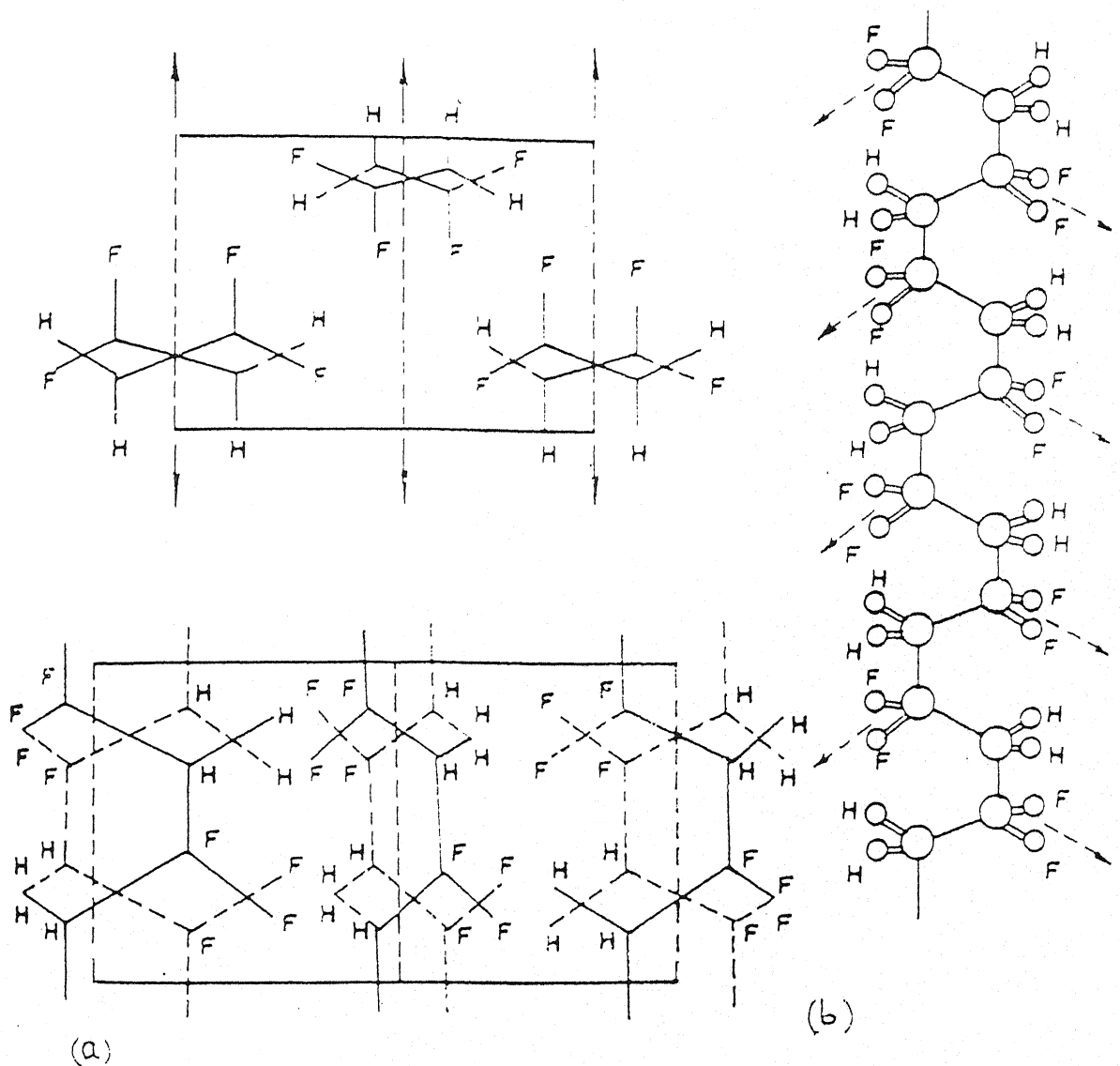


Fig 1.10: Configuration of the α PVDF crystalline from :

(a) Unit cell according to the structure of Bachman and Lando Down and up chains are depicted by solid and broken lines respectively.

(b) TG^+ TG^- chain conformation dipolar moments are indicated

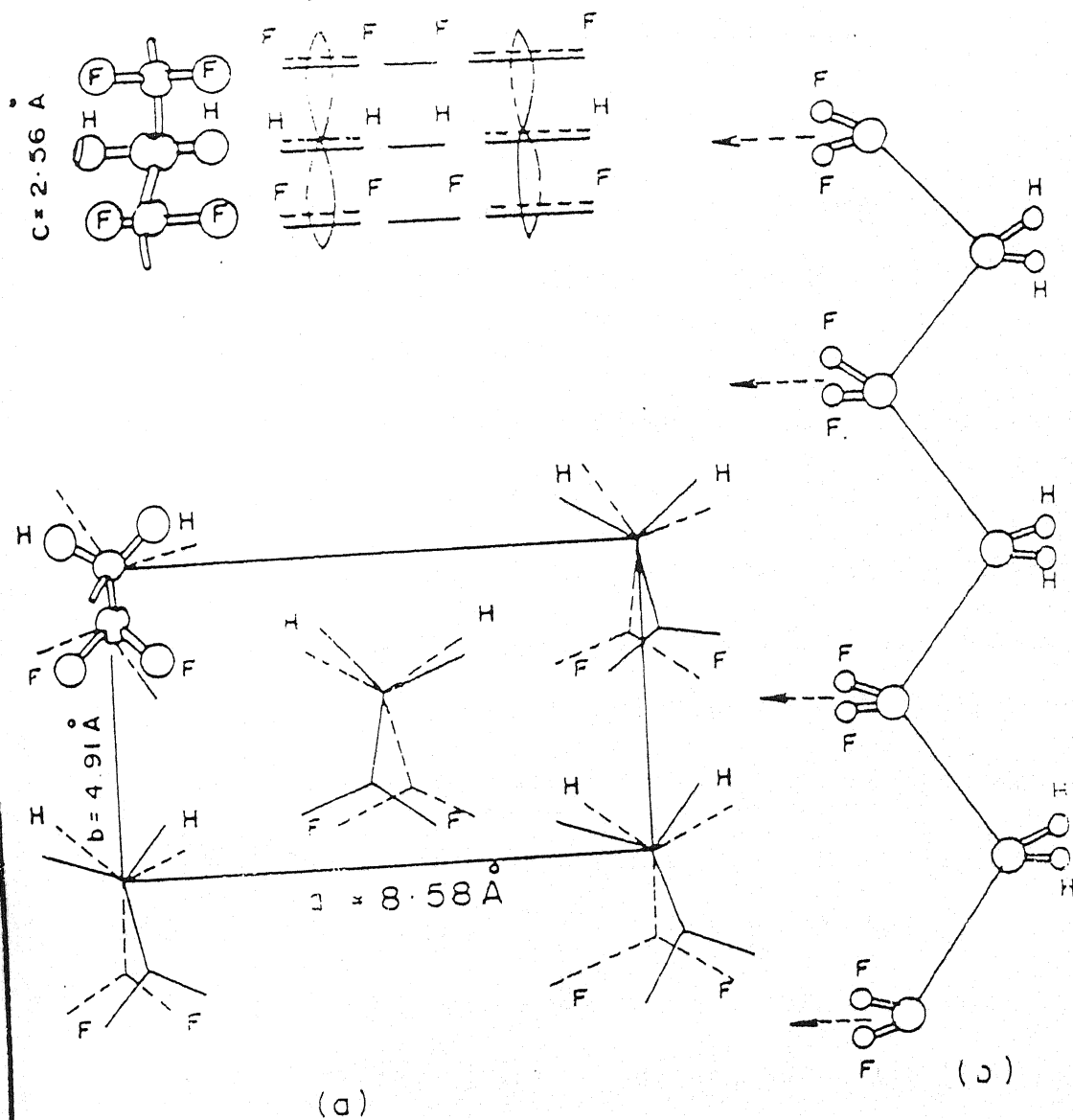


Fig.1.11 : Configuration of the β PVDF crystalline from.
 (a) Unit cell (b) TT zig-zag chain conformation (dipole moments are indicated)

extraordinarily large [233]. Depolarization studies of unstretched, stretched, solvent cast and doped PVDF films have been done by Tara [234].

Murayama and Hashizume [235] studied depolarization and pyroelectricity of thermoelectrets prepared from β form PVDF. Depolarization current and pyroelectric activity depends on poling time, field and temperature. The depolarization spectra obtained from different electrets have five peaks. The first peak P_1 is obtained around 60°C as a weak shoulder. This peak is related to characteristic molecular motion at this temperature [236]. The second peak depends on polarizing temperature and shifts towards higher temperature with increasing poling field E_p . Therefore, it is due to trapped charges, P_3 and P_4 appear near the melting temperature, P_3 is polarization responsible for piezo-electricity, P_4 gives negative depolarization current because of space charge caused by migration of charges over microscopic distances. The last peak P_5 appears in the melting temperature region and is related to phase transition. Charge storage capacity of PVDF films can be increased by doping [237].

The electrical conductivity by PVDF depends on ionic impurity concentration, which in turn depends on sample history [238] and field strength [239]. Typically the resistivity ρ is 10^{14} – 10^{15} cm for PVDF at room temperature and the relative permittivity ϵ_s is 10-15 [236].

The high dielectric constant of PVDF and its copolymers make them potential candidates for energy storage devices [240]. Recently, Jow and

Cygan have found that dc breakdown strength of PVDF is very high and ac breakdown strength is very low. Low ac breakdown strength of PVDF relative to its dc breakdown strength can be attributed to its specific dielectric properties, namely the piezoelectricity and ferroelectricity. The injected space charge that exists at the surface of polarized zones is the reason for PVDF's high dc breakdown strength. Large interval stress existing at the boundaries of the polarized zones plus the space charge mentioned will induce breakdown near any defect in the sample under ac conditions.

PVDF exhibits extraordinary piezoelectric, dielectric, ferroelectric and pyroelectric properties [241]. Piezoelectricity means change in polarization on application of stress or strain. The electrets of PVDF show a piezoelectric strain constant more than 10^{-6} cgs esu [242]. The β phase has the highest piezoelectric activity. The piezoelectricity depends on crystal form and stretching conditions. The piezoelectricity of PVDF electrets is quite stable at room temperature [243].

It was suggested by Murayama [244] that piezoelectricity can be explained on the basis of trapped charge theory. Recently, Schaffner and Jungnickel [245] have studied the dielectric moment contribution to the piezoelectricity of PVDF.

Pyroelectricity is the effect which exhibits a change in polarization when the temperature of the sample is changed. Pyroelectricity in PVDF is studied by many workers [246-248]. Pyroelectric material exhibits a

spontaneous polarization. True (reversible) pyroelectricity originates from the temperature dependence of spontaneous polarization. As the polar pyroelectric materials are also piezoelectric, a strain originating from a thermal expansion may also provide a secondary pyroelectric effect which is, however, small in comparison with the primary pyroelectric effect.

Ferroelectrics constitute a special class of dielectrics which has a spontaneous polarization which can be switched by action of an external electric field. Ferroelectrics belong to a subgroup of pyroelectrics which belong to a subgroup of piezoelectrics. PVDF and its copolymers with other polymers exhibit ferroelectricity. Ferroelectricity in PVDF and copolymers of PVDF and TrFE (Trifluoro ethylene) has been studied using different methods [249].

/ ***** /

TABLE - 1.1

CHARACTERISTICS OF 5-CRYSTALLINE FORMS OF PVDF :

α , β , γ , δ and ϵ

	α form	β form	γ form	δ form	ϵ form
Crystalline form	Ortho-rhombic	Ortho-rhombic	Mono-clinic	Ortho-rhombic	Mono-clinic
Space group	P2 cm	CM2M	Cc	P2cm	Cc
Chain conformation	TG ⁺ TG ⁻	TT	T3G ⁺ T3G ⁻	TG ⁺ TG ⁻	T3G ⁺ T3G ⁻
Polar conformation	Antipolar	Polar	Polar	Polar	Antipolar
Dipolar moment/ monomer	$\mu = 3.4 \times 10^{-30}$ cm $\mu = 4.0 \times 10^{-30}$ cm	$\mu = 0$ $\mu = 7.00 \times 10^{-30}$ cm	$\mu = 3.4 \times 10^{-30}$ cm $\mu = 4.0 \times 10^{-30}$ cm	—	—
Elementary cell	a = 4.96 Å b = 9.64 Å c = 4.62 Å	a = 8.59 Å b = 4.91 Å c = 2.56 Å	a = 4.96 Å b = 9.58 Å c = 9.23 Å	a = 4.96 Å b = 9.64 Å c = 4.62 Å	a = 4.96 Å b = 9.58 Å c = 9.23 Å
Density	1.92 g/cm ³	1.97 g/cm ³	1.94 g/cm ³	1.92 g/cm ³	1.94 g/cm ³

REFERENCES

1. Chen, R. and Kirsh, Y., Analysis of Thermally Stimulated, Pergamon Press Limited (1981).
2. Gowariker, V.R., Viswanathan, N.V. and Shreedhar, Jayadev, Polymer Science, Wiley Eastern Limited (1987).
3. Sessler, G.M. (Ed.), Acoust. Soc. Am., **34**, 1787 (1962).
4. Zhongfu and Hongyan, Z. (Eds.), Proc. 9th International Symposium on Electrets (ISE 9), Shanghai (1996).
5. Schaffert, R.M., Electrophotography (Wiley, New York) (1975).
6. Turnhout, J. van, Bochove, C. van and van, G.J., Staub. Reinhalt Luft., **36**, 36 (1975).
7. Andryuschchemks, V.A., Autom. Remote Control (USSR), **21**, 93 (1960).
8. Hine, G.H. and Brownell, G.L. (ed.), Radiation Dosimetry (Academic Press, New York) (1956).
9. Lines, M.E. and Glass, A.M., "Principles and Applications of Ferroelectrics and Related Materials" (Clarendon Press, Oxford) (1977).
10. Hennian, C. and Lewiner, J., J. Acoust. Soc. Am., **63**, 1229 (1978).
11. Jefimenko, O.D., "Electrostatic Motors, Electrostatics and its Applications", Ed. by A.D.Moore (Wiley, New York) (1973), pp. 131-142.
12. Wider, H. H. and Kaufman, S., Elect. Engg. (USA), **72**, 511 (1953).
13. Turnhout, J. van, J. Electrostat., **1**, 147 (1975).

14. Holland, E.R. *et al.*, J. Appl. Phys., **75**, 12 (1994).
15. Yasufusa, Tada, IEEE Trans. on Electrical Insulation, **28(3)**, 402 (1993).
16. Debye, P., Polar Molecules, Dover Publications, London (1945).
17. Frohlich, H., Theory of Dielectrics, Oxford University Press, London (1958).
18. Haroop, R.J., Dielectrics, John Wiley, New York (1972).
19. Cole, K.S. and Cole, R.H., J. Chem. Phys., **9**, 341 (1941).
20. Havriliak, S. and Negami, H., Polymer, **8**, 161 (1967).
21. Ishida, Y., Kolloid Z., **174**, 124 (1961).
22. Masayuki Ieda, IEEE Trans. Elec. Insul., Vol. **EI-15**, No.3, 206, June (1980).
23. Mahendru, P.C., Singh Ramadhar, Panwar, V.S. and Gupta, N.P., J. Phys. D. Appl. Phys., **17**, pp L 61-64 (1984).
24. Pathmanathan, Dissado, L.A. and Hill, R.M., J. Mat. Sci., **20**, 3716 (1985).
25. Narula, G.K. and Pillai, P.K.C., J. Mat. Sci. Lett., **8**, 608 (1989).
26. Tripathi, A., Tripathi, A.K. and Pillai, P.K.C., J. Mat. Sci. Lett., **9**, 443 (1990).
27. Singh Ramadhar, Panwar, V.S., Tandon, R.P., Gupta, N.P. and Subhash Chandra, J. Appl. Phys., **72(8)**, 3410 (1992).
28. Jow, T.R. and Cygan, P.J., J. Appl. Phys., **73(10)**, 5148 (1993).
29. Kozakov, A. *et al.*, J. Phys. D. Appl. Phys., **26**, 967 (1993).

30. Turnhout, J. Van, "Thermally Stimulated Discharge of Polymer Electrets", Elsevier, Amsterdam, 1975.
31. Sessler, G.M. (Ed.), "Electrets", Topics in Applied Physics, **33**, Springer-Verlag, New York, 1980.
32. Eguchi, M., Japan J. Appl. Phys., **1**, 10 (1922).
33. Eguchi, M., Phil. Mag., **49**, 178 (1925).
34. Perlman, M.M., Electrochem. Technol., **6**, 95 (1968).
35. Pillai, P.K.C., Jain, K. and Jain, V.K., Phys. Status Solidi (a), **13**, 341 (1972).
36. Nadzhnikov, G., Chem. Rev., **204**, 1865 (1937).
37. Fridkin, V.M. and Zheludev, I.S., Photoelectrets and the Electrophotographic Process, Consultants Bureau, New York, 1960.
38. Pillai, P.K.C. and Goel, Malti, Phys. Status Solidi (a), **6**, 9 (1971).
39. Padgett, E.P., Radio Electronics, **2**, 61 (1955).
40. Pillai, P.K.C., Balakrishnanand, K.G. and Jain, V.K., J. Appl. Phys., **42**, 525 (1974).
41. Murphy, P.V., J. Chem. Phys., **38**, 2400 (1963).
42. Murphy, P.V., J. Phys. Chem. Solids, **24**, 329 (1963).
43. Bhatnagar, C.S., Indian J. Pure Appl. Phys., **2**, 331 (1964); **4**, 355 (1966).
44. Khare, M.L. and Bhatnagar, C.S., Indian J. Pure Appl. Phys., **3**, 356 (1965).
45. Pillai, P.K.C., Jain, K. and Jain, V.K., J. Electrochem. Soc., **448**, 1675 (1974).

46. Heaviside, O., Electrical Papers (U.S.A.), **4**, 488 (1949).
47. Gemant, A., Phil. Mag., **20**, 929 (1935).
48. Mikola, S., Z. Phys., **32**, 476 (1925).
49. Adams, E.P., J. Franklin Inst., **204**, 469 (1927).
50. Gross, B., J. Chem. Phys., **17**, 866 (1949).
51. Gross, B., Brit. J. Appl. Phys., **4**, 259 (1950).
52. Perlman, M.M. and Meunier, J.M., J. Appl. Phys., **36**, 420 (1965).
53. Bucci, C. and Fieschi, R., Phys. Rev. Lett., **12**, 16 (1964).
54. Campos, M., Mascarenhas, S. and Ferreira, G.L., Phys. Rev. Lett., **27**, 1432 (1974).
55. Sessler, G.M. and West, J.E., J. Electrochem. Soc., **115**, 836 (1968).
56. Schaffert, R.M., Electrophotography, Focal Press, London, 1971.
57. Wintle, H.J., J. Acoust. Soc. Am., **53**, 1578 (1973).
58. Gross, H. and DeMoraes, R.J., Phys. Rev., **126**, 930 (1962).
59. Fable, G.W. and Henisch, H.K., Phys. Status Solidi (a), **6**, 535 (1971).
60. Kunze, I., Starbov, N. and Buroff, A., Phys. Status Solidi (a), **16**, K59 (1973).
61. Agarwal, S.C. and Fritzsche, H., Phys. Rev. B., **10**, 4340 (1974).
62. Martin, G.M., Eogarassy, E. and Fabre, E., J. Appl. Phys., **47**, 264 (1976).
63. Srivastava, A.P. and Agarwal, S.R., Indian J. Pure Appl. Phys., **13**, 869 (1975).

64. P. Devaux and Schott, M., Phys. Status Solidi, **20**, 301 (1967).
65. Caserata, G. and Serra, A., J. Appl. Phys., **42**, 3778 (1971).
66. Perlman, M.M., J. Appl. Phys., **42**, 2645 (1971).
67. Tachibana, T., Takamatsu, T. and Fukada, E., Chem. Lett., 907 (1973).
68. Bini, S. and Gapelletti, R., in "Electrets, Charge Storage and Transport in Dielectrics", (Ed. M. M. Perlman), Electrochemical Society, Princeton, 1973, p. 66.
69. G. Boster and Abkowitz, M.A., J. Appl. Phys., **45**, 1001 (1974).
70. Pillai, P.KC., Jain, K. and Jain, V.K., Indian J. Pure Appl. Phys., **11**, 597 (1973).
71. Mazur, K., Japan J. Appl. Phys., **17**, 265 (1978).
72. Gupta, M.P., Jain, K. and Mahendru, P.C., Thin Solid Films, **61**, 297 (1979).
73. Linkens, A. and Vanderschuren, J., J. Electrostatics, **3**, 149 (1977).
74. Mahendru, P.C., Jain, K., Chopra, V.K. and Mahendru, P., J. Phys. D., **8**, 305 (1975).
75. Jain, K., Kumar, N. and Mahendru, P.C., J. Electrochem. Soc., **126**, 1958 (1979).
76. Sharp, E.J. and Garn, L.E., J. Appl. Phys., **29**, 480 (1976).
77. Takamatsu, T. and Fukuda, E., Polym. J., **1**, 101 (1970).
78. Singh Ranjit and Datt, S.C., Thin Solid Films, **70**, 235 (1980).
79. Shrivastava, S.K., Ranade, J.D. and Srivastava, A.P., Japan J. Appl. Phys., **18**, 2303 (1979).

80. Alexandrovich, P., Karasz, F.E. and MacKnight, W.J., J. Appl. Phys., **47**, 425 (1976).
81. Linkens, A., Vanderschueren, J., Choi, S.H. and Gasoit, J., Eur. Polym. J., **12**, 137 (1976).
82. Gupta, N.P., Jain, K. and Mahendru, P.C., J. Chem. Phys., **69**, 1785 (1978).
83. Chatain, D., Lacabanne, C., Maitrot, M., Seytre, G. and May, J.F., Phys. Status Solidi(a), **16**, 225 (1973).
84. Guillet, J., Seytre, G., Chatain, D., Lacabanne, C. and Monpagnens, J.C., J. Polym. Sci. Polym. Phys. Ed., **15**, 541 (1977).
85. Reichle, M., Nedetzka, T., Mayer, A. and Vogel, H., J. Phys. Chem., **74**, 2659 (1970).
86. Gutman, F., Rev. Mod. Phys., **20**, 457 (1948).
87. Johnson, V.A., Electrets - A State of the Art Survey, Part I (p. 48); Part II, A Bibliography (p. 124); Office of the technical service, U.S. Deptt. of Commerce Publications AD 299 259 and AD 299 256 (1962).
88. J. Vanderschueren, J. Polym. Sci. Polym. Phys. Ed., **12**, 991 (1974).
89. Mahendru, P.C., Jain, K. and Mahendru, P., J. Phys. D., **19**, 729 (1977).
90. Beeler, J.R., Jr., Stranathan, J.D. and Wiseman, G.C., J. Chem. Phys., **32**, 442 (1960).
91. Sawa, G., Nakamura, S., Nishio, Y. and Ieda, M., Japan J. Appl. Phys., **17**, 1507 (1978).
92. Sheppard, G.E. and Stranathan, J.P., Phys. Rev., **60**, 360 (1941).

93. Draughan, R.A. and Catlin, A., J. Electrochem. Soc., **115**, 391 (1968).
94. Palaia, F.L., Jr. and Catlin, A., J. Chem. Phys., **52**, 3651 (1970).
95. Bowlt, C., Contemp. Phys., **17**, 461 (1976).
96. Khanna, S.L., J. Chem. Phys., **46**, 4989 (1967).
97. Perlman, M.M., J. Appl. Phys., **42**, 2465 (1971).
98. Pillai, P.K.C., Jain, K. and Jain, V.K., Phys. Lett. A., **35**, 403 (1971).
99. Lilly, A.C. Jr., Stewart, L.L. and Henderson, R.M., J. Appl. Phys., **41**, 2001 (1970).
100. Nath, R. and Bhawlikar, D.R., Czech. J. Phys., **25B**, 210 (1975).
101. Feaster, G.R., Prossak, F.W. and Wiseman, G.C., Rev. Sci. Instrum., **23**, 768 (1952).
102. Kojima, S. and Kato, K., J. Phys. Soc. Japan, **6**, 207 (1951).
103. Reedyk, C.W. and Perlman, M.M., J. Electrochem. Soc., **115**, 49 (1968).
104. Murray, J.J., J. Appl. Phys., **33**, 1525 (1962).
105. Gray, S., Philos. Trans. R. Soc. London Ser. **A.37**, 285 (1732).
106. Faraday, M., Experimental Researchers in Electricity (Richard and John Edward Taylor, London 1839).
107. Heaviside, O., Electrical Paper (Chelsea, New York), (1892), pp. 408-493.
108. Eguchi, M., Philos. Mag., **49**, 178 (1925).

109. Carlson, C.F., "History of Electrostatic Recording in Xerography and Related Processes", Ed. by J.H. Dessauer, H.E. Clark (Focal Press, London) (1965), pp. 15-49.
110. Nadjakoff, G., E. R. Acad. Sci., **204**, 1865 (1937).
111. Fridkin, V.M. and Zheludev, I.S., Photoelectrets and the Electrophotographic Process (Consultants Bureau, New York) (1961).
112. Tyler, R.W., Webb, J.H. and York, W.C., J. Appl. Phys., **26**, 61 (1955).
113. Creswell, R.A. and Perlman, M.M., J. Appl. Phys., **41**, 2365 (1970).
114. Gross, B., Z. Phys., **107**, 217 (1937).
115. Gerson, R. and Rohrbaugh, J.H., J. Chem. Phys., **23**, 2381 (1955).
116. Randall, T.J. and Wilkins, M.H.F., Proc. R. Soc. London A **184**, 347, 366, 390 (1945).
117. Bucci, C. and Fieschi, R., Phys. Rev. Lett., **12**, 16 (1964).
118. Bucci, C., Fieschi, R. and Guidi, G., Phys. Rev., **148**, 816 (1966).
119. Januzzi, N. and Mascarenhas, S., J. Electrochem. Soc., **115**, 382 (1968).
120. Sessler, G.M. and West, J.E., Phys. Rev., **10**, 4488 (1974).
121. Turnhout, J. van, Polym. J., **2**, 173 (1971).
122. Gross, B., J. Electrochem. Soc., **119**, 855 (1972).
123. Creswell, R.A., Perlman, M.M. and Kabayama, M.A., In "Dielectric Properties of Solids", Ed. by F.E. Karsz (Plenum, New York) (1972), pp. 295-312.

124. Turnhout, J. van, Thermally Stimulated Discharge of Polymer Electrets (Elsevier, Amsterdam) (1975).
125. Gross, B., Charge Storage in Solid Dielectrics (Elsevier, Amsterdam) (1964).
126. Lupu, A., Giurgea, M., Baltog, I. and Gluck, P., J. Polym. Sci. Polym. Phys. Ed., **12**, 2399 (1974).
127. Bloss, P., De Reggi, A.S. and Yang, G.M., J. Phys. D. Appl. Phys., **33(6)**, 719 (2000).
128. Sessler, G.M., Schafer, H., Frayes, J. and Planes, J., Phys. Stat. Sol., **218(1)**, 16 (2000).
129. Sessler, G.M., 'Electrets', Chap 1, p.2 (Springer Verlag, Berlin) (1980).
130. Karanja, P. and Nath, R., IEEE Trans., **1,2**, 213 (1994).
131. Ochiai, S. *et al.*, IEEE Trans., **3**, 487 (1994).
132. Mizutani, T., IEEE Trans., **1,5** 923 (1995).
133. Suh, K.S. *et al.*, IEEE Trans., **2,1** 1 (1995).
134. Suh, K.S. *et al.*, IEEE Trans., **1,2**, 224 (1994).
135. Eguchi, M., Jap. J. Phys., **1**, 10 (1922).
136. Sessler, G.M., Electrets (Springer Verlag) (1980).
137. Gross, B., J. Chem. Phys., **17**, 866 (1949).
138. Sessler, G.M. and West, J.E., Appl. Phys., **17**, 507 (1970).
139. Sessler, G.M. and West, J.E., Appl. Phys., **43**, 922 (1972).
140. Murphy, P.V. and others, Jour. Chem. Phys., **38**, 2400 (1963).

141. Gross, B., Sessler, G.M. and West, J.E., Jour. Appl. Phys., **47**, 968 (1976).
142. Gross, B., Phys. Rev., **107**, 368 (1957).
143. Nadzhakov, G., Z. Physik., **39**, 225 (1938).
144. Nadzhakov, G., Comp. Rend., **204**, 1864 (1937).
145. Fridkin, V.M. and Zheludev, I.S., "Photo-electric and Electrophotographic Process", (Focal Press, New York) (1973).
146. Kallmann, H. and Rosenberg, H., Phys. Rev., **97**, 1596 (1955).
147. Kallmann, H. *et al.*, Rev. Mod. Phys., **33**, 553 (1961).
148. Padgett, E.D., Radio electronics, **2**, 61 (1955).
149. Bhatnagar, C.S., Ind. J. Pure Appl. Phys., **2**, 33 (1964).
150. Khare, M.L. and Bhatnagar, C.S., Ind. J. Pure Appl. Phys., **7**, 160 (1969).
151. Shrivastava, R.K., Quereshi, M.S. and Bhatnagar, C.S., Jpn. J. Appl. Phys., **17**, No. 9, 1537 (1978).
152. Andreich, R. and Kolomietev, Sov. Phys. Sol. State, **4**, 598 (1962).
153. Ohera, K., Wear, **48**, 409 (1978).
154. Tarev, B., Phys. of Dielectric Materials (Mir Publishers, Moscow) (1979).
155. Lyubin, V.M., Tverdogo Tela (USSR), **5**, 3367 (1963).
156. Gibbons, D.J., Nature, **198**, 177 (1963).
157. Pillai, P.V.C., Jain, K. and Jain, V.K., J. Electrochem. Soc., **118**, 1617 (1971).

158. Goldade, V.A., Pinechuk, L.S. and Voronezhstsev, Yu. I., Proc. 6th International Symosium on Electrets, ISE-6, Oxford England, Sept. 1-3 (1988) (available IEEE Services Centre, Piscataway, New Jersey, USA) 419.
159. Goldade, V.A., Voronezhstsev, Yu., Pinchuk, I. and L.S., Int. Conf. "Plastko-90", Ostrava (1990) 76.
160. Eguchi, M., Proc. Phys. Math. Soc. Japan, **1**, 326 (1919).
161. Eguchi, M., Japan J. Phys., **1**, 10 (1922).
162. Page, R.H. *et al.*, J. Opt. Soc. Am., **B7**, 1239 (1990).
163. Martiniz, D.R. *et al.*, J. Appl. Phys., **75**, 8, 4273 (1994).
164. Turnhout, J. Van, Advances in Static Electricity, Vol. I by W. de Geed (Auxilia Brussels) (1971), pp. 56-81.
165. Sessler, G.M. and West, J.E., Rev. Sci. Instrum., **42**, 15 (1971)
166. Zisman, W.A., Rev. Sci. Instrum., **3**, 367 (1932).
167. Freedman, L.A. and Rosenthal, L.A., Rev. Sci. Instrum., **21**, 896 (1950).
168. Sessler, G.M. and West, J.E., J. Electrochem. Soc., **115**, 836 (1968).
169. Sessler, G.M., West, J.E., Berkley, D.A. and Morgnstern, G., Phys. Rev. Lett., **38**, 368 (1977).
170. Gross, B., Sessler, G.M. and West, J.E., J. Appl. Phys., **45**, 2841 (1974).
171. Thiessen, P.A., Winkel, A. and Hermann, K., Phys. Z., **37**, 511 (1936).

172. Antenen, K. and Anjew, Z., Math. Phys., **6**, 478 (1955).
173. Moore, W. and Silver, M., J. Chem. Phys., **33**, 1671 (1960).
174. Badian, L., Ai, B., Lacoste, R. and Mayoux, C., C. R. Acad. Sci. Paris, **261**, 2181 (1965).
175. Harrah, L.A., Appl. Phys. Lett., **17**, 421 (1970).
176. Turnhout, J. van, "Thermally Stimulated Discharge of Electrets", Springer-Verlag, Berlin, Heidelberg (1980).
177. Sessler, G.M. and West, J.E., 1970 Annu. Rep. Conf. Electr. Insul. Dielectric Phenom. (NAS Washington, D.C.) (1971), p.8-16.
178. Collins, R.E., Applied Phys. Lett., **26**, 675 (1975); J. Appl. Phys., **47**, 1801 (1976); Rev. Sci. Instrum., **48**, 83 (1977).
179. Sessler, G.M. and West, J.E., Phys. Rev. Lett., **38**, 46 (1977).
180. Spear, W.E., J. Non Cryst. Solids, **1**, 197 (1969).
181. Kepler, R.G., Phys. Rev., **119**, 1126 (1960).
182. Davies, D.K., J. Phys., **D6**, 1017 (1973).
183. Thielen, A. *et al.* I and II, J. Appl. Phys., **75**, 8 (1994).
184. Vanderschueren, J. and Linkens, A., J. Appl. Phys., **49**, 7 (1978).
185. Kao, K.C. and Hwang, H.W., "Electr. Transport in Solids", Pergamon Press, Oxford (1981).
186. Wintle, H.J., "Theory of Electrical Conductivity of Polymers in The Radiation Chemistry of Macromolecules", Academic Press, London (1972).
187. Adamec, V. and Calderwood, J.H., J. Appl. Phys., **11**, 781 (1978).
188. Moliton, A. *et al.*, Philos. Mag., **B69**, 6, 1155 (1994).

189. Chandra, A. and Chandra, S., J. Phys. Appl. Phys., **27**, 2171 (1994).
190. Ieda, M. *et al.*, IEEE Trans. Dielect. Insul., **1**, 5, 934 (1994).
191. Gutmann, F. and Lyons, L.E., "Organic Semiconductors", Wiley, New York, 1967.
192. Saegusa, H., Sci. Rept. Iohoku Imp. Univ., **15**, 795 (1926).
193. Clark, J.D. and Williams, J.W., J. Phys. Chem., **37**, 119 (1933).
194. Fuoss, R.M., J. Am. Chem. Soc., **63**, 369 (1941).
195. Akamatu, H., Inokuchi, H. and Matsunga, Y., Nature, **173**, 168 (1954).
196. Acker, D.S., Harder, R.J., Hertler, W.R., Mahler, W., Melby, L.R., Benson, R.E. and Mochel, W.E., J. Am. Chem. Soc., **82**, 6408 (1960).
197. Shirakawa, H., Louis, E.J., MacDiarmid, A.G., Chiang, C.K. and Heeger, A.J., J. Chem. Soc. Chem. Commun., 578 (1977).
198. Walatka, V.V., Jr., Labes, M.M. and Peristein, J.H., Phys. Rev. Lett., **31**, 1139 (1973).
199. Little, W.A., Phys. Rev. A., **134**, 1416 (1964).
200. Meier, H., "Organic Semiconductors", Verlag Chemie, Berlin, 1974.
201. Kepler, E.G., in "Treatise on Material Science and Technology" (Ed. J.H.Schultz), Vol. 10B, Academic, New York, 1977, p. 637.
202. Boguslavskii, L.I. and Vannikov, A.V., "Organic Semiconductors and Biopolymers", Plenum, New York, 1970.
203. Seanor, D.A. (Ed.), "Electrical Properties of Polymers", Academic Press, New York, 1982.

204. Skotheim, T.A. (Ed.), Hand Book of Conducting Polymers, Vol. 1,2, Marcel Dekker, New York, 1986.
205. Roggen, A. Van, Phys. Rev. Lett., **9**, 368 (1962).
206. Ieda, M., Takeuchi, R. and Swan, G., Japan J. Appl. Phys., **9**, 727 (1970).
207. Kosaki, M., Sugiyama, K. and Ieda, M., J. Appl. Phys., **42**, 3388 (1971).
208. Fuoss, R.M., J. Am. Chem. Soc., **61**, 2329 (1939).
209. Eley, D.D. and Spivey, D.I., Trans. Faraday Soc., **57**, 2280 (1961).
210. Dewsbarry, R., J. Phys. D., **9**, 265 (1976).
211. Bashara, N.M. and Doty, C.T., J. Appl. Phys., **35**, 3498 (1964).
212. Farmer, F.T. and Fowler, J.F., Nature, **171**, 1020 (1952).
213. Myiohisi, Y. and Chino, K., Japan J. Appl. Phys., **6**, 181 (1967).
214. Takashima, S., J. Mol. Biol., **7**, 455 (1965).
215. O'Konsky, C.T., Rev. Mod. Phys., **35**, 721 (1963).
216. Kins, G. and Medly, J.A., J. Colloid. Sci., **4**, 1 (1949).
217. Baxter, J., Tran. Faraday Soc., **39**, 207 (1958).
218. Rosenberg, B., J. Chem. Phys., **36**, 816 (1962).
- 218a. Haijboar, J., British Polymer, **1**, 3 (1969).
- 218b. Guicking, D. and Suss, H.J., Z. Angew. Phys., **28**, 238 (1970).
- 218c. Tanaka, A., Uemura, B and Ishida, Y., J. Polym. Sci. A-2, **8**, 1585 (1970).

- 218d. Ashcraft, C.R. and Boyd, R.H., J. Polym. Sci. Polym. Phys. Ed., **14**, 2153 (1976).
- 218e. Kosaki, M. and Ieda, M., J. Phys. Soc. Japan, **27**, 1604 (1969).
- 218f. Kawamura, Y., Nagai, S., Hirose, J. and Wada, Y., J. Polym. Sci. Pt. A-2, Polym. Phys., **7**, 1, 559 (1969).
- 218g. Pochan, J.M. and Hinman, D.F., J. Polym. Sci. Polym. Phys. Ed., **14**, 2285 (1976).
- 218h. Ito, M., Nakatani, S., Gokan, A. and Tanaka, K., J. Polym. Sci. Polym. Phys. Ed., **15**, 605 (1977).
- 218i. Barkley, M. and Zimm, D., Ann. Chem. Soc. Polym. Prep., **9**, 317 (1968).
- 218j. Broadhurst, M.G., Ann. Rep. Conf. Electrical Insul. and Dielectric Phenomena, Nat. Acad. Sci. Washington, (1970), p. 48.
- 218k. Patrosian, V.P., Vysokomol - Soedin, **13**, 761 (1971).
- 218l. Cook, M., Wats, C.D. and Williams, C., Trans. Faraday Soc., **67**, 2503 (1971).
- 218m. Pollak, M., J. Chem. Phys., **43**, 908 (1965).
- 218n. Ishida, Y., Kogyokugaku Zasshi, **73**, 1318 (1970).
- 218i Lovinger, A.J., Development in Crystalline Polymers - 1, Ed. D.C. Basset, Pub. Appl. Sc. London (1982), Ch. 5.
- 218ii Peterlin, A. and Hollbrook, J.D., Kolloid Z., **203**, 68 (1965).
- 218iii Peterlin, A., Hollbrook, J.D. and Elwell, J., J. Mater. Sci., **2**, 1 (1967).
- 218iv Yano, S., J. Polym. Sc. A-2, **8**, 1057 (1970).

- 218v Sasabe, H., Saito, S., Asahina, M. and Kakutani, H., J. Poly. Sc. A-2, **7**, 1405 (1969).
- 218vi Osaki, S. and Ishida, Y., J. Poly. Sc. Poly Phys., **12**, 1727 (1974).
- 218vii Nakagawa, K. and Ishita, Y., J. Poly. Sci. Poly Phys., **11**, 1503 (1973).
- 218viii Brierty, M.C., Douglass, D.C. and Weber, T.A., J. Poly. Sci. Phys., **14**, 1271 (1976).
- 218ix Ishida, Y., Wataabe, M. and Yamafuli, K., Kolloid Z., **200**, 48 (1964).
- 218x Yamada, K., Oie, M. and Takayanagi, M., J. Poly. Sci. Poly. Phys., **22**, 245 (1984).
- 218xi Wen, J.X., Polym. J., **171**, 399 (1985).
- 218xii Grubb, O.T. and Keorney, F.R., J. Poly. Sci. Pat-6, **28**, 2071 (1990).
- 218xiii Seh, V.H., Midt. Ferroelectni., **13**, 333 (1981).
- 218xiv Toshiro, K., Koboyashi, M., Chutani, Y. and Tadokra, H., Ferroelectric, **57**, 297 (1984).
219. Lovinger, A.J., Developments in Crystalline Polymers, 1982, Ch. 5, Ed., D.C. Basset, Allied Science Publisher, London.
220. Tashiro, K., Todakoro, H. and Kobayushi, M., Ferroelectrics, **32**, 103 (1981).
221. Roerdink, E. and Challa, G., Polymer, **21**, 509 (1980).
222. Paul, D.R., Barlow, J.W., Bensten, R.E. and Wabruand, D.R., Polym. Engng. Sci., **18**, 1225 (1978).
223. Wendroff, J.H., J. Polym. Sci. Polym. Lett. Edn., **18**, 439 (1980).

- 224. Easegawa, R., Takahashi, Y., Chatani, Y. and Tadokoro, H., Polym. J., **3**, 600 (1972).
- 225. Yutaka Ando, Tomomi Handa, Kumiko Saitoh, J. Polym. Sci. Part-B, Polym. Phys., **32**, 185 (1994).
- 226. McFee, J.H., Bergman, J.G. and Crane, G.R. Jr., Ferroelectrics, **3**, 305 (1972).
- 227. Luonngo, J.P., J. Polym. Sci., **A-2**, 10, 1119 (1972).
- 228. Davis, G.T., Mckinney, J.E., Broadhurst, M.G. and Roth, S.C., J. Appl. Phys., **49(10)**, 4998 (1978).
- 229. Okuda, K., Yoshida, T., Sugita, M. and Asahina, M., Polym. Lett., **5**, 165 (1967).
- 230. Prest, W.M. Jr. and Luca, D.J., J. Appl. Phys., **46**, 4136 (1975).
- 231. Takamatsu, T., Fukada, E and Riken Hokoku, **45**, 49 (1969).
- 232. Nakamura, K. and Wada, Y., J. Polym. Sci. Pt. A-2, **9**, 161 (1971).
- 233. Wada, Y. and Oyobutsuri, Appl. Phys., **38**, 296 (1969).
- 234. Kaura, Tara, Ph.D. Thesis Indian Institute of Technology, Delhi (1983).
- 235. Murayama, N. and Hashizume Hideynki, J. Polym. Sci., **14**, 989 (1976).
- 236. Kautani, H., J. Polym. Sci. Pt. A-2, **8**, 1177 (1970).
- 237. Suresh Chand and Naresh Kumar, Ind. J. Pure Appl. Phys., **26**, 579 (1988).
- 238. Uemura, S., J. Polym. Sci. Polym. Phys. Ed. **10**, 2155 (1972).

- 239. Sussner, H. and Yoon, D.Y., Organic Coatings Plast. Chem., **38**, 331 (1978).
- 240. Murayama, N., Kakutani, H., Mizano, T., Nakamura, K. and Terasaki, S., U. S. Patent 4 656 234, Issued Apr. 7 (1987).
- 241. Wang, T.T., Herbert, J.M. and Glass, A.M., The Applications of Ferroelectric Polymer, Chapman and Hall, New York (1987).
- 242. Murayama, N., Microsymposium on Electrical Properties of Polymers, Tokyo (Jan. 1972).
- 243. Murayama, N., J. Polym. Sci. Poly. Phys. Ed., **13**, 929 (1975).
- 244. Murayama, N., Takao Oikawa, Katto Tayayuki, Nakamura, K., J. Poly. Sci. Poly. Phys. Ed., **13**, 1033 (1975).
- 245. Schaffner, F. and Jungnickel, B.J., IEEE Trans. Dielectr. Electr. Insul. **1**, No. 4, 553 (1994).
- 246. Broadhurst, M.G., Davis, G.T. and Mckinney, J.E., J. Appl. Phys., **19(10)**, 4992 (1978).
- 247. Pfister, G., Abkowitz, M. and Crystal, R.G., J. Appl. Phys., **44**, No. 5, 2064 (May 1973).
- 248. Kepler, R.G. and Anderson, R.A., J. Appl. Phys., **49(2)**, 4490 (Aug. 1978).
- 249. Latour, M., Key Eng. Materials, **92** (1994), Chap-3, p. 81-82.

/ ***** /

CHAPTER II

EXPERIMENTAL

DETAILS

2.1 INTRODUCTION

With rapid technological advances in the preparation of film with controlled reproducible and well defined structures, thin films are expected to play an increasingly important role in the studies of variety of solid state phenomena of basic and practical interest. The properties of a large variety of new and exotic materials obtained by thin film technique will undoubtedly draw considerable attention in the future. A multitude of thin film optical, magnetic, electronic and super conductive devices have been successfully operated. With increasing flexibility and diversity of the application oriented industry, a natural course of growth and selection of new promising devices based on complete and careful utilization of the science and technology of thin film will dominate future developments.

2.2 DIFFERENT METHODS OF FILM FORMATION

There are various methods for preparing thin solid films. The deposition techniques for thin films may be broadly classified under the headings, which are as follows [1,4] :

- (a) Glow discharge polymerization,
- (b) Polymerization by electron bombardment,
- (c) Photolytic polymerization using ultraviolet radiation,
- (d) Vacuum evaporation, and
- (e) Films from polymer solution.

2.2(a) GLOW DISCHARGE POLYMERIZATION

At low pressure, the organic monomer vapour is subjected to a continuous discharge of suitable radio frequency. The polymerization occurs from monomer gas molecules and the film is deposited either on the electrode or on the substrate kept near the electrode [5,6].

Under relatively high pressure and low current density, films formed are clear, transparent, soft and often tacky showing incomplete polymerisation. However, films formed with high current density and low pressure are mechanically hard and often discoloured yellow brown, but pin holes are not present in the films formed by this technique [7,8].

2.2(b) POLYMERIZATION BY ELECTRON BOMBARDMENT

In this technique, an electron beam obtained from an electron gun is made to sweep the surface of a substrate exposed to the monomer vapour at a pressure of 10^{-3} torr. A continuous flow of monomer vapour is maintained through the reaction zone and the film is deposited on the exposed surface of the substrate. The film obtained by this method is also free from pin holes [9,10].

2.2(c) PHOTOLYTIC POLYMERIZATION USING ULTRAVIOLET RADIATION

Ultraviolet rays are focused through a quartz window on a substrate at a controlled temperature. The substrate is kept in a belljar which can be evacuated to a pressure of about 10^{-6} torr. Photolysis takes place when the monomer is made to flow in the reaction zone at a partial pressure of 2 torr.

The films so formed are simpler in structure than those by glow discharge polymerization [11-13].

2.2(d) VACUUM EVAPORATION

Hogarth *et al.* [14,15] prepared polypropylene thin films by vacuum evaporation technique. Polypropylene was evaporated at a pressure of 6×10^{-5} torr. from a stainless steel boat which was maintained at a temperature of 335°C . The film was deposited on a previously deposited copper or aluminium based electrode. The polymer films formed by this technique are generally not free from pin holes.

2.2(e) FILMS FROM POLYMER SOLUTION

The techniques of film formation described above involve immediate polymerization as such these are not expected to give useful films for research purposes. Further, the polymer films formed by these techniques may have different degree of polymerization and may contain undesired impurities. Polymer films formed by vacuum deposition technique are also not quite useful as these have pin holes. Films of doped polymer cannot be obtained by above mentioned methods since it is difficult to control the quality of dopant both during evaporation as well as during polymerization. Film with uniform degree of polymerisation and high purity can be prepared from polymer solution using highly pure polymer as solute and inert solvents of AR grade. The doping percentage can be controlled easily by dissolving known amount of dopant in the solution.

There are two main methods available for preparing thin films from polymer solution :

(i) Isothermal immersion technique

Solution of suitable concentration is kept at a desirable temperature and substrate is immersed into it vertically for a given period of time depending upon the required film thickness. When the film is deposited, the substrate is slowly taken out and dried by hot air. The deposited film is then gently detached using a sharp knife edge [16,17]. Doped films can also be prepared using desired quantity of dopant in solution. Rastogi and Chopra [17] found that the thickness of film depends upon concentration of the solution, its temperature, nature of the substrate, and the time for which the substrate is kept immersed in the solution.

This method requires a great care in selecting the temperature and concentration of the solution. Also, sophisticated mechanical instrumentation is required for taking out the substrate from the solution and keeping them exactly vertical to the solution surface. Lack of proper instrumentation and precautions may result into the films containing air bubbles and non-uniform thickness.

(ii) Casting from the solution :

Polymer solution of known concentration and quantity is spread over an optically plane clear glass plate of known surface area which is made to float in a mercury pool. Solvent is allowed to evaporate at a suitable

constant temperature and the resulting film is gently detached from the substrate. Films of different thickness may be obtained using solution of different concentrations. The films obtained by this technique are of uniform thickness and perfectly plane. Also, an elaborate cleaning procedure must be adopted for substrate in order to eliminate any possible impurity and deformation.

In the present investigation, plane glass plates were used as substrate for deposition of polymer films. The glass plates were cleaned carefully by acid, water and finally in soap water. Subsequently, these were rinsed in the distilled water. The cleaned substrate were then dried up in hot air.

Plane circular glass plates were made to float in mercury pools in petri dishes which were kept inside an oven at temperature between 60-70°C. Chemically pure PVDF (Robert Johnson) were weighed, then dissolved in dimethyl formaldehyde (from Robert Johnson) in 30% solution. This solution was stirred at 65°C in a magnetic stirrer for a minimum four hours. Thereafter, the homogeneous solution thus obtained was poured over the glass plates floating in the mercury pools kept inside the oven. Great care was taken to avoid air bubbles during the settling of polymer solution over the plates. The solvent was made to evaporate for a minimum 12 hours (i.e. overnight). The glass plates were taken out carefully, films were detached from the glass plates using a sharp edge knife or blade. The films were preserved between paper leaves so that these are not damaged.

2.3 MEASUREMENT OF THICKNESS OF THE FILM

The thickness of polymer thin films can be measured accurately by any of the following techniques :

- (a) Optical,
- (b) Electrical, and
- (c) Mechanical.

2.3(a) OPTICAL TECHNIQUES

Under this technique, there are following three methods :

(i) Ellipsometric method :

In this, thickness of transparent films is measured by mathematically analysing the difference in polarization of light reflected from the film and the substrate [1,16]. This is a nondestructive method.

(ii) Interferometric method :

In this, optical devices like Michelson's interferometer, Fabry-Perot Etalon or Newton's rings are used to measure the shift in the interference pattern between film surface and the substrate. These methods demand optical smoothness of the film [17].

(iii) Light sectioning method :

In this method, light is projected at an angle of 45° from a slit over an optically smooth film formed on a substrate. If the film is opaque, then a step is made between the film and the substrate. For transparent films, the slit image is formed from the top and bottom surfaces of the film. An observing microscope with a micrometer eyepiece placed at an angle of 45° to the

sample is used for observing the separation of the slits [17,18]. This method can be utilized for measuring the film of more than one mm thickness but the method become inaccurate for the films of non-uniform thickness.

2.3(b) ELECTRICAL TECHNIQUE

In this method, vacuum evaporated electrodes are deposited on both the surfaces of the film specimen and the capacitance of the film condenser so formed is measured using a sensitive LCR Bridge [19-23]. If the high frequency dielectric constant, area of metallic electrodes, etc. are known then the thickness of a sample can be very accurately known provided the film is of uniform thickness with no pin holes. This method, therefore, is the most suitable for solution grown samples [24].

2.3(c) MECHANICAL TECHNIQUES

It has the following three methods :

(i) Stylus method

In this, a fine stylus is moved over a stepped surface formed by the edge of the film and the substrate. This stylus undergoes transverse vibrations at the step which is recorded and amplified after being fed into an electronic circuit [25,26]. This method is unsuitable for the film of non-uniform thickness and suffers from low accuracy.

(ii) Weighting method

This method uses the relation between the thickness, mass, density and area of the film. Since the mass is defined as the density multiplied by

the volume and the area and mass of the film can be measured precisely using physical balance and vernier callipers. The thickness, t , of the film can be computed using the following formula :

$$t = M/d \cdot A$$

where, M = mass, d = density and A = area of the film.

The sensitivity of the method depends upon the accuracy of the mass and area measurements. Also, it is not always possible to cut the substrate in well-defined areas [27,28].

(iii) Micrometer gauge method

This is the simplest method of measuring the thickness of a film. A number of observations are averaged to find out the exact thickness.

2.4 ELECTRICAL CONTACTS

Electrical contacts play a very important role in heterogeneous materials. Poor electrical contacts results into breakdown and depending upon the voltage applied and in case adequate precautions are not taken, accidents may also take place. Electrical contacts differ significantly in case of polymers as compared to those with metals. The work function of metal electrode ϕ_m and that of the insulator (polymer) ϕ_i are not equal when their contact for applying an electric field is made. Once these are brought into contact, charge transfer between metal and insulator takes place and continues until the Fermi level of both are aligned to the same height. The

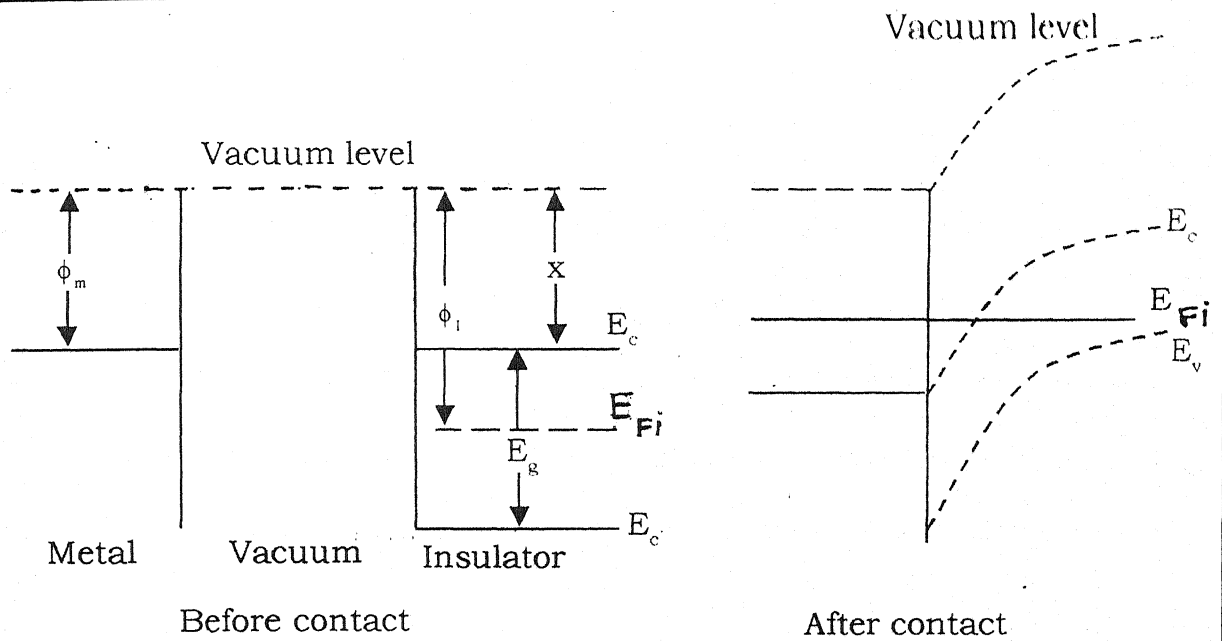
electrical contacts between a metal insulator interface fall into the following three types :

- (a) Ohmic contacts,
- (b) Neutral contacts, and
- (c) Blocking contacts.

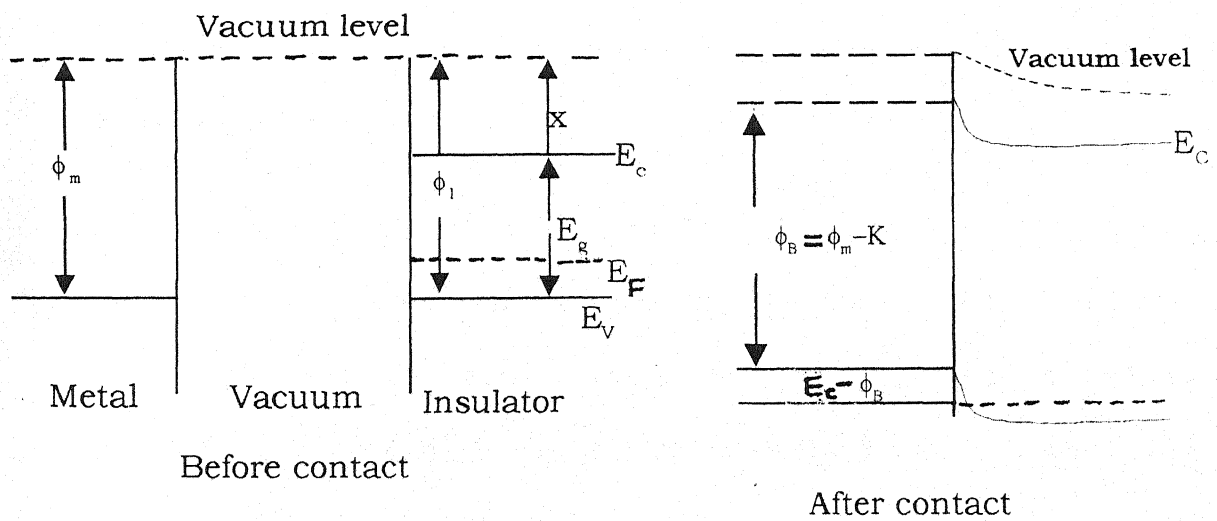
2.4(a) OHMIC CONTACTS

An ohmic contact is defined as the one which injects carriers so copiously that the current flowing through the specimen upon application of forward bias is space charge limited. Ohmic carrier injection can be accomplished by applying suitable electrode material or by generating carriers in a surface layer on exposing it to an intense light beam. In case of dark injection contact, when the work function of electrode material ϕ_m is lower than that of the insulator ϕ_i as shown in Fig. 2.1(a), in order to satisfy the thermal equilibrium requirements, electrons are injected from the electrode into the conduction band of the insulator, thus giving rise to a space charge region in the insulator. If the electronic work function is greater, the band bends upwards and a hole injecting contact is formed as shown in Fig. 2.1(b).

Since an ohmic contact acts as a reservoir of free charge carriers, the electric conduction is controlled by the impedance of the bulk of the insulator and is, therefore, bulk controlled.



(a) Election - blocking contact ($\phi_m > \phi_i$)



(b) Hole ohmic contact

Fig. 2.1 :Energy level diagrams for an ohmic contact

2.4(b) NEUTRAL CONTACTS

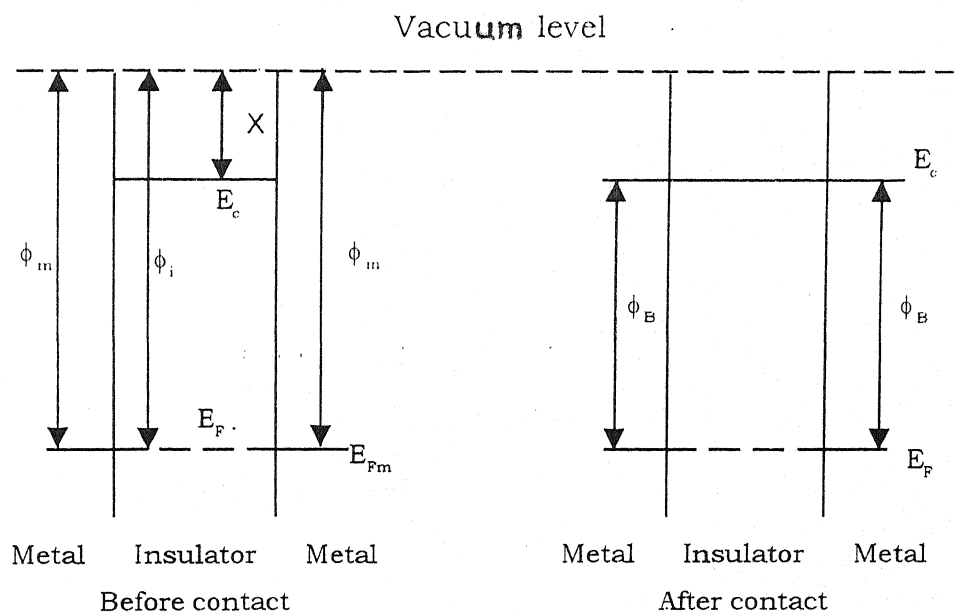
A neutral contact is defined as the one in which the carrier concentration at the contact is equal to that in the bulk of the material, i.e., there is no reservoir of charge carriers at the contact ($Q_0 = 0$). This implies $\phi_m = \phi_i$ which means no space charge exists and no band bending takes place so that both conduction and valence band edges are flat right up to the interface as shown in Fig. 2.2 (a). This condition is sometimes referred to as flat band condition.

When $\phi_m = \phi_i$ at low temperature or with an electron trapping level at a distance sufficiently above the Fermi level, E_F , in a wide band material, the contact can be neutral because of the trapped space charge in the trap will be too small under these conditions to cause significant band bending as shown in Fig. 2.2(b).

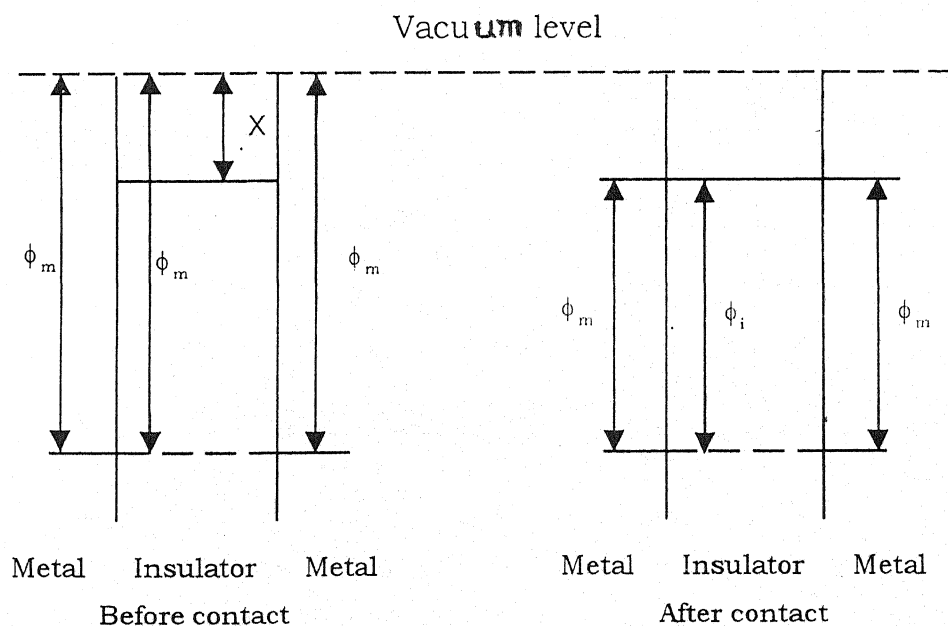
Such a contact is sometimes referred as a rectifying contact because under forward bias electrons can flow from insulator to metal, while under the reverse bias, the flow of electron from the metal is limited by electrons available over the Schottky barrier, the density of which is much smaller than in the bulk of the insulator.

2.4(c) BLOCKING CONTACTS

Energy level diagrams for blocking contacts are shown in Fig. 2.3. A blocking contact occurs when ϕ_m is greater than ϕ_i . Electrons flow from the insulator into the metal to establish thermal equilibrium conditions. A space charge region of positive charge (the depletion region) is created in

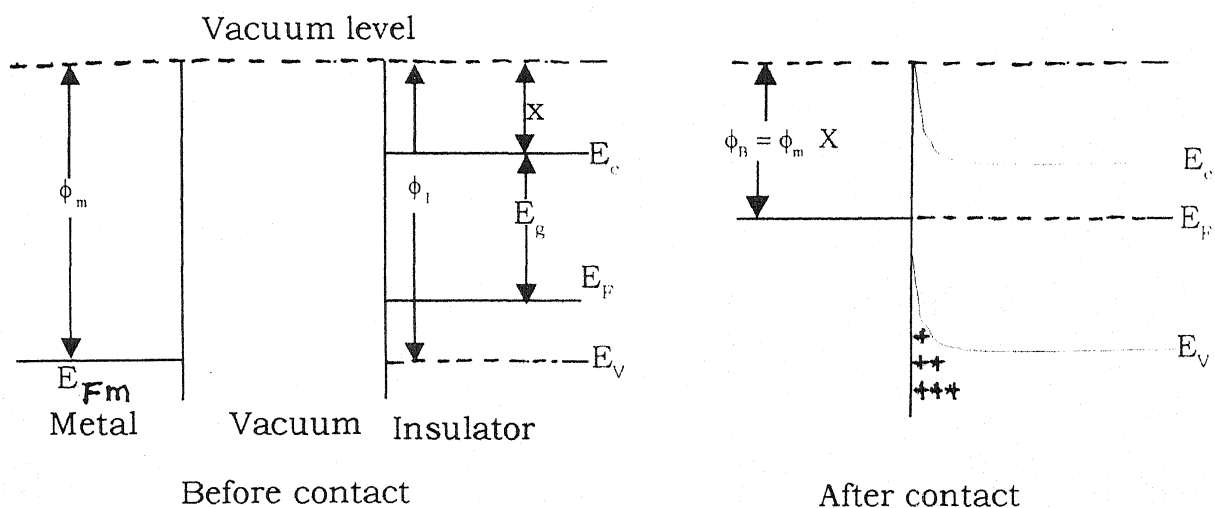


(a) Condition $\phi_m = \phi_i$

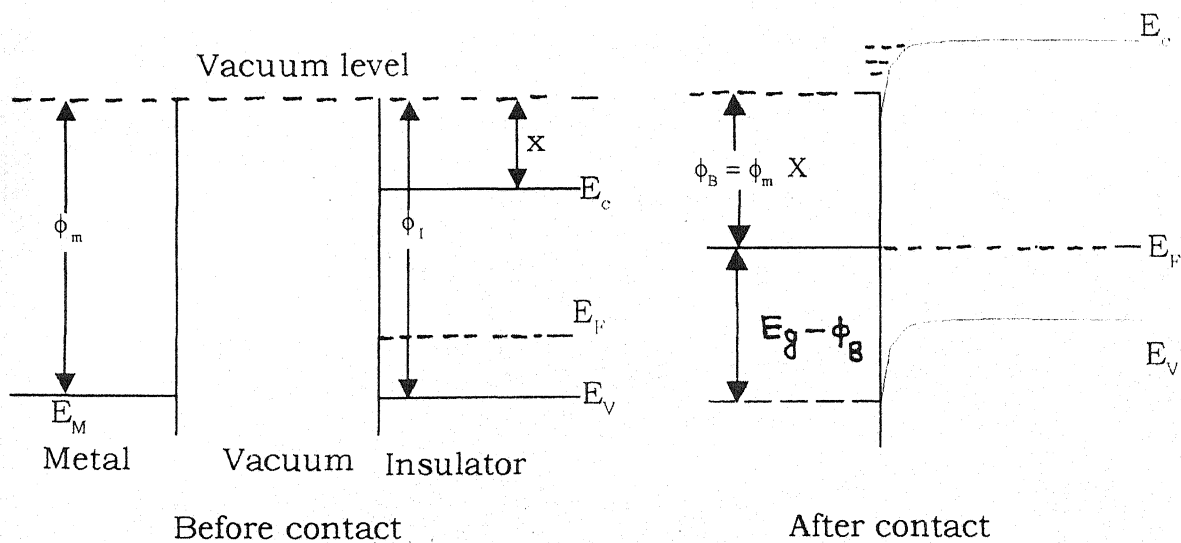


(b) Condition $\phi_m \neq \phi_i$ or $\phi_m < \phi_i$

Fig. 2.2 : Energy band diagrams for a neutral contact



(a) Electron - blocking contact ($\phi_m > \phi_i$)



(b) Hole- blocking contact ($\phi_m > \phi_i$)

Fig. 2.3 :Energy level diagrams for a blocking contact

the insulator and an equal negative charge resides on metal electrode. As a result of the electrostatic interaction between the oppositely charged regions, a local field exists within the surface of the insulator. This causes the bottom of the conduction band to bend downwards until the Fermi level within the bulk of the insulator lies below the vacuum level. As the density of the electrons in an intrinsic insulator is very small, it would have to be very thick to satisfy the above condition. Therefore, the conduction band of an insulator at a blocking contact bends only slightly downwards as shown in Fig. 2.3(a) so that we have essentially a neutral contact.

2.5 ELECTRODES

The polymer and electrode contact plays an important role in all electrical measurements [28,29]. The shape of energy band near dielectric and electrode interface decides which one of the three categories of contacts is at work. When energy band is completely horizontal, it is called a neutral contact; if a band bends downwards helping in injection of carriers of the opposite sign then the electrode is an ohmic electrode; when the energy band bends upwards hindering the injection and neutralisation of charges, the contact made is called a blocking contact. These contacts are explained in detail later in this chapter.

Following four types of electrodes can be used for making electrical contacts with polymer films for the purpose of studying the charging and discharging phenomena

- (a) Painted electrodes,
- (b) Liquid contact electrodes,
- (c) Vacuum deposited electrodes, and
- (d) Pressed metal foil electrodes.

2.5(a) PAINTED ELECTRODES

Conducting material paste can be used for painting the polymer film which can be used as the electrodes. Such materials are graphite, silver and epoxy paints. Such paints may react with the polymer and can damage it also. Therefore, use of such painted electrodes is restricted to only those polymer which do not react with these.

2.5(b) LIQUID CONTACT ELECTRODES

In this, non-metallised surface of an unilaterally metallised film specimen is kept in contact with a liquid, such as water or ethyl alcohol so that a thin uniform layer of liquid rests over the film surface. A potential is applied between the metallic electrode and rear unmetallised surface of the film. A double charge layer is formed at the solid-liquid interface and as a result of interaction between electrostatic and molecular forces, charge transfer to polymer film takes place. Electrode should be withdrawn and liquid evaporated before removal of the voltage to ensure charge retention of the specimen surfaces. Recently, nonwetting liquid insulator contact electrodes have also been employed. Monocharge electrets have also

been prepared using liquid contact electrodes obtained by filling one side metal-polymer gap with liquid and leaving other filled by air.

2.5(c) PRESSED METAL FOIL ELECTRODES

In this, polymer film is sandwiched between two plane metallic foil electrodes of the desired shape and area. Springs are used to ensure uniform pressure throughout the film for proper contacts. However, in case of polymers, following precautions need to be taken :

- (a) Measurements at high temperatures should not be carried out. At high temperatures, the polymer is softened. Due to the pressure of the spring loaded electrodes on the film, its thickness is reduced and sometimes it results in the breakdown of the film.
- (b) Metallic surface of the foil needs to be cleaned or else the foil electrode itself should be changed. Under ambient humid atmospheric conditions, practically all metallic electrodes form oxides except those of gold or platinum. This disturbs the experimental results by contaminating the film surface as improper transfer of charges takes place through the contaminated surfaces.

2.5(d) VACUUM DEPOSITED ELECTRODES

This is probably one of the best and convenient methods of depositing metallic electrodes of desired sizes and shapes. Metal can be evaporated in vacuum or any metallic or nonmetallic substrate of the film

specimen under study. No air gap exists between the evaporated electrodes and the substrate. The electrodes so obtained can be very conveniently used for measurements at low as well as high temperatures provided the melting point of electrode metal is higher than the temperature of measurements.

The author has used vacuum deposited aluminium electrodes in the present investigation. The process is described in detail later.

2.6 VACUUM COATING OF POLYMER FILMS

During the present investigation, polymer films were deposited with metal electrodes using a vacuum coating unit. The details of the unit and its operation for electrode deposition are described below.

2.6-1 VACUUM COATING UNIT

Aluminium electrodes were deposited on polymer films using a Hind High Vacuum Coating Unit, Model 12A-4. The schematic line diagram of the unit is given in Fig. 2.4.

Main parts of the unit are described below :

- (a) Vacuum chamber : It consists of -
 - (i) Hemispherical glass bell jar with a L-shaped rubber gasket for air sealing.
 - (ii) Support for substrate or specimen to be coated.

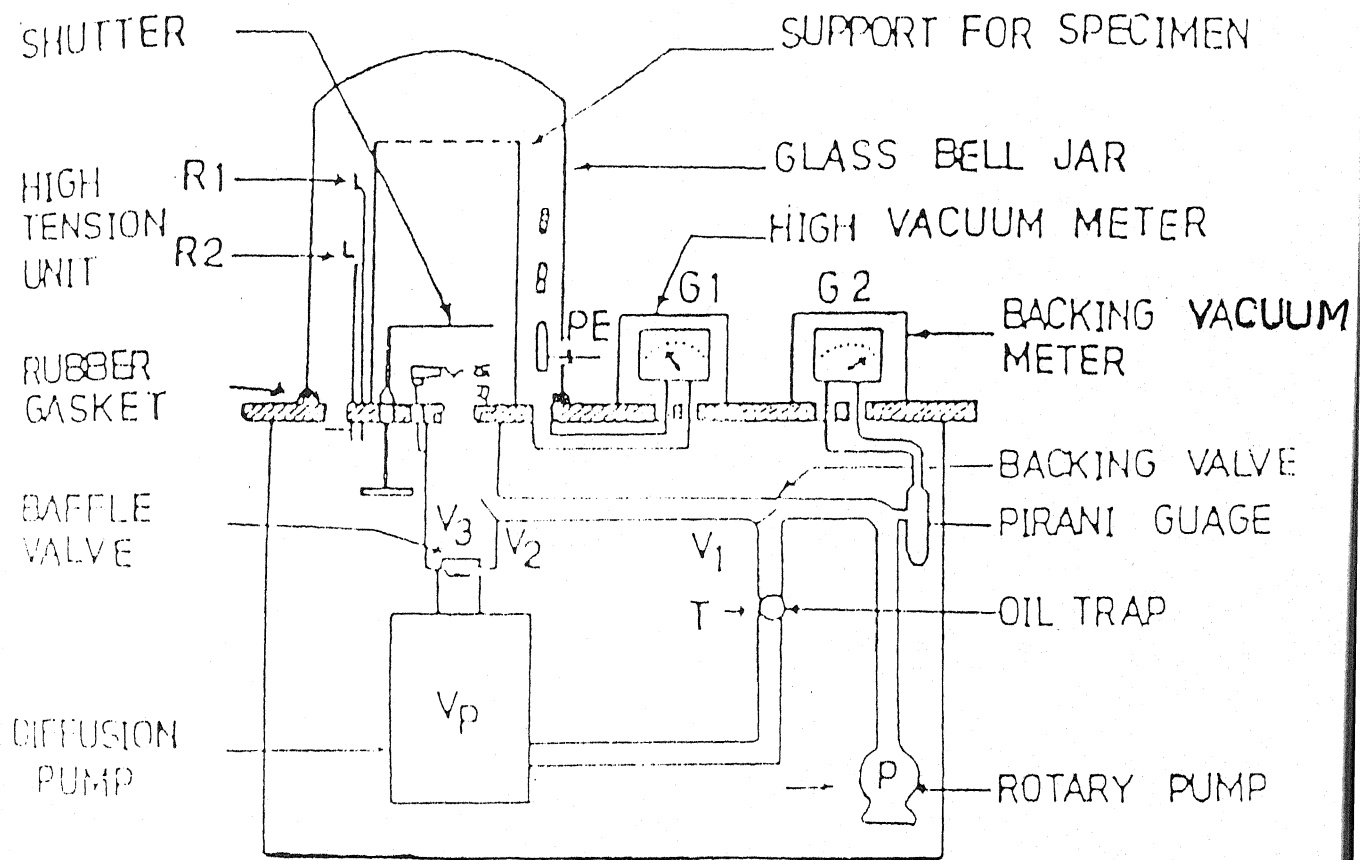


FIG. 2.4 VACUUM COATING UNIT

- (iii) Molybdenum boat or a tungsten filament for heating the material to be evaporated,
 - (iv) Hinged metallic shield for controlling the deposition rate of the material,
 - (v) High tension discharge unit (electrodes) for ionic bombardments, and
 - (vi) Substrate rotator.
- (b) Rotary pump
- (c) Diffusion pump
- (d) Pirani gauge (for measuring coarse vacuum).
- (e) Penning gauge (for measuring high vacuum).
- (f) Electric supplies to the chamber -
- (i) A low tension (LT) supply - for filament and boat.
 - (ii) A high tension (HT) supply - for glow discharge cleaning of the substrate, and
 - (iii) Variac for LT and HT supply.
- (g) Valves -
- (i) Backing valve (V_1) connecting the rotary pump with the diffusion pump,

- (ii) Roughing valve (V_2) connecting the rotary pump with the vacuum chamber,
- (iii) Baffle valve (V_3) for connecting the diffusion pump with the vacuum chamber,
- (iv) Air admittance valve (V_4) for allowing air to enter the vacuum chamber, and
- (v) Gas inlet valve (V_5) for allowing the gas to enter the chamber at the desired rate.

2.6-2 OPERATION FOR ELECTRODE DEPOSITION

In the beginning all the five valves are closed. The rotary pump is switched ON. It initially evacuates the tubes connecting the rotary pump and the junction of the backing and roughing valves V_1 and V_2 . When the pressure shown by the pirani gauge attains a value less than 0.5 torr, the backing valve V_1 is opened for connecting the rotary pump with the oil diffusion pump. Circulation of water in the tubes surrounding the diffusion pump is started and the heater of the diffusion pump is turned ON.

After about half an hour, with the diffusion ready, the backing valve V_1 is closed and the roughing valve V_2 is operated for connecting the vacuum chamber directly with the rotary pump. The pressure inside the vacuum chamber is allowed to fall to 10^{-2} – 10^{-3} torr. After this, the HT supply is switched ON. This causes ionisation of the rarefield air inside the

vacuum chamber with the net result that the substrate is cleaned by ionic bombardment. The HT supply is switched OFF after about five minutes.

The pressure inside the vacuum chamber is now allowed to fall up to 0.002 torr, so as to establish a tough vacuum. Thereafter, roughing valve V_2 is closed and backing valve V_1 is opened again so that the rotary pump is connected to the diffusion pump for maintaining the backing vacuum. With backing valve V_1 open, the baffle valve V_3 is opened to connect the diffusion pump with the vacuum chamber. The vacuum is maintained by reading the pressure on the Penning gauge. When the vacuum reaches a pressure of 10^{-5} torr, the LT supply is switched ON. When the aluminium pellet kept in the spiral tungsten filament starts evaporating, the hinged metallic shield is swung out to allow the deposition of metal vapours on the surface of the specimen.

With the deposition over, the filament and heater currents are switched OFF. Baffle valve V_3 is closed and fine vacuum Penning gauge is switched OFF. After about 10 minutes or so, the air admittance valve V_4 is opened to leak air into the vacuum chamber making the bell jar free to be removed and the electrode deposited film is taken out. The coating unit is closed down by first turning OFF the diffusion pump heater with the rotary pump still running and the backing valve V_1 open. After 15 minutes, when the boiler of the diffusion pump is cooled, the backing valve V_1 is closed

and the rotary pump switched OFF. Finally water circulation in the diffusion pump is stopped.

2.7 CIRCUITRY AND INSTRUMENTATION

Instrumentation was common to most of the studies undertaken in the present investigation. Sample holder has been designed for carrying out accurate measurement with ease. Other instrument, e.g. electric amplifier, high voltage unit, Keithley electrometer and temperature programmer etc. were used at various places depending upon the experimental requirements.

(a) Keithley Electrometer :

Keithley 610C electrometer was used for measuring the current. The range of the electrometer in the ammeter mode is 10^{-14} amp. of full scale to 0.3 amp. in twenty eight 1x and 3x ranges.

Accuracy : $\pm 2\%$ of full scale on 0.3 to 10^{-11} amp. ranges using the smallest available multipliers setting : $\pm 4\%$ of full scale on 3×10^{-12} to 10^{-14} amp. ranges.

The electrometer in ohm meter mode has a range 100 ohm full scale to 10^{14} ohm in twenty five linear 1x and 3x ranges. Accuracy is $\pm 5\%$ of full scale on 3×10^{10} ohm to 10^{14} ohm ranges. This electrometer in the voltmeter mode has a range from 0.001 V to 1000 V of full scale in eleven 1x and 3x ranges with an accuracy of $\pm 5\%$. As a Coulomb meter this

electrometer has a range from 10^{-13} Coulomb full scale to 10^{-5} Coulomb in seventeen 1x and 3x ranges.

(b) Hewlett Packard (HP) 4192 A Low Frequency (LF) Impedance Analyzer :

The HP 4192 LF Impedance Analyzer is a fully automatic high performance test instrument designed to measure wide range of impedance parameters - Capacitance (C); Dissipation factor (D-tan θ), absolute value of impedance ($|Z|$), absolute value of admittance ($|Y|$), phase angle (θ), resistance (R), reactance ($|X|$), conductance (G), susceptance (B), inductance (L) and quality factor (Q). The frequency can be swept with a built in frequency synthesizer. The measuring frequency can be swept either in auto mode or in manual mode with a maximum resolution of 1 MHz (10^6 Hz). Oscillator (OSC) level is variable from 5 mV to 1.1 mV rms and can also be varied either with the auto mode or with manual mode with 1 mV resolution. Measurement range of C is 0.1 pF to 100 mF; D is 0.0001 to 19.999; $|Z|/R/X$ is 0.1 m to 1.299 M; $|Y|/G/B$ is 1 ns to 12.999 ns, θ is $-180^\circ.00$ to $180^\circ.00$, Q is 0.1 to 1999.9. All have a basic accuracy of $\pm 0.1\%$ and resolution $48\frac{1}{2}$ digits (number of digits depends on the measuring frequency and OSC level setting).

(c) High voltage power supply :

A high voltage DC regulated power supply of Electronic Corporation, Model 4800 D was used to apply the field to the sample in transient, dark conduction and TSDC measurements.

(d) The Measurement Cell :

The measurement cell for D.C. conductivity, A.C. dielectric bridge measurements and TSDC studies was fabricated in the laboratory. It consists of a heating coil as heating element and detachable lid. A Jumo contact thermometer and a Jumo electronic relay were used to maintain the temperature as required. The accuracy of the contact thermometer was $\pm 0.3^{\circ}\text{C}$. An aluminium lid fixed with UHF Teflon sockets was placed on the top of the cell. The electrical connections of the sample were taken with the help of these sockets. The sample sandwiched between two aluminium electrodes were held tightly in a sample holder as shown in Fig. 2.5.

(e) Contact Thermometer :

A contact thermometer (Jumo, Germany) along with an electronic relay unit was used to control the temperature of the measurement cell. The system is capable of controlling the temperature within $\pm 3^{\circ}\text{C}$.

(f) Micrometer Screw :

Micrometer screw made by Mitutoyo, Japan, was used to measure the thickness of the sample films.

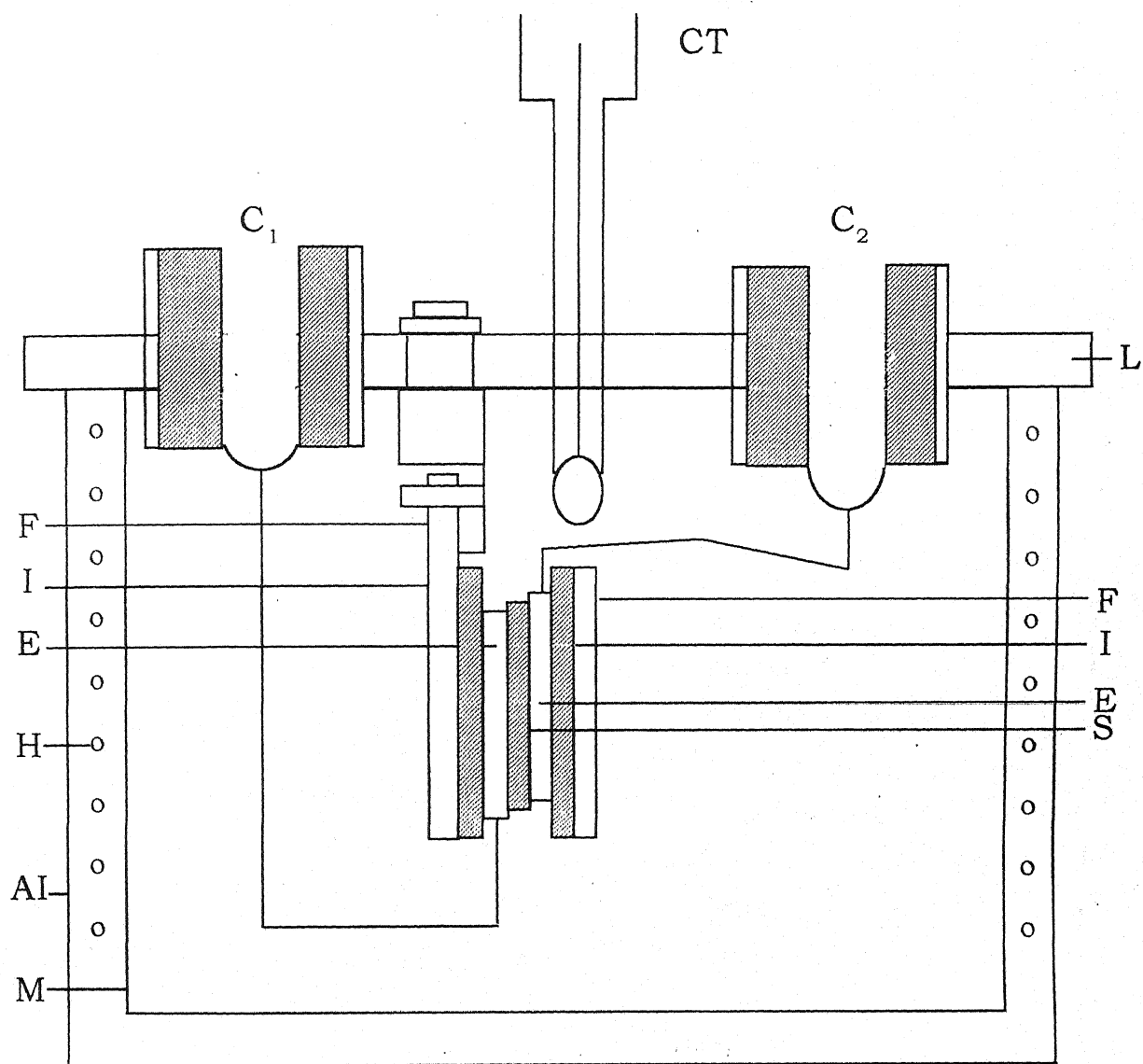
(g) Vacuum Coating Unit :

A vacuum coating unit assembled in the laboratory was used to coat the metal electrodes on the sample films.

2.8 MEASUREMENT TECHNIQUES

(a) Transient and D.C. Conductivity Measurements :

The block diagram of the experimental set up for transient and D.C. conductivity studies is shown in Fig. 2.6.



INDEX

CT	: Contact thermometer
$C_1 C_2$: Teflon insulated connectors
F	: Brass frame of sample holder
I	: Teflon insulation
E	: Aluminium Electrode
H	: Heating coil
AI	: Asbesros cloth insulation
M	: Metal Box (brass)
S	: Sample

Fig. 2.5 : Measurement Cell

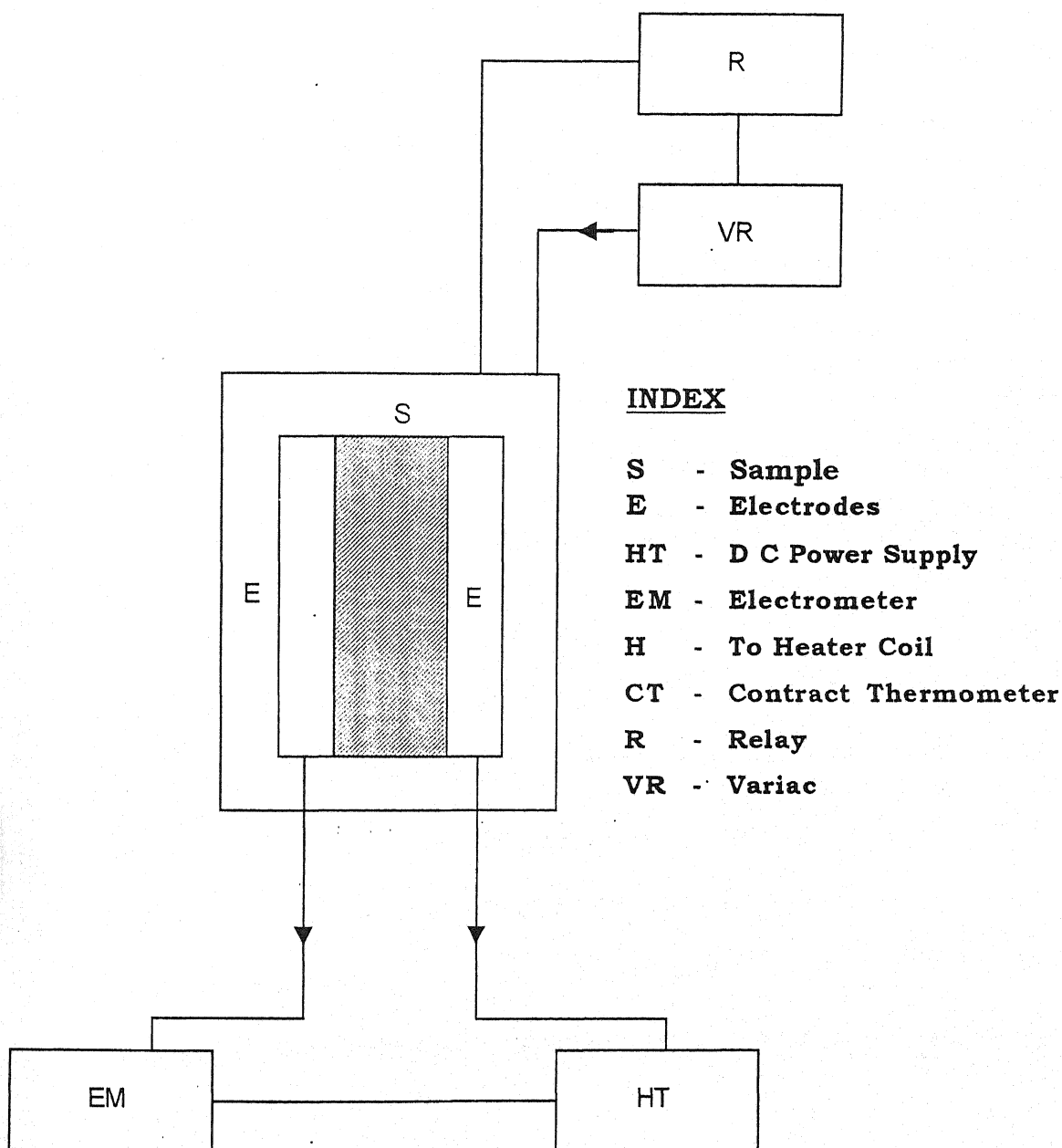


Fig. 2.6 : Block diagram of the experimental set up used for Electrical conductivity measurements.

The electrical conductivity measurements were carried out by measuring the steady state current, with Keithley 610-C electrometer, as a function of voltage at different temperatures. The temperature was electronically controlled with the help of a thermoregulating system with a Jumo contact thermometer and electronic relay.

The conductivity was calculated by using the equation :

$$\sigma = \left(\frac{d}{AV} \right) I \quad \dots (2.1)$$

where d is the thickness of the sample, A is the area of the sample, V is the voltage applied across the material, and I is the conduction current.

(b) Dielectric Measurements :

The capacitance and loss tangents of materials were measured with HP 4192 LF Impedance Analyzer at different fixed temperatures. The measurement cell is the same one which is used for D.C. conductivity measurements. Schematic arrangement used for this study is shown in Fig. 2.7. Using measured values of capacitance C and loss tangent, $\tan \delta$; the dielectric constant and loss factor were calculated. The relations used are following :

Dielectric constant,

$$\epsilon' = \frac{C \cdot d}{\epsilon_0 A} \quad \dots (2.2)$$

and Loss Tangent,

$$\tan \delta = \frac{\epsilon''}{\epsilon'} \quad \dots (2.3)$$

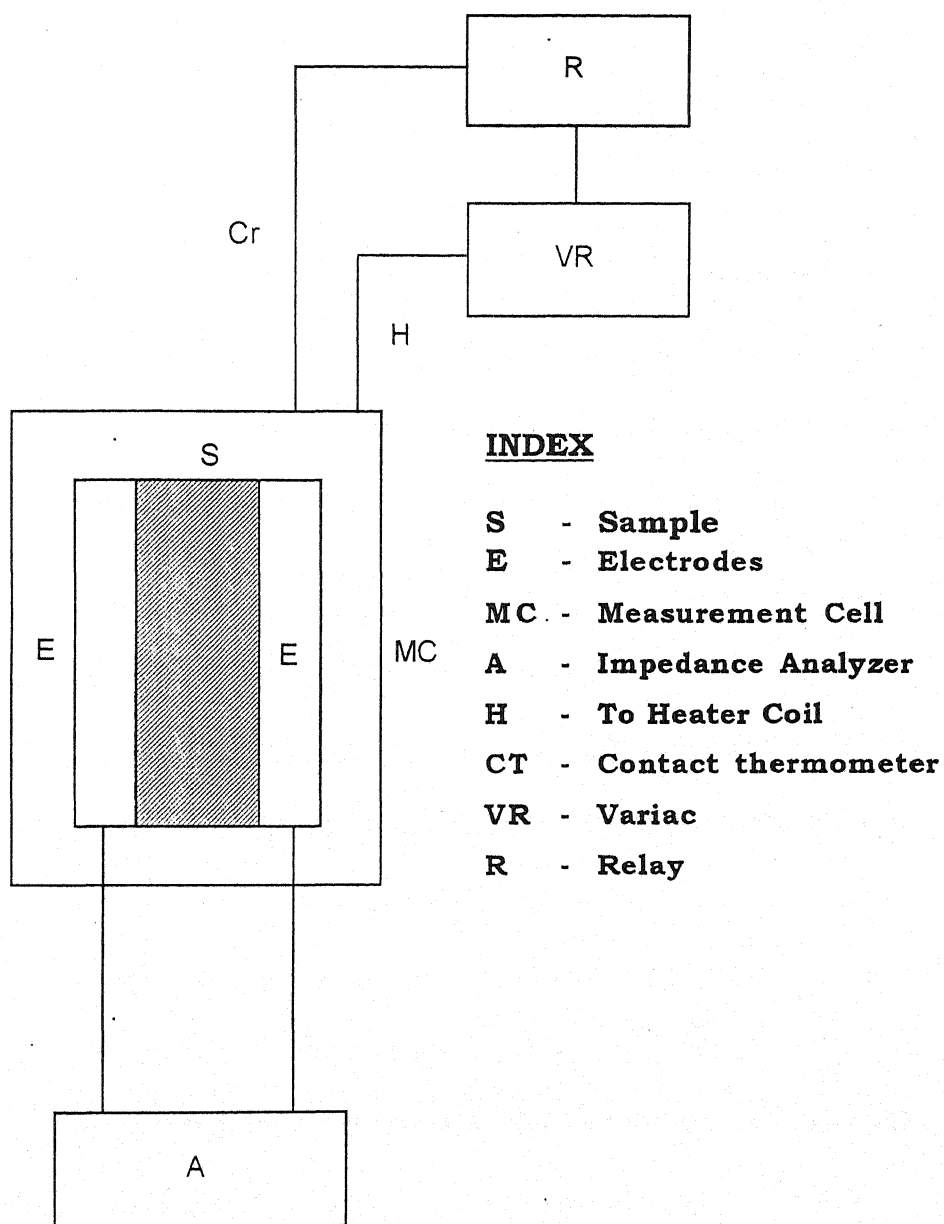


Fig. 2.7 : Schematic arrangement for Dielectric AC Bridge Measurement

where,

C is the measured value of the capacitance,

ϵ_0 is permittivity of free space,

$\tan \delta$ is the measured value of the loss tangent,

d is the thickness of the sample, and

A is the area of the sample.

(c) Thermally Stimulated Discharge Current (TSDC) Measurements:

The experimental set up used for TSDC measurements is the same as used for D.C. conductivity measurements. The circuit diagram for polarization and depolarization measurements is shown in Fig. 2.8.

Samples were polarized by keeping the specimen at an elevated temperature (T_p) under polarizing field (E_p) for certain time (t_p) and then cooling the specimen down to room temperature with the field on. In the present investigation, field E_p was applied at an elevated temperature for 30 minutes. After the temperature was switched off and field was kept on for 69 minutes. Then the field was switched off and the sample was short circuited for 30 minutes in order to discharge the stray charges. Then the sample was reheated at a linear rate of $3^\circ\text{C}/\text{min}$ and the discharge current was recorded with Keithley 610-C electrometer. The scheme for thermoelectret formation and TSDC is shown in Fig. 2.9. TSDC spectra was recorded for different parameters T_p and E_p .

To obtain reliable result in accurate measurement of current, the specimen must be kept in the sample holder which is dry, rigid and well

Two way switch

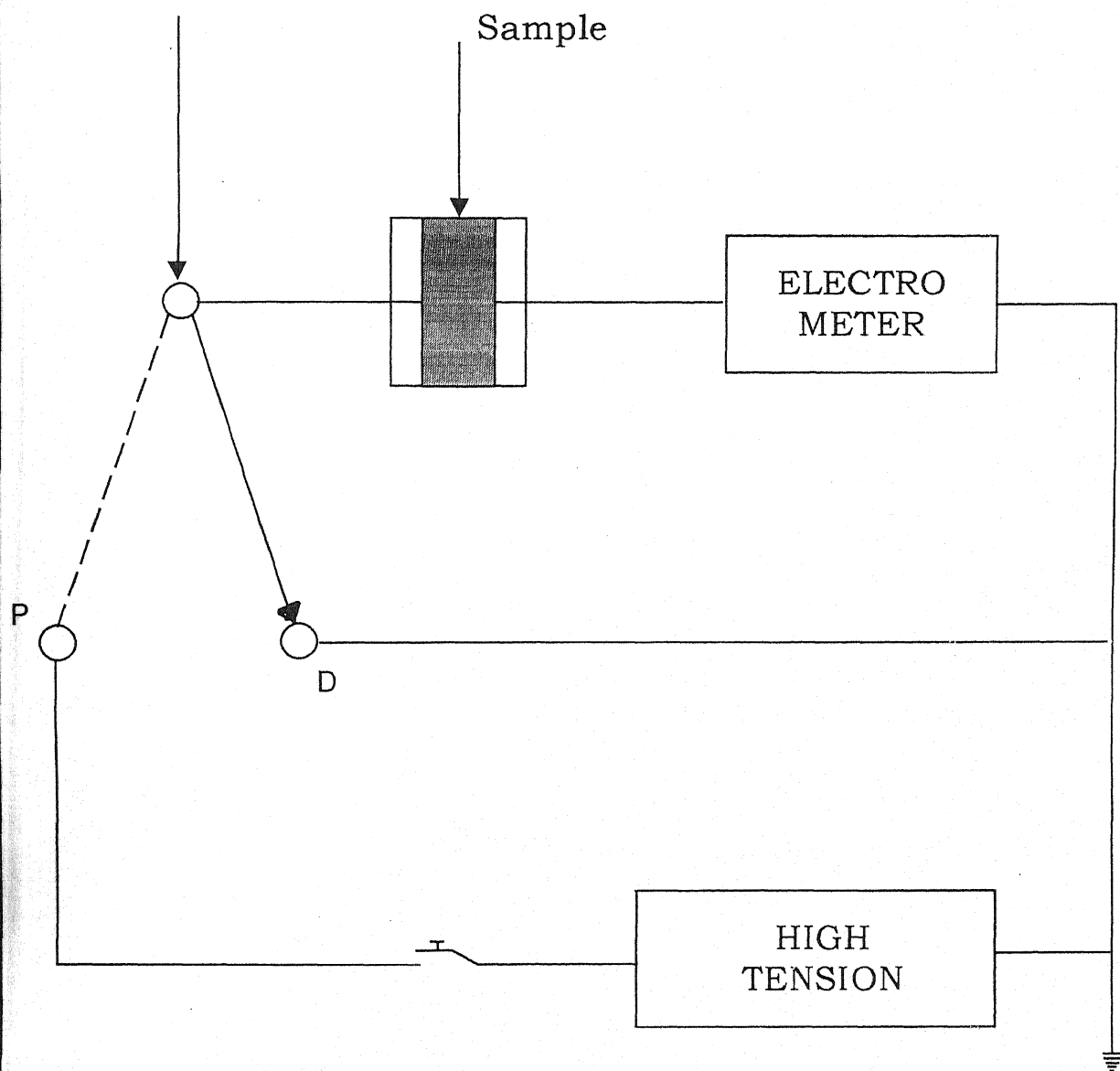


Fig. 2.8 : Circuit Diagram for the Polarization and Depolarization

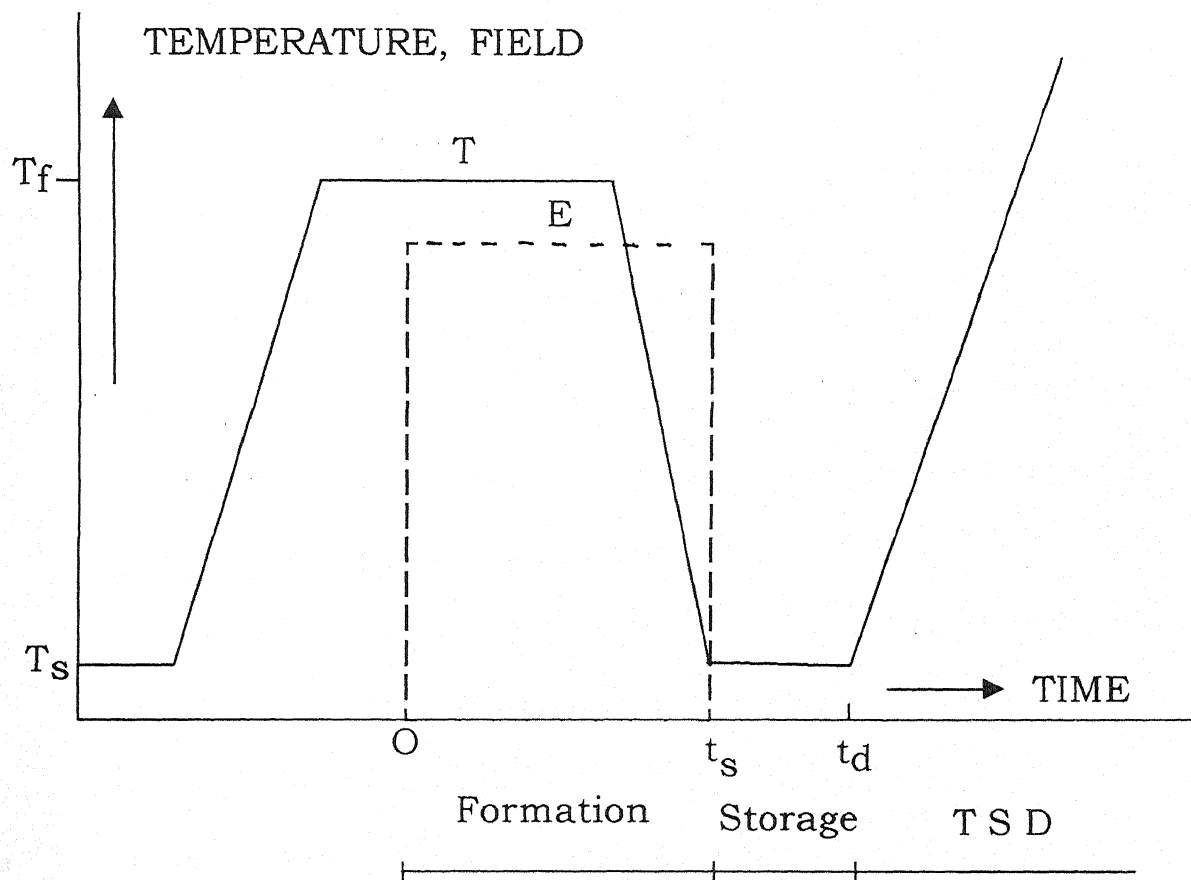


Fig. 2.9 : Field - Temperature scheme for thermo electret formation.

shielded from spurious currents. A good sample holder has high insulation resistance, possesses freedom from spurious voltage, induced charges, microphonics and has no leakage of current. Rigidity is required to avoid picking up of undesired induction.

In the present investigation, the insulators of high resistivity were used as test specimen. In almost all the studies, high values of voltage and low values of currents were involved. During the measurement of very low currents produced due to high voltage drop across a high resistance, insulation of the leads, fixture and voltmeter must be several orders of magnitude greater than the resistance of the specimen. In the absence of such insulation the current will start flowing through leads and other less insulating parts. Keeping this in mind, best insulating material teflon-FEP was used wherever the insulation was required. Teflon-FEP has a very high volume resistivity and a surface on which water/moisture film is not readily formed. Its insulation properties remain unaffected by humidity of the air, perspiration and finger oil due to normal manual handling. It is chemically inert to various organic solvents and can be cleaned by many liquids and also can be machined in the desired shape. This is possible because of its excellent mechanical and thermal properties. However, to avoid surface conduction through the deposited dust, solid flux and oil or water film on the surface, attention was constantly paid for keeping the insulation clean and dry. Methyl alcohol or benzene was used for cleaning purposes.

Spurious voltage are always expected to affect the system performance in high resistance circuits. These may be caused either due to internal electrical disturbances or due to the internal induced signals. Line disturbances were avoided using highly stabilised voltage to drive electrical instruments and the induced signals were avoided using electrostatic shielding. To achieve this, all leads were surrounded by grounded conducting surfaces and the high resistance circuit was enclosed in a shielded aluminium enclosure inside the oven.

In any high resistance circuitry, physical motion of the system and leads may distort the result in the following two ways :

- (a) If the coaxial cables are moved during the measurements, friction between the braid and the insulator surrounding the central conductor or piezoelectric effect in insulator may develop voltage across the electrometer input, thus distorting the result. This was greatly minimised by using "low noise cables" type RC 58 A/u. In these cables the surface under the shielded braid is coated with graphite powder to provide a conducting equipotential cylinder around the insulator and a conducting path for any charge that is generated.
- (b) The movements of coaxial cables may also change the capacitance between the shield and input lead, as a small charge is always present in this capacitance. This change in capacitance ΔC may produce a voltage change, ΔV , where

$$\Delta V = Q/\Delta C$$

... (2.4)

which should be seen by the electrometer. Rigid connection and firm mechanical support to the flexible cables were found to be necessary to minimise these effects.

/ ***** /

REFERENCES

1. Glong, R., "Handbook of Thin Film Technology", Eds. L.T. Maissel, R. Glong, McGraw Hill, New York (1970).
2. Campbell, D.S., "Physics of Non-Metallic Films", Plenum Press, London (1976).
3. Chapman, B.N. and Anderson, J.C., "Science and Technology of Surface Coating", Academic Press, London (1974).
4. Harper, C.A., "Handbook of Thin Film Hybrid Microelectronics", McGraw Hill, New York (1975).
5. Denaro, A.R. *et al.*, Europ. Polym. Jour., **4**, 93 (1968).
6. Williams, T. and Hayes, M.W., Nature, **209**, 769 (1966).
7. Rose, A., J. Appl. Phys., **35**, 2664 (1964).
8. Weash, R.C., Selby, S.M. and Hodgeman, C.D., "Handbook of Chemistry and Physics", Chemical Rubber Co. Pub. (1964) 517.
9. Lyons, L.E., J. Chem. Soc., 5001 (1957).
10. Kallmann, H. and Pope, M., Nature, **186**, 31 (1960).
11. Kallmann, H. and Pope, M., J. Chem. Phys., **36**, 2482 (1962).
12. Silver, M., Organic Semiconductors, McMillan Co., New York (1962) 27.
13. Lind, S.C. and Livingstone, J. Am. Chem. Soc., **52**, 4613 (1930).
14. White, P., Proc. Chem. Soc., 327 (1961).
15. White, P., Microelectron Reliability, **2**, 161 (1963).
16. Hogarth, C.A. and Iqbal, T., Thin Solid Films, **51**, 45 (1978).

CHAPTER III

**THEORETICAL
BACKGROUND
OF
STUDIES**

In this chapter we discuss the theoretical background of the various studies proposed for the present investigation.

3.1 THERMALLY STIMULATED DISCHARGE CURRENT

The basic principle of TSD is to study the process of charge decay by heating the electret at a constant rate. The decay processes are investigated as a function of temperature instead of time. During its short history, TSD has evolved into a basic tool for the identification and evaluation of dipole orientation processes and of trapping and recombination levels. Its rapid growth has been spurred on by the fact that charge trapping and charge transport phenomena are not only of vital importance for electrets but also for materials used in thin films.

In TSD measurements, a charged/polarised sample is heated up from some low temperature T_0 (usually in the absence of an external field), while its electrodes are short circuited through a sensitive current detector. The current which appears in the external circuit due to depolarisation processes is recorded as a function of temperature. Each depolarisation process becomes detectable when its relaxation time is short enough, by producing a depolarisation current which increases at first with the temperature, then reaches a maximum and drops to zero as the equilibrium distribution is accomplished [1].

In an ideal case, a separate peak is produced for each relaxation process. If partial overlapping between two peaks occurs, separation of

high temperature peaks can be perused by the usual thermal cleaning. Let the maximum temperature of the two peaks be T_1 and T_2 and $T_1 < T_2$. Heating the crystal to an intermediate temperature T' (where $T_1 < T' < T_2$) and subsequently cooling it, erases the low temperature peak. Then the sample is heated again to exhibit the second peak which is now nearly clear.

Early experiments of TSD were carried out without programmed heating since their main purpose was to measure the total related charge. Since mid-sixties, however, investigators have applied linear increase in temperature.

3.2 FACTORS GOVERNING THE TSD SPECTRA

There are a number of observations to the fact that poling conditions used for the formation of an electret and deliberately added impurities prior to the formation of an electret, play an essential role on the shape and size of the TSD spectra. Essentially, there are three poling parameters which affect the TSD spectra, they are : poling temperature, poling field and poling time.

3.2-i EFFECT OF POLING TEMPERATURE

Of the three poling parameters, poling temperature (T_P) has a special significance on the position and intensity of the TSD spectra. An electret may have a non-distributed (single relaxation) or distributed polarization and this can be detected from the shift in position of TSD

spectra with variation of T_p . The position of the current maxima in the TSD spectra remains unaltered. While the magnitude of current increases with increase in T_p , in the case of non-distributed polarization, the position of current maxima shifts to higher temperature and magnitude of current maxima increases for the distributed polarization [2,3]. At lower value of T_p , only the fast activated carriers contribute to the magnitude of current but as T_p increases more and more carriers, even those with higher relaxation times will be activated and current maxima will increase.

3.2-ii EFFECT OF POLING FIELD

The distinction between uniform and non-uniform polarizations can be made with variation of poling field (E_p). For uniform polarizations, charge increases linearly [4] while for non-uniform polarizations charge increases non-linearly [5] with E_p . Generally, the peak position is not affected by a change in field. However, there are reports regarding the shift in the position of current maxima towards lower temperature with E_p . This has been explained on the basis of field-assisted detrapping due to Poole-Frenkel effect [6] and on the mobility induced TSD where recombination factor is neglected. Lowering of activation energy with increase in E_p but without a shift in the current maxima has been observed [7]. This has been attributed to the lowering of barrier height of the charge traps with the increase in E_p . Shrivastava *et al.* [8] have observed a linear relation

between peak current and square root of the polarizing field and they have explained this on the basis of charge injection from the electrodes.

3.2-iii EFFECT OF POLING TIME

Effect of poling time (t_p) on the TSD spectra is similar to that of poling temperature. However, poling time should be changed logarithmically in order to obtain the changes of the same magnitude as that of poling temperature [9].

3.2-iv EFFECT OF DELIBERATELY ADDED IMPURITIES

Magnitude of peak current in the TSD spectra increases many fold and peak position shifts to lower temperature side on introducing impurities into the specimen [10-14]. Both inorganic and organic doping agents have been used for this purpose. According to some authors [15], life and charge stability of polymer electrets increases with doping. This has been attributed to the modification of trap levels in the presence of impurity. the decrease in activation energy of the discharge process with doping has been observed by Gupta *et al.* [10]. It is surprising to find that sometimes the electret can be formed just by the incorporation of impurity and without the application of the field [16] which has been attributed to the formation of charge transfer complexes between dopant and the main molecular chain of polymer.

3.2-v EFFECT OF HEATING RATE

The TSDC peak shifts to higher temperature and their magnitudes increase with increasing heating rate. By varying the heating rate, activation energy of the dielectric relaxation process can be obtained [17].

Humidity can also affect the polarization. Effects of pressure and high energy radiations [18] on the charge storage have also been studied.

3.3 THEORY OF TSD

The disorientation of dipoles, on thermal stimulation can take place in the following two ways which are discussed in subsections.

- (a) TSD of dipoles with one relaxation time, and
- (b) TSD for a distribution of relaxation time.

(a) TSD OF DIPOLES WITH ONE RELAXATION TIME

In this discharge, the TSD peak appears in a narrow temperature interval and that its shape and position are unaffected by changes in polarisation conditions. The discharge of frozen in dipole polarisation, $P(t)$ in a short circuited polar electret under a linear heating rate, r , is considered here. Assuming that the polarisation $P(t)$ decays with a single temperature dependent relaxation frequency on reciprocal relaxation time $\alpha(T)$, according to the Debye rate equations, we have

$$\frac{dP(t)}{dt} + \alpha(T) \cdot P(t) = 0 \quad \dots (3.1)$$

Integrating above yields

$$P(t) = P_d \exp \left[- \int_d^t \alpha(T) dt \right] \quad \dots (3.2)$$

where, t_d is the time of commencement of TSD.

P_d is the attained equilibrium polarisation before the start of the TSD and could be expressed by

$$P_d = N_p \overline{\cos \theta} \quad \dots (3.3)$$

where N is the density of dipoles, p is the electric dipole moment and θ is the angle the dipoles subtend with the applied field. For a low concentration of dipoles, the average orientation can be expressed as

$$\cos \theta = \frac{pE_p}{3kT_p} \quad \dots (3.4)$$

where E_p is applied field, k is the Boltzman's constant and T_p is polarisation temperature.

The current density, $j(t)$ due to the decay of the polarisation is

$$\begin{aligned} j(t) &= \frac{dP(t)}{dt} \\ &= \alpha(T) \cdot P(t) \end{aligned} \quad \dots (3.5)$$

Substituting $P(t)$ in eqn. (3.5), we get

$$j(t) = \alpha(T) P_d \exp \left[- \int_{t_d}^t \alpha(T) dt \right] \quad \dots (3.6)$$

In a TSD run, the temperature T is raised at a rate $r = dT/dt$, and the released current is expressed as

$$j(T) = \alpha(T) P_d \exp \left[- \frac{1}{r} \int_{T_d}^T \alpha(T) dT \right] \quad \dots (3.7)$$

using the condition that at the start of the TSD run, i.e. at $t = t_d$, we have $T = T_d$.

The relaxation frequency for the dipole disorientation, $\alpha(T)$ is often envisaged to follow an Arrhenius shift, therefore

$$\alpha(T) = \alpha_0 \exp(-A/kT) \quad \dots (3.8)$$

where α_0 is the characteristic relaxation frequency ($T \rightarrow \infty$) and A is the activation energy for dipole disorientation. Eqn. (3.8) can be applied to describe the temperature shift of the relaxation frequency of well characterised dipole groups normally associated with the β -type of relaxations. For dipole groups, where disorientation are brought about by the segmental and cooperative movements of segments of the main chains, the frequency shift can be better described by the Williams Landel Ferry (WLF) shift (applicable for $T > T_g$).

$$\alpha(T) = \alpha_s \exp[2.303] C_1 (T - T_s) \cdot (C_2 + T - T_s)^{-1} \quad \dots (3.9)$$

where for most of the amorphous polymers $\alpha_s = 7 \times 10^{-3} \text{ sec}^{-1}$, $C_1 = 17.44$ and $C_2 = 51.6 \text{ K}$.

Combining eqns. (3.7) and (3.8), we get the following expression for current density :

$$j(T) = \alpha_0 \exp[-A/kT] P_d - \exp \left[-\frac{1}{r} \int_{T_d}^T \alpha(T) dT \right] \quad \dots (3.10)$$

expressed as

$$\cos \theta = \frac{p E_p}{3 k T_p} \quad \dots (3.11)$$

where E_p and T_p are the applied field and temperature respectively. Using eqns. (3.3) and (3.11)

$$j(T) = \frac{\alpha_0 N_p^2 \epsilon_0 E_p}{3kT_p} \left[\{-A/kT\} \cdot \exp \left\{ -\frac{\alpha_0}{r} \int_{t_d}^t \exp(-A/kT) dT \right\} \right] \quad \dots (3.12)$$

here ϵ_0 is the permittivity of free space.

Equation (3.12) describes the depolarisation current density released due to dipolar depolarisation in a shorted electret. The first exponential, which dominates the expression at low temperatures, describes the initial increase of the depolarisation current as the frozen in dipoles gradually become disoriented. The second exponential which dominates at high temperatures will gradually depress the current released until a maximum output current is reached, after which the current rapidly falls as the induced polarisation is exhausted. The current peak is thus asymmetric, having a steep slope on its high temperature side. The theory of TSD due to dipolar disorientation as described above, can be extended to include systems with a distribution in relaxation times.

The peak temperature, T_m , for the current peak can be found by differentiating eqn. (3.10) and substituting for $\alpha(T)$ from eqn. (3.8), we get

$$T_m = \left[\frac{rA}{k\alpha_0} \exp(A/kT_m) \right]^{1/2} \quad \dots (3.13)$$

From the above equation it can be seen that T_m will shift towards a higher temperature if a higher heating rate, r , is employed. Also, for a fixed heating rate, the position of the peak (i.e. along the temperature axis) will be an increasing function of A , the activation energy for disorientation as well as the natural relaxation time, $1/\alpha_0$, for the process. It may also be

noted that T_m is independent of the forming conditions, E_p and T_p , provided the equilibrium polarisation has been attained.

(b) TSD FOR A DISTRIBUTION OF RELAXATION TIME

In the essentially non-crystalline polymeric solid, different conformations that the macromolecules may adopt, will result in an environment that can offer, differing resistance to the disorientating or rotating dipoles in different areas of the bulk. The dipoles will then have to surmount different activation energies resulting in different relaxation frequencies, $\alpha_i(T)$. Assuming that they still obey an Arrhenius shift, this can be written as

$$\alpha_i(T) = \alpha_o \exp(A_i/kT) \quad \dots (3.14)$$

Different relaxation frequencies may also arise from different values of α_o , for which we have

$$\alpha_i(T) = \alpha_{oi} \exp(A_i/kT) \quad \dots (3.15)$$

A distribution of the type described by eqn. (3.14) is usually encountered in β -type relaxation. The type described by eqn. (3.15) is more likely to arise from relaxation associated with movements of the dipolar groups that move in unison with the micro-Brownian motions of the main chain segment, like the α -relaxation near T_g . Here, different masses for the relaxing segments are most likely to be involved.

Assuming that distributions in α_0 and A are continuous, their contributions towards the polarisation, $P(t)$, could be expressed as

$$P(t) = P_d \int_0^{\infty} f(\alpha_0) \cdot \exp \left[-\alpha_0 \int_{t_d}^t \exp(-A/kT) dt \right] d\alpha_0 \quad \dots (3.16)$$

for a distribution in α_0 . For a distribution in A , this can be given as

$$P(t) = P_d \int_0^{\infty} g(A) \cdot \exp \left[-\alpha_0 \int_{t_d}^t \exp(-A/kT) dt \right] dA \quad \dots (3.17)$$

The distributions are also normalised such that

$$\int_0^{\infty} f(\alpha_0) d\alpha_0 = \int_{t_d}^{\infty} g(A) dA = 1 \quad \dots (3.18)$$

The corresponding expressions for the current can be found by differentiating eqns. (3.16) and (3.17) which yields

$$j(t) = P_d \exp(-A/kT) \int_0^{\infty} f(\alpha_0) \cdot \exp \left[-\alpha_0 \int_{t_d}^t \exp(-A/kT) dt \right] d\alpha_0 \quad \dots (3.19)$$

and

$$j(t) = P_d \exp(-A/kT) \int_0^{\infty} g(A) \cdot \exp \left[-\alpha_0 \int_{t_d}^t \exp(-A/kT) dt \right] dA \quad \dots (3.20)$$

Above equations also show that the TSD currents are independent of the forming conditions provided that the fullest possible polarisation has been reached. If this condition is not achieved, say due to too short a polarisation time t_p , or too low a temperature, T_p , then an effective distribution can be defined by

$$f^*(\alpha_0) = f(\alpha_0) FS(\alpha_0) \quad \dots (3.21)$$

$$g^*(A) = g(A) FS(A) \quad \dots (3.22)$$

where $FS(\alpha_0)$ or $FS(A)$ refers to the filling state of the polarisation. For a completely filled state, i.e. one where the electret has been polarized to its equilibrium polarisation value, P_d , the parameter FS equals unity.

3.4 MECHANISM OF TSD

TSD is actually the mirror image of the charging process contributing to the discharge of electrets but the driving force of all of these is the restoration of charge neutrality. In electrets, prepared from polar materials, disorientation of dipoles play an important role. This disorientation tends to destroy the persistent dipole polarisation by distributing all dipoles at random.

The disorientation of dipoles involves the rotation of coupled pair of positive and negative charges and requires a certain energy. It is for this reason that the discharge by dipole disorientation is thermally activated and, therefore, can be speeded up by heating. Often disorientation energy is not the same for all dipoles. The current-temperature plot, therefore, consists of several peaks because the dipoles with low activation energy will disorient at low temperatures, while those with a high activation energy will respond at higher temperatures. If the difference in the various activation energies is not large, it is appropriate to assume a continuous distribution of activation energies, for which all the individual peaks overlap and average into a single peak. Such broad peaks often result as a disorientation of polar side groups in a polymer at low temperature. Another

possible cause for the appearance of broad peaks is a difference in the rotational mass of the dipoles. These differences occur in a polymer when heated to its softening temperature, where the dipoles are disoriented by the motion of main chain segments. This disorientation is responsible for the peaks which are located near glass transition.

In addition to dipoles, the electret usually contains immobile space charges which are distributed randomly, often near the electrodes. During the heating process, these get mobilised and neutralised either at the electrodes, or in the sample by recombination with charges of opposite sign. The forces driving the charges are their '*drift*' in the local electric '*field*' and '*diffusion*', which tends to remove concentration gradient. The space charge peak appears at a higher temperature than the dipolar peak. This is because the disorientation of dipoles merely requires local rotation, whereas the neutralisation of space-charge requires them to move over many atomic distances.

If the space charges are ions, these are generally considered to be free to move with a thermally activated mobility. One can visualise them as trapping from one vacancy to another across a potential barrier equal to the activation energy. If, however, the charges are electrons or holes, it is more appropriate to visualise them as being immobilised in local traps, from which the heating releases them into a band of energies in which these are freely diffused to the electrodes.

At a higher temperature, the motion of space charge is accompanied by a second neutralisation mechanism, namely, recombination with thermally generated carriers. These carriers are generated uniformly in the entire bulk of the specimen by dissociation of neutral entities. These are responsible for conductivity of the specimen which can be either electronic or ionic. In polymers, it seems to be the impurity ions which contribute to the ohmic conduction because polymers show appreciable conduction only above T_g where enough free volume is available for the ions to move.

Usually, the detrapping of electronic carriers is analysed with the band gap model developed for crystalline solids. However, most electret materials are amorphous or at most partially crystalline. The high degree of positional (and compositional) disorder in these materials results in many localised states in the forbidden energy gap [19]. These trapping states differ in number and depth, the higher the order, the fewer these are and the deeper they tail off into the energy gap. The energy gap is thus replaced by a pseudo-gap, in which the density of states remains finite. As a result, the band edges are blurred, so that it is difficult to mark the energy at which a carrier is completely nonlocalised.

Mott *et al.* [1] have, therefore, proposed to base the definition of the transport bands in amorphous materials on the mobility of the carriers. This is illustrated in Fig. 3.1, the critical energy E_c , at the mobility edge (where the mobility drops by three orders of magnitude) separates localised from

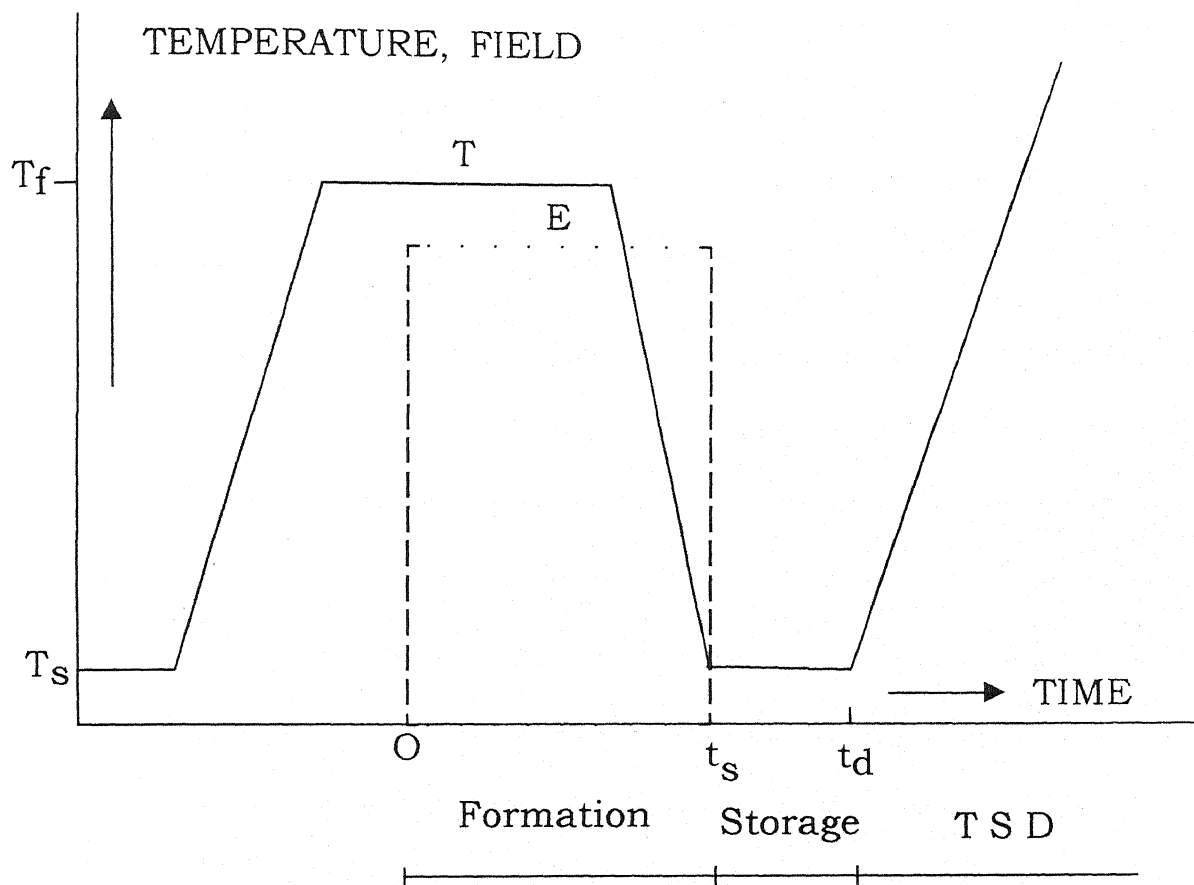


Fig. 3.1 : Field - Temperature scheme for thermo electret formation.

delocalised states. Clearly, it is only above E_c that electrons can move through the solid without the help of thermal energy. In addition to the disorder-induced band-tail states (which stretch out monotonically from the band edges), clearly recognisable gap states may be formed by intrinsic structural defects. In polymers, intrinsic defects are branching, chain entanglements, chain ends, pendant groups, etc.

However, the actual situation being unknown for most amorphous materials, the conventional band gap model is still used as a first approximation. With this model, it is easy to visualise the other two processes that a carrier may undergo after its thermal release from a trap. It is a retrapping, when on its way to the electrodes it meets another trapping centre, and recombines with an opposite charge when it is caught by a recombination centre. At low temperatures, the multitude of trapping sites in disordered materials allows the electronic carriers to move in the direction of the field by hopping across the localised gap state instead of moving freely along extended band states.

3.5 TSD PARAMETERS

3.5-i ACTIVATION ENERGY

Theoretically the activation energy of non-distributed relaxation process can be calculated from a single TSD curve by means of some characteristic elements of the peak such as its half width, inflection point or initial part of the current rise. Other methods based on utilizing the whole

current-temperature curve or that which use several heating rates are also available. Most of these methods, except for one using the whole TSD plot are derived from methods based on the early works on thermoluminescence or thermally stimulated conductivity [19].

Methods for calculation of activation energies are explained in succeeding subsections.

(a) INITIAL RISE METHOD

This method is accredited to Garlick and Gibson [20] and is based on the fact that the second integral term in the $j(T)$ expression is negligible at temperatures $T < T_m$. Thus, differentiating with respect to $1/T$, the following expression for the initial portion of the current rise is obtained

$$\frac{d}{d(1/T)} \log j(T) = -\frac{A}{k} \quad \dots (3.23)$$

By plotting $\log j(T)$ versus $1/T$, activation energy A can be determined. This procedure is generally advocated to be satisfactory and is widely used. It does not necessitate a linear heating rate nor a precise knowledge of the absolute temperature.

The approximation that at $T < T_m$, the TSD current can be simplified into $j(T) = \text{constant} \exp(-A/kT)$ may not be true if the magnitude of the TSD current in the rising portion of the plot is large when compared to the peak height. When this happens, the plot of $\log j(T)$ versus $1/T$ ceases to be linear and the value of A (obtained from the slope) has to be corrected as

$$A_{\text{corrected}} = (1 + 0.74d_1 + 0.092d_2)A - (2d_1 + 0.22d_2)kT_m \quad \dots (3.24)$$

where A is the value obtained from the least squares fitted plot of $\log j(T)$ versus $1/T$ with experimental values of $j(T)$ that had been called between two values of the current $j(T_2)$ and $j(T_1)$, where $T_1 < T_2 < T_m$. The parameters d_1 and d_2 are defined as

$$d_1 = \frac{j(T_1)}{j(T_m)} \quad \dots (3.25a)$$

$$d_2 = \frac{j(T_2)}{j(T_m)} \quad \dots (3.25b)$$

The ranges of applicability of eqn. (3.23) are $d_2 \leq 0.5$, $d_2/d_1 \geq 5$.

$$10 \leq \frac{A_{\text{corrected}}}{kT_m} \leq 100 \quad \dots (3.26)$$

(b) GRAPHICAL INTEGRATION METHOD

The relaxation time can be written as [21]

$$\tau(T) = \frac{P(T)}{j(T)} = \frac{1}{r} \left[\int_T^\infty J(T') dT' \right] \frac{1}{J(T)} \quad \dots (3.27)$$

$$\log \tau(T) = \log \left[\frac{1}{r} \int_T^\infty J(T') dT' \right] - \log J(T) \quad \dots (3.28)$$

Assuming an Arrhenius shift for $\tau(T)$, we have

$$\log \tau(T) = \log \tau_0 + A/kT \quad \dots (3.29)$$

The quantity $\tau(T)$ can be calculated by using eqn. (3.28) where we have taken the integral term to be easily evaluated by graphical integration of the area of the TSD peak from $T \rightarrow \infty$. Knowing $\log \tau(T)$ and plotting it

against $1/T$, a straight line may be obtained, yielding the activation energy A . The straight line is usually called the BFG plot after Bucci *et al.* [22]. Like the initial rise method, this procedure does not presume a linear heating rate, but unlike the former, it utilises data from the whole of the TSD peak. The BFG plot is to be preferred if the TSD plot exhibit larger parasitic background currents which may be difficult to eliminate from the small current signal portion of the initial rise.

(c) METHODS BASED ON THE VARIATION OF HEATING RATES

These methods are based on the shifts of the TSD current maximum with the heating rates employed. Several ways of plotting the results have been proposed [23,24]. It can be seen that

$$A = \frac{k T_{m1} T_{m2}}{T_{m1} - T_{m2}} \log \left(\frac{r_1 T_{m1}^2}{r_2 T_{m1}^2} \right) \quad \dots (3.30)$$

i.e. if the heating rate is changed from r_1 to r_2 , the activation energy for the relaxation can be calculated from the corresponding shift of the peak temperature T_{m1} to T_{m2} .

A better procedure utilising a series of heating rates, r (resulting in corresponding T_m s), was also suggested by Hoogenstraaten whereby the plot of $\log(T_m^2/r)$ against $1/T_m$ should yield a straight line, from the slope of which the activation energy can be found [25]. The accuracy of these methods will depend on the accurate control of the heating rates employed and also on the magnitude of the actual shifts of the T_m s. Therefore, that

the method is less suitable for relaxations with large activation energies, A , because the shifts of the current maxima will be smaller and experimentally more difficult to measure.

Several other methods to calculate the activation energy based on utilising the shape or symmetry of the TSD peak can also be found [26-28]. More recently, a new procedure has been proposed for a more accurate determination of activation energy [29].

(d) **ACTIVATION ENERGY FOR DISTRIBUTED PROCESSES**

The methods described hitherto to calculate the activation energy only holds good strictly for relaxations of a single, well-defined frequency. For a distributed relaxation, the initial rise method for calculation of activation energy would theoretically yield too low a value by over emphasising the role of the components with the slowest relaxation times. The graphical integration method will also have the same systematic error as a result of taking into account too high a number of components.

It has been shown that the initial rise method can still be applied to the case where there is a symmetrical distribution in $1/\alpha_0$ [30]. Up to the lower half width temperature, the TSD current was shown to obey, approximately

$$\log J(T) \sim \text{constant} - \frac{WA}{kT} \quad \dots (3.31)$$

where W is a constant whose value will depend on the type of the distribution describing $1/\alpha_0$. Above equation will also show that A can still be calculated by the initial rise plot.

The methods based on the variations of the heating rates are still theoretically applicable without modification, for the distributed process. This is so because the peak of the TSD current plot is determined essentially by the components with the average value of the activation energy. However, a problem would exist in the exact determination of T_m s and their shifts due to the broader nature of the TSD plots of the distributed systems.

The determination of other relaxation parameters, such as characteristics frequency, equilibrium polarisation and relaxation strength is little affected by the existence of a distribution in relaxation times [31]. The quantities can still be approximated by equation given in the graphical integration method [32].

3.5-ii RELAXATION TIME (τ_0)

The low temperature tail equation is given by

$$\log i(T) = \text{Const} \left(-\frac{A}{kT} \right) \quad \dots (3.32)$$

Thus, from equation (3.20) the activation energy A of the discharge process responsible for the peak can be obtained from a plot of $\log I$ versus $1/T$.

On differentiating of low temperature tail equation with respect to temperature and equating it to zero ($di/dT = 0$), one obtains the temperature (T_m) where maximum current occurs. T_m is given by

$$\tau_0 = \frac{k T_m^2}{\beta A \exp\left(\frac{A}{k T_m}\right)} \quad \dots (3.33)$$

Finding T_m from current versus temperature plots, one can calculate τ_0 . Knowing τ_0 we can easily calculate the relaxation time at T_m and at any temperature, i.e.

$$\tau(\tau_m) = \tau_0 \exp\left(\frac{A}{k T_m}\right) \quad \dots (3.34)$$

Calculations of $\tau(\tau_m)$ from equation (3.22) requires the value of τ_0 one can, however, calculate $\tau(\tau_m)$ without knowing τ_0 . From equation (3.33), we have

$$\begin{aligned} k T_m^2 &= \beta A \tau_0 \exp(A / k T_m) \\ &= \beta A \tau(\tau_m) \\ \text{or } \tau(\tau_m) &= \frac{k T_m^2}{\beta A} \quad \dots (3.35) \end{aligned}$$

Knowing T_m from experimental plots $\tau(\tau_m)$ can be obtained directly from 3.35.

3.5-iii CHARGE RELEASED (Q)

Charge released (Q) during the discharge was calculated by integrating the current versus temperature/time curves using Simson's rule.

Polymers are generally good dielectrics which are capable of storing the charge in them permanently when subjected to field temperature treatment. Such dielectric materials bearing persistent charge are called thermoelectrets. When thermoelectrets are subjected to a programmed

heat treatment, they give rise to a current in the external circuit and this is called thermally stimulated discharge current (TSDC). Thermally stimulated discharge current technique is a convenient and sensitive method for studying the charging and discharging process in dielectrics. These currents are due to dielectric relaxation behaviour and motion of free charges in the polymer. Hence, the TSDC technique can be used to understand the low frequency dielectric relaxation in solids and the relaxation between dielectric behaviour and process on the atomic scale. Because of the high sensitivity of this technique, it is also used to investigate the low concentration of dipolar impurities.

3.6 TRANSIENT CURRENTS IN CHARGING AND DISCHARGING MODES

The charge of electrets may be generated by various mechanisms : orientation of permanent dipoles (in polar materials), trapping of charges by structural defects and impurity centres, and build up of charge near heterogeneity such as the amorphous-crystalline interfaces in semi-crystalline polymers and the grain boundaries in polycrystalline materials.

At room temperature, charge decay measurements are rather time consuming, because at such temperatures, the dipoles and charges remain virtually immobile. However, when an electret is heated, the dipoles and charges quickly regain their freedom of motion. Thermal stimulation of the discharge, therefore, shortens the measurement considerably. During such a heat stimulated discharge, an electret connected to two electrodes

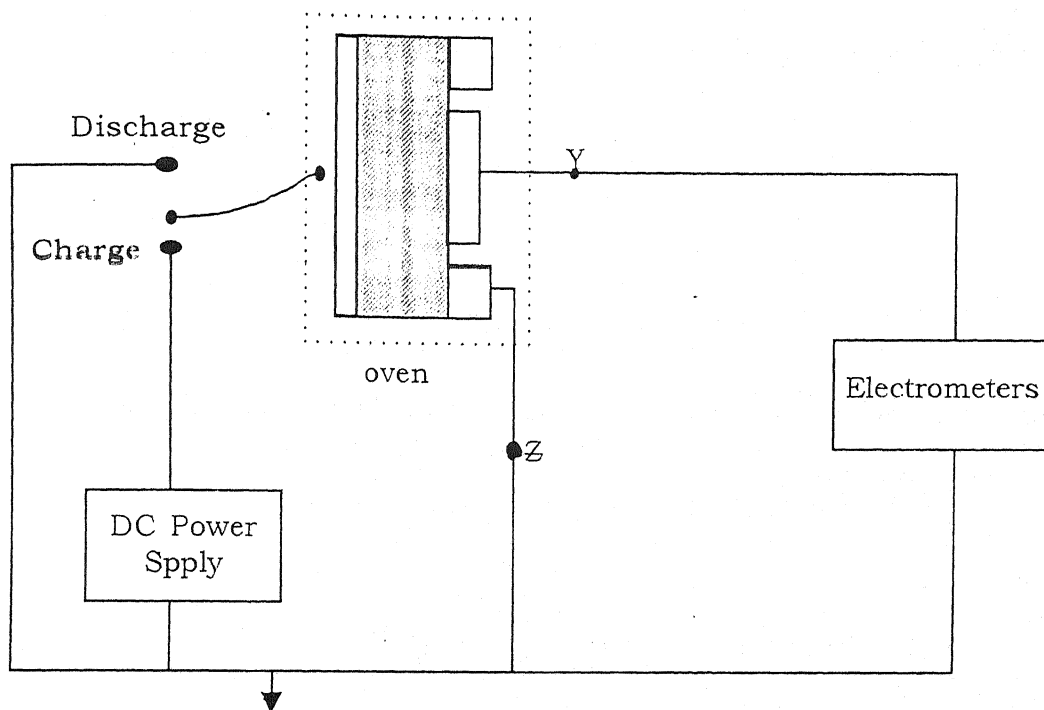
generates a weak current that shows a number of peaks when recorded as a function of temperature. The shape and location of these peaks are characteristics of the mechanisms by which electrets store their charges. Analysis of the curves yield detailed information on the dipoles (density, relaxation and activation energy) [33,34] and trapping parameters (energies, concentration and capture cross section of traps). In spite of the fact that the charge of the electret is destroyed, the method has come into extensive use for the analysis of electrets as well as the development of electrets having a longer lifetime. Schematic diagram of measuring system for the DC transient current experiment and typical charging-discharging cycle are shown in Figure (x).

3.7 THEORY OF TRANSIENT CHARGING AND DISCHARGING CURRENTS IN POLYMERS

On applying an electric field to a polymer sample, a charging current flows in the external circuit. This current is composed of two components, namely, the polarization current component and the conduction current component. On assuming that the polarization current is due to the dipole of a single relaxation frequency $\alpha(T)$, it can be expressed as

$$dP_s(t)/dt + \alpha(T) P_s(t) = \epsilon_0(\epsilon_s - \epsilon_\infty) \cdot \alpha(T) \cdot E \quad \dots (3.36)$$

where T is the absolute temperature, t is the time, ϵ_0 the permittivity of free space, E the steady charging field, ϵ_s and ϵ_∞ are the static and high



Schematic diagram of measuring system for the DC transient current experiment.

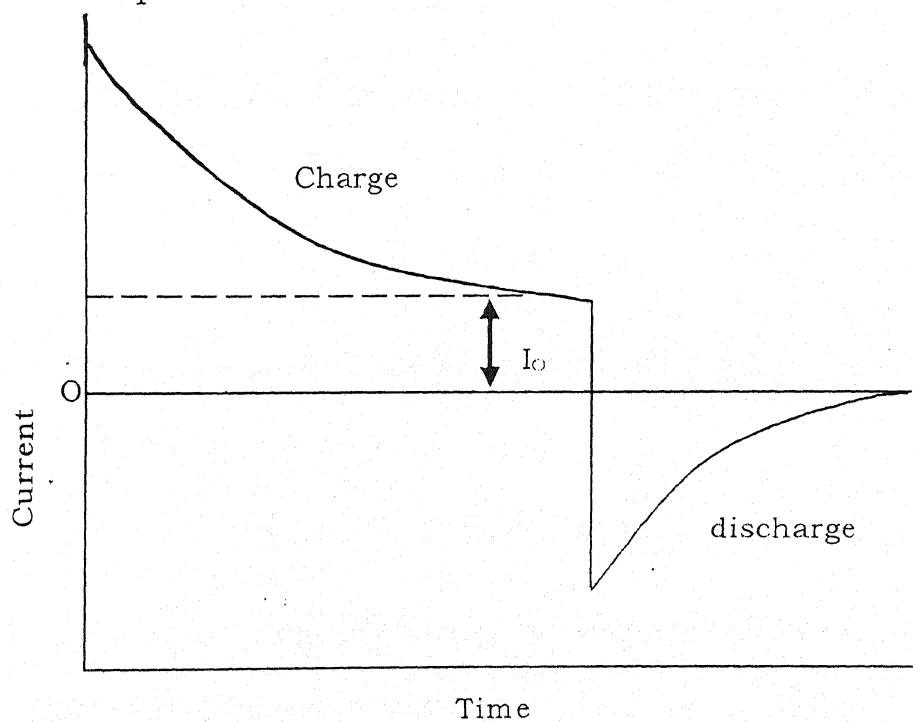


Fig. (X) : Typical charging - discharging cycle.

frequency dielectric constants respectively. The current density generated by decay in polarisation is given by

$$\begin{aligned} i_p(t) &= dP(t)/dt \\ &= -\alpha(T) P_s(t) + \epsilon_0 (\epsilon_s - \epsilon_\infty) \cdot \alpha(T) \cdot E \end{aligned} \quad \dots (3.37)$$

the conduction current i_c at a fixed temperature T and the field E is defined as

$$i_c = \sigma(T) \cdot E \quad \dots (3.38)$$

where $\sigma(T)$ is the conductivity of the material at a fixed temperature T . Thus, the total absorption current will be the sum of both the components, i.e.,

$$\begin{aligned} i_{ab} &= i_c + i_p(t) \\ &= [\epsilon_0 (\epsilon_s - \epsilon_\infty) \cdot \alpha(T) + \sigma(T)]E - \alpha(T) \cdot P_s(T) \end{aligned} \quad \dots (3.39)$$

The discharging current is obtained when the sample is short circuited and the field is made zero. Thus, from eqn. (3.37), we have

$$dP_s(t)/dt + P(t) \cdot \sigma(T) = 0 \quad \dots (3.40)$$

The above is a differential equation with constant coefficients. Its isothermal solution can be written as

$$P_s(t) = P_0 \exp \left[- \int \alpha(T) dt \right] \quad \dots (3.41)$$

The current generated during disorientation of dipoles is only due to polarisation. There is no conduction current present since the external field is zero. The discharge current is thus given by

$$\begin{aligned}
i_d(t) &= -dP_s(t)/dt \\
&= \epsilon_0 \cdot E \cdot f(t) \\
&= \alpha(T) \cdot P_0 \cdot \exp[-\alpha(T) t_0] \quad \dots (3.42)
\end{aligned}$$

where $f(t)$ is the dielectric response function, P_0 is the initial polarization and $\alpha(T)$ the dielectric response loss peak in frequency domain.

Alternatively, this can also be expressed in terms of the frequency response of the complex dielectric constant, $\epsilon(\omega)$

$$\epsilon(\omega) = \epsilon'(\omega) - i\epsilon''(\omega) \cdot (1+i\omega t)^{-1} \quad \dots (3.43)$$

where $\epsilon'(\omega)$ and $\epsilon''(\omega)$ are the real and imaginary part of the dielectric constant, ω the angular frequency and t the relaxation time.

Thus, the isothermal discharge current measurements offer an alternative technique for dielectric constant and dielectric loss measurements as a function of temperature and frequency.

Frequency dependence of dielectric loss factor can also be obtained using Hamon's approximation,

$$\epsilon^H(t) = i(t)/2 \pi f \cdot c \cdot V \quad \dots (3.44)$$

where $i(t)$ is the magnitude of the transient current at time t , c is the geometrical capacitance of the electrode assembly without the sample, V the applied voltage and f is the Hamon's frequency ($= 0.1/t$). This

approximation gives adequately good accuracy in calculation of the dielectric loss provided there is a broad distribution of relaxation times.

The time dependence of transient currents can be expressed according to the Curie von Schweidler law [35] expressed as

$$i(t) = k \cdot t^{-n} \quad \dots (3.45)$$

In the optimum time range if the charging phenomenon persists for a time t_p , then according to the principle of superposition, time dependence of the transient currents can be expressed by the following equation.

$$i_d(t) \propto (t) = i_p(t) - i_p[\alpha(t) + t] \quad \dots (3.46)$$

Using eqn. (3.46), we have

$$-i_d(t) \propto (t) = -k t^{-n} [1 - \{\alpha(t)/(t+1)\}^{-n}] \quad \dots (3.47)$$

For $t \ll 1/\alpha(T)$, eqn. (3.47) gives

$$i_d \propto (T) (t) = -k t^{-n} \quad \dots (3.48)$$

and for $t \gg 1/\alpha(T)$.

$$i_d \propto (T) (t) = -n \alpha(T) k t^{-n-1} \quad \dots (3.49)$$

where $0 < n < 1$.

3.8 THEORY OF ELECTRICAL CONDUCTION MECHANISM IN POLYMER FILMS

To explain the transport of charge carrier in a thin polymeric films sandwiched between metal electrodes, there appears to be six separate

conduction mechanisms used. They are (i) Ionic conduction, (ii) Tunnelling mechanism, (iii) Hopping mechanism, (iv) Richardson-Schottky emission, (v) Poole-Frenkel effect, and (vi) Space charge limited current. Brief theoretical details of each mechanisms is discussed below :

(i) IONIC CONDUCTION

The concept of ionic conduction due to lattice defects has been understood for some time [36-38] and it depends principally on the rate of drift of the defects in an applied electric field. The actual conduction mechanism of this drift is jump of ions (or vacancies) over a potential barrier from one site to the next. If F is the electric field and l the distance between successive defect sites, then the current density J at high fields for ionic conduction is given by [39]

$$J = J_0 \exp[-(\Phi/kT - Fel/2kT)] \quad \dots (3.50)$$

where Φ is the potential barrier height. Eqn. (3.50) explains satisfactorily the observed results in thin insulating films [40,41].

(ii) TUNNELLING MECHANISM

Consider a thin insulating film sandwiched between two metal electrodes. If the potential barrier is thin enough, electrons can flow through the barrier between the electrodes by quantum mechanical tunneling [42]. The energy level diagram of an insulator having an arbitrary potential barrier is shown in Fig. 3.2. The relationship connecting the current density

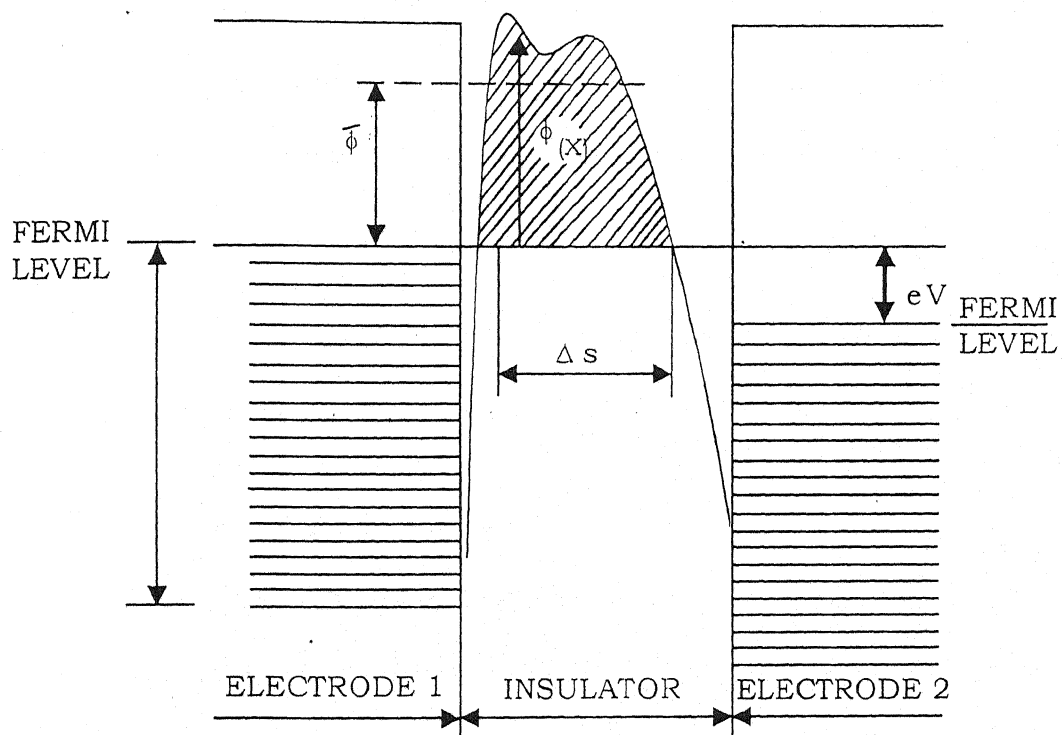


Fig. 3.2 : Tunneling process in an insulator.

due to electrons tunneling through an arbitrary potential barrier with applied voltage V , is given by [43]

$$J = J_0 [\Phi \exp(-A\Phi^{1/2}) - (\Phi + eV) \exp(-A(\Phi + eV)^{1/2})] \quad \dots (3.51)$$

In eqn. (3.38), $J_0 = e/2\pi\hbar (\beta\Delta s)^2$ and $A = 4\pi\beta\Delta s (2m)^{1/2}/\hbar$, where Δs is the width of the barrier at the Fermi level, Φ is the mean barrier height, \hbar is the Planck's constant, β is a function of barrier shape, m and e are mass and charge of electron, respectively.

The above equation (3.51) is readily applicable to potential barriers of arbitrary shape and to all practical voltage ranges.

(iii) HOPPING MECHANISM

In solids with broad intermolecular barriers, electron can migrate from one molecule to the other by moving over the barrier via an activated rate and this process is called hopping [44]. An electron in an occupied state with energy below Fermi level receives energy and hops to the nearby state above Fermi level. A generalized relation between hopping conductivity and temperature is given by [45].

$$\sigma = a_0 \exp(-E'/kT) \quad \dots (3.52)$$

where a_0 is a constant and E' is the hopping activation energy.

Equation (3.52) suggests that conductivity varies exponentially as a function of T^{-1} and E' decreases with temperature. This expression is valid generally at higher temperatures. Mott [46] pointed out that at low

temperatures the most hopping would not be to the nearest neighbour. His analysis resulted an expression for the conductivity (Fig. 3.3).

$$\sigma = A \exp(-B/T^{1/4}) \quad \dots (3.53)$$

where A and B are constants.

(iv) RICHARDSON-SCHOTTKY EMISSION

This type of electron emission from the metal at negative potential is analogous to thermionic emission except that the applied field lowers the barrier height, essentially by reducing the metal-insulator work function as shown in Fig. 3.4.

When an electric field exists at a metal-insulator interface, it interacts with the image force and lowers the potential barrier. The line CD in Fig. 3.4 represents the potential due to a uniform field F, which when added to the barrier $\Phi(x)$ produces the potential step shown by the dotted line, which is seen to be $\Delta\Phi_s$ lower than that without the electric field. The change in the barrier height due to this interaction of the applied field with the image potential is given by

$$\Delta\Phi_s = (e^3/4\pi \epsilon \epsilon_0)^{1/2} F^{1/2} = \beta_{RS} F^{1/2} \quad \dots (3.54)$$

$$\text{where } \beta_{RS} = (e^3/4\pi \epsilon \epsilon_0)^{1/2} \quad \dots (3.55)$$

Equation (3.43), e is the electronic charge, ϵ_0 the permittivity of the free space and ϵ is the dielectric constant of the material. Because of image

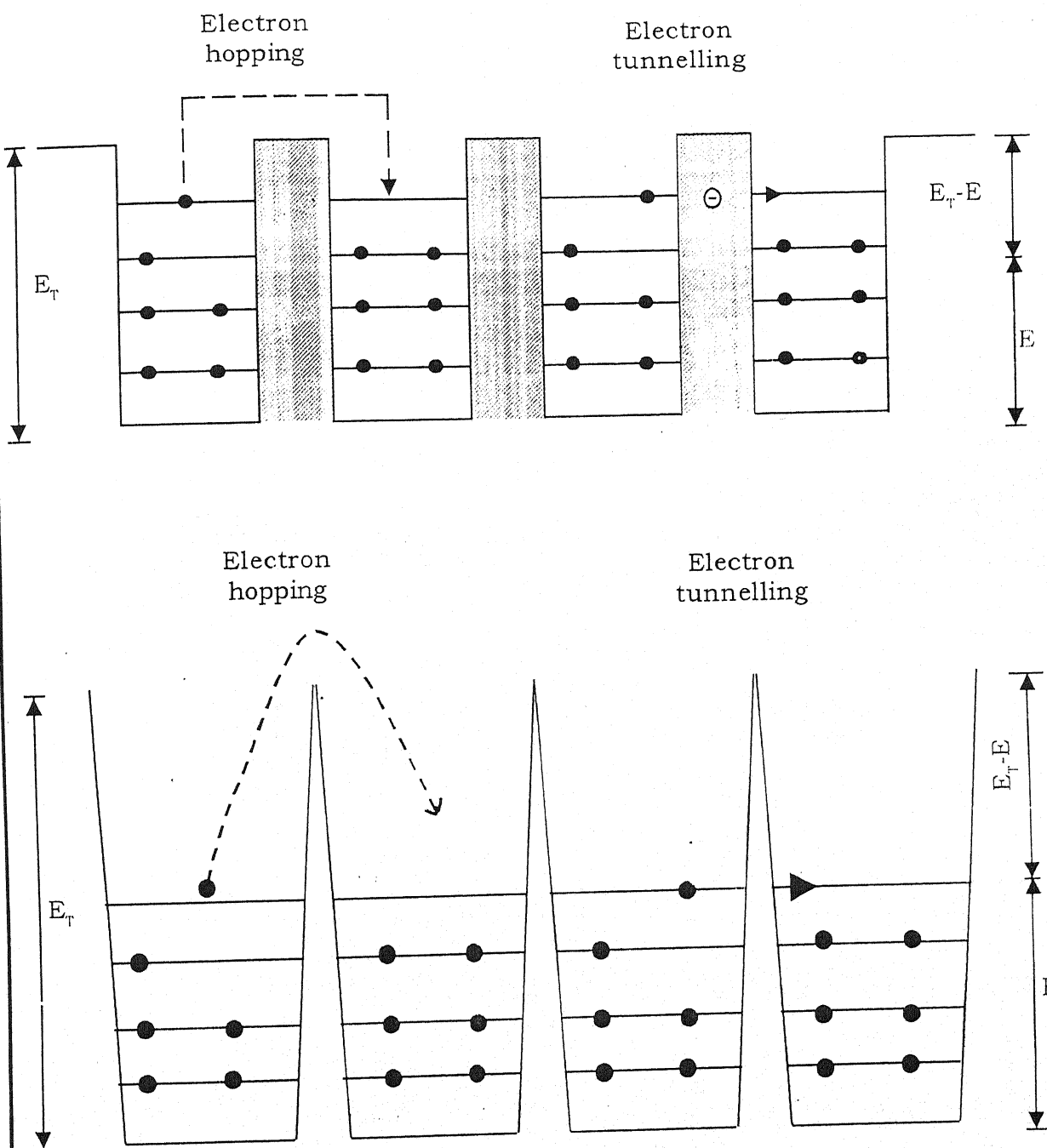


Fig. 3.3 : Schematic diagrams illustrating the electron hopping across and the electron tunnelling through a square and a triangular potential barrier. The electron hopping or tunnelling in one direction is equivalent to the hole hopping or tunnelling in the opposite direction.

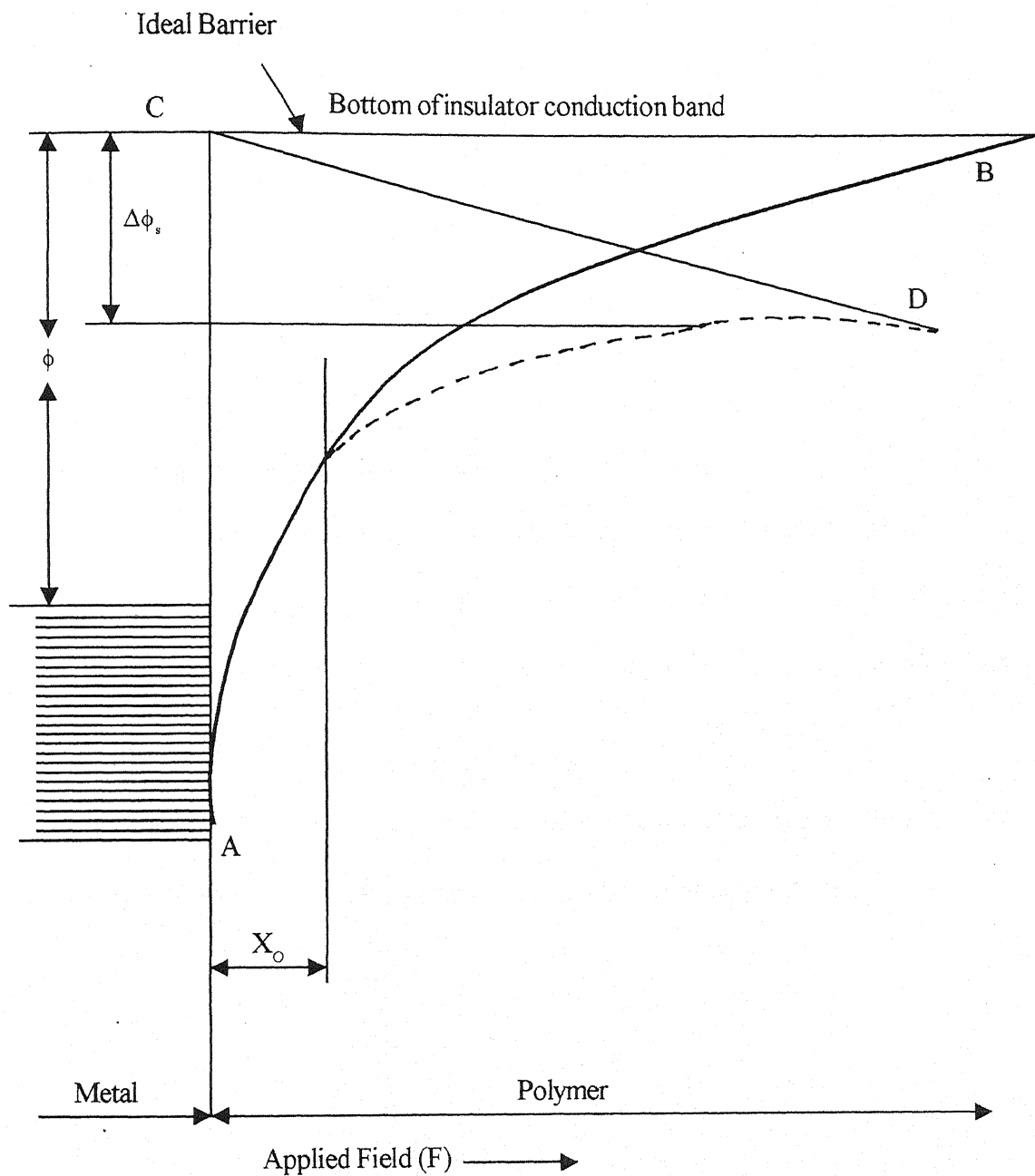


Fig. 3.4 : The Schottky effect. Reduction in barrier height ($\Delta\phi_s$) on application of the applied field (F) due to the image charges operative in the distance X_0

force lowering of the barrier, the electrode limited current does not saturate even at high fields and obeys the Richardson-Schottky law [37]

$$J = AT^2 \exp(-\phi_0/kT) \exp(\beta_{RS} F^{1/2}/kT) \quad \dots (3.56)$$

where,

$$A = 4\pi me k^2/h^3 = 120 \text{ A cm}^{-2} \cdot \text{deg}^{-1}$$

(v) POOLE-FRENKEL EFFECT

The Poole-Frenkel [47,48] effect (field assisted thermal ionization) is lowering of a Coulombic potential barrier when it interacts with an electric field as shown in Fig. 3.5. This process is analogous to Schottky effect at an interfacial barrier.

The Poole-Frenkel attenuation of a Coulombic barrier Φ_{PF} in a uniform electric field is twice that due to the Schottky effect at a neutral barrier.

$$\Delta\Phi_{PF} = (e^3/\pi\epsilon\epsilon_0)^{1/2} F^{1/2} = \beta_{PF} F^{1/2} \quad \dots (3.57)$$

$$\text{where } \beta_{PF} = (e^3/\pi\epsilon\epsilon_0)^{1/2} \quad \dots (3.58)$$

It is interesting to note from eqns. (3.55) and (3.57) that

$$\beta_{PF} = 2\beta_{RS} \quad \dots (3.59)$$

The current density in the case of Poole-Frenkel effect is given by [48]

$$J = J_0 \exp(\beta_{PF} F^{1/2}/kT) \quad \dots (3.60)$$

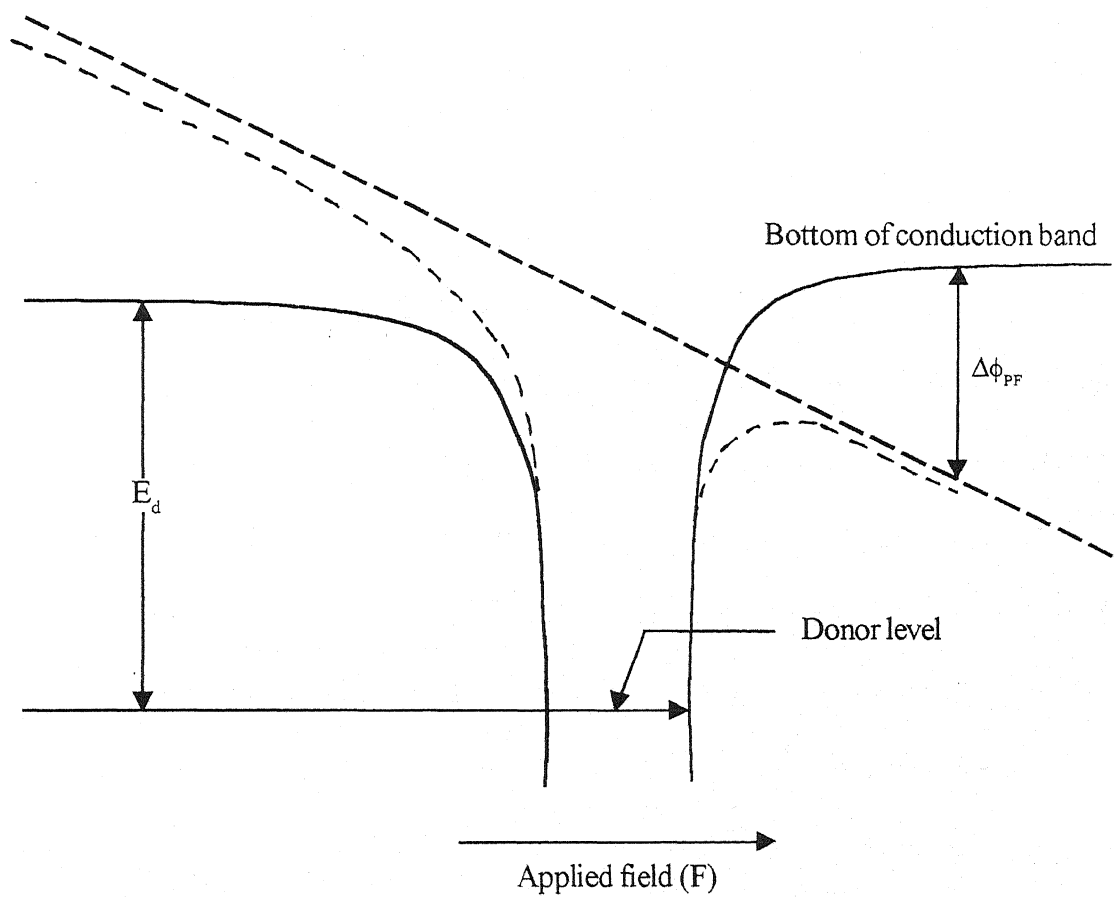


Fig. 3.5 : The Poole Frankel effect. Reduction in coulombic potential ($\Delta\phi_{PF}$) on application of the applied field (F). Here E_d is the trap depth below the conduction band.

where $J_0 = \sigma_0 F$ is the low field current density and σ_0 is the low field conductivity. Mead [49] was the first to report the field dependent conductivity apparently of the form given by eqn. (3.60) in thin insulating films.

(vi) SPACE CHARGE LIMITED CURRENT

In the case of polymers, the mobility of charge carriers is usually very low and hence their drift velocity under the applied electric field is also quite small. Thus, when charges are injected from the electrode into the insulator they tend to accumulate and tend to form space charge at the inter-electrode region. The formation of space charge also takes place due to the presence of large number of traps in the bulk of the material [39].

For simplicity, let us consider a perfect trap free insulator, with no intrinsic carriers, of thickness d . Assuming the current density is only due to the charges injected from the electrode, then the current density is given by [39].

$$J = 9/8 \mu \epsilon V^2/d^3 \quad \dots (3.61)$$

where μ is the mobility of the charge carriers, V the applied voltage, and ϵ the high frequency dielectric constant. The interesting feature of eqn. (3.52) is that it predicts that SCL currents is directly proportional to V^2 and inversely to d^3 .

If now thermally generated free carriers with density, n_o are included, then at low voltages where the injected carrier density is less than n_o Ohm's law will be obeyed, i.e.

$$J = e n_o \mu V/d \quad \dots (3.62)$$

The transition from Ohm's law, [eqn. 3.62] to Mott and Gurney law [50], [eqn. 3.38] takes place at the so called transition voltage, V_{tran} which is given by

$$e n_o \mu V_{tran}/d = 9/8 \mu \epsilon V_{tran}^2/d^3$$

$$V_{tran} = 8/9 e n_o d^2/c \quad \dots (3.63)$$

This suggests that transition voltage V_{tran} is directly proportional to d^2 .

Equations (3.61) and (3.63) are applicable to trap-free insulators. However, when a more realistic insulator, that is, which contains traps, is considered, the above equations get modified. The modified equations for current density, J and V_{tran} for shallow traps are [51]

$$J = 9/8 \mu \epsilon \theta V^2/d^3 \quad \dots (3.64)$$

$$\text{and} \quad V_{tran} = 8/9 e n_o d^2/\epsilon \theta \quad \dots (3.65)$$

where θ is a constant and for shallow traps, it is the ratio of the free carrier density to the trapped carrier density, i.e.

$$q = n/n_t \quad \dots (3.66)$$

Equation (3.65) clearly shows that the smaller the value of θ , the more effective are the traps in immobilizing the injected carriers. θ can be as slow

as 10^{-7} . Thus, the very large effect of shallow traps on SCL current is obvious.

3.9 CONDUCTION PARAMETERS

(i) POWER 'm'

The variation of current with applied DC voltage is important because power law given below is obeyed.

$$I = KV^m \quad \dots (3.67)$$

m determines the degree of linear relationship between $\log I$ and $\log V$.

Taking logarithm of above eqn.

$$\log I = \log K + m \log V \quad \dots (3.68)$$

Putting $\log I = y$; $\log V = x$ and $\log K = c$,

$$\text{We have } y = mx + c \quad \dots (3.69)$$

It is an equation of straight line. The problem has now reduced to the problem of fitting a straight line to a set of points on the XY plane and thus to a simple problem of least squares as follows.

$$m = \frac{\Sigma X \cdot \Sigma Y - n \Sigma (XY)}{(\Sigma X)^2 - n \Sigma X^2} \quad \dots (3.70)$$

The values obtained from above equation are some what different from those obtained by solving original least square equation, but these differences are small.

(ii) CONDUCTIVITY

The conductivity was calculated by using the equation

$$\sigma = \left[\frac{d}{A \times V} \right] \times I \quad \dots (3.71)$$

where d is the thickness of the sample (cm), A is the area (cm^2), V is the voltage applied across the material and I is the conduction current.

(iii) ACTIVATION ENERGY

Relation between conductivity and temperature governed by the eqn. (3.71). On the basis of this eqn., activation energy can be calculated as

$$E = \frac{K (\log_e \sigma_1 - \log_e \sigma_2)}{1/T_2 - 1/T_1} \quad \dots (3.72)$$

where K is the Boltzmann constant $= 8.617 \times 10^{-5}$ eV. σ_1 and σ_2 are the values of conductivity at two points corresponding to temperature $1/T_1$ and $1/T_2$.

3.10 EFFECT OF ENVIRONMENT AND OTHER FACTORS ON ELECTRICAL CONDUCTION OF POLYMERS

Electrical properties of polymers are highly sensitive to the environmental conditions such as temperature, pressure, humidity, ambient gases, high energy radiations, etc. and also to number of material parameters such as structure, crystallinity, mol. wt., orientation, deliberately added impurities. The variation of conductivity with temperature is of great importance and can be made as a basis of differentiating between metals

and semiconductors. Electrical conductivity of all polymers increases exponentially with temperature and follows the Arrhenius relation [52]

$$\sigma = \sigma_0 \exp(-E/kT) \quad \dots (3.73)$$

where σ is the conductivity measured, E the activation energy for conduction, σ_0 a pre-exponential factor, k the Boltzmann constant and T the absolute temperature.

A linear relation between logarithm of pre-exponential factor ($\log \sigma_0$) and activation energy in eqn. (3.61) has been observed for a class of substances and has been termed the "compensation effect" [53,54]. The linear relation is of the form

$$\log \sigma_0 = a E + b \quad \dots (3.74)$$

where a and b are constants for a class of substances. A more detailed study of compensation effect for polymeric semiconductors has been carried out by Gelfman and Larzan [55]. It is interesting to note that impurities introduced into a polymer alter both $\log \sigma_0$ and E values but the linear relation between them remains valid [56].

The pressure dependence of electrical conductivity has been the subject of several papers [57-59]. The conductivity of polymeric films increases with increase in pressure. This has been attributed to the orbital overlaps between adjacent molecules during compression. According to some workers [59,60] logarithm of conductivity of polymers is proportional to the square root of the pressure. However, there is a certain amount of

evidence [58] that the conductivity tends to level off and become pressure independent after certain value.

If the polymer is exposed to humid atmosphere its conductivity increases considerably [61-63]. The effect of water on the conduction process is by no means clear. Water may act as an electron donor and source of charge carriers. Rosenberg [64] observed a change in conduction from electron to ionic in hydrated proteins as the water content increases.

Adsorbed and absorbed gases exert a profound influence on the conductivity. The effect of ambient gases on the electrical properties of polymers has been studied by many workers [65-67]. Hydrogen, oxygen, and nitrogen were found to be active. It is known that polyacrylonitrile which is a hole semiconductor in the air, changes not only in magnitude but also the type of conduction when its surface is degassed [67]. Adsorbed oxygen on polyphenylacetylene suppresses the electrical conductivity [68]. The influence of various gases on electrical conductivity has been used to establish whether the semiconductor is n-type or p-type [52].

When a polymer is exposed to high energy radiation (Gamma rays, X-rays, electron beams) changes often occur which significantly alter the physical, chemical and mechanical properties of the polymer [69-71]. The type and degree of change may vary over a wide range and can be easily controlled by the type of radiation, exposure time, temperature, environment and the composition of the material [69]. The large effect of

radiation on polymers is due to the sensitivity of the material properties to molecular weight [72]. Only a few scissions or cross links per polymer molecule are sufficient to change markedly the tensile strength, solubility, melting point, glass transition temperature and so on. The decrease or increase in conductivity of a polymer depends on whether it is degrading or crosslinking on irradiation [73].

It is shown that conduction is strongly structure sensitive and it may differ between samples of the same material prepared by different methods as between samples of different materials [74]. In spite of extensive experimentation, the knowledge of relationship between conductivity and structure is still fragmentary. According to Seanor [75] polymer structure may be considered in three levels. The first level is the basic chemical composition of the monomer unit, the second level is the special arrangement of the basic polymer units within the individual polymer molecules and the third level is the special arrangement of polymer chains in the solid state. Eley and Parfitt [76] observed in a series of polycyclic aromatics differing in the number of condensed rings, that electrical conductivity increases with the number of condensed aromatic rings.

Wilk [77] argued that current flows mainly along the longitudinal axis of the molecule and that angular joints represent a disturbance which reduces the conductivity. He also found an empirical relation between activation energy E and number of linearly joined rings n , as

$$E = (17 - n)^2/100 \quad \dots (3.75)$$

which holds quite well up to 5 rings. In the study of effects of substituents on the electrical conductivity of anils, Gooden [78] found a correlation between conductivity and the Hammett substituent constant for both the meta and para series of substituents.

The dependence of the conductivity on the degree of crystallinity differs from one polymer to another [79]. It has been shown in polyacetylene [80,81] that a highly crystalline polymer has a conductivity four orders of magnitude greater than that of an amorphous polymer. However, conductivity of polytrifluorochloroethylene or polyethylene decreases on transition from amorphous to crystalline [82,83].

There are reports of study of the effect of molecular weight on the conductivity of polymers [84-86]. However, the relationship between molecular weight and conductivity has not yet been quantitatively determined. Increased mol. wt. of polyhydroquinone, polystyrene and poly(vinyl acetate) showed an increase in conductivity. Increased mol. wt. of cis-polyacetylene showed no change in conductivity and increased mol. wt. of trans-polyacetylene showed a decrease in conductivity [84].

Induced orientation of the macromolecules affects the conductivity of polymers in a complex manner. For instance, the conductivity of polyacrylonitrile increased [87] while that of polyvinyl alcohol remains unchanged [88] and that of polyethylene terephthalate decreased [89].

Considerable interest has been devoted to the problem of change in conductivity of polymers due to intentional doping with low mol. wt. compounds [90]. The carrier mobility can be greatly influenced by impregnating the polymer with suitable dopants [91]. Depending on their chemical structure and the way in which they react with the macromolecular matrix, doping substance increases the conductivity of the polymer to different degrees.

The doping of polymers is usually accomplished by chemical [92] or electrochemical [93] means. It has been suggested that the conduction mechanism in polyacetylene is independent of the method of doping [94].

3.11 MODELS EXPLAINING STEADY STEADY CONDUCTION

The steady state current is generated due to intrinsically generated charge carriers and charge injection from contacts. These phenomenon can be explained by the following model/theory/effects.

(a) Block band theory :

Charge transport in the solids having a negative temperature coefficient of carrier drift mobility is usually described in terms of Bloch band theory. The basic assumptions of the band theory are :

- (i) Use of one electron in the periodic potential one electron approximation,
- (ii) Neglect of multiple structure on individual atoms, and
- (iii) Treatment of electron lattice interaction as small perturbation.

The basic mechanism of charge transport in solids depends on nature of the electron exchange interactions and the electron phonon interactions. In inorganic semiconductors the electron exchange interactions are much larger than the electron phonon interactions, so that the electron behaves as a quasi free particle occasionally scattered by phonons and, therefore, the charge transport is coherent [95]. In polymeric substances the electron exchange interactions are much smaller than the inorganic solids, so that there is always a possibility that the electron phenomena on interactions may dominate in such solids. Thus, the small mean free path and the small carrier mobility in polymeric solids make the assumption of coherent charge transport barely self consistent.

(b) The Tunnelling Method :

Another important model of charge transport is the tunnelling of charge carrier, proposed and discussed by Eley [96]. Tunnelling is the process in which charge carriers can cross the barrier without having energy equal to the barrier height. This model assumes that an electron in a π -molecular orbital on one molecule, when excited to a higher energy level, can tunnel through a potential barrier to an unoccupied state of a neighbouring molecule with energy conserved in the process. The electron in the excited state may tunnel to its neighbouring molecule or return to its ground state but, in general, the probability for the former is much greater than the latter.

Tunnelling process is shown in Fig. 3.2. For a square potential barrier, E_T can be assumed to be the ionization potential of the molecule. In reality, the tunnelling electron would experience a potential which is the sum of the approximate coulomb potential attracting the electron to a positive ion and the potential of electron affinity of the originally neutral molecule. These potentials vary smoothly and are more correctly approximated by a triangular rather than a square barrier. Perhaps the triangular barrier shape facilitates the intermolecular electron transport as the barrier width becomes smaller for the excited electron at a higher level.

(c) The Hopping Model :

The charge transport can also be described in terms of the hopping model which may be preferable to the band model under certain circumstances. A carrier can move from one molecule to another by jumping over the barrier via an excited state as shown in Fig. 3.3. The criterion to determine whether the charge transport in the molecular crystals takes place coherently according to the band model or by random jumps according to the hopping model depends on the electron lattice interactions. It depends on whether the strongest coupling exists with intermolecular (lattice) or intramolecular (nuclear) vibrations, it is linear or quadratic in the phonon coordinates and it is strong or weak compared with the intermolecular electron exchange interactions. The vibration period are typically 10^{-12} sec for intermolecular modes and 10^{-11} sec for

intramolecular period and intermolecular vibration period by τ , τ_{vi} and $\tau_{v\eta}$, respectively, we have the following two important cases :

Case I : $\tau < \tau_{v\eta} < \tau_{vi}$:

In this case the electron motion is so rapid that the vibration motion can be regarded as stationary and as a perturbation to the motion of the electrons. The electron can be thought of travelling over several lattice sites before being scattered. The band model is applicable to this case.

Case II : $\tau_{v\eta} < \tau < \tau_{vi}$:

In this case the molecule vibrates (intermolecular vibration) while the electron remains on a particular lattice site. This implies that during the time when electron remains on the lattice site, the nuclei of the molecule on this particular lattice site moves to a new equilibrium position. This gives rise to the formation of a polaron. The interaction of electron and phonon in the lattice site may lead to self-trapping in which the electron polarises the molecule and is trapped in self induced potential well. This case may lead either to random hopping transport or to coherent band transport. For the former, the electron trapped in such a potential well requires an activation energy to surmount a barrier of height equal to the binding energy of the polaron in order to move to the neighbouring site. Thus, for the hopping transport the electron-phonon interaction must be strong.

(d) Richardson-Schottky Effect :

The observable conduction in polymeric solids is usually explained in terms of charge injection from the metal contacts. Injection current which is smaller than the bulk current is observed due to Schottky field emission (i.e., electrode limited current flows with heteropolar space charge and depletion layer formation in front of electrode).

Schottky emission of electrons may occur from the metal contact of negative potential into conduction band of the dielectric. The fact that the electrons are emitted into the dielectric instead of vacuum is taken care of by multiplying the Richardson's formula for thermionic emission of electrons with the dielectric constant of solids. At very low voltage the conduction is due to field assisted thermionic emission of electrons from negative biased electrode (or holes from positively biased electrodes) over the interfacial barrier. The presence of electric field at the barrier modifies the emission current as it reduces the work function (as shown in Fig. 3.4) separating the two materials and is known as Schottky effect. For a trap free insulator the current density J is given by [97,98]

$$J = AT^2 \exp(-\phi_s/kT) \exp(\beta_s V^{1/2}/kT) \quad \dots (3.76)$$

where β_s , known as Schottky coefficient $= (e^{3/4} \epsilon \epsilon_0 d)^{1/2}$, d is the thickness, ϵ_0 is the permittivity of free space, ϵ is the dielectric constant, e is electronic charge, A (Richardson Dushman constant) $= 4 \pi m e k^2/h^3$, T is the absolute temperature, ϕ_s is the metal dielectric potential barrier height, V is the applied voltage and k is the Boltzmann's constant.

The above equation predicts a linear relationship between $\ln J$ and $V^{1/2}$ of slope β_s/kT at constant temperature. To a first approximation, a plot of $\ln (J/T^2)$ versus $1/T$ for a constant voltage can yield ϕ_s , the barrier height.

Thus, Schottky emission is the thermionic emission of electron under the application of electric field due to the lowering of constant barrier height, leading to a strong temperature dependent Schottky current.

(e) Poole-Frenkel Effect :

The application of an electric field on the dielectric material will either change the rate of carrier generation or injection, or change the distribution function and the mobility of the carriers. Sometimes both changes occur. The former change causes 'Electrode Effect' due to the Schottky type thermionic emission, and the latter produces "Bulk Effects" caused by the field dependent carrier mobility due to various scatterings and also by the field dependent carrier density due to field dependent detrapping process which is known as the "Poole-Frenkel Effect".

Poole-Frenkel Effect (abbreviated as P-F effect) sometimes called internal Schottky effect describes the electron transfer by field enhanced thermal excitation (or detrapping) of trapped electrons into the conduction band of the dielectric. The interaction between the positively charged trap and electron gives rise to the Coulombic barrier [99], the P-F effect (field assisted thermal ionisation) is the lowering of this Coulombic potential

barrier when it interacts with an electric field. This is usually associated with the lowering of trap barrier in the bulk of dielectric.

The P-F bulk limited conductivity is given by the following equation [100,101].

$$J = AT \exp(-\phi_{PF}/kT) \exp(\beta_{PF} V^{1/2}/kT) \quad \dots (3.77)$$

where ϕ_{PF} is the barrier associated with the promotion of an electron from a donor level to the conduction state or alternatively, with the promotion of an electron from a valence state to an acceptor level, A is a constant, V is the applied potential, k is the Boltzmann's constant, β_{PF} is P-F the coefficient and T is the absolute temperature.

The factor $(\beta_{PF} V^{1/2})$ in the above equation is the amount by which the coulombic barrier is lowered due to its interaction with the field.

Usually $\beta_{PF} = 2 \beta_S$, it can, however, become comparable to β_S under certain conditions [102,103]. Hence, quite often it becomes difficult to distinguish between the R-S and P-F type of conduction from the analysis of J-V characteristics. However, the use of different electrode materials modifies significantly the R-S current but not the P-F current [104].

(f) **Space Charge Limited Current (SCLC) :**

This mode of conduction can have a pronounced effect on the electrical properties of insulators. Space charge limited current is important because the injected current is independent of the mechanism of carrier

generation and their trapping within the solid. Space charge is generally referred to as the space field with a net positive or negative charge and appears in a variety of insulators. Space charge polarisation occurs in the direction of the field and also due to direct injection of charge carriers from the electrodes at high field.

There are, in fact, several variations of space charge limited flow depending on whether the current is due to electrons only (i.e., single injection), or electrons and holes both (i.e., double injection) and whether the traps and recombination centres are present.

Single carrier injection currents are necessarily space charge limited. In a perfect trap free insulator, all the injected carriers remain free. They contribute to the space charge and the current flow is exactly analogous to that in a vacuum diode. Under double injection, i.e., with electrons, injected from cathode and holes injected from anode, space charge conditions are partially overcome and for intermediate injection level charge neutrality can be assumed throughout the insulator. However, at high and low injection levels, the space charge again becomes important.

The magnitude of current response and the actual form of the current-voltage characteristics are determined by the interaction of the injected carriers with localized defect states, which can trap and store charge in equilibrium with the free charge. In fact, some injected charge is trapped at these localized defects. Therefore, due to reduction of injected

current through trapping, the appearance of SCLC is inhibited until a sufficiently large field is applied. Further, the transition from ohmic region to SCLC region depends mainly on the distribution of trapping levels.

The role of traps in study of SCLC was realised by Rose [105] and Lampert [106]. As long as the concentration of traps is not very large, an increase in the applied field and so in the concentration of carriers injected into the dielectric will shift the equilibrium between occupied and unoccupied traps and in case of unipolar SCLC the current density is given by [107]

$$J = \frac{V^2}{d^3} \mu \theta (\epsilon \epsilon_0 / d^3) \quad \dots (3.78)$$

where J is the current density, d is the thickness of the sample, V is the applied potential, ϵ is the dielectric constant, μ is the carrier mobility, ϵ_0 is the permittivity of free space and $q = n_o/n_t$, where n_o is the effective density of free carriers and n_t is the effective density of the trapped carriers.

Assuming that carriers are trapped at shallow levels of average depth E_t , that remains in the thermal equilibrium with the concerned energy band, we have

$$q = n_o/n_t = N_c/N_t \exp(-E_t/kT) \quad \dots (3.79)$$

where N_c is the density of states in the conduction band and N_t is the density of shallow traps within the quadratic region of SCLC, the current density is given by :

$$J = v^2 \mu (\epsilon \epsilon_0 / d^3) (N_C / N_t) \exp(-E_t / kT) \quad \dots (3.80)$$

$$\text{or } J = V^2 \mu_0 (\epsilon \epsilon_0 / d^3) (N_C / N_t) \exp[-(E_t - E_\mu) / kT] \quad \dots (3.81)$$

where $\mu = \mu_0 \exp E_\mu / kT$ is the temperature activated carrier mobility. Deviation from eqn. (3.81) and dependence of J on some higher power of V has been described as due to existence of deep traps and continuous distribution of trapping levels in the forbidden gap [105-108]. The slope of $\log J$ and $1/T$ plot gives $-E_t/k$ while the intercept for the limit $1/T \rightarrow 0$ gives $(m \epsilon \epsilon_0 V^2 / d^3) (N_C / N_t)$, from which $(m N_C / N_t)$ and N_t can be calculated.

The fact that only few organic solids show an ohmic region [109,110] has led to the belief that the conduction in organic solids is mainly extrinsic. The hole [111] and electron injection in organic solids have been achieved using special electrodes and their correlation with ionization energies have been studied [112].

3.12 DIELECTRIC MEASUREMENT

When solid polymeric materials are subjected to an electric field, an induced electric moment is produced. This induced electric moment persists, whenever the field is present. In case, when the permanent dipoles are present, an electric field brings about their orientation and polarizes the material. The displacement of polar groups require some time and is thus dependent on frequency and temperature, which lead to different dispersion [113,114] phenomena. Actually at frequencies and

temperatures where dispersion occurs, only a part of electrical energy is stored, while some of it is dissipated as heat.

There are different types of polarization has already been described in Chapter I. Dipolar polarization occurs in the frequency range 10^3 to 10^6 Hz. Atomic and electronic polarizations are observed in the IR and optical frequency ranges.

The displacement of polar group of polymers requires some time and is thus dependent on the frequency and temperature which lead to different dispersion phenomena according to the segmental motion of the polymer chain or orientation of the polar side groups.

The loss factor exhibits a maximum at frequencies at which dielectric permittivity, ϵ' shows a dispersion (Fig. 3.10). The maxima in dielectric loss occurs at temperatures at which motion of large segments of polymer chain or different side groups begins. Dielectric behaviour of polymers is characterized by distribution in relaxation times. The detailed study of dielectric behaviour of polymers has given valuable insight into their macromolecular motion.

3.12-i DIELECTRIC RELAXATION IN POLYMERS

Valuable informations could be obtained from the dielectric relaxation [115-144] studies, made in polar and non polar linear polymers using various techniques. Various mechanism for the charge storage in polymers could be easily classified as a result of these studies.

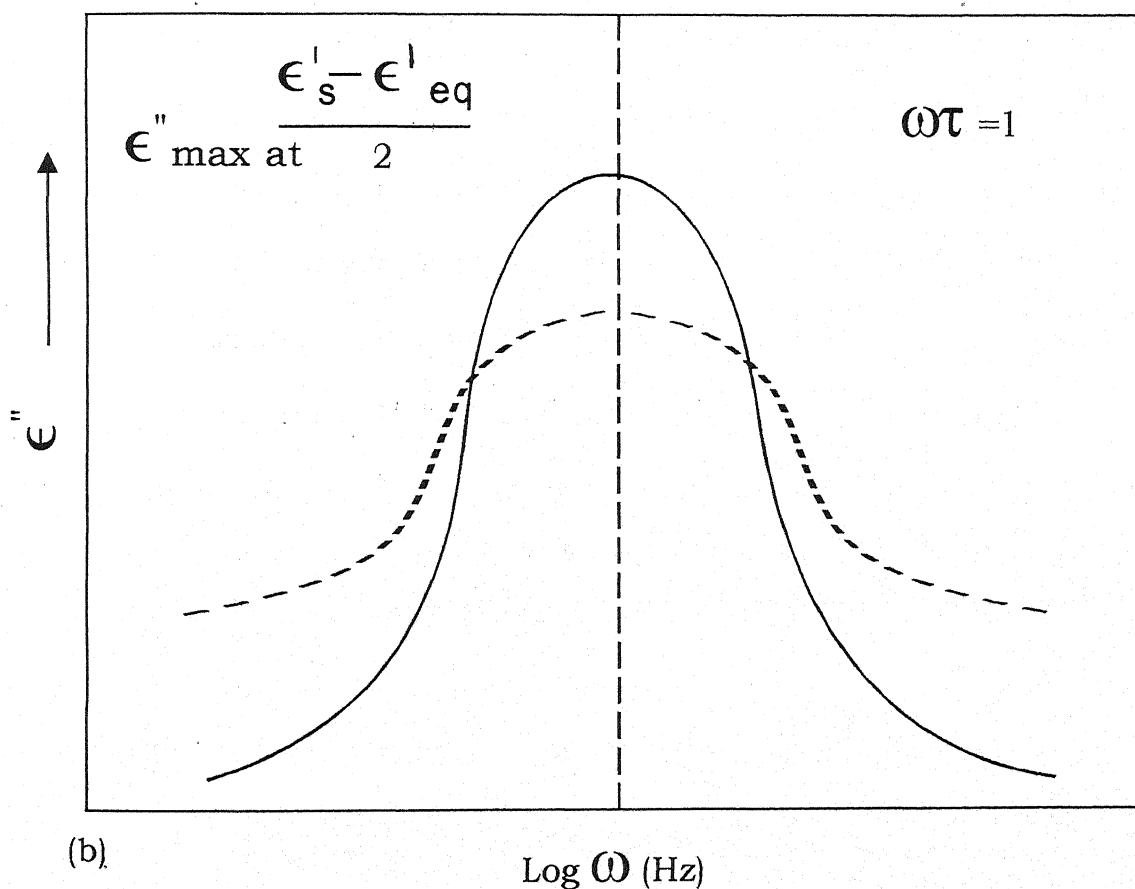
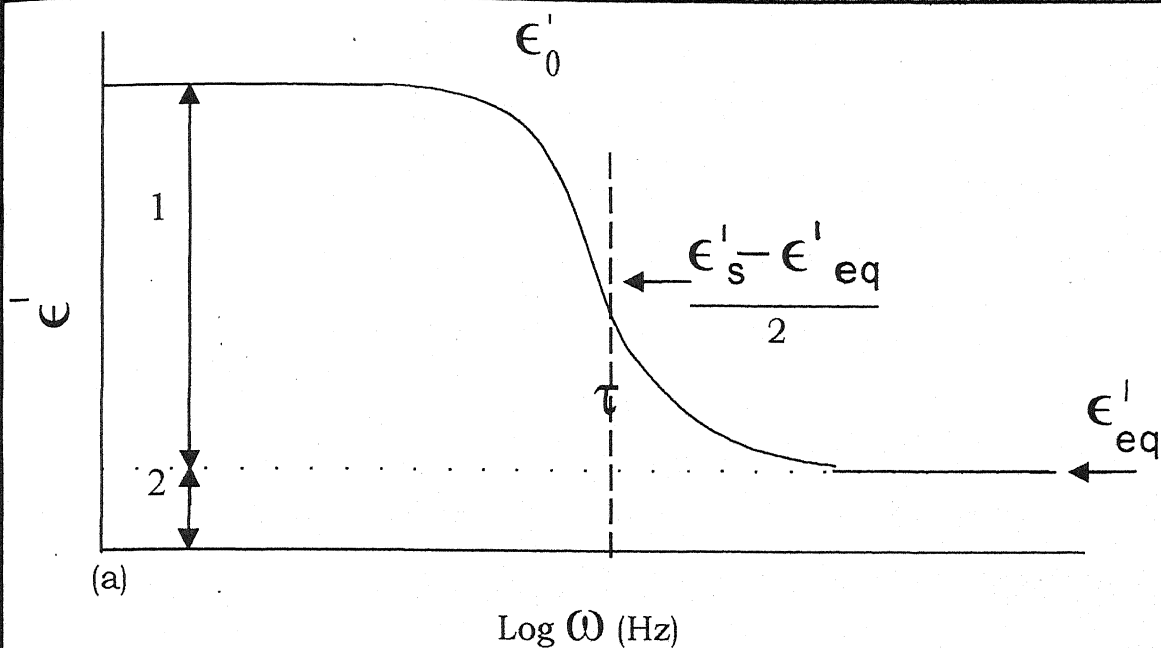


Fig. 3.6 Behavior of dielectric constant (ϵ') and loss factor (ϵ'') for polar polymers as a function of frequency (broadening of loss curve is caused by multiple relaxation times and is shown by the dotted line)

- ϵ'_s - Static dielectric constant
- ϵ'_{eq} - High frequency dielectric constant
- τ = Dielectric relaxation time.
- 1 - Dipole contribution
- 2 - Electronic contribution

It has been observed that total charge stored in a polymer electret [145] and the different mechanism which contribute to this charge are very sensitive to the structure of the forming material. It was also observed that charge can be produced by making some structural changes in the polymer matrix itself by doping with certain impurities [146-148].

Polymers are complex dielectric materials. The use of polymers as dielectrics is being increasingly important. Choice of the polymeric dielectric for each concrete case depends on its dielectric and other physical properties over a wide range of temperatures, electric field and frequencies [149-160]. Investigation of dielectric properties is one of the most convenient and sensitive methods of studying polymer structure. Dielectric studies in polymers provide vital [161-172] information on the molecular configuration of a system; for example - movement of dipoles, losses of energy, segmental motion, conduction mechanism, latent heat, etc. It is, therefore, important that their dielectric behaviour should be fully understood. Dielectric properties of several polymers [173-179], polar and non-polar have been investigated.

3.12-ii DIELECTRIC PROPERTIES [180-193]

(a) MACROSCOPIC DESCRIPTION OF STATIC DIELECTRIC CONSTANT [194]

As an introduction to the concept of the static dielectric constant of a substance, consider the following well-known experimental result.

Two plane parallel plates of area A and separated by d cm are charged with a surface charge density q , one plate being positive and other negative. If the space between the plates is evacuated and if d is small compared with the dimensions of the plates, this will result a homogeneous electric field between the plates, the field strength being given by

$$E_{vac} = 4 \pi q = D \quad \dots (3.82)$$

in e.s.u. is called the electric displacement or flux density. The potential difference between the plates is equal to

$$f_{vac} = E_{vac} \cdot d \quad \dots (3.83)$$

and the capacitance of the system is defined by

$$C_{vac} = A q / \phi_{vac} = \phi / \phi_{vac} \quad \dots (3.84)$$

Suppose now that the space between the plates is filled with an insulating substance, the charge of the plates being kept constant. It is observed that the new potential difference ϕ is lower than ϕ_{vac} and similarly the capacitance C of the system is increased. The static dielectric constant ϵ_s is then defined by

$$\epsilon_s = \phi_{vac} / \phi = C / C_{vac} \quad \dots (3.85)$$

Thus, as a result of introducing the substance, the field strength is reduced from the value E_{vac} to the value E , where

$$E_{vac} = D = \epsilon_s E \quad \dots (3.86)$$

In other words, the effective surface charge density on the plates is now $q' = E/4\pi$ rather than $q = E_{vac}/4\pi$, and one may say that introducing the dielectric is equivalent to reducing the surface charge density by an amount

$$P = q - q' = (E_{vac}/4\pi)(1 - 1/\epsilon_s) = (\epsilon_s - 1)E/4\pi \quad \dots (3.87)$$

Thus, under the influence of the external field, the dielectric facing the positive charge acquires a negative induced surface-charge density P and vice versa. This is illustrated in Fig. 3.7. P is called the polarisation of the substance. One may write

$$D = E - 4\pi P = \epsilon_s E \quad \dots (3.88)$$

3.12-iii DIELECTRIC PROPERTIES OF INSULATORS IN ALTERNATING FIELDS

When an ideal dielectric is subjected to an alternating field, current - I , would be ahead of voltage - V , precisely by 90° and current would be purely reactive. In actual fact, the phase angle ϕ is slightly less than 90° ; total current through the capacitor can be resolved into two components - active I_a and reactive I_r currents, we see that

$$\delta = 90^\circ - \phi \quad \dots (3.89)$$

where δ is called the dielectric loss angle.

3.13 THE COMPLEX DIELECTRIC CONSTANT AND DIELECTRIC LOSSES [194]

When a dielectric is subjected to an alternating field, the polarisation P , also varies periodically with time and so does the displacement D . In

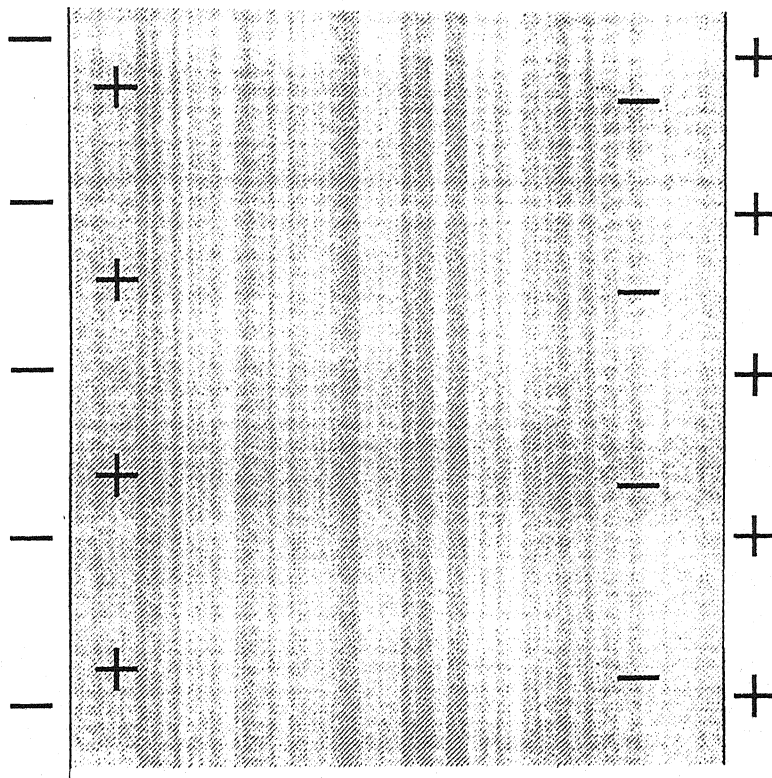


Fig. 3.7 : SCHEMATIC ILLUSTRATION OF CHARGES INDUCED AT THE SURFACE OF A DIELECTRIC.

general, however, P and D may lag behind in phase-relative to E, so that, for example if

$$E = E_0 \cos \omega t \quad \dots (3.90)$$

we have

$$\begin{aligned} D &= D_0 \cos (\omega t - \delta) \\ &= D_1 \cos \omega t + D_2 \sin \omega t \quad \dots (3.91) \end{aligned}$$

$$\text{Clearly, } D_1 = D_0 \cos \delta$$

$$\text{and } D_2 = D_0 \sin \delta$$

For most dielectric D_0 is proportional to E_0 , but the ratio D_0/E_0 is generally frequency-dependent. To describe this situation, one may thus introduce two frequency dependent dielectric constants :

$$\epsilon'(\omega) = D_1/E_0 = (D_0/E_0) \cos \delta \quad \dots (3.92)$$

$$\epsilon''(\omega) = D_2/E_0 = (D_0/E_0) \sin \delta \quad \dots (3.93)$$

It is frequently convenient to lump these two constants into a single complex dielectric constant,

$$\epsilon^* = \epsilon' - i\epsilon'' \quad \dots (3.94)$$

because the relation between D and E, both expressed as complex quantities, is then simply

$$D = \epsilon^* E_0 e^{i\omega t} \quad \dots (3.95)$$

as may readily be verified.

It may be noted that according to equation (3.92) and (3.93), there exists the relation

$$\tan \delta = \epsilon''(\omega)/\epsilon'(\omega) \quad \dots (3.96)$$

and because both ϵ' and ϵ'' are frequency-dependent, the phase angle δ is frequency-dependent. $\epsilon''(\omega)$ represents the losses in the system of bound charges exactly in the same way as the free charges are responsible for the conductivity losses [195]. Now, it will be shown that the energy dissipated in the dielectric in the form of heat is proportional to ϵ'' .

3.14 DIELECTRIC LOSSES AND RELAXATION TIME

Let us consider a dielectric for which the total polarisation P_s in a static field is determined by three contributions

$$P_s = P_e + P_a + P_d \quad \dots (3.97)$$

where the subscripts e, a and d refer respectively to electronic, atomic and dipolar polarisation. It will be assumed that values of P_e and P_a are attained instantaneously. Let P_{ds} denote the saturation value of P_d obtained after a static field E has been applied for a long time. It will be assumed that the value of P_d as a function of time after the field has been switched on is given by

$$P_d(t) = P_{ds} (1 - e^{-t/\tau}) \quad \dots (3.98)$$

Hence,

$$dP_d/dt = (1/\tau) [P_{ds} - P_d(t)] \quad \dots (3.99)$$

In the case of an alternating field $E = E_0 e^{i\omega t}$, eqn. (3.89) may be employed if we make the following change.

P_{ds} must be replaced by a function of time $P_{ds}(t)$ representing the saturation value which would be obtained in a static field and is equal to instantaneous value $E(t)$. Hence, for alternating fields we shall employ the differential equation

$$dP_d/dt = (1/\tau) [P_{ds}(E) P_d] \quad \dots (3.100)$$

we shall define the "instantaneous" dielectric constant ϵ_{ea} by

$$P_e + P_a = \frac{\epsilon_{ea} - 1}{4\pi} E \quad \dots (3.101)$$

We may then write

$$\begin{aligned} P_{ds} &= P_s - (P_e + P_a) \\ &= \frac{\epsilon_s - \epsilon_{ea}}{4\pi} E \end{aligned} \quad \dots (3.102)$$

This yields

$$\frac{dP_d}{dt} = \frac{1}{\tau} \left(\frac{\epsilon_s - \epsilon_{ea}}{4\pi} \cdot E_0 e^{i\omega t} P_d \right) \quad \dots (3.103)$$

Solving this equation, we obtain

$$P_d(t) = C e^{-t/\tau} + \frac{1}{4\pi} \cdot \frac{\epsilon_s - \epsilon_{ea}}{1 + \omega\tau} \cdot E_0 e^{i\omega t} \quad \dots (3.104)$$

The total polarisation is now also a function of time and is given by $P_e + P_a + P_d(t)$.

Hence, for displacement one obtained

$$\begin{aligned}
 D(t) &= \epsilon^* E(t) \\
 &= E(t) + 4 \pi P(t) \quad \dots (3.105)
 \end{aligned}$$

From the last two equations and from the definition $\epsilon^* = \epsilon' - i\epsilon''$ the following expressions result :

$$\epsilon'(\omega) = \epsilon_{ea} + \frac{\epsilon_s - \epsilon_{ea}}{1 + \omega^2 \tau^2} \quad \dots (3.106)$$

$$\epsilon''(\omega) = (\epsilon_s - \epsilon_{ea}) \frac{\omega \tau}{1 + \omega^2 \tau^2} \quad \dots (3.107)$$

These equations are frequently referred to as the Debye equations.

When the dielectric polarisation is studied as a function at frequency, it is found that at low frequencies all the three polarisation contribution and ϵ' at such frequencies represent the static dielectric constant (Fig. 3.8). At higher frequencies, the orientation polarisation stops contributing the ϵ' and only contribution is from electronic and atomic polarisation. Above IR frequencies, even atomic polarisation stops contributing (Fig. 3.9).

3.15 DIFFERENT TYPE OF RELAXATION IN POLYMERS

In polymers normally two types of relaxations α and β are observed. The α -relaxation is due to the reorientation of the segmental groups and it takes place at temperatures around and above glass transition temperature (T_g) and is very much dependent on the intra and inter-molecular interactions. The β -relaxation is due to the micro-Brownian motion of the dipoles in the side groups attached to the main chain and it occurs at

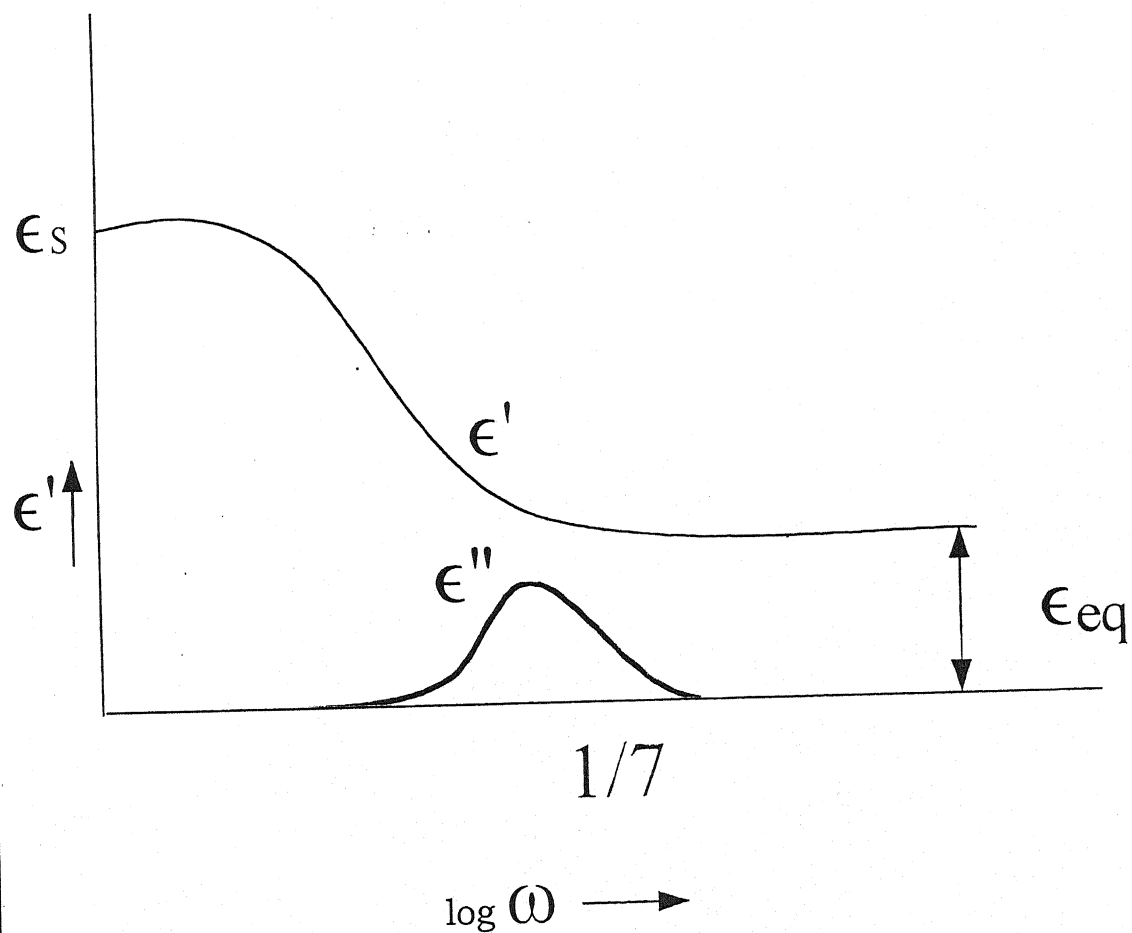
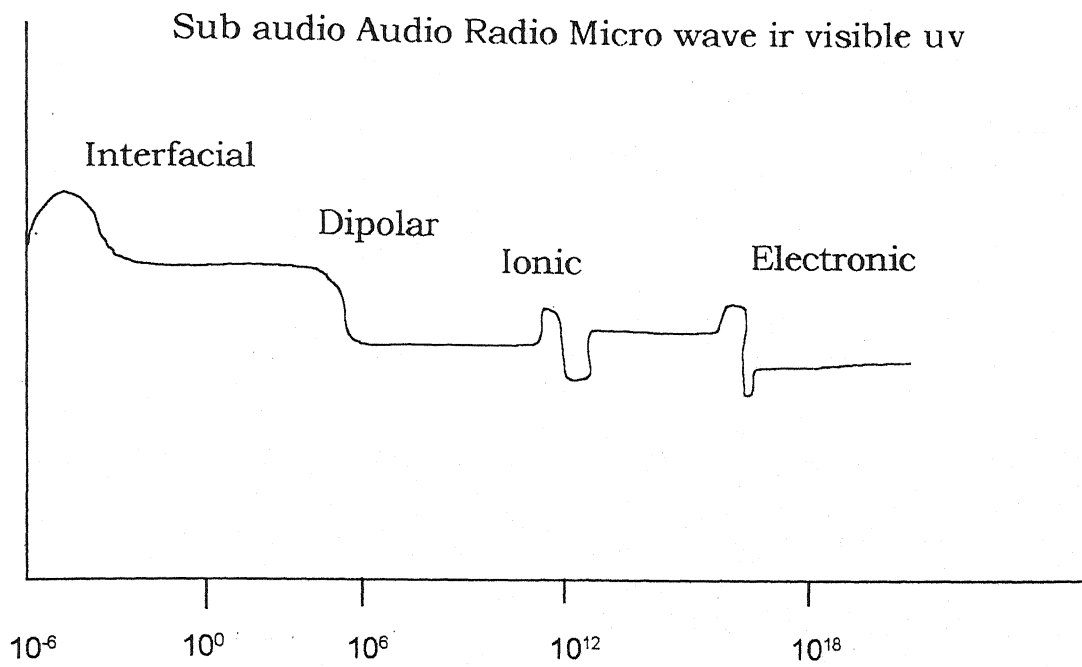
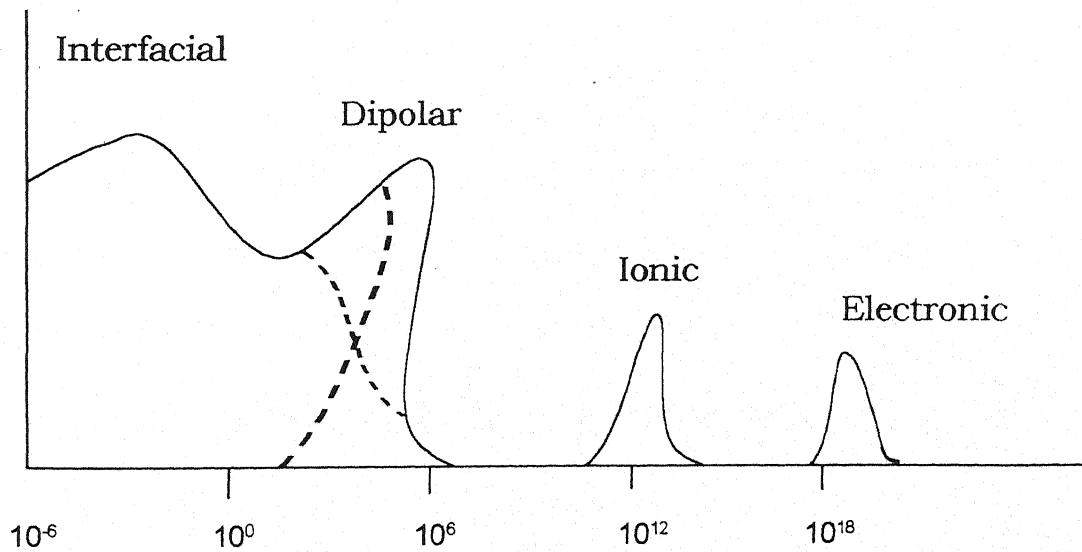


Fig. 3.8 : DEBYE CURVES FOR ϵ' AND ϵ'' AS FUNCTIONS OF FREQUENCY FOR A DIELECTRIC WITH A SINGLE RELAXATION TIME.



(a)



(b)

Fig. 3.9: (a) Variation of permittivity with frequency for simple dielectric

(b) Variation of loss tangent with frequency for simple dielectric.

temperatures below T_g . In polymers like poly(methyl methacrylate) (PMMA), both α and β relaxation coalesce to give single relaxation and is known as β -relaxation process [196].

3.16 FACTORS AFFECTING DIELECTRIC BEHAVIOUR OF POLYMERS

(a) Effects of Polar Groups :

The α -relaxation is basically dependent on the intra- and inter-molecular interactions. The greater the inter-molecular interaction the less mobile are the molecules and higher is the relaxation temperature at which loss maximum occurs and longer is the relaxation time. Exchange of non-polar substitutes increases dipole-dipole interaction.

(b) Effect of Substituents :

Introduction of very bulky substituents into the side chains or increasing the side chains decreases the mobility sharply. Introduction of chlorine considerably increases the magnitude of α -relaxation in poly(methyl α -chloroacrylate) but it has not altered β -relaxation [197].

(c) Effect of Side Group Isomerism :

The magnitude of α - and β -relaxations of isomers have been significantly different. For example, the magnitude of α -relaxation for poly(vinyl acetate) (PVAC) is much higher than that of poly(methyl acrylate) (PMA), whereas the magnitude of β -relaxation of PMA is seven times

higher than that of PVAc [198,199]. This arises because of the attachment of ester oxygen to the main chain in PVAc.

(d) Effect of Stereoregularity :

The dielectric properties of polymers are substantially dependent on the stereoregular nature of the polymer because the percentage, the length and quantitative proportion of syndiotactic and isotactic sections have a significant effect on the molecular mobility of polymers [200]. The molecular mobility of syndiotactic polymers is more restricted than of isotactic polymers [200,201].

(e) Effect of Plasticizers :

Dielectric relaxation of polymers shift towards lower temperature side on the addition of plasticizers. This is because plasticizers

- (i) increase molecular mobility
- (ii) increase free volume
- (iii) decrease T_g of the polymer

Effect of plasticizer on dielectric relaxation of polymers reveals that at low concentrations of plasticizers the loss peak occurs mainly from the motions of polymers segment as modified by the plasticizer molecules which are bound to the polymer molecules by the dipole-dipole interactions, till the critical composition is achieved. Beyond that the loss peak arises largely from the plasticizer molecules [200,202].

(f) Effect of copolymerization :

Dielectric properties of copolymers vary according to the constitution/composition and the ratio of the monomeric units [203-205].

(g) Effect of CrossLinking :

Cross-linking always decreases molecules mobility and increases temperature and relaxation time of α -process [200].

(h) Effect of Pressure :

Pressure influences the relaxation times of the process in which the inter-molecular interaction plays an important role. Thus, increasing the pressure results in the increase of α -relaxation process and that of β -process to a lesser degree [196].

3.17 PARAMETERS AFFECTING DIELECTRIC CONSTANT

(a) Temperature [206-229] :

According to the classical mechanics, the total molecular polarizability α is the sum of electronic polarizability α_e and polarizability arising due to molecular motion $P^2/3kT$ and is given by

$$\alpha = \alpha_e + \frac{P_{\text{perm}}^2}{3kT} \quad \dots (3.108)$$

where P_{perm} is the permanent dipole moment, k is Boltzman constant and T the absolute temperature. The dielectric constant of simple elemental dielectrics show relatively small temperature dependence since there occurs very small change in electronic structure. For ionic dielectrics, substantial increase in dielectric constant is brought about at high

temperature because of the loosening of the bonds which hold the ions in place.

Debye's equation relating the dielectric constant ϵ with structure and temperature of a substance is

$$\frac{\epsilon - 1}{\epsilon - 2} = \frac{4\pi N}{3} \left(\alpha_0 + \frac{\mu^2}{3kT} \right) \quad \dots (3.109)$$

where,

N = No. of molecules per c.c.

α_0 = Polarizability of the molecule

μ = Permanent electric dipole moment of the molecule.

This suggests that the dielectric constant of polar substance is temperature dependent and that of non-polar substances temperature independent.

(b) Frequency [230-241] :

One of the most striking features of the dielectric is the relationship between dielectric constant, dielectric losses and frequency. Each type of polarization has a particular frequency range at which it responds quickly. Only in this range they show proper variations in dielectric constants and losses.

When a dielectric is subjected to an alternating field, the polarization and displacement vectors vary periodically but due to absorption they lag

behind in phase with the applied field resulting in the complex form of dielectric constant. We know that

$$\tan \delta = \epsilon''/\epsilon' \quad \dots (3.110)$$

where δ is the phase angle between displacement and field. The energy dissipated in the dielectric in the form of heat is proportional to ϵ'' and, therefore, $\tan \delta$ is termed loss tangent and δ as loss angle.

In eqns. (3.96) and (3.97) If $\omega \ll 1/\tau$, then ϵ' approaches ϵ_s and $\omega \ll 1/\tau$ then ϵ' approaches ϵ_{ea} which follows that the dipoles are no longer able to follow the field. Thus, with increase in frequency the relaxation spectrum is characterised by a constant value followed by a slow fall of ϵ' to a low value and ϵ'' shows a broad peak.

(c) Field [242-248] :

An electric field orients the dipoles of the polar dielectric in all possible directions, parallel, antiparallel or others, depending upon the applied field strength. High dielectric constant and high dielectric losses appear when dipoles align parallel to the field. However, their perpendicular alignment with field produces almost no dielectric constant.

(d) Humidity :

Water molecules present inside the dielectric configuration increase the dielectric constant to a considerable amount [249]. Chatterjee [250] has done a detailed study on the variation of dielectric constant with varying amount of moisture in the ebonite and fibre specimens in frequency range

of 214 to 750 mc/s. Bhargava [233] has also reported increase in dielectric constant of polystyrene with humidity in low temperature region.

(e) Impurity :

Impurity in polymer produces changes in dielectric constant and dielectric losses of the polymer. Effect of chloronil on polystyrene is observed by Shrivastava and Kulshetra [251]. Relaxation behaviour of doped polycarbonate their film has been studied by Mahendru and Agarwal [252].

(f) Nature of the Polymer :

Polymer can be divided as polar and non-polar materials. For non-polar substances containing no ionic impurities, the measured loss factor is very small but it is not actually zero in the liquid state and rather it increases with frequency in micro wave region.

The dielectric constant exhibits a sharp drop when transition from liquid to the solid state occurs in the polar substances. Dielectric losses are also approximately zero for such non-rotating polar molecules.

/ ***** /

REFERENCES

1. Mott, N.F. and Davis, E.A., Electronic Processes in Non Crystalline Materials (Clarendon Press), Oxford (1971).
2. Hino, T., J. Appl. Phys., **46**, 1956 (1975).
3. Fischer, P. and Rohl, P., J. Polym. Sci. Polym. Phys. Ed., **14**, 531 (1976).
4. Gutman, F., Rev. Mod. Phys., **20**, 457 (1948).
5. Sawa, G., Kawade, M. and Ieda, M., J. Appl. Phys., **44**, 5397 (1973).
6. Chen, R., J. Appl. Phys., **47**, 2988 (1976).
7. Talwar, L.M. and Sharma, D.L., J. Electrostat., **9**, 49 (1980).
8. Shrivastava, S.K., Ranade, J.D. and Srivastava, A.P., Thin Solid Films, **67**, 201 (1980).
9. Turnhout, J. Van, "Thermally Stimulated Discharge of Polymer Electrets", Elsevier, Amsterdam, 1975.
10. Gupta, C.L. and Tyagi, R.C., Indian J. Pure Appl. Phys., **16**, 428 (1978).
11. Shrivastava, S.K., Ranade, J.D. and Srivastava, A.P., Phys. Lett. A., **65**, 465 (1979).
12. Jain, V.K., Gupta, C.L., Jain, R.K., Agarwal, S.K. and Tyagi, R.C., Thin Solid Films, **30**, 245 (1975).
13. Jain, V.K., Gupta, C.L., Jain, R.K. and Tyagi, R.C., Thin Solid Films, **48**, 175 (1978).
14. Mahendru, P.C. and Suresh Chand, J. Phys. D., **16**, L 185 (1983).

15. Shrivastava, S.K., Ranade, J.D. and Srivastava, A.P., Phys. Lett. A., **72**, 185 (1979).
16. Tiwari, A.R., Shrivastava, S.K., Saraf, R.K. and Srivastava, A.P., Thin Solid Films, **70**, 191 (1980).
17. Hino, T., Jpn. J. Appl. Phys., **12**, 611 (1973).
18. Vanderschueren, J. and Linkens, A., J. Polym. Sci. Polym. Phys., **16**, 223 (1978).
19. Sessler, G.M., Electrets, Springer Verlag (1980).
20. Garlick, C.F.J. and Gibson, A.F., Proc. Phys. Soc., **A60**, 574 (1948).
21. Berge, B., C.R. Acad. Sci. Paris, **B263**, 380 (1966).
22. Bucci, C., Fieschi, R. and Guidi, G., Phys. Rev., **148**, 816 (1966).
23. Both, A.M., Can. J. Chem., **32**, 214 (1954).
24. Bohun, W., Czech. J. Phys., **4**, 91 (1954).
25. Hoogenstraaten, W., Philips Res. Rep., **13**, 515 (1958).
26. Grossweiner, I., J. Appl. Phys., **14**, 1306 (1953).
27. Halperin, A. and Branes, A.A., Phys. Rev., **117**, 408 (1960).
28. Chen, R., J. Appl. Phys., **40**, 520 (1960).
29. Christodoulides, C., J. Phys. D., **18**, 1501 (1985).
30. Mazurin, O.V., J. Non Cryst. Solids, **25**, 130 (1977).
31. Stunzian, V. Biederman, J. Appl. Phys., **34(4)**, 430 (2000).
32. Vanderschuren, J. and Gariot, J., Thermally Stimulated Relaxation in Solids, Springer Verlag, Berlin (1979).
33. Singh, R. and Narula, A.K., J. Appl. Phys., **82**, 4362 (1997).

34. Singh, R., Narula, A.K., Tandon, R.P, Mansingh, A. and Chandra, S., Philos. Mag., **B75**, 419 (1997).
35. Schiveidler, E. Von, Ann. Physik., **LP3**, 24, 711 (1907).
36. Frankel, J., Z. Physik., **35**, 652 (1926).
37. Schottky, W. and Wagner, C., Z. Physik. Chem. B., **11**, 163 (1930).
38. Wagner, C., Z. Physik. Chem. B., **22**, 181 (1933).
39. Lamb, D.R., "Electrical Conduction Mechanism on Thin Insulating Films", Methuen, London, 1967.
40. Vermilyen, D.A., J. Electrochem. Soc., **102**, 655 (1955).
41. Stevels, J.M., "Encyclopedia of Physics", Springer, **30**, 352 (1963).
42. Simmons, J.G. in "Handbook of Thin Film Technology", Ed. I. I. Maissel and R. Glang, McGraw Hill, New York, 1970.
43. Simmons, J.G., J. App. Phys., **34**, 1793, 2581 (1963).
44. Meier, H. in "Topics in Current Chemistry", **61**, "Dyestuffs", Springer-Verlag, Berlin, 1976.
45. Mott, N.F., "Conduction in Non-Crystalline Materials", Clarendon, New York, 1987.
46. Mott,N.F., J. Non Cryst. Solids, **1**, 1 (1968).
47. Frankel, J., Tech. Phys., **5**, 685 (1938).
48. Frankel, J., Phys. Rev., **54**, 647 (1938).
49. Mead, C.A., Phys. Rev., **128**, 2088 (1962).
50. Mott, N.F. and Gurney, R.W., "Electronic Processes in Ionic Crystals", Oxford University Press, New York, 1940.

51. Lampert, M. and Mark, A., "Current Injection in Solids", Academic, New York, 1970.
52. Sessler, G.M., Electrets, Springer Verlag (1980).
53. Eley, D.D., J. Polym. Sci. C., **17**, 73 (1967).
54. Rosenberg, G., Bhowmik, B.B., Harder, H.C. and Postow, E., J. Chem. Phys., **49**, 4108 (1968).
55. Gelfman, A.Y. and Luzan, R.G., Dokl. Akad. Nauk. SSSR, **168**, 1371 (1966).
56. Wacławek, W. and Zabowski-Wacławek, M., Thin Solid Films, **146**, 1 (1987).
57. Sasabe, H. and Saito, S., J. Polym. Sci. A-2, **6**, 1401 (1968).
58. Andersen, T.W., Wood, D.W., Livingstone, R.C. and Eyring, H., J. Chem. Phys., **44**, 1259 (1966).
59. Samara, G.A. and Drickamer, H.G., J. Chem. Phys., **37**, 474 (1962).
60. Phol, H.A., Rembaum, A. and Henry, A., J. Am. Chem. Soc., **84**, 2699 (1962).
61. Crowley, J.R., Wallace, R.A. and Bube, R.H., J. Polym. Sci. Polym. Phys. Ed., **14**, 1769 (1976).
62. Labes, M.M., Pure Appl. Chem., **12**, 275 (1976).
63. Wallace, R.A., J. Appl. Polym. Sci., **18**, 2855 (1974).
64. Rosenberg, B., Nature, **193**, 364 (1964).
65. Epstein, A. and Wildi, J. Chem. Phys., **32**, 324 (1960).
66. Meier, H., Z. Electrochem., **59**, 1029 (1955).
67. Assor, I.M. and Harrison, S.E., J. Phys. Chem., **68**, 872 (1964).

68. Mylnikov, V.S., Dokl. Akad. Nauk. SSSR, **164**, 622 (1965).
69. Charlesby, A., "Atomic Radiation and Polymers", Pergamon, New York, 1960.
70. Chapiro, A., "Radiation Chemistry and Polymers Systems", Interscience, New York, 1962.
71. Makhlis, P.A., "Radiation Physics and Chemistry of Polymers", John Wiley, New York, 1975.
72. O'donnel, J.H. in "Polymer Science in the Next Decade : An International Symposium Honoring Herman, F. Mark on his 90th Birthday", Eds. O. Vogl and E.H. Immergut, John Wiley, New York, 1987, p. 203.
73. Hedvig, P., in "Radiation Chemistry of Macromolecules", **1**, Ed. M. Dole, Academic, New York, 1972, Chap. 8.
74. Antoun, S., Karasz, F.E. and Lenz, R.W., J. Polym Sci. Polym. Chem. Ed., **26**, 1809 (1988).
75. Seanor, D.A. (Ed.), Electrical Properties of Polymers, Academic Press, New York, 1982.
76. Eley, D.D. and Parfitt, G.D., Trans. Faraday Soc., 1529 (1955).
77. Wilk, M., Z. Elektrochem., **64**, 930 (1960).
78. Gooden, E.W., Australian J. Chem., **18**, 637 (1965).
79. Dulov, A.A., Russ. Chem. Rev., **35**, 773 (1966).
80. Hatano, M., Kambara, S. and Okamoto, S., J. Polym. Sci., **51**, 26 (1961).
81. Watson jun, W.M., McMordie jun, W.C. and Lands, L.Y., J. Polym. Sci., **55**, 137 (1961).

82. Sazhin, B.I. and Podosenova, N.G., Polym. Sci. USSR, **6**, 162 (1964).
83. Sazhin, B.I. and Podosenova, N.G., Sov. Phys. Solid State, **6**, 1755 (1965).
84. Khahilor, S.K. and Nurullaer, Y.G., "Neravnovesnye Protessy Tverdotelnykh Gazon. Plazmakh", Ed. B. M. Askerov, USSR, 1983, p.35.
85. Kolesov, S.N., Balaban, N.P. and Kildeep, I.A., Elektrichestvo, **4**, 83 (1972).
86. Chien, J.C.W., Warakowski, J.M., Karasz, F.E. and Schen, M.A., Macromolecules, **18**, 2380 (1985).
87. Gelfman, A., Bidnaya, D., Buravleva, M. and Luzan, R.O., Doklady Akad. Nauk. SSSR, **150**, 833 (1963).
88. Craig, D.P. and Fantoni Sarti, P., Chem. Commun., 742 (1966).
89. Amborski, L., J. Polym. Sci., **62**, 331 (1962).
90. Simon, J. and Andre, J.J., "Molecular Semiconductors", Springer-Verlag, Berlin, 1985.
91. Mortensen, K., Thewalt, L.W. and Tomkiewicz, Y., Phys. Rev. Lett., **45**, 490 (1980).
92. Deits, W., Cukor, P., Rubner, M. and Jopson, H., J. Electro. Mat., **10**, 683 (1981).
93. Nigrey, P.J., MacDiarmid, A.G. and Heeger, A.J., J. Chem. Soc. Chem. Commun., 594 (1979).
94. Druy, M.A., Rubner, M.F., Sichel, E.K., Tripathy, S.K., Emma, T. and Cukor, P., Mol. Cryst. Liq. Cryst., **105**, 109 (1984).

95. Ioffe, A.E., J. Phys. Chem. Solids, **8**, 6 (1959).
96. Eley, D.D., J. Polym. Sci., **17**, 73 (1967).
97. Inuishi, Y., IEEE Trans. Electr. Insul. E-1, **15**, 139 (1980).
98. Schottky, W., J. Physics, **15**, 872 (1914).
99. Simmon, J. G. Phys. Rev., **3**, 155 (1938).
100. Frankel, J. Phys. Rev., **54**, 647 (1938).
101. Jonscher, A.K., Thin Solid Films, **1**, 213 (1967).
102. Hill, R.M., Phil. Mag., **23**, 59 (1971).
103. Yeaigan, J.R. and Jayler, H.L., J. Appl. Phys., **39**, 5600 (1968).
104. Ghosh, S.K. and Kaveer, D.J., Polym. Sci. Polym. Phys., **10**, 2305 (1972).
105. Rose, A., Concepts in Photoconductivity and App. Problems (InterScience, New York), 70 (1963).
106. Lampert, M.A. and Mark, P., "Current Injection in Solids", Acad. Press, London (1970).
107. Cole, K.S. and Cole, R.H., J. Chem. Phys., **10**, 98 (1942).
108. Tredgold, R.H., Space Charge Conduction in Solids, Elsevier Pub. Co., New York (1966).
109. Mar, P. and Helfrich, W., J. Appl. Phys., **33**, 205 (1962).
110. Eley, D.D. and Newmann, Trans. Faraday Soc., **66**, 1106 (1970).
111. Croanacher, I., Solid State Commun., **2**, 365 (1964).
112. Adolf, J. *et al.*, Phys. Rev. Lett., **1**, 36 (1963).

113. Grum, N.G.M.C., Read, B.E. and Williams, G., An Elastic and Dielectric Effects in Polymeric Solids, Willey London (1967).
114. Block, H. and North, A.M., Advan. Mol. Relaxation Processes, **1**, 300 (1970).
115. Symth, C.P., "Dielectric Behaviour and Structure", McGraw Hill Pub., N.Y. (1955).
116. Symth, C.P. in "Physics and Chemistry of the Organic Solid State", Eds. D. Fox *et al.*, Interscience Pub., N.Y., **1**, Chapt. 12 (1963).
117. Hara, T. and Okamoto, S., J. Phys. Soc., Japan, **20**, 7, 1291 (1965).
118. Jaffrin, M., J. Chim. Phys. (France) **63**, 1, 77 (1966).
119. Saiki, K. and Okamoto, Y., Jap. J. Appl. Phys., **5**, 10, 962 (1966).
120. Rao, K.S.R., Ind. J. Pure Appl. Phys., **4**, 12, 447 (1966).
121. Rao, K.S.R., Ind. J. Pure Appl. Phys., **5**, 8, 353 (1967); **4**, 447 (1966).
122. Hara, T., Jap. J. Appl. Phys. **6**, 2, 135 (1967).
123. Hippel, A. Von, "Dielectric Materials and Applications", John Wiley and Sons (1964).
124. McCrum, N.G., Read, B.E. and Willami, G., "An Elastic and Dielectric Effects in Polymer Solids", John Willey & Sons, N.Y. (1967).
125. Ishida, Y., J. Polym. Sci. Part A-2 (7) L 1835, (1969).
126. Philips, W.A., Proc. Roy. Soc. A (G.B.), **319**, 565 (1978).
127. Barkley, M. and Zimm, B., Ann. Chem. Soc. Polym. Prep., **9**, 317 (1968).

128. Broadhurst, M.G., Ann. Rep. Cont. Electrical Insul. and Dielectric Phenomena, Nat. A. Cad. Sci., Washington, (1970), p. 48.
129. Patrosian, V.P., Vysokomot Socdin, **13**, 761 (1971).
130. Cook, M., Wats, C.D. and Williams, G., Trans. Faraday Soc., **67**, 2503 (1971).
131. Pollak, M., J. Chem. Phys., **43**, 908 (1965).
132. Ishida, Y., Kogyokugaku Zasshi, **73**, 1318 (1970).
133. Uembra, S., J. Polym. Sci., Polym. Phys., **12**, 1177 (1974).
134. Ikado, E. and Watande, J., J. Polym. Sci. Polym., **11**, 1503 (1973).
135. Link, G.L., J. Electro Chem. Soc., **120C**, 84 (1973).
136. Jonscher, A.K., Physics of Thin Films, Vol. 11, The Universal Dielectric Resonance (Chelesa Dielectic Group) : Academic Press, 205 (1980).
137. Budenstein, P.P. (Ed.), Digest of Literature on Dielectric, 36 (1972).
138. Parkel, T.G. in Polymer Sci. Vol. II, Ed. A.D. Jenkins, North Holland Pub. Co.
139. Jonscher, A.K. (R. Holloway and Bedford New Coll., Egham, UK), IEEE Electr. Insul. Mag. (USA), Vol.6, No.2, pp. 16-22 (March-April, 1990).
140. Bohmer, R., J. Chem. Phys. (USA), **91**, No. 5, 3111 (1989).
141. Gupta, M., J.P.S., J. Mol. Liq. (Netherlands), **44**, No.1, 9 (1989).
142. Sharma, G.L. and Gandhi, J.M., J. Mol. Liq. (Netherlands), **44**, No.1, 17 (1989).
143. Murthy, S.S.N., J. Chem. Phys. (USA), **92**, No. 4, 2684 (1990).

144. Uvarov, N.F. and Hairetdinov, E.F., Proc. Indian Natl. Sci. Acad. A. (India), **55**, No. 5, 709 (1989).
145. Hara, T., Nozaki, M. and Okamoto, S., Jap. J. Appl. Phys., **6**, 9, 1138 (1967).
146. Fuoss, R.M., J. Am. Chem. Soc., **59**, 1703 (1937); **60**, 451 (1936); Ann. N. Y. Acad. Sci., **40**, 429 (1940).
147. Schollosser, E. and Horn, G., Exper. Tech. der Phys. (Ger.), **11**, 2, 145 (1963).
148. Schollosser, E. and Horn, G., Deutschen Akad. Wiss., Berlin (Ger.), **5**, 1, 57 (1963).
149. Heijboer, J., British Polymer, **1**, 3 (1969).
150. Bahri, R. and Singhi, H.P., Thin Solid Films, **62**, 291 (1979).
151. Uemura, S., J. Polym. Sci. Polym. Phys., **12**, 1177 (1974).
152. Cummins, S.E. and Cross, L.E., Appl. Phys. Lett., **10**, 14 (1967).
153. Cummins, S.E. and Cross, L.E., J. Appl. Phys., **30**, 2268 (1968).
154. Cross, L.E. and Pohanka, R.C., J. Appl. Phys., **39**, 3992 (1968).
155. Pulvari, C.F., Proc. Intern. Mtg. Ferroelectricity, **1**, 347 (1966).
156. Krajnik, N.N., Mylnikova, I.E. and Kolesnicenko, S.F., Fiz. Tverd. Tela, **10**, 260 (1968).
157. Seitz, M.A. and Holliday, T.B., J. Electro. Chem. Soc., **121**, 163 (1974).
158. Seitz, M.A. and Holliday, T.B., J. Electro. Chem. Soc., **121**, 122 (1974).
159. Jonscher, A.K., Philos. Mag. (Part) **B38**, 587 (1978).

160. Gupta, A.K. and Singhai, P., J. Appl. Polym. Sci., **26**, 3599 (1981).
161. Debye, P., Polar Molecules, Fever Publications, London (1945).
162. Frohlich, H., "Theory of Dielectrics", Oxford University Press, London (1958).
163. Hedvig, C.D., "Dielectric Spectroscopy of Polymers", Adam Hilger, Bristol (1977).
164. Jang, Y.T. and Philips, P.J., Journal of Applied Polymers Science, **28**, 1137 (1983).
165. Williams, G. and Watts, D.C., "Dielectric Properties of Polymers", Ed. F.E. Karasz, Plenum Press, New York (1971).
166. Yoshisa Miyamoto, Polymer, **25**, 63, January (1984).
167. Pillai, P.K.C., Narula, G.K. and Tripathi, A.K., Jap. J. Appl. Phys., **23(9)**, 1251 (1984).
168. Natrajan, R. and Dube, D.C., Ind. J. Pure Appl. Phys., **19**, 675 (1981).
169. Mahendru, P.C., Agarwal, J.P., Jain, K. and Jain, P .C., Ind. J. Pure Appl. Phys., **19**, 217 (1981).
170. Das, D.K. and Doughty, K., Ferroelectrics, **28**, 307 (1980).
171. Perlman, M.M. and Unger, S., J. Appl. Phys., **45(6)**, (1974).
172. Ngai, K.L. and Rendell, R.W., Phys. Rev. B. Condens. Mat. (USA), **41**, No. 1, 754 (1990).
173. Kawamura, Y., Nagai, S., Hirose, J. and Wada, Y., J. Polym. Sci. Pt. A-2, Polym. Phys., **7**, 1559 (1969).

174. Knizhnik, E.I. and Mamchich, C.D., *Vysokomolek Soed.*, **11**, 1665 (1969) (in Russian).
175. Sasabe, H., Saito, S., Asahina, M. and Kakutani, H., *J. Polym. Sci. Pt. A-Z, Polym. Phys.*, **7**, 1405 (1969).
176. Kakutani, H. and Asahina, M., *J. Polym. Sci. Pt. A-2, Polym. Phys.*, **7**, 1473 (1963).
177. Link, I.G.L., *Dielectric Properties of Polymers*, Vol.2, North Holland Publ. Co., Amsterdam (1972).
178. Ashcraft, C.R. and Boyd, R.H., *J. Polym. Sci. Polym. Phys. Ed.*, **14**, 2153 (1976).
179. Pochan, J.M. and Hinan, D.F., *J. Polym. Sci. Polym. Phys. Ed.*, **14**, 2285 (1978).
180. Kosaki, M. and Ieda, M., *J. Phys. Soc., Japan*, **27**, 1604 (1969).
181. Kawamura, Y., Nagai, S., Hirose, J. and Wada, Y., *J. Polym. Sci. Pt. A-Z Polym. Phys.*, **7**, 1559 (1969).
182. Pochan, J.M. and Hinman, D.F., *J. Polym. Sci. Polym. Phys. Ed.*, **14**, 2285 (1976).
183. Ifo, M., Nakafani, S., Gokan, A. and Tanaka, K., *J. Polym. Sci. Polym. Phys. Ed.*, **15**, 605 (1977).
184. Kulshrestha, Y.K. and Shrivastava, A.P., *Thin Solid Films*, **71** (1980).
185. Shrivastava, S.K., Ranade, J.D. and Shrivastava, A.P., *Ind. J. Pure Appl. Phys.*, **19**, 953 (1981).
186. Yamafuji, K., *J. Phys. Soc., Japan*, **15**, 2295 (1960).
187. Tripathi, A., Tripathi, A.K. and Pillai, P.K.C., *J. Mater. Sci. Lett. (U.K.)*, **9**, No. 4, 443 (1990).

188. Aliev, A.E., Akramor, A.Sh. and Tashmukhamedova, N.Kh., Sov. Phys. - Solid State (USA), **31**, No. 2, 328 (1989); Translation of Fiz. Tverd. Tela (USSR), **31**, No. 2, 263 (1989).
189. Ravez, J., Simon, A., Bonnet, J.P. , Denage, C. and Miane, J.L., J. Phys. Chem. Solids (UK), **50**, No. 10, 1041 (1989) (In French).
190. Choudhary, B.K., Choudhary, R.N.P. and Rao, K.V., Phys. Status Solidi A (East Germany), **115**, No. 1, 301 (1989).
191. Lopathi, V.V. and Kabyshev, A.V., Phys. Status Solidi A (East Germany), **116**, No. 1, 221 (1989).
192. Prasad, C.D., Tewari, H.S., Kumar, D. and Prakash, O., Bull. Mater. Sci. (India), **11**, No. 4, 307 (1988).
193. Dharamprakash, S.M. and Mohan Rao, P., J. Mater. Sci. Lett. (UK), **8**, No. 10, 1167 (1989).
194. Dekkar, A.J., "Solid State Physics", Macmillan (1970).
195. Kubo, R. and Nagamiya, T., Solid State Physics, McGraw Hill (1969).
196. Sasape, H. and Saito, S., J. Polym. Sci. Pt. A-Z, **6**, 1401 (1968).
197. Mikhailov, G.P., Borisova, T.I. and Druitrochenko, D.A., J. Tech. Phys. (USSR), **26**, 1924 (1956).
198. Mikhailov, G.P., J. Tech. Phys. (USSR), **21**, 1365 (1951).
199. Ishida, Y., Kolloid Z., **174**, 124 (1961).
200. McCrum, N.G., Read, B.E. and Williams, G., "An Elastic and Dielectric Effects in Polymeric Solids", John Wiley and Sons, London (1967).
201. Mikhailov, G.P. and Borisova, T.I., Polym. Sci. USSR, **2**, 387 (1961).

202. Tager, A., Physical Chemistry of Polymer, Mir Publications, Moscow (1978).
203. North, A.M., Pethrick, R.A. and Wilson, A.D., Polymer, **19**, 913 (1978).
204. Gupta, A.K., Chand, N., Singh, R. and Singh Man, A., Eur. Polym. J., **15**, 129 (1979).
205. Gupta, A.K., Singhal, R.P., Bajaj, P. and Agarwal, V.K., J. Appl. Polym. Sci., **28**, 1167 (1983).
206. Sawaguchi, E. *et al.*, J. Phys. Soc. Japan, **17**, 1666 (1962).
207. Beam, W.R., "Electronics of Solids", McGraw Hill Book Co., N.Y., 386 (1965).
208. Panchenko, V.V., Fiz. Tverd Tela, **6(2)**, 584 (1964).
209. Havinga, E.E., J. Phys. Chem. Sol., **8**, 253 (1961).
210. Boseman, A. and Havinga, E.E., Phys. Rev. Letts., **10**, 29 (1963).
211. Debye, P., "Polar Molecules", Chemical Catalogue Co., N.Y. (1929).
212. Symth, C.P. and Norgan, S.O., J. Am. Chem. Soc., **50**, 1547 (1928).
213. Reddish, W., J. Poly Sci. Pt. C, **14**, 123 (1966).
214. Symth, C.P. and Hitchcock, C.H., J. Am. Chem. Soc., **55**, 1030 (1933).
215. Dornte, R.W. and Symth, C.P., J. Am. Chem. Soc., **52**, 3546 (1930).
216. Hara, T. and Okamoto, S., J. Phys. Soc. Japan, **20**, 1291 (1965).
217. Hersping, A., Angew Z., Phys. (Germany), **20**, 369 (1966).
218. Brosowski, G., Luther, G. and Muser, H.E., Phys. Status Solidi (A), **14**, 15 (1972).

219. Deyour, J. *et al.*, Acad. Sci. B. (France), **276**, 111 (1973).
220. Havinga, E.E., J. Phys. Chem. Sol., **18**, 253 (1961).
221. Tareev, B., "Physics of Dielectric Materials", Mir Publishers, Moscow (1975).
222. Talwar, I.M., Shina, H.C. and Shrivastava, A.P., J. Mat. Sci. Lett., **4**, 448 (1985).
223. Idem, Thin Solid Films, **113**, 331 (1984).
224. Polizko, S. and Hoffman, G., J. Appl. Polym. Sci., **30**, 799 (1985).
225. Pox, T.G. and Flory, P.J., J. Amer. Chem. Soc., **70**, 2384 (1950).
226. Roberts, G.E. and White, E.F.T., "The Physics at Glassy Polymers", Ed. R.M.Haward, London (1973).
227. Turnhout, Van J., "Thermally Stimulated Discharge of Polymer Electrets", Elsevier, Amsterdam (1974).
228. Turnhout, Van J., "Topics in Applied Physics Electrets", Ed. G.M. Sessler, Springer-Verlag, N.Y. (1980).
229. Amitin, E.B., Bessergenv, V.G., Varchenko, A.A., Ilyasov, S.S. and Yudanov, N.F., Phys. Scr. (Sweden), **40**, No. 6, 759 (1989).
230. Von Hippel, A.R., "Tables of Dielectric Materials", Massachussetts, Institute Technology, Vol.I, 1944; Vol. II, 1945, Vol. III, 1948; Vol. IV, 1953 and in "Dielectric Materials and Applications", Ed. Technology Press of N.I.I. and John Wiley, New York (1954).
231. Agarwal, D.P., Ph.D. Thesis, University of Sagar (India), 1974.
232. Pateria, A.P., Ph.D. Thesis, University of Sagar (India), 1975.
233. Bhargava, B., Ph.D. Thesis, University of Sagar, 1976.

234. Shrivastava, S.K., Ph.D. Thesis, University of Saugor (India), 1980.
235. Tiwari, A.R., Ph.D. Thesis, University of Sagar (India), 1983.
236. Sharma, A.D., Ph.D. Thesis, I.I.T., New Delhi (India), 1981.
237. Cole, K.S. and Cole, R.H., J. Chem. Phys., **18**, 1417 (1951).
238. Rastogi, A.C., Ph.D. Thesis, I.I.T., New Delhi, 1975.
239. Jenkins, A.D., "Polymer Science, Vol. 2, North-Holland Publishing Company, Amsterdam, London (1972).
240. Purohit, H.D., Lunker, H.C. and Sengwa, R.J., Ind. J. Pure Appl. Phys. (India), **27**, No. 6, 296 (1989).
241. Dube, D.C., Mathur, S.C., Jang, S.J. and Bhalla, A.S., Mater. Lett. (Netherlands), **8**, No. 11-12, 451 (1989).
242. Chatterji, S.D. and Bhandra, T.C., Phys. Rev., **98**, 1728 (1955).
243. Bhandra, T.C., Ind. J. Phys., **32**, 281 (1956).
244. McMohan, W., J. Am. Chem. Soc., **78**, 14, 3290 (1956).
245. Elgard, A.M., Fiz. Tverd. Tela, **4**, 1320 (1962).
246. Robert, S., Phys. Rev., **71**, 890 (1947).
247. Lal, H.B., Ind. J. Pure Appl. Phys., **7**, 5, 370 (1969).
248. Agarwal, S.R., Ph.D. Thesis, University of Sagar (India), 1975.
249. Kittel, C., Introduction to Solid State Physics, 2nd Ed., John Wiley and Sons, N.Y. (1956).
250. Chatterjee, S.K., Ind. J. Phys., **22**, 259 (1948).
251. Kulshrestha, Y.K. and Shrivastava, A.P., Thin Solid Films, **71**, 41 (1980).
252. Mahendru, P.C., Agarwal, J.P. and Jain, K., Thin Solid Films, **78**, 251 (1981).

CHAPTER IV

**THERMALLY STIMULATED
DISCHARGE CURRENT
STUDY**

4.1 INTRODUCTION

In order to qualify for scientific recognition, a material has to have a reasonably well-defined chemical composition (even unknown) and possess physical characteristics. Of all the solids scientifically identifiable in this sense, it is doubtful whether anyone is truly amorphous. Even in a highly disordered material, the immediate environment of any given type of atom will not vary a great deal from one site to another. One might follow Mott and Davis and define an amorphous solid as one in which three dimensional periodicity is absent. However, a departure from perfect periodicity is induced by crystal surfaces, thermal vibrations and chemical impurities at low concentration - none of which features one would normally consider productive of an amorphous solid. Accordingly, one should use the more correct definition of structural disorder in the high-density limit. This definition does not, of course, imply anything about the density of the material itself, but serves to distinguish this type of disorder from dislocations, isolated voids and other structural imperfections present in relatively low concentrations. Materials that can be made in relatively stable amorphous phases are termed glasses.

Polymer glasses, in which the intramolecular bonding is covalent and the intermolecular forces are of Vander Waals type or hydrogen - bond type, constitute an important field of study. The characteristic features of these solids are largely due to extra rotational degrees-of-freedom compared with the other solid types.

From the view point of physical kinetics, the glassy state of polymers can be interpreted as a state in which segmental mobility is frozen. If the temperature of a polymer in the rubbery state is lowered, then the equilibrium state corresponding to the new temperature will set in only after a certain finite time which in the first approximation can be considered as the structure relaxation time. The structure relaxation time will grow with decreasing temperature, and at a sufficiently low temperature it will become so great that the equilibrium state of the polymer and the structure corresponding to it will practically never be reached. It is this state that is called the glassy state. Thus, the glassy state is a state of relative equilibrium, i.e., a metastable state [1]. A feature of this state, however, consists in that a polymer may remain in it for a very long time, which is practically unlimited. Such a long existence of polymer in a state of relative equilibrium is apparently due to the presence in them of sufficiently stable supermolecular formations. Different theories exist on the glass-transition of polymers [2].

A well known work of Gibbs and Marzio [3] is devoted to the nature of polymer glass transition. Different aspects of this work were discussed in detail by Staverman [4], Eisenberg and Saito [5], Shen and Eisenberg [2] and Moacanin and Simha [6]. Gibbs and Marzio [3] showed that the transition to the glassy state is characterized by two very important factors which determine many physical properties of polymer in this state. The first one is the change in the flexibility of the polymer chains in the glass

transition, and the second one is the change in the energy of intermolecular interaction. The concept of the glass transition temperature of polymers was introduced by Lieberreiter [7]. By the glass transition temperature is meant the temperature at which the viscosity of a polymer is 10^{13} Poise [4]. On the other hand, it is interpreted as the temperature below which segmental motion of the polymer molecules is frozen.

Polyvinylidene fluoride (PVDF) has been chosen for the present work due to its excellent thermal and electrical properties. It offers good opportunities for practical applications in different devices. Its bulk structure is relatively well known. Clusters [8-10] are the regions (domains) that have a denser packing of the molecules (or their parts) and a more ordered arrangement of them in comparison with the main, looser and disordered mass of a substance. It is natural that the density of a cluster should be somewhat greater than the average density of a substance. At the same time clusters are less ordered and less densely packed domains than crystallites.

It has been observed that energy of several photons is stored at an active centre comprising an uniquely situated impurity molecules through mechanism of energy transfer between molecules of host material. This is what happens when solar energy is put to use for synthesis in nature's laboratory. If it is possible to prepare a rigid matrix and embed impurity molecules in it, then conditions for putting solar energy for useful purpose

could be found. Rigid matrix will prevent molecules from losing energy in radiationless transitions. It has been seen that many organic molecules when illuminated in a rigid environment such as a frozen glassy solvent give rise to long lived emission or after glow. Such rigid glasses can be made by dispersing organic compounds in polymeric matrix.

Heaviside [11] first used the term 'electret'. Around 1890 he wrote, "the study of electrification is in some respects more important than of magnetization, on account of its greater generality it is more instructive". Thirty years later Eguchi [12] succeeded in producing bodies with electrical properties analogous to properties of permanent magnets. Gemant [13] repeated, confirmed and extended Eguchi's results. But the strange behaviour of electrets revealed by the early experiments, reinforced by Gemant's view that for theoretical reasons 'they should not exist', did much to shroud the electret effect in mystery. It took much fundamental research to establish the basic facts and to show that the electret effect, far from being an anomaly, is a general property of solid dielectrics, varying in degree rather than in nature. Technical developments have now led to practical applications [14-17].

The electret is, in effect, an insulator which will store charge over an extended period of time, where applications are concerned, the electret has useable external electric field. The greatest interest lies in the polymer film electrets. Many proposals have been made for the use of electrets in

electrostatic measuring instruments, electrostatic voltage generators, piezoelectric devices, air filters, radiation dosimeters and electrophotography. Its use in microphones is world known. Attempts have been made to use electrified polymer as blood compatible materials in prosthetic devices. The blood components which are likely to cause clotting in contact with the plastic tubing used to replace arteries, in particular, the platelets, are negatively charged. For platelets charge densities of about 5×10^{12} electronic charges cm^{-2} have been reported; similar values can be obtained with electrets. A negative surface charge of the inner walls of the tubes which are used as inserts and are in contact with the blood flow should prevent or atleast reduce platelet deposition and thus help to prevent clotting. Experiments *in vitro* have been inconclusive; but *in vivo* experiments have given encouraging results [18]. Thus, a wide and rewarding area of research is available.

Thermally stimulated discharge current (TSDC) technique is generally considered as particularly well suited for the study of dielectric relaxations [19-21]. This is mainly because the technique is characterized by a very low equivalent frequency (10^{-2} to 10^{-4} Hz) as compared to the dielectric loss method (1 to 10^{12} Hz). and consequently leads to a better resolution of the different relaxation processes [22-26]. As a matter of fact, the α and β -relaxations arising from the conformational motions of main chain or side groups respectively are more or less superimposed at the common measurement frequencies of few Hz. and thus the values of the

characteristic parameters determined from the loss curves are often the hybrid values [27]. Much uncertainty results from this and there are numerous discussions concerning the detailed mechanism of the motions involved [27,28], the discrete or continuous nature of the possibly associated distribution of relaxation times [21,23] and also physical significance of such a distribution [28], because of above problems in view, the thermally stimulated current (TSC) method appears very useful owing to its exceptional ability to resolve multicomponent peaks by techniques such as thermal cleaning or fractional polarization [20,29]. TSC is an electrical spectroscopy and have practical application to electrical quality control. It elucidates decay mechanisms and charging processes. It throws light on conduction properties of dielectrics. Air gap TSC can be utilized to study the decay of electrostatically charged polymers about the decay of which little is known.

Charging of polymers can be achieved with a variety of methods. Among these are thermal procedures [30-33] using simultaneous application of heat and an electric field, Corona and Townsend discharge methods [34-36], electron bombardment using penetrating beams (range of the electrons greater than the thickness of the polymer), as well as nonpenetrating beams [37-39] and γ -irradiation [40].

Phenomenological theories of the thermoelectret states, based on the two-charge theory, have been reported [41-43]. It seems that the

behaviour of the two-charges - a hetero-charge and a homo-charge depend on the kind of the polymer used. Bucci and Fieschi [44] have proposed an ionic thermal current method. Perlman and Creswell [45,46], Turnhout [21] and others [47] have used this method for analysing the electret effect qualitatively which has been generalized by Gross [48], Perlman and Crewwell [45,46] and others.

In recent years, a good amount of work on TSC studies of polymers [49-57] has appeared in literature covering both polar and nonpolar materials. The occurrence of TSC-spectra and of isothermal currents have been generally interpreted in terms of either detrapping of electronic charge carriers or in terms of dipolar processes, i.e. an orientation of permanent dipoles or annihilation of dipoles due to ionic motion. Ong and Turnhout [32] have concluded in favour of the existence of dipolar processes having a continuous distribution of relaxation times. Similar conclusions have been inferred by Fischer and Bohl [58,59] and Hino [60]. Chaitan *et al.* [61], however, have found that the low temperature peak could generally be decomposed in several discrete Debye processes. Perlman [62] has classified different trapping levels in polymers as primary, secondary and tertiary on the basis of degree of discharging, electron affinity and unique crystalline-amorphous structure of them.

Various factors affect TSC spectra. It has been shown by theoretical argument [63] and by experiments [64] also that only in the case of a first

order kinetics of polarization do the TSD peak occur invariably at a fixed temperature. Otherwise their position shifts in a characteristic way with changing initial polarization. In the case of space charge release, for example, the peak temperature increases with polarizing temperature and time. Thus, peak position data for varying polarizing conditions allows one to decide in particular whether a peak is due to a first order depolarization process, e.g. complex reorientation or to the release of a space charge. Heating rate affects the height and the position of the thermograms. Dipolar peaks are not influenced by the choice of electrode material but the space charge peaks get modified due to the different charge exchange rate at the metal-polymer interface.

Comparatively few reports [65-67] exist on TSC-studies of PS films that too emphasising particularly low temperature relaxations. This chapter comprises of a detailed study of TSD-currents in solution grown PVDF films as a function of polarizing field and temperature. It also reports the effect of electrode material on TSC-spectra of PVDF films.

Many kinds of polymer films [68-79] polarized in a high d.c. field at an elevated temperature and cooled in that field, have semi-permanent charges which exist for many years at room temperature. Depolarization currents at room temperature are frequently too small to be easily measured. To increase them one must speed up the depolarization process by heating the electret up to or above the polarization temperature.

The ensuing current has been called thermally stimulated current (TSC) since it is produced by heating without an external voltage [80]. TSC is now generally considered as particularly well suited to the study of dielectric relaxations [81,82]. This is mainly because this technique is characterised by a very low equivalent frequency as compared to the dielectric loss method and consequently leads to a better resolution of the different relaxation processes [83].

As a matter of fact, the α , β -relaxations arising from the conformational motions of main chain segments and from the local motions of main chain or side groups respectively are more or less superimposed at the common measurement frequencies of a hertz and thus the values of the characteristic parameters determined from the loss curves are often hybrid values [84]. Much uncertainty results from this, and numerous discussions are found in the literature especially concerning the detailed mechanism of the motions involved [85,86], the discrete or continuous nature of the possibly associated distribution of relaxation times [82] and the physical significance of such a distribution [86]. With these latest problems in view, the TSC technique appears also very useful, owing to its exceptional ability for resolving multicomponent peaks by techniques such as thermal cleaning or partial polarization [87].

A wide literature [88-99] is available on TSC in polymers. The technique has been widely used in the study of trapping parameters in

luminescent and photo-conducting materials. Lilly *et al.* [100] investigated TSC in mylar and teflon. Stupp and Carr [101] suggested an ionic origin for high temperature discharge currents in poly acrylic nitrile. Guillet and Seytre [102] conducted a detailed study of the complex relaxation modes observed in poly-L-proline. Takeda and Naito [103] studied temperature change of dielectric constant of polystyrene using TSC measurement. TSC in corona charged polymers have been investigated by Perlman [93] and those in electron beam irradiated. Polymers have been investigated by Sessler [104]. Ong and Turhnout [81] have concluded in favour of the existence of a continuous distribution of relaxation times. Recently, similar conclusions have been inferred by Fischer and Rohl [105] and Hino [106] from studies on secondary peaks of polyethylene and polyethylene terephthalate respectively. Chaïtan *et al.* [89], however, have found in polyamides that the low temperature peaks could generally be decomposed in several discrete Debye processes.

It has been shown by theoretical argument and by experiment [107] that only in the case of a first order kinetics polarization do the TSC peaks occur invariably at a fixed temperature. Otherwise their position is shifting in a characteristic way with changing initial polarization. In the case of a space charge release, for example, the maximum temperature is increasing with polarization temperature and polarizing time. Thus, peak position data for varying polarization conditions allow one to decide in particular whether

a peak is due to a first order depolarization process, e.g. complex reorientation or to the release of a space charge.

TSC of polar materials [108] shows several bands or peaks. This indicates that the depolarization is realized by several different processes. Two such processes are well known, the relaxation of aligned dipoles and the relaxation of a space charge caused by mobile carriers accumulated at the electrodes. But there are still other processes which cause TSC peaks and have not yet been identified. It is one of the fundamental problems of any TSC investigation to relate the observed peaks to specific depolarization processes. TSC peak may be characterized by the maximum positions, the magnitude of the peak and the slope of initial rise of the peak. The magnitude of the peak is eventually a measure of the number of defects causing the polarization. The determination of activation is a delicate task if the peaks overlap too much, possibly no meaningful value can be obtained at all. Dependence of peak position on initial polarization provides information on the depolarization processes.

TSC spectra are unique to the material under study. They are fingerprints of them and are sensitive to impurities, additives, discharges, humidity, i.e. to any chemical or morphological change. They provide a sensitive analytical tool that could be used to guide the production of materials with fixed electrical properties. TSC is an electrical spectroscopy and have practical application to electrical quality control. Recently, several

workers [109,110] have used TSC technique to investigate changes produced in polymers due to doping of them with suitable impurities. Gupta and Tyagi [109] doped polyvinyl fluoride with rhodamine, alizarine, dichlorofluorescein and iodine and utilized TSC to find out the changes produced by doping. Srivastava *et al.* have reported relaxation parameters by doping polystyrene with copper-phthalocyanine, ferrocene, anthracene, pyrene, iodine and chloranil [110].

Mahendru *et al.* [111] have reported TSC in PVAc films. They observed three TSC peaks at 53, 116 and 195°C and studied the effect of film thickness on TSC spectra of PVAc. 53°C peak was found to grow slightly with thickness. The magnitude of 116°C peak was observed to increase with film thickness and 195°C remain uninfluenced with the thickness. Total charge under all the three peaks grew linearly with the film thickness which led them to conclude uniform volume polarization in PVAc. Effect of iodine doping on TSC spectra of PVAc has been considered by Mahendru *et al.* [112].

4.2 POLING OF THE FILM

A time-temperature and time-field scheme [] for polarization and observation of TSC from the polymer film is shown in Fig. 4.2. The sample was heated to an elevated temperature (T_p) usually $< T_g$, by which permanent dipoles and free charges were mobilized. When the constant temperature was achieved, say at time t_1 , the static electric field (E_p) was

applied from a regulated power supply (ECIL, India) which causes an alignment of the permanent dipoles and a drift of free charges towards the electrodes. After certain time, say at t_2 , while the poling field (E_p) is still on, the charge sample was cooled down to room temperature (T_r) upto time, t_3 by which most of the permanent dipoles and charges were frozen-in and main chains of the polymer were immobilized. After switching off the field (E_p) at time t_3 , most of the charge stored at T_p was retained. Thus, the charging process was completed in time, t_p which was from time t_1 to t_3 . In order to eliminate the accumulated electric charges caused by the applied field during polarization, the electrodes were short-circuited for an arbitrary time from t_3 to t_4 before the start of heating.

The TSD technique because of its high sensitivity and high resolving power has become a powerful tool for obtaining information on trap depth and relaxation processes in polymeric materials. This method is analogous to thermoluminescence (TL) [113-115]. TL is suitable for those materials which show natural phosphorescence, or which have been made phosphorent by coping with activators (acceptors) and coactivators (donors) [116,117].

The TSD current method involves the following steps : Electrodes should be made on both the sides of a polymeric films (any dielectric in general), elevate its temperature, apply an electric field across the electrodes, cool the specimen to room temperature keeping the field on.

The specimen now possesses polarization. If the temperature of the specimen increased at a linear heating rate, the discharge current is generated. A plot of this current as a function of temperature is a TSD thermogram.

TSD gives a complete picture of temperature dependent relaxation and allows the parameter of dipolar relaxation time and activation energy to be determined from a single measurement with higher accuracy than the conventional dielectric measurements.

There are numerous ways of analysing the TSD spectra. They are based on the nature of the curve on the low temperature side [118], the precise shape of the [119,120] and the way it moves with different heating rates [121].

4.3 METHODS USED FOR STUDYING TSD

Thermally stimulated discharge current (TSDC) of an electret can be studied by the following methods :

(a) Measurement of TSDC with shorted electrodes :

The dipole reorientation and the motion of the excess charges are observed in this technique. This method, whose general principle is depicted in Fig. 4.1 (a), was developed for two-sided metallised specimens by Frei's [122] and subsequently successfully applied by other workers. Owing to the virtual short circuit, the mean electric fields E_p and mean ohmic conduction current within the electret are very small, so that only a

displacement current is generated. In other words, the external current is due to image charges escaping from the evaporated electrodes where they are previously induced by dipoles and space charges.

(b) Measurement of TSDC with open circuit (air gap) electrodes :

To study the decay of one sided metallised homoelectrets, van Turnhout modified Frei's method by introducing an air gap between nonmetallised side of the specimen and adjacent metal electrode as shown in Fig. 4.1(b). When such a two layer assembly is heated, a displacement current is generated by image charges, released from the noncontacting electrodes as the air gap prevents the electret charges from recombining with the image charges of the upper electrode. Since the electret itself is not shorted, the electric field within the electric is no longer zero and in fact becomes quite large. Consequently, the ohmic conduction current flowing through the electret produces an appreciable external displacement current, whereas it remains obscured in TSDC of shorted electrets.

(c) Measurement of TSD charge by transferring the induced charge to an electrometer

Methods have been developed to investigate TSD charge by employing an air gap between nonmetallised side of the dielectric and adjacent electrode. A common method is to move the nonadhering electrode periodically away in order to transfer the image charges induced on it to an integrating electrometer as shown in Fig. 4.1(c). However, no

continuous record of decaying charge can be obtained and hence it is difficult to determine accurately the temperature of the fastest discharge.

(d) Measurement of TSD charge by field cancellation method

Measurements of TSDC have been found unfavourable in case one side metallised homoelectret foils for which the ratio between the air gap electret thickness cannot be made small. In such a case, the discharging/decaying electret induces most of its image charge on the grounded electrode instead of probing electrode. A novel version of air gap charge TSD developed by van Turnhout. Fig. 4.1(d) is now generally used. This method allows a continuous monitoring of decaying charge and is based on the field cancellation technique, according to which the external field of the foil is nullified by driving noncontacting electrode with an adjustable bias voltage of the same value and polarity as the equivalent voltage of the electret. Since the upper electrode in such a system is virtually floating, the external current is zero and, therefore, the method is referred to as the charge TSD measurement in open circuit.

4.4 DETECTION EFFICIENCY OF VARIOUS TSD METHODS

The magnitude of the TSDC depends on the effective charge retained by the electret but all the decay processes do not contribute fully to the external current. For example, in decay processes that involve space charges, only a part of the decay is observed between the shorted

electrodes. This experimental characteristics may be due to either one or a combination of the reasons mentioned below.

Some of the charge could be neutralised by an internal ohmic conduction which will pass unnoticed in the external circuit. This will be especially true for materials of relatively high intrinsic conductivity like polar polymers.

Some of the charges may recombine with their image charges at the nonblocking electrodes. Only a part of total induced image charges will, therefore, be made to flow in the external circuit. The nature of the dielectric-electrode interface will thus play an important role in the efficiency of the TSD current measured.

Current released by diffusion of the excess charges will depend on the blocking nature of the electrodes. A zero external current would result if completely nonblocking or open electrodes are used.

In general, the detection efficiency for various processes involving neutralisation of space charges may be improved by incorporating a highly blocking layer between the sample and the electrode such that any charge exchange across the electrode dielectric interface will be blocked. Such an electrical arrangement can be easily obtained by utilizing an air gap as the blocking layer. Also, as the net field in the solid is now nonzero, the decay of the excess charges by ohmic conduction will also be observed. It has been shown that for such electrical systems, decay of the excess charges

by the external ohmic conduction will dominate that of the drift or diffusion TSD measurement of this type is called air gap TSD or open circuit TSD.

Alternatively, in such systems, measurements of the voltage induced or the noncontacting electrode would also be useful in the study of persistent polarisation in the sample bulk. This method may be named "charge TSD" because it now measures the evolution of the effective surface charge on the electret as it is being heated up. Compared with the TSD current measurements where the measured signals are very small (typically 10^{-13} to 10^{-17} Amp) charge TSD has the advantage of measuring large signal (10 - 10^3 V) [123].

Excellent review on this subject, both theoretical and experimental have appeared in the literature [124]. Some other important results on the polymer electrets have been reported by Perlman [125], Caserta and Serra [126], Pillai *et al.* [127], Mahendru [128], Latour and Murphy [129], Jain *et al.* [130], Talwar and Sharma [131], Kojima and Maeda [132], Tokai *et al.* [133], Shrivastava *et al.* [134], Shrivastava and Mathur [135], Tanaka *et al.* [136], Iqbal and Hogarth [137], Rao and Das [138], Rao and Kalpalatha [139], Christodoulides *et al.* [140], Fraile *et al.* [141], Vaezi-Najad [142], Rychkov *et al.* [143], Kamarulzaman *et al.* [144], Weijun *et al.* [145], Lewandowski [146], Vanderschueren and Gasiot [147], etc.

4.5 THERMALLY STIMULATED DISCHARGE CURRENT (TSDC) MEASUREMENT

For polarization the whole assembly was placed inside an oven and heated to a polarizing temperature, T_p , and then polarizing voltage (E_p)

was applied across the electrodes. The electric stress was maintained at polarizing temperature for 60 min, after which the sample was cooled to room temperature without removing the polarization voltage. The cooling process was completed in 1.5 h.

In order to exclude a confusing contribution of unstable charges which stay on the electret surface, the sample is kept in short circuited condition for 5 min after the completion of polarization. For monitoring TSDC, the sample was depolarised by heating at a rate of 3°C per min. The depolarization current was manually recorded at convenient intervals of time for complete depolarization. The sample was heated to about 190°C .

4.6 RESULTS AND DISCUSSION

The experimental conditions under which the thermally stimulated discharge currents were measured are summarised below -

Polarizing field strength	-	10 kV/cm to 100 kV/cm
Polarizing temperature	-	40°C to 80°C
Heating Rates	-	$3^{\circ}\text{C}/\text{min}$
Electrode materials	-	Aluminium, Silver, Copper and Tin

The thermally stimulated discharge current (TSDC) spectra for polyvinylidene fluoride (PVDF) films polarized with 10, 25, 50, 75 and 100 kV/cm at fixed temperatures 40°C , 50°C , 60°C , 70°C and 80°C are illustrated in Figs. 4.1 to 4.20 and 4.21 to 4.35 for similar electrodes (i.e. Al-Al, Cu-Cu,

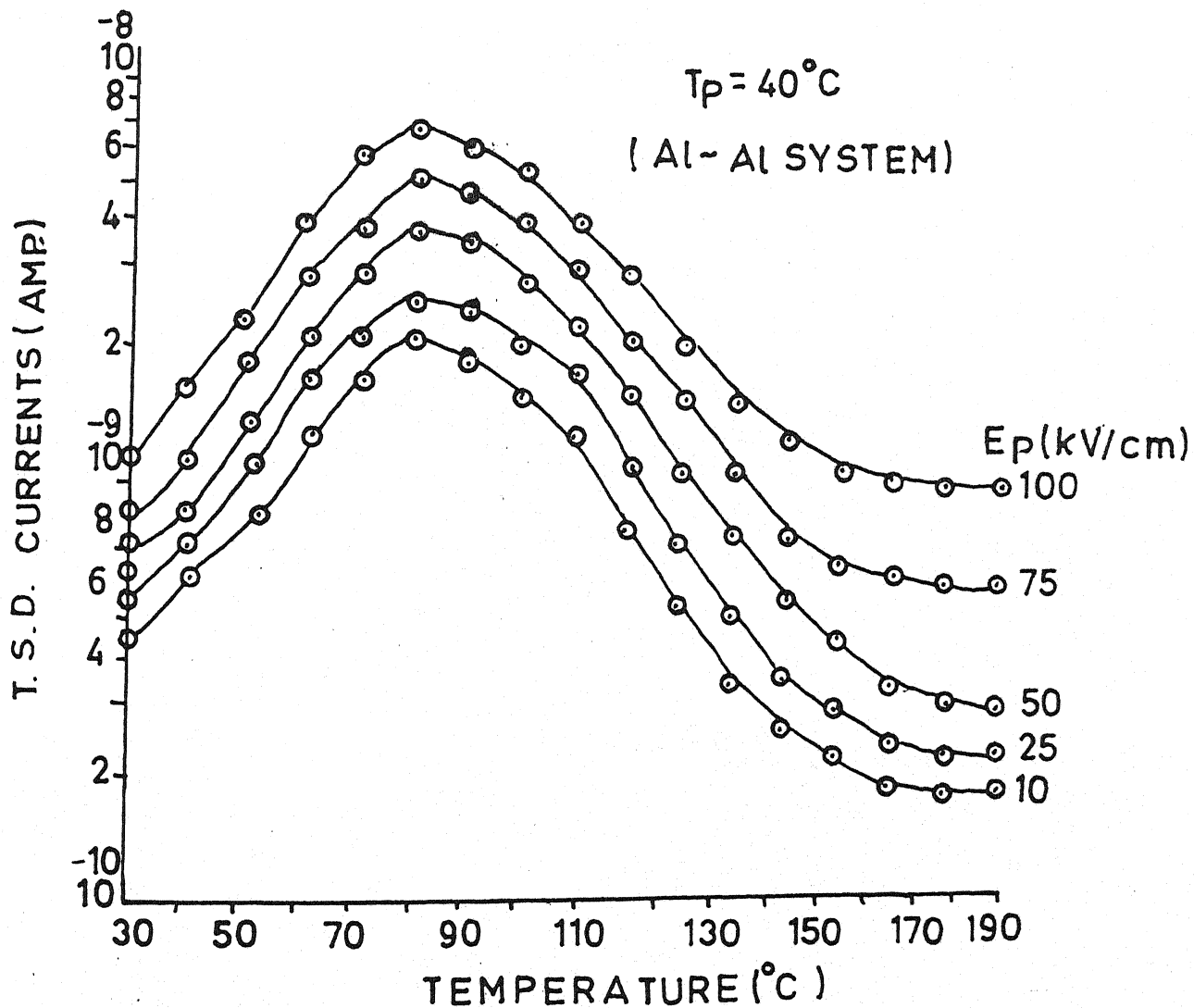


Figure No. 4.1

Thermally Stimulated Discharge Currents (T.S.D.C.) for Polyvinylidene fluoride Samples ($20\ \mu\text{m}$) poled at $T_p = 40^\circ\text{C}$ with different polarisation fields (i.e. 10, 25, 50, 75 and 100 kV/cm) for Al-Al system.

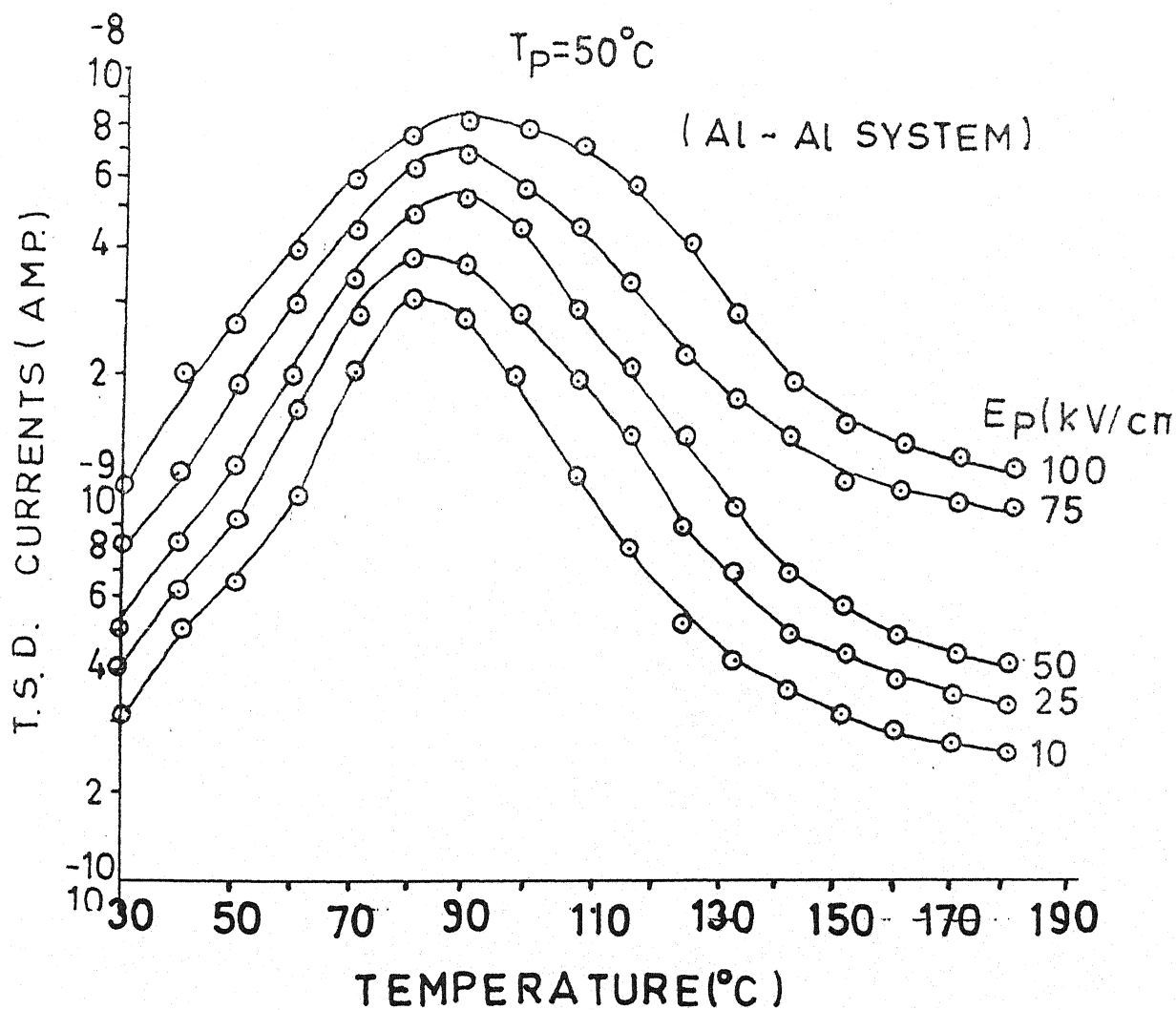


Figure No. 4.2
Thermally Stimulated Discharge Currents (T.S.D.C.) for Polyvinylidene fluoride Samples ($20\ \mu\text{m}$) poled at $T_p = 50^\circ\text{C}$ with different polarisation fields (i.e. 10, 25, 50, 75 and 100 kV/cm) for Al - Al system.

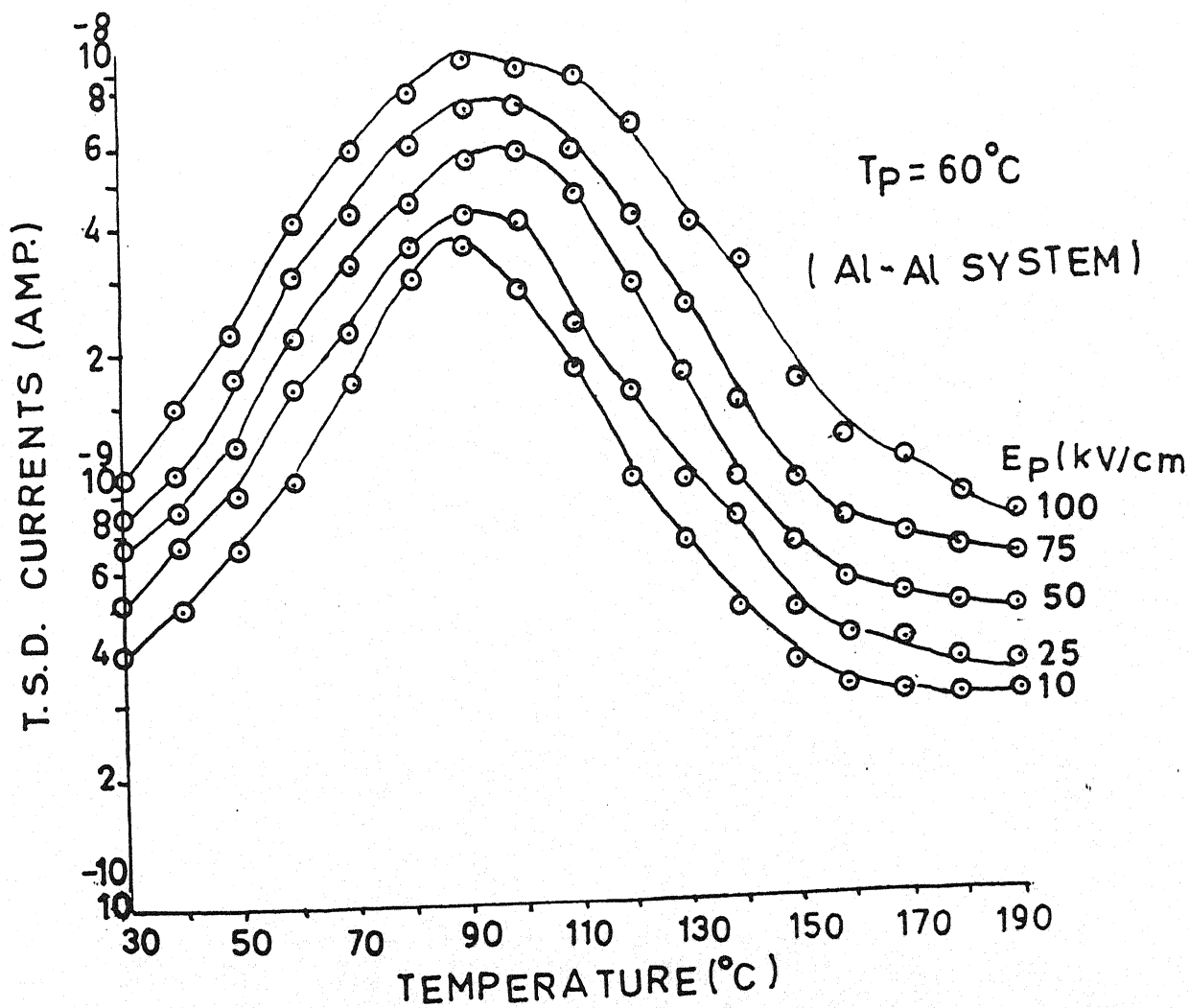


Figure No. 4.3

Thermally Stimulated Discharge Currents (T.S.D.C.) for Polyvinylidene fluoride Samples (20 μm) poled at $T_p = 60^{\circ}\text{C}$ with different polarisation fields (i.e. 10, 25, 50, 75 and 100 kV/cm) for Al-Al system.

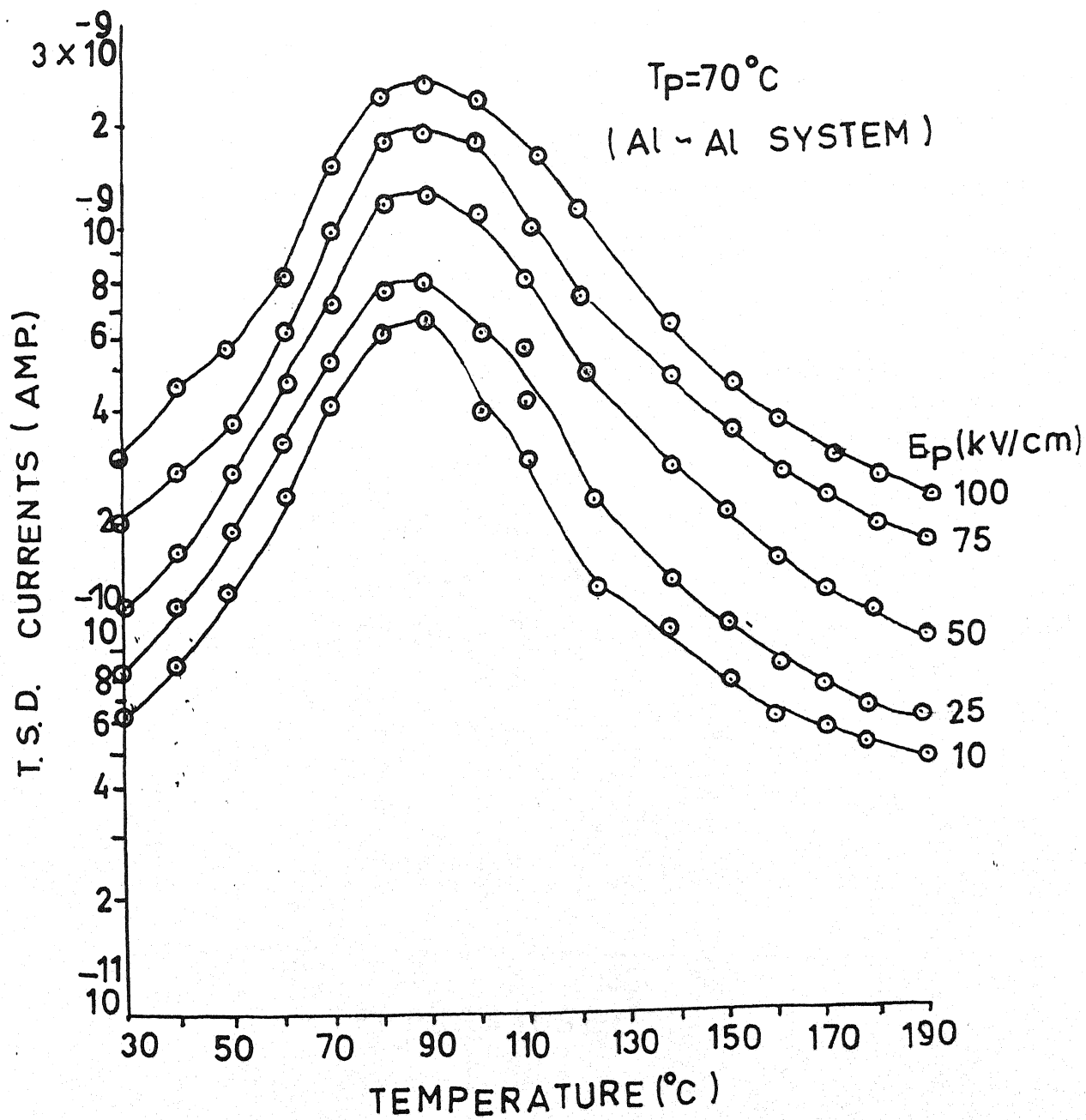


Figure No. 4.4
Thermally Stimulated Discharge Currents (T.S.D.C.) for Polyvinylidene fluoride Samples ($20\ \mu\text{m}$) poled at $T_p = 70^\circ\text{C}$ with different polarisation fields (i.e. 10, 25, 50, 75 and 100 kV/cm) for Al-Al system.

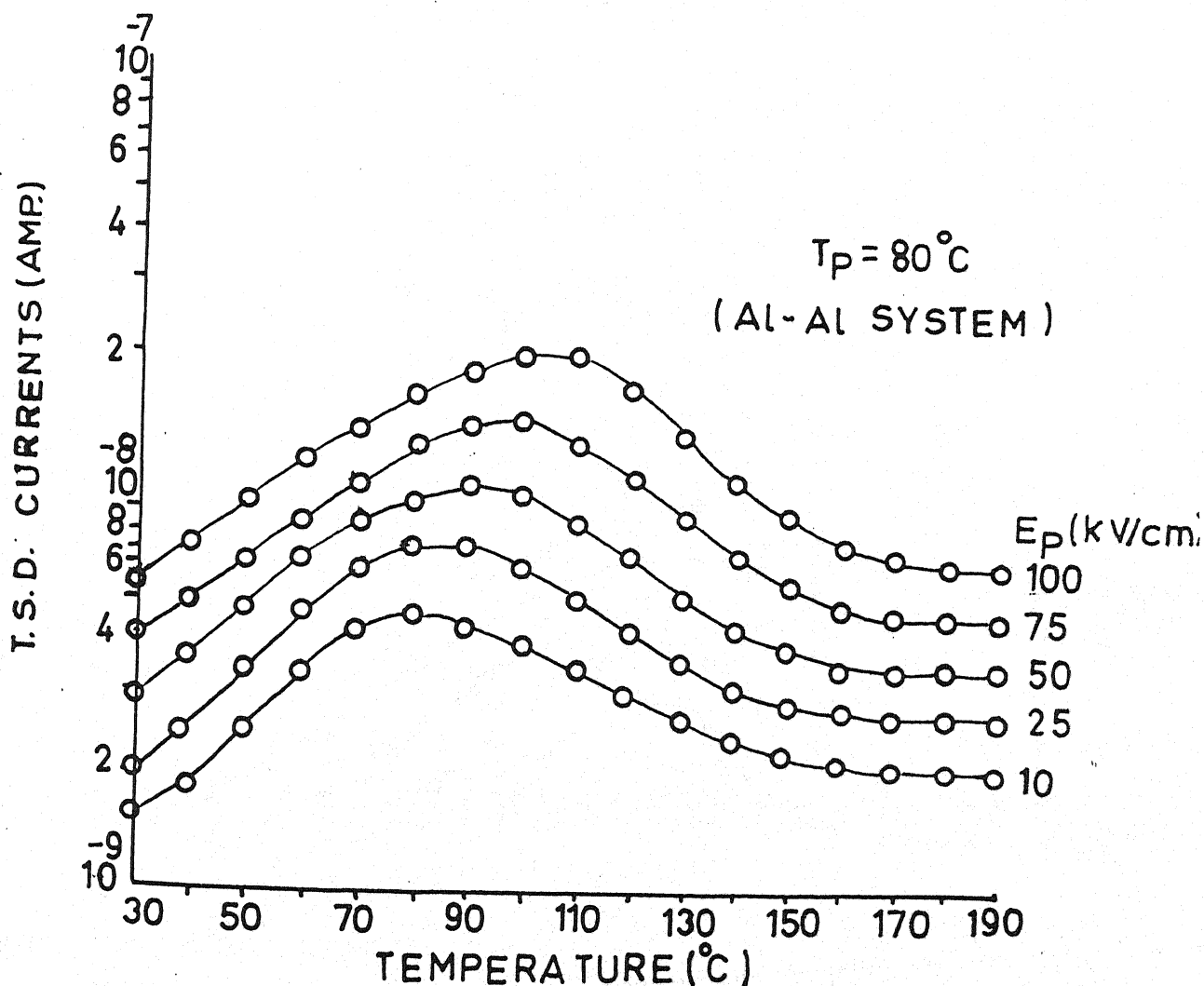


Figure No. 4.5

Thermally Stimulated Discharge Currents (T.S.D.C.) for Polyvinylidene fluoride Samples ($20\ \mu\text{m}$) poled at $T_p = 80^\circ\text{C}$ with different polarisation fields (i.e. 10, 25, 50, 75 and 100 kV/cm) for Al-Al system.

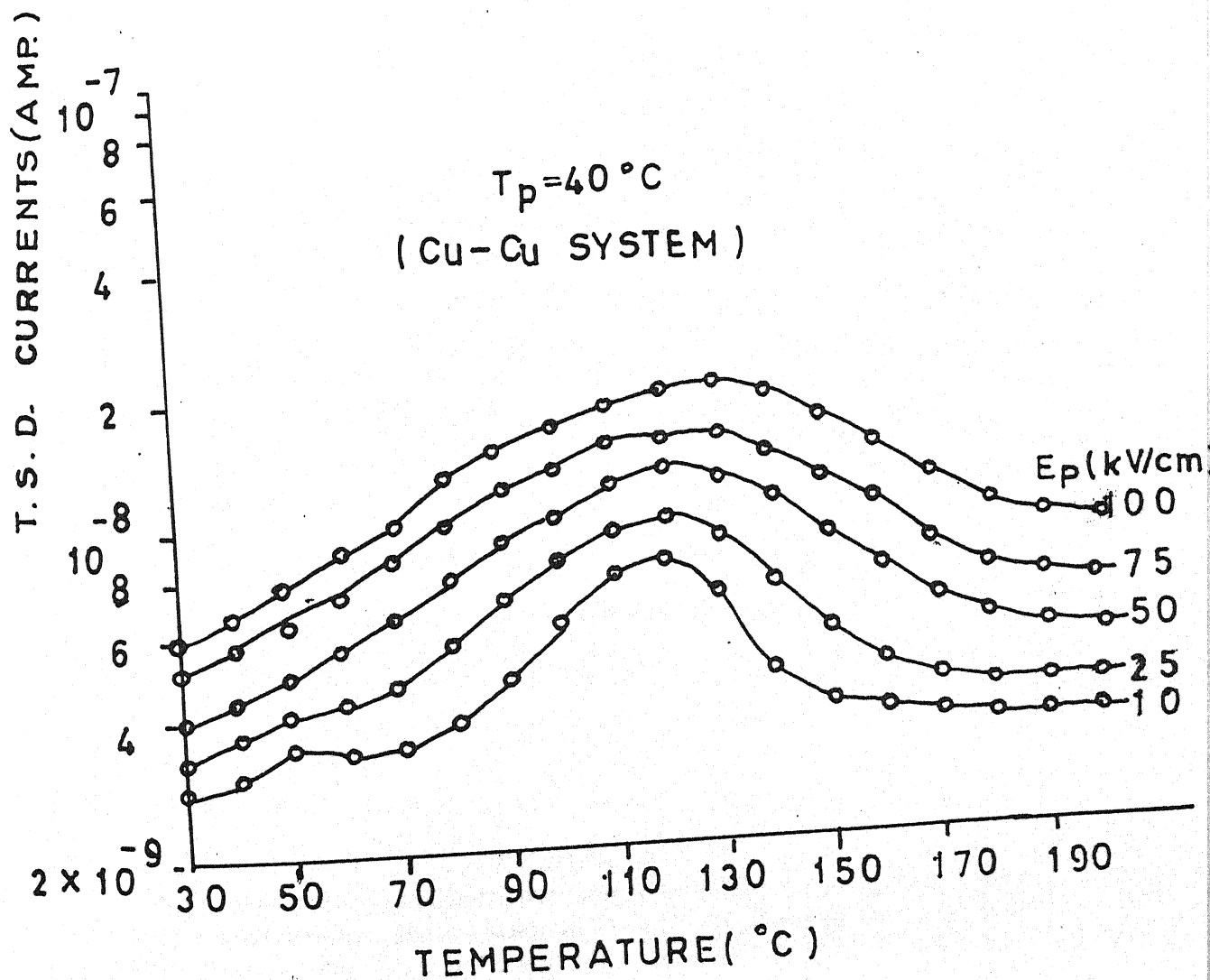


Figure No. 4.6
Thermally Stimulated Discharge Currents (T.S.D.C.) for Polyvinylidene fluoride Samples ($20\ \mu\text{m}$) poled at $T_p = 40^\circ\text{C}$ with different polarisation fields (i.e. 10, 25, 50, 75 and 100 kV/cm) for Cu - Cu system.

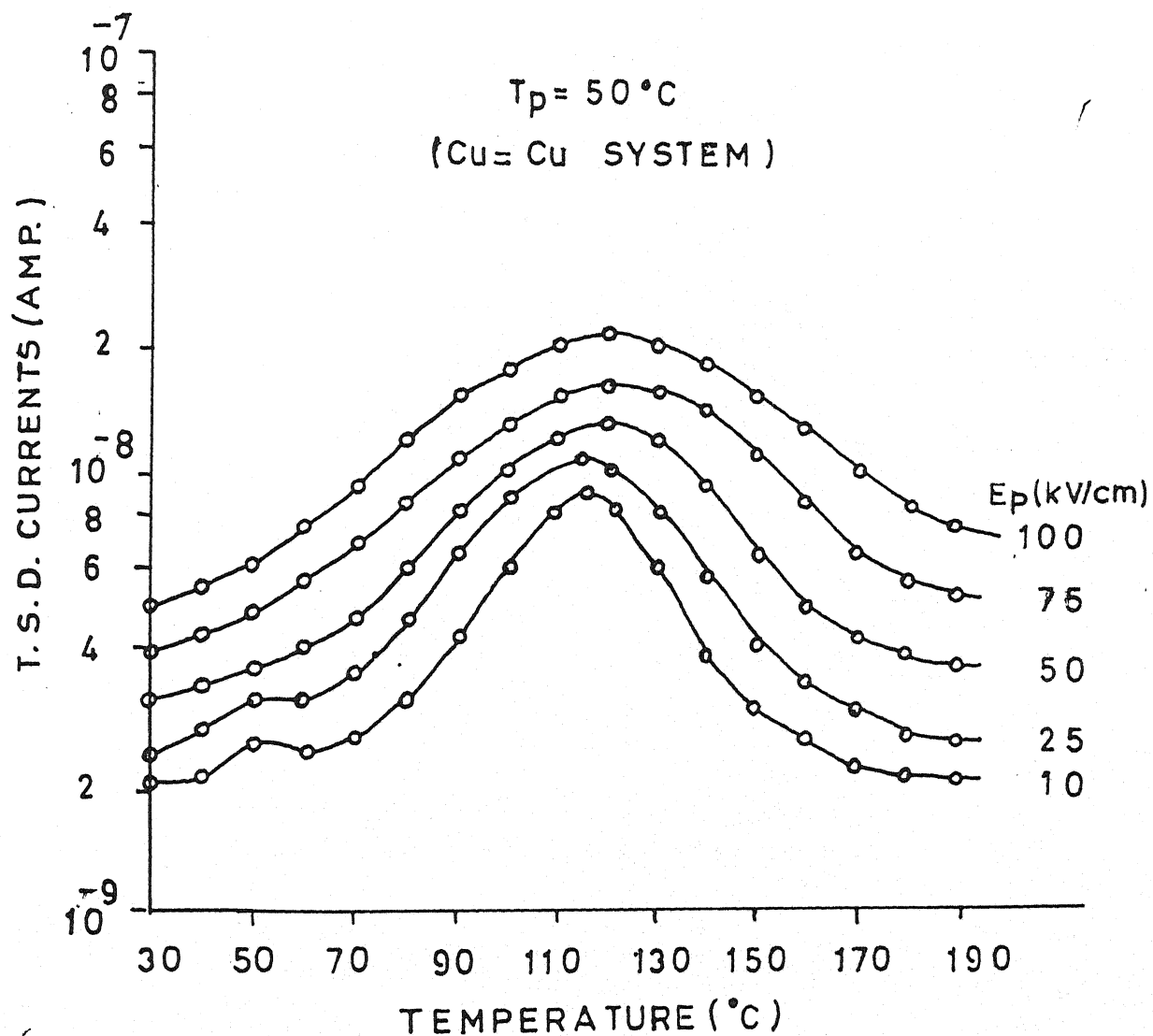


Figure No. 4.7
Thermally Stimulated Discharge Currents (T.S.D.C.) for Polyvinylidene fluoride Samples ($20\ \mu\text{m}$) poled at $T_p = 50^\circ\text{C}$ with different polarisation fields (i.e. 10, 25, 50, 75 and 100 kV/cm) for Cu - Cu system.

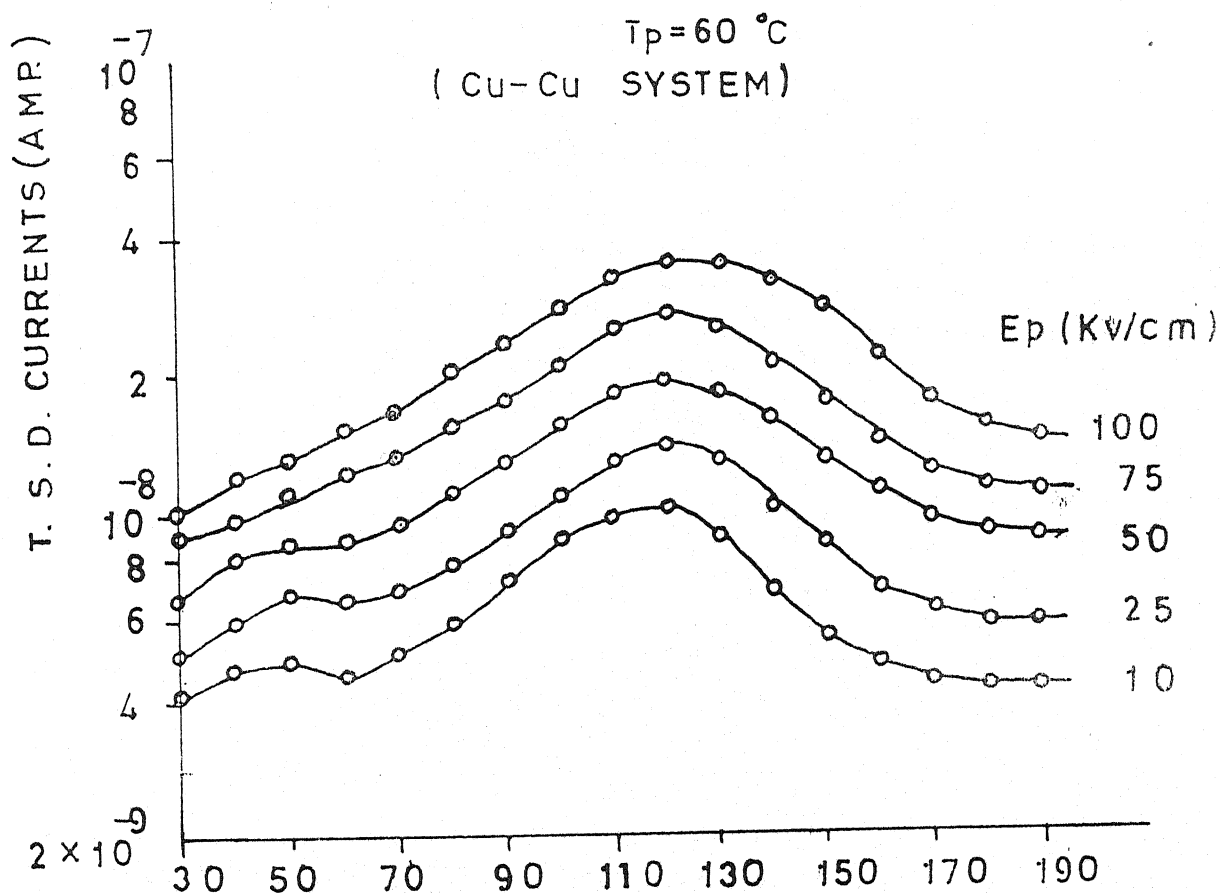


Figure No. 4.8
Thermally Stimulated Discharge Currents (T.S.D.C.) for Polyvinylidene fluoride Samples ($20\ \mu\text{m}$) poled at $T_p = 60^\circ\text{C}$ with different polarisation fields (i.e. 10, 25, 50, 75 and 100 kV/cm) for Cu - Cu system.

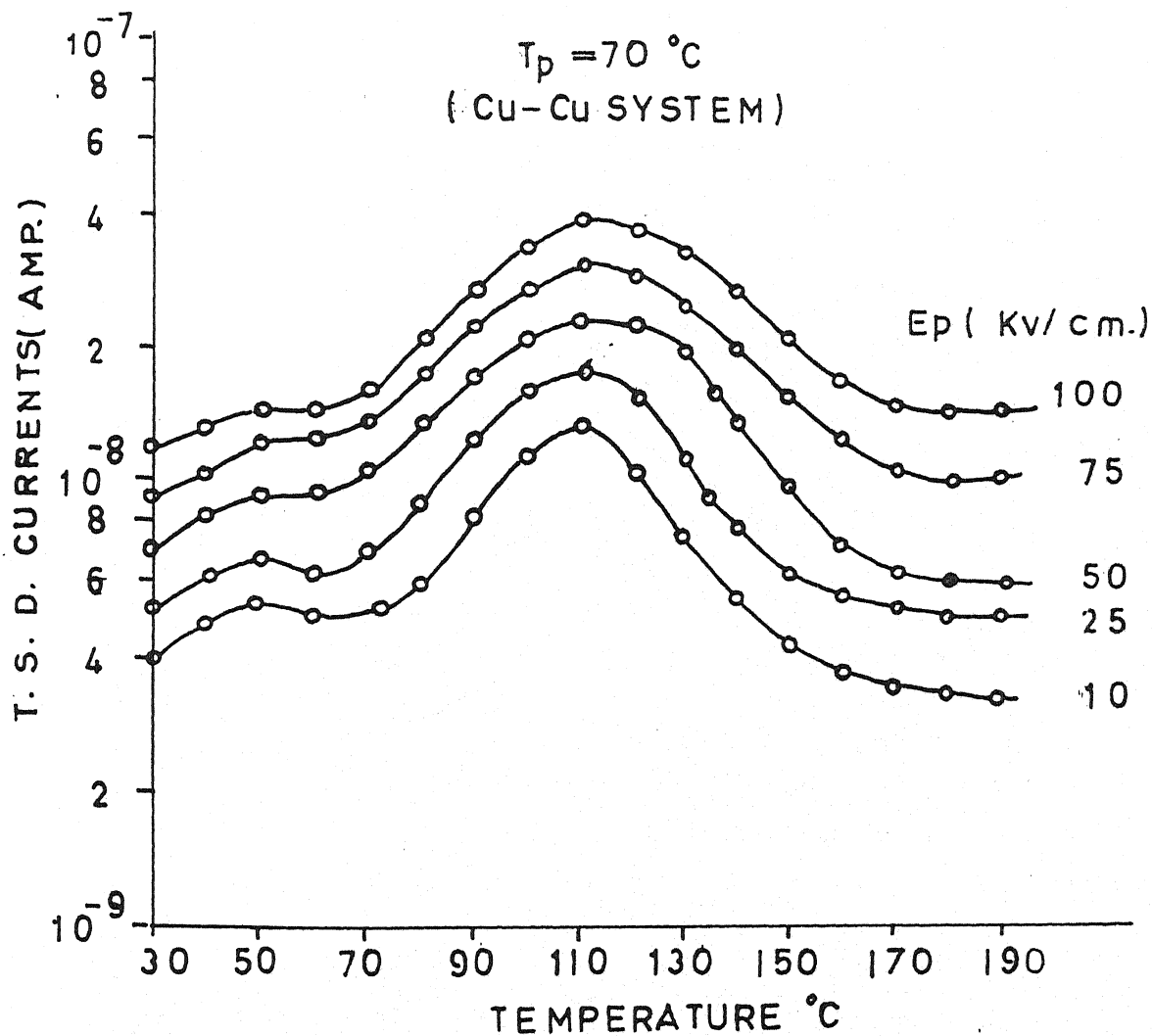


Figure No. 4.9
Thermally Stimulated Discharge Currents (T.S.D.C.) for Polyvinylidene fluoride Samples ($20\ \mu\text{m}$) poled at $T_p = 70^\circ\text{C}$ with different polarisation fields (i.e. 10, 25, 50, 75 and 100 kV/cm) for Cu - Cu system.

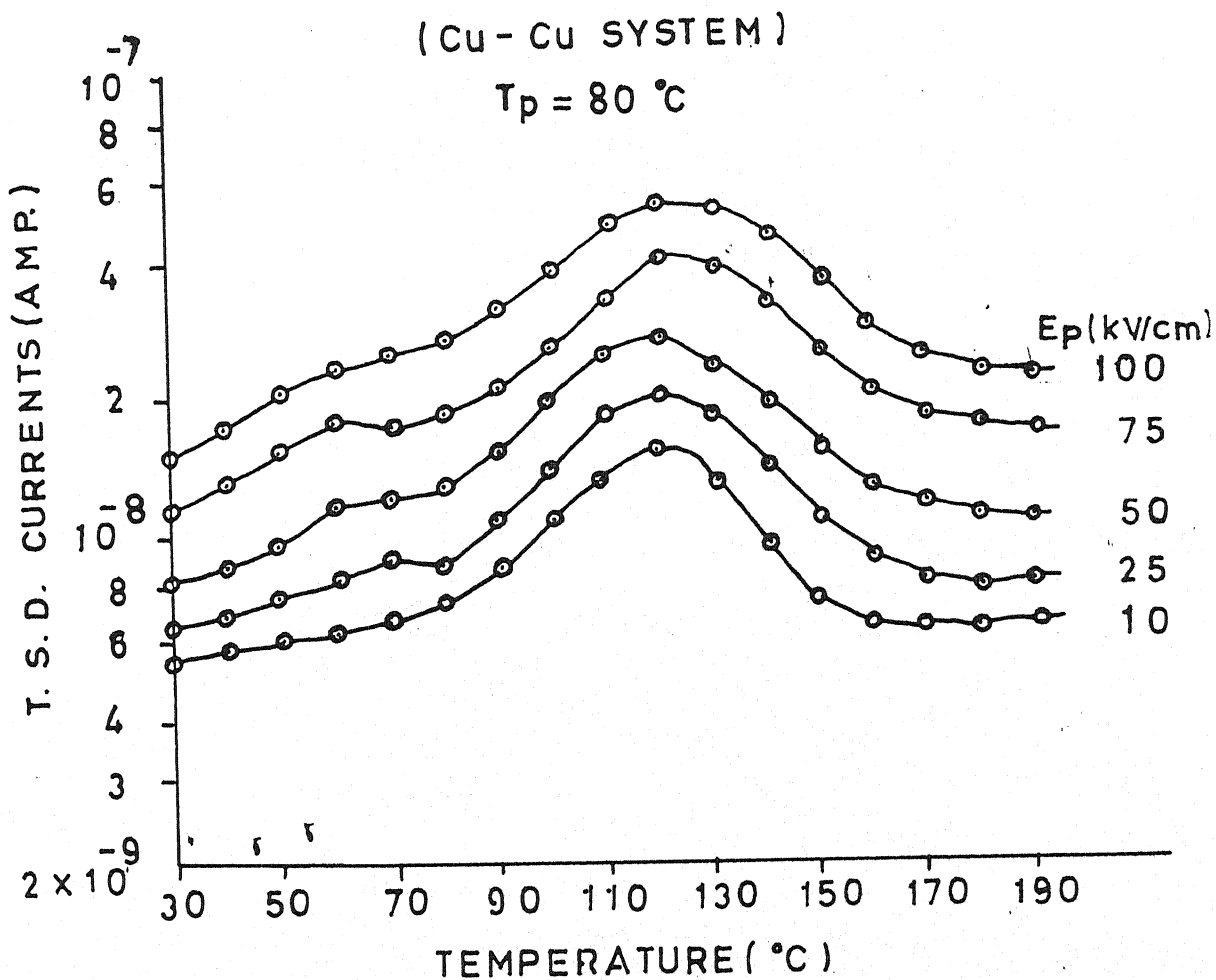


Figure No. 4.10
Thermally Stimulated Discharge Currents (T.S.D.C.) for Polyvinylidene fluoride Samples ($20\ \mu\text{m}$) poled at $T_p = 80^\circ\text{C}$ with different polarisation fields (i.e. 10, 25, 50, 75 and 100 kV/cm) for Cu - Cu system.

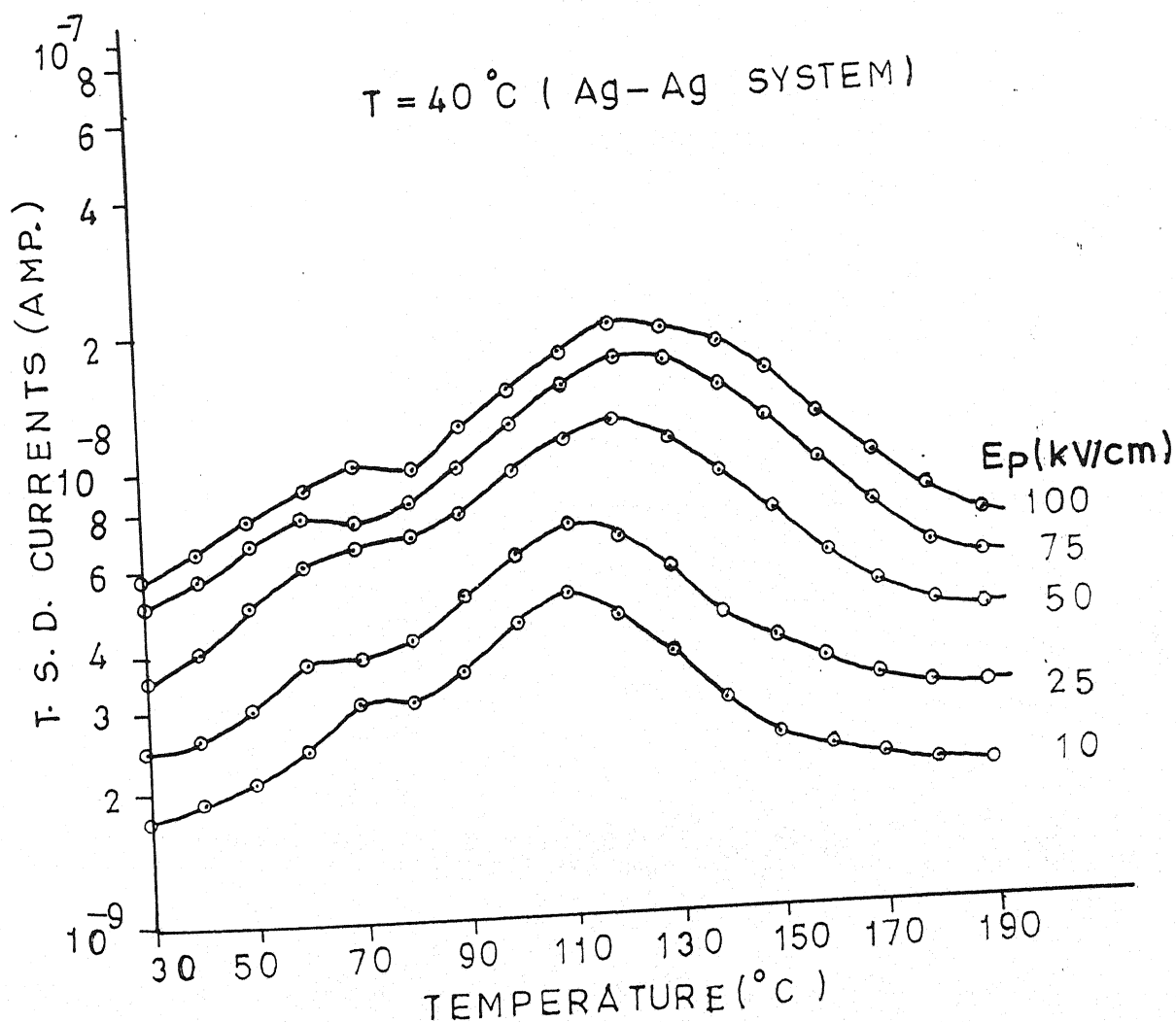


Figure No. 4.11
 Thermally Stimulated Discharge Currents (T.S.D.C.) for Polyvinylidene fluoride Samples ($20\ \mu\text{m}$) poled at $T_p = 40^\circ\text{C}$ with different polarisation fields (i.e. 10, 25, 50, 75 and 100 kV/cm) for Ag - Ag system.

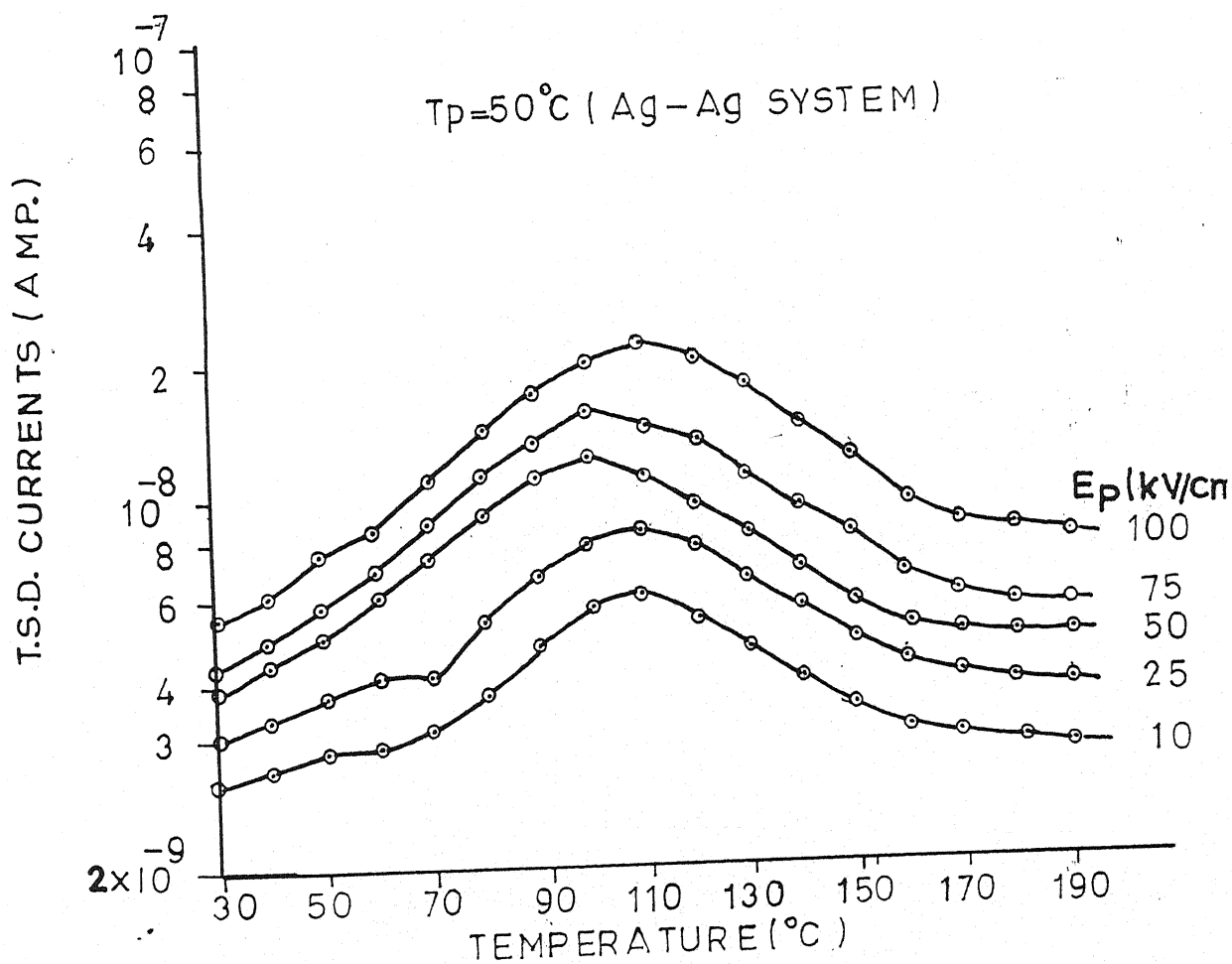


Figure No. 4.12
 Thermally Stimulated Discharge Currents (T.S.D.C.) for Polyvinylidene fluoride Samples ($20\ \mu\text{m}$) poled at $T_p = 50^\circ\text{C}$ with different polarisation fields (i.e. 10, 25, 50, 75 and 100 kV/cm) for Ag - Ag system.

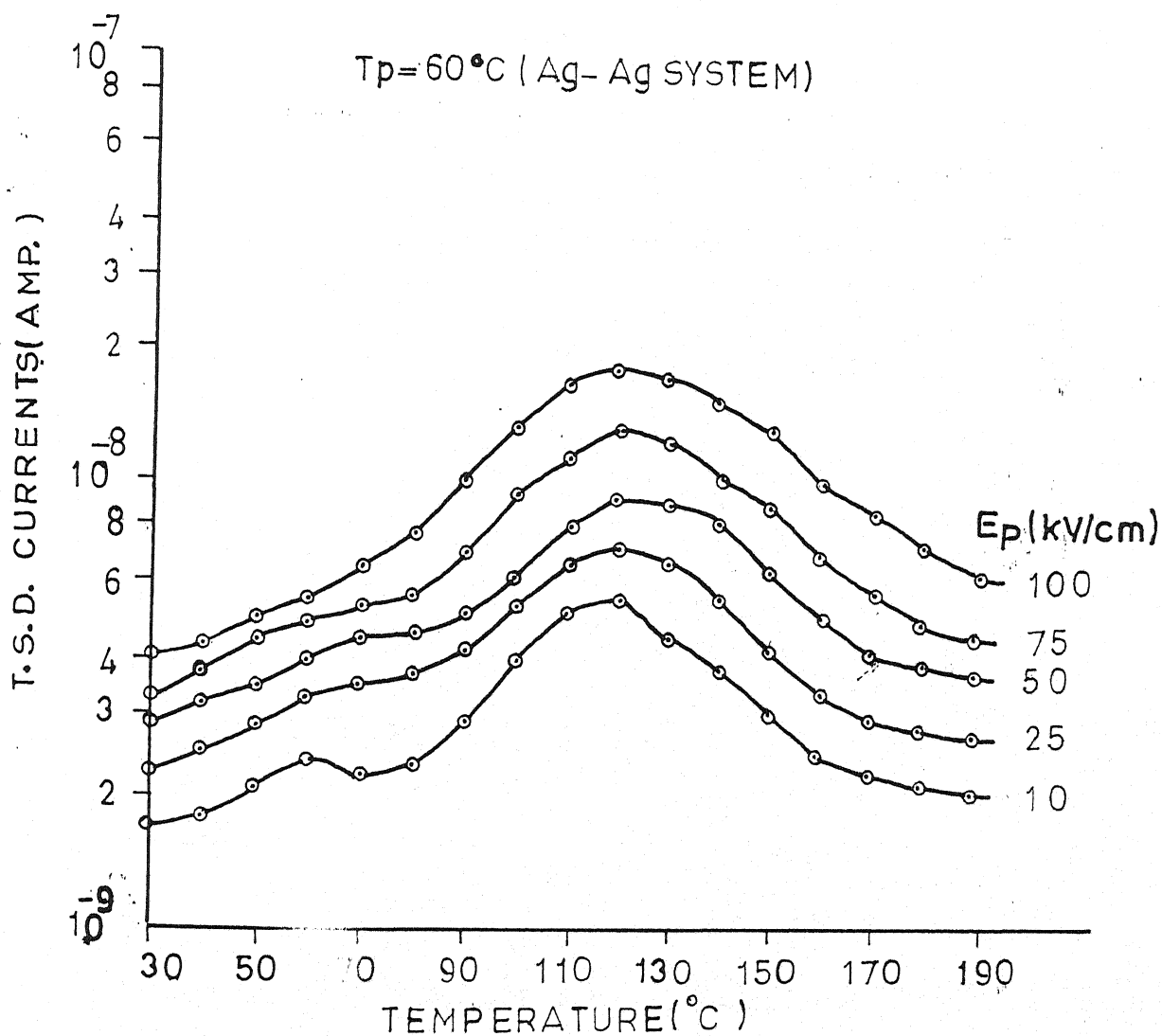


Figure No. 4.13

Thermally Stimulated Discharge Currents (T.S.D.C.) for Polyvinylidene fluoride Samples ($20\ \mu\text{m}$) poled at $T_p = 60^\circ\text{C}$ with different polarisation fields (i.e. 10.25.50.75 and 100 kV/cm) for Ag-Ag system.

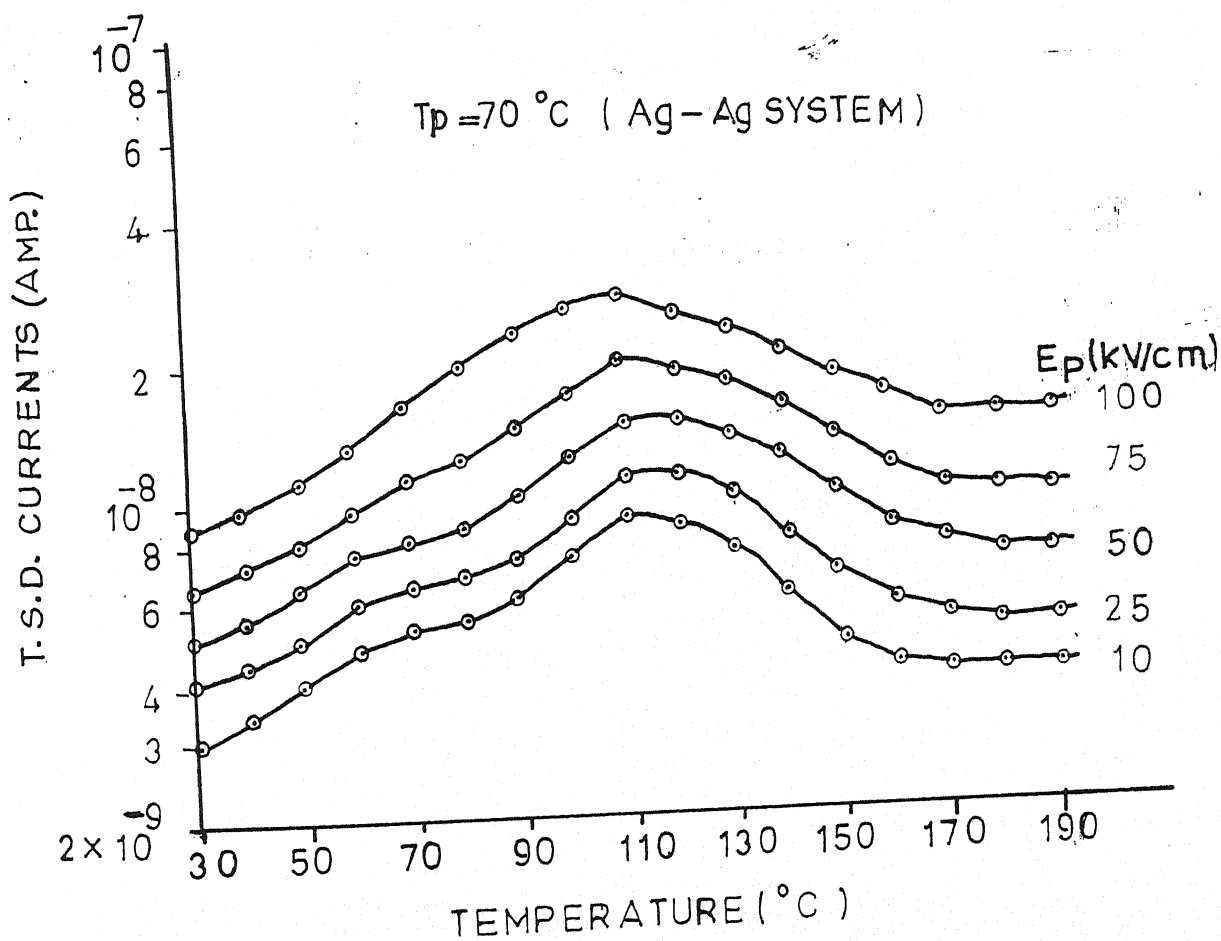


Figure No. 4.14
Thermally Stimulated Discharge Currents (T.S.D.C.) for Polyvinylidene fluoride Samples ($20\ \mu\text{m}$) poled at $T_p = 70^\circ\text{C}$ with different polarisation fields (i.e. 10, 25, 50, 75 and 100 kV/cm) for Ag-Ag system.

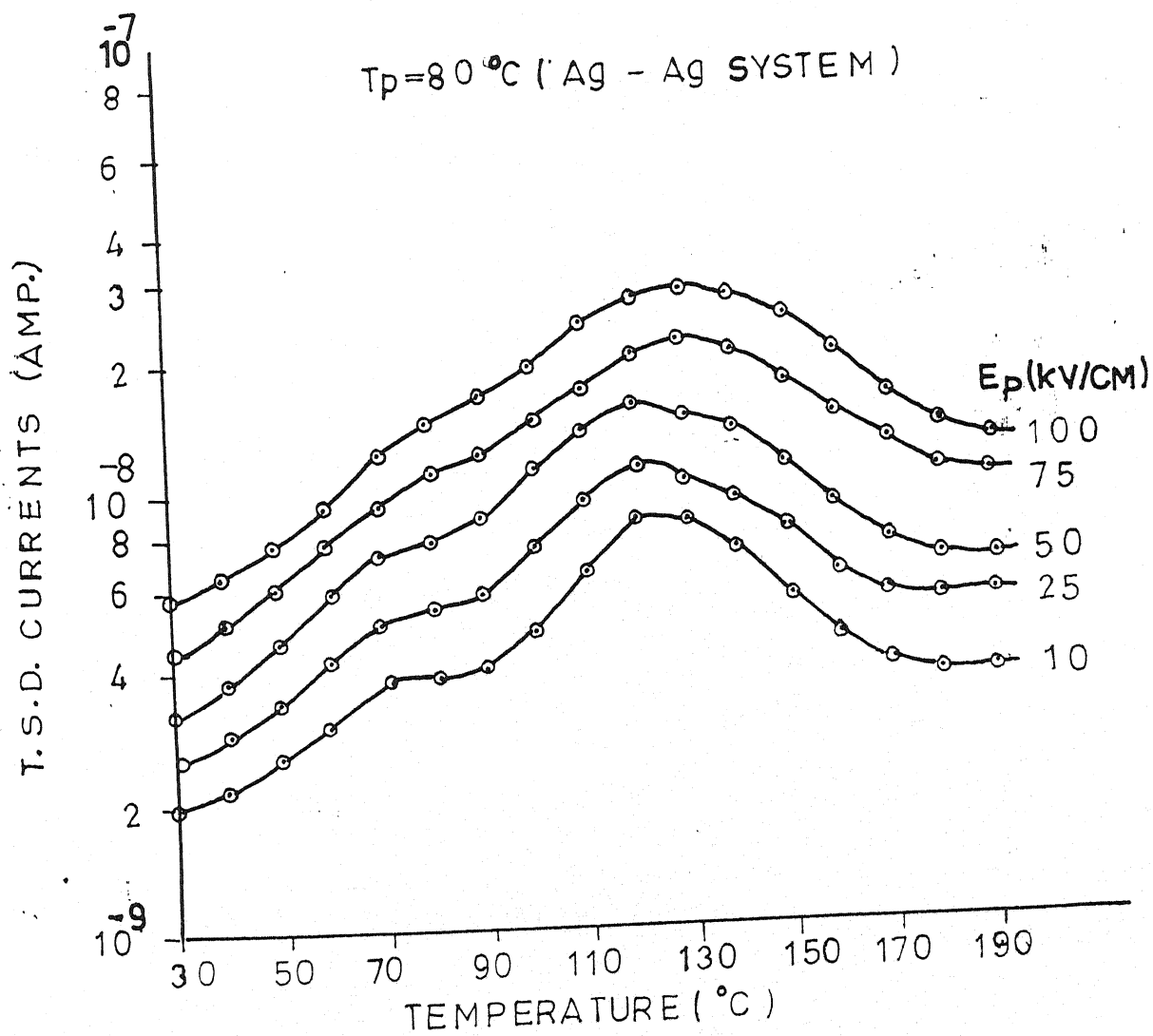


Figure No. 4.15
 Thermally Stimulated Discharge Currents (T.S.D.C.) for Polyvinylidene fluoride Samples ($20\ \mu\text{m}$) poled at $T_p = 80^\circ\text{C}$ with different polarisation fields (i.e. 10, 25, 50, 75 and 100 kV/cm) for Ag-Ag system.

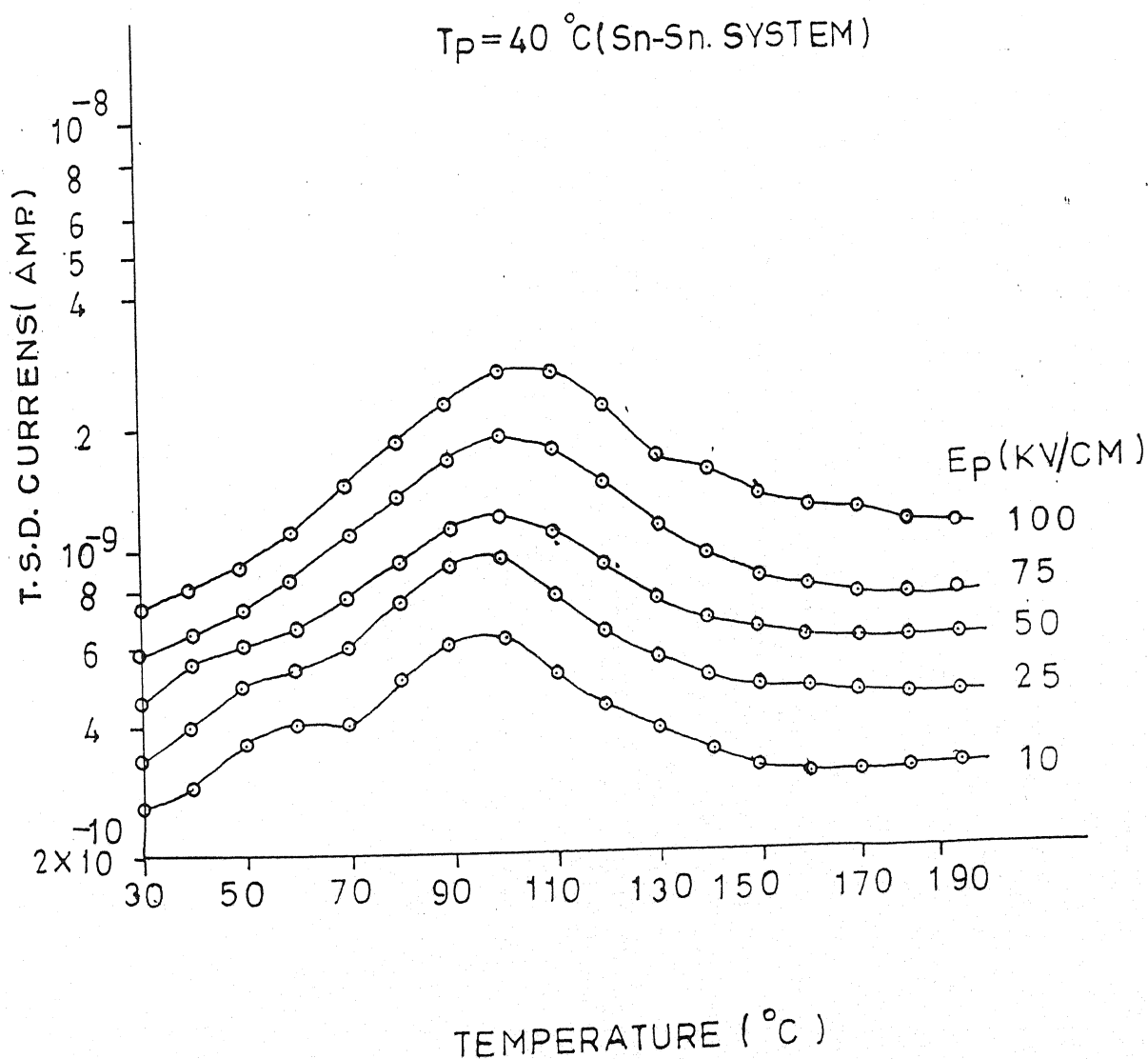


Figure No. 4.16
 Thermally Stimulated Discharge Currents (T.S.D.C.) for Polyvinylidene fluoride Samples ($20 \mu\text{m}$) poled at $T_p = 40^\circ\text{C}$ with different polarisation fields (i.e. 10, 25, 50, 75 and 100 kV/cm) for Sn - Sn system.

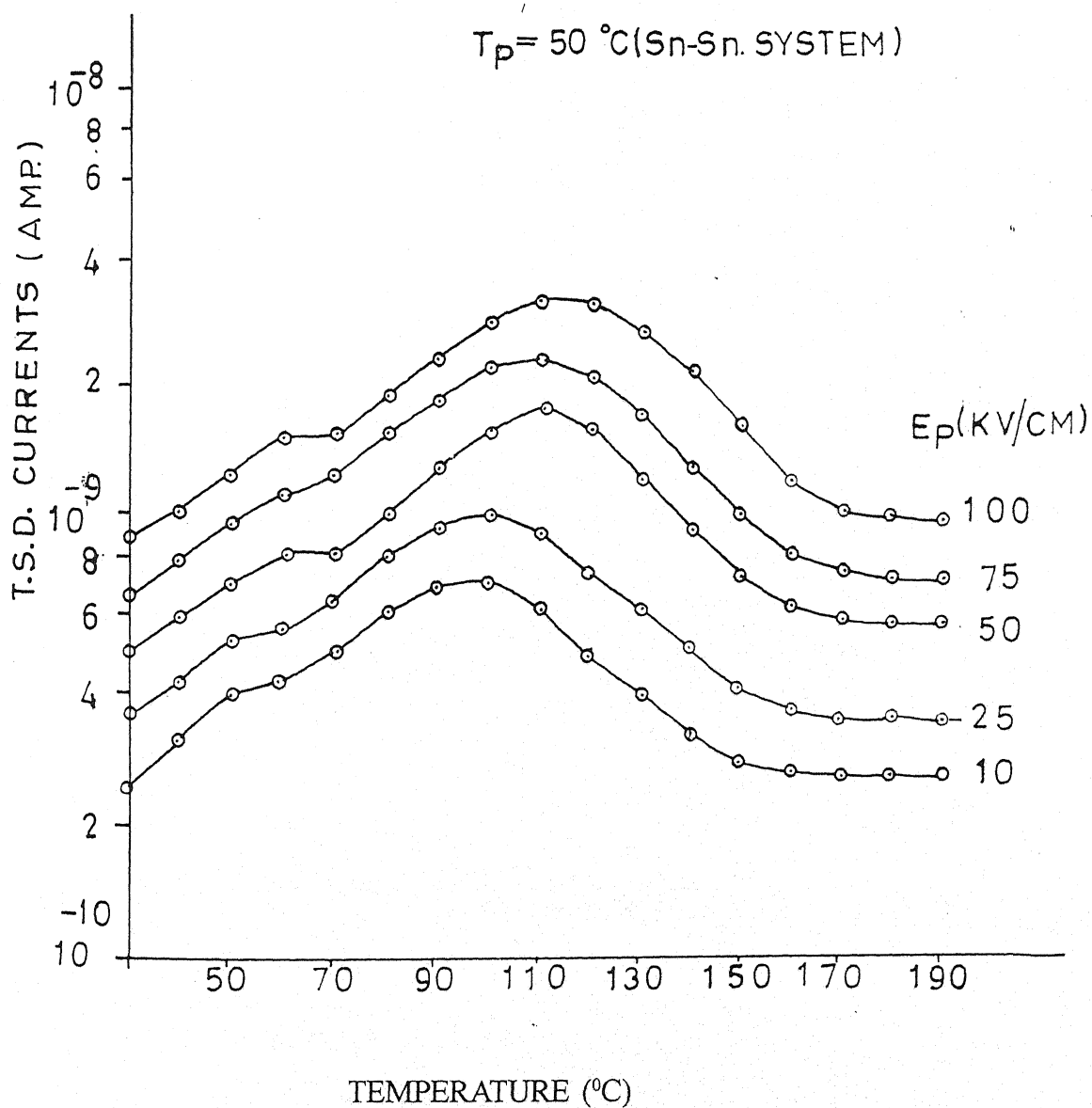


Figure No. 4.17

Thermally Stimulated Discharge Currents (T.S.D.C.) for Polyvinylidene fluoride Samples ($20\ \mu\text{m}$) poled at $T_p = 50^\circ\text{C}$ with different polarisation fields (i.e. 10, 25, 50, 75 and 100 kV/cm) for Sn - Sn system.

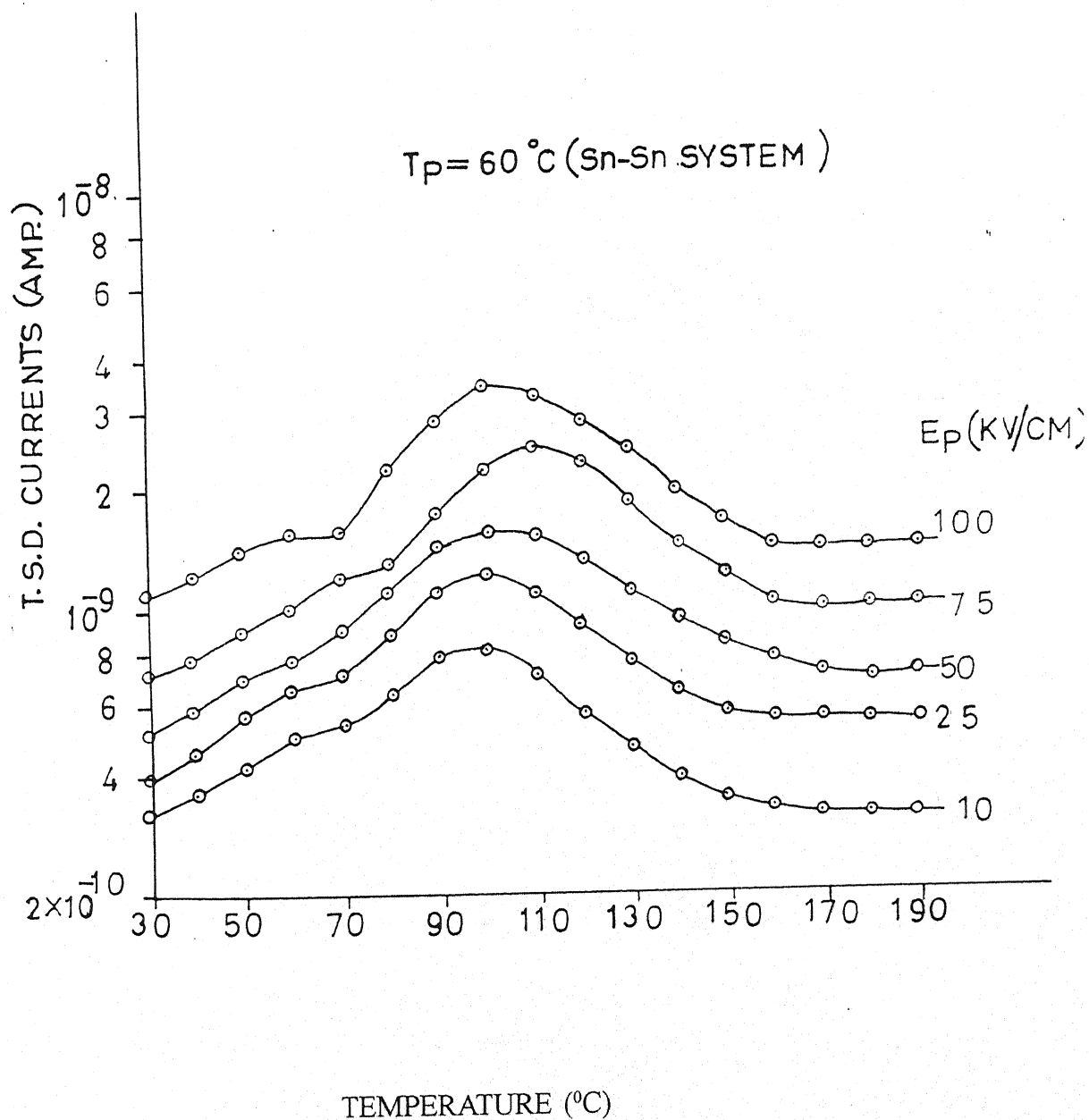


Figure No. 4.18

Thermally Stimulated Discharge Currents (T.S.D.C.) for Polyvinylidene fluoride Samples ($20\ \mu\text{m}$) poled at $T_p = 60^\circ\text{C}$ with different polarisation fields (i.e. 10, 25, 50, 75 and 100 kV/cm) for Sn - Sn system.

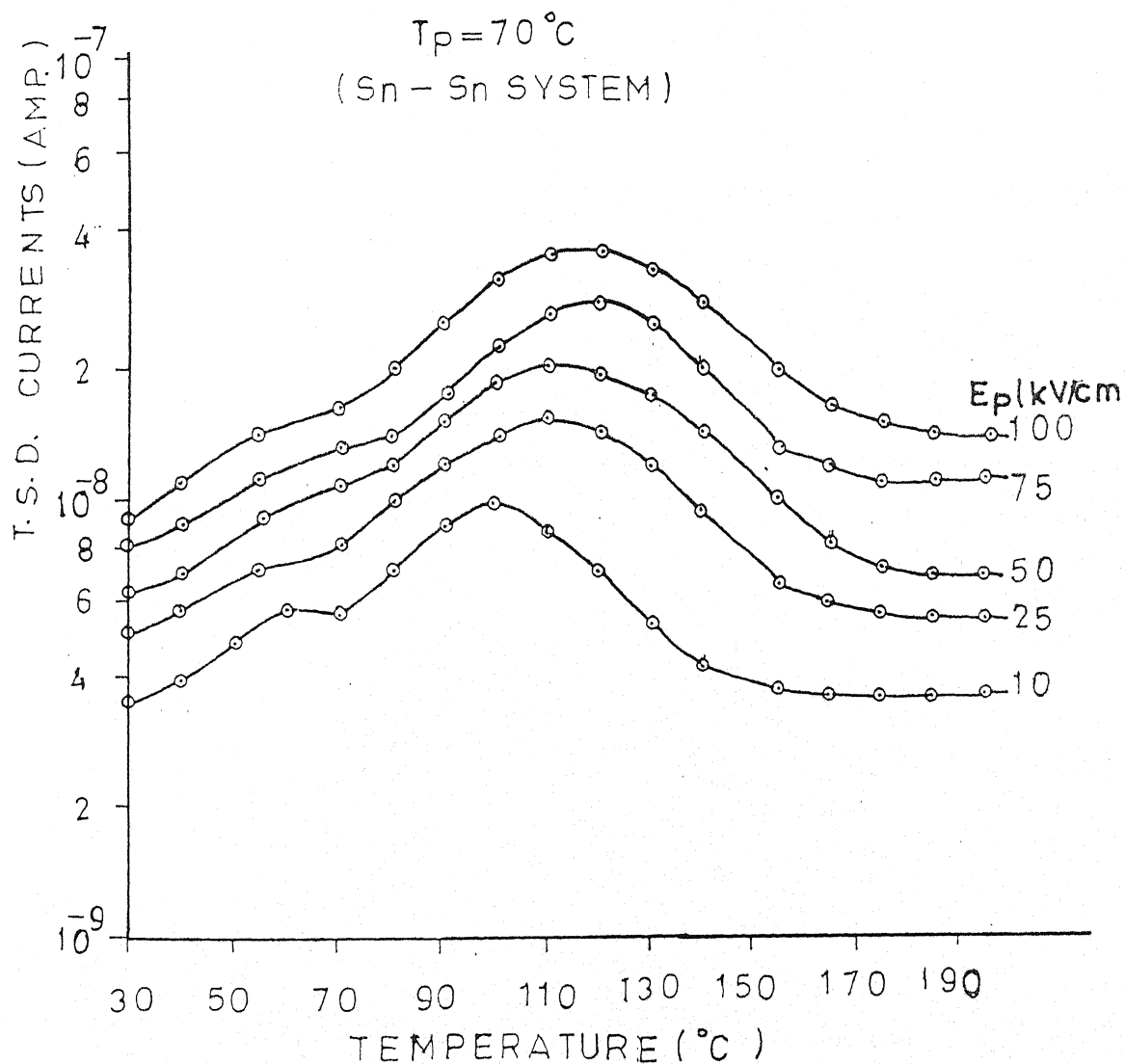


Figure No. 4.19
Thermally Stimulated Discharge Currents (T.S.D.C.) for Polyvinylidene fluoride Samples ($20\ \mu\text{m}$) poled at $T_p = 70^\circ\text{C}$ with different polarisation fields (i.e. 10, 25, 50, 75 and 100 kV/cm) for Sn - Sn system.

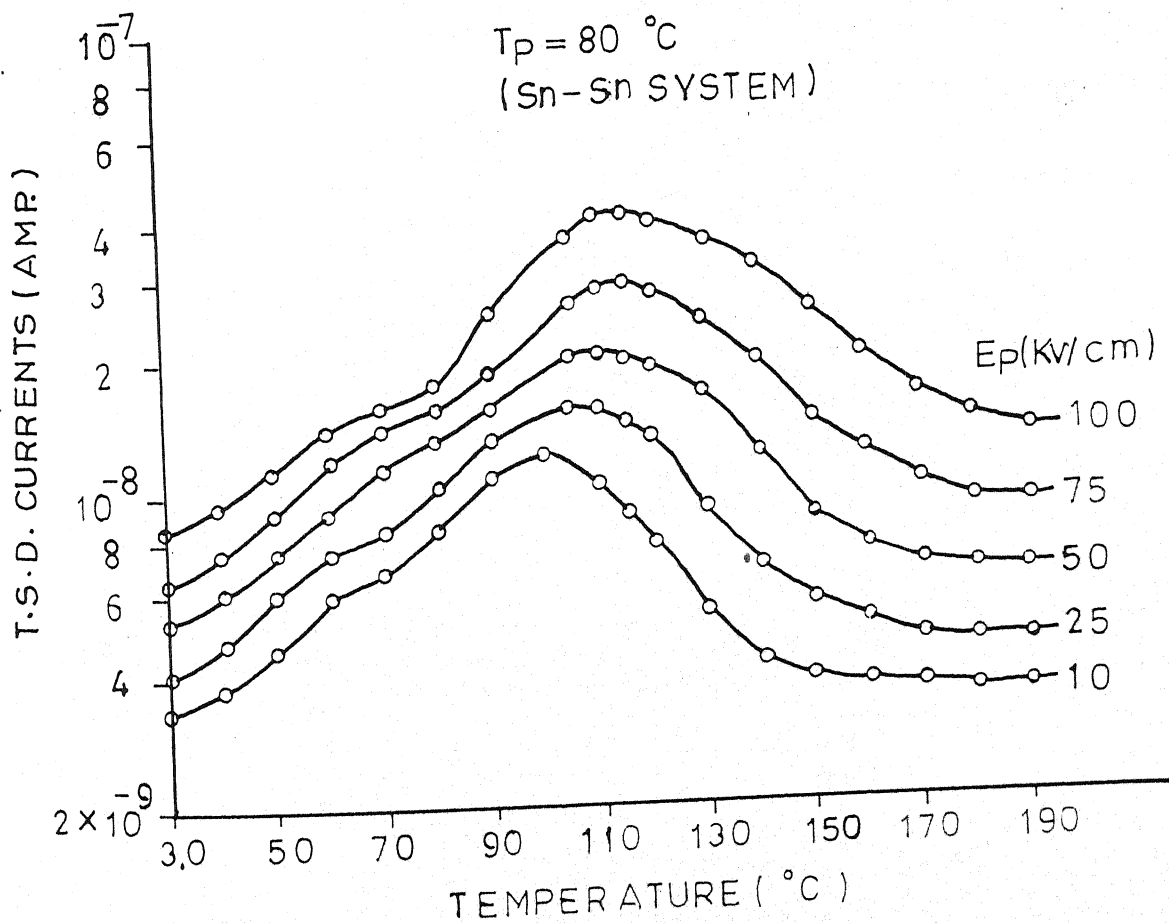


Figure No. 4.20

Thermally Stimulated Discharge Currents (T.S.D.C.) for Polyvinylidene fluoride Samples ($20\ \mu\text{m}$) poled at $T_p = 80^\circ\text{C}$ with different polarisation fields (i.e. 10, 25, 50, 75 and 100 kV/cm) for Sn - Sn system.

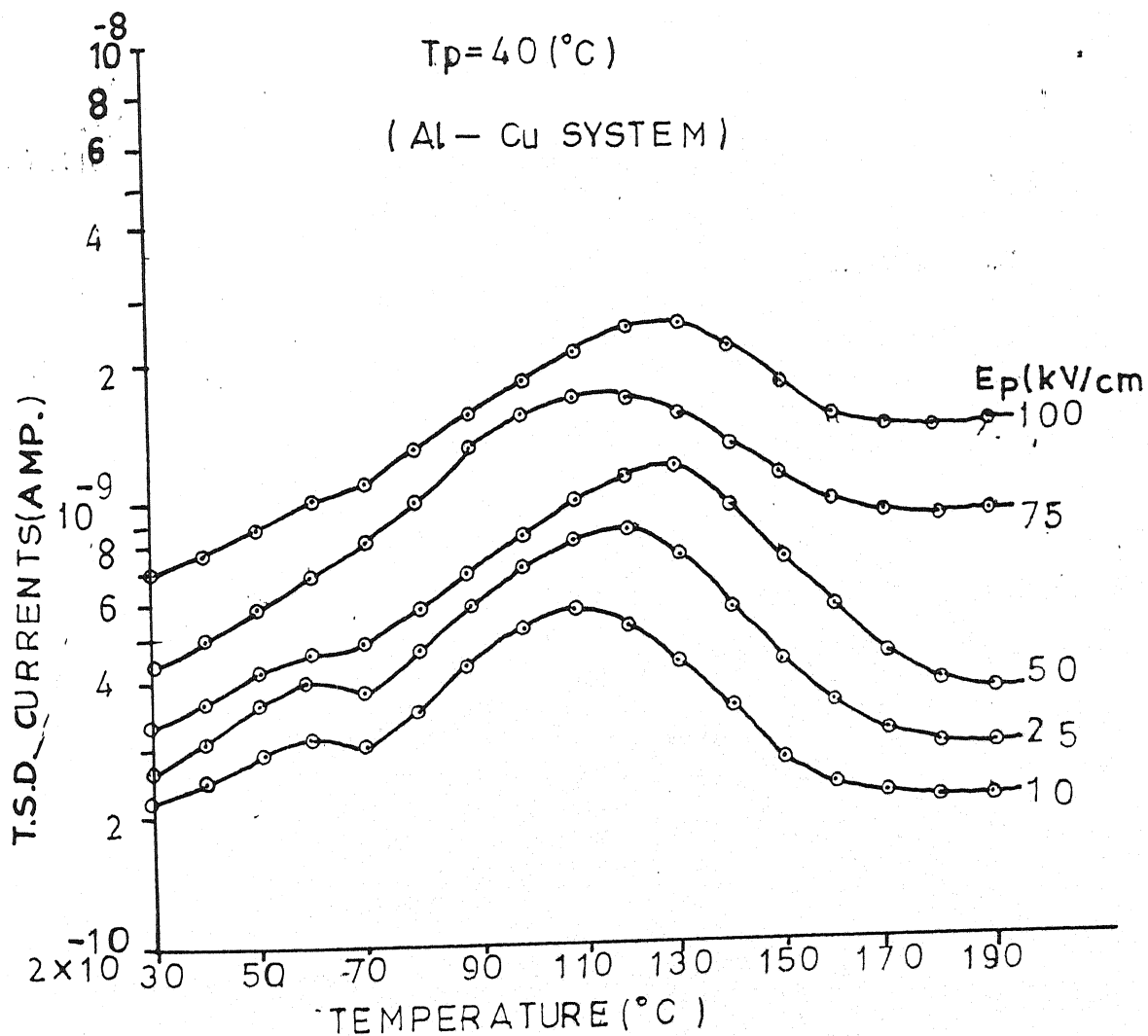


Figure No. 4.21

Thermally Stimulated Discharge Currents (T.S.D.C.) for Polyvinylidene fluoride Samples ($20 \mu\text{m}$) poled at $T_p = 40^{\circ}\text{C}$ with different polarisation fields (i.e. 10, 25, 50, 75 and 100 kV/cm) for Al - Cu system.

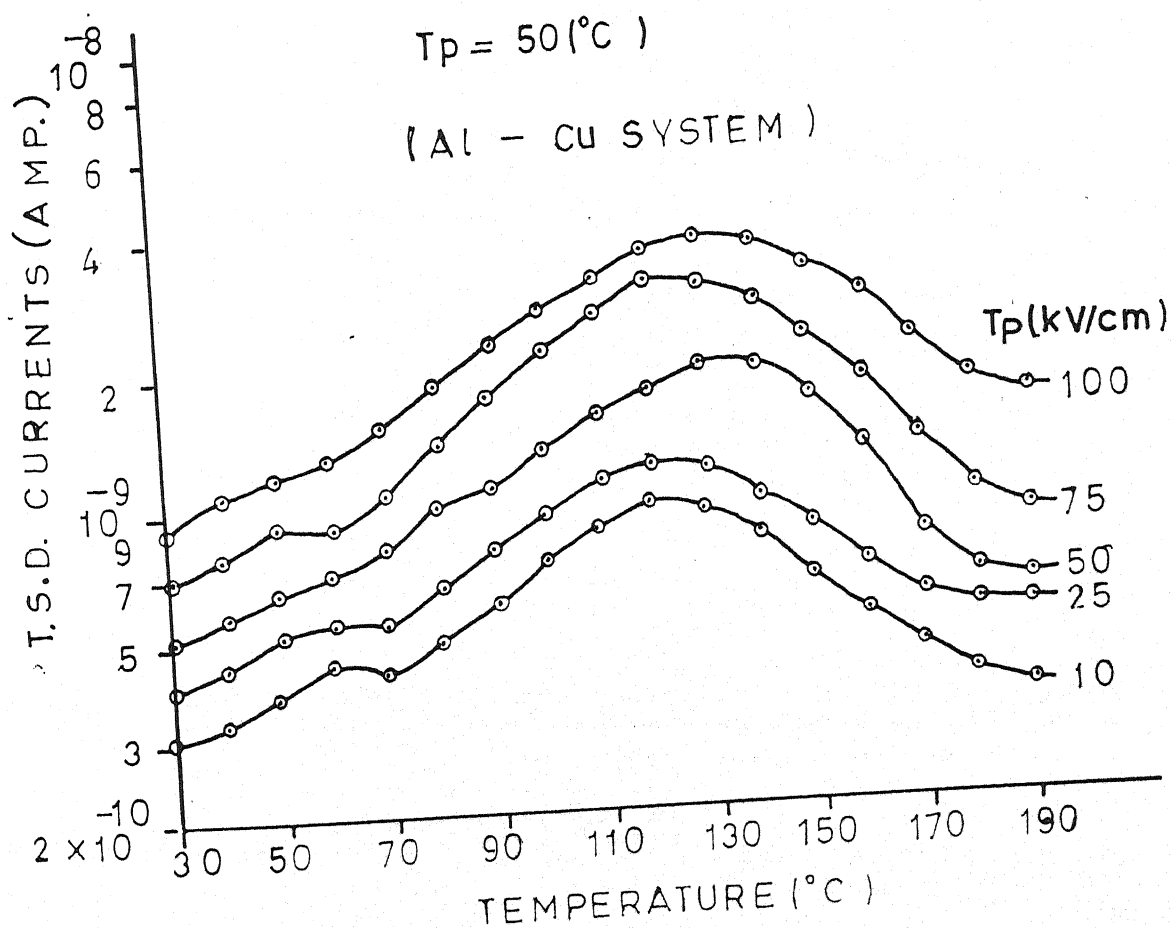


Figure No. 4.22
Thermally Stimulated Discharge Currents (T.S.D.C.) for Polyvinylidene fluoride Samples ($20\text{ }\mu\text{m}$) poled at $T_p = 50^{\circ}\text{C}$ with different polarisation fields (i.e. 10, 25, 50, 75 and 100 kV/cm) for Al - Cu system.

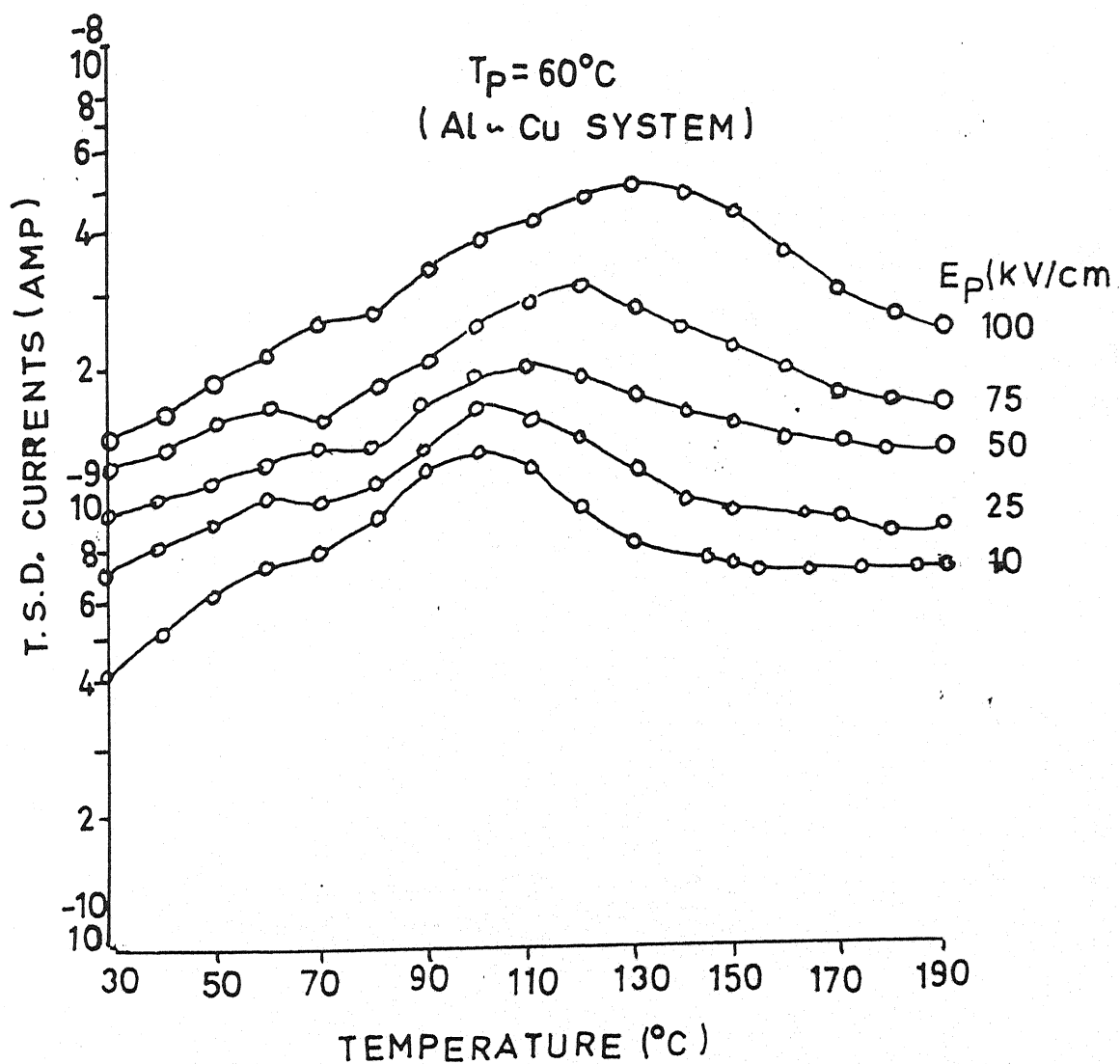


Figure No. 4.23

Thermally Stimulated Discharge Currents (T.S.D.C.) for Polyvinylidene fluoride Samples ($20\ \mu\text{m}$) poled at $T_p = 60^\circ\text{C}$ with different polarisation fields (i.e. 10, 25, 50, 75 and 100 kV/cm) for Al - Cu system.

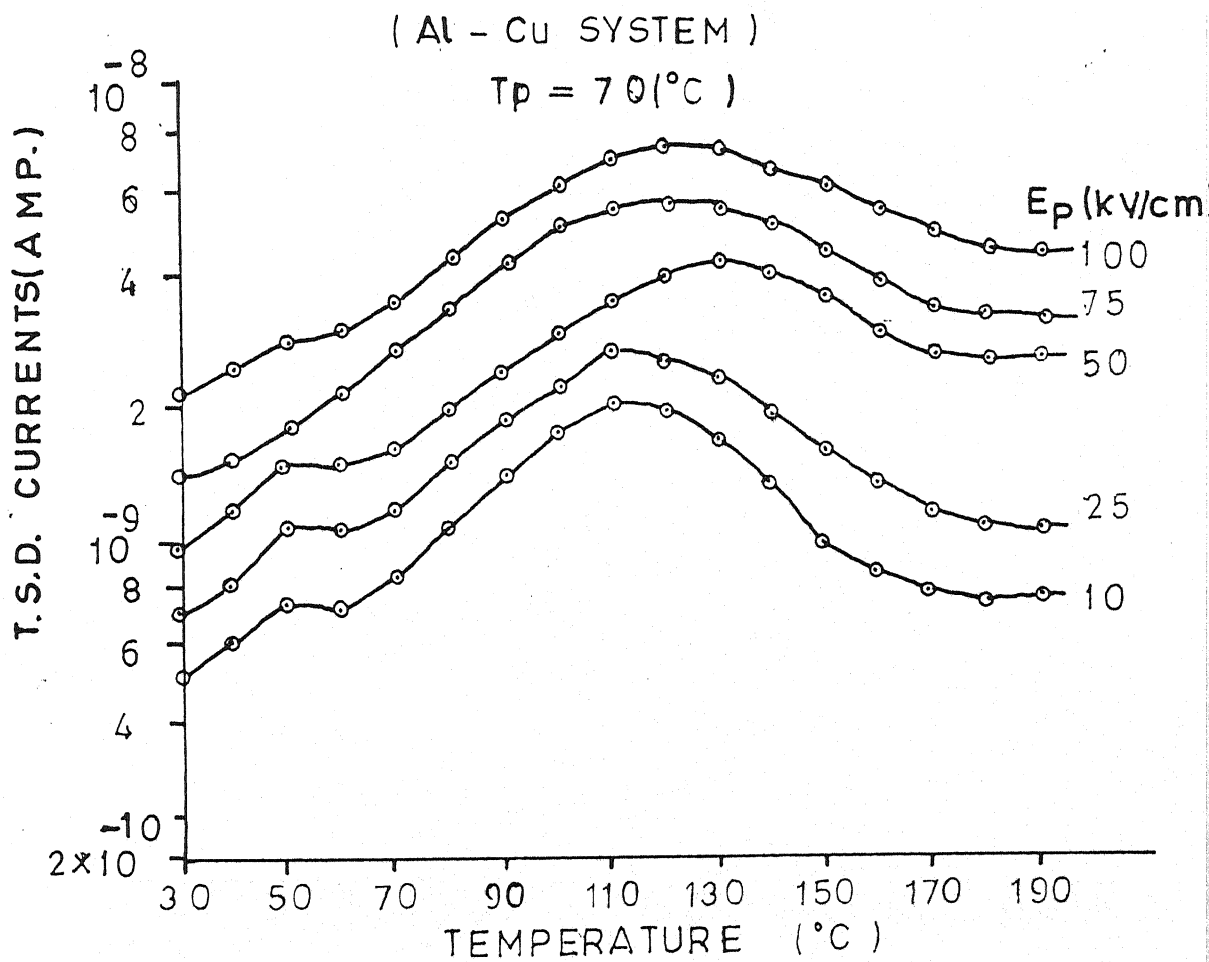


Figure No. 4.24
 Thermally Stimulated Discharge Currents (T.S.D.C.) for Polyvinylidene fluoride Samples ($20\ \mu\text{m}$) poled at $T_p = 70^{\circ}\text{C}$ with different polarisation fields (i.e. 10, 25, 50, 75 and 100 kV/cm) for Al - Cu system.

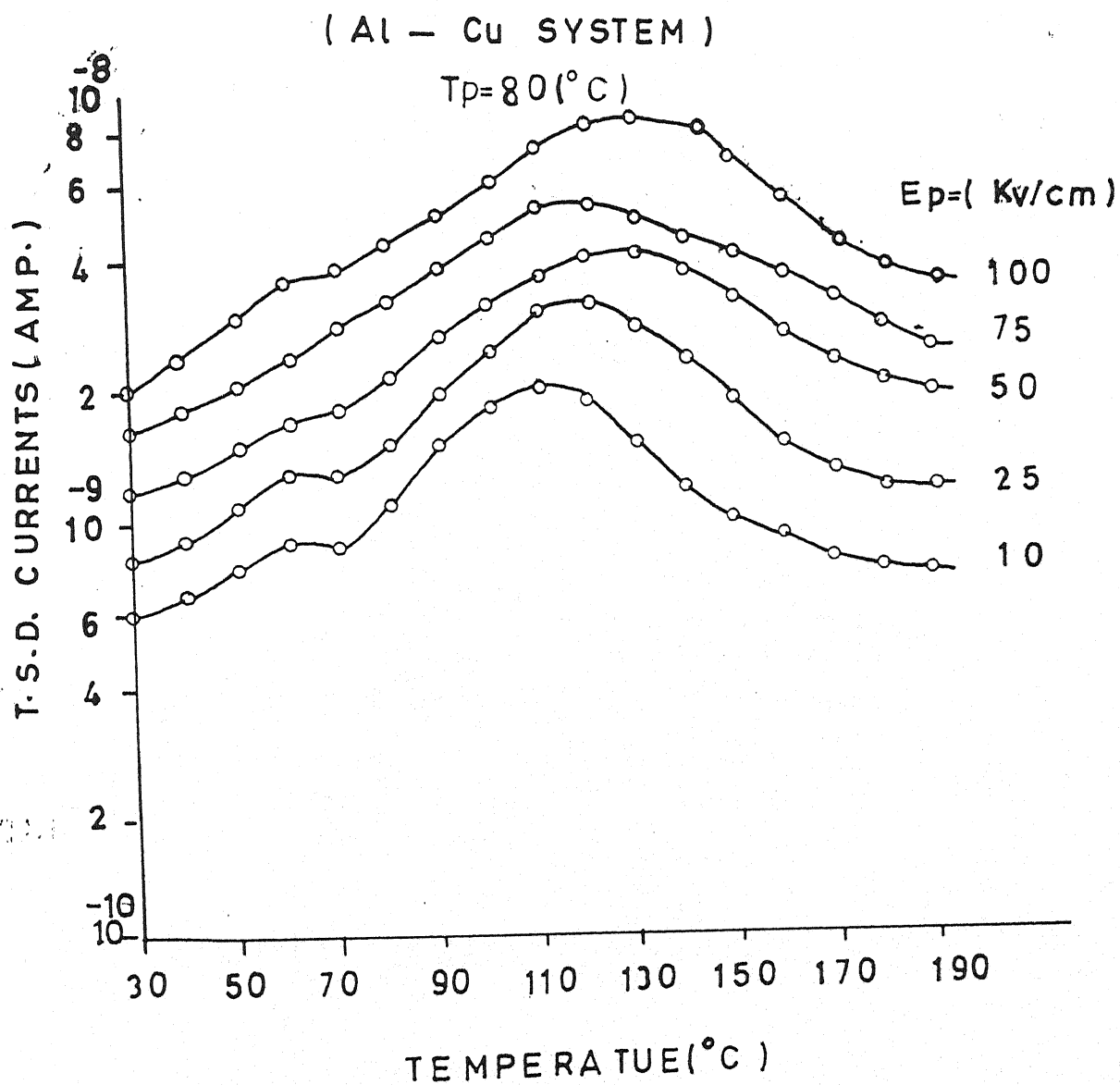


Figure No. 4.25

Thermally Stimulated Discharge Currents (T.S.D.C.) for Polyvinylidene fluoride Samples ($20 \mu\text{m}$) poled at $T_p = 80^{\circ}\text{C}$ with different polarisation fields (i.e. 10, 25, 50, 75 and 100 kV/cm) for Al - Cu system.

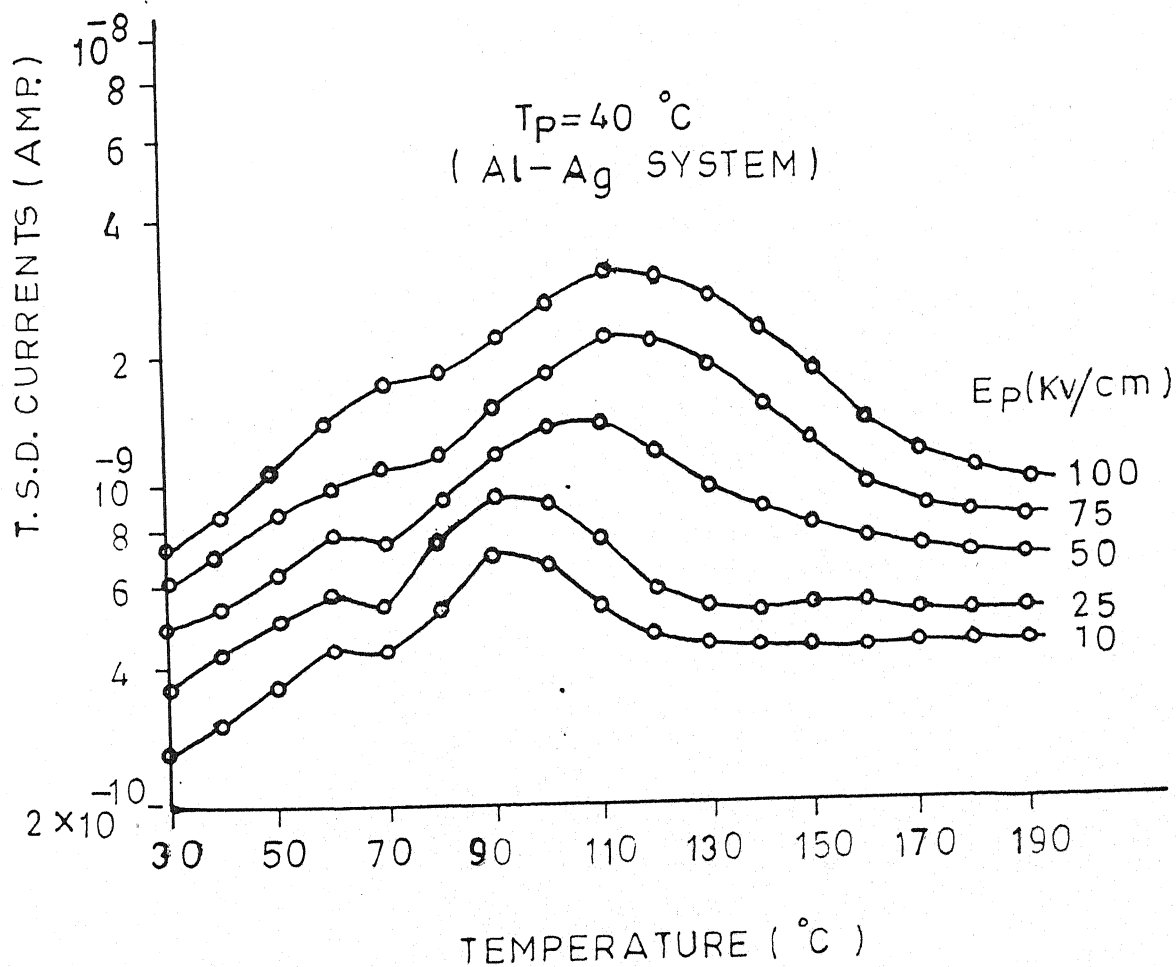


Figure No. 4.26
Thermally Stimulated Discharge Currents (T.S.D.C.) for Polyvinylidene fluoride Samples ($20 \mu\text{m}$) poled at $T_p = 40^\circ\text{C}$ with different polarisation fields (i.e. 10, 25, 50, 75 and 100 kV/cm) for Al - Ag system.

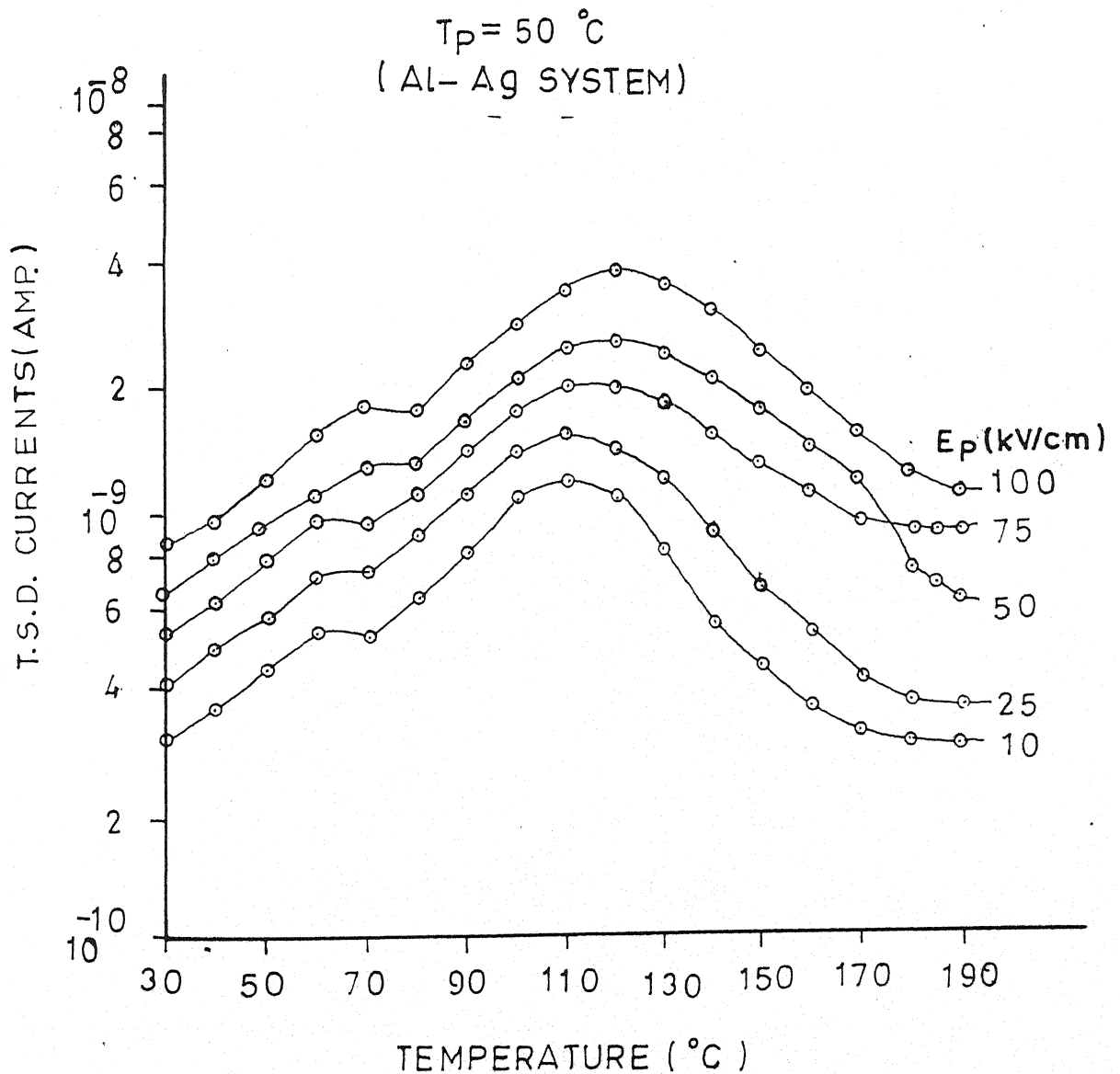


Figure No. 4.27
Thermally Stimulated Discharge Currents (T.S.D.C.) for Polyvinylidene fluoride Samples ($20\ \mu\text{m}$) poled at $T_p = 50^\circ\text{C}$ with different polarisation fields (i.e. 10, 25, 50, 75 and 100 kV/cm) for Al - Ag system.

$T_p = 60^\circ\text{C}$ (Al-Ag SYSTEM)

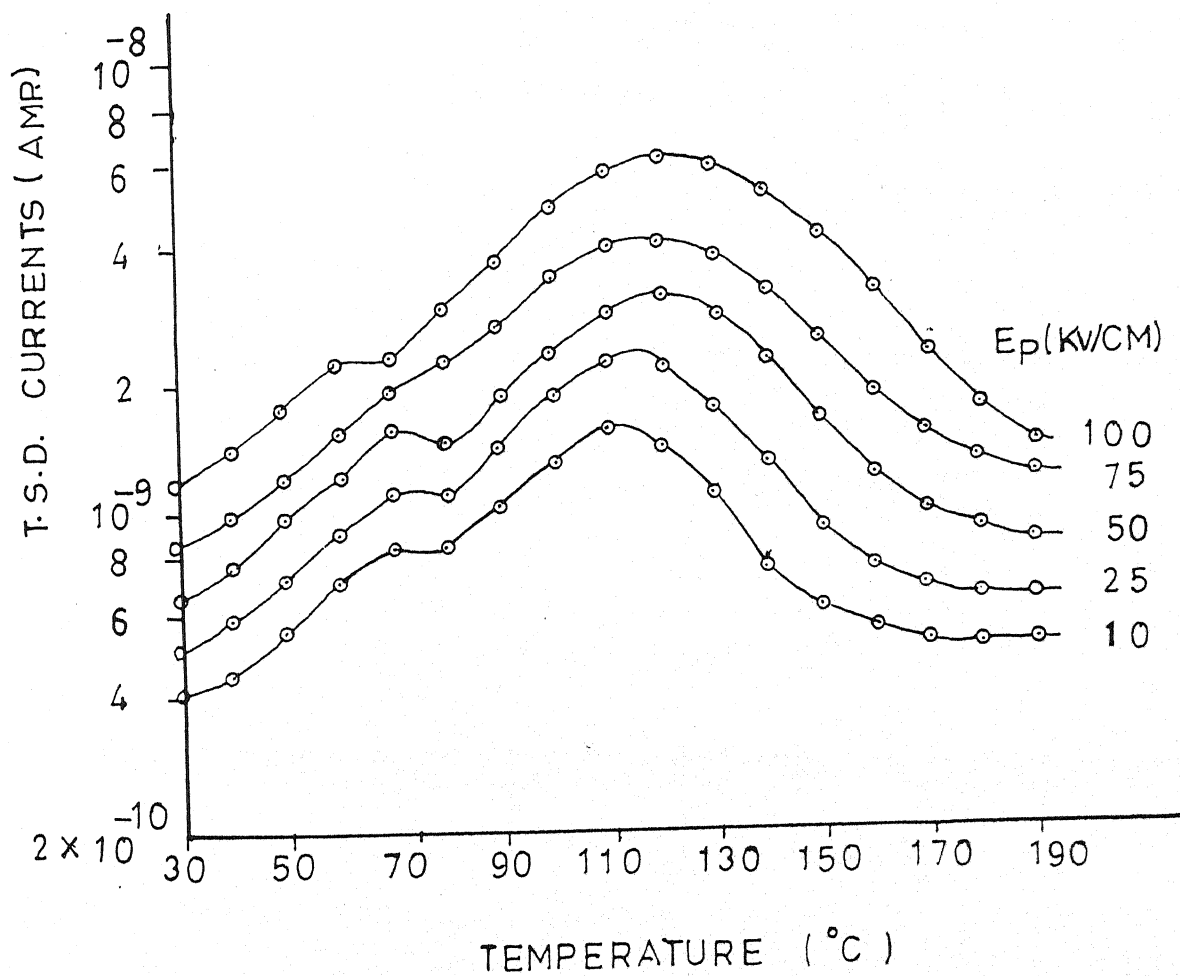


Figure No. 4.28

Thermally Stimulated Discharge Currents (T.S.D.C.) for Polyvinylidene fluoride Samples ($20\ \mu\text{m}$) poled at $T_p = 60^\circ\text{C}$ with different polarisation fields (i.e. 10, 25, 50, 75 and 100 kV/cm) for Al - Ag system.

$T_p = 70^\circ\text{C}$ (Al-Ag SYSTEM)

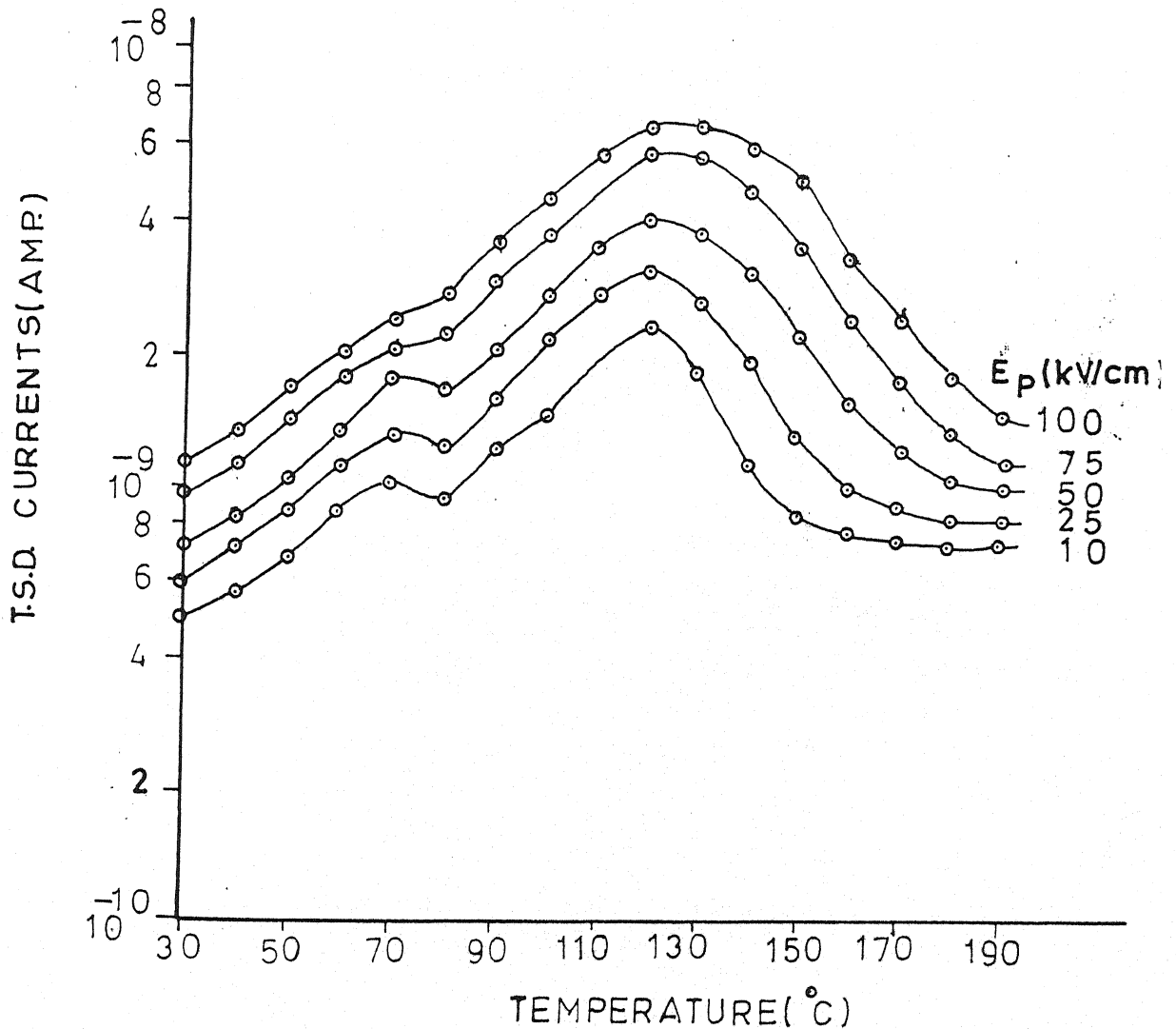


Figure No. 4.29

Thermally Stimulated Discharge Currents (T.S.D.C.) for Polyvinylidene fluoride Samples ($20\ \mu\text{m}$) poled at $T_p = 70^\circ\text{C}$ with different polarisation fields (i.e. 10, 25, 50, 75 and 100 kV/cm) for Al - Ag system.

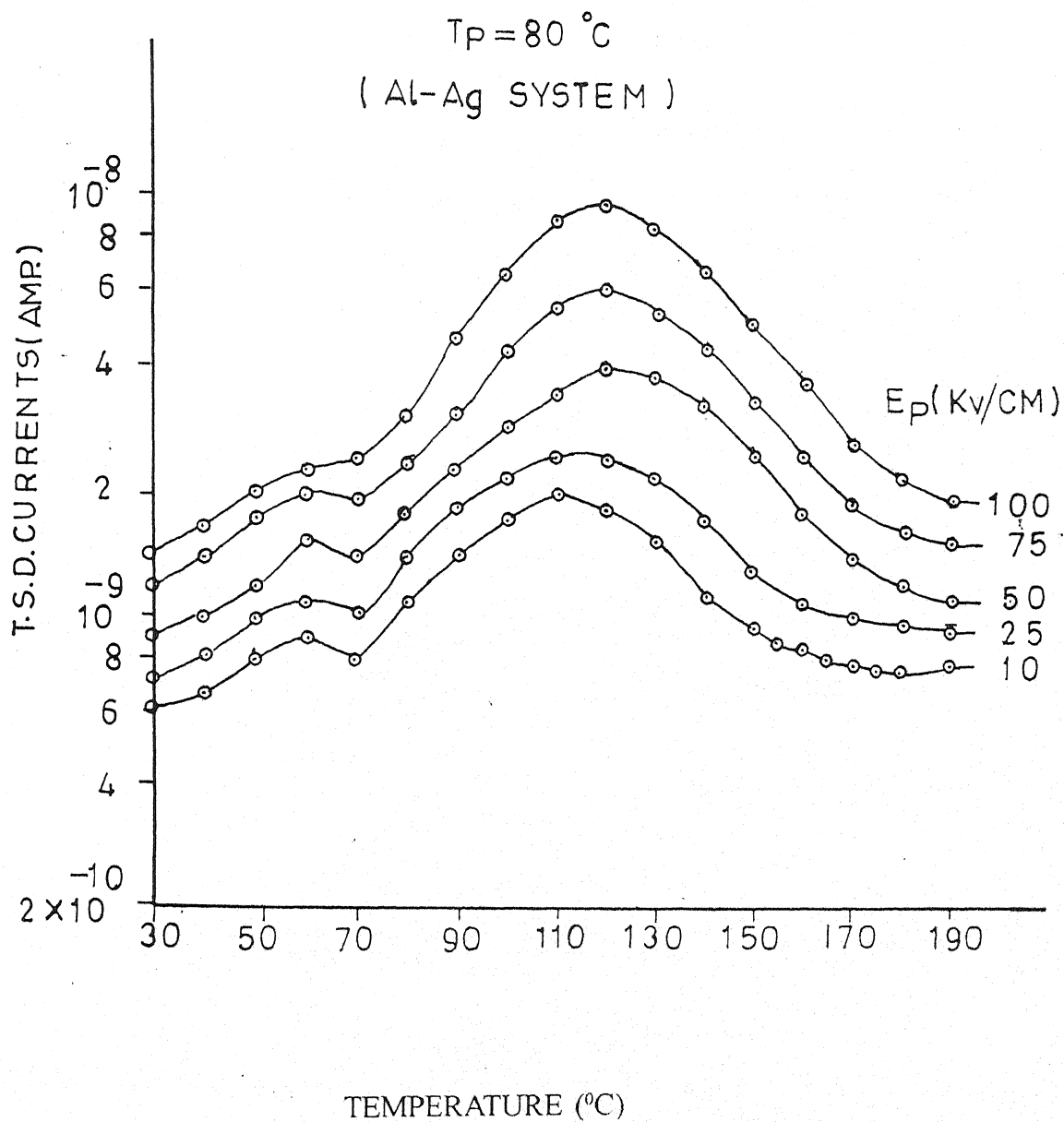


Figure No. 4.30

Thermally Stimulated Discharge Currents (T.S.D.C.) for Polyvinylidene fluoride Samples ($20\ \mu\text{m}$) poled at $T_p = 80^\circ\text{C}$ with different polarisation fields (i.e. 10, 25, 50, 75 and 100 kV/cm) for Al - Ag system.

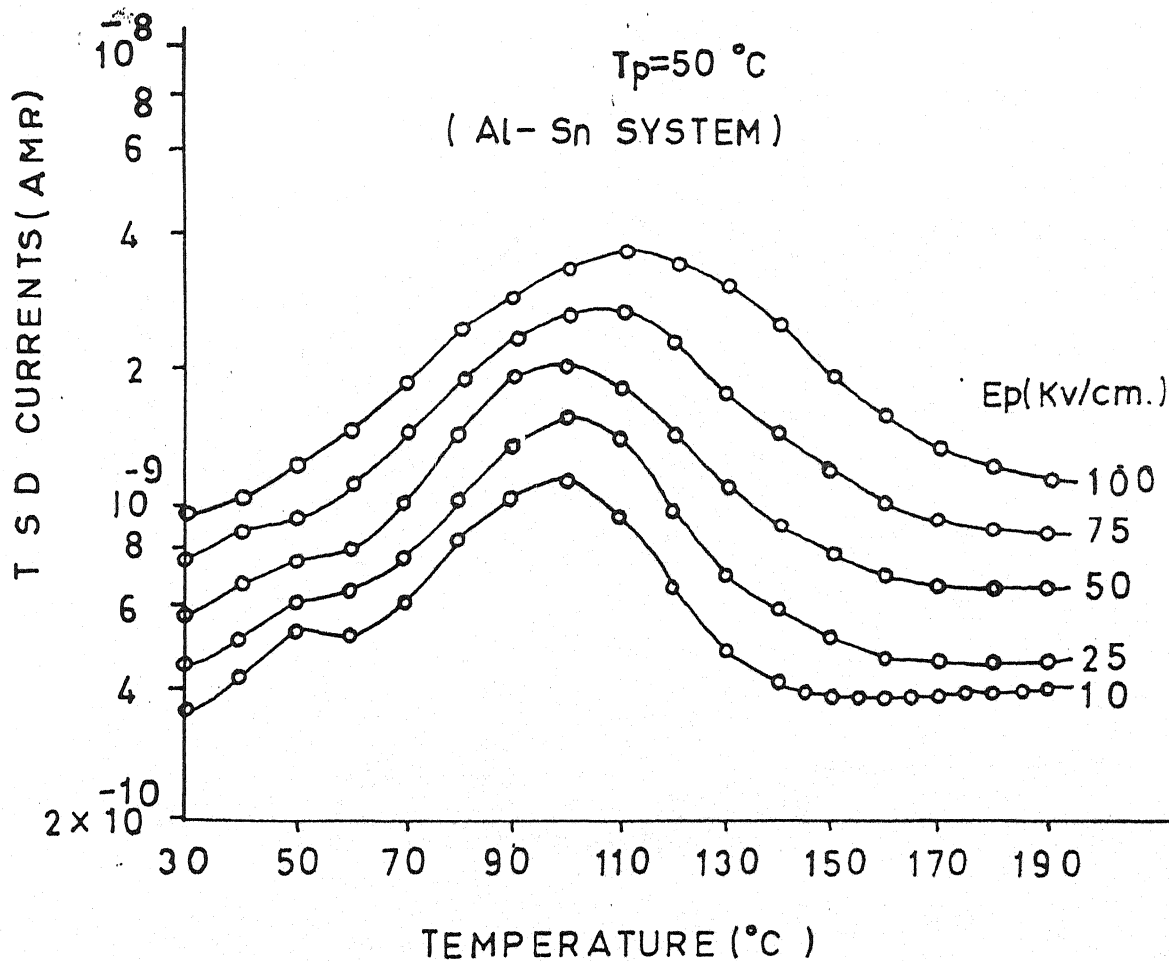


Figure No. 4.31
Thermally Stimulated Discharge Currents (T.S.D.C.) for Polyvinylidene fluoride Samples ($20\ \mu\text{m}$) poled at $T_p = 50^\circ\text{C}$ with different polarisation fields (i.e. 10, 25, 50, 75 and 100 kV/cm) for Al - Sn system.

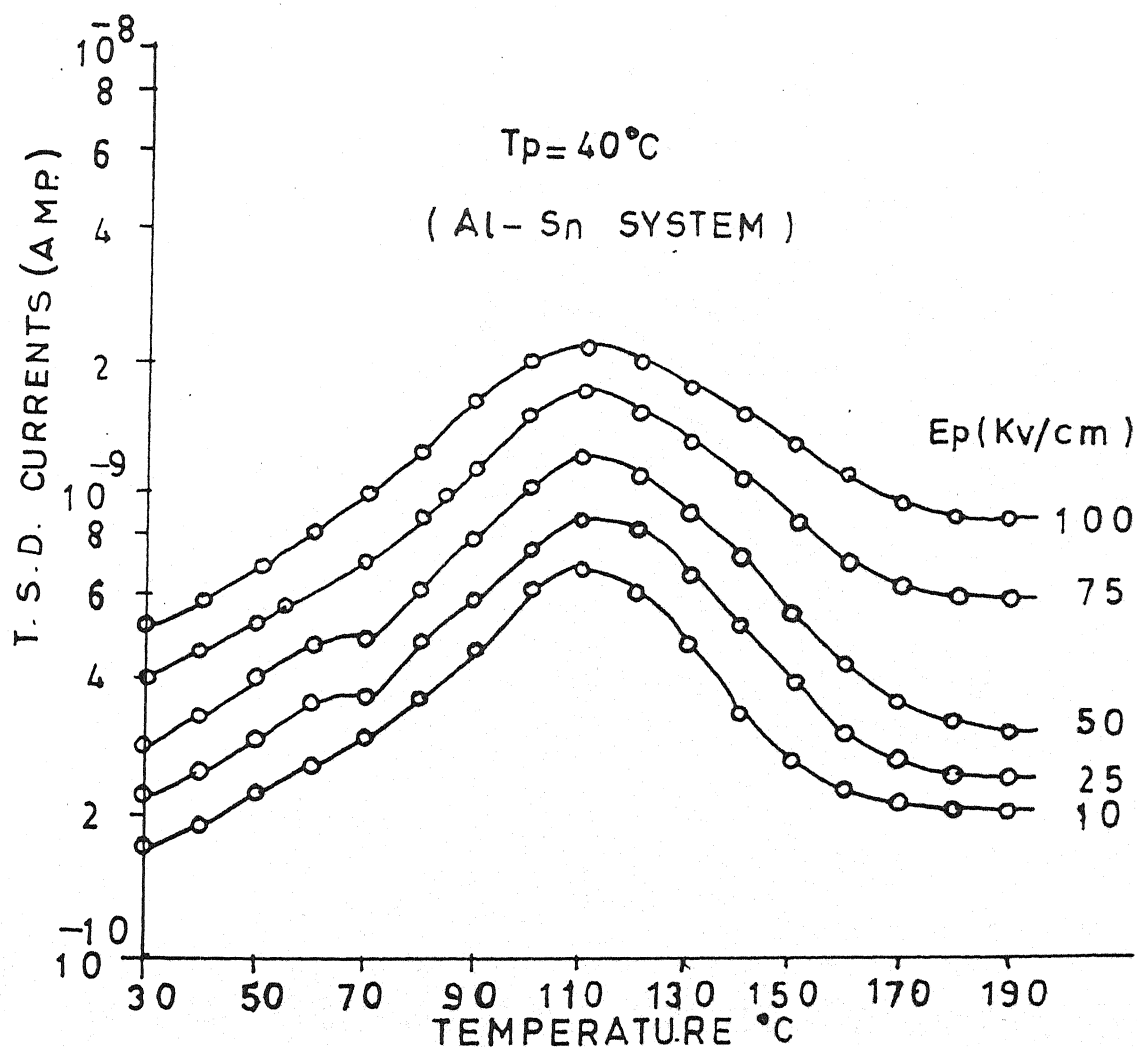


Figure No. 4.32
Thermally Stimulated Discharge Currents (T.S.D.C.) for Polyvinylidene fluoride Samples (20 μm) poled at $T_p = 40^\circ\text{C}$ with different polarisation fields (i.e. 10, 25, 50, 75 and 100 kV/cm) for Al - Sn system.

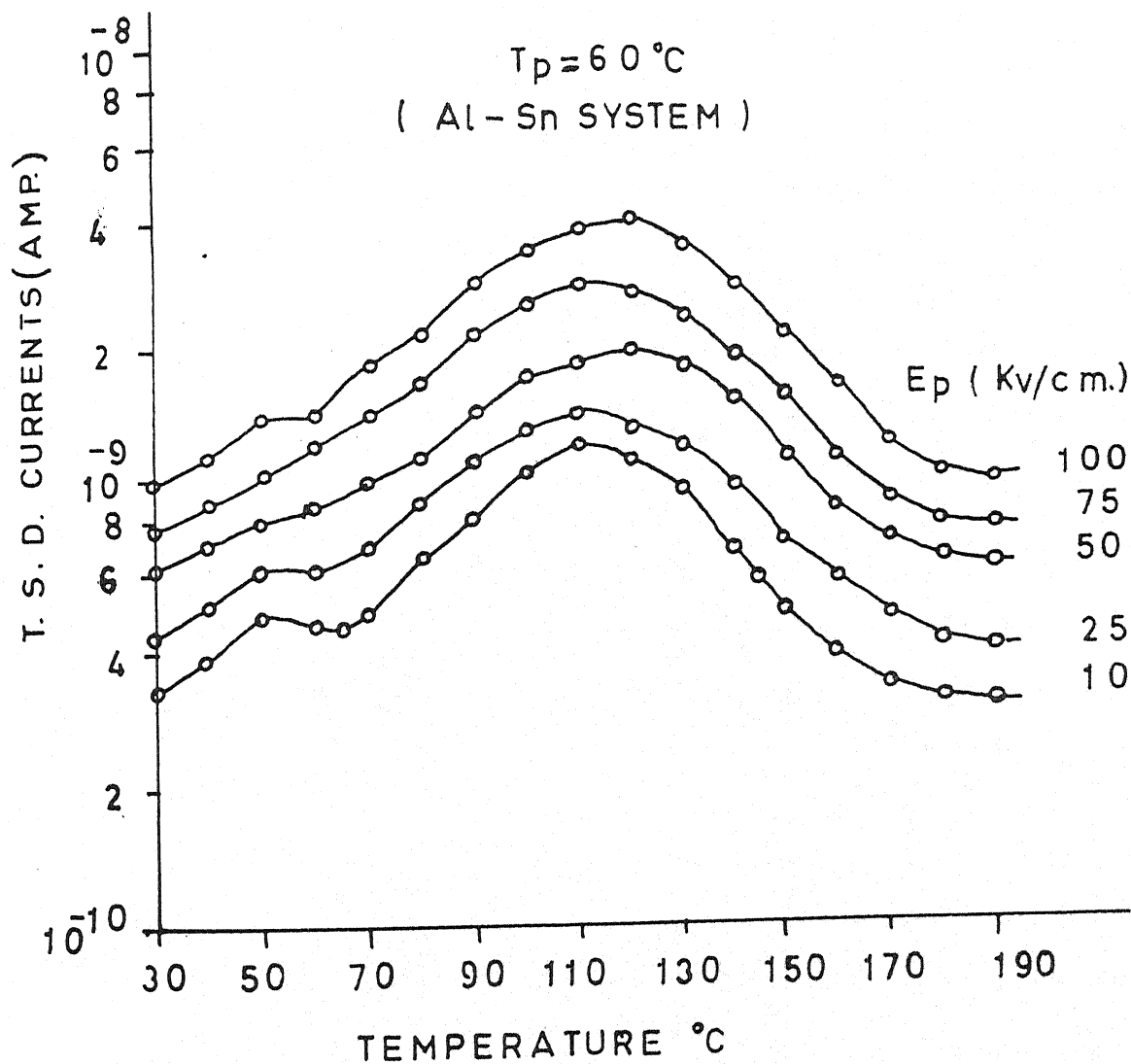


Figure No. 4.33
Thermally Stimulated Discharge Currents (T.S.D.C.) for Polyvinylidene fluoride Samples ($20\ \mu\text{m}$) poled at $T_p = 60^\circ\text{C}$ with different polarisation fields (i.e. 10, 25, 50, 75 and 100 kV/cm) for Al - Sn system.

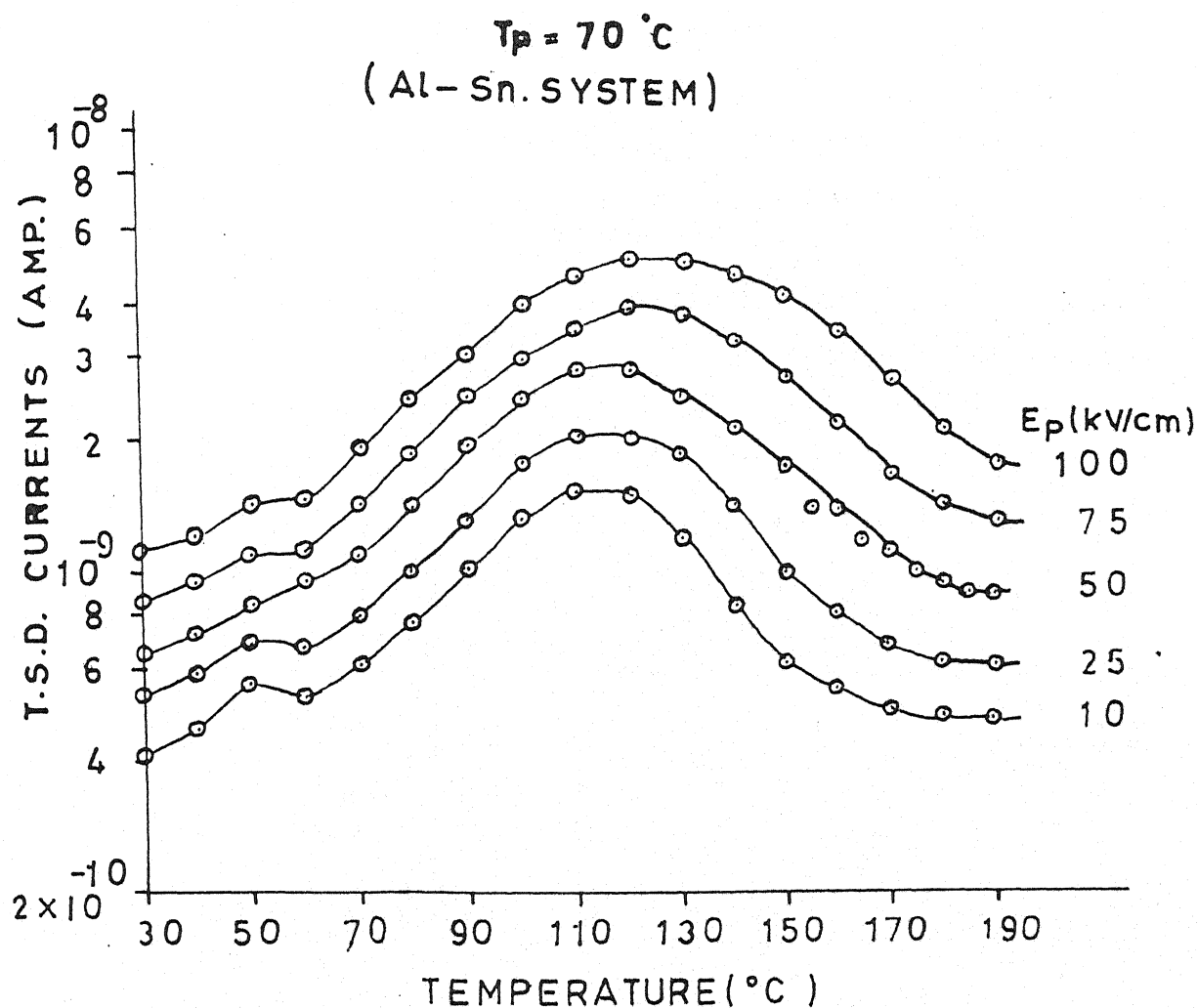


Figure No. 4.34
Thermally Stimulated Discharge Currents (T.S.D.C.) for Polyvinylidene fluoride Samples ($20\ \mu\text{m}$) poled at $T_p = 70^\circ\text{C}$ with different polarisation fields (i.e. 10, 25, 50, 75 and 100 kV/cm) for Al - Sn system.

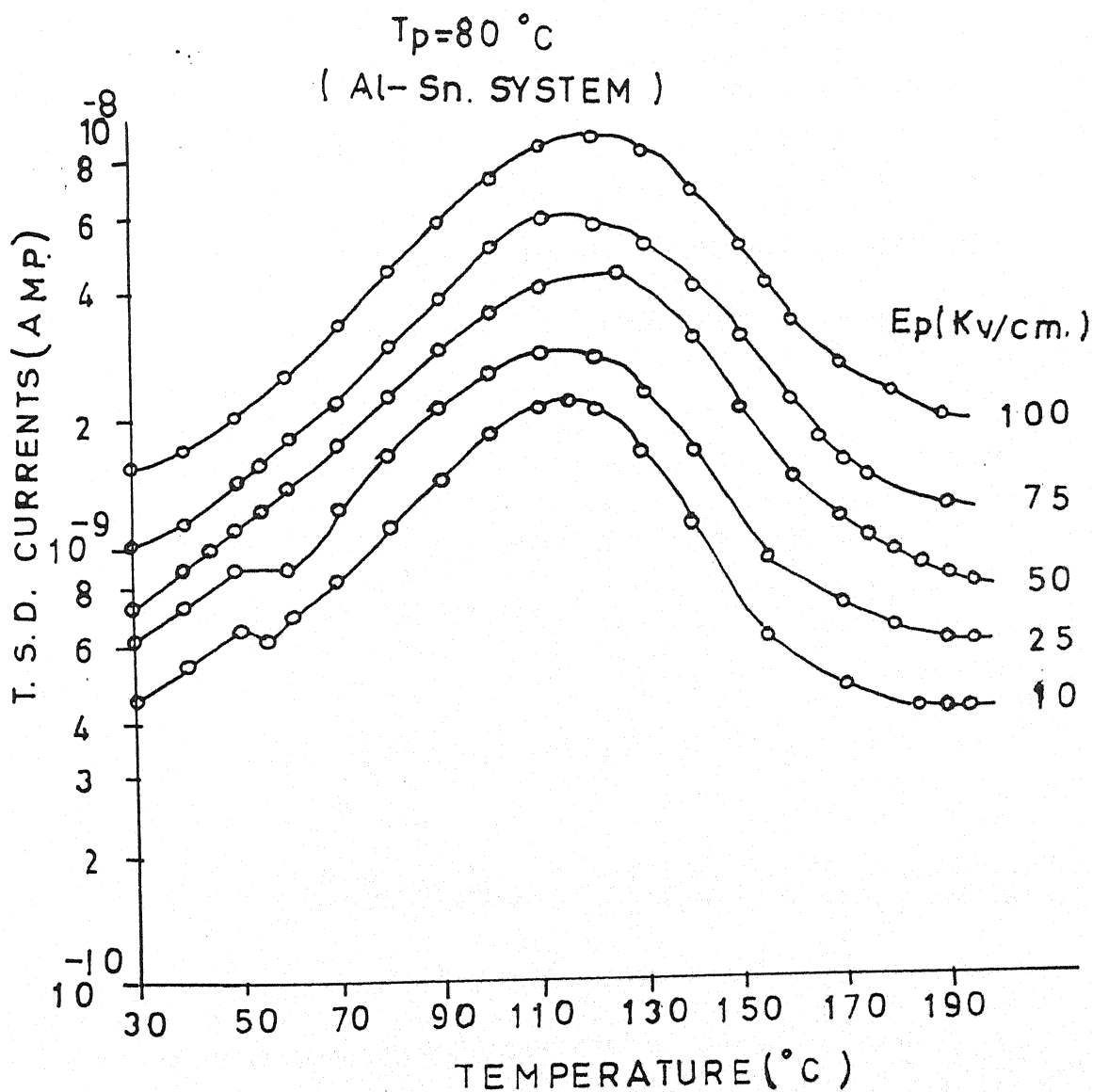


Figure No. 4.35
Thermally Stimulated Discharge Currents (T.S.D.C.) for Polyvinylidene fluoride Samples ($20\ \mu\text{m}$) poled at $T_p = 80^\circ\text{C}$ with different polarisation fields (i.e. 10, 25, 50, 75 and 100 kV/cm) for Al - Sn system.

Ag-Ag and Sn-Sn) and dissimilar electrodes (Al-Cu, Al-Ag and Al-Sn) combinations respectively. Similarly, Figs. 4.36–4.55 and 4.56–4.70 represent TSDC spectra for PVDF films with constant poling fields, i.e. 10, 25, 50, 75 and 100 kV/cm) at different temperatures, i.e. 40, 50, 60, 70 and 80°C for similar (i.e., Al-Al, Cu-Cu, Ag-Ag and Sn-Sn) and dissimilar (i.e., Al-Cu, Al-Ag and Al-Sn) electrode configurations respectively. For comparison purpose and to observe the electrode effects at constant poling temperature and poling field, TSD spectra are shown in Figs. 4.71–4.75.

The initial rise (i.e., current versus $10^3/T$) curves for constant poling fields (i.e. 10, 50 and 100 kV/cm) at different poling temperature for Cu-Cu, Ag-Ag and Sn-Sn electrode systems and Al-Cu, Al-Ag and Al-Sn electrodes combinations are shown in Figs. 4.76–4.93. Also, Figs. 4.94–4.102 and 4.103–4.111 exhibit the initial rise curves for constant poling temperature (i.e. 40, 60 and 80°C) with various poling fields (i.e., 10, 25, 50, 75 and 100 kV/cm) for Cu-Cu, Ag-Ag, Sn-Sn, Al-Au, Al-Ag and Al-Sn electrode configurations. The values of activation energy are calculated with the help of these curves.

All the TSDC spectra of specimen polarized at different temperatures with different poling fields, consist of only one broad peak. The peak currents increased with increase in field strength. The variation of peak currents as a function of field strength shows a linear behaviour. The charge released can be computed by integrating the area under the TSDC

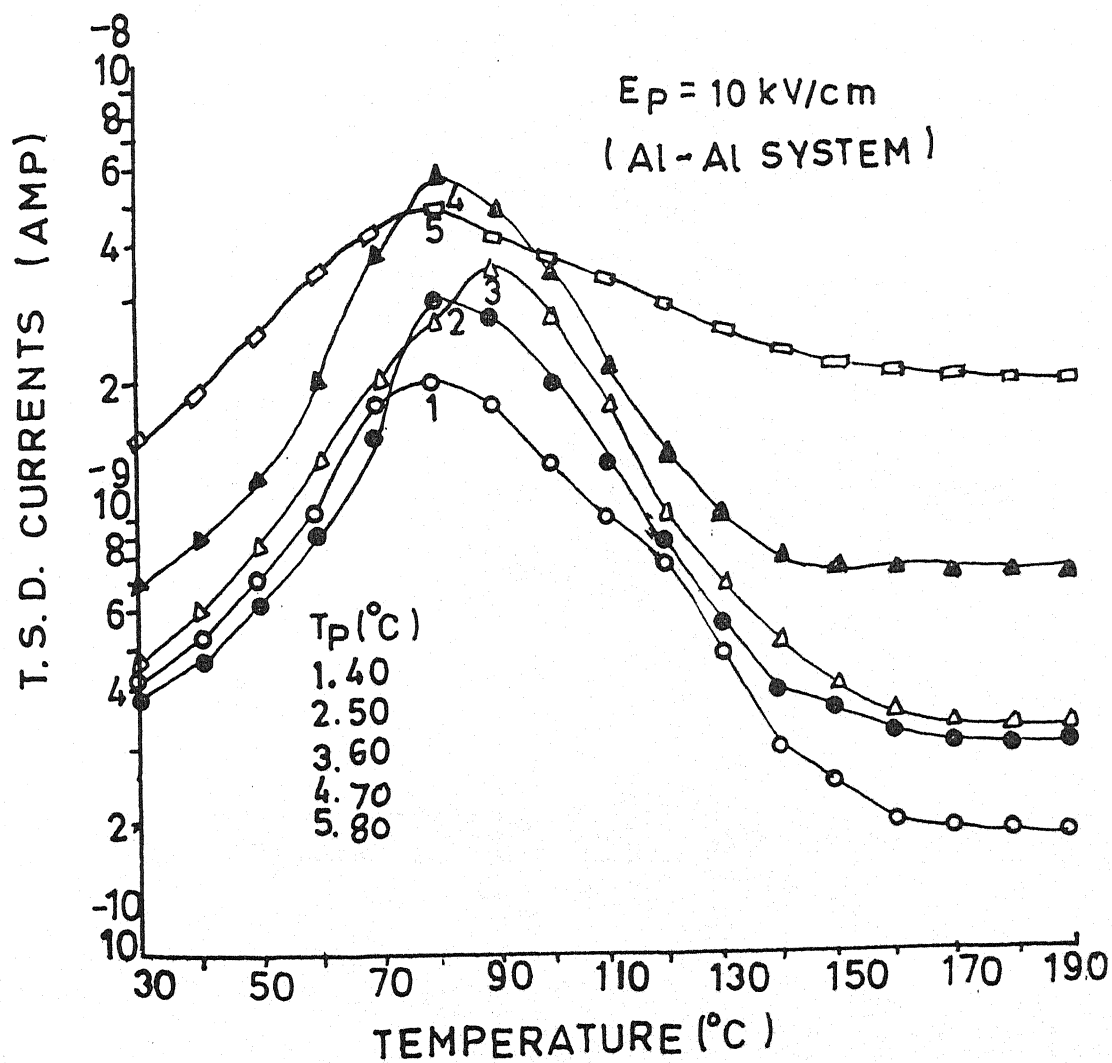


Figure No. 4.36

Thermally Stimulated Discharge Currents (T.S.D.C.) for Polyvinylidene fluoride Samples ($20 \mu\text{m}$) poled at $E_p = 10 \text{ kV/cm}$ with different polarisation Temperature (i.e. 40, 50, 60, 70 and 80°C) for Al-Al system.

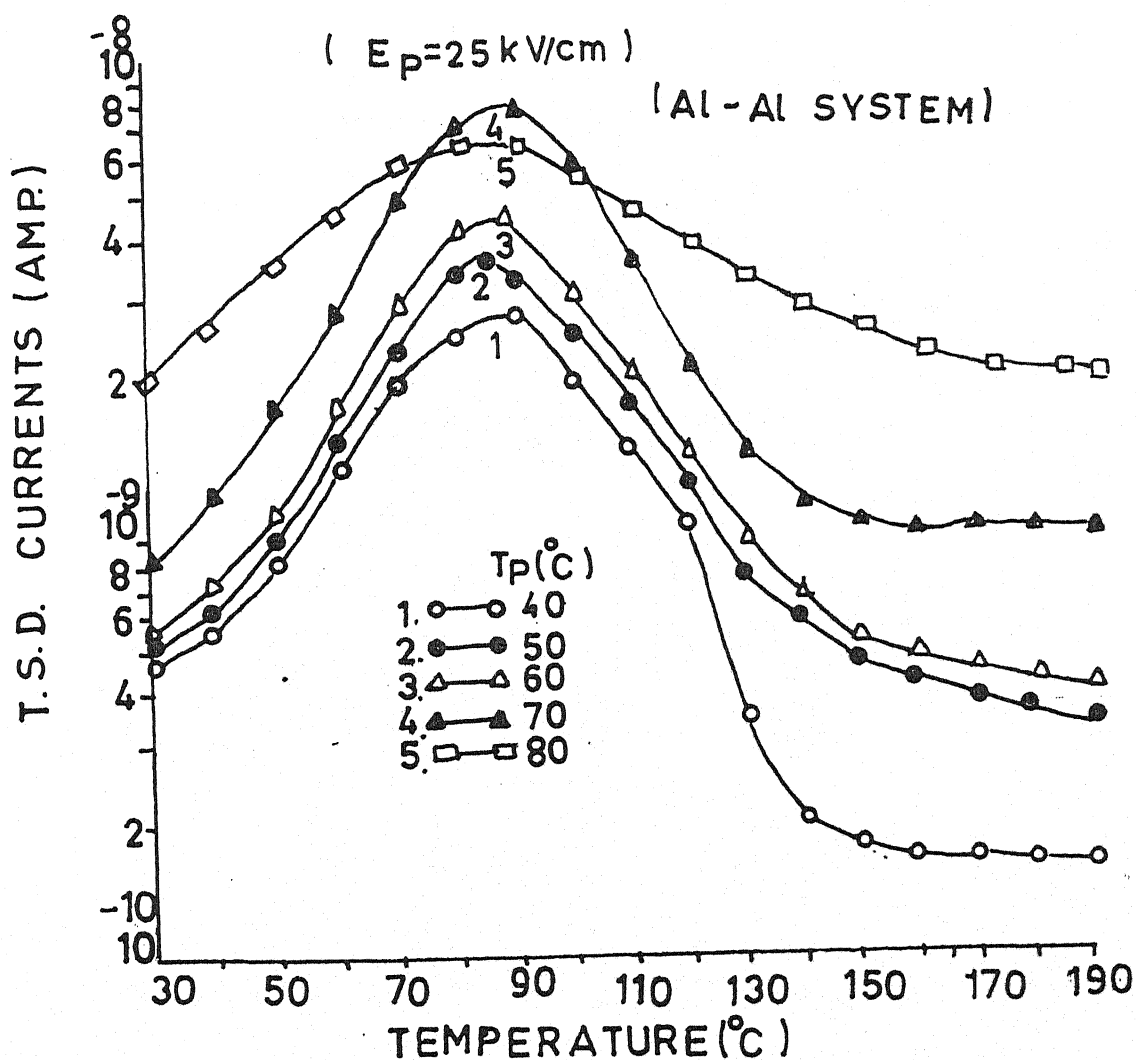


Figure No. 4.37

Thermally Stimulated Discharge Currents (T.S.D.C.) for Polyvinylidene fluoride Samples ($20 \mu\text{m}$) poled at $E_p = 25 \text{ kV/cm}$ with different polarisation Temperature (i.e. $40, 50, 60, 70$ and 80°C) for Al~Al system.

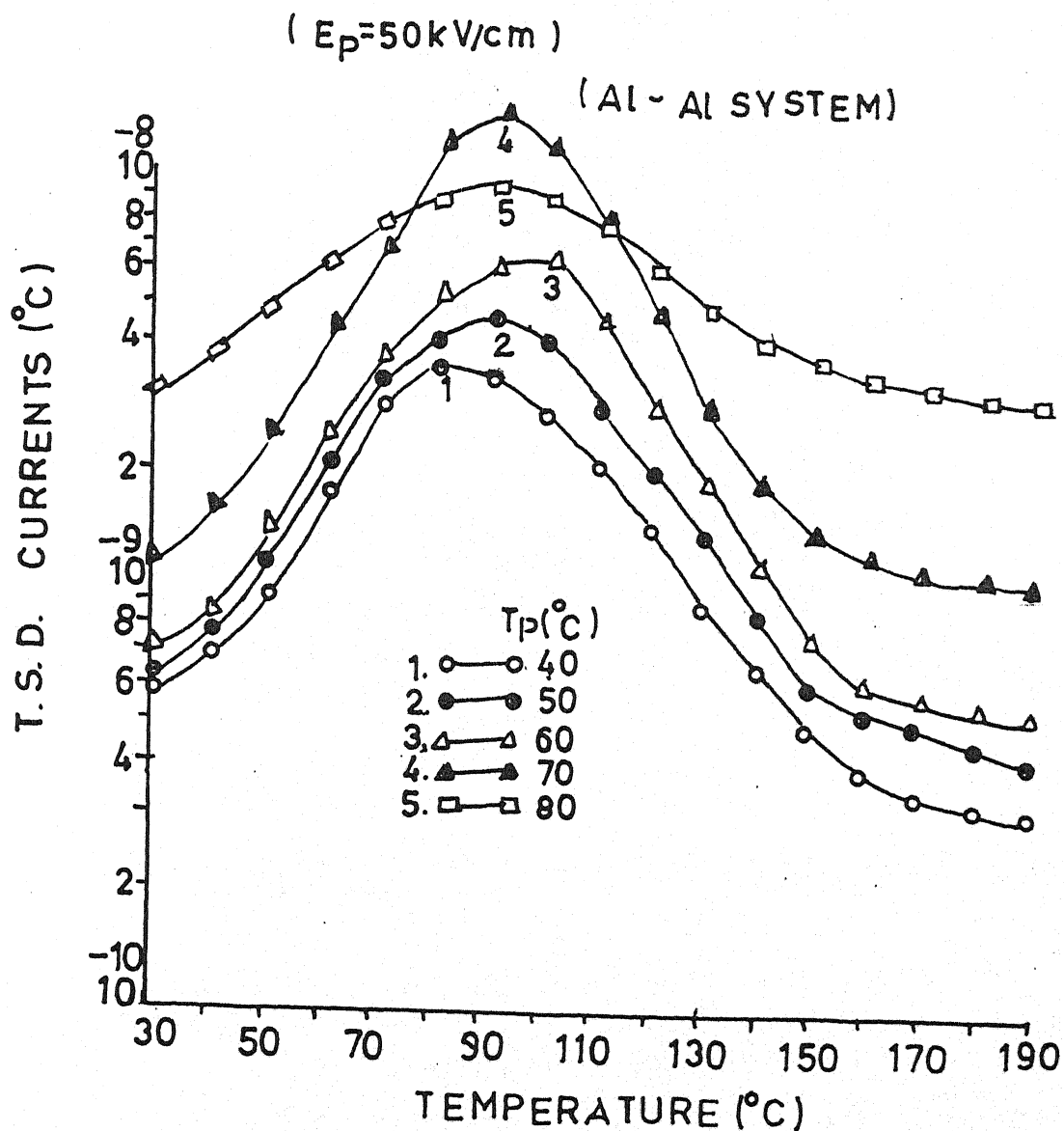


Figure No. 4.38

Thermally Stimulated Discharge Currents (T.S.D.C.) for Polyvinylidene fluoride Samples ($20 \mu\text{m}$) poled at $E_p = 50 \text{ kV/cm}$ with different polarisation Temperature (i.e. $40, 50, 60, 70$ and 80°C) for Al~Al system.

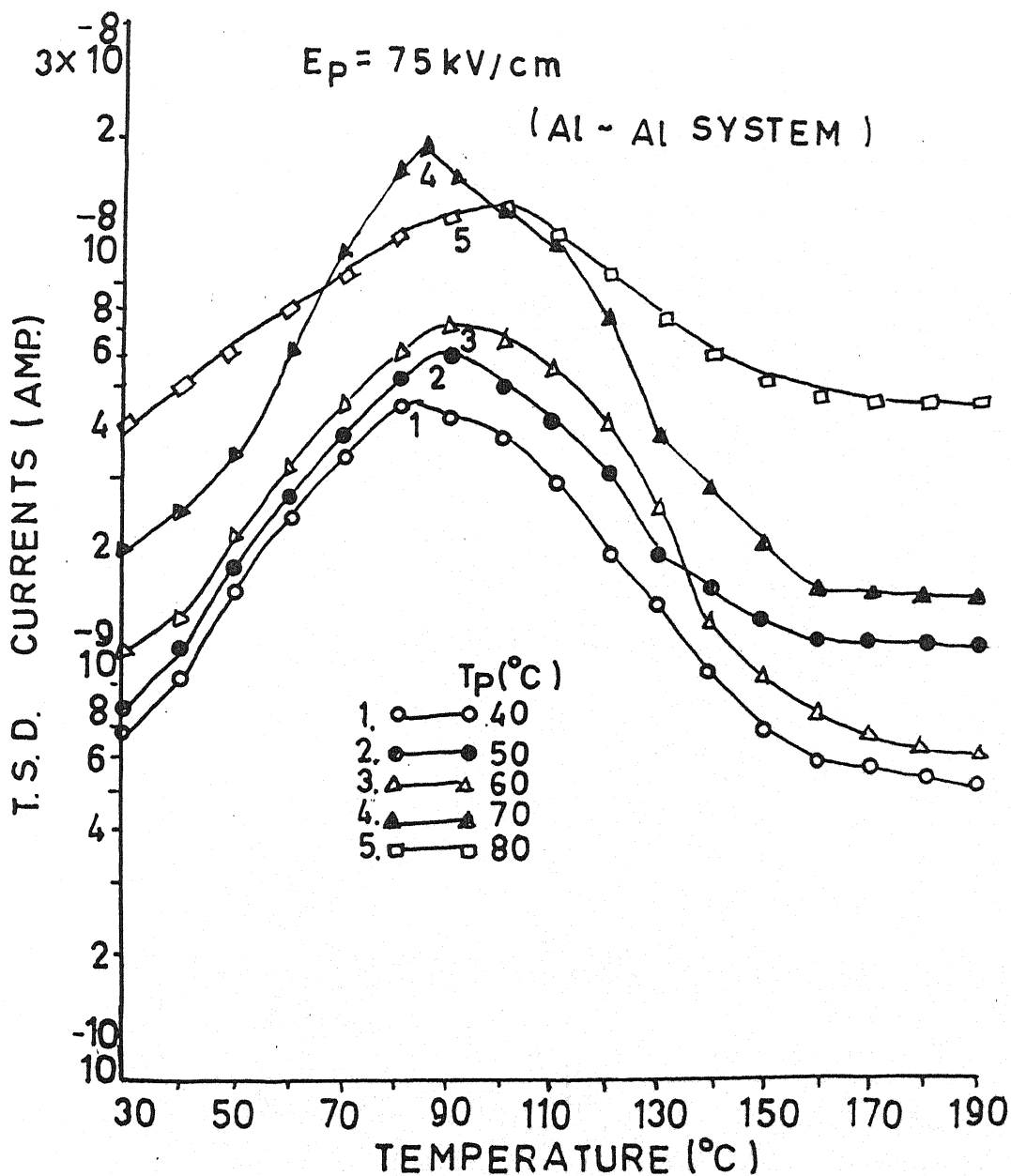


Figure No. 4.39

Thermally Stimulated Discharge Currents (T.S.D.C.) for Polyvinylidene fluoride Samples ($20 \mu\text{m}$) poled at $E_p = 75 \text{ kV/cm}$ with different polarisation Temperature (i.e. 40, 50, 60, 70 and 80°C) for Al~Al system.

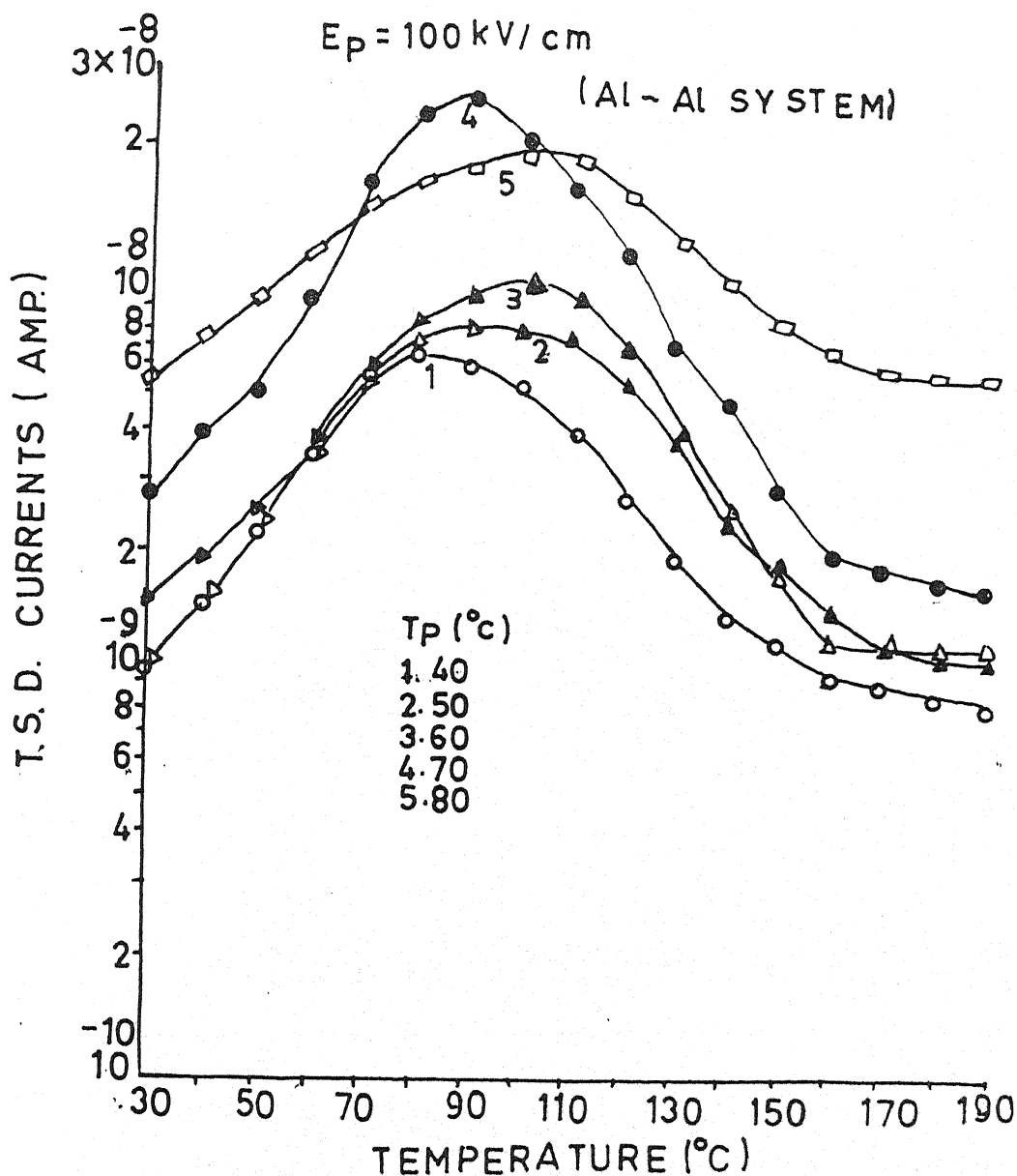


Figure No. 4.40
 Thermally Stimulated Discharge Currents (T.S.D.C.) for Polyvinylidene fluoride Samples ($20 \mu\text{m}$) poled at $E_p = 100 \text{ kV/cm}$ with different polarisation Temperature (i.e. 40, 50, 60, 70 and 80°C) for Al~Al system.

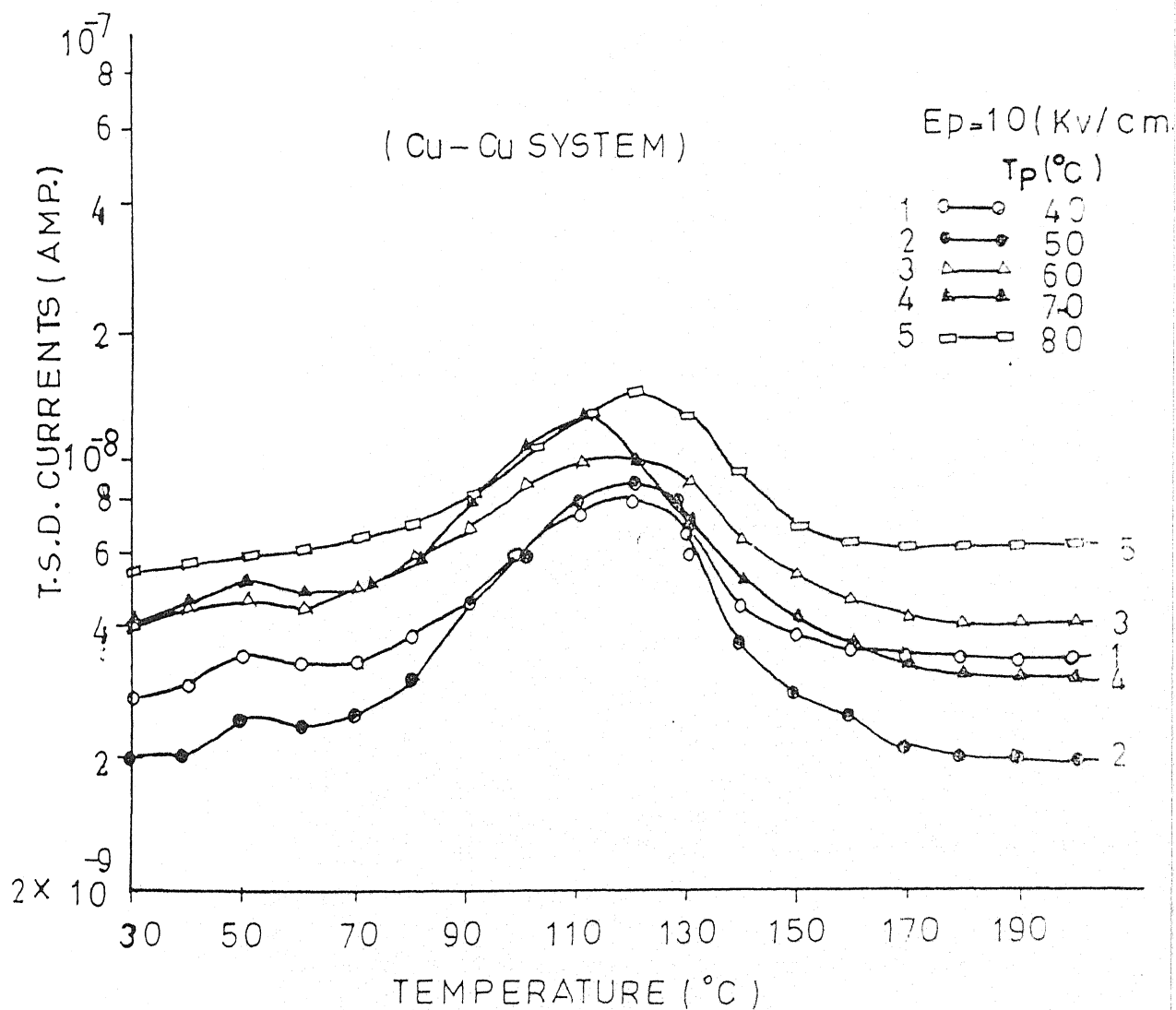


Figure No. 4.41
Thermally Stimulated Discharge Currents (T.S.D.C.) for Polyvinylidene fluoride Samples ($20 \mu\text{m}$) poled at $E_p = 10 \text{ kV/cm}$. with different polarisation Temperetures (i.e. 40, 50, 60, 70 and 80°C) for Cu-Cu system

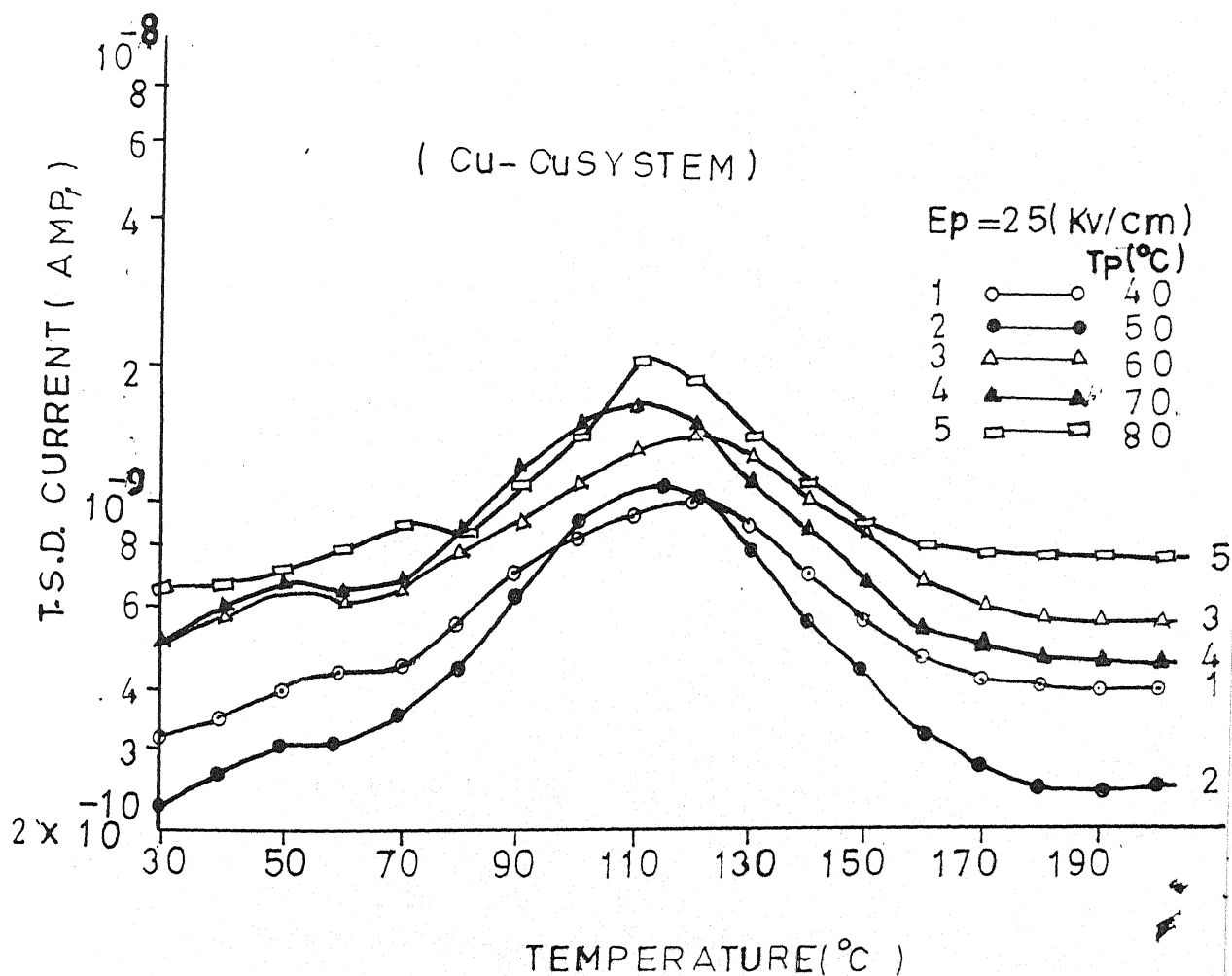


Figure No. 4.42

Thermally Stimulated Discharge Currents (T.S.D.C.) for Polyvinylidene fluoride Samples ($20 \mu\text{m}$) poled at $E_p = 25 \text{ kV/cm}$ with different polarisation Temperature (i.e. 40, 50, 60, 70 and 80°C) for Cu - Cu system.

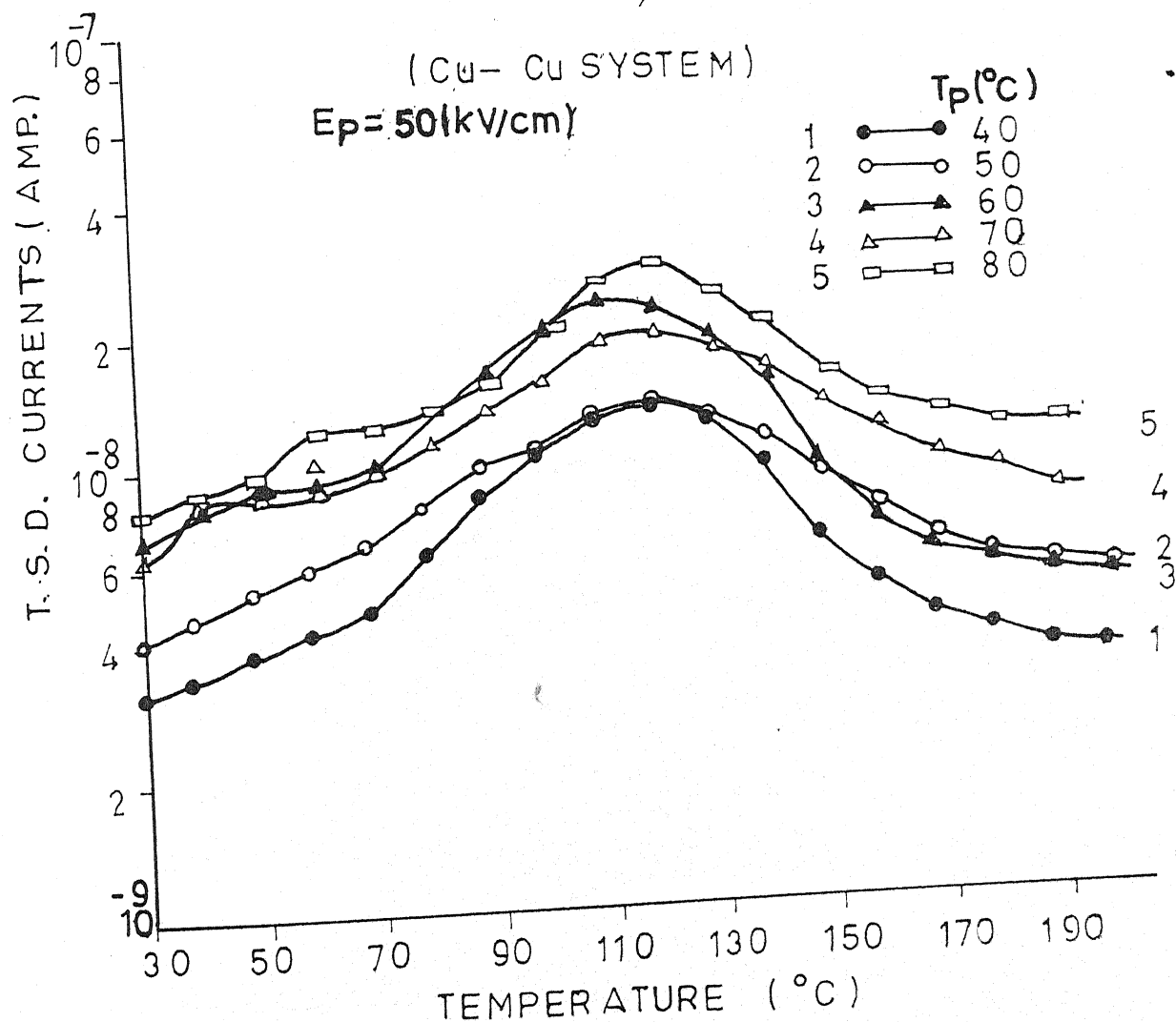


Figure No. 4.43
 Thermally Stimulated Discharge Currents (T.S.D.C.) for Polyvinylidene fluoride Samples ($20 \mu\text{m}$) poled at $E_p = 50 \text{ kV/cm}$ with different polarisation Temperature (i.e. 40, 50, 60, 70 and 80°C) for Cu - Cu system.

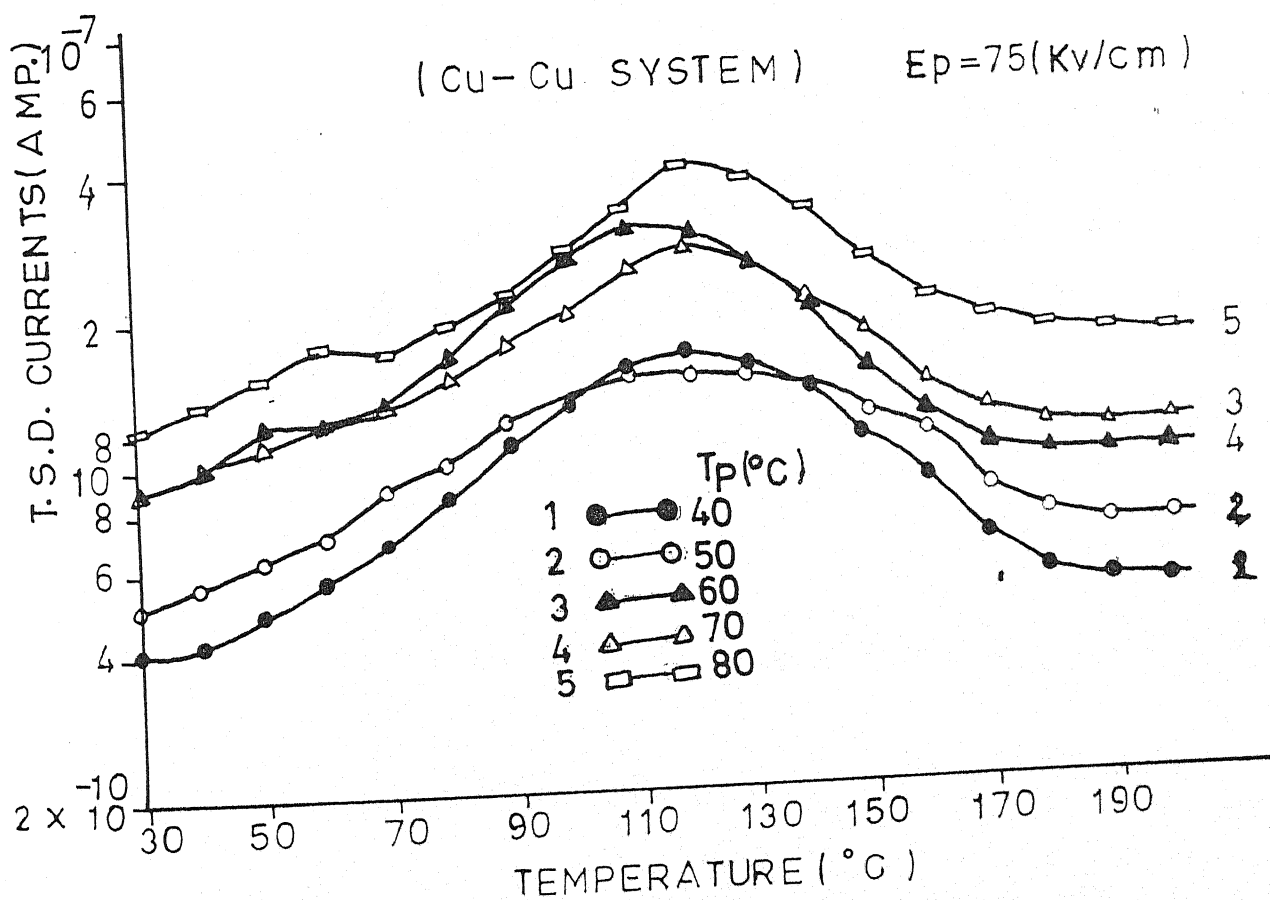


Figure No. 4.44
Thermally Stimulated Discharge Currents (T.S.D.C.) for Polyvinylidene fluoride Samples ($20 \mu\text{m}$) poled at $E_p = 75 \text{ kV/cm}$ with different polarisation Temperature (i.e. 40, 50, 60, 70 and 80°C) for Cu - Cu system.

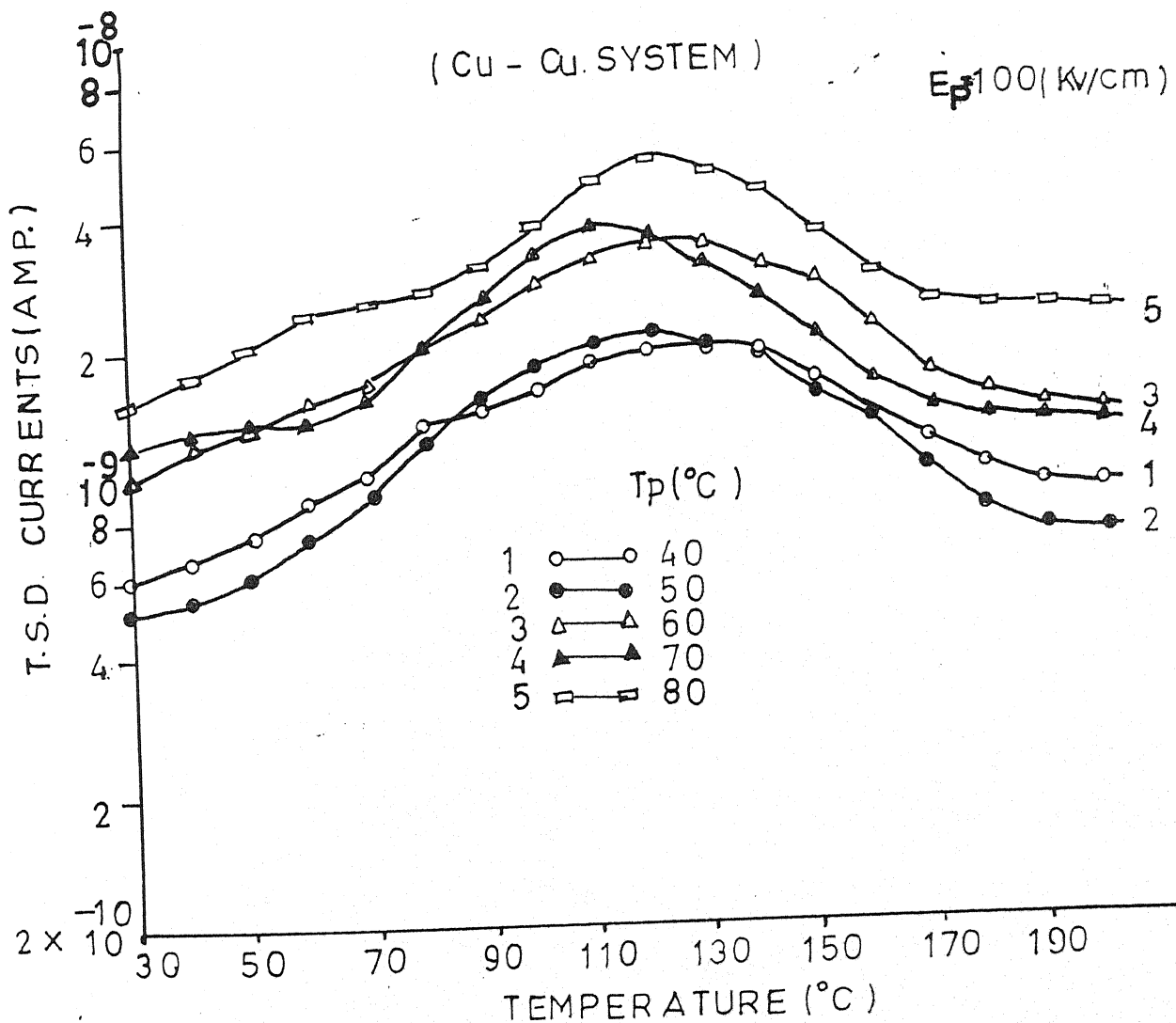


Figure No. 4.45
 Thermally Stimulated Discharge Currents (T.S.D.C.) for Polyvinylidene fluoride Samples (20 μ m) poled at $E_p = 100$ kV/cm with different polarisation Temperature (i.e. 40, 50, 60, 70 and 80° C) for Cu - Cu system.

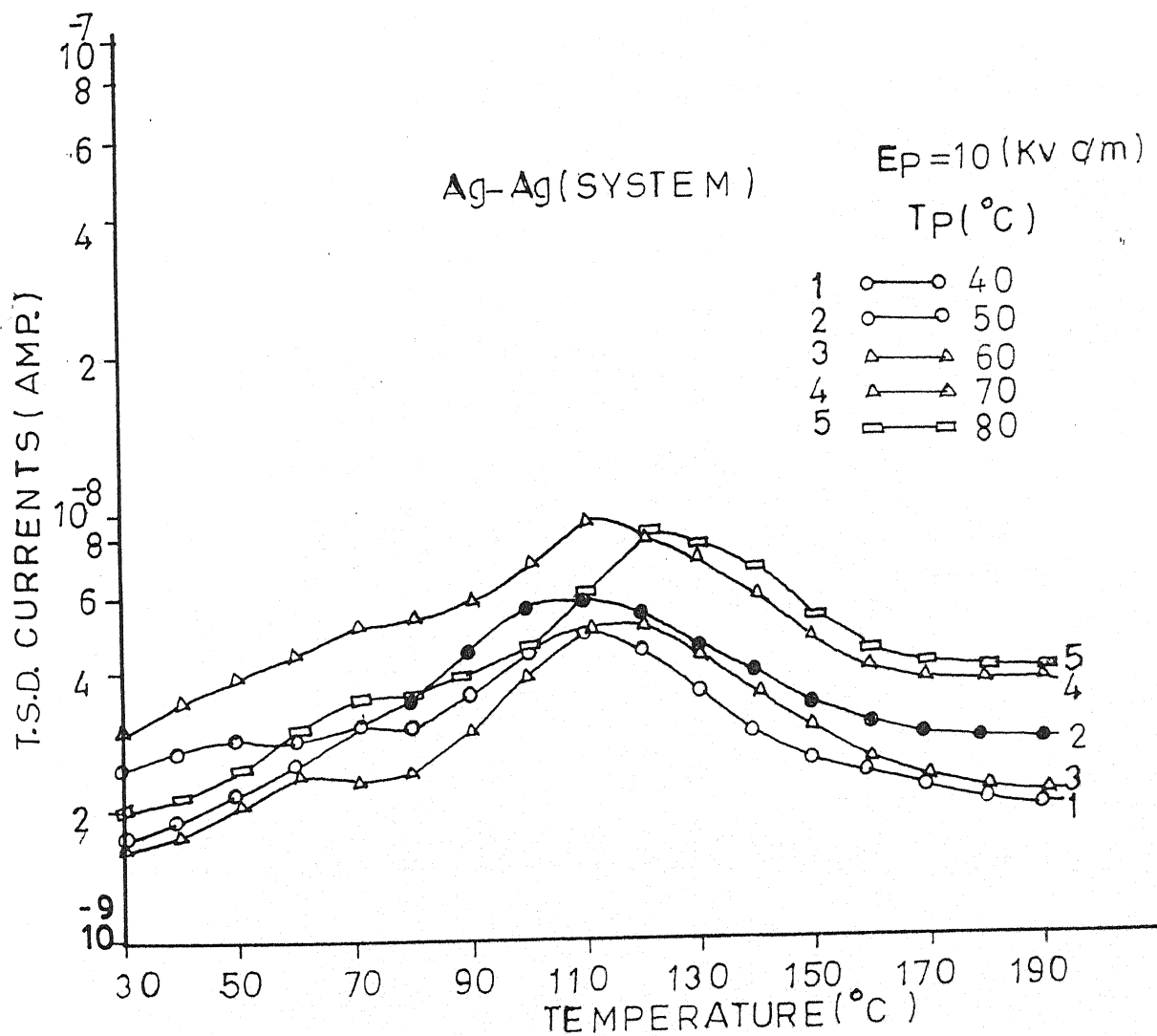


Figure No. 4.46
Thermally Stimulated Discharge Currents (T.S.D.C.) for Polyvinylidene fluoride Samples ($20 \mu\text{m}$) poled at $E_p = 10 \text{ kV/cm}$ with different polarisation

Temperature (i.e. $40, 50, 60, 70$ and 80°C) for Ag-Ag system.

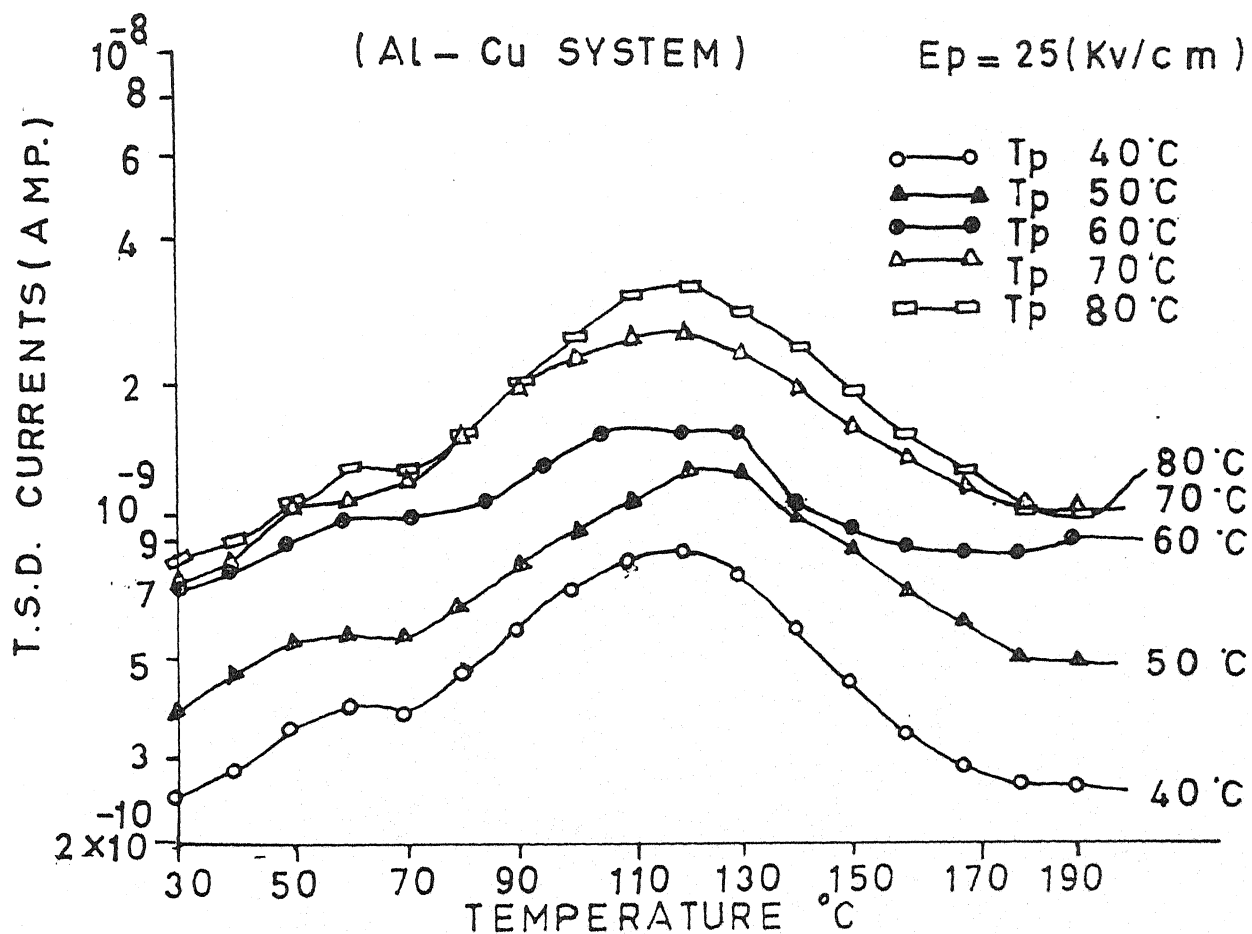


Figure No. 4.47.
 Thermally Stimulated Discharge Currents (T.S.D.C.) for Polyvinylidene fluoride Samples ($20 \mu\text{m}$) poled at $E_p = 25 \text{ kV/cm}$ with different polarisation Temperature (i.e. 40, 50, 60, 70 and 80 °C) for Al - Cu system.

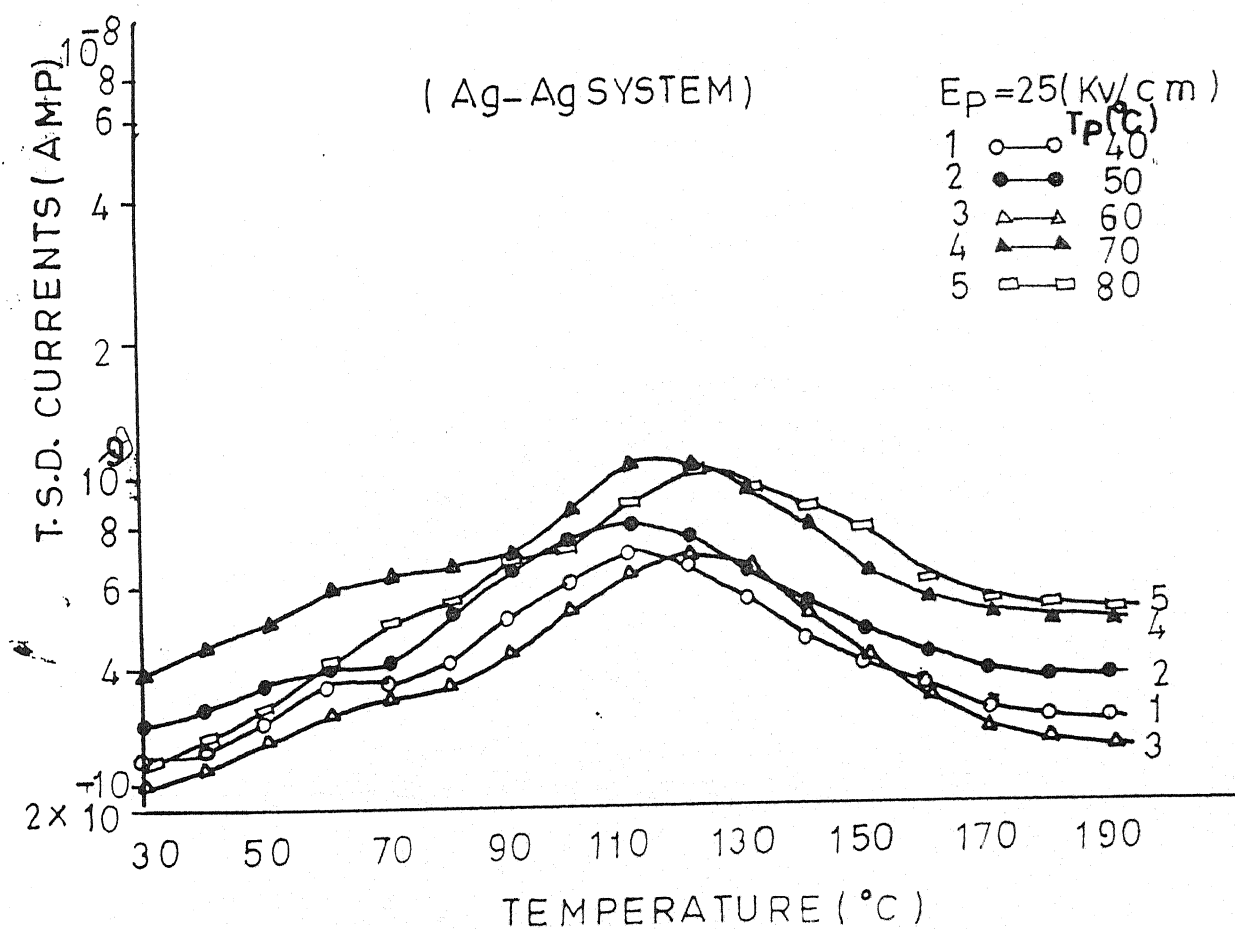


Figure No. 4.48

Thermally Stimulated Discharge Currents (T.S.D.C.) for Polyvinylidene fluoride Samples ($20 \mu\text{m}$) poled at $E_p = 25 \text{ kV/cm}$ with different polarisation Temperature (i.e. $40, 50, 60, 70$ and 80°C) for Ag-Ag system.

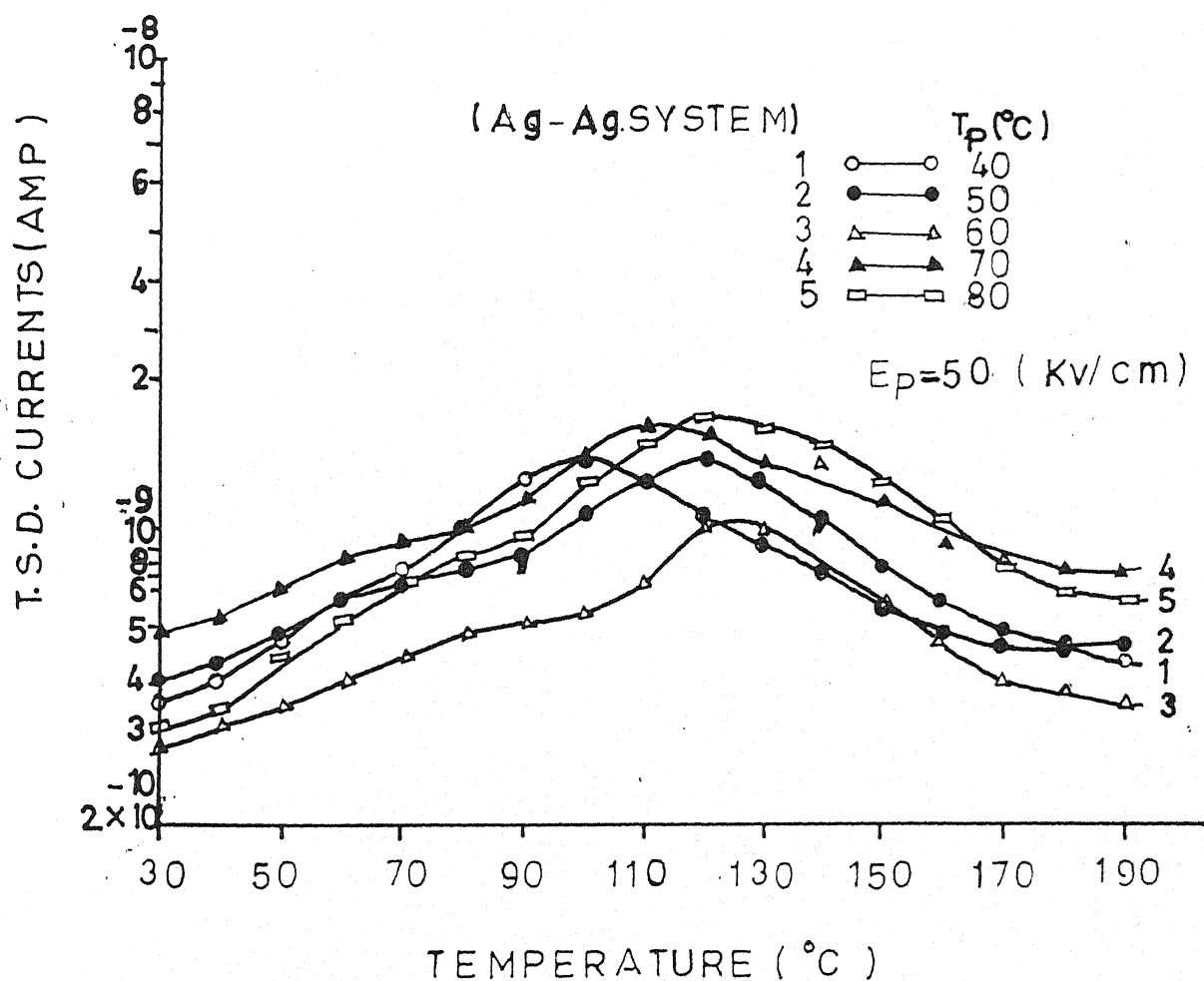


Figure No. 4.49

Thermally Stimulated Discharge Currents (T.S.D.C.) for Polyvinylidene fluoride Samples ($20 \mu\text{m}$) poled at $E_p = 50 \text{ kV/cm}$ with different polarisation Temperature (i.e. $40, 50, 60, 70$ and 80°C) for Ag-Ag system.

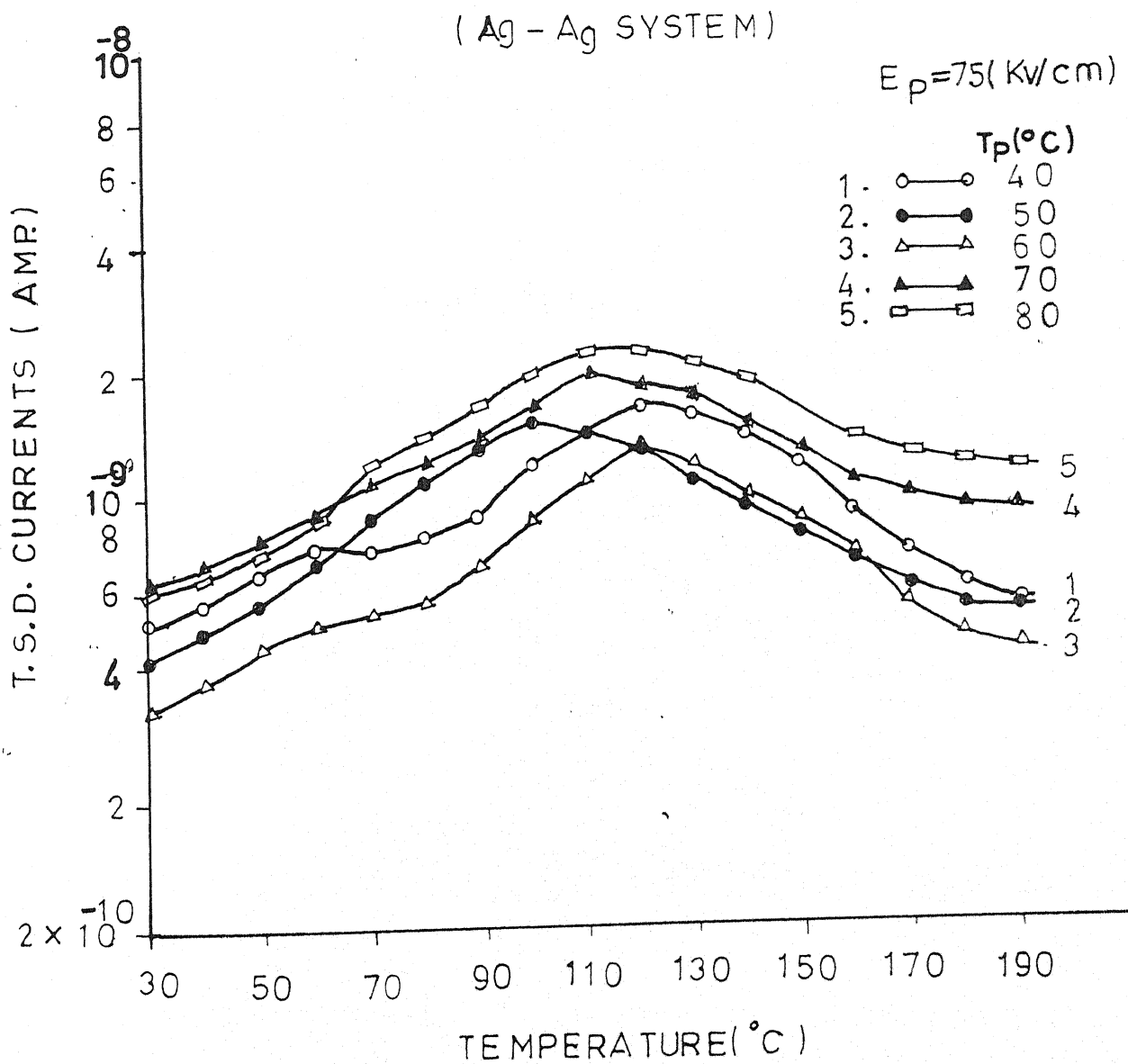


Figure No. 4.50
Thermally Stimulated Discharge Currents (T.S.D.C.) for Polyvinylidene fluoride Samples (20 μm) poled at $E_p = 75 \text{ kV/cm}$ with different polarisation Temperature (i.e. 40, 50, 60, 70 and 80 $^{\circ}\text{C}$) for Ag-Ag system.

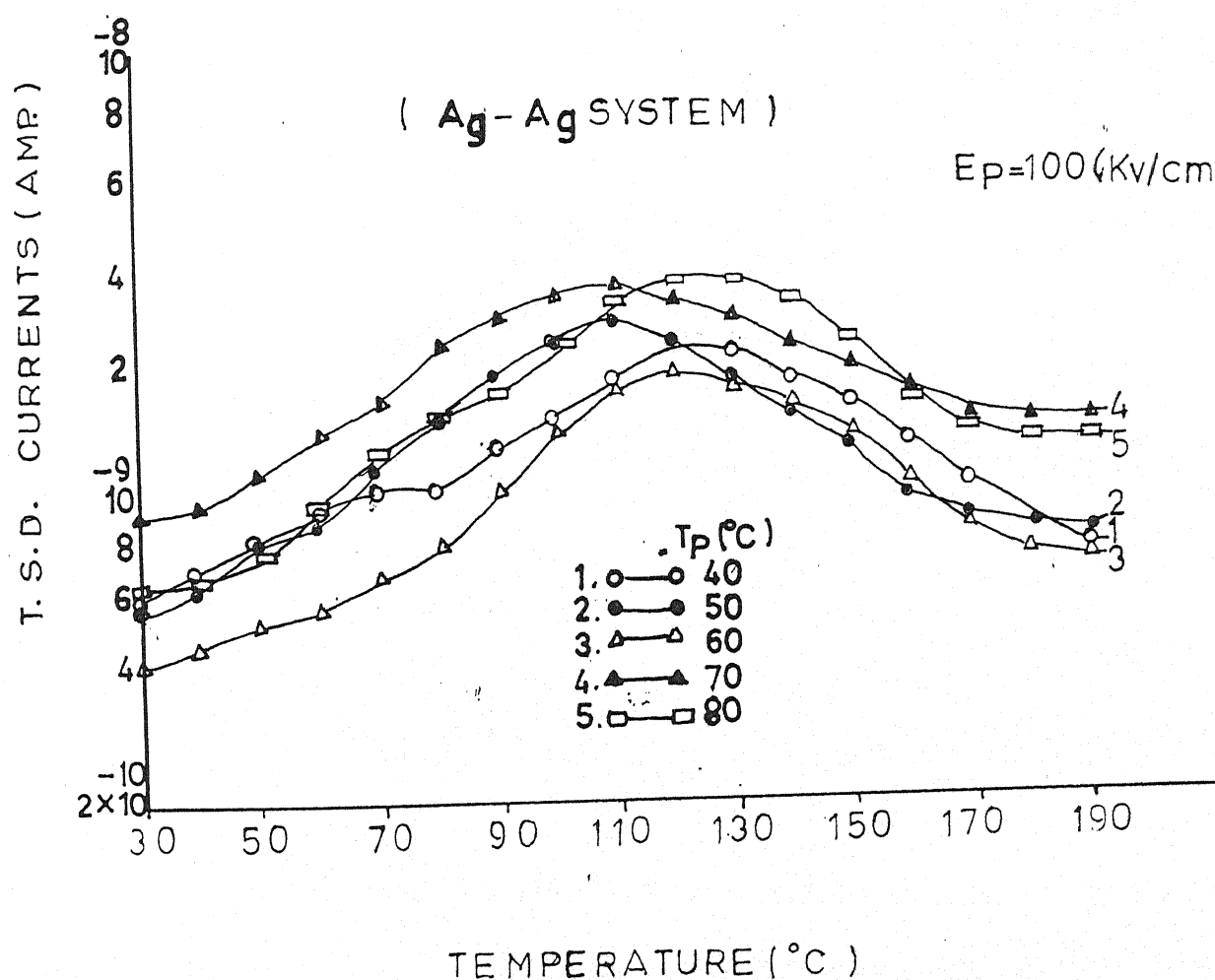


Figure No. 4.51
 Thermally Stimulated Discharge Currents (T.S.D.C.) for Polyvinylidene fluoride Samples ($20 \mu\text{m}$) poled at $E_p = 100 \text{ kV/cm}$ with different polarisation Temperature (i.e. 40, 50, 60, 70 and 80°C) for Ag-Ag system.

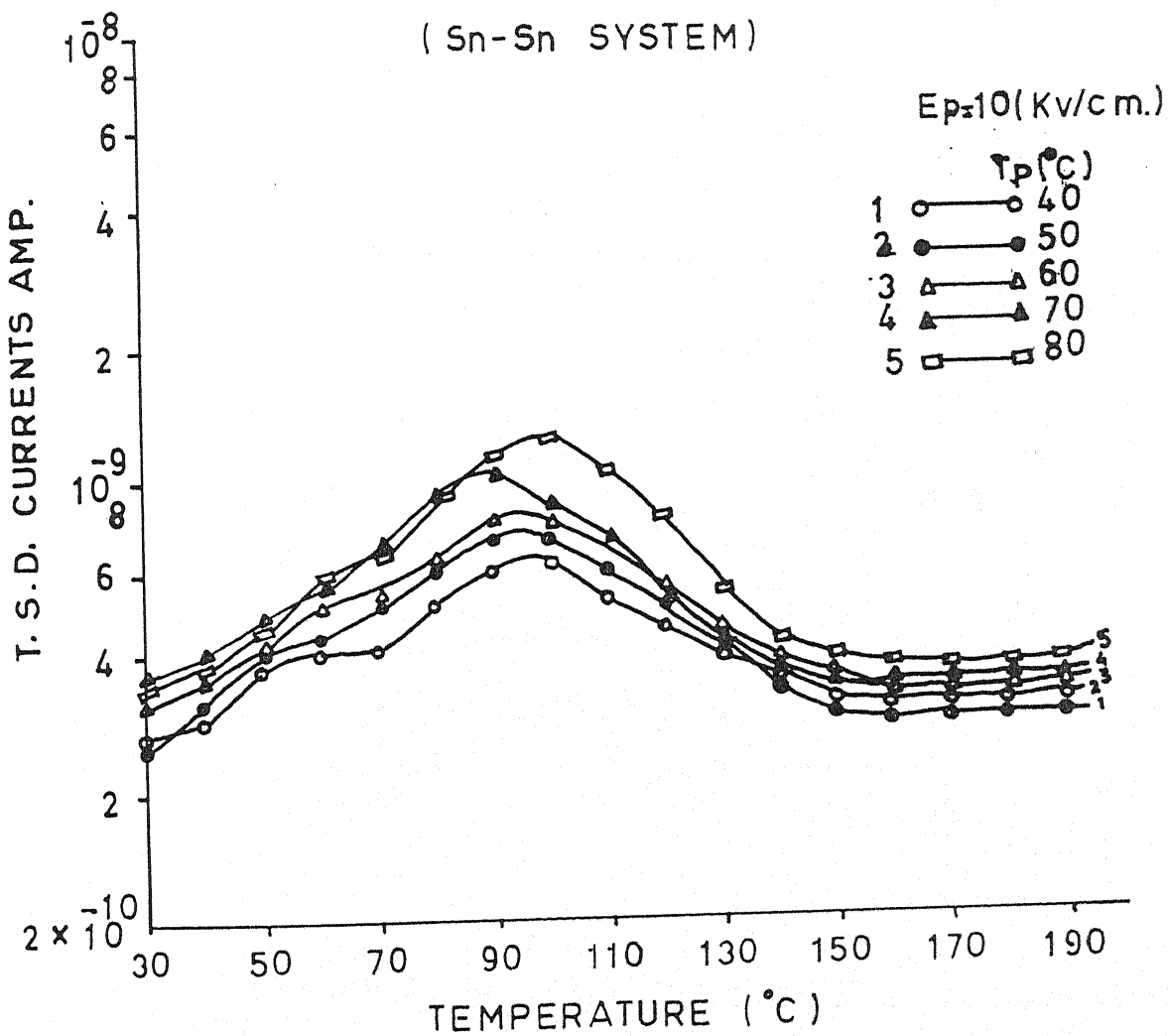


Figure No. 4.52

Thermally Stimulated Discharge Currents (T.S.D.C.) for Polyvinylidene fluoride Samples ($20 \mu\text{m}$) poled at $E_p = 10 \text{ kV/cm}$ with different polarisation Temperature (i.e. 40, 50, 60, 70 and 80°C) for Sn - Sn system.

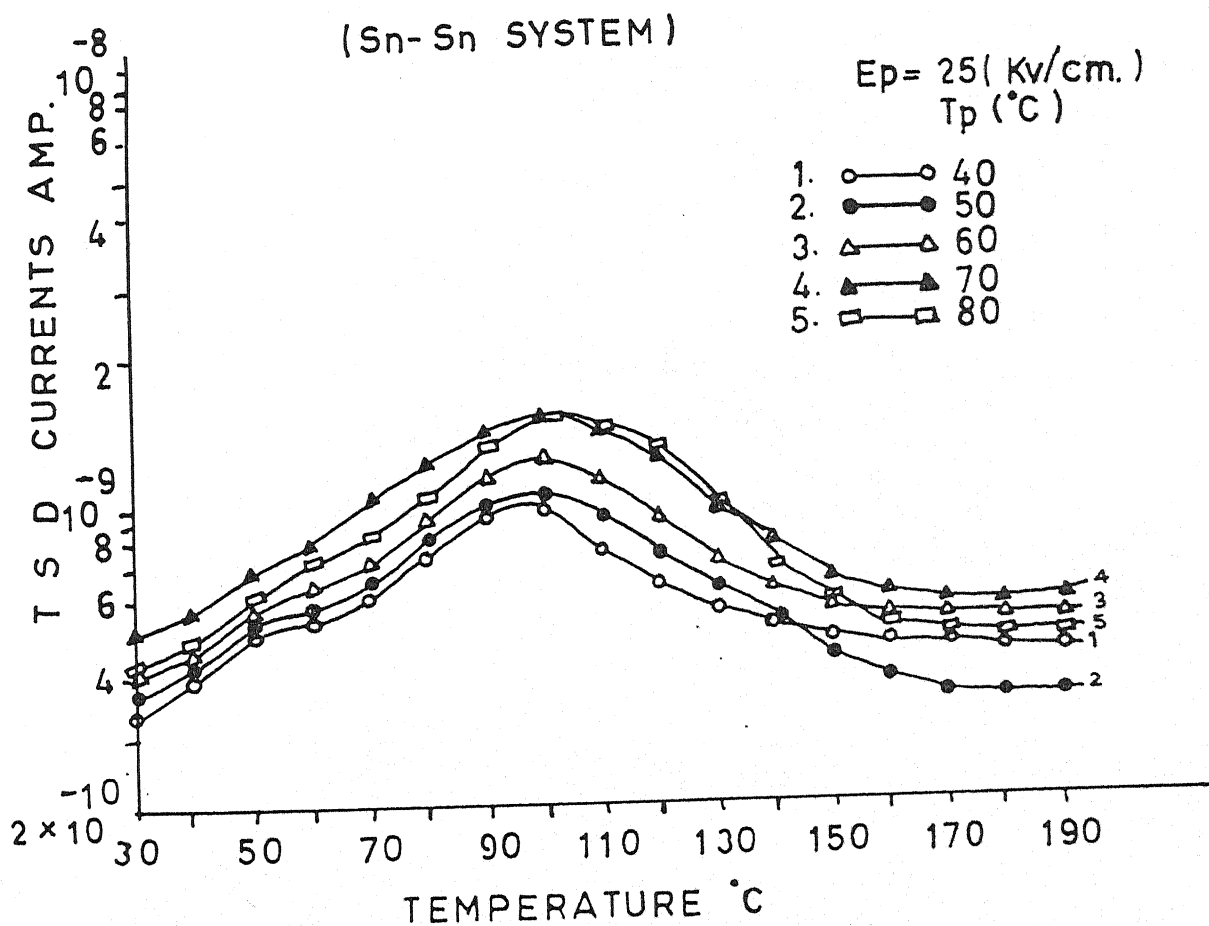


Figure No. 4.53

Thermally Stimulated Discharge Currents (T.S.D.C.) for Polyvinylidene fluoride Samples ($20 \mu\text{m}$) poled at $E_p = 25 \text{ kV/cm}$ with different polarisation Temperature (i.e. 40, 50, 60, 70 and 80°C) for Sn - Sn system.

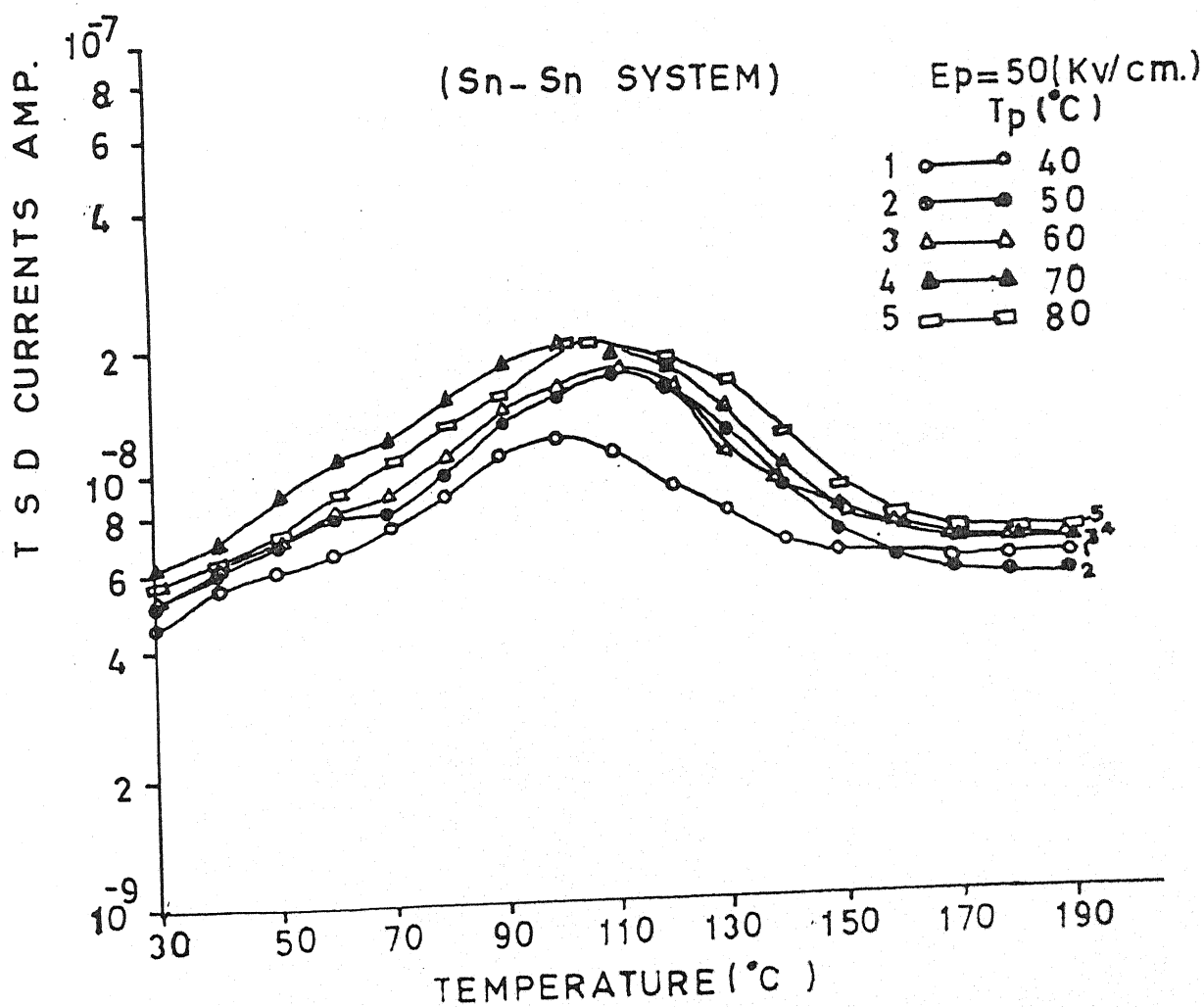


Figure No. 4.54

Thermally Stimulated Discharge Currents (T.S.D.C.) for Polyvinylidene fluoride Samples ($20 \mu\text{m}$) poled at $E_p = 50 \text{ kV/cm}$ with different polarisation Temperature (i.e. 40, 50, 60, 70 and 80°C) for Sn - Sn system.

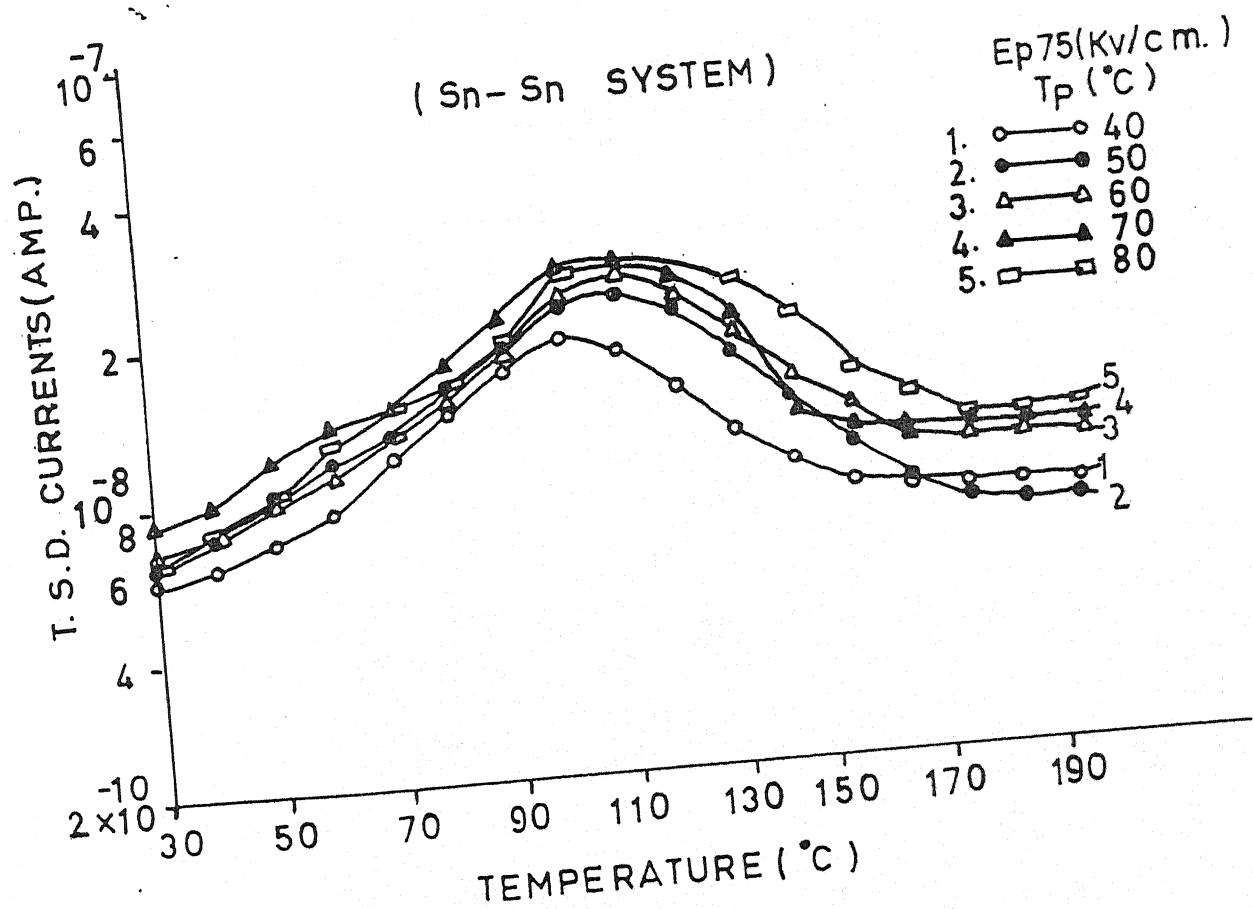


Figure No. 4.55
Thermally Stimulated Discharge Currents (T.S.D.C.) for Polyvinylidene fluoride Samples (20 μ m) poled at $E_p = 75$ kV/cm with different polarisation Temperature (i.e. 40, 50, 60, 70 and 80°C) for Sn - Sn system.

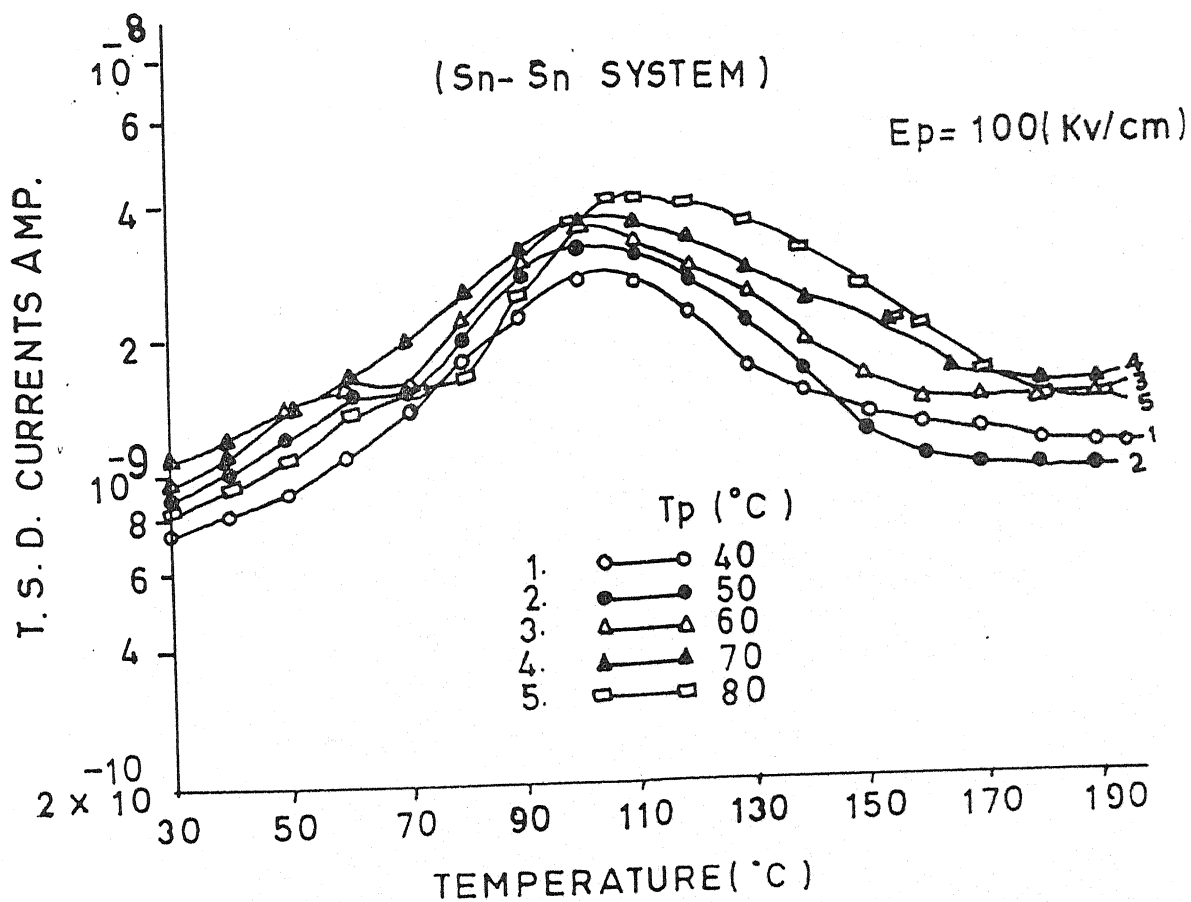


Figure No. 4.56
Thermally Stimulated Discharge Currents (T.S.D.C.) for Polyvinylidene fluoride Samples ($20 \mu\text{m}$) poled at $E_p = 100 \text{ kV/cm}$ with different polarisation Temperature (i.e. $40, 50, 60, 70$ and 80°C) for Sn - Sn system.

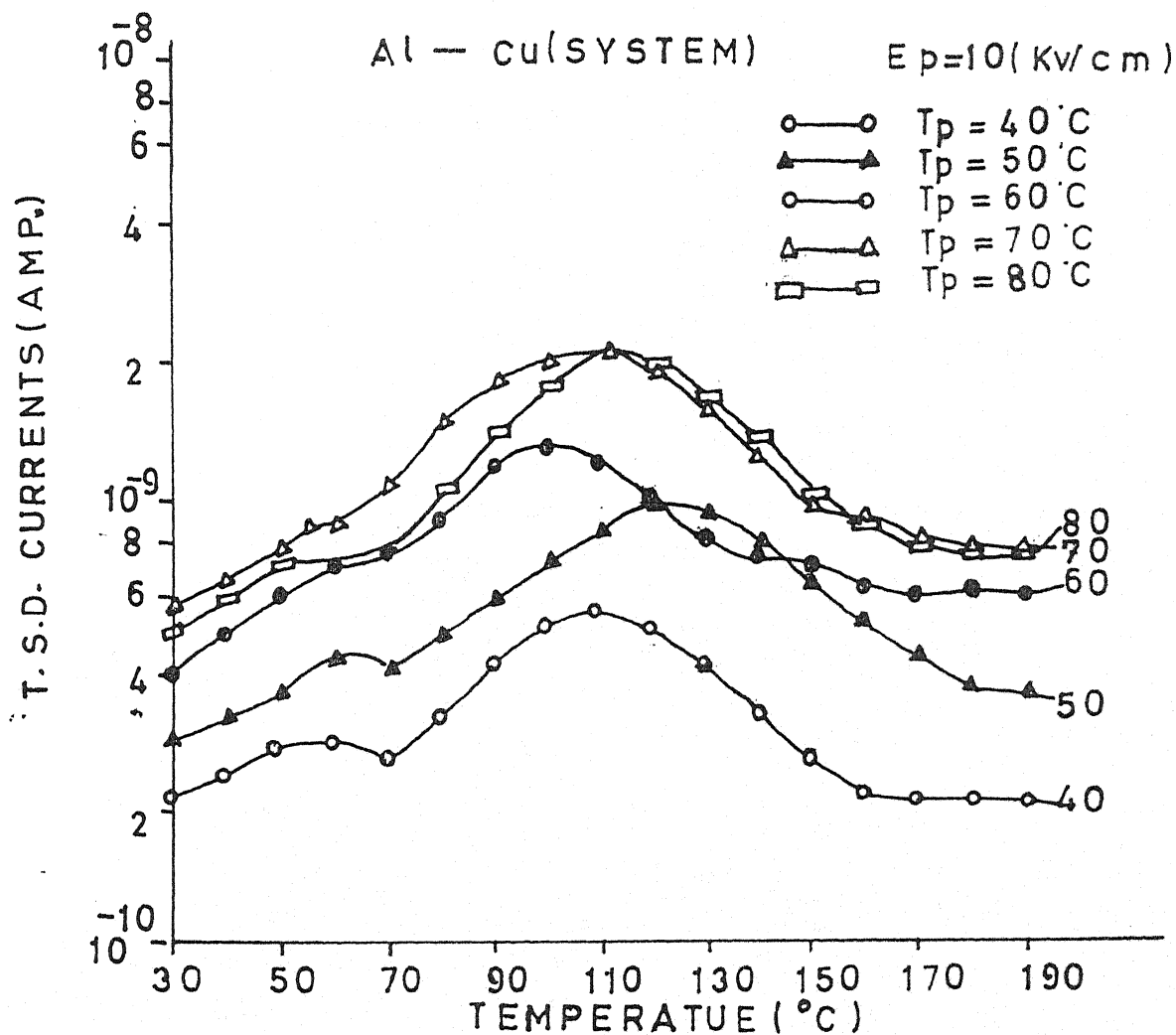


Figure No. 4.57

Thermally Stimulated Discharge Currents (T.S.D.C.) for Polyvinylidene fluoride Samples ($20 \mu\text{m}$) poled at $E_p = 10 \text{ kV/cm}$ with different polarisation Temperature (i.e. $40, 50, 60, 70$ and 80°C) for Al - Cu system.

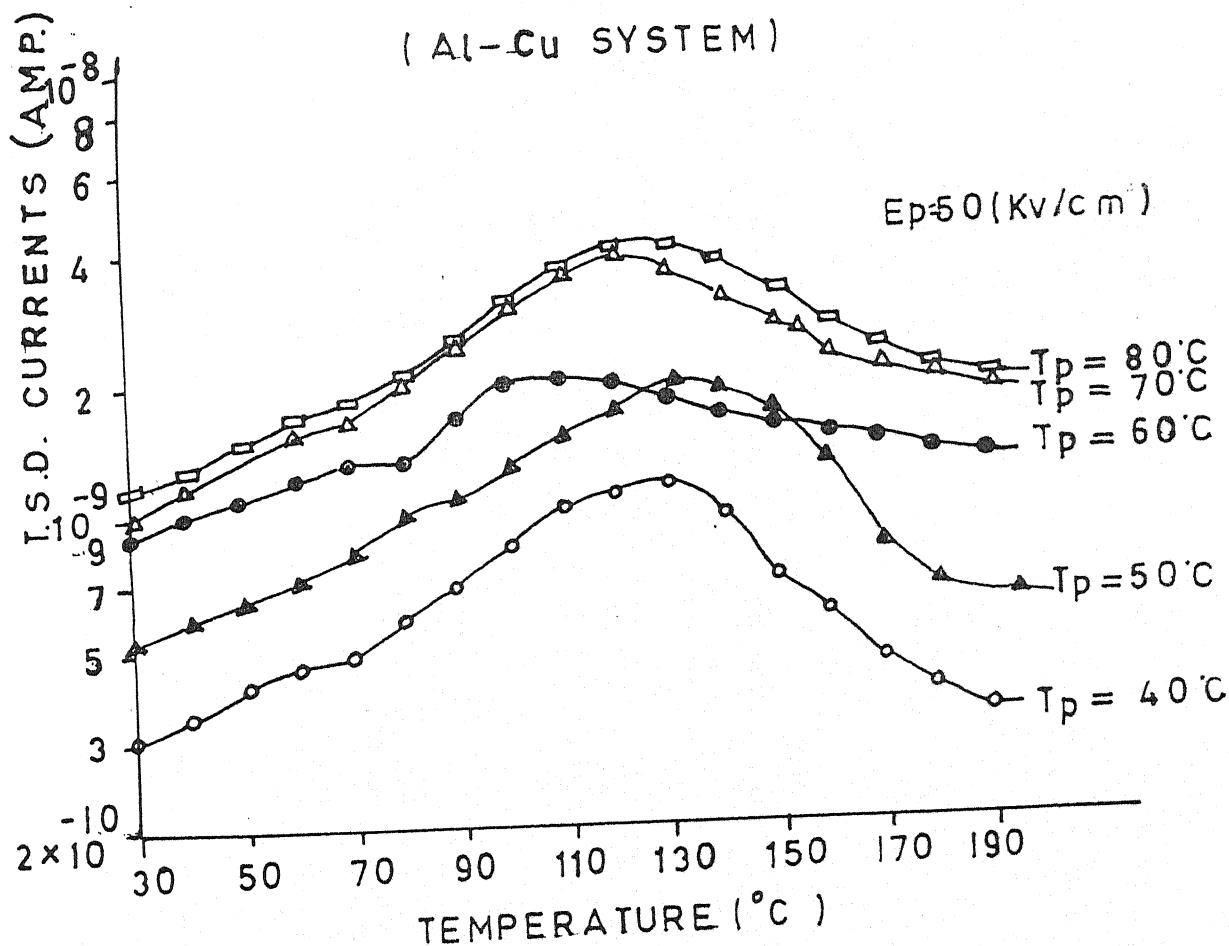


Figure No. 4.58
 Thermally Stimulated Discharge Currents (T.S.D.C.) for Polyvinylidene fluoride Samples ($20 \mu\text{m}$) poled at $E_p = 50 \text{ kV/cm}$ with different polarisation Temperature (i.e. $40, 50, 60, 70$ and 80°C) for Al - Cu system.

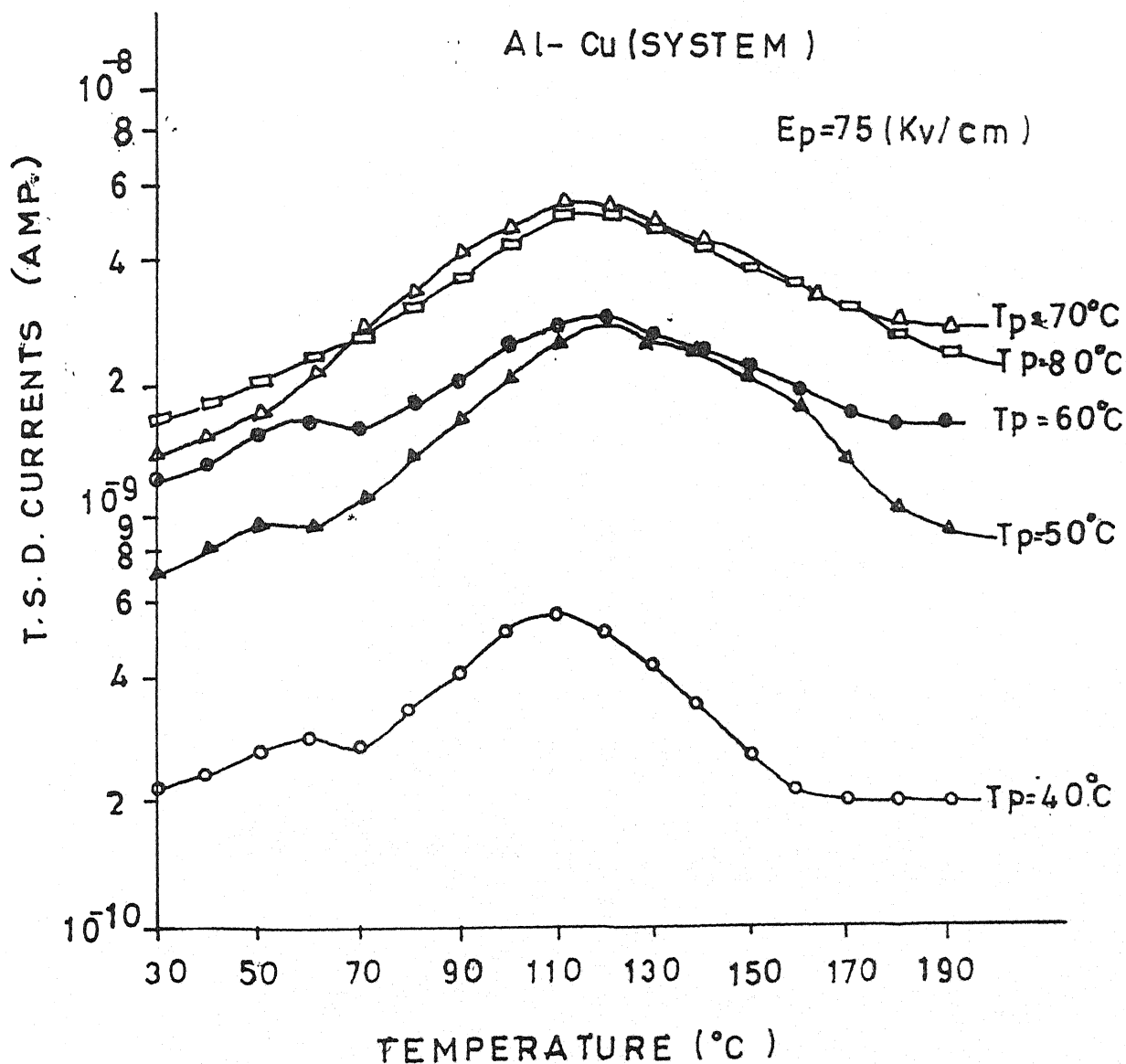


Figure No. 4.59

Thermally Stimulated Discharge Currents (T.S.D.C.) for Polyvinylidene fluoride Samples ($20 \mu\text{m}$) poled at $E_p = 75 \text{ kV/cm}$ with different polarisation Temperature (i.e. 40, 50, 60, 70 and 80° C) for Al - Cu system.

Ep-100(Kv/cm)

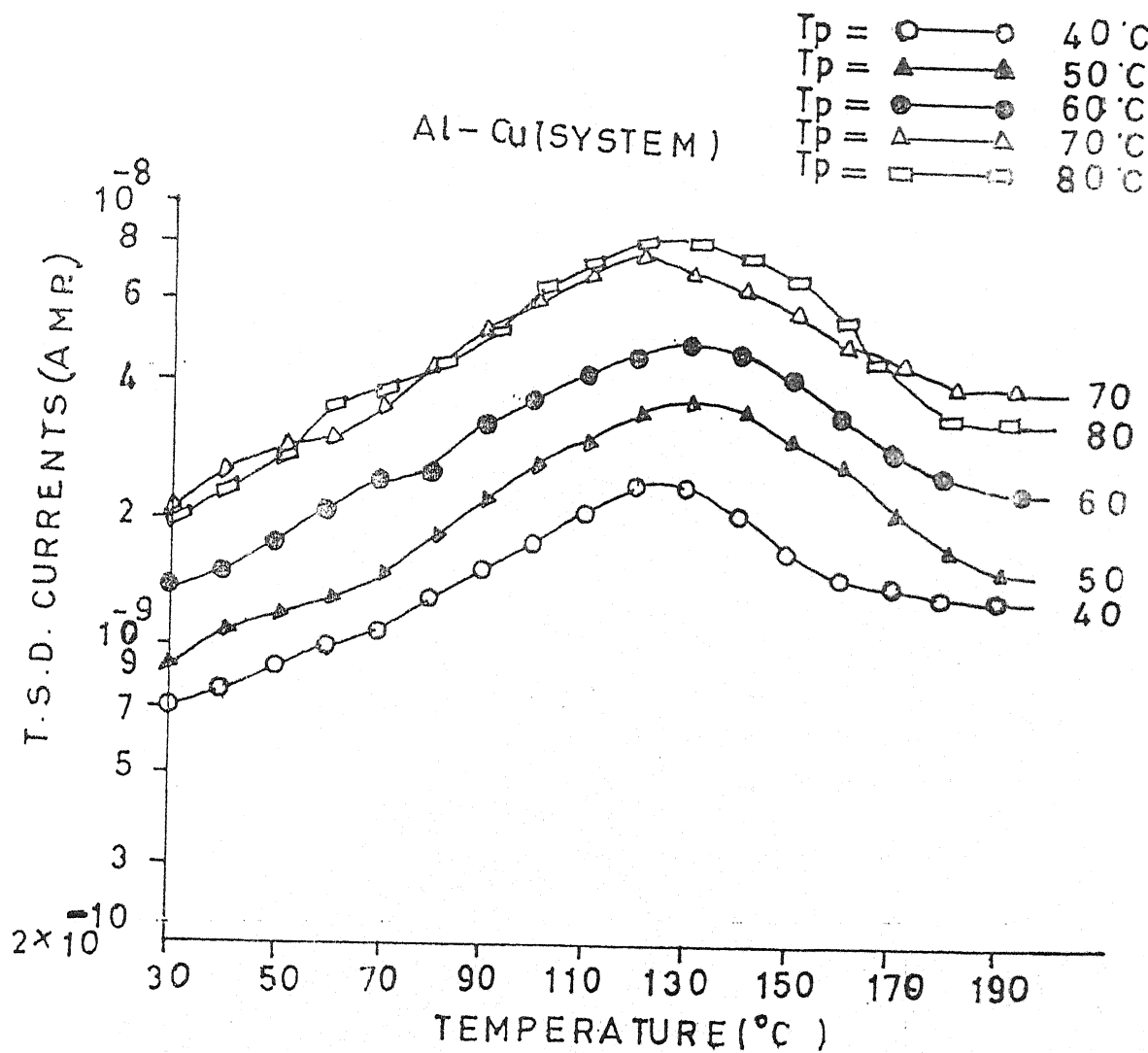


Figure No. 4.60

Thermally Stimulated Discharge Currents (T.S.D.C.) for Polyvinylidene fluoride Samples ($20 \mu\text{m}$) poled at $E_p = 100 \text{ kV/cm}$ with different polarisation Temperature (i.e. 40, 50, 60, 70 and 80 °C) for Al - Cu system.

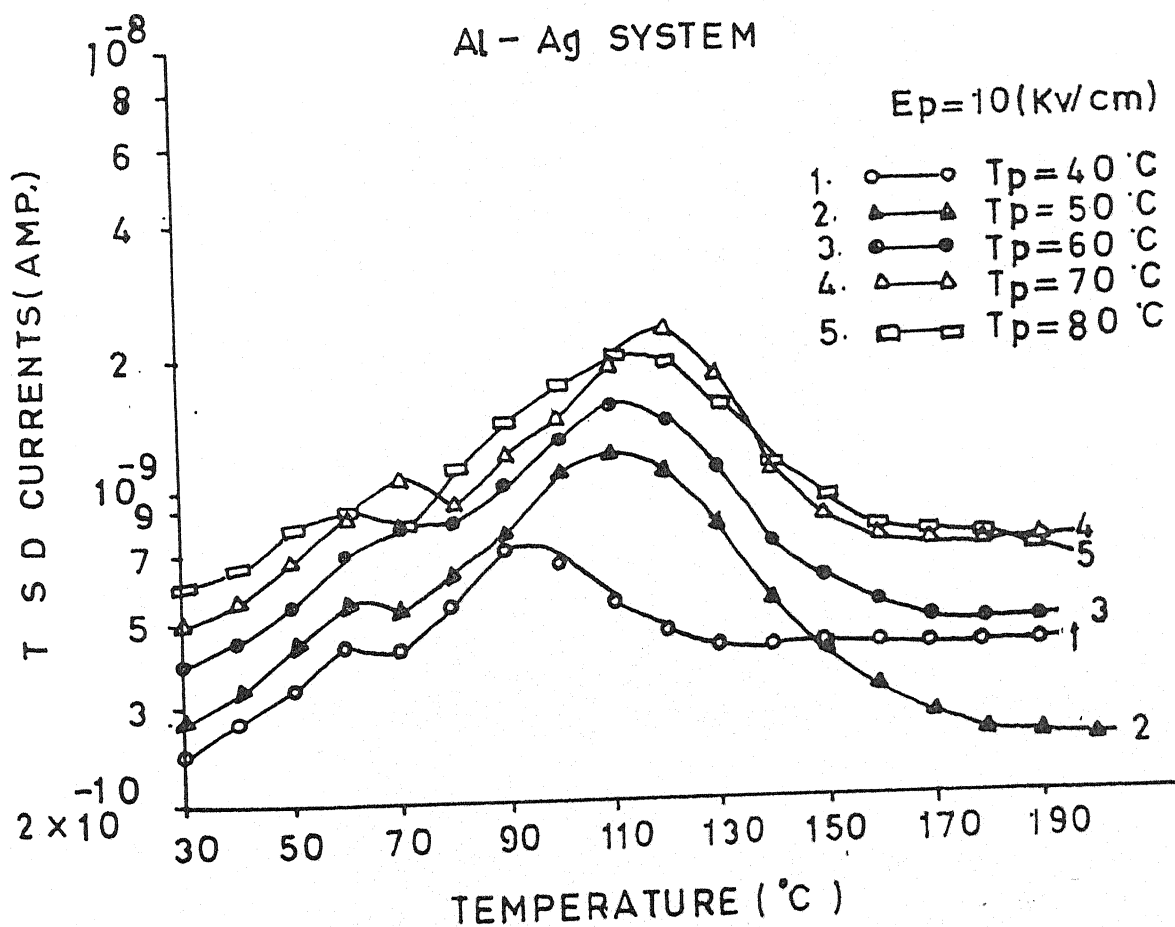


Figure No. 4.61

Thermally Stimulated Discharge Currents (T.S.D.C.) for Polyvinylidene fluoride Samples ($20 \mu\text{m}$) poled at $E_p = 10 \text{ kV/cm}$ with different polarisation Temperature (i.e. $40, 50, 60, 70$ and 80°C) for Al - Ag system.

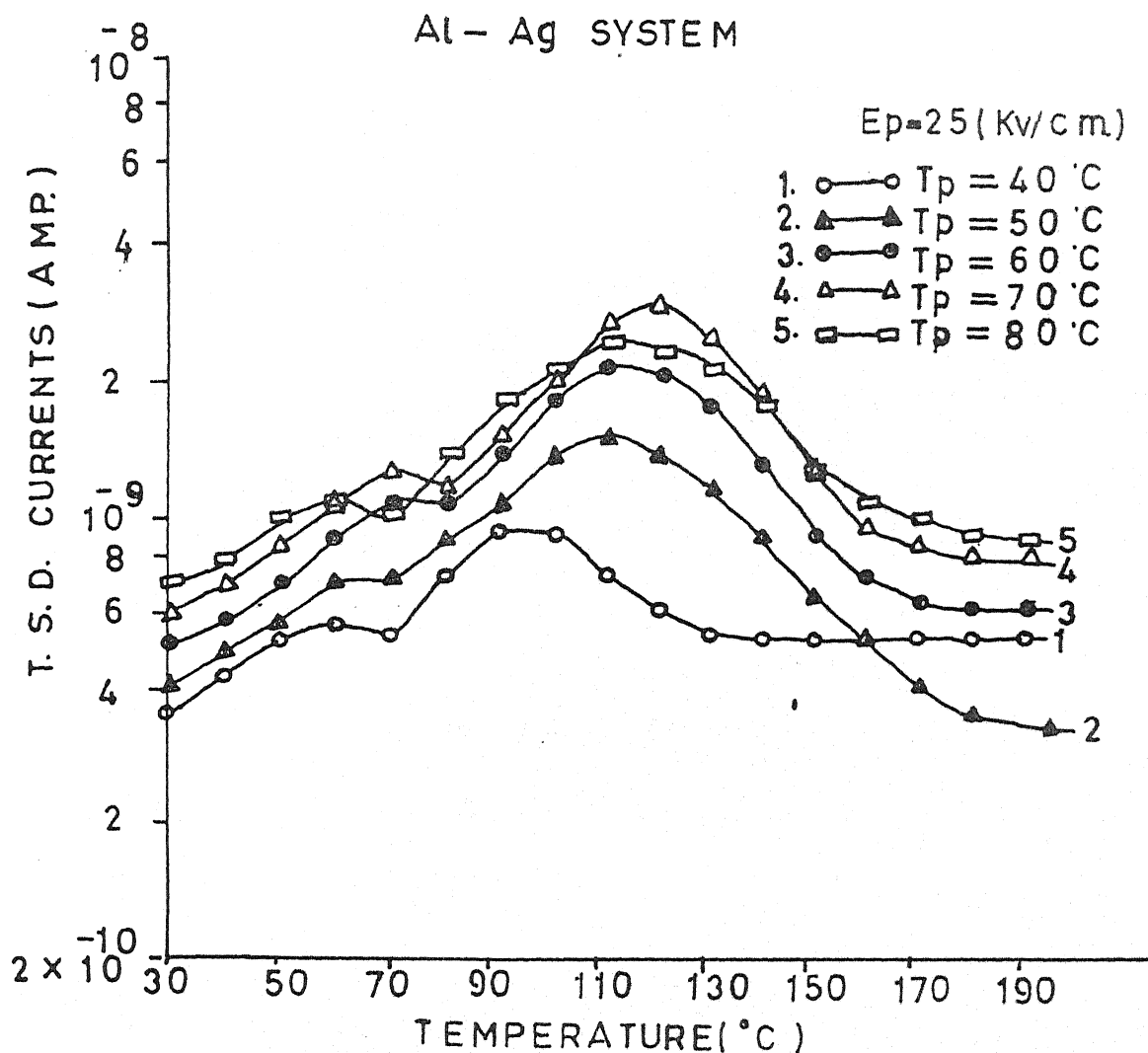


Figure No. 4.62

Thermally Stimulated Discharge Currents (T.S.D.C.) for Polyvinylidene fluoride Samples ($20 \mu\text{m}$) poled at $E_p = 25 \text{ kV/cm}$ with different polarisation Temperature (i.e. 40, 50, 60, 70 and 80°C) for Al - Ag system.

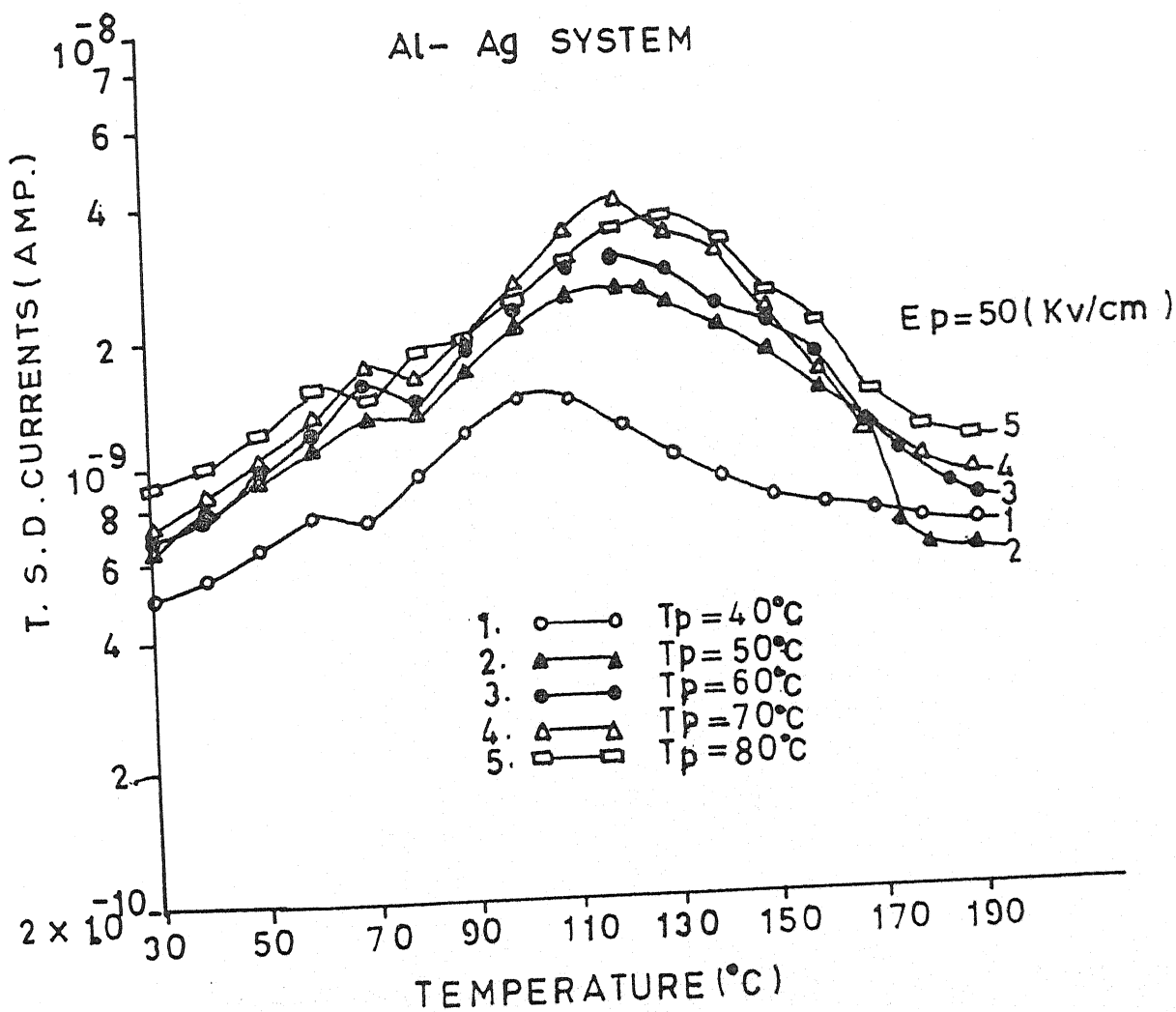


Figure No. 4.63

Thermally Stimulated Discharge Currents (T.S.D.C.) for Polyvinylidene fluoride Samples ($20 \mu\text{m}$) poled at $E_p = 50 \text{ kV/cm}$ with different polarisation Temperature (i.e. $40, 50, 60, 70$ and 80°C) for Al - Ag system.

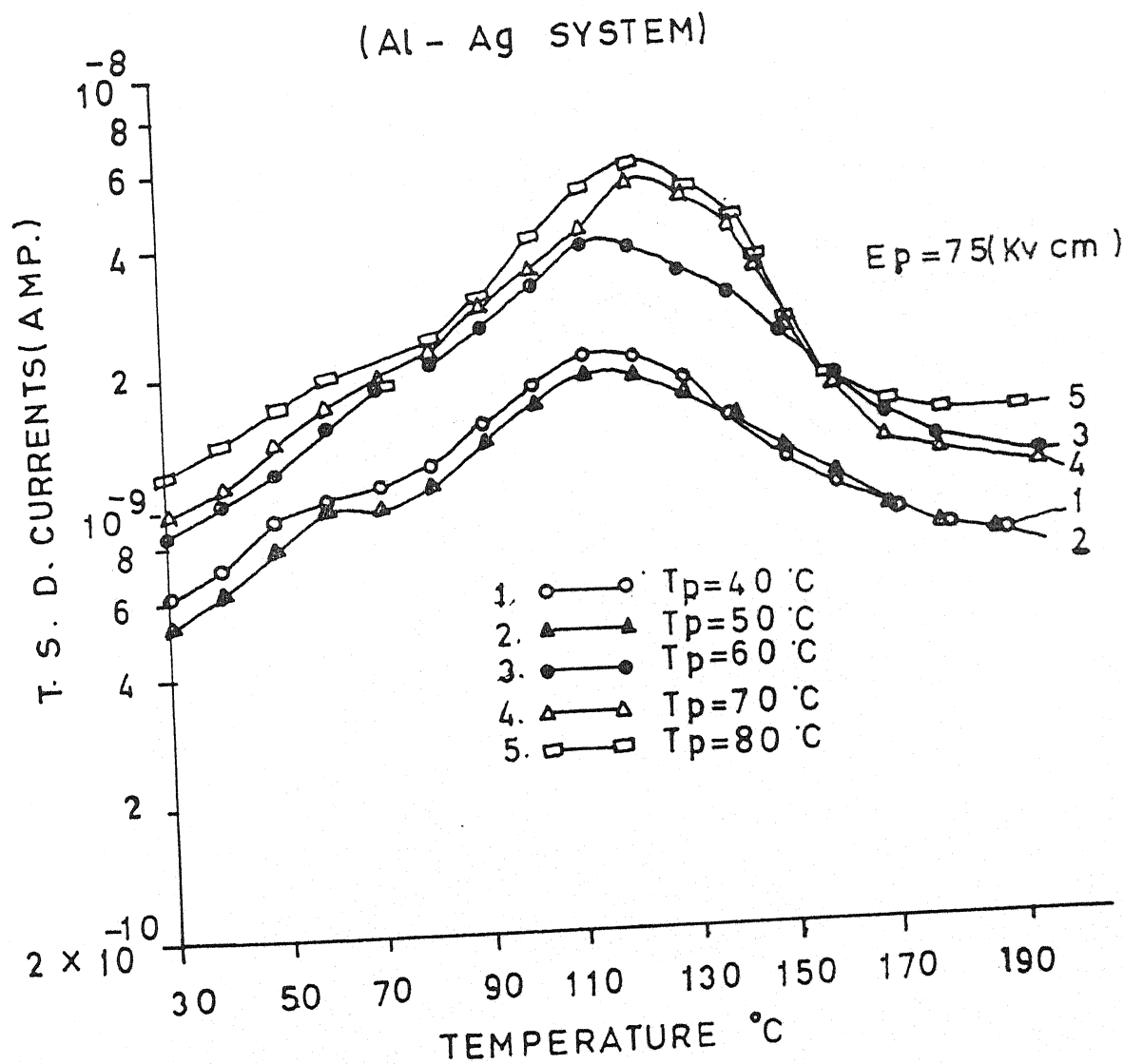


Figure No. 4.64
Thermally Stimulated Discharge Currents (T.S.D.C.) for Polyvinylidene fluoride Samples ($20 \mu\text{m}$) poled at $E_p = 75 \text{ kV/cm}$ with different polarisation Temperature (i.e. $40, 50, 60, 70$ and 80°C) for Al - Ag system.

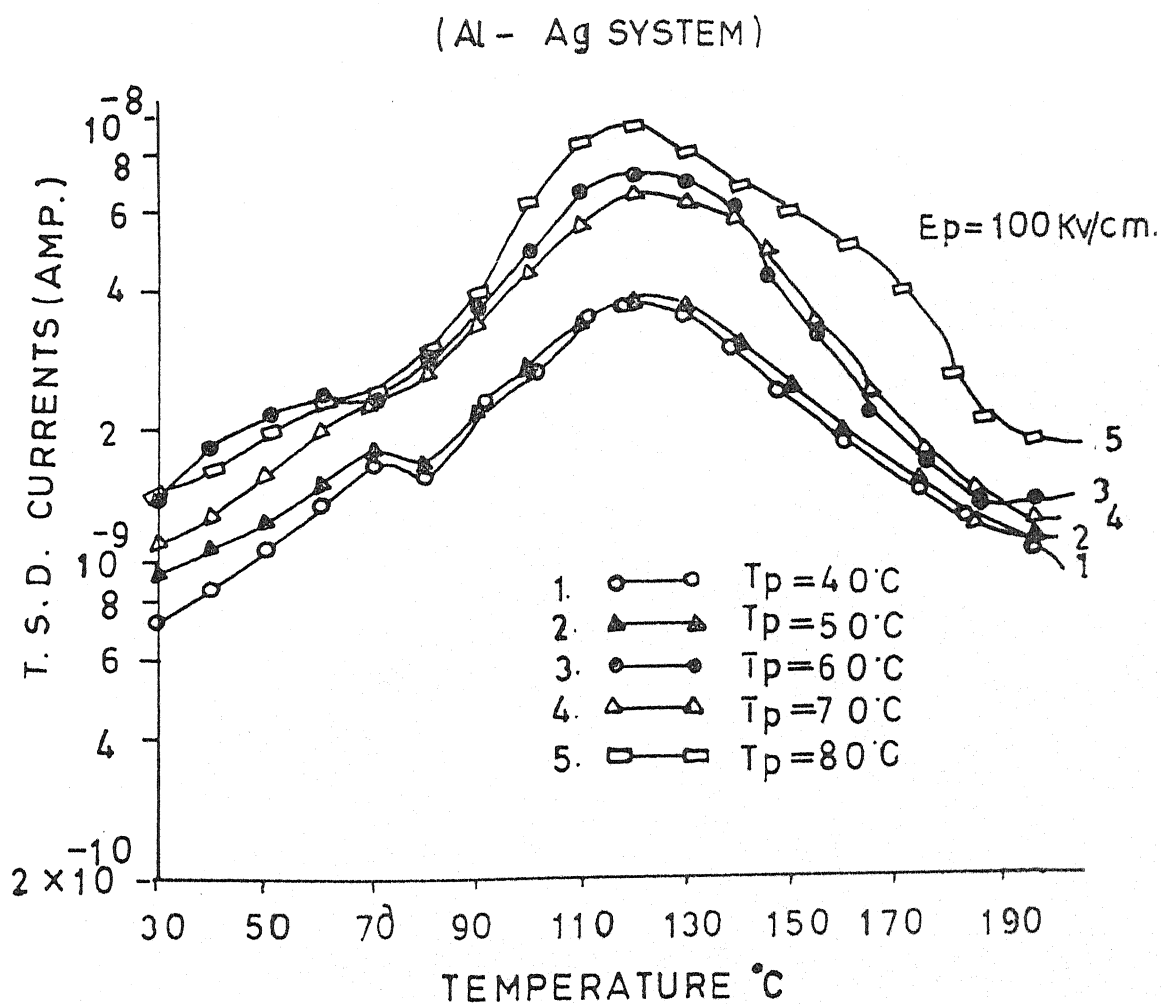


Figure No. 4,65

Thermally Stimulated Discharge Currents (T.S.D.C.) for Polyvinylidene fluoride Samples ($20 \mu\text{m}$) poled at $E_p = 100 \text{ kV/cm}$ with different polarisation Temperature (i.e. 40, 50, 60, 70 and 80°C) for Al - Ag system.

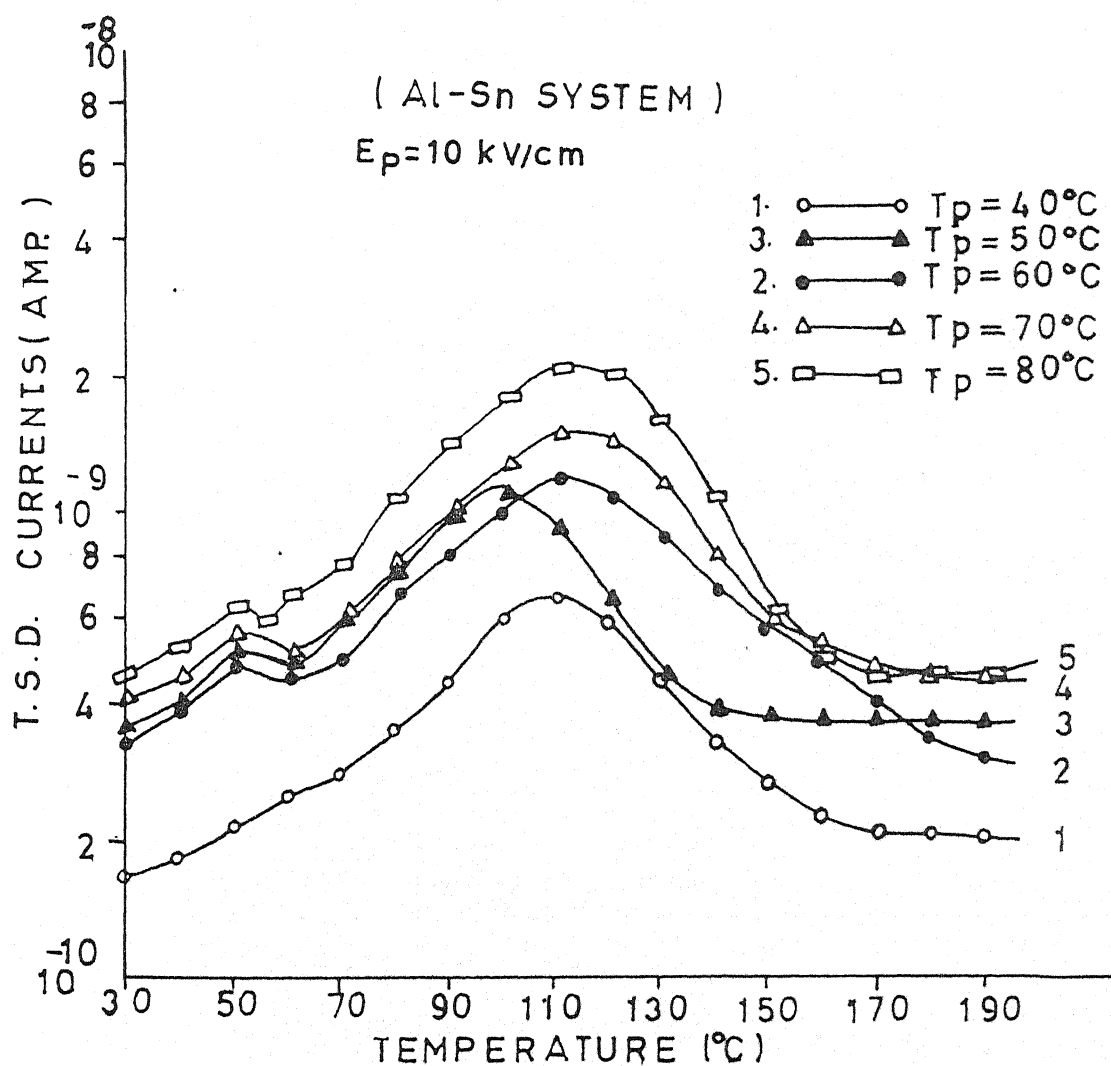


Figure No. 4.66

Thermally Stimulated Discharge Currents (T.S.D.C.) for Polyvinylidene fluoride Samples ($20 \mu\text{m}$) poled at $E_p = 10 \text{ kV/cm}$ with different polarisation Temperature (i.e. $40, 50, 60, 70$ and 80°C) for Al - Sn system.

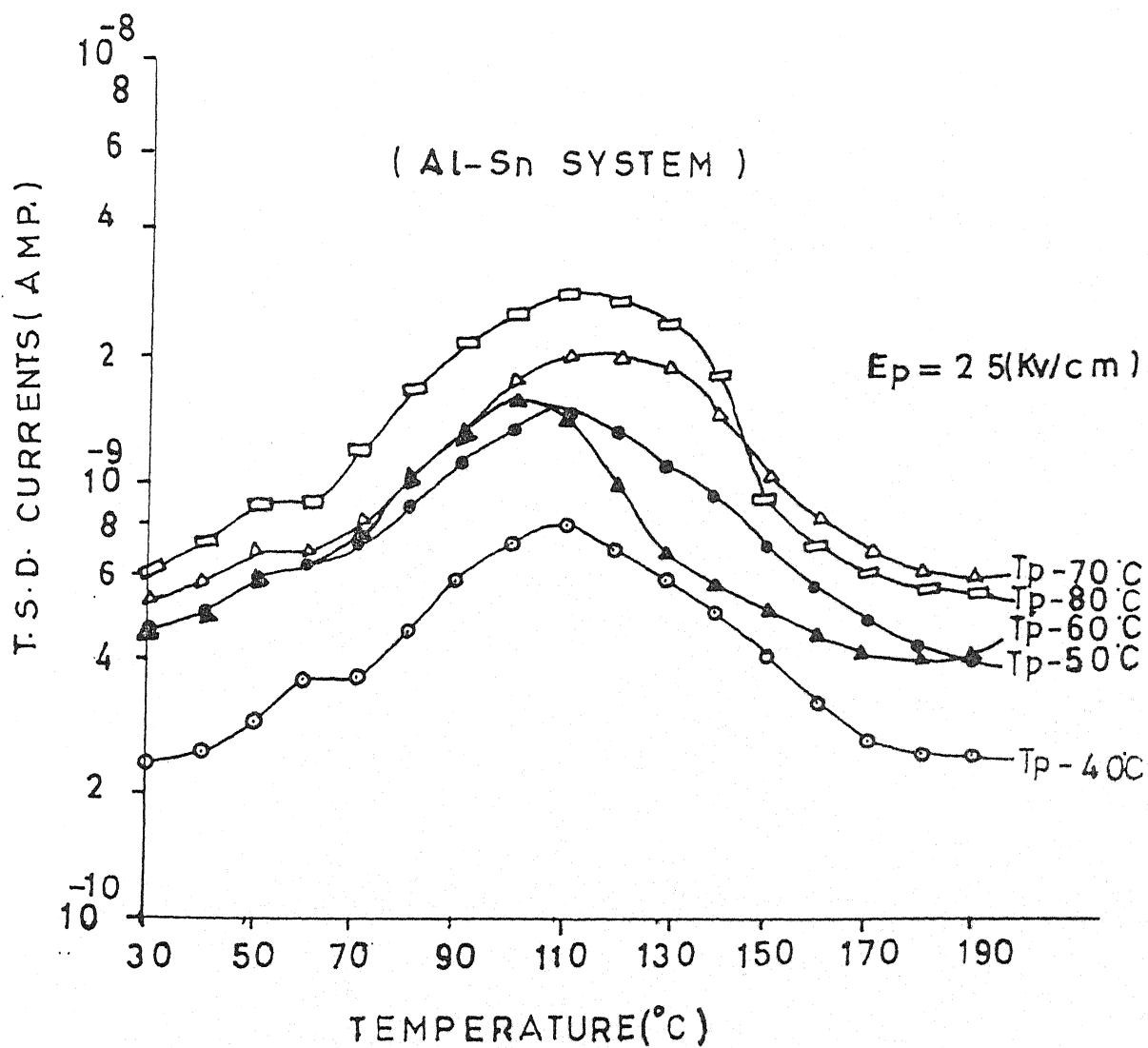


Figure No. 4.67

Thermally Stimulated Discharge Currents (T.S.D.C.) for Polyvinylidene fluoride Samples ($20 \mu\text{m}$) poled at $E_p = 25 \text{ kV/cm}$ with different polarisation Temperature (i.e. $40, 50, 60, 70$ and 80°C) for Al - Sn system.

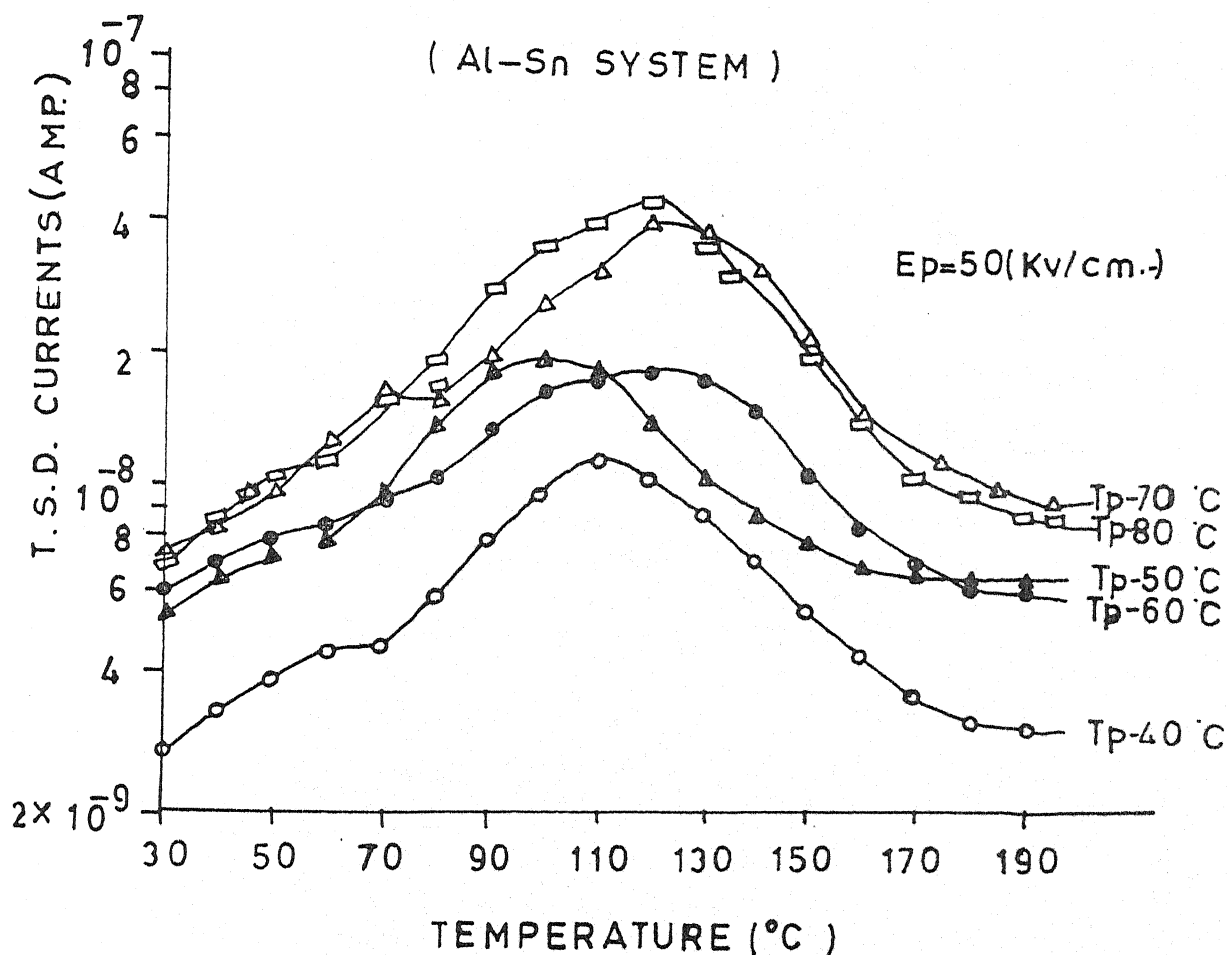


Figure No. 4.68

Thermally Stimulated Discharge Currents (T.S.D.C.) for Polyvinylidene fluoride Samples ($20 \mu\text{m}$) poled at $E_p = 50 \text{ kV/cm}$ with different polarisation Temperature (i.e. 40, 50, 60, 70 and 80° C) for Al - Sn system.

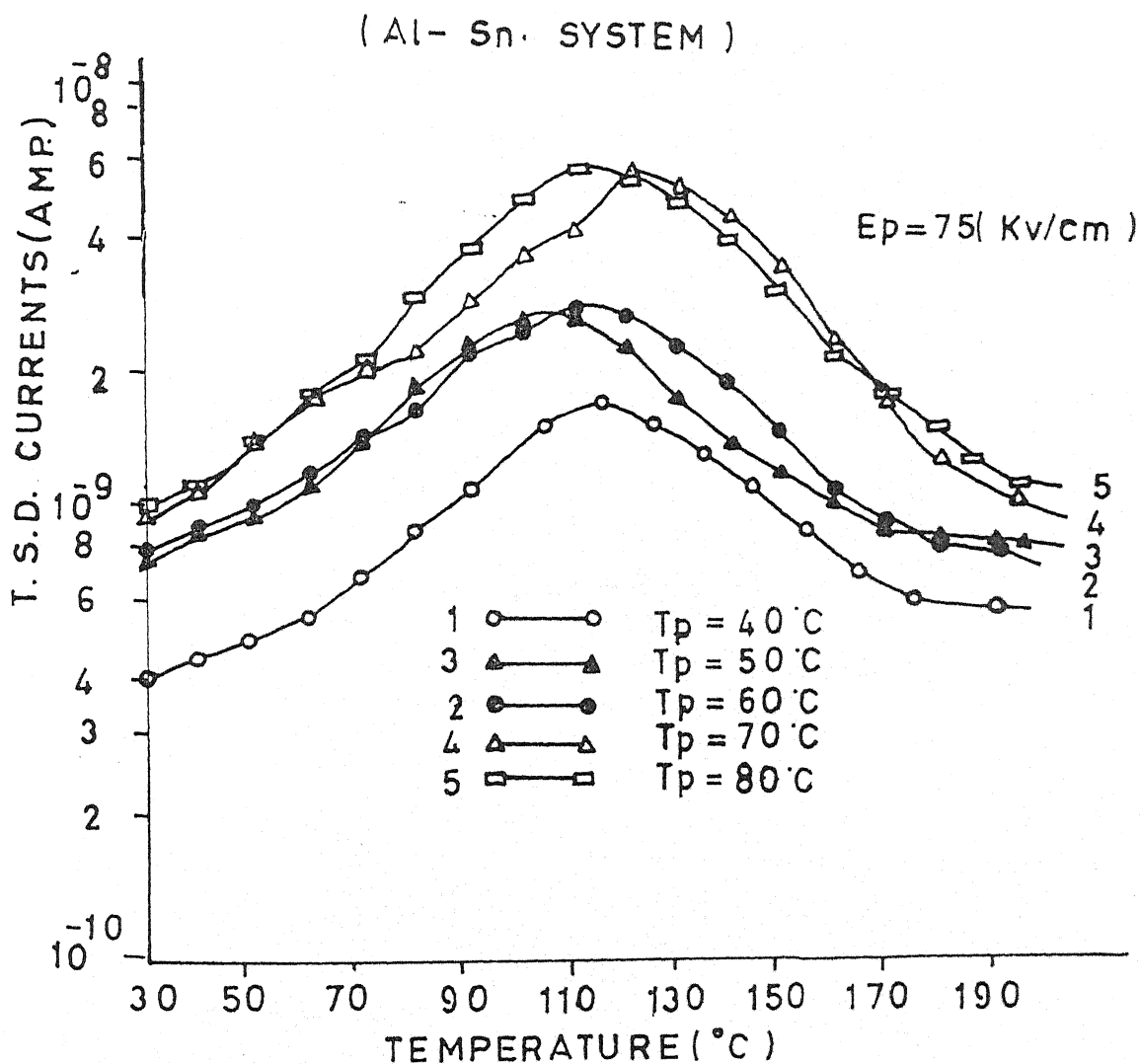


Figure No. 4.69

Thermally Stimulated Discharge Currents (T.S.D.C.) for Polyvinylidene fluoride Samples ($20 \mu\text{m}$) poled at $E_p = 75 \text{ kV/cm}$ with different polarisation Temperature (i.e. $40, 50, 60, 70$ and 80°C) for Al - Sn system.

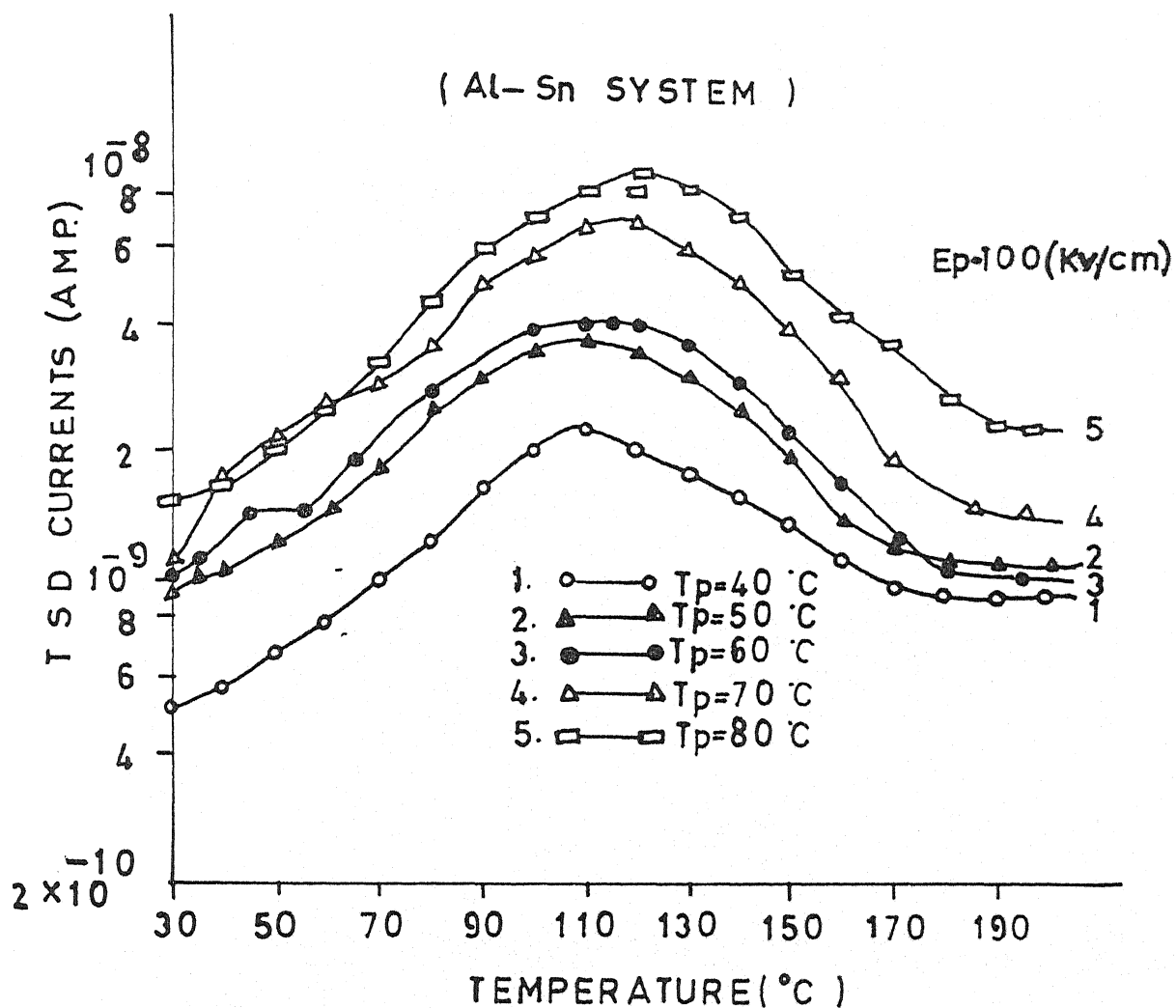


Figure No. 4.70

Thermally Stimulated Discharge Currents (T.S.D.C.) for Polyvinylidene fluoride Samples ($20 \mu\text{m}$) poled at $E_p = 100 \text{ kV/cm}$ with different polarisation Temperature (i.e. $40, 50, 60, 70$ and 80°C) for Al - Sn system.

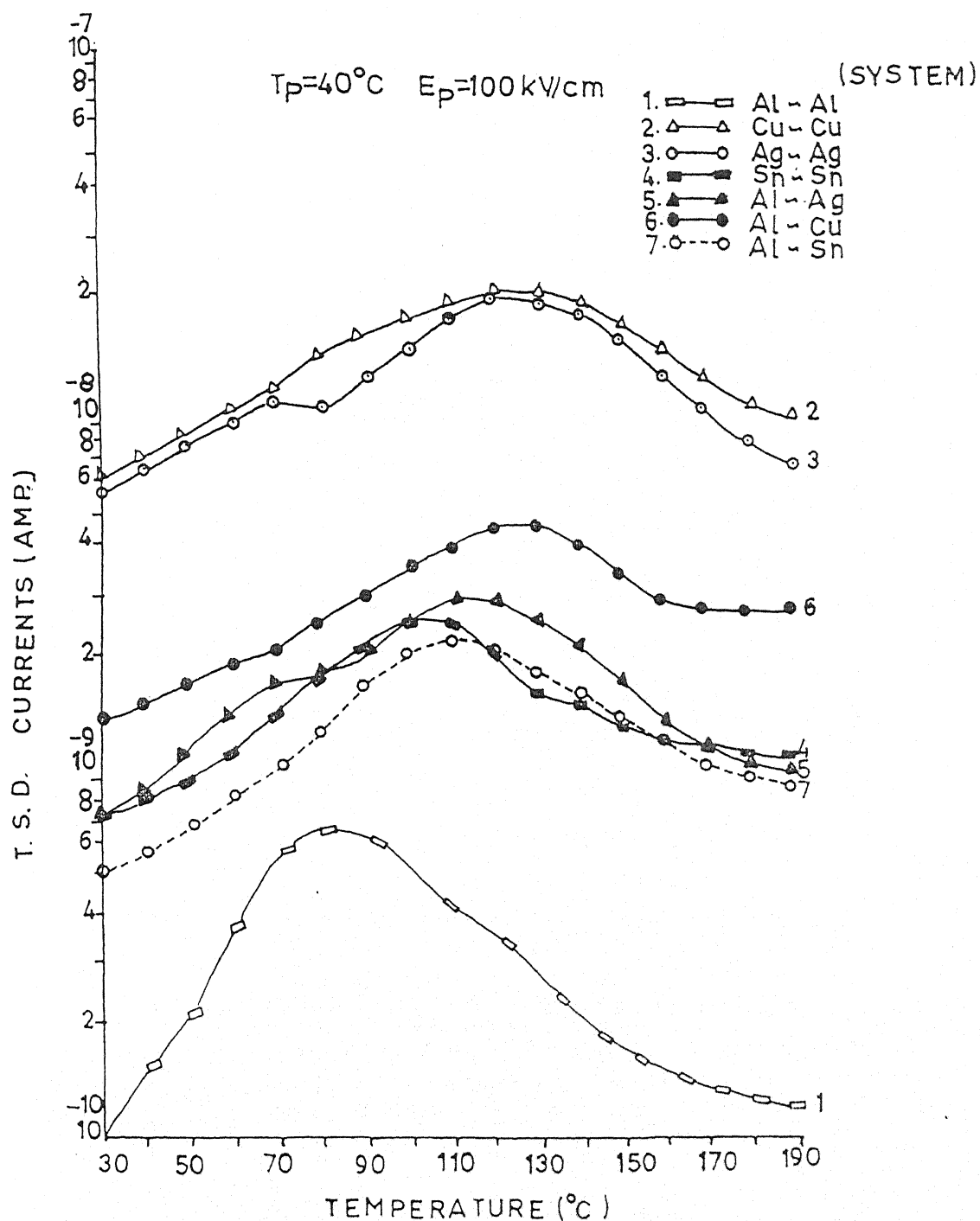


Figure No. 4.71

Thermally Stimulated Discharge Currents (T.S.D.C.) for Polyvinylidene fluoride Samples ($20\mu\text{m}$) poled at $T_p = 60^\circ\text{C}$ and $E_p = 100\text{ kV/cm}$. with different electrodes system (i.e. Al-Al-, Cu-Cu, Ag-Ag, Sn-Sn, Al-Ag, Al-Cu and Al-Sn)

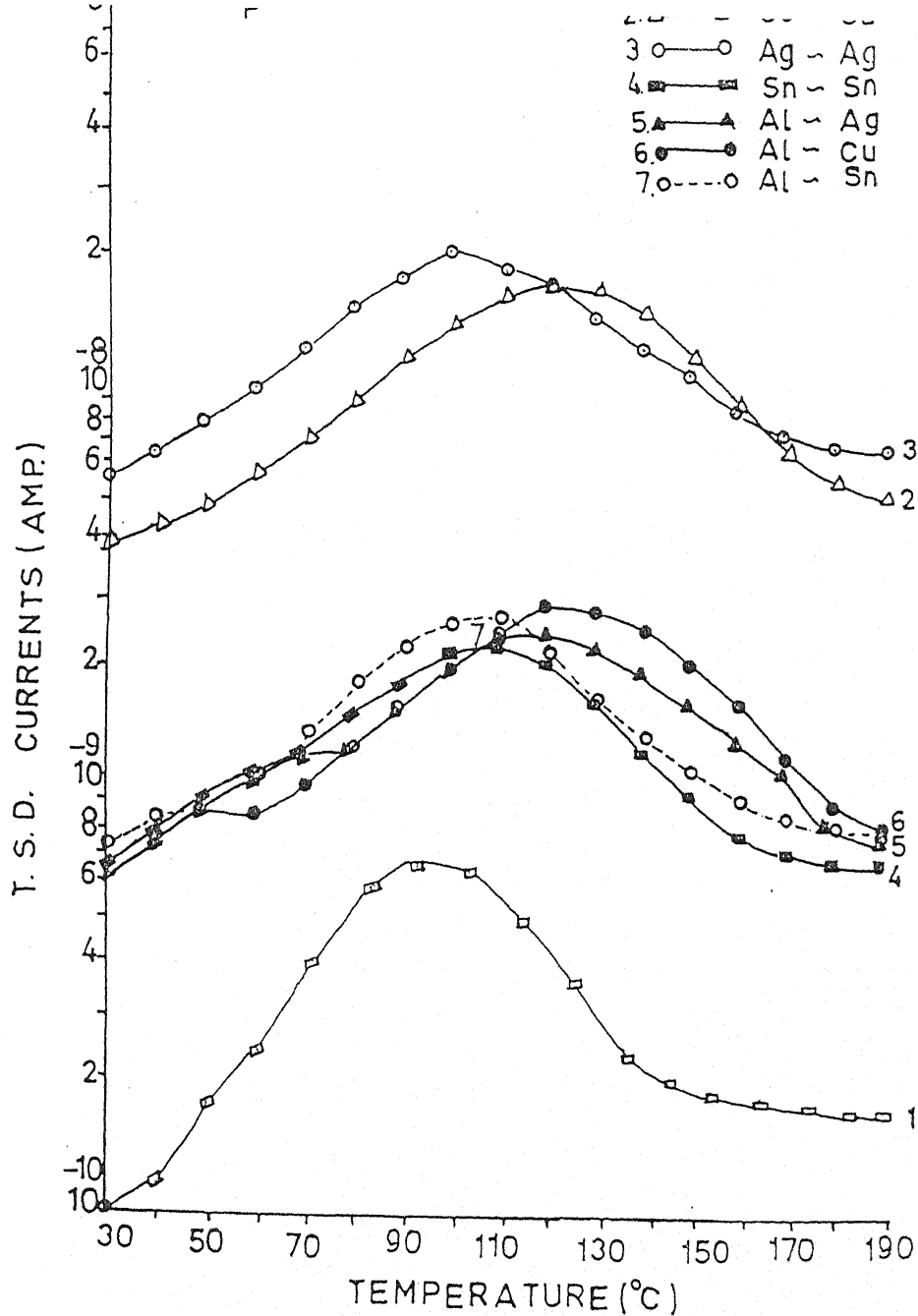


Figure No. 4.72

Thermally Stimulated Discharge Currents (T.S.D.C.) for Polyvinylidene fluoride Samples ($20\mu\text{m}$) poled at $T_p = 50^\circ\text{C}$ and $E_p = 75\text{ kV/cm}$. with different electrodes system (i.e. Al-Al-, Cu-Cu, Ag-Ag, Sn-Sn, Al-Ag, Al-Cu and Al-Sn)

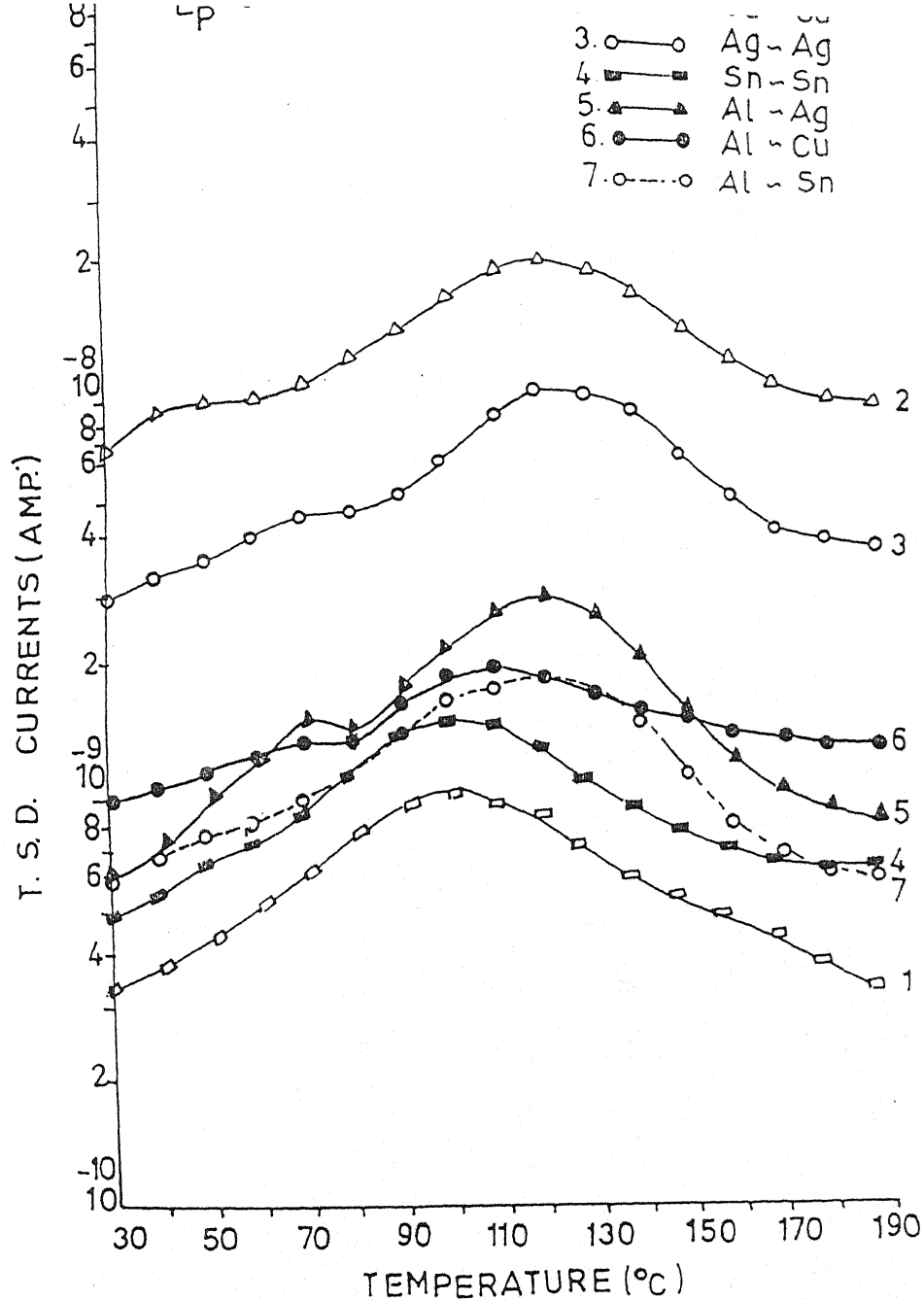


Figure No. 4.73

Thermally Stimulated Discharge Currents (T.S.D.C.) for Polyvinylidene fluoride Samples ($20\mu\text{m}$) poled at $T_p = 60^\circ\text{C}$ and $E_p = 50\text{ kV/cm}$. with different electrodes system (i.e. Al-Al-, Cu-Cu, Ag-Ag, Sn-Sn, Al-Ag, Al-Cu and Al-Sn)

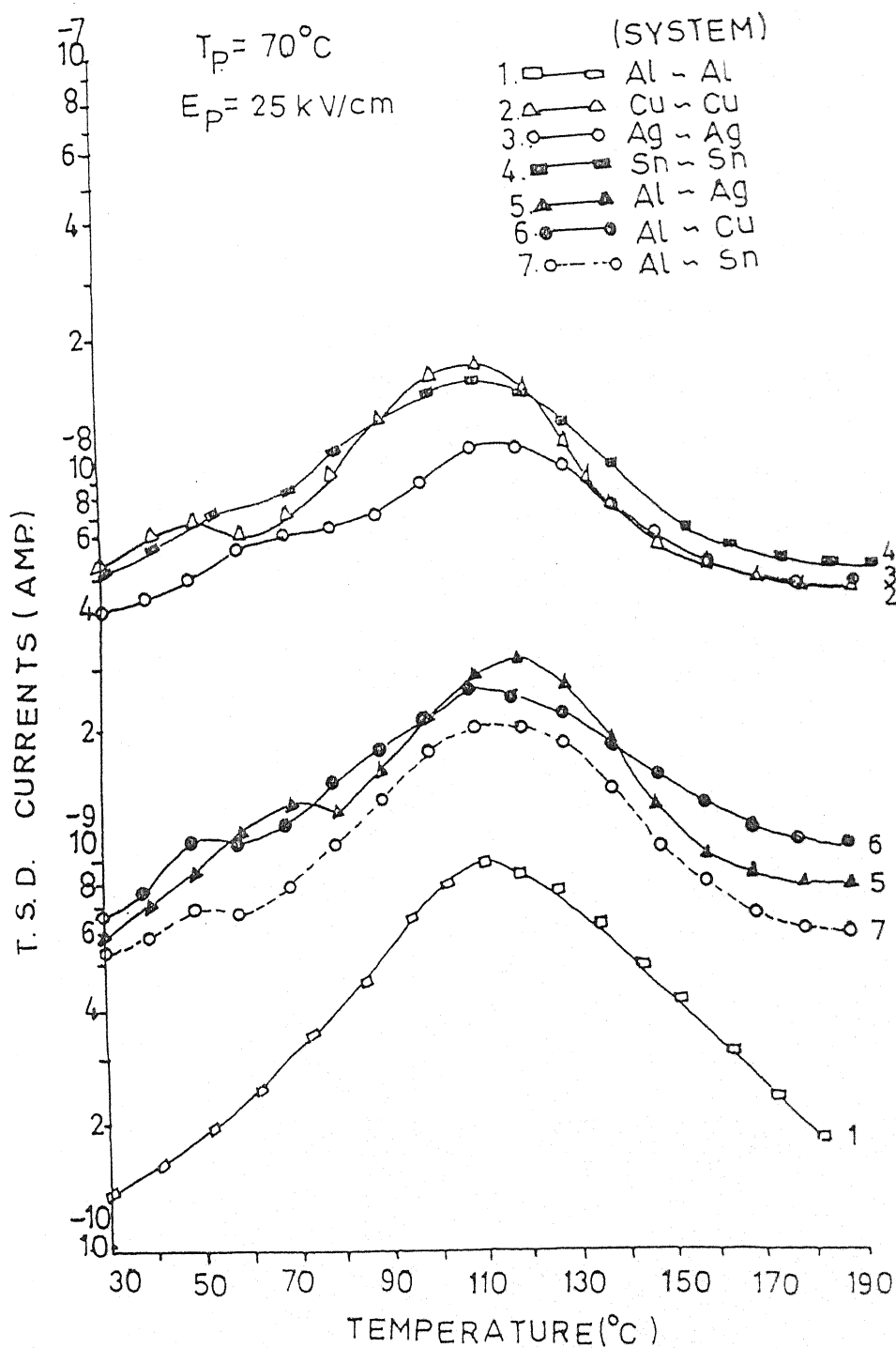


Figure No. 4.74

Thermally Stimulated Discharge Currents (T.S.D.C.) for Polyvinylidene fluoride Samples ($20\mu\text{m}$) poled at $T_P = 70^\circ\text{C}$ and $E_P = 25 \text{ kV/cm}$. with different electrodes system (i.e. Al-Al, Cu-Cu, Ag-Ag, Sn-Sn, Al-Ag, Al-Cu and Al-Sn)

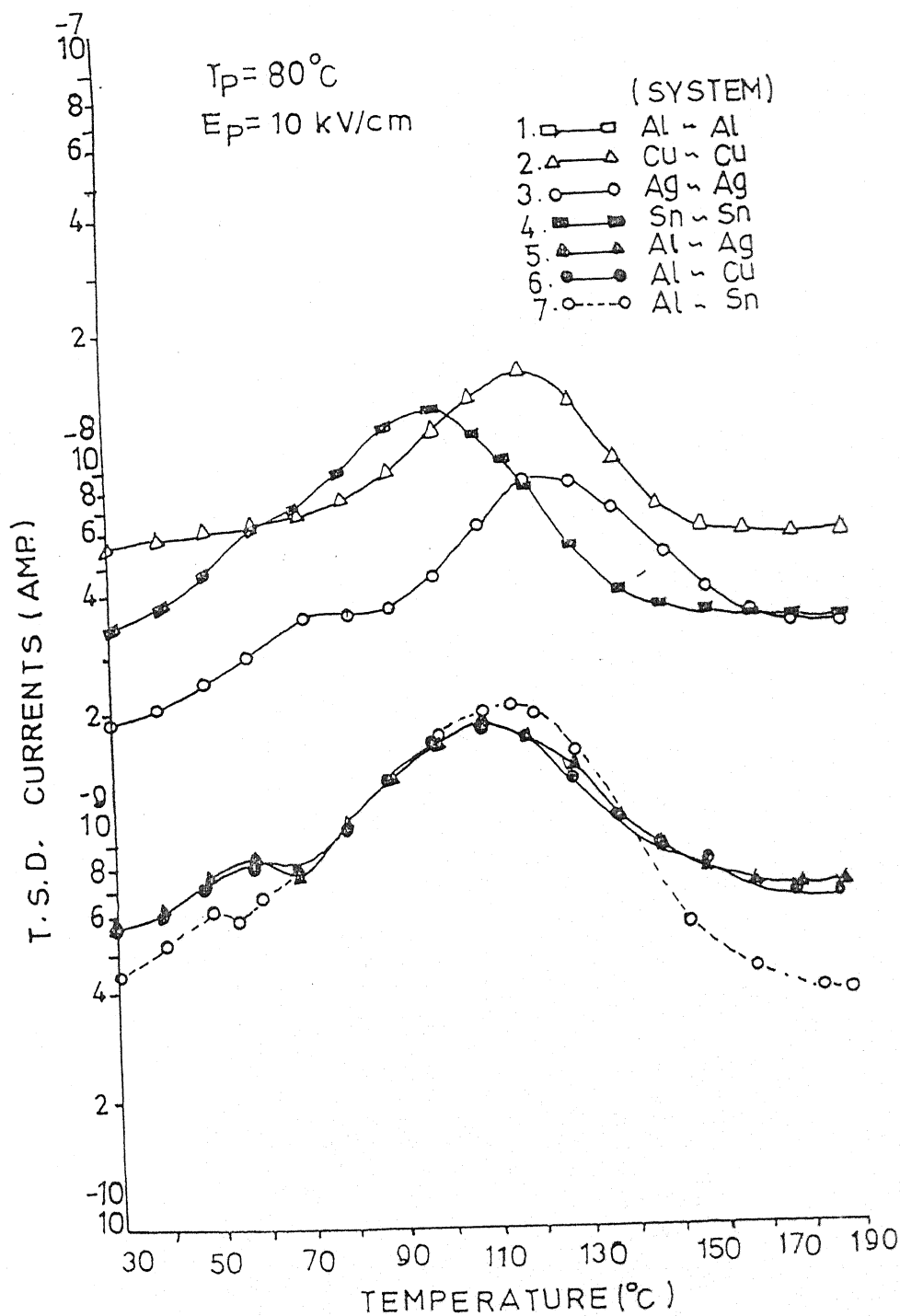


Figure No. 4.75
 Thermally Stimulated Discharge Currents (T.S.D.C.) for Polyvinylidene fluoride Samples ($20\mu\text{m}$) poled at $T_p = 80^\circ\text{C}$ and $E_p = 10 \text{ kV/cm}$. with different electrodes system (i.e. Al-Al, Cu-Cu, Ag-Ag, Sn-Sn, Al-Ag, Al-Cu and Al-Sn)

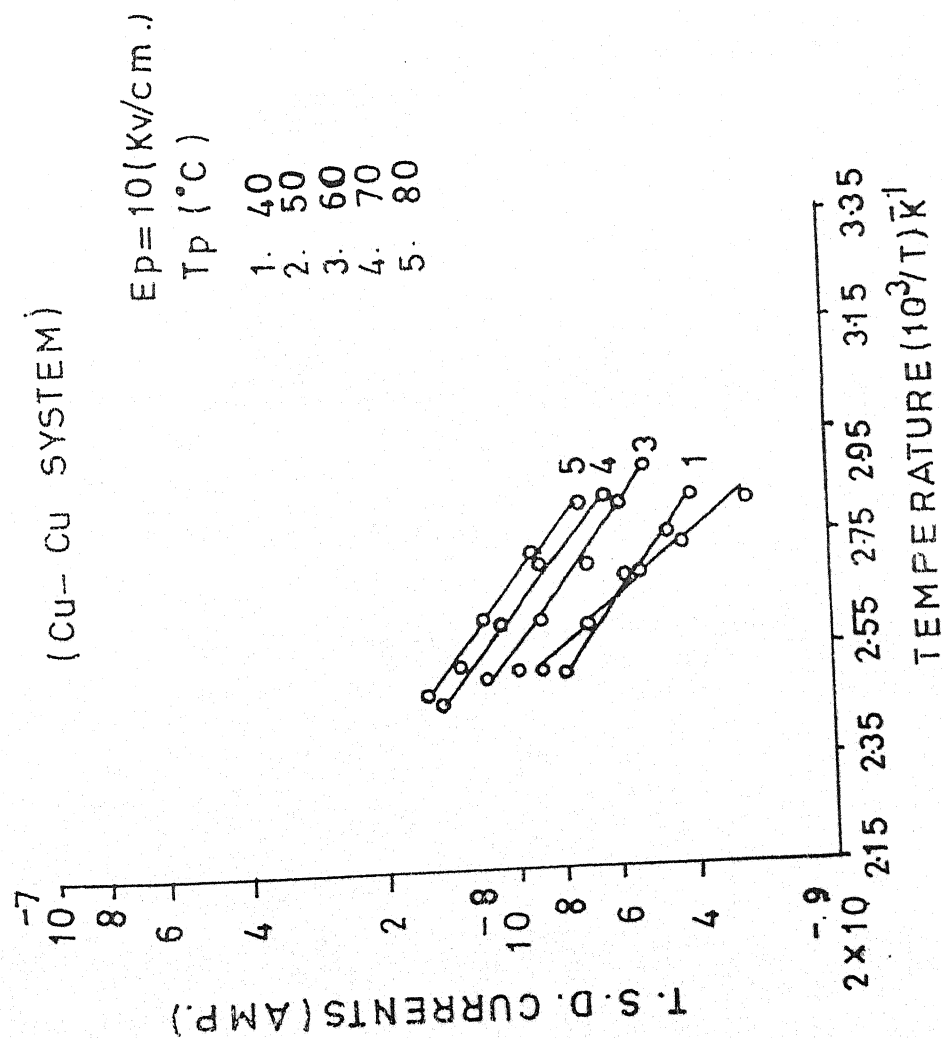


Figure No. 4.76
Initial rise plots of Fig. No. 4.41

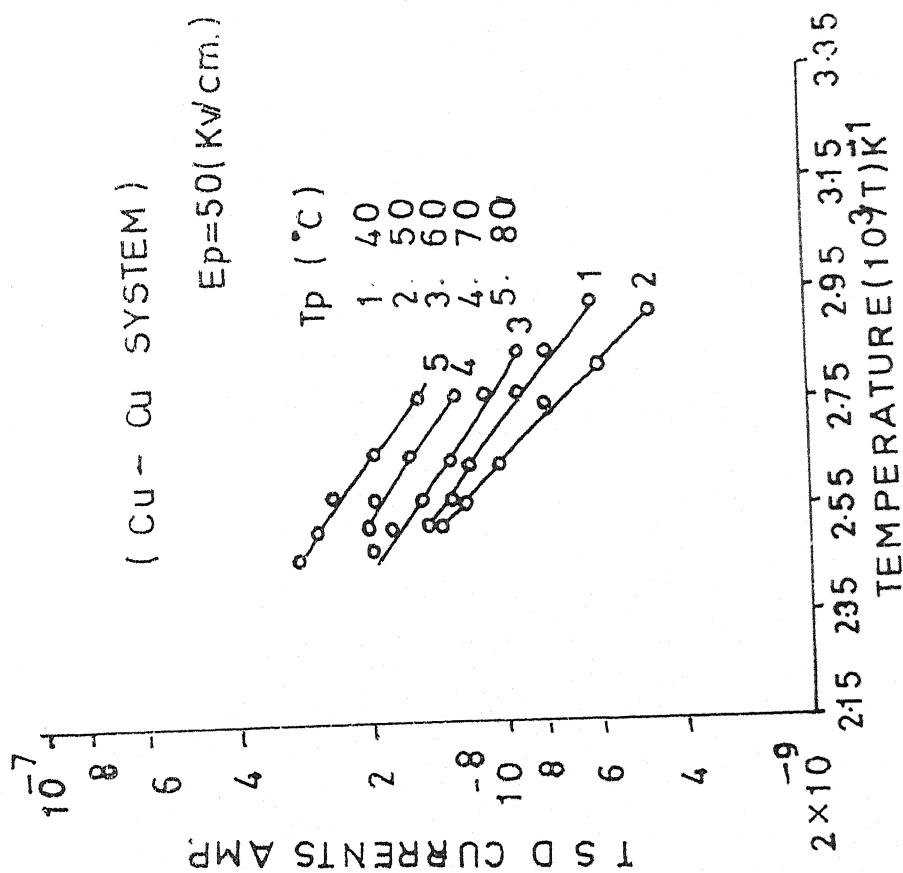


Figure No. 4.77
Initial rise plots of Fig. No. 4.43

(Cu-O₂ SYSTEM)

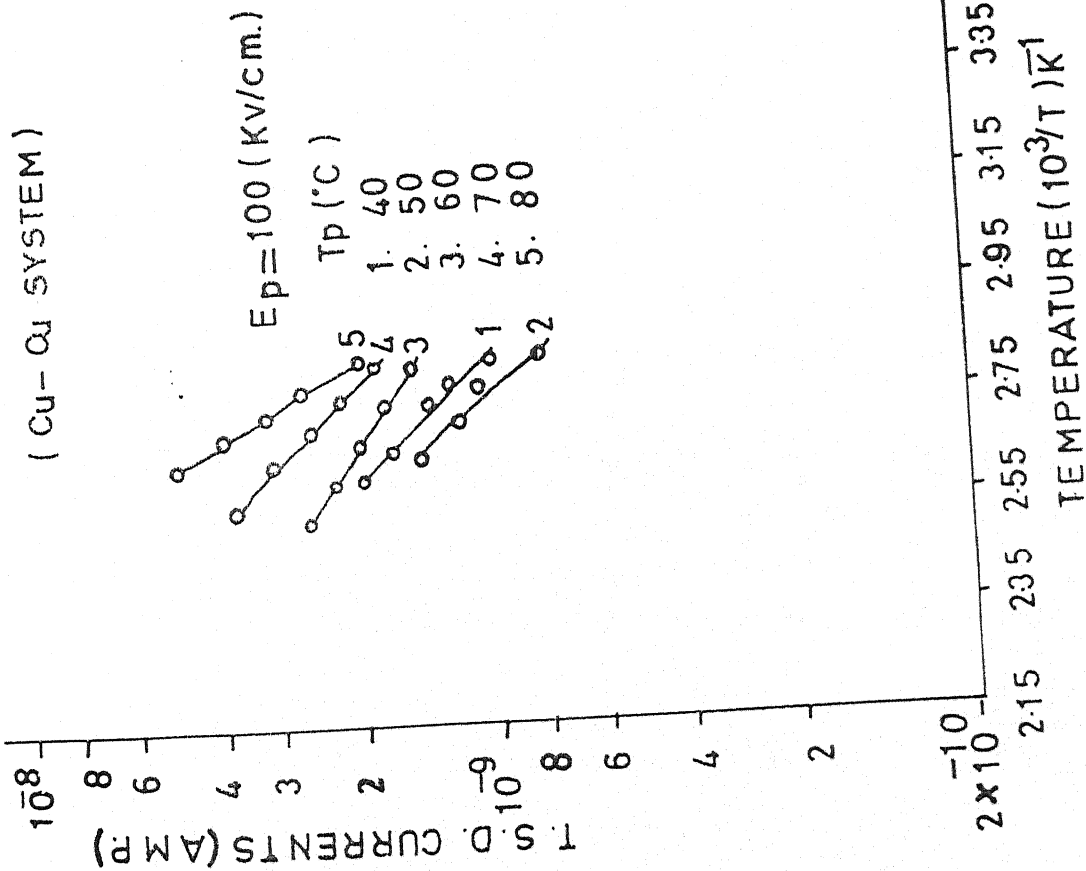


Figure No. 4.78

Initial rise plots of Fig. No. 4.45

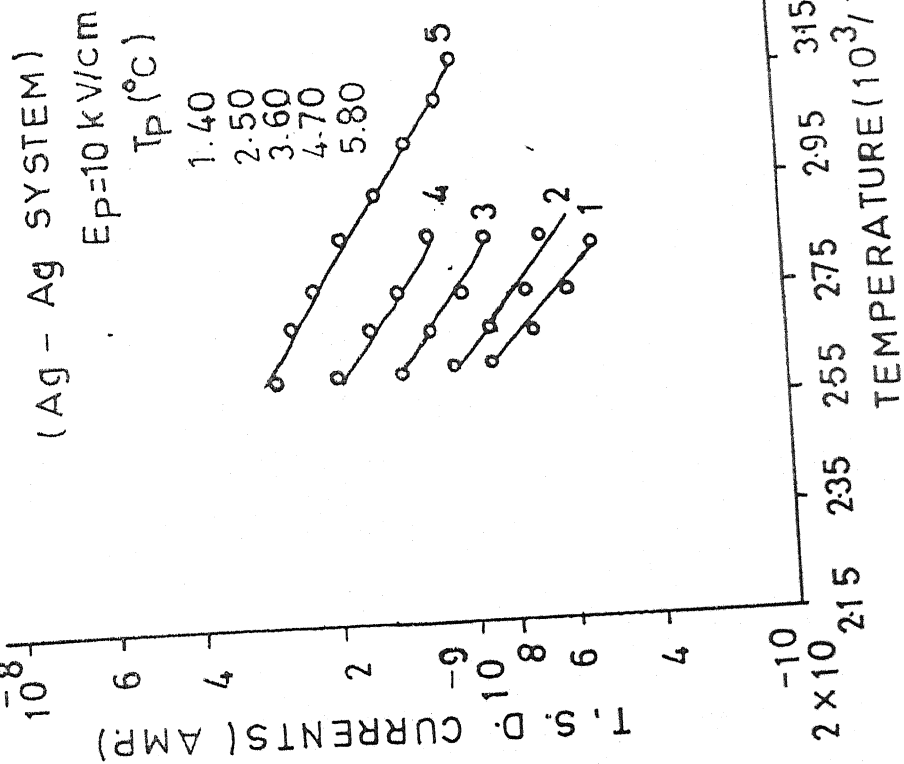


Figure No. 4.79

Initial rise plots of Fig. No. 4.46

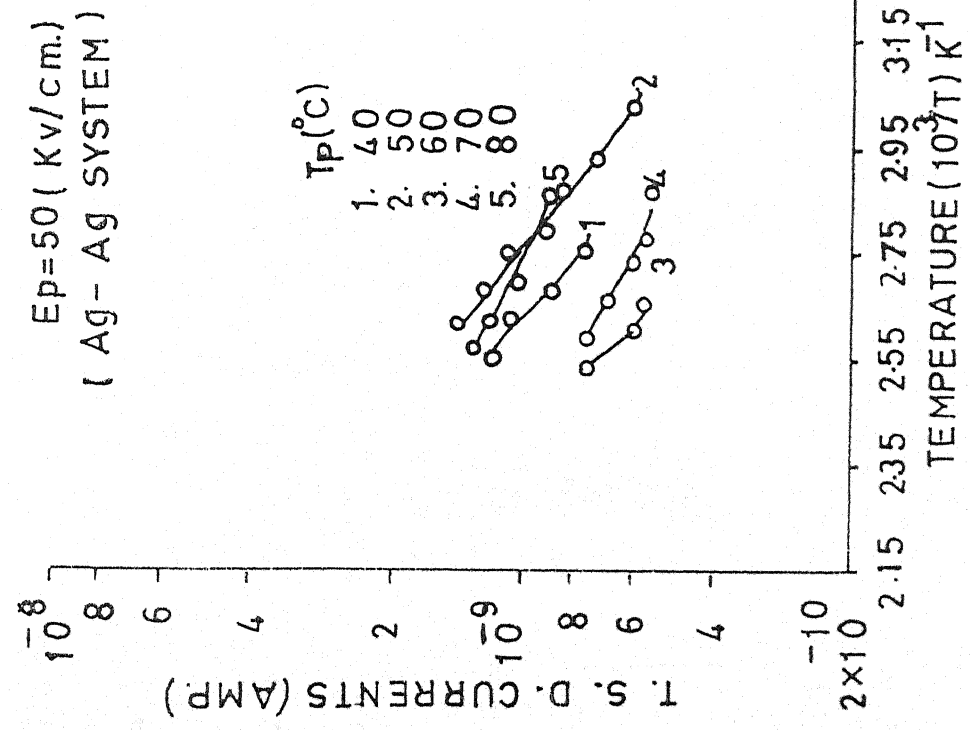


Figure No. 4.80
Initial rise plots of Fig. No. 4.48

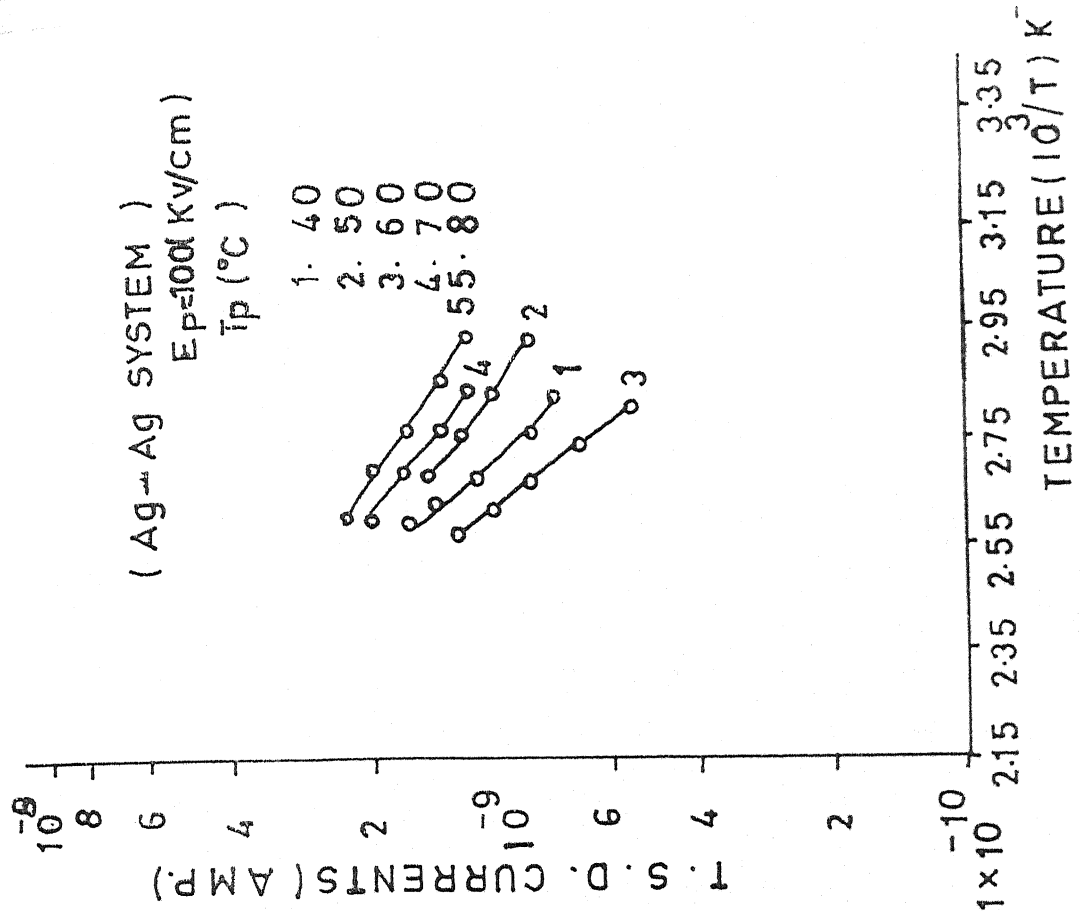


Figure No. 4.81
Initial rise plots of Fig. No. 4.50

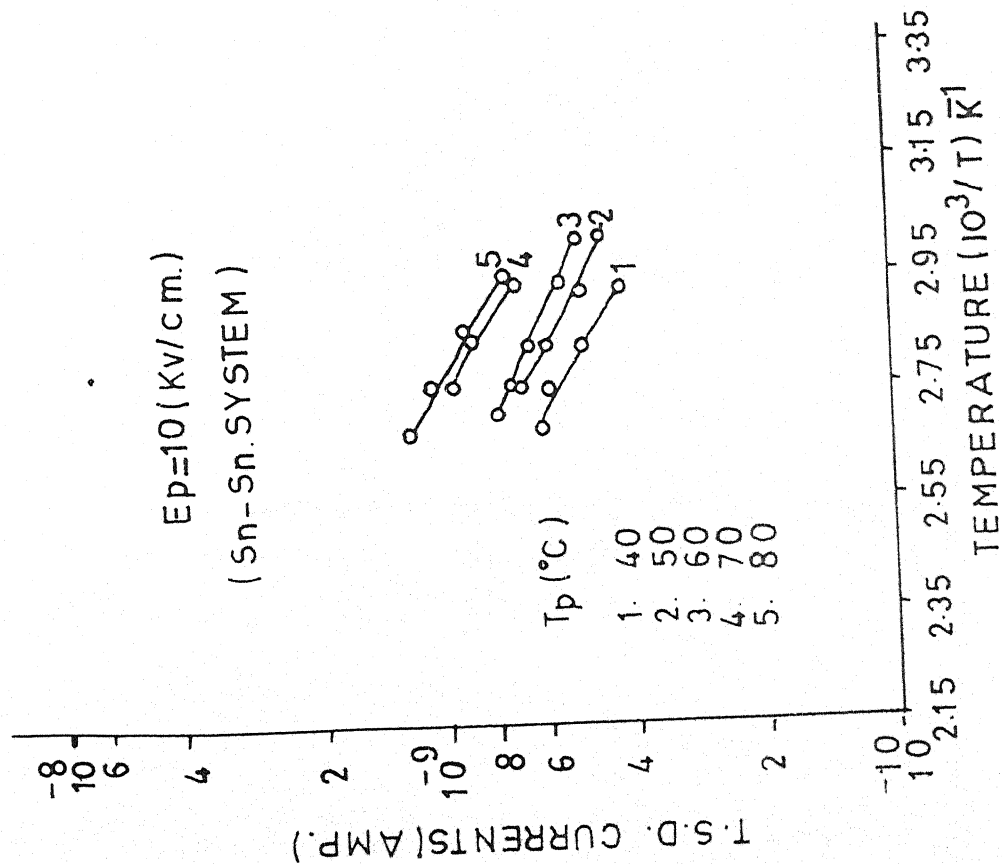


Figure No. 4.82
Initial rise plots of Fig. No. 4.51

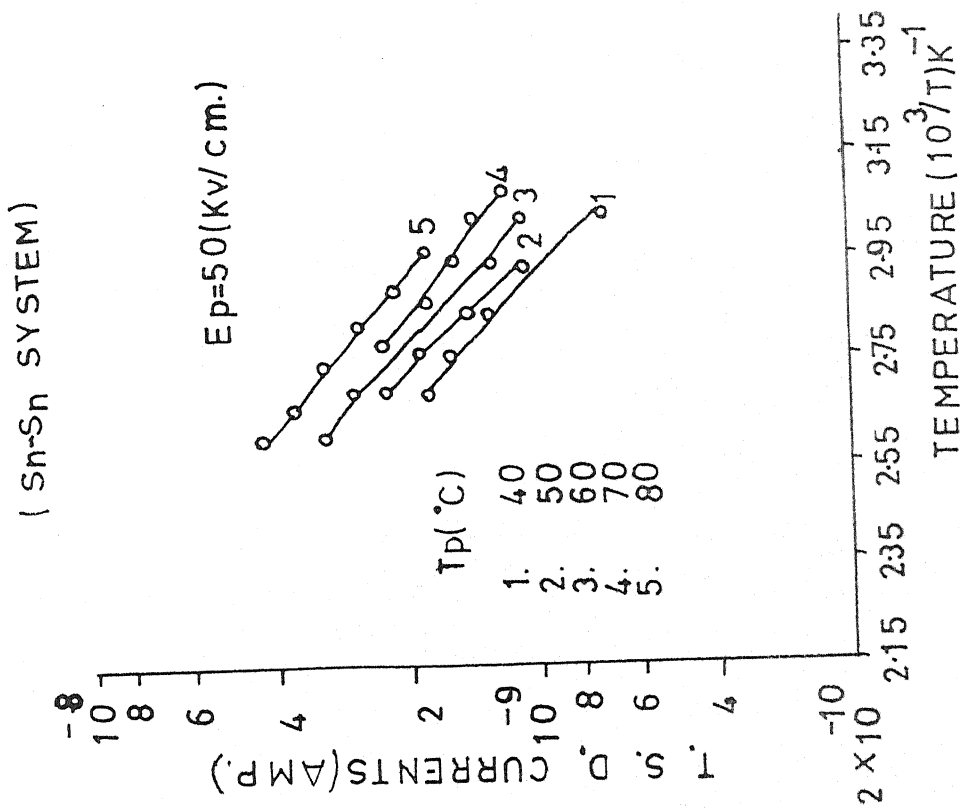


Figure No. 4.83
Initial rise plots of Fig. No. 4.53

(Al - Cu SYSTEM)

$E_p = 10 \text{ (Kv/cm.)}$

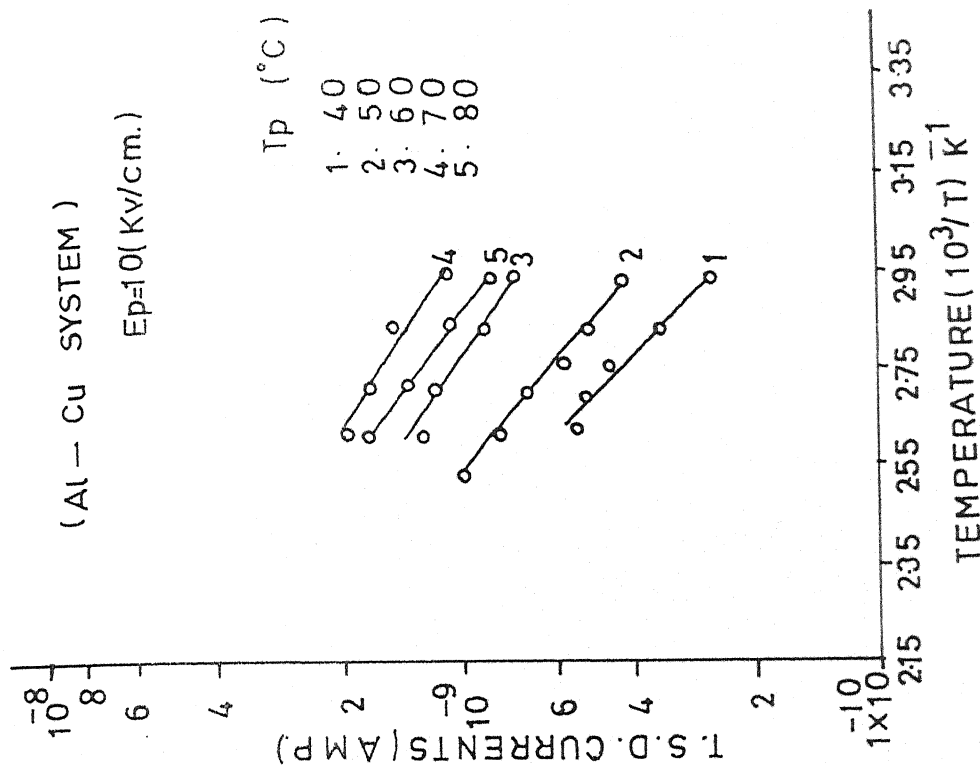


Figure No. 4.85

Initial rise plots of Fig. No. 4.56

(Sn-Sn SYSTEM)

$E_p = 100 \text{ (Kv/cm.)}$

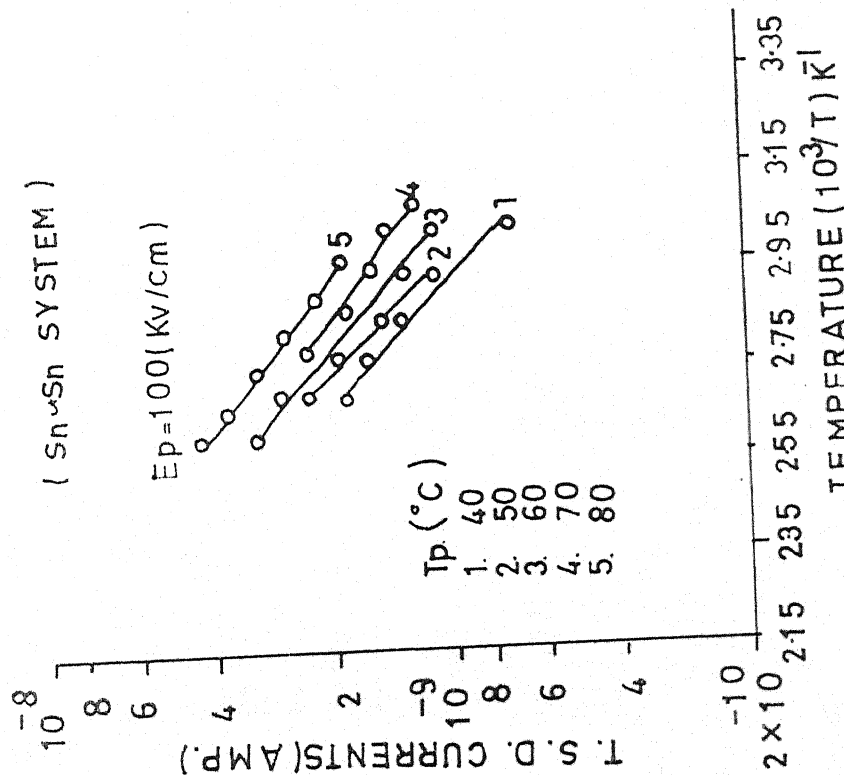


Figure No. 4.84

Initial rise plots of Fig. No. 4.55

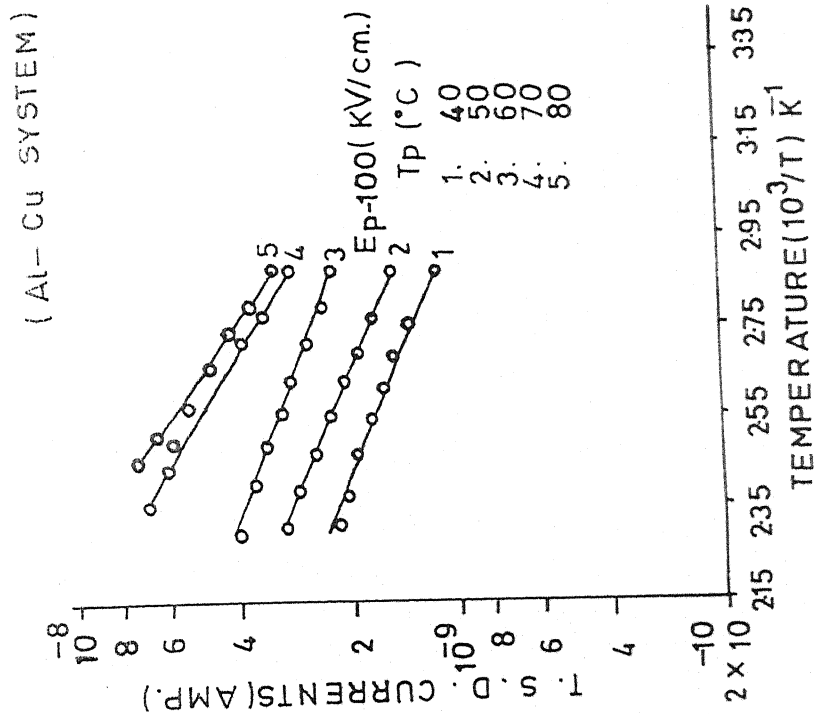


Figure No. 4.87
Initial rise plots of Fig. No. 4.60

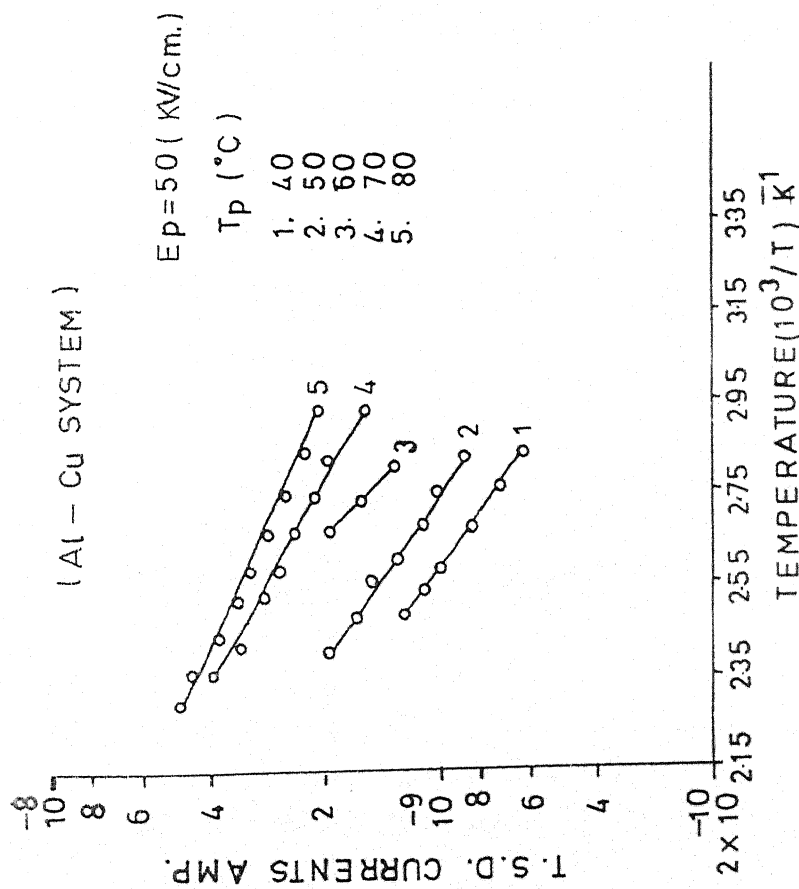


Figure No. 4.86
Initial rise plots of Fig. No. 4.58

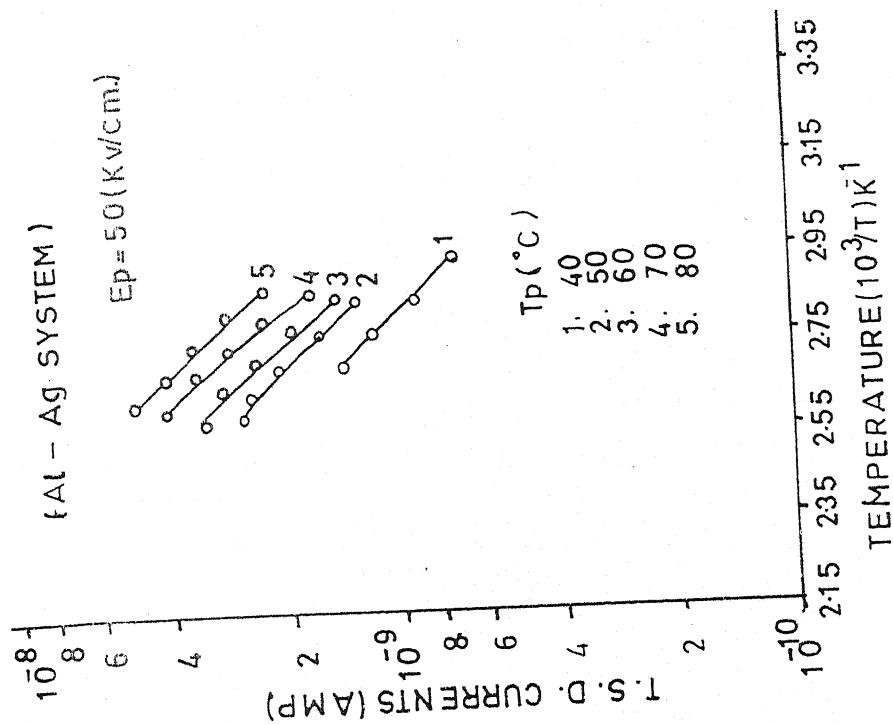


Figure No. 4.89
Initial rise plots of Fig. No. 4.63

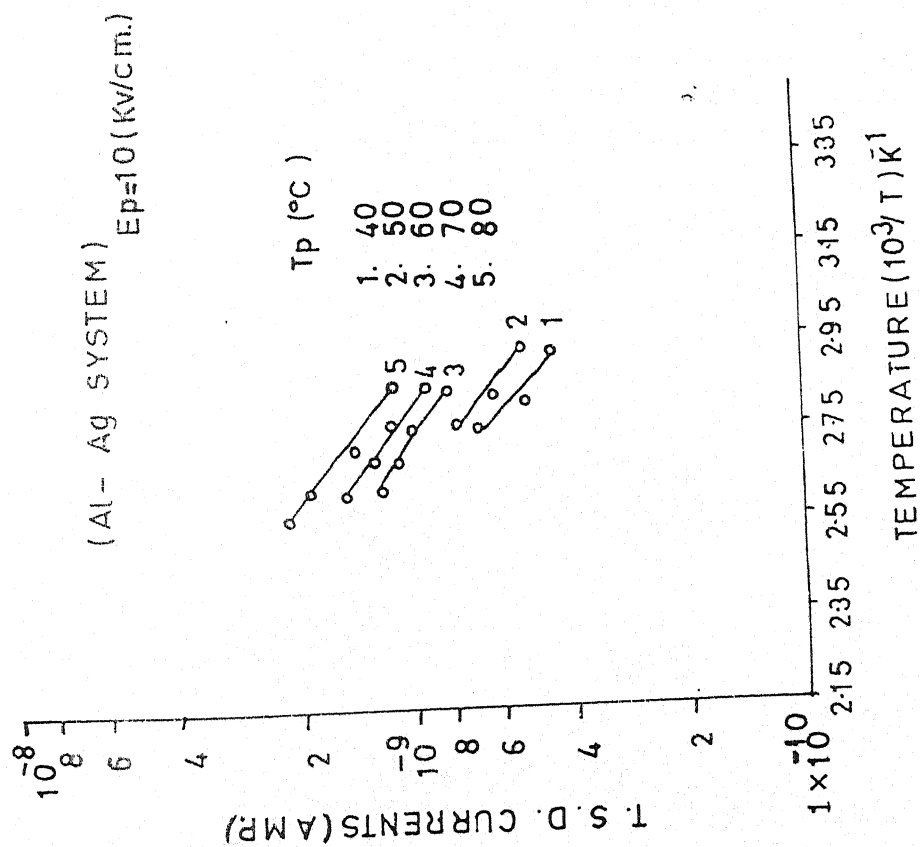


Figure No. 4.88
Initial rise plots of Fig. No. 4.61

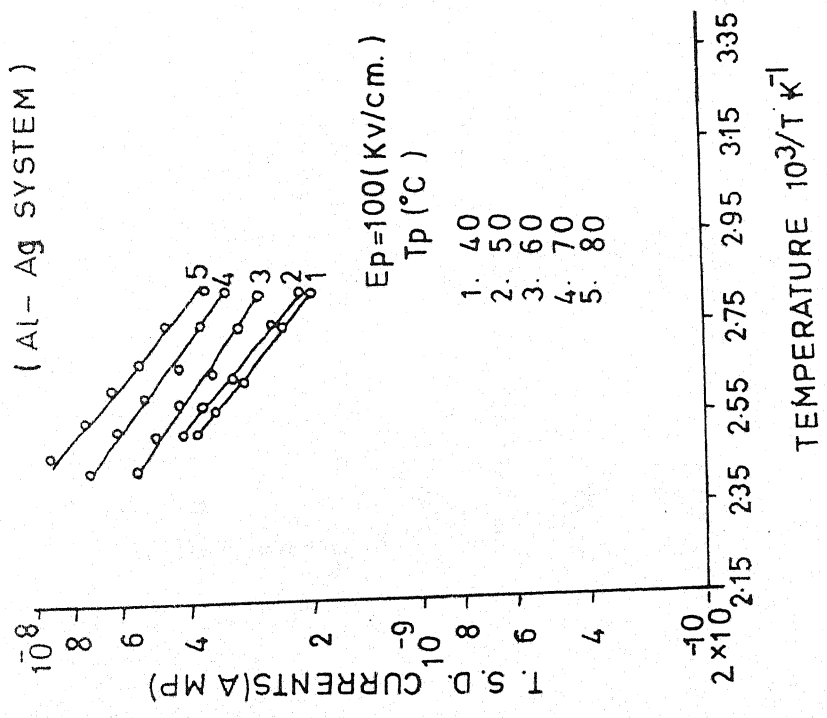


Figure No. 4.90
Initial rise plots of Fig. No. 4.65

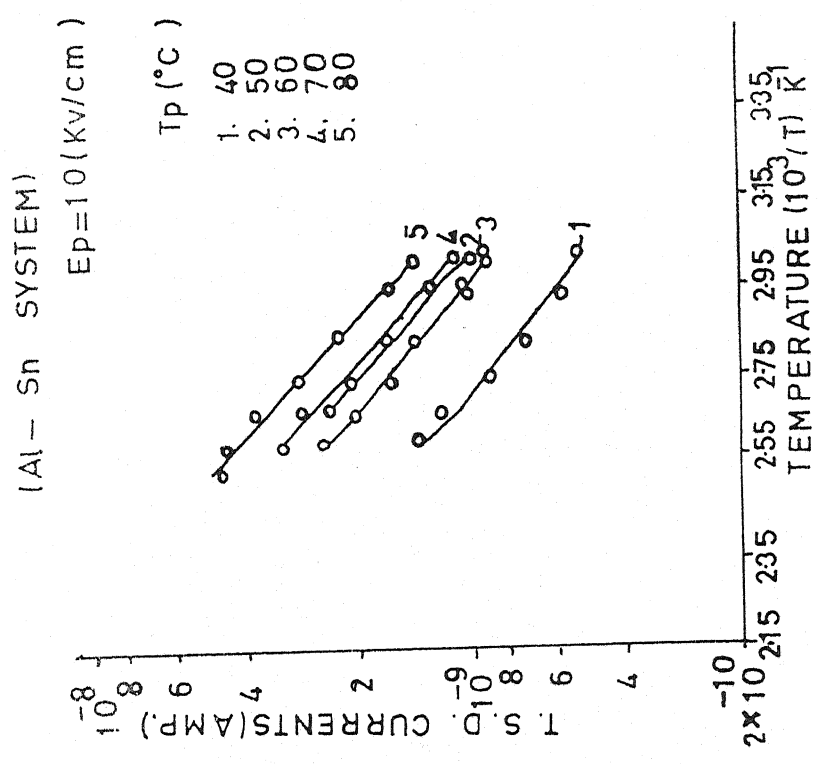


Figure No. 4.91
Initial rise plots of Fig. No. 4.66

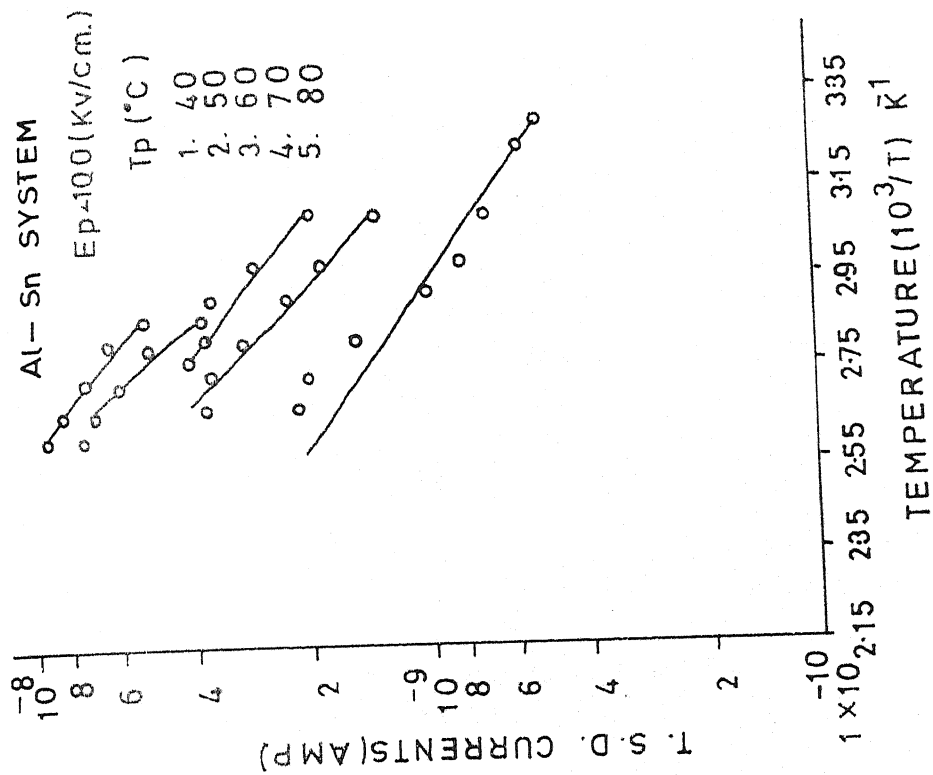


Figure No. 4.93
Initial rise plots of Fig. No. 4.70

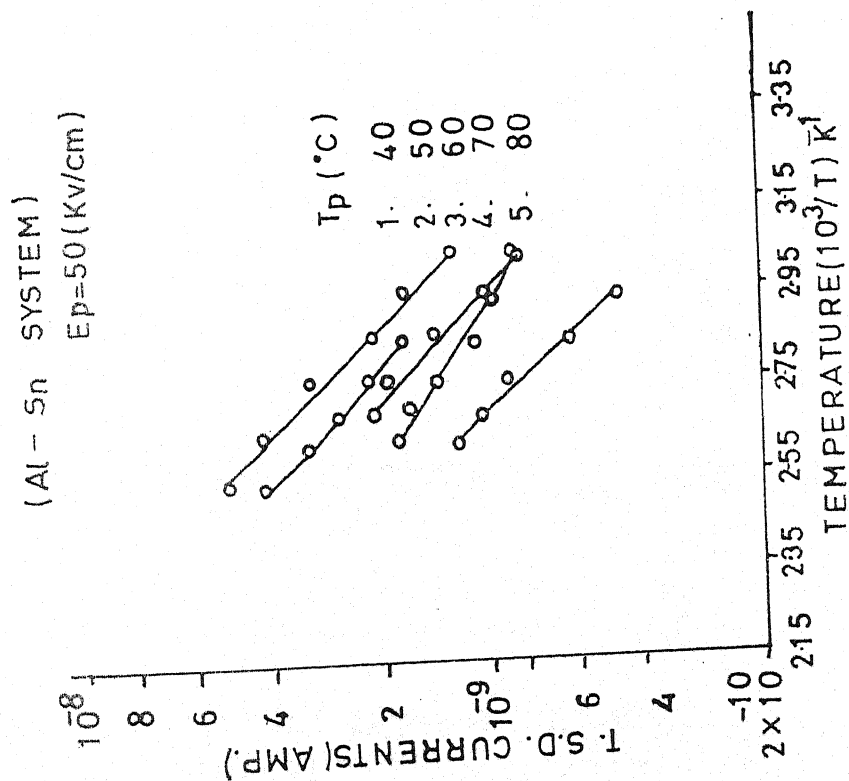


Figure No. 4.92
Initial rise plots of Fig. No. 4.68

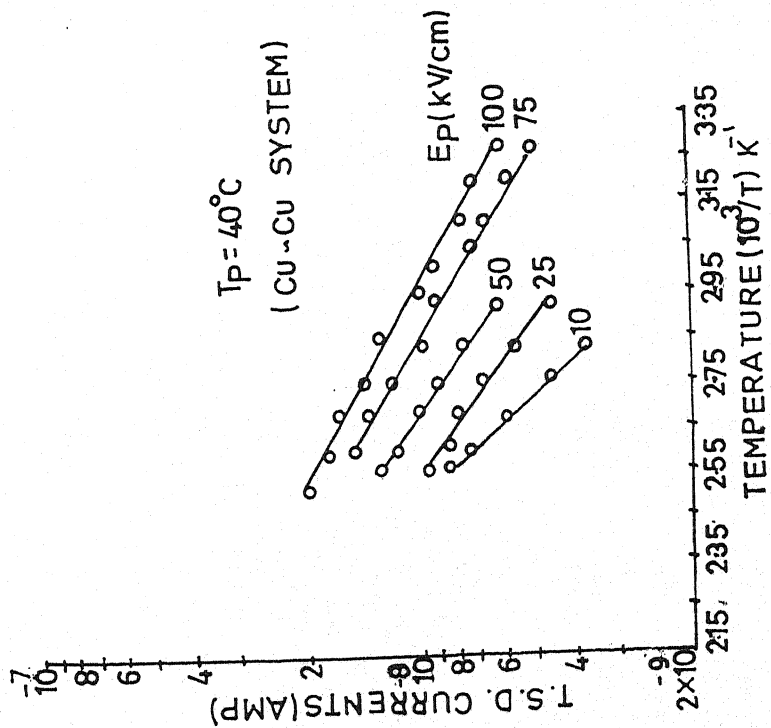


Figure No. 4.94
Initial rise plots of Fig. No. 4.6

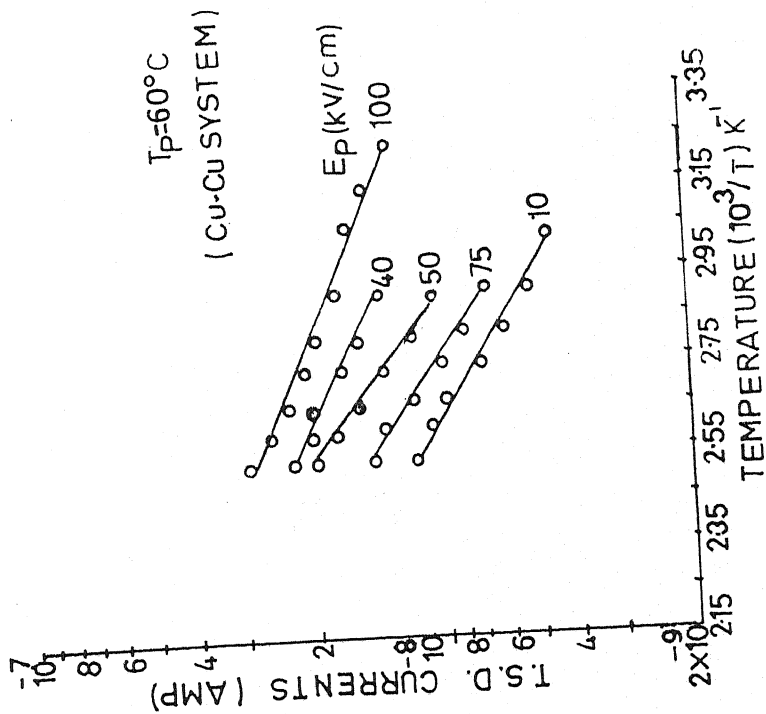


Figure No. 4.95
Initial rise plots of Fig. No. 4.8

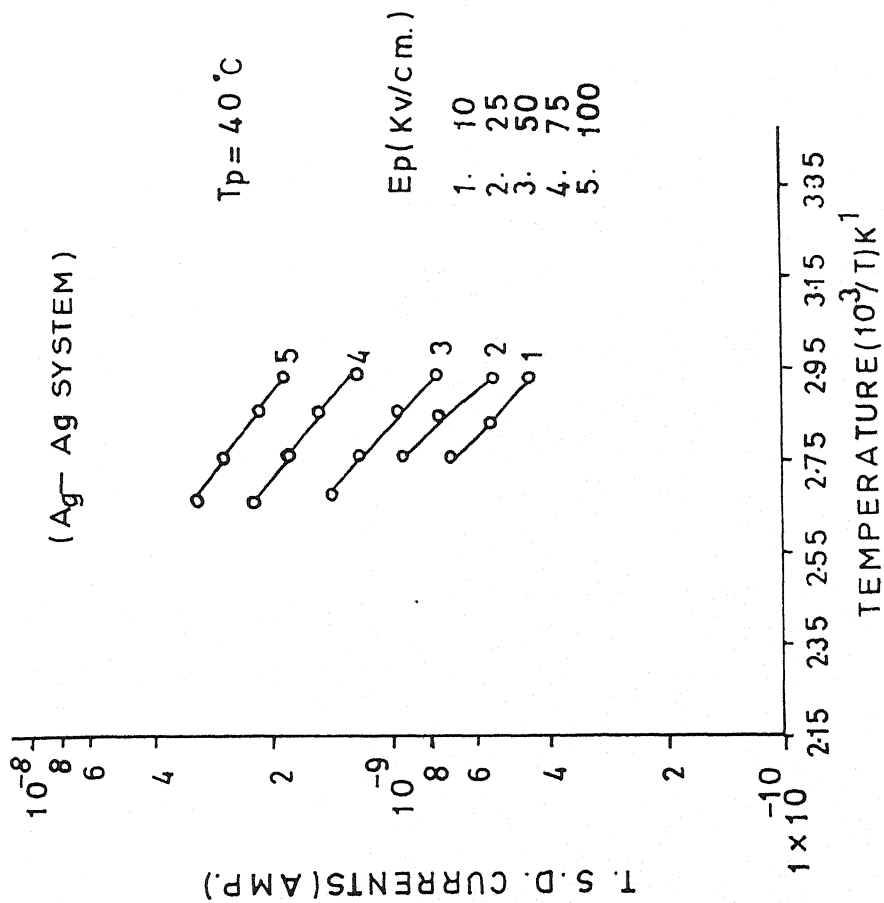


Figure No. 4.97
Initial rise plots of Fig. No. 4.11

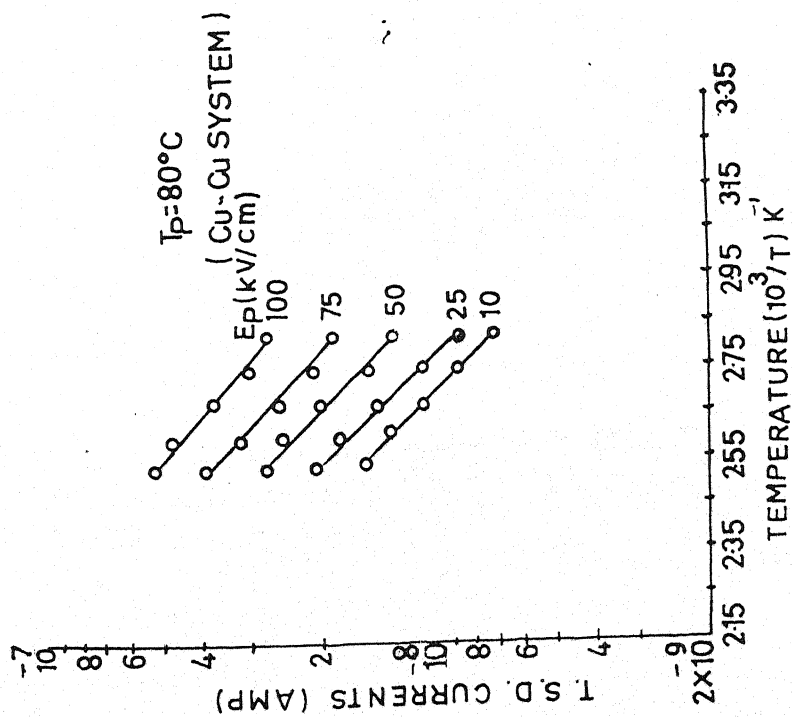


Figure No. 4.96
Initial rise plots of Fig. No. 4.10

(Ag - Ag SYSTEM)

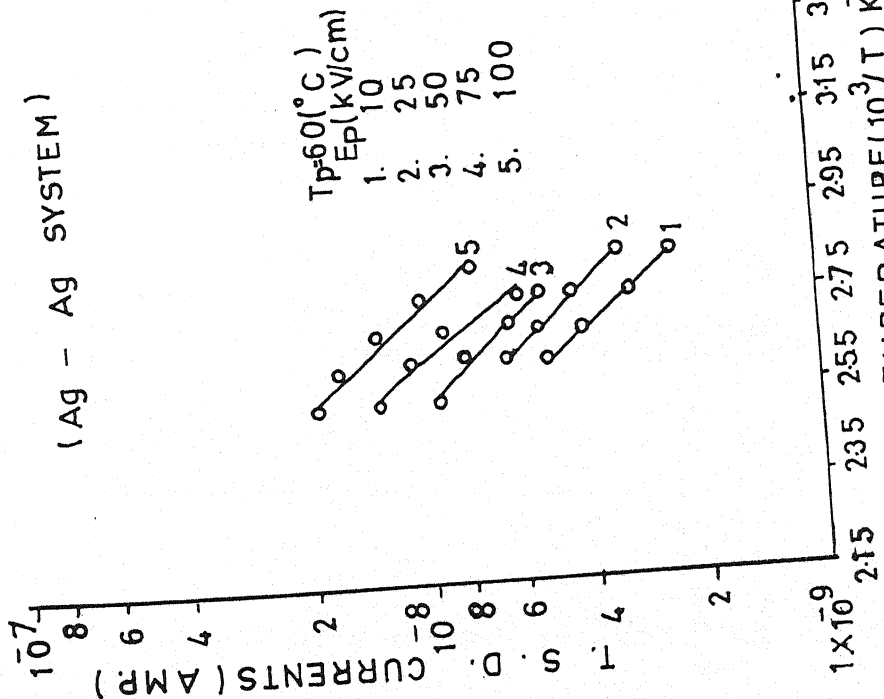


Figure No. 4.98
Initial rise plots of Fig. No. 4.13

(Ag - Ag SYSTEM)
 $T_p = 80^\circ C$

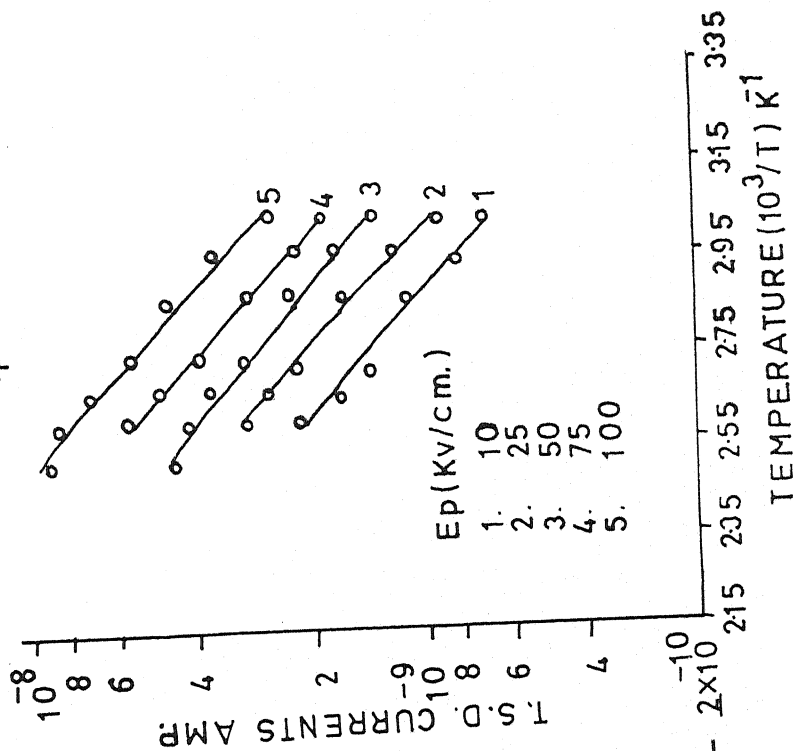


Figure No. 4.99
Initial rise plots of Fig. No. 4.15

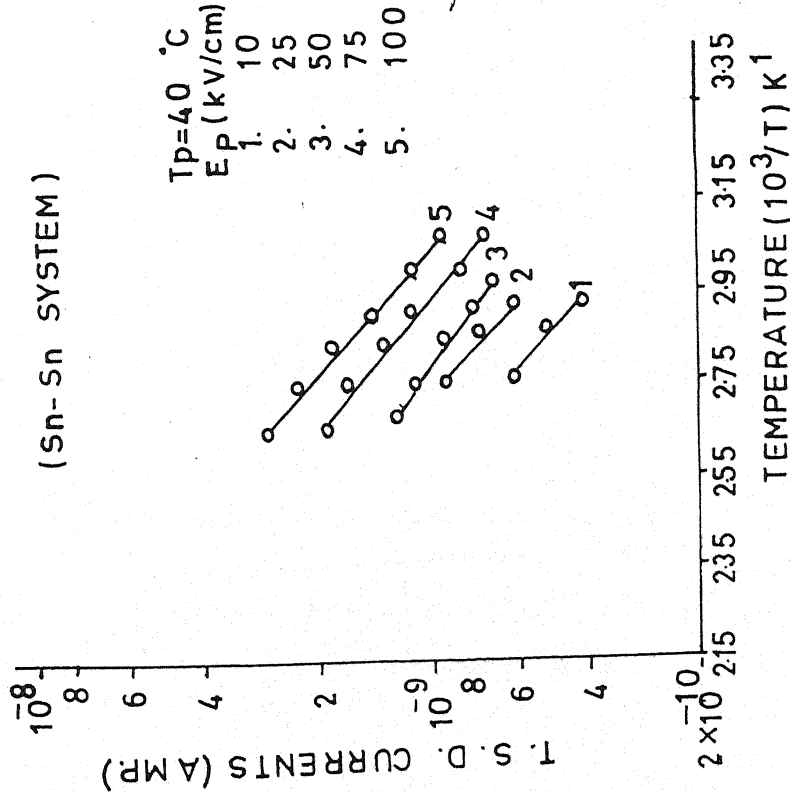


Figure No. 4.100
 Initial rise plots of Fig. No. 4.16

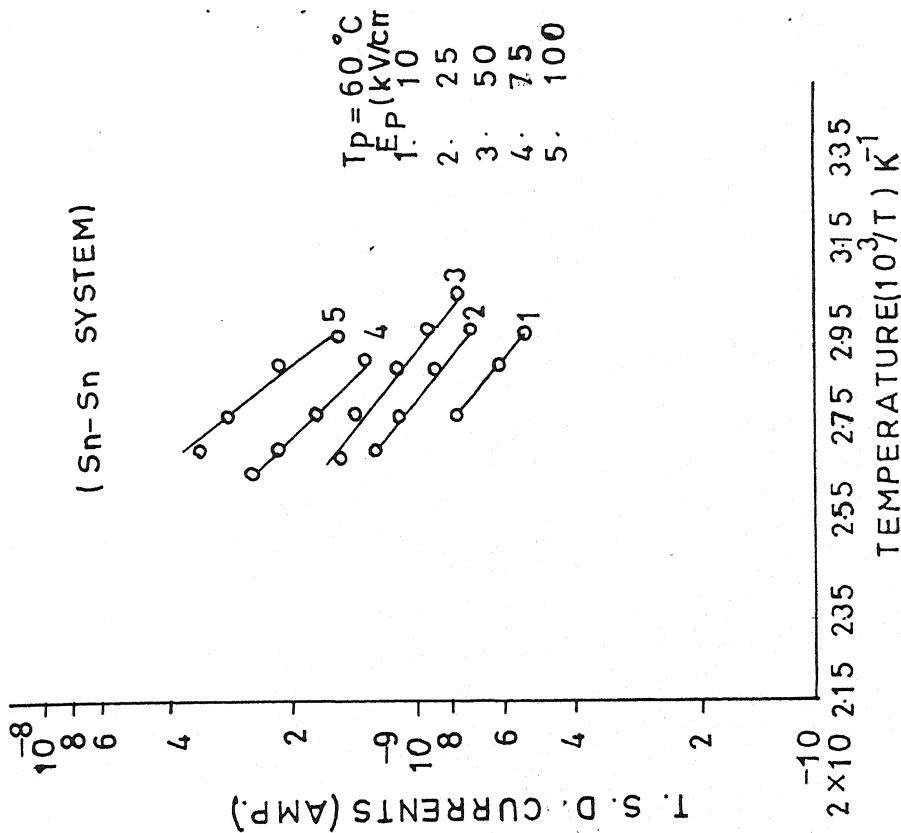


Figure No. 4.101
 Initial rise plots of Fig. No. 4.18

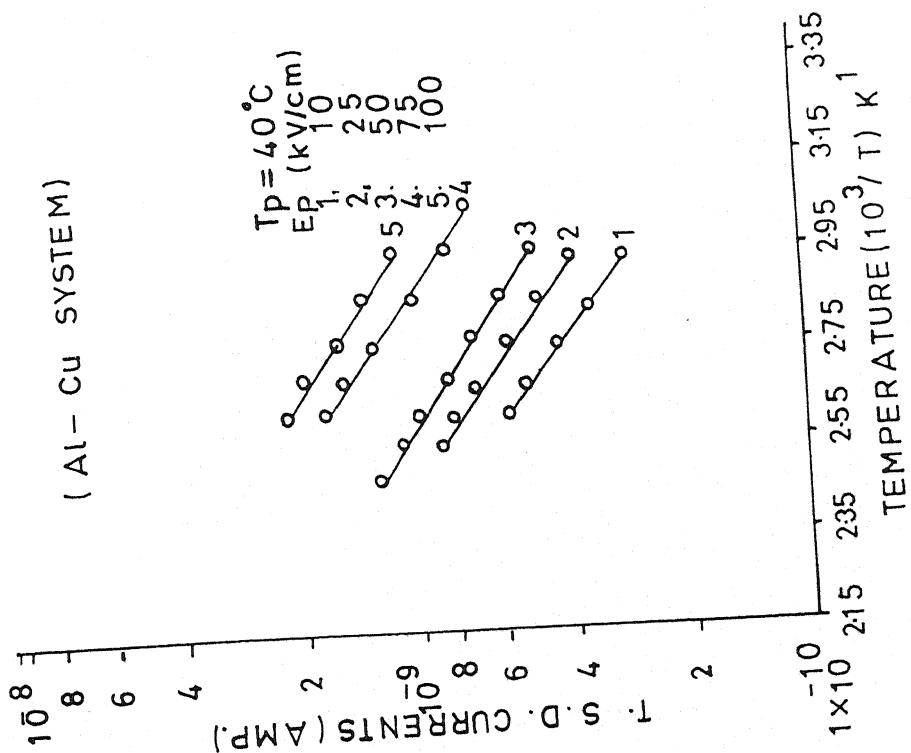


Figure No. 4.103
 Initial rise plots of Fig. No. 4.21

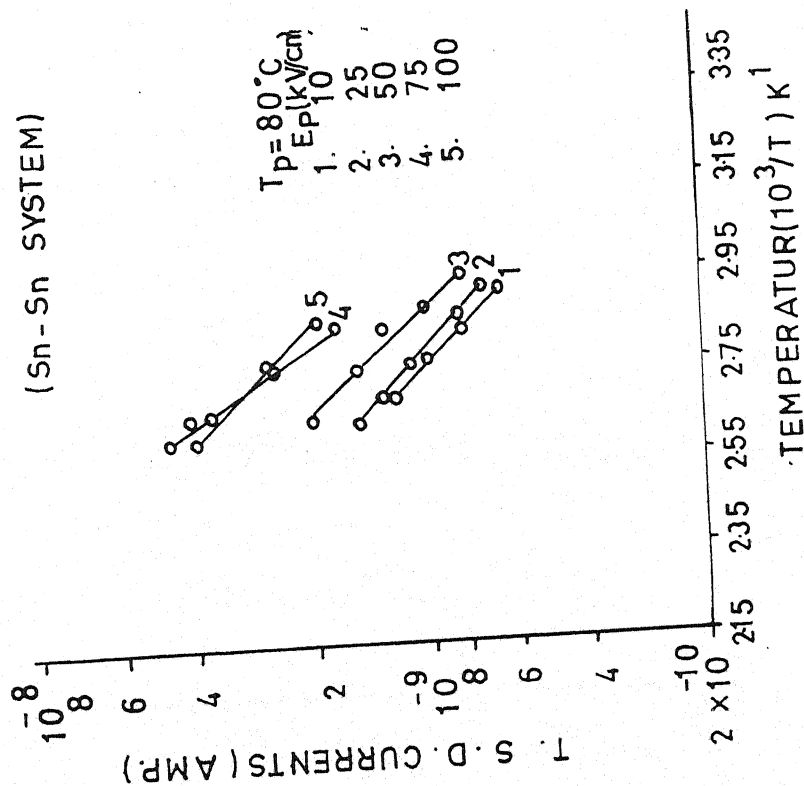


Figure No. 4.102
 Initial rise plots of Fig. No. 4.20

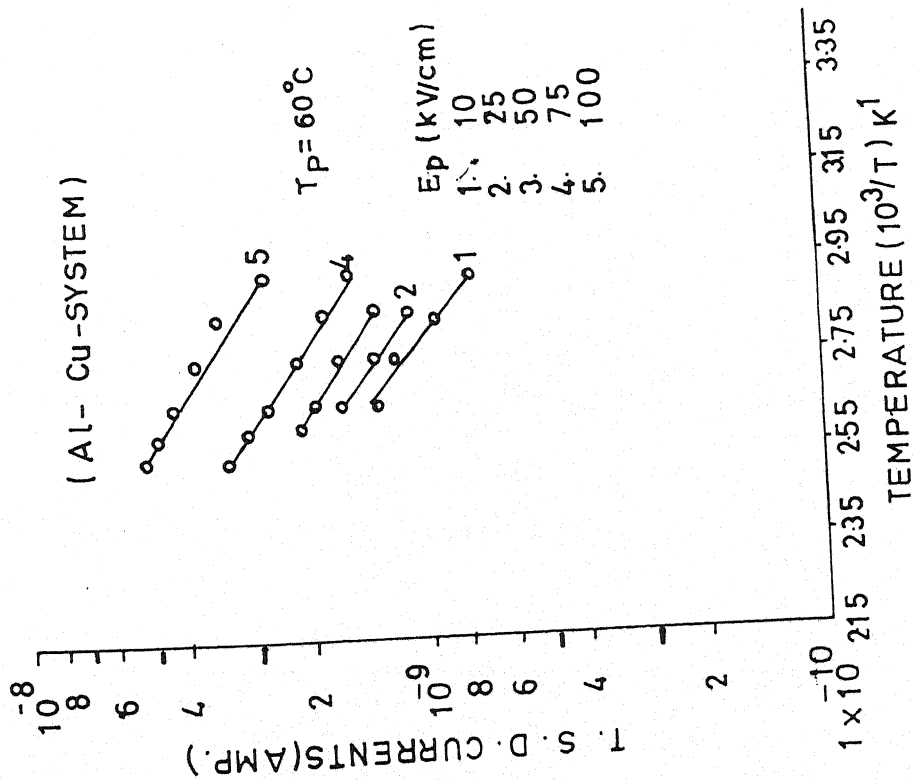


Figure No. 4.104
Initial rise plots of Fig. No. 4.23

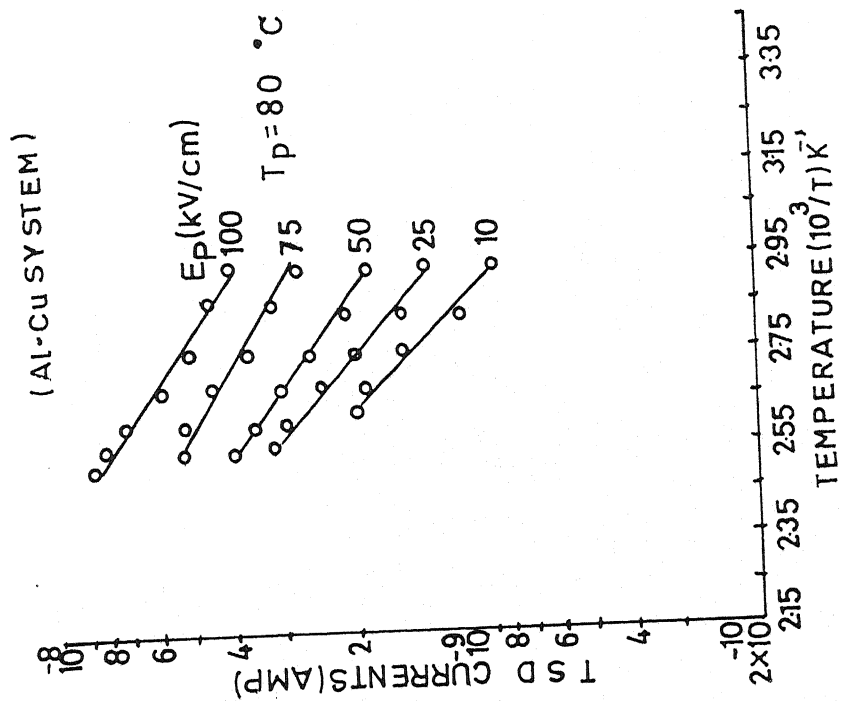


Figure No. 4.105
Initial rise plots of Fig. No. 4.25

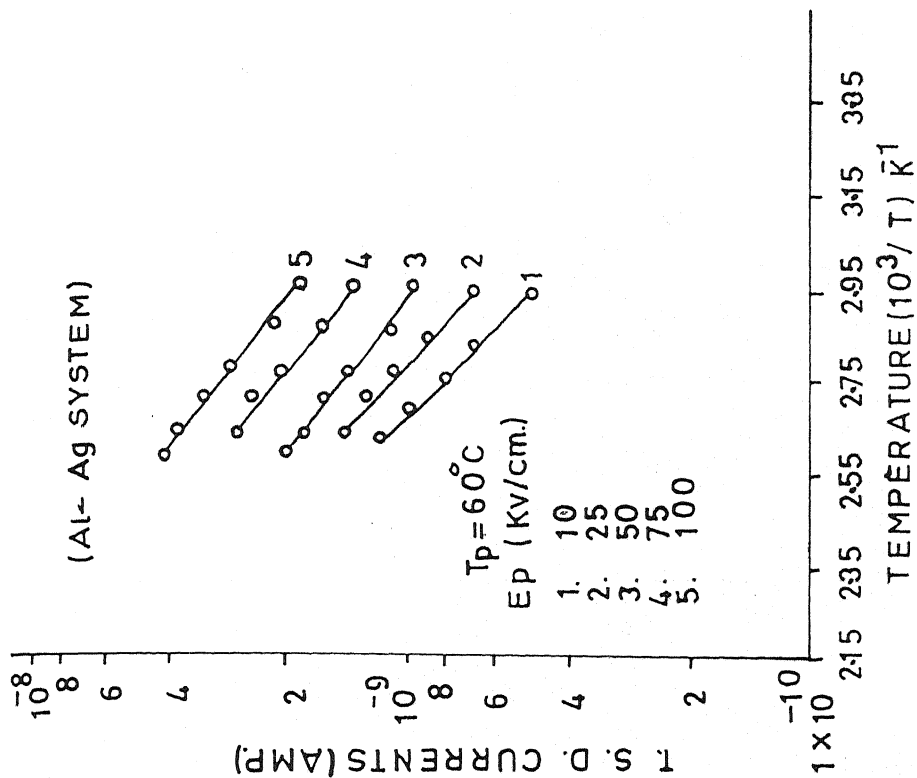


Figure No. 4.107
Initial rise plots of Fig. No. 4.28

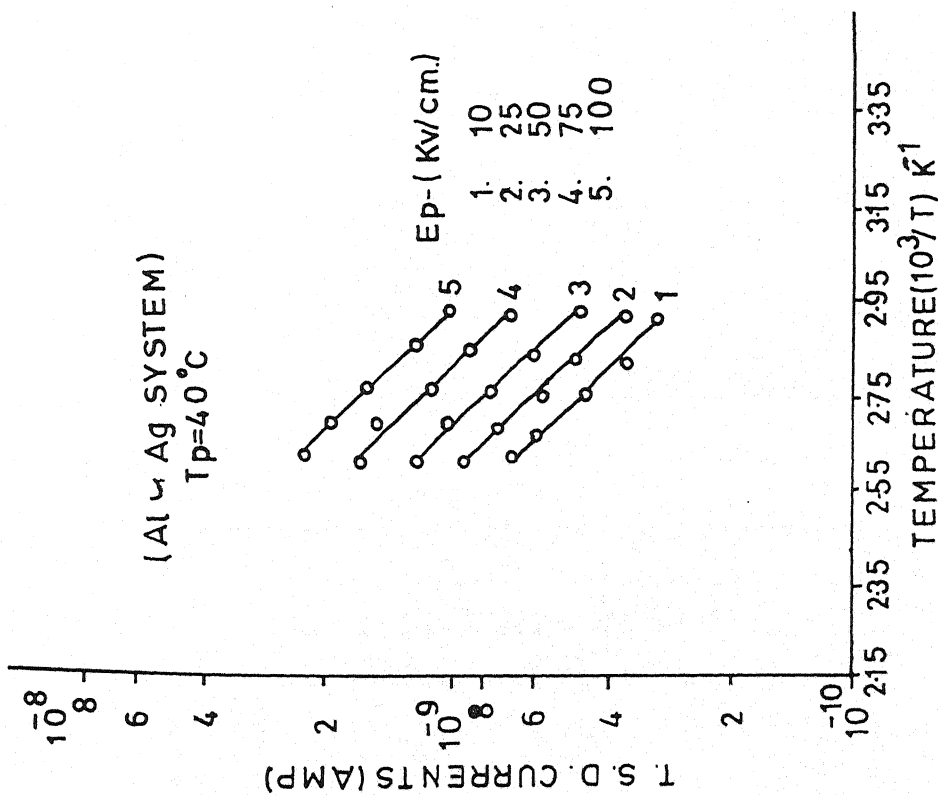


Figure No. 4.106
Initial rise plots of Fig. No. 4.26

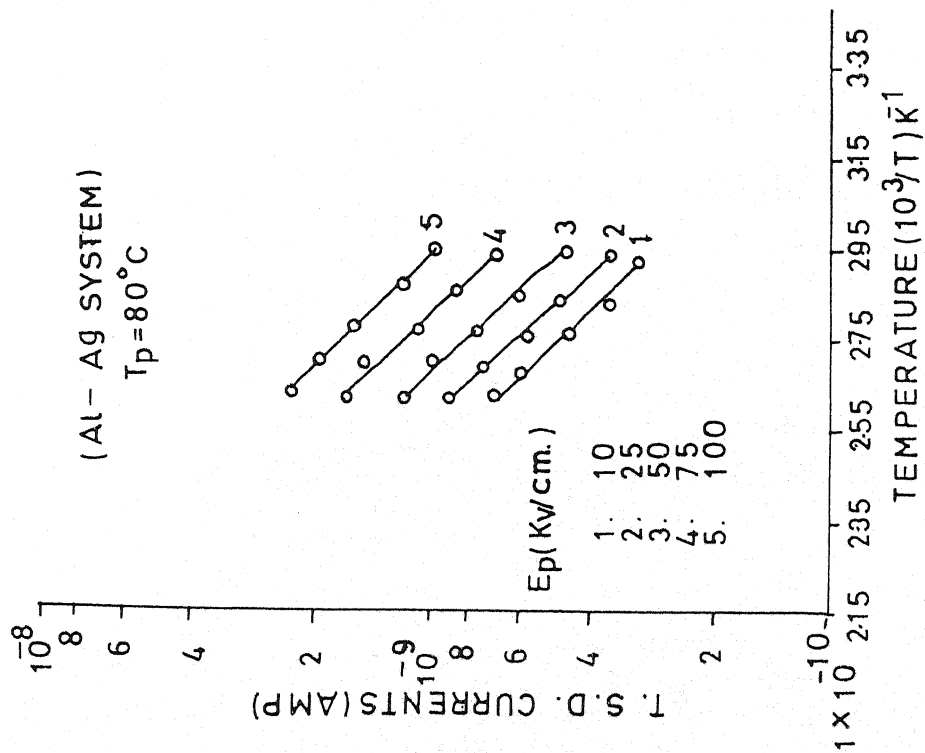
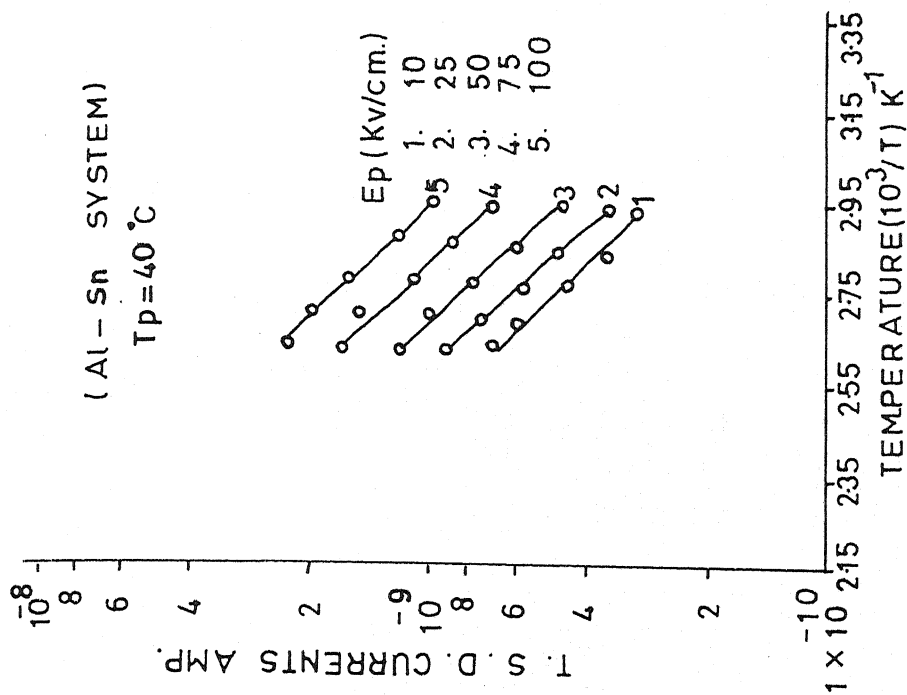


Figure No. 4.109
Initial rise plots of Fig. No. 4.31

Figure No. 4.108
Initial rise plots of Fig. No. 4.30

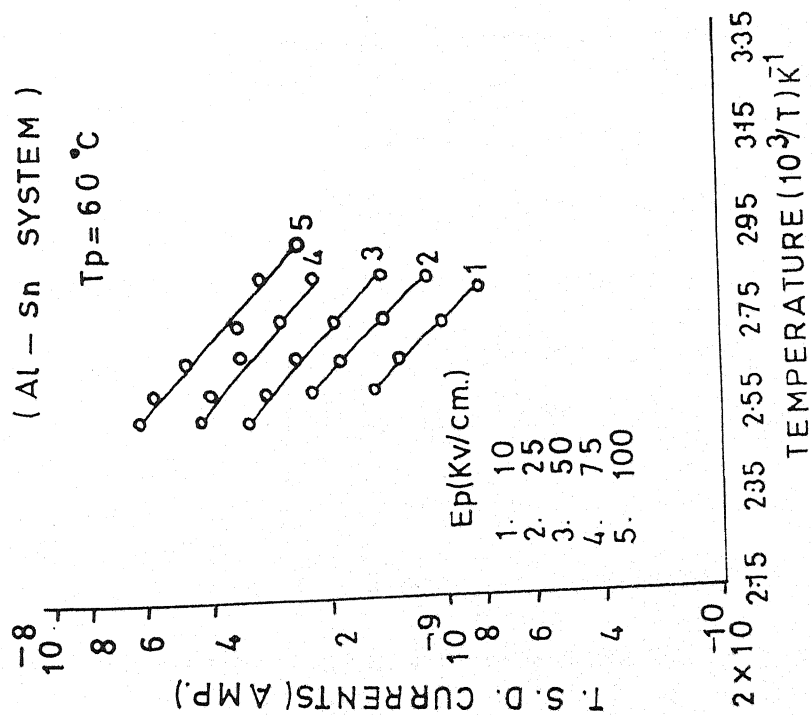


Figure No. 4.110
Initial rise plots of Fig. No. 4.33

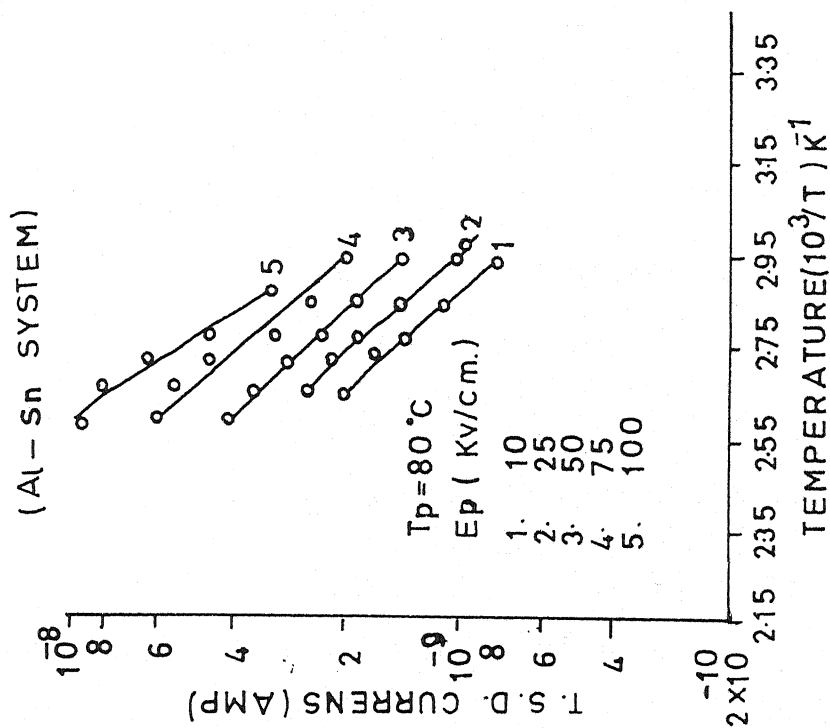


Figure No. 4.111
Initial rise plots of Fig. No. 4.35

spectra and are plotted as a function of field strength for electret polarized under different poling temperatures and show a linear relationship with field strength (results not shown). TSDC characteristics of PVDF films have also been recorded as a function of polarizing temperature under identical conditions of polarization. It is evident from the figures that with the variation in electrodes the magnitude of TSD current increases in general. It is also clear from the figures that the peak current increases and the peak shifts towards the higher temperature with increasing polarizing temperatures for a given polarizing field strength.

The depolarization kinetic data for polyvinylidene fluoride, samples poled at various temperatures with different polarizing fields are shown in Tables 4.1 to 4.7.

Application of an electric field always produces a small movement of charges within the atoms of a dielectric, displacing the negative electronic cloud relative to the positive nucleus and thus temporarily generating a small dipole moment and a consequent atomic or deformation polarization. This effect occurs within very short times, its time scale cannot be changed from outside. Thus, its influence on the persistent polarization of the electret can be disregarded. Many dielectrics, including polymers, contain molecules that have an electric moment. An applied field tends to align these elementary dipoles along its own direction and thus produce an

electric moment of the whole body giving rise to dipole polarization, essentially a volume effect.

All dielectrics contain a small number of free charge carriers, ions or electrons or both. An electric field tends to separate positive from negative charges and to move them towards the electrode. The structure of many polymers is not homogeneous, there exist microscopic domains or grains separated by highly resistive interfaces. In this case the charge carriers can move relatively freely only within single grains, piling up along the barriers which they are unable to surmount as they lack the necessary energy. Alternatively, when the dielectric contains many irregularly distributed traps with widely different well depths, carriers might move in the direction of the field until they fall into deep traps from which they do not have enough energy to escape unless reactivated by a temperature increase. Both these interfacial polarization effects constitute again a volume polarization.

Ionic conduction currents in homogeneous dielectrics usually lead to the formation of space charge clouds in the electrode regions. The effect results in a macroscopic space charge polarization of the dielectric.

The sources of the internal polarization described so far have been charges originating from and remaining within the dielectric, but a polarization can also be caused by the deposition or injection of charge carriers from outside. Deposition of equal and opposite charges on opposing surfaces of a dielectric produces an external polarization. The

distinction between internal and external polarization is due to Mikola [148]. Charges can also be shot into the dielectric using penetrating electron beams. Such electron charged dielectrics now are also called electrets, a rather loose use of the term.

The degree of polarization and its rate of decay depend on the nature of the dielectric and the experimental conditions, in particular the temperature. A dielectric becomes an electret when the rate of decay can be slowed down so much that a significant fraction of the field induced polarization is preserved long after the polarizing field has been removed.

Dipole orientation is strongly temperature dependent; at high temperature the forces opposing rotation are lessened. Thus, a high degree of polarization can be achieved in a short time by application of an electric field at a high temperature. If the dielectric is cooled and the field removed only after a low temperature has again been reached, dipoles return to the original disordered state very slowly because rotation is hindered by strong viscous forces. The polarization is thus frozen-in. A similar behaviour is found in the case of space charge and interfacial polarization. The mobility of charge carriers is very low at room temperature, but increases strongly with temperature. Thus, the previous reasoning applies here too. Space charge clouds and charges accumulated along interfaces can be frozen-in.

All types of internal polarization lead to surface charges which have the opposite polarity to that of the corresponding polarizing electrodes.

Therefore, heterocharge formation should be, and is a very general effect. Every decrease of the internal polarization due to rotation of dipoles or recombination of ions within the dielectric frees image charges which flow back through the external circuit where a discharge current is recorded. Analogously every increase of polarization gives a charging current. Therefore, build-up and dissipation of internal polarization can be investigated by means of current measurement. Current peaks are observed at temperatures where dipole orientation or carrier release from traps is activated.

The processes taking place during discharge are similar to those occurring during charging. Generally speaking, they only behave in an opposite way. The net charge of an electret usually arises from aligned dipoles and space charges. The latter are excess charges which cause the electret to be not locally neutral. However, before the electret formation the neutral polymer already contained free charges, they manifest themselves in a conduction current when a field is applied. So in addition to the excess charges there are free equilibrium charges in the electret. These do not contribute to its net charge, but are responsible for its ohmic conductivity. In heteroelectrets, the excess charges are intrinsic and bipolar. They originate from those charges that first take part in conduction and were accumulated near the electrodes during formation. This field motion is opposed by diffusion. Moreover, during their transport a part of the charges is lost by recombination with opposite carriers.

The decay of the charge of an electret during TSC results from dipole reorientation, excess charge motion and ohmic conduction. The first process will be clear, the thermal agitation will reorient the aligned dipoles at random. The motion of excess charges originates from space charge limited drift and diffusion. The first motion is due to the local electric fields forcing the mobilized excess charges to drift towards opposite charges, where by electric neutrality is restored. The excess charges will eventually recombine either with their opposed image charges or with opposite excess charges within the polymer, whichever is the case, their gross motion should generate a discharge current opposed to the charging current [149].

The temperature dependence of the dipole reorientation can be differed from the motion of excess charges. The latter will conform closely to that of ohmic conduction, from which the charges often originate. In particular, we may expect the current maxima for dipole reorientation to occur at lower temperature than that of the excess charge motion. The first process requires only a rotational motion of molecular groups, whereas the latter process involves a motion of molecular groups (ions) over macroscopic distances. The activation energy predicted theoretically by Reddish [150] for the relaxation process resulting from the local twisting of the main chain or the orientation of the side groups in a polymer is about 0.2 eV. The relaxation process associated with the peak is the orientation of the side groups and or local twisting of the main chain. It is difficult, however, to differentiate whether the low temperature relaxation in PVAc is

due to the local twisting of the main chain only or it is also due to the motion of the side groups in the polymer chain.

When PVDF film is poled at different T_p 's, a single peak at $80 \pm 10^\circ\text{C}$ is observed in the thermogram. The dipolar contribution calculated from Debey's equation does not respond to the high value of charge released. To account for the charge released probably the displacement of charges during polarization with their subsequent trapping is also responsible [151]. The charges may also be injected from electrodes into the polymer film. It is only at temperatures above the glass transition of the polymer that the molecular chains are sufficiently agitated to release the charges stored in them.

The TSDC spectra may arise due to various mechanisms such as (i) dipolar orientation, (ii) displacement of ions by a microscopic distance with trapping, (iii) ionic space charge due to slow discharge rate of ions at their counter electrodes, (iv) space charge injected from electrodes, and (v) hopping of charge carrier from one localised state to another [152,153]. Processes (II), (III) and (IV) may be related to space charge polarization. Perlman [154] pointed out that the shape of spectra may be same in all the cases. One of the arguments advocated for distinguishing a dipolar polarization and space charge polarization is based on the field dependence of the TSDC properties; such as the peak current, peak temperature and charge released. The linear dependence of charge

released and the peak current on polarization field strength is a characteristic of dipolar origin whereas in the case of space charge polarization, the peak current and charge released will show a non-linear variation with polarizing field strengths. For a dipolar peak, the peak temperature will be independent of polarizing field strength and polarizing temperature whereas the peak temperature depends on the poling fields and temperatures of the space charge polarization. The linear field dependence of peak current suggests that the TSDC spectra may be either due to dipolar origin or migration of charge carriers through microscopic distances with trapping [155]. The increasing value of peak current with poling field and the observed activation energy values indicate that the peak may be contributed significantly by dipolar and ionic polarizations. Also, the contribution from the migration of charge carriers through microscopic distances with trapping is possible. The linear dependence of charge released from electrets on the polarizing field strengths suggest that the depolarization process throughout the volume of the electret is uniform which is a characteristic of dipolar origin or due to migration of charge carriers through microscopic distance with trapping [156]. The activation energies evaluated from initial rise method and Bucci-Fieshi method are in good agreement and are very small in magnitude when compared to 1 eV, which is for the movement of ions. Hence, the present TSDC spectra may not be due to movement of ions. Hence, the observed TSDC may not be

completely due to alignment of dipoles. In addition to dipolar contribution, there must be some contribution from the heterocharge also.

The study of the influence of electrode material is one of the most reliable ways of distinguishing not only between dipolar and space charge processes but also to differentiate the two types of space charge polarizations. Metals used as contacting electrodes introduces various amount of free charge carriers which contribute to TSDC. The TSDC spectra are recorded for different electrode materials (aluminium, silver, copper and tin) polarized at 40-80°C with fields 10-100 kV/cm.

PVDF is of fundamental interest for its different crystalline phases and phase transitions. PVDF can present in five distinct crystalline structures depending on the formation conditions of the polymer. Four of these phases designated as α , β , γ and δ respectively, by form I, II, III and IV are stable at room temperature, a fifth form ϵ could exist just below the melting point [157]. The α -phase of PVDF crystallizes from the melt [158]. The β -phase is normally obtained by mechanical deformation of α -form [159]. The β -form may also be grown from solution under special conditions [160]. Growth from solutions such as dimethyl sulfoxide or dimethyl acetamide usually leads to γ form [161]. PVDF is inherently polar. The hydrogen atoms are positively charged and the fluorine atoms negatively charged with respect to the carbon atom in the polymer. The net moment of a group of molecules in a liquid region of PVDF will be zero in the absence

of an applied field because of random orientation of individual dipoles. PVDF has attracted considerable attention due to unique electroactive properties induced by high field exposure.

The PVDF is a polar polymer, the contribution to the polarization may be due to alignment of the dipoles under the effect of the electric field. In the present investigation, TSDC thermograms exhibits a broad peak. This peak gets centered around $100 \pm 10^{\circ}\text{C}$. Broad peaks represent presence of multiplicity of relaxation mechanism. The multiplicity of relaxation in PVDF may be because of presence of trapping levels of different depths. Two peaks were reported [162] for PVDF. The first peak reported at 30°C (related to the charging temperature) and at 52°C due to release of charges trapped at crystalline/amorphous boundaries. In the present case, the appearance of peak in the high temperature region imply that the injection of ions may be significant in this polymer. It is also possible that PVDF contains a high number of impurity molecules prior to field treatment and these molecules are dissociated into various ionic species by a combination of the high internal and external fields. The charge trapping in a polymer takes place at the molecular main chain, the side chain and at the interface of crystalline and amorphous regions of the polymer [163]. The high field applied during electret formation may also produce some additional trapping sites.

The charge released from these traps occurs because of the thermal excitation and motion of the molecular chain that causes the lowering of trap depth. The released charge can recombine, retrapped in trapping sites, or may get discharged at the electrodes. The chances of retrapping of the released charge are high in a polymer having a large number of trapping sites and it is expected that the discharge will give complex TSC spectra with broad peaks indicating a distribution of activation energies. Ong and Turnhout [164] have also assigned the broadness of a TSDC peak to the distribution of relaxation frequencies. The high values of activation energies have been observed can only be associated with the ionic and electronic trapping [165]. The superlinear behaviour of peak current versus poling field in the higher field region indicates the space charge phenomena. The peak observed in the thermograms is not due to single relaxation but seems to be complex and may arise due to the release of the frozen dipoles by their cooperative motion with adjoining segments of the main polymer chain. The superlinear increase of peak current and release charge versus poling field (not reported) in the higher field region suggests that the peak is contributed both by electronic and ionic processes, arising in the bulk and injected from the electrodes which are subjected to a higher field. It is not a simple process but a complicated one of Maxwell-Wagner type [166].

The values of activation energy, E_a , peak current I_m , peak temperature T_m , relaxation time τ_0 and charge released during the process

for the electrode series are given in Table 4.1 to 4.7. All these values are different for samples prepared with different electrodes. Such electrode dependence has also been found by quite few workers [167,168]. Table reveals a close relationship between the surface charge and TSD currents of PVDF foil electrets on the metal electrodes. The results support the Gross's theory [169] of homocharge which attributes it either to electrode dielectric interface breakdown (ruled out in our case due to experimental arrangement used) or to the charge injection from the electrodes. The electrons and holes migrate from the electrodes onto the surface of the dielectric [170,171]. When the polymer is polarized under identical conditions of polarisation with electrodes (Al, Cu, Ag, Sn) of different work function determined by contact potential method [172], but less than that of PVDF, the metal with higher work function injects a large number of charge carriers than that with lower work function [173]. Since the injection of charge carriers from the electrodes to the polymer results in a reduction of the contribution of the heterocharge (due to the charge carriers present in the bulk of the material) so the charge released to the external circuit and the magnitude of the peak current I_m , should decrease with the work function of the metal [174]. Slight difference in peak positions for different metal-electrode-metal combinations were observed. These results suggest that the liberated opposite part of ions and carriers may be slightly affected by the work function different of different combinations. In these results, a possibility seems to be present that the internal field of PVDF may get

modified by the difference in the work function of different electrodes. Peak value of the current seems to be controlled effectively by the work function for metal-insulator-metal interfaces.

It is clear from the Table 4.1 to 4.17 that the activation energies associated with the process responsible for TSDC and relaxation times are found to vary slightly, with that of the polarizing temperatures. Further, the dependence of TSDC peak on the polarizing temperature also suggest the distribution in relaxation times. Such relaxation process of activation energy and for a fixed rate of heating the position of the peak is independent of polarizing temperature. Hence, it may be concluded that the TSDC spectra may be of dipolar origin with contribution from space charges.

/ ***** /

Table 4.1. Depolarization kinetic data for the observed peaks of polyvinylidene fluoride films at different polarizing temperatures with various poling fields (Al-Al system).

S. No.	Polarizing Temp. (°C)	Polarizing Fields (kV/cm)	Activation Energy (eV)	Peak Current (Amp.)	Charge Released (Coul.)	Relaxation time (sec.)
1.	40	10	0.612	2.0×10^{-10}	3.2×10^{-7}	6.76×10^5
		25	0.623	2.0×10^{-10}	4.0×10^{-7}	4.78×10^6
		50	0.621	3.6×10^{-10}	8.0×10^{-7}	7.85×10^7
		75	0.622	5.0×10^{-10}	9.0×10^{-7}	8.24×10^6
		100	0.623	6.6×10^{-10}	9.8×10^{-7}	9.55×10^8
2.	50	10	0.602	3.0×10^{-10}	6.0×10^{-7}	4.78×10^7
		25	0.605	3.8×10^{-10}	8.8×10^{-7}	8.76×10^6
		50	0.627	5.6×10^{-10}	1.2×10^{-7}	5.33×10^7
		75	0.628	6.8×10^{-10}	2.0×10^{-7}	9.87×10^8
		100	0.627	8.0×10^{-10}	2.4×10^{-7}	2.48×10^9
3.	60	10	0.600	3.6×10^{-10}	1.8×10^{-8}	2.467×10^5
		25	0.613	4.0×10^{-10}	2.2×10^{-8}	3.48×10^8
		50	0.618	6.0×10^{-10}	3.2×10^{-8}	7.98×10^7
		75	0.620	8.0×10^{-10}	5.0×10^{-7}	8.24×10^8
		100	0.628	1.0×10^{-9}	6.0×10^{-7}	9.44×10^7
4.	70	10	0.584	6.0×10^{-10}	3.0×10^{-8}	5.78×10^6
		25	0.597	8.0×10^{-10}	3.8×10^{-8}	4.47×10^7
		50	0.618	1.2×10^{-9}	5.6×10^{-7}	9.32×10^8
		75	0.627	2.0×10^{-9}	6.8×10^{-7}	2.46×10^7
		100	0.629	2.6×10^{-9}	8.0×10^{-8}	3.57×10^7
5.	80	10	0.594	4.6×10^{-9}	5.0×10^{-8}	8.78×10^6
		25	0.601	6.8×10^{-9}	6.4×10^{-8}	7.65×10^7
		50	0.615	9.40×10^{-9}	7.8×10^{-8}	9.87×10^6
		75	0.631	1.04×10^{-9}	9.5×10^{-7}	7.34×10^5
		100	0.631	2.00×10^{-9}	9.78×10^{-7}	4.47×10^5

Table 4.2. Depolarization parameters for polyvinylidene fluoride samples (~20 μm thick) poled at different temperatures with different polarizing fields (Ag-Ag system)

S. No.	T_p ($^{\circ}\text{C}$)	E_p (kV/cm)	Peak Temp. T_m ($^{\circ}\text{C}$)	Peak Current I_m (Amp.)	Activation Energy (eV)	Relaxation Time (sec.)	Charge Released (Coul.)
1.	40	10	110	5.0×10^{-9}	0.478	4.85×10^{-4}	3.37×10^{-8}
		25	110	7.0×10^{-9}	0.482	9.87×10^{-5}	4.38×10^{-7}
		50	120	1.2×10^{-8}	0.480	4.32×10^{-4}	3.99×10^{-7}
		75	120	1.5×10^{-8}	0.479	7.65×10^{-5}	4.27×10^{-7}
		100	120	2.0×10^{-8}	0.476	8.76×10^{-6}	6.67×10^{-6}
2.	50	10	110	6.0×10^{-9}	0.482	8.78×10^{-7}	4.87×10^{-8}
		25	110	8.0×10^{-9}	0.491	2.48×10^{-6}	8.86×10^{-7}
		50	100	1.2×10^{-8}	0.497	8.53×10^{-6}	7.79×10^{-6}
		75	100	1.5×10^{-8}	0.499	4.33×10^{-5}	8.54×10^{-5}
		100	110	2.2×10^{-8}	0.501	3.89×10^{-5}	7.65×10^{-4}
3.	60	10	120	5.1×10^{-9}	0.497	2.27×10^{-8}	3.47×10^{-8}
		25	120	7.0×10^{-9}	0.501	4.56×10^{-7}	4.88×10^{-7}
		50	120	9.0×10^{-8}	0.511	7.77×10^{-7}	7.65×10^{-6}
		75	120	1.3×10^{-8}	0.522	4.77×10^{-6}	3.88×10^{-5}
		100	120	1.7×10^{-8}	0.530	9.87×10^{-7}	7.66×10^{-5}
4.	70	10	110	9.0×10^{-9}	0.501	3.47×10^{-8}	8.47×10^{-8}
		25	110	1.1×10^{-8}	0.521	5.43×10^{-6}	9.47×10^{-8}
		50	110	1.4×10^{-8}	0.533	4.78×10^{-5}	3.28×10^{-7}
		75	110	2.0×10^{-8}	0.539	3.78×10^{-4}	8.88×10^{-7}
		100	110	2.6×10^{-8}	0.541	8.76×10^{-5}	9.32×10^{-6}
5.	80	10	120	8.0×10^{-9}	0.511	4.47×10^{-7}	8.78×10^{-7}
		25	120	1.1×10^{-8}	0.533	3.37×10^{-5}	7.65×10^{-6}
		50	120	1.5×10^{-8}	0.522	4.78×10^{-6}	8.47×10^{-6}
		75	120	2.1×10^{-8}	0.545	8.76×10^{-4}	3.38×10^{-5}
		100	120	2.7×10^{-8}	0.556	3.37×10^{-3}	8.76×10^{-5}

Table 4.3. Depolarization parameters for polyvinylidene fluoride samples (~20 μm thick) poled at different temperatures with different polarizing fields (Cu-Cu system)

S. No.	T_p ($^{\circ}\text{C}$)	E_p (kV/cm)	Peak Temp. T_m ($^{\circ}\text{C}$)	Peak Current I_m (Amp.)	Activation Energy (eV)	Relaxation Time (sec.)	Charge Released (Coul.)
1.	40	10	120	8.0×10^{-9}	0.491	3.78×10^{-4}	1.47×10^{-8}
		25	120	1.0×10^{-8}	0.497	8.76×10^{-8}	3.60×10^{-7}
		50	120	1.3×10^{-8}	0.501	9.54×10^{-6}	7.80×10^{-6}
		75	120	1.5×10^{-8}	0.508	8.76×10^{-4}	2.57×10^{-5}
		100	130	2.0×10^{-8}	0.510	7.77×10^{-8}	3.88×10^{-5}
2.	50	10	115	9.0×10^{-9}	0.513	5.48×10^{-5}	2.56×10^{-8}
		25	115	1.1×10^{-8}	0.508	6.78×10^{-4}	9.98×10^{-8}
		50	120	1.3×10^{-8}	0.519	7.88×10^{-7}	7.65×10^{-7}
		75	120	1.6×10^{-8}	0.521	8.54×10^{-6}	8.75×10^{-6}
		100	120	2.2×10^{-8}	0.531	2.58×10^{-3}	4.78×10^{-6}
3.	60	10	120	1.0×10^{-9}	0.527	3.37×10^{-6}	4.95×10^{-8}
		25	120	1.4×10^{-9}	0.531	7.65×10^{-7}	6.43×10^{-8}
		50	120	1.8×10^{-9}	0.540	4.77×10^{-5}	8.76×10^{-7}
		75	120	2.6×10^{-8}	0.539	7.95×10^{-6}	9.99×10^{-6}
		100	120	3.5×10^{-8}	0.547	8.76×10^{-4}	6.98×10^{-6}
4.	70	10	110	1.3×10^{-8}	0.540	7.67×10^{-4}	7.65×10^{-8}
		25	110	1.7×10^{-8}	0.541	8.87×10^{-5}	8.48×10^{-8}
		50	110	2.3×10^{-8}	0.549	7.98×10^{-6}	2.36×10^{-6}
		75	110	3.0×10^{-8}	0.550	5.78×10^{-6}	5.79×10^{-6}
		100	110	3.6×10^{-8}	0.559	8.79×10^{-5}	9.87×10^{-6}
5.	80	10	120	1.5×10^{-8}	0.547	6.68×10^{-5}	3.36×10^{-7}
		25	120	2.0×10^{-8}	0.552	7.89×10^{-6}	5.66×10^{-7}
		50	120	2.6×10^{-8}	0.562	8.99×10^{-5}	6.68×10^{-6}
		75	120	4.0×10^{-8}	0.566	9.47×10^{-4}	8.76×10^{-6}
		100	120	5.1×10^{-8}	0.566	3.27×10^{-3}	2.47×10^{-5}

Table 4.4 Depolarization parameters for polyvinylidene fluoride samples ($\sim 20 \mu\text{m}$ thick) poled at different temperatures with different polarizing fields (Sn-Sn system)

S. No.	T_p ($^{\circ}\text{C}$)	E_p (kV/cm)	Peak Temp. T_m ($^{\circ}\text{C}$)	Peak Current I_m (Amp.)	Activation Energy (eV)	Relaxation Time (sec.)	Charge Released (Coul.)
1.	40	10	100	6.0×10^{-10}	0.513	3.67×10^{-6}	2.78×10^{-8}
		25	100	9.0×10^{-10}	0.527	5.48×10^{-7}	7.78×10^{-7}
		50	100	1.2×10^{-9}	0.529	6.54×10^{-6}	3.26×10^{-6}
		75	100	1.9×10^{-9}	0.532	8.78×10^{-5}	7.65×10^{-6}
		100	100	2.6×10^{-9}	0.547	9.45×10^{-4}	9.32×10^{-6}
2.	50	10	100	7.0×10^{-10}	0.526	7.67×10^{-7}	3.85×10^{-7}
		25	100	1.0×10^{-9}	0.537	8.76×10^{-8}	4.78×10^{-6}
		50	110	1.7×10^{-9}	0.543	9.78×10^{-7}	8.76×10^{-6}
		75	110	2.3×10^{-9}	0.556	2.59×10^{-6}	9.35×10^{-6}
		100	120	3.0×10^{-9}	0.563	4.37×10^{-5}	1.27×10^{-5}
3.	60	10	100	8.0×10^{-10}	0.529	6.54×10^{-6}	7.76×10^{-6}
		25	100	1.2×10^{-9}	0.532	7.88×10^{-7}	8.78×10^{-6}
		50	100	1.5×10^{-9}	0.539	9.54×10^{-5}	9.54×10^{-6}
		75	110	2.5×10^{-9}	0.533	3.78×10^{-6}	3.37×10^{-5}
		100	100	3.4×10^{-9}	0.547	8.78×10^{-7}	8.42×10^{-5}
4.	70	10	100	1.0×10^{-8}	0.456	4.48×10^{-7}	9.54×10^{-6}
		25	110	1.5×10^{-8}	0.558	6.54×10^{-6}	1.32×10^{-5}
		50	110	2.0×10^{-8}	0.563	8.35×10^{-5}	5.55×10^{-5}
		75	120	2.3×10^{-8}	0.573	9.74×10^{-7}	7.65×10^{-5}
		100	120	3.5×10^{-8}	0.577	7.77×10^{-6}	9.78×10^{-5}
5.	80	10	100	1.2×10^{-8}	0.498	7.45×10^{-6}	1.37×10^{-5}
		25	110	1.5×10^{-8}	0.499	7.43×10^{-5}	7.65×10^{-5}
		50	110	2.0×10^{-8}	0.571	8.78×10^{-6}	9.67×10^{-5}
		75	115	2.9×10^{-8}	0.587	9.54×10^{-5}	1.35×10^{-4}
		100	115	4.0×10^{-8}	0.592	3.75×10^{-4}	4.33×10^{-4}

Table 4.5. Depolarization parameters for polyvinylidene fluoride samples ($\sim 20 \mu\text{m}$ thick) poled at different temperatures with different polarizing fields (Al-Ag system)

S. No.	T_p ($^{\circ}\text{C}$)	E_p (kV/cm)	Peak Temp. T_m ($^{\circ}\text{C}$)	Peak Current I_m (Amp.)	Activation Energy (eV)	Relaxation Time (sec.)	Charge Released (Coul.)
1.	40	10	90	7.0×10^{-10}	0.482	3.85×10^{-6}	4.781×10^{-7}
		25	90	9.0×10^{-10}	0.497	4.78×10^{-5}	8.87×10^{-7}
		50	110	1.4×10^{-9}	0.502	8.35×10^{-4}	2.56×10^{-6}
		75	120	2.1×10^{-9}	0.512	9.47×10^{-7}	4.78×10^{-6}
		100	120	3.0×10^{-9}	0.522	7.66×10^{-6}	8.54×10^{-6}
2.	50	10	110	1.2×10^{-9}	0.496	9.65×10^{-7}	7.65×10^{-7}
		25	110	1.5×10^{-9}	0.514	4.78×10^{-6}	9.43×10^{-6}
		50	120	2.0×10^{-9}	0.522	5.44×10^{-5}	3.26×10^{-5}
		75	120	2.5×10^{-9}	0.534	7.77×10^{-5}	8.78×10^{-5}
		100	120	3.6×10^{-9}	0.539	8.46×10^{-5}	4.88×10^{-5}
3.	60	10	110	1.5×10^{-9}	0.486	7.65×10^{-6}	8.765×10^{-8}
		25	110	2.1×10^{-9}	0.491	8.65×10^{-7}	2.565×10^{-7}
		50	120	3.0×10^{-9}	0.501	9.47×10^{-6}	6.654×10^{-6}
		75	120	4.0×10^{-9}	0.513	4.31×10^{-5}	7.78×10^{-6}
		100	120	6.0×10^{-9}	0.522	3.88×10^{-5}	2.478×10^{-5}
4.	70	10	120	2.4×10^{-9}	0.494	5.66×10^{-6}	2.485×10^{-7}
		25	120	3.0×10^{-9}	0.521	9.87×10^{-6}	6.599×10^{-7}
		50	120	4.0×10^{-9}	0.517	3.35×10^{-5}	9.543×10^{-7}
		75	130	5.2×10^{-9}	0.523	9.88×10^{-5}	3.378×10^{-6}
		100	130	6.2×10^{-9}	0.533	3.22×10^{-5}	4.888×10^{-6}
5.	80	10	110	2.0×10^{-9}	0.503	4.78×10^{-5}	7.654×10^{-6}
		25	120	2.5×10^{-9}	0.533	6.66×10^{-5}	8.794×10^{-6}
		50	120	4.0×10^{-9}	0.545	8.56×10^{-6}	2.34×10^{-5}
		75	120	6.0×10^{-9}	0.556	9.78×10^{-6}	6.654×10^{-5}
		100	120	9.0×10^{-9}	0.559	3.34×10^{-5}	9.876×10^{-5}

Table 4.6. Depolarization parameters for polyvinylidene fluoride samples ($\sim 20 \mu\text{m}$ thick) poled at different temperatures with different polarizing fields (Al-Cu system)

S. No.	T_p ($^{\circ}\text{C}$)	E_p (kV/cm)	Peak Temp. T_m ($^{\circ}\text{C}$)	Peak Current I_m (Amp.)	Activation Energy (eV)	Relaxation Time (sec.)	Charge Released (Coul.)
1.	40	10	110	5.5×10^{-10}	0.544	4.54×10^{-6}	6.65×10^{-6}
		25	120	8.0×10^{-10}	0.594	5.45×10^{-4}	9.87×10^{-6}
		50	130	1.2×10^{-9}	0.562	2.62×10^{-3}	3.58×10^{-5}
		75	120	1.5×10^{-9}	0.569	7.65×10^{-4}	6.48×10^{-5}
		100	130	2.5×10^{-9}	0.571	8.65×10^{-6}	9.37×10^{-5}
2.	50	10	120	1.0×10^{-9}	0.566	9.54×10^{-8}	8.48×10^{-6}
		25	120	2.0×10^{-9}	0.582	3.78×10^{-7}	9.65×10^{-6}
		50	130	3.0×10^{-9}	0.572	8.85×10^{-6}	2.78×10^{-5}
		75	130	3.0×10^{-9}	0.587	9.47×10^{-5}	8.76×10^{-5}
		100	130	3.5×10^{-9}	0.567	8.88×10^{-6}	9.99×10^{-5}
3.	60	10	100	1.3×10^{-9}	0.569	4.48×10^{-8}	9.32×10^{-6}
		25	100	1.6×10^{-9}	0.578	7.67×10^{-7}	2.75×10^{-5}
		50	110	2.1×10^{-9}	0.583	8.43×10^{-6}	3.98×10^{-5}
		75	120	3.0×10^{-9}	0.597	7.48×10^{-5}	6.87×10^{-5}
		100	130	5.0×10^{-9}	0.602	4.89×10^{-4}	8.54×10^{-5}
4.	70	10	110	2.1×10^{-9}	0.578	8.54×10^{-8}	2.78×10^{-5}
		25	110	2.6×10^{-9}	0.583	7.67×10^{-7}	4.78×10^{-5}
		50	130	4.1×10^{-9}	0.586	6.48×10^{-6}	7.87×10^{-5}
		75	120	5.4×10^{-9}	0.595	7.88×10^{-5}	8.43×10^{-5}
		100	120	7.0×10^{-8}	0.608	9.78×10^{-5}	9.98×10^{-5}
5.	80	10	110	2.0×10^{-9}	0.582	3.38×10^{-7}	6.43×10^{-6}
		25	120	2.1×10^{-9}	0.593	4.98×10^{-6}	8.78×10^{-6}
		50	130	4.0×10^{-9}	0.612	9.85×10^{-5}	9.78×10^{-6}
		75	120	5.1×10^{-9}	0.607	8.76×10^{-4}	3.24×10^{-5}
		100	130	6.1×10^{-9}	0.618	3.37×10^{-3}	8.78×10^{-5}

Table 4.7. Depolarization parameters for polyvinylidene fluoride samples (~20 μm thick) poled at different temperatures with different polarizing fields (Al-Sn system)

S. No.	T_p ($^{\circ}\text{C}$)	E_p (kV/cm)	Peak Temp. T_m ($^{\circ}\text{C}$)	Peak Current I_m (Amp.)	Activation Energy (eV)	Relaxation Time (sec.)	Charge Released (Coul.)
1.	40	10	110	6.8×10^{-10}	0.563	3.65×10^{-7}	2.57×10^{-7}
		25	110	8.5×10^{-10}	0.572	2.78×10^{-8}	3.99×10^{-7}
		50	110	1.2×10^{-9}	0.579	3.95×10^{-8}	6.54×10^{-6}
		75	110	1.7×10^{-9}	0.581	6.47×10^{-6}	7.84×10^{-6}
		100	110	2.3×10^{-9}	0.589	5.48×10^{-5}	9.53×10^{-6}
2.	50	10	100	1.1×10^{-9}	0.557	7.65×10^{-8}	4.89×10^{-7}
		25	100	1.5×10^{-9}	0.592	9.54×10^{-7}	9.84×10^{-6}
		50	100	2.0×10^{-9}	0.601	8.76×10^{-6}	2.53×10^{-5}
		75	110	2.6×10^{-9}	0.644	9.98×10^{-5}	6.67×10^{-5}
		100	110	3.0×10^{-9}	0.638	5.55×10^{-5}	8.88×10^{-5}
3.	60	10	110	1.2×10^{-9}	0.561	1.65×10^{-7}	8.765×10^{-7}
		25	110	1.4×10^{-9}	0.578	7.58×10^{-6}	8.45×10^{-6}
		50	120	2.0×10^{-9}	0.582	2.85×10^{-5}	9.56×10^{-6}
		75	110	2.6×10^{-9}	0.592	9.25×10^{-6}	3.87×10^{-5}
		100	120	4.0×10^{-9}	0.601	6.01×10^{-5}	8.56×10^{-5}
4.	70	10	120	1.5×10^{-9}	0.558	8.55×10^{-6}	2.958×10^{-6}
		25	120	2.0×10^{-9}	0.569	9.56×10^{-5}	3.876×10^{-6}
		50	120	2.8×10^{-9}	0.589	5.76×10^{-4}	7.659×10^{-6}
		75	120	4.0×10^{-9}	0.605	3.39×10^{-5}	9.948×10^{-6}
		100	120	5.0×10^{-9}	0.614	7.78×10^{-6}	3.256×10^{-5}
5.	80	10	115	2.1×10^{-9}	0.562	2.65×10^{-7}	6.547×10^{-6}
		25	120	2.6×10^{-9}	0.569	6.58×10^{-6}	9.987×10^{-6}
		50	125	4.1×10^{-9}	0.572	3.45×10^{-7}	7.758×10^{-5}
		75	120	5.2×10^{-9}	0.589	8.59×10^{-6}	6.543×10^{-5}
		100	120	6.8×10^{-9}	0.593	3.95×10^{-5}	8.864×10^{-5}

REFERENCES

1. Frenkel, S.Ya and Klyashevich, G.K., Vysokomol. Soed., **13A**, 493 (1971).
2. Shen, M.C. and Eisenberg, A., Progr. Solid State Chem., **3**, 407 (1967).
3. Gibbs, J.H. and Di Marzio, E.A., J. Chem. Phys., **28**, 373 (1958).
4. Staverman, A.J., Rheol. Acta., **5**, 283 (1968).
5. Eisenberg, A. and Saito, Sh., J. Chem. Phys., **45**, 1673 (1966).
6. Moacenin, J. and Sisha, S., J. Chem. Phys., **45**, 964 (1966).
7. Uberreiter, K., Phys. Chem., Leipzig, **B45**, 361 (1970).
8. Kirk-Othmer Encyclopedia of Chemical Technology, II Ed., Vol. 19, p. 89, Wiley, New York.
9. Perepechko, I.I., Evacheva, L.A., Ushakov, L.A., Evetov, A.Ya and Grechishkin, V.A., Plast. Massy, **8**, 43 (1970).
10. Ubbelohde, A.R., Melting and Crystal Structure, Clarendon Press, Oxford (1965).
11. Heaviside, O., Electrical Papers, I, p. 488, Macmillan, London (1993).
12. Eguchi, M., Proc. Phys. Meth. Soc. Japan, **1**, 326 (1919).
13. Gemant, A., Phil. Mag., **20**, 929 (1935).
14. Gutmann, W.F., Rev. Mod. Phys., **20**, 457 (1948).

15. Fridkin, V.M. and Sheludev, I.S., Photoelectrets and the Electrophotographic Process, Consultants Bureau, New York (1960).
16. Gross, B., Charge Storage in Solid Dielectrics, Elsevier Publ. Co., Amsterdam (1964).
17. Baxt, L. and Perlman, M.H. (Eds.), Electrets and Related Electrostatic Charge Storage Phenomena, Electrochem. Soc., New York (1968).
18. Murphy, P.V. and Holly, J., Electrets and Related Electrostatic Charge Storage Phenomena, 5, p. 109, Electrochem. Soc., New York (1968).
19. Bucci, C. and Fieschi, R., Phys. Rev. Lett., **12**, 16 (1964).
20. Creswell, R.A. and Perlman, M.M., J. Appl. Phys., **41**, 2369 (1970).
21. Turnhout J. Van, Polym. J., **2**, 173 (1972).
22. Ong, P.H. and Turnhout J. Van, Electrets, Charge Storage and Transport in Dielectrics, Ed. M.M.Pearlman, Electrochem. Soc., New Jersey, p. 214 (1973).
23. Chatain, D., Gautier, P. and Lacebanne, C., J. Polym. Sci. Polym. Phys. Ed., **11**, 1631 (1973).
24. Guillet, J. and Seytre, G., J. Polym. Sci. Polym. Phys. Ed., **15**, 541 (1977).
25. Hino, T., Suzuki, K. and Yamashite, K., Jap. J. Appl. Phys., **12**, 651 (1973).
26. Hino, T. and Kitamura, Y., Jap. Electr. Engng., **95**, 24 (1975).

27. McCrum, N.G., Read, B.E. and Williams, G., *An Elastic and Dielectric Effects in Polymeric Solids*, Wiley, London (1967).
28. Jonscher, A.K., *Coll. Polym. Sci.*, **253**, 231 (1975).
29. Gobrecht, H. and Hofman, D., *J. Phys. Chem. Solids*, **27**, 509 (1966).
30. Sessler, G.M. and West, J.E., *J. Electrochem. Soc.*, **115**, 836 (1968).
31. Perlman, M.M. and Reedyk, C.W., *J. Electrochem. Soc.*, **115**, 45 (1968).
32. Pillai, P.K.C., Jain, V.K. and Vij, G.K., *J. Electrochem. Soc.*, **116**, 836 (1969).
33. Murphy, P.V. and Fraim, F.W., *J. Audio Engng. Soc.*, **16**, 450 (1968).
34. Tyler, R.W., Webb, J.H. and York, W.C., *J. Appl. Phys.*, **26**, 61 (1955).
35. Rieser, A., Lock, M.W.B. and Knight, J., *Trans. Faraday Soc.*, **65**, 2168 (1969).
36. Seiwatz, H. and Brophy, J.J., *Annual Report Conf. on Electr. Insul.*, pp. 1-3 (1965).
37. Sessler, G.M. and West, J.E., *Polym. Letts.*, **7**, 367 (1969).
38. Monteith, L.K., *J. Appl. Phys.*, **37**, 2623 (1966).
39. Gross, B., Sessler, G.M. and West, J.E., *J. Appl. Phys.*, **45**, 2841 (1974).
40. Gross, B., Sessler, G.M. and West, J.E., *J. Appl. Phys.*, **47**, 968 (1976).

41. Wiseman, G.G. and Feaster, O.R., J. Chem. Phys., **26**, 521 (1957).
42. Perlman, M.M. and Meunier, J.L., J. Appl. Phys., **36**, 4200 (1965).
43. Tilly, J.E., J. Appl. Phys., **38**, 2543 (1967).
44. Bucci, C., Fieschi, R. and Guidi, G., Phys. Rev., **148**, 816 (1966).
45. Perlman, M.M. and Creswell, R.A., J. Appl. Phys., **43**, 531 (1971).
46. Perlman, M.M., J. Appl. Phys., **42**, 2465 (1971).
47. Clilly, A. Jr., Steward, L.L. and Henderson, R.H., J. Appl. Phys., **41**, 2001 (1970); **42**, 2007 (1970).
48. Gross, B., J. Electrochem. Soc., **115**, 376 (1968).
49. Vanderschueren, J., J. Polym. Sci. Polym. Phys. Ed., **15**, 873 (1977).
50. Ikezaki, K., Hattori, M. and Arimoto, Y., Jap. J. Appl. Phys., **16**, 863 (1977).
51. Mizutani, T. and Ieda, M., J. Phys. D. Appl. Phys., **11**, 185 (1978).
52. Swiatek, J., Phys. Stat. Sol. A. **52**, K69 (1979).
53. Lee, D.C., J. Korean Inst. Electr. Engng., **27**, 225 (1978).
54. Mahendru, P.C., Chani, S. and Pathak, N.L., Thin Solid Films, **44**, 13 (1977).
55. Kojima, K., Maeda, A. and Ieda, M., Jap. J. Appl. Phys., **15**, 2657 (1977).
56. Suzuki, Y., Migutani, T. and Ieda, M., Jap. J. Appl. Phys., **15**, 929 (1976).
57. Comstock, R.J., Stupp, S.I. and Carr, S.H., J. Macromol. Sci. Phys., **B13**, 101 (1977).

58. Fischer, P. and Rohl, P., J. Polym. Sci. Polym. Phys. Ed., **14**, 531 (1976).
59. Fischer, P. and Rohl, P., J. Polym. Sci. Polym. Phys. Ed., **14**, 543 (1976).
60. Hino, T., Jap. J. Appl. Phys., **11**, 1573 (1972); **12**, 611 (1973).
61. Chatain, D., Lacabanne, C. and Maitrot, M., Phys. Stat. Sol. A, **13**, 303 (1972).
62. Perlman, M.M., J. Electrochem. Soc., **119**, 892 (1972).
63. Kessler, A., J. Electrochem. Soc., **123**, 1236 (1976).
64. Turnhout, J. Van, Thermally Stimulated Discharge of Polymer Electrets, Elsevier Publ. Co., Amsterdam (1975).
65. Ranicer, J.H. and Fleming, R.J., J. Polym. Sci., **10**, 1979 (1972).
66. Bui, L., Carchano, H., Gaustevino, J., Chatain, D., Gautier, P. and Lacabanne, C., Thin Solid Films, **21**, 313 (1974).
67. Takeda, S. and Naito, M., Proc. 7th Inter. Vac. Congr. and 3rd Inter. Conf. Solid Surfaces, Vienna, pp. 2007-10 (1977).
68. Perlman, M.M. and Reedyk, C.W., J. Electrochem. Soc., **115**, 45 (1968).
69. Pillai, P.K.C., Jain, V.K. and Vij, G.K., J. Electrochem. Soc., **116**, 836 (1969).
70. Murphy, P.V. and Fraim, F.W., J. Audio. Eng. Soc., **16**, 450 (1968).
71. Reiser, A., Lock, M.W.B. and Knight, J., Trans. Faraday Soc., **65**, 2168 (1969).
72. Sessler, G.M. and West, J.E., Polym. Letts., **7**, 367 (1969).

73. Sessler, G.M. and West, J.E., Bull. Am. Phys. Soc., **15**, 307 (1970).
74. Matsuzaki, K., Okada, M. and Uryu, T., J. Polym. Sci., A-1, **9**, 1701 (1971).
75. Hinrichsen, G., J. Polym. Sci. C, **38**, 303 (1972).
76. Pillai, P.K.C., Jain, K. and Jain, V.K., Ind. J. Pure Appl. Phys., **11**, 597 (1973).
77. Gohil, R.M., Patel, K.C. and Patel, R.D., Polymer, **15**, 403 (1974).
78. Jain, V.K., Gupta, C.L., Jain, R.K., Agrawal, S.K. and Tyagi, R.C., Thin Solid Films, **30**, 245 (1975).
79. Kaneko, F. and Hino, T., J. Inst. Elect. Engrs. Japan, **98A**, 45 (1978) (in Japanese).
80. Bucci, C. and Fieschi, R., Phys. Rev. Lett., **12**, 16 (1964).
81. Ong, P.H. and Turnhout, J. Van, Electret Charge Storage and Transport in Dielectrics, Electrochem. Soc., Princeton, New Jersey (1973).
82. Chatain, D., Gautier, P. and Lacabanne, C., J. Polym. Sci. Polym. Phys. Ed., **11**, 1631 (1973).
83. Vanderschuren, J., J. Polym. Sci. Polym. Phys. Ed., **15**, 873 (1977).
84. McCrum, N.G., Read, B.E. and Williams, G., An Elastic and Dielectric Effects in Polymeric Solids, Wiley, London (1967).
85. Williams, G. and Watta, D.C., Dielectric Properties of Polymers, Plenum, New York (1972).
86. Jonscher, A.K., Coll. Polym. Sci., **253**, 231 (1975).
87. Creswell, R.A. and Perlman, M.M., J. Appl. Phys., **41**, 2365 (1970).

88. Hino, T., Jap. J. Appl. Phys., **12**, 611 (1973).
89. Chatain, D., Lacabanne, C. and Maitrot, M., Phys. Stat. Sol. A, **13**, 303 (1972).
90. Fischer, P. and Rohl, P., Annual Report Conf. Electrical Insulation and Dielectric Phenomena, NAS, Washington (1975).
91. Blake, A.E., Charlesby, A. and Randle, K.J., J. Phys. D. : Appl. Phys., **7**, 759 (1974).
92. Nishitani, T., Yoshino, K. and Inuishi, Y., Jap. J. Appl. Phys., **14**, 721 (1975).
93. Perlman, M.M., Kao, K.J. and Bamji, S.S., J. Appl. Phys., **50**, 3622 (1979).
94. Cantaloube, B., Dreyfus, G. and Lewiner, J., J. Polym. Sci. Polym. Phys. Ed., **17**, 95 (1979).
95. Singh, R. and Datt, S.C., J. Electrostat. (Netherlands), **8**, 279 (1980).
96. Chara, K., J. Electrostat., **8**, 299 (1980).
97. Mahendru, P.C., Chand, S. and Jain, K., Ind. J. Pure Appl. Phys., **18**, 183 (1980).
98. Jain, K., Agrawal, J.P. and Mahendru, P.C., Nuovo Cimento, B. (Italy), **558**, 123 (1980).
99. Lacabanne, C., Chatain, D. and Monpagens, J.C., J. Appl. Phys., **50**, 2723 (1979).
100. Lilly, A.C., Jr., Henderson, H.M. and Sharp, P.S., J. Appl. Phys., **41**, 2001 (1970).
101. Stupp, S.I. and Carr, S.H., J. Appl. Phys., **46**, 4120 (1975).

102. Guillet, J. and Seytre, G., J. Polym. Sci., Poly. Phys. Ed., **15**, 541 (1977).
103. Takeda, S. and Naito, M., 3rd Intern. Conf. Solid Surface, Vienna, 2007 (1977).
104. Sessler, G.M. and West, J.E., Phys. Rev., **B10**, 4488 (1974).
105. Fischer, P. and Rohl, P., J. Polym. Sci. Polym. Phys. Ed., **14**, 543 (1976).
106. Hino, T., J. Appl. Phys., **46**, 1956 (1975).
107. Kessler, A., J. Electrochem. Soc., **123**, 1236 (1976).
108. Takamatsu, T. and Fukada, E., Electrets Charge Storage and Transport in Dielectrics, Electrochem. Soc. Inc., New York (1973).
109. Gupta, C.L. and Tyagi, R.C., Ind. J. Pure and Appl. Phys., **16**, 428 (1978).
110. Kulshrestha, Y.K. and Srivastava, A.P., Polym. J. Jap., **11**, 515 (1979).
111. Mahendru, P.C., Jain, K., Choptra, V.K. and Mahendru, P., J. Phys. D. : Appl. Phys., **8**, 305 (1975).
112. Mahendru, P.C., Jain, K. and Mahendru, P., J. Phys. D. : Appl. Phys., **9**, 83 (1976).
113. Partridge, R.H., "TL in Polymers" in "Radiation Chemistry of Macromolecules", Vol. 1, Ed. M. Dole, Academic Press, New York, 1972, pp. 193-222.
114. Curie, D., "Luminescence in Crystals", Wiley, New York, 1963, Chap. 6.
115. Bucci, C., Phys. Rev., **164**, 1200 (1967).

116. Wang, S., "Solid State Electronics", McGraw-Hill, New York, 1966, Chap. 14.
117. Ray, B., "II-VI Compounds", Pergamon, Oxford, 1969, Chap. 4.
118. Garlick, G.F.J. and Gibson, A.F., Proc. Phys. Soc. (London), **60**, 574 (1948).
119. Keating, P.N., Proc. Phys. Soc. (London), **78**, 1408 (1961).
120. Halperin, A. and Braner, A.A., Phys. Rev., **117**, 408 (1960).
121. Haering, R.R. and Adams, W.N., Phys. Rev., **117**, 451 (1960).
122. Frei, H. and XXXXXXXXXXXX,
123. Mahendru, P.C., Phys. Stat. Sol.(a), **42**, 403 (1977).
124. Mahendru, P.C., Chandra, S. and Pathak, N.L., Thin Solid Films, **44**, 13 (1977).
125. Perlman, M.M., J. Electro. Chem. Soc., **119**, 892 (1972).
126. Caserta, G. and Serra, A., J. Appl. Phys., **42**, 3778 (1972).
127. Pillai, P.K.C., Jain, K. and Jain, V.K., Phys. Stat. Sol.(a), **17**, 221 (1973).
128. Mahendru, P.C., J. Phys. D. Appl. Phys., **8**, 305 (1975).
129. Latour, M. and Murphy, P.V., J. Electro. State, **3**, 163 (1974).
130. Jain, K., Rastogi, A.C. and Chopra, K.L., Phys. Stat. Sol. (a), **21**, 2, 685 (1974).
131. Talwar, M. and Sharma, D.L., J. Electrochem. Soc., **125**, 434 (1978).
132. Kojima, K. and Maeda, Jpn. J. Appl. Phys., **17**, 1735 (1978).

133. Tokai, Y., Mori, K., Mizitani, T and Leda, M., Jpn. J. Appl. Phys., **16,11**, 1937 (1977).
134. Shrivastava, S.K., Ranade, J.D. and Shrivastava, A.P., Thin Solid Films, **67**, 201 (1980).
135. Shrivastava, A.P. and Mathur, O.N., Indian J. Phys., **57A**, 91 (1979).
136. Tanaka, T., Hirabayashi, S. and Shribayama, K., J. Appl. Phys., **49**, 784 (1978).
137. Iqbal, T. and Hogarth, C.A., Thin Solid Films, **61**, 23 (1979).
138. Rao, V.V.R. Narsimha and Das, N. Narsing, J. Vac. Sci. Technol., **A4**, 1 (1986).
139. Rao, V.V.R. Narsimha and Kalipalatha, A., Materials Chem. and Phys., **17**, 317 (1987).
140. Christodoulides, C. *et al.*, Phys. Stat. Sol. (a), **11**, 325 (1989).
141. Fraile, T. *et al.*, Journ. Mat. Sci., **24**, 33 (1989).
142. Vaezi-Najad, S.M. *et al.*, Journ. Mat. Sci., **27**, 437 (1992).
143. Rychkov, A.A. *et al.*, J. Phys. D. Appl. Phys., **25**, 986 (1992).
144. Kamarulzaman, B.M.Z. *et al.*, Journ. Mat. Sci., **27**, 4316 (1992).
145. Weijun, Yin *et al.*, IEEE Trans. on Dielectrics and Electrical Insulation, **1,2**, 169 (1994).
146. Lewandowski, A.C. *et al.*, Phys. Rev., **B-49**, 8029 (1994).
147. Vanderschueven, J. and Gasiot, J., "Thermally Stimulated Relaxation in Solids", Springer Verlag, Berlin (1979).
148. Mikolo, S., Z. Phys., **32**, 475 (1925).

149. Kulshrestha, Y.K. and Srivastava, A.P., Polym. J. Japan, **11**, 515 (1979).
150. Reddish, W., Trans. Faraday Soc., **46**, 459 (1950).
151. Wiseman, G.G. and Feaster, G.R., J. Chem. Phys., **26**, 521 (1957).
152. Gupta, N.P., Jain, K. and Mahendru, P.C., Thin Solid Films, **61**, 297 (1979).
153. Perlman, M.M., J. Appl. Phys., **42**, 2645 (1971).
154. Khare, P.K. and Srivastava, A.P., Ind. J. Pure Appl. Phys., **30**, 102 (1992).
155. Khare, P.K., Surinder, P. and Srivastava, A.P., Ind. J. Pure and Appl. Phys., **30**, 165 (1992).
156. Turnhout, J. Van, "Thermally Stimulated Discharge of Polymer Electrets", Elsevier, Amsterdam, 1975.
157. Lovinger, A.J., Development in Crystalline Polymers, Ch.5, Allied Science, London, 1982.
158. Tashiro, K., Todakora, H. and Kobayushi, M., Ferroelectrics, **32**, 103 (1981).
159. Roerdink, E. and Challa, G., Polymer, **21**, 509 (1980).
160. Paul, D.R., Barlow, J.W., Bensten, R.E. and Wahrmuand, D.R., Polym. Eng. Sci., **18**, 1225 (1978).
161. Wendroff, J.H., J. Polym. Sci. Polym. Lett., **18**, 439 (1980).
162. Dasgupta, D.K. and Doughty, K., J. Appl. Phys., **11**, 2415 (1978).
163. Perlman, M.M. and Cresswell, R.A., J. Appl. Phys., **42**, 531 (1971).

165. Jonscher, A.K., Thin Solid Films, **1**, 213 (1967).
166. Pillai, P.K.C., Gupta, B.K. and Malti Goel, J. Polym. Sci. Phys., **19**, 1461 (1981).
167. Srivastava, S.K., Rande, J.D. and Srivastava, A.P., Phys. Lett., **72A**, 185 (1979).
168. Srivastava, S.K., Rande, J.D. and Srivastava, A.P., Jap. J. Appl. Phys., **18**, 2303 (1979).
169. Talwar, I.M., Ph.D. Thesis, University of Sagar, Sagar (1968).
170. Khare, P.K. and Srivastava, A.P., Indian J. Pure and Appl. Phys., **30**, 131 (1992).
171. Bogroditskii, N.P. and Tairova, D.A. *et al.*, Fizika. Tverad. Tela, **6**, 2301 (1954).
172. American Institute of Physics Handbook, New York, McGraw Hill Book Co., (1965), p. 9-14.
173. Gupta, N.P., Jain, K. and Mahendru, P.C., Thin Solid Films, **61**, 297 (1979).
174. Grepstad, J.K., Gartland, P.O. and Stagsvold, B.J., Surf. Sci., **57**, 348 (1976).

/ ***** /

CHAPTER V

TRANSIENT CURRENTS IN CHARGING AND DISCHARGING MODES

5.1 INTRODUCTION

If we take a polymeric sample and apply a step field to it, the field interacts with the bound and free charge causing their motion. The motion of charges manifests itself as a current flow in the external circuit. Generally, this current known as absorption or charging current, depends on the time elapsed after the application of potential to the electrodes; usually it falls off at first and then becomes steady. After the step voltage has been removed, there is still a current flowing in the external circuit, which is called desorption or discharging current. We find that under isothermal conditions both absorption as well as desorption currents decay approximately in most of the cases as t^{-n} , where t is the time elapsed after the application of the step voltage and ' n ' is an exponent whose value may be greater or less than 1, depending upon the properties of the material chosen and the experimental conditions [1-12]. The discharge current may be the mirror image of the charging current except that a steady state current is not reached. The isothermal desorption current decays for a long time, depending upon the internal phenomena taking place irrespective of the steady state current level.

Desorption currents can yield much useful information about the charging process even when the corresponding absorption current is masked by the conduction current during charging. The analysis of the experimental conditions can lead to a quantitative as well as qualitative idea of the mechanisms. The results can be compared with some other

studies like thermally stimulated discharge current (TSDC), etc., to arrive at coherent and cogent conclusion. Transient current measurements are tedious - on being carried out over a long time is not a regular study but nevertheless it is a very useful one, giving far more consistent results than the others. This being so on account of electrical and other perturbing influences affecting the charging process far less than in other experiments involving decay processes.

The fact that electronic conduction plays a role in polymers has been established experimentally by Seanor [13]. To discuss electronic condition, it is necessary to investigate the generation of free carriers and their transport through the material.

In polymers at low temperature, the density of free charge carriers is extremely low and with an electric field, non-equilibrium conditions can be achieved, which can be easily enhanced by injecting a charge through an ohmic contact. Current-voltage curves is generally non-linear on account of two basic causes. At high fields the charges are accumulated between the electrodes. The density, energy distribution and nature of the traps have a determining influence on current-voltage characteristics which also depend on type of charges involved in the conduction process.

Trapping sites exert strong influence on the current flow, i.e. the concentration of free carriers and their mobility if the activation energy values are low 0.2 to 0.3 eV, hopping is contacted with charge jumps

brought about by motion of chain elements while great values (0.5 eV) the so-called trap hopping mechanism is involved.

5.2 TIME DEPENDENCE CURRENT MODELS

Many scientists have attempted to explain the mechanisms of the charging and discharging in polymers. A number of models incorporating charging and discharging related processes have been evolved to explain the mechanism. The important ones are given in succeeding subsections.

(a) Electrode polarisation :

Free charge are frequently available in the polymer bulk and have thermally activated mobilities. These charges move towards electrodes of opposite polarities on application of a polarising voltage and start piling up near the electrode. The electrode polarization or blocking mechanism (occurring in ionic materials) is characterised by linear dependence of the isochronal current on the field (though theory predicts a nonlinear region at low field), and a current that is thermally activated. It has been observed that the isochronal current at constant field does not depend upon the thickness on the sample. The current fall is initially proportional to $t^{-1/2}$ followed by a steep change where $n > 1$. The charging and discharging currents are mirror images of each other [14,15].

(b) Dipole orientation :

Randomly arranged dipoles in the polymer bulk do not contribute any definite dipole moment to the polymer specimen. They possess a

definite relaxation time and activation energy, however, relaxation time is a thermally activated parameter. On applying an external electric field and raising the temperature, relaxation of dipole is activated and they start orienting in the field direction. Fast polarisation responds immediately to the orientational effect of the field. The rate of orientation is thermally activated as the relaxation time gradually decreases on increasing the temperature. Like accumulation of space charges, orientation of dipoles is also field dependent as more and more electrostatic force is available for dipole alignment on increasing the polarisation field. Image charges are induced on metal electrode surface during the orientation of dipoles, causing a net current to flow in the external circuit. The value of this current depends on the rate of dipole orientation and decreases gradually with time at a fixed temperature and field, thus causing fall in the value of absorption current with time. The exact behaviour of the decay of absorption current depends upon relaxation time, activation energy, distribution function and the experimental conditions. The current density of absorption current is unaffected by the specimen thickness and this type of polarisation is polar dielectrics is a volume or bulk phenomenon.

After removal of the polarising field, dipoles start disorienting to acquire their original configuration. The fast dipoles are disoriented earlier than the slow dipoles. The rate of depolarisation also depends on the temperature, maximum charge attained and some inherent properties like activation energy and distribution function. This again causes a definite

amount of desorption current to flow in the external circuit, which is expected to be a mirror image of absorption current provided that the value of steady state conduction current is negligible and the experimental conditions are identical to those during polarisation.

(c) Hopping mechanism :

In certain materials, a large number of localised states are present inside their molecular arrangement, with a wide distribution in their activation energy or trap depths. These states are usually filled by the charge carriers, which are electrons in most of the cases. On applying an external electric field, some of the charge carriers may jump from one localised state to another causing disturbance in the internal charge distribution. Hopping of the charge carriers is thermally activated as their mobility and detrapping from the traps increase with the thermal energy. However, field can play an important role in detrapping of charge carriers causing field assisted thermal excitation of impurity centres. It can also provide a directive force to the charge carriers. Thus, the absorption current in the process is expected to be field and temperature dependent. However, it is independent of the electrode material and the specimen thickness as the trapped charge carriers are intrinsic and uniformly distributed in the polymer bulk. The absorption and desorption currents are expected to be the mirror image of each other as the trapping and detrapping are perfectly reversible mechanisms [16,17]. Farriera and Morena [18] observed that a time dependent, effective medium,

approximation essentially explains the time behaviour of the polarisation reversals obtained in doped copolymers of vinylidene fluoride and trifluoroethylene.

(d) Tunnelling model :

This model [14,15] assumes the presence of the trap level (s) in the dielectric. It may so happen that the charge carriers may lack enough energy to overcome the potential barrier existing between the traps and hence take part in the current process. This model [19] assumes that an electron in a π -molecular orbital on one molecule, when excited to a higher energy level (in our case by application of an external field at a higher temperature) can tunnel through a potential barrier to a non-occupied state of a neighbouring molecule. Traps are an essential part of the tunnelling model. It has been observed that the current-time curve is mainly due to the trap level closest to the Fermi level of the injecting electrode whereas trap levels which are deep and located well inside the band gap have been postulated. Deep traps have been reported [20] in corona charged samples, which in fact may be ion traps. The lack of substantial evidence on the presence of deep traps may be due to an inhomogeneous distribution leading to a weaker concentration of deep traps in the bulk.

The tunnelling model points to a field (up to 10^5 V/cm) and which is directly proportional to the isochronal current at moderate field (up to 10^5 V/cm) and is inversely proportional to the thickness. The current is

strongly dependent on the electrode material and is independent of the temperature. It is dependent on time as $I \propto t^{-n}$ with $0 \leq n \leq 2$ and the charging and discharging currents are mirror images of each other.

(e) Charge injection leading to trapped space charge effects :

There are usually a high concentration of trapping sites in the forbidden energy gap of polymer. These trapping sites are the outcome of impurities or the internal molecular arrangements in macromolecules. The application of a electric field to the polymer sandwiched between two metallic electrodes causes electrons or holes to be injected which get trapped in the trapping sites available, their distribution depending upon the energy and trap depths. The charges which get trapped inside the bulk form a space charge, further oppose trapping of charge carriers. The trapping process causes the charging current to flow while removal of the external field produces the discharging current. Nagashima and Faria [21] have developed a model for space charge migration in discharge current measurements.

The space charge model needs a sufficiently high concentration of deep trapping levels to be present. Under this model, the isochronal current at constant field is independent of thickness. We find that the transient current shows a field dependence, temperature effect and electrode material dependence which is related to the charge injection mechanism

prevalent. The transient current is proportional to t^{-n} , where $0 \leq n \leq 1$ and the charging and discharging currents are totally dissimilar to each other.

The process of charging and discharging a polymer sample is a complex process which is attributed to the generation of the charge carriers. The charging and discharging processes exhibit electrical properties of a polymer dielectric and thus help in its better understanding. The current across a polymer dielectric immediately after applying a field is called the transient charging or absorption current and the same immediately after removing the field is called transient discharge or desorption current. Under isothermal conditions, charging and discharging currents decay approximately as t^{-n} , where t is the time elapsed after the application of the field and 'n' is the constant depending upon the properties of the material and the experimental conditions. The discharge current may be the mirror image of the charging current except that a steady state current is not reached.

The discharge current can yield very useful information about the charging process even when the corresponding charging current is masked by the conduction current during charging. The analysis of experimental conditions can lead to a quantitative as well as a qualitative idea of the mechanisms at work. The result can then be compared with some other studies like TSDC etc. to arrive at some useful conclusions.

Although many transient measurements have so far been made [22-24] and subjected to detailed analysis, the origin of charging and discharging currents is still afflicted with doubts and controversies. This is

because more extensive study on the effects of various parameters like field, temperature and electrode material is still desired. To take a step forward, i.e. to reach a clear, irrefutable and concrete explanation for the mechanisms involved in transient charging and discharging current flow, the present work takes up the studies of PVDF.

5.3 EXPERIMENTAL

The sandwiched sample (metal-PVDF-metal) was placed in a specially designed cell. The temperature of the cell was controlled with an accuracy of ± 1 K by adjusting the input voltage from the variac for which the calibration has been made. The d.c. voltage across the sample were fed from a regulated power supply (ECIL, India) and currents in the circuit were recorded by means of a Keithley Electrometer Model 610C. After making proper electrical connections, the sandwiched sample mounted on electrode assembly was placed inside the thermostat and allowed to attain required temperature. It took about 1.5 hours. When the sample attained the desired temperature, a dc voltage was applied. A sudden burst of current observed in the beginning decreases with time. Its initial as well as steady state value was recorded. At lower voltages and temperature it took longer period to reach the steady state while at higher voltages and temperatures, steady state was obtained in considerable low period. The effect of voltage variation in current was noted by increasing the voltage at fixed temperatures while temperature variation was measured keeping

voltage constant and increasing the temperature. Measurements were taken in the voltage and temperature ranges of 10-100 kV/cm and 40-70 °C, respectively. A fresh sample is used for each set of observation.

5.4 RESULTS AND DISCUSSION

The results of transient currents in charging and discharging modes are analyzed and interpreted.

The time dependence of the charging and discharging transient currents in polyvinylidene fluoride (PVDF) samples have been investigated over a period of time 1-80 min. The Figs. 5.1 to 5.30 show the variation of discharging transient currents with time at different temperatures, i.e. 40, 50, 60, 70 and 80 °C with polarizing fields of 10, 25, 50, 75, 100 kV/cm, respectively. It is evident from the figures that the current decays at a faster rate for a few minutes and then the decay rate slows down. Curves illustrating the time-dependence of transient discharging currents are, in general, characterized with two regions which are designated as the short-time and the long-time regions, respectively.

Figures 5.31 to 5.60 illustrate the charging characteristics of PVDF films at different temperatures, i.e. 40, 50, 60 and 70 °C with different polarizing fields (10, 25, 50, 75 and 100 kV/cm). From the above characteristics, it is clear that at least two distinct mechanisms should be responsible for the observed transient currents. One mechanism is operative in the short-time range with a particular value of decay constant

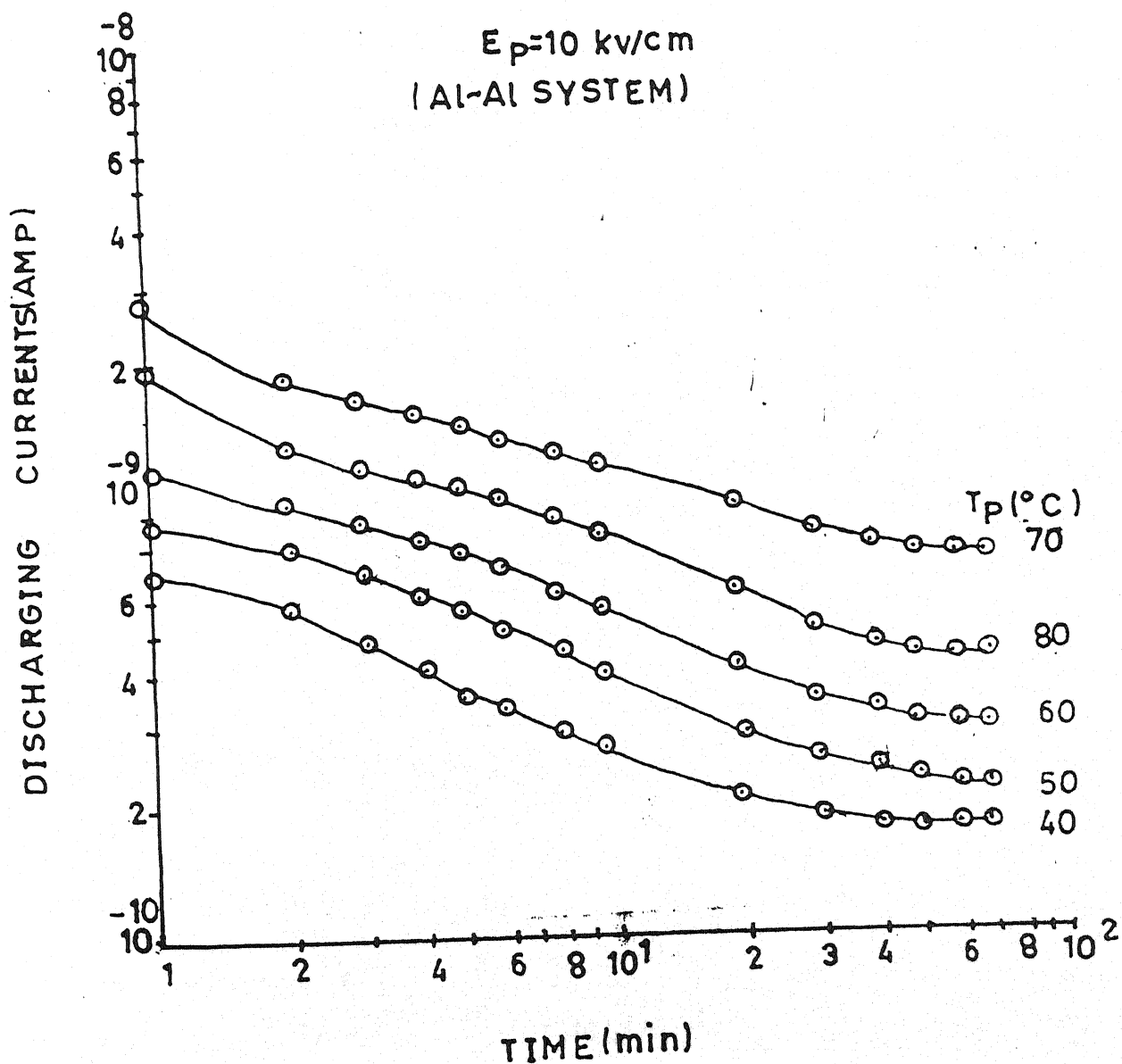


Fig. 5.1

Transient currents in Discharging mode for polyvinylidene fluoride sample ($20 \mu\text{m}$) poled with polarization field 10 kv/cm with different polarization temperature i.e. $40, 50, 60, 70$ and 80°C for Al - Al Electrode system.

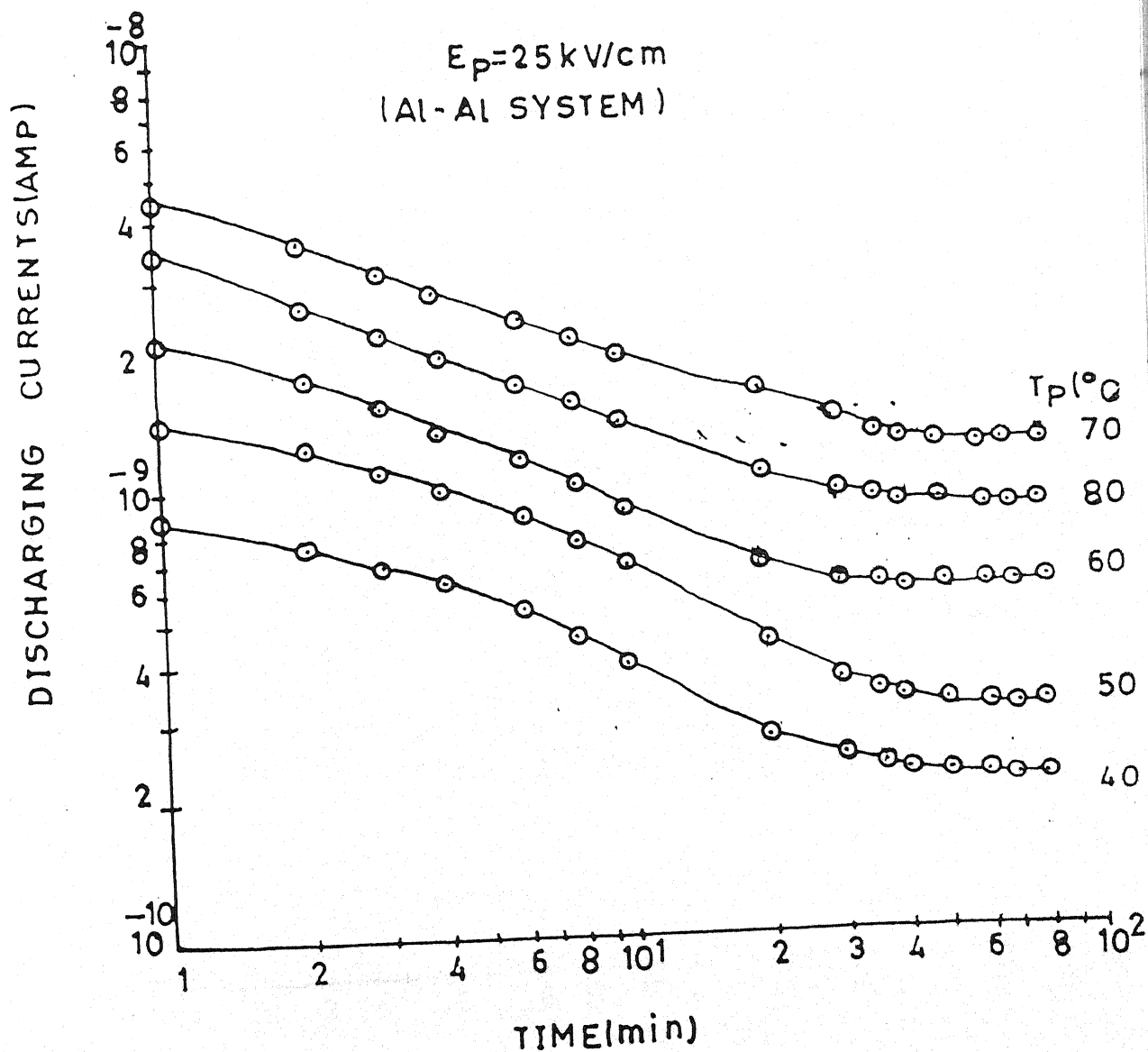
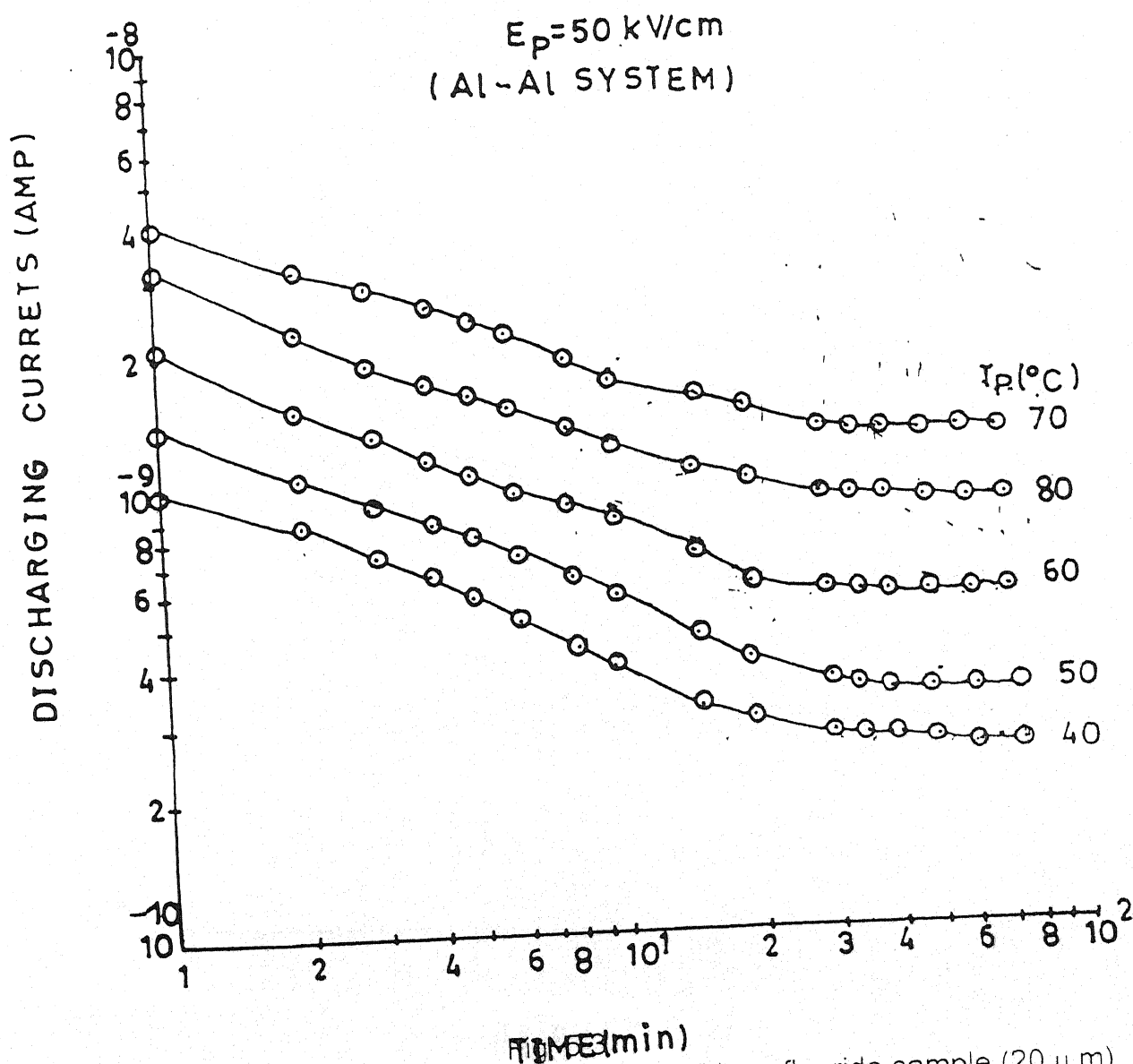


Fig. 5.2
Transient currents in Discharging mode for polyvinylidene fluoride sample ($20 \mu\text{m}$)
poled with polarization field 25 kV/cm with different polarization temperature i.e. 40°C ,
 60°C , 70°C and 80°C for Al - Al Electrode system.



Transient currents in Discharging mode for polyvinylidene fluoride sample ($20 \mu\text{m}$) poled with polarization field 50 kV/cm with different polarization temperature i.e. $40, 50, 60, 70$ and 80°C for Al - Al Electrode system.

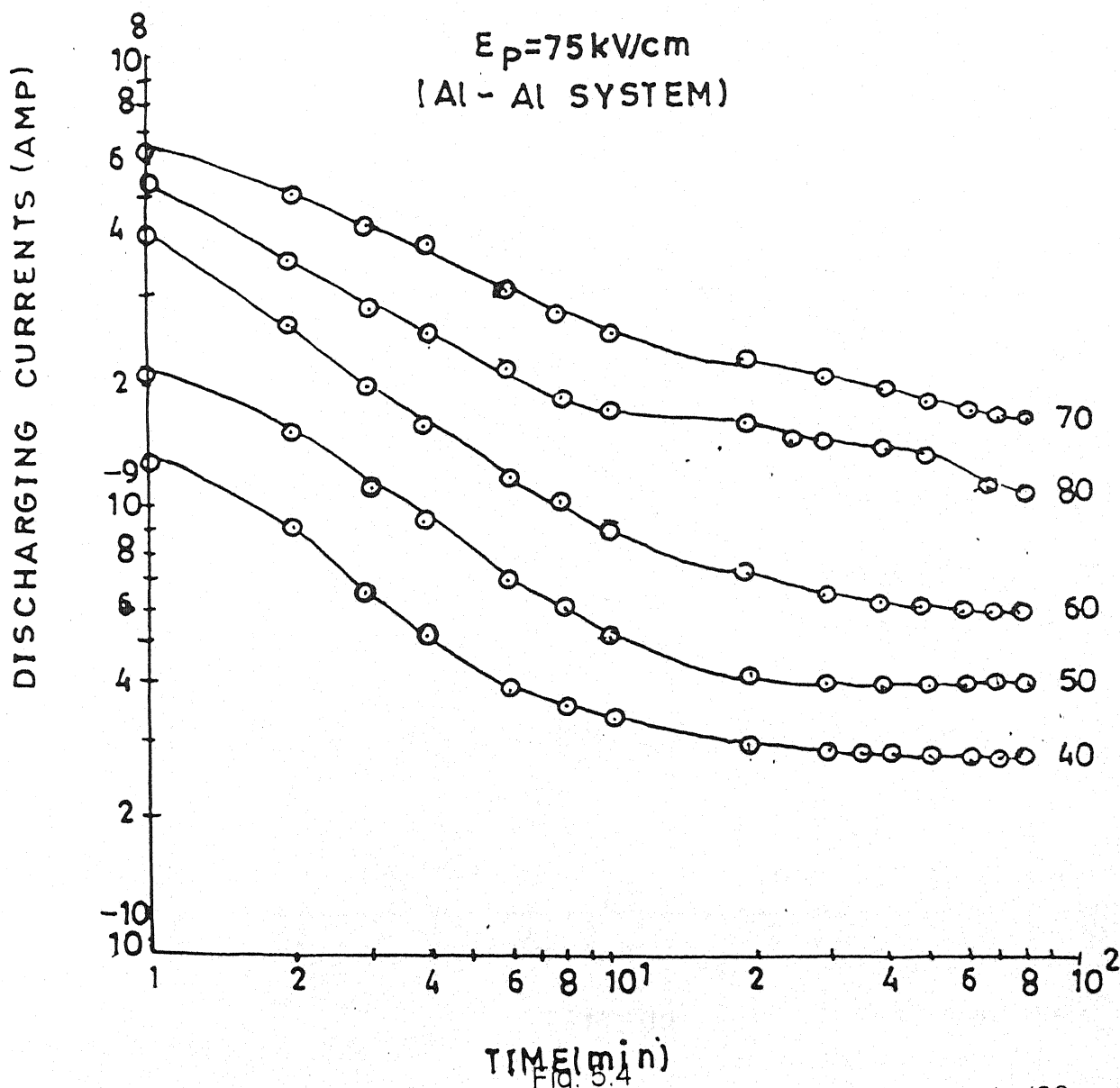


Fig. 5.4
Transient currents in Discharging mode for polyvinylidene fluoride sample ($20 \mu\text{m}$) poled with polarization field 75 kV/cm with different polarization temperature i.e. $40, 50, 60, 70$ and 80°C for Al - Al Electrode system.

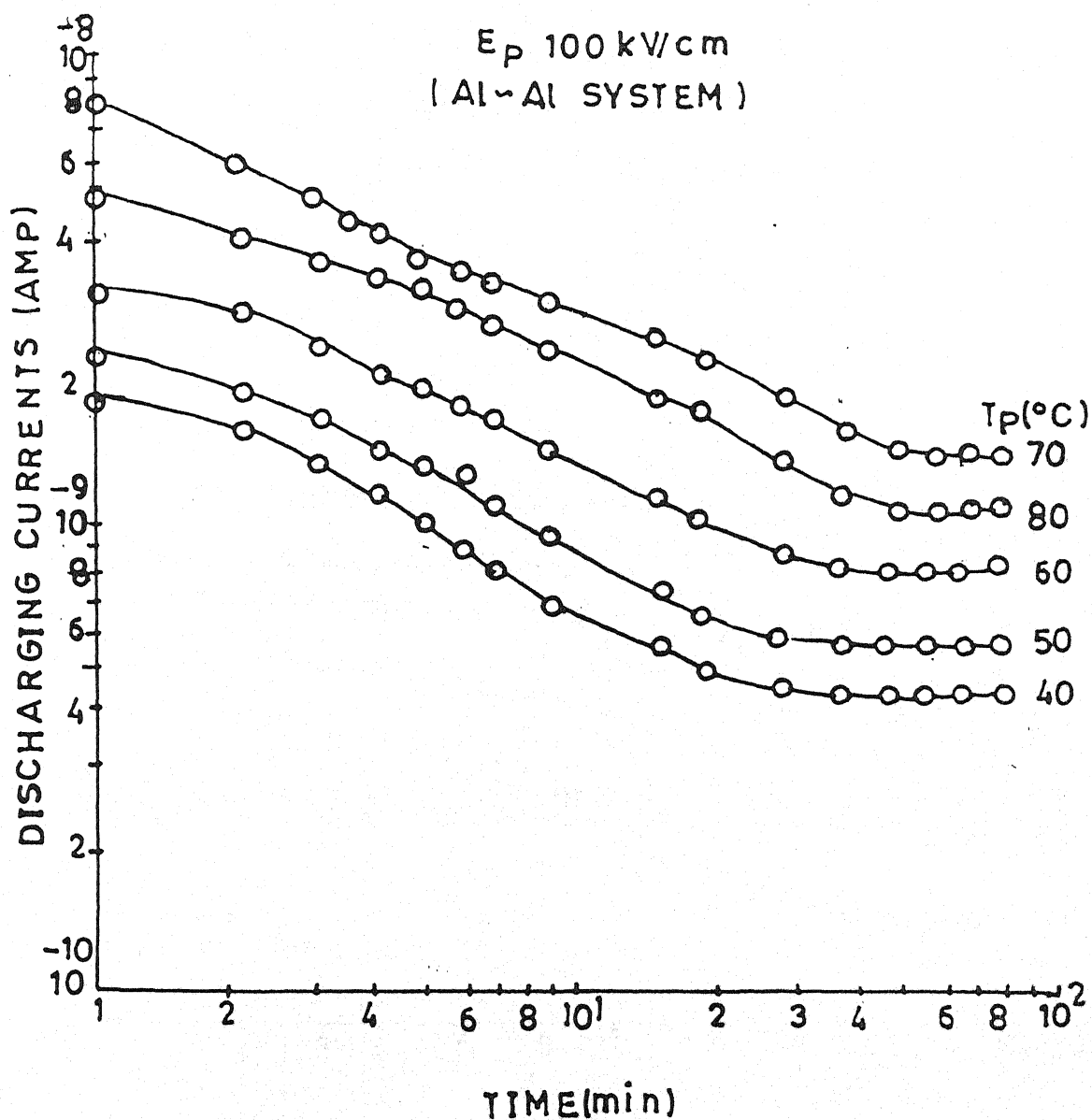


Fig. 5.5
Transient currents in Discharging mode for polyvinylidene fluoride sample (20 μ m) poled with polarization field 100 kV/cm with different polarization temperature i.e. 40, 50, 60, 70 and 80 $^{\circ}$ C for Al-Al Electrode system.

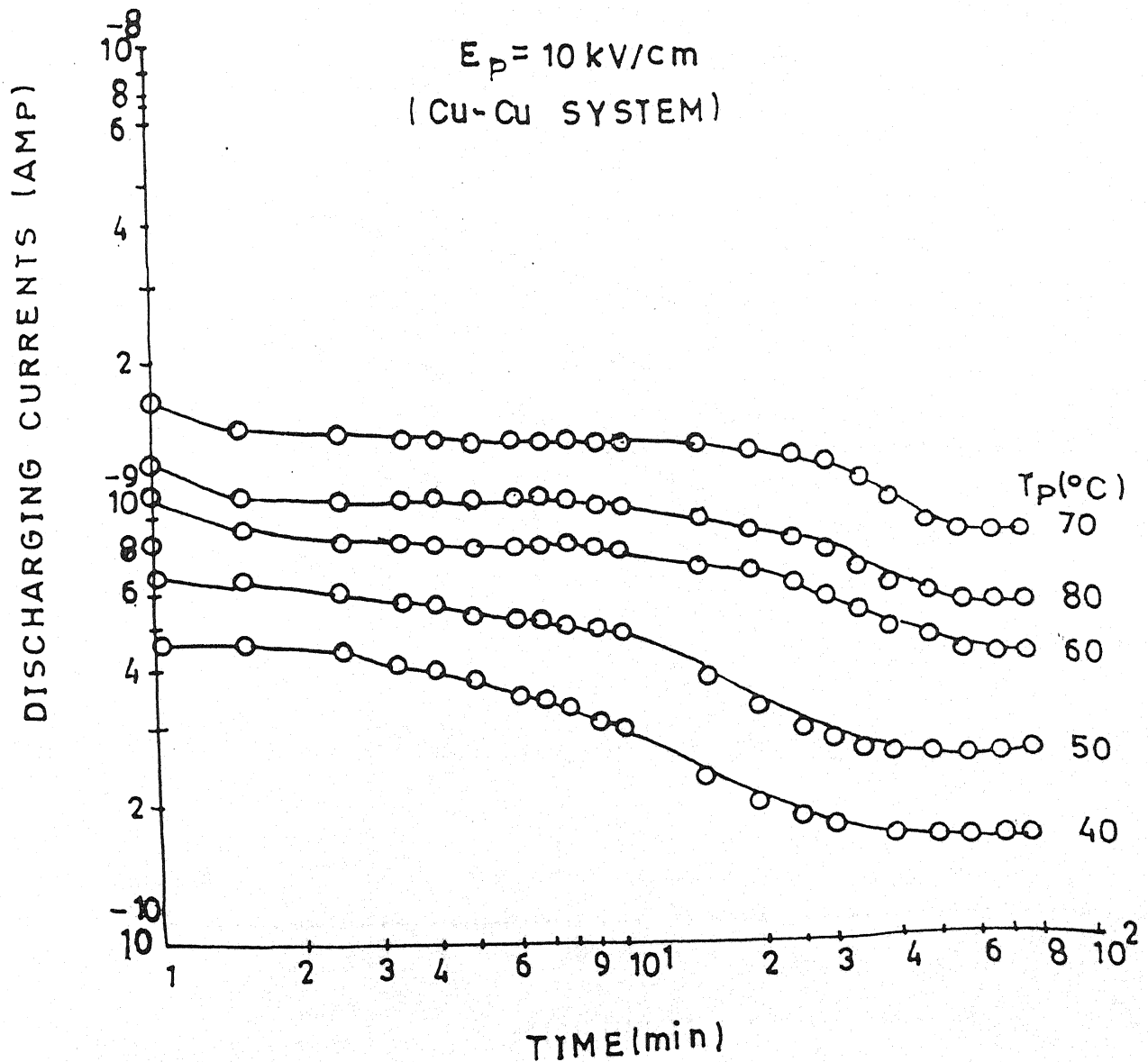


Fig. 5.6
Transient currents in Discharging mode for polyvinylidene fluoride sample (20 μm) poled with polarization field 10 kV/cm with different polarization temperature i.e. 40, 50, 60, 70 and 80°C for Cu-Cu Electrode system.

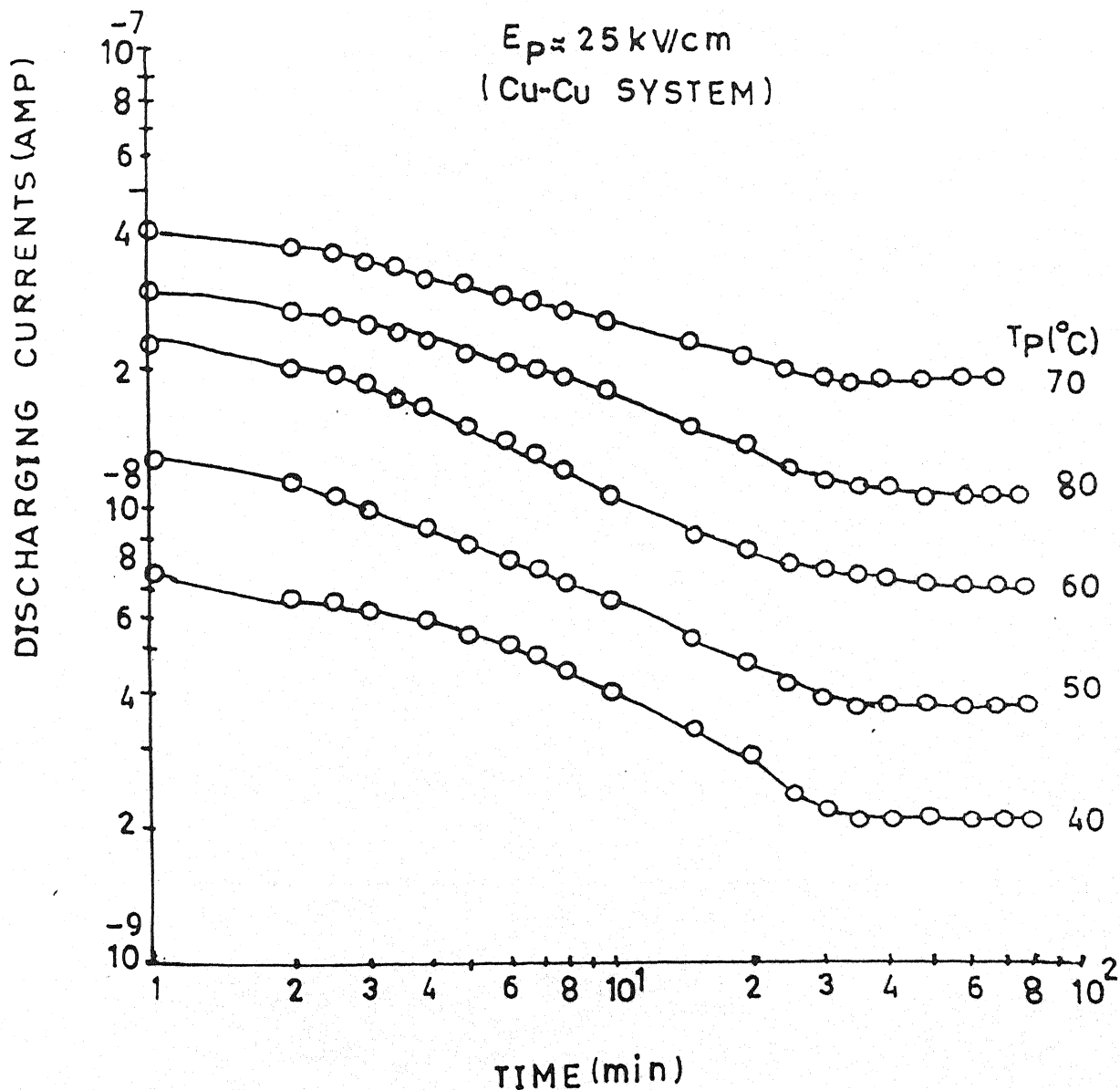


Fig. 5.7

Transient currents in Discharging mode for polyvinylidene fluoride sample (20 μm) poled with polarization field 25 kV/cm with different polarization temperature i.e. 40, 50, 60, 70 and 80°C for Cu-Cu Electrode system.

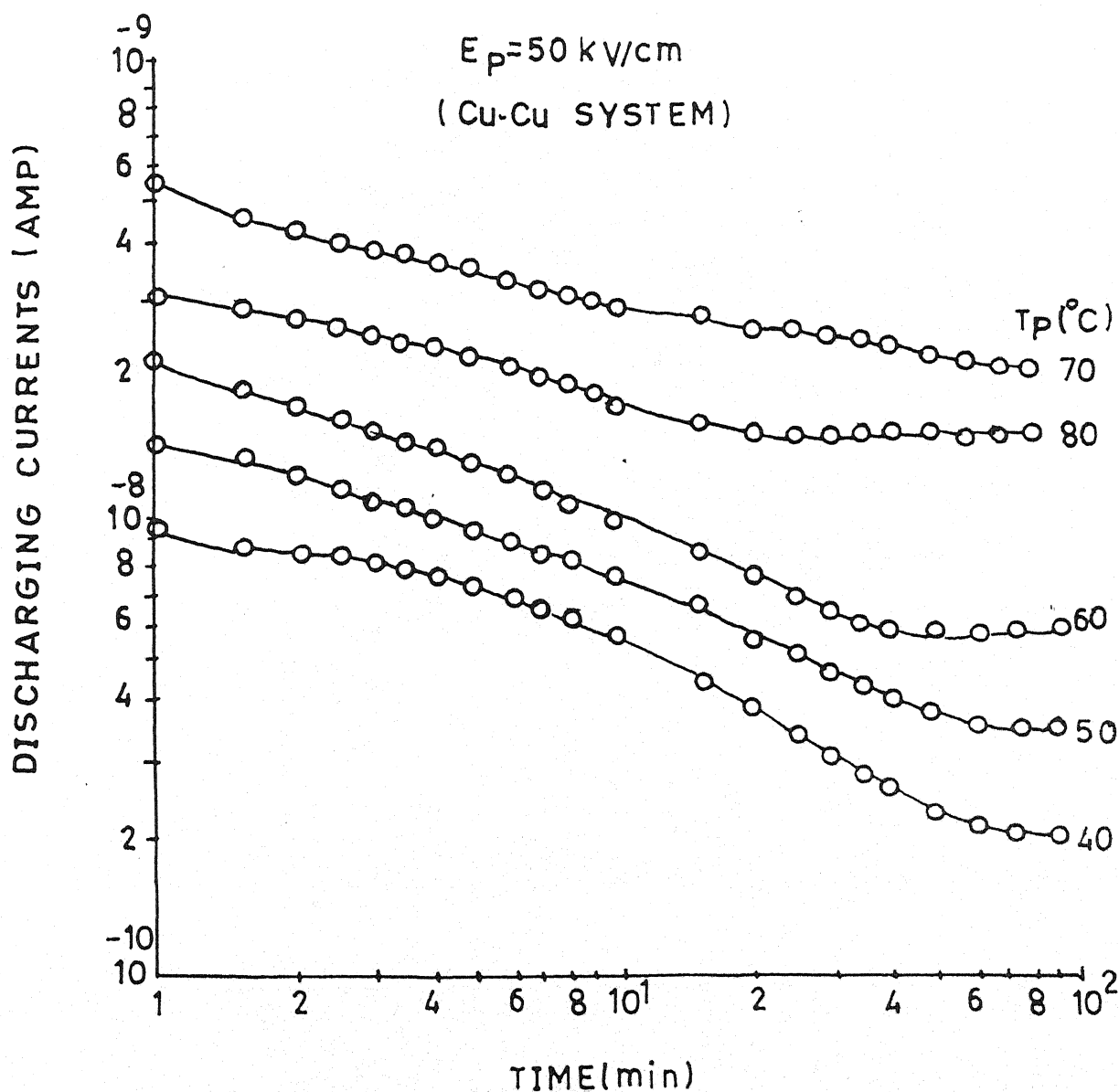


Fig. 5.8
Transient currents in Discharging mode for polyvinylidene fluoride sample (20 μm) poled with polarization field 50 kV/cm with different polarization temperature i.e. 40, 50, 60, 70 and 80°C for Cu-Cu Electrode system.

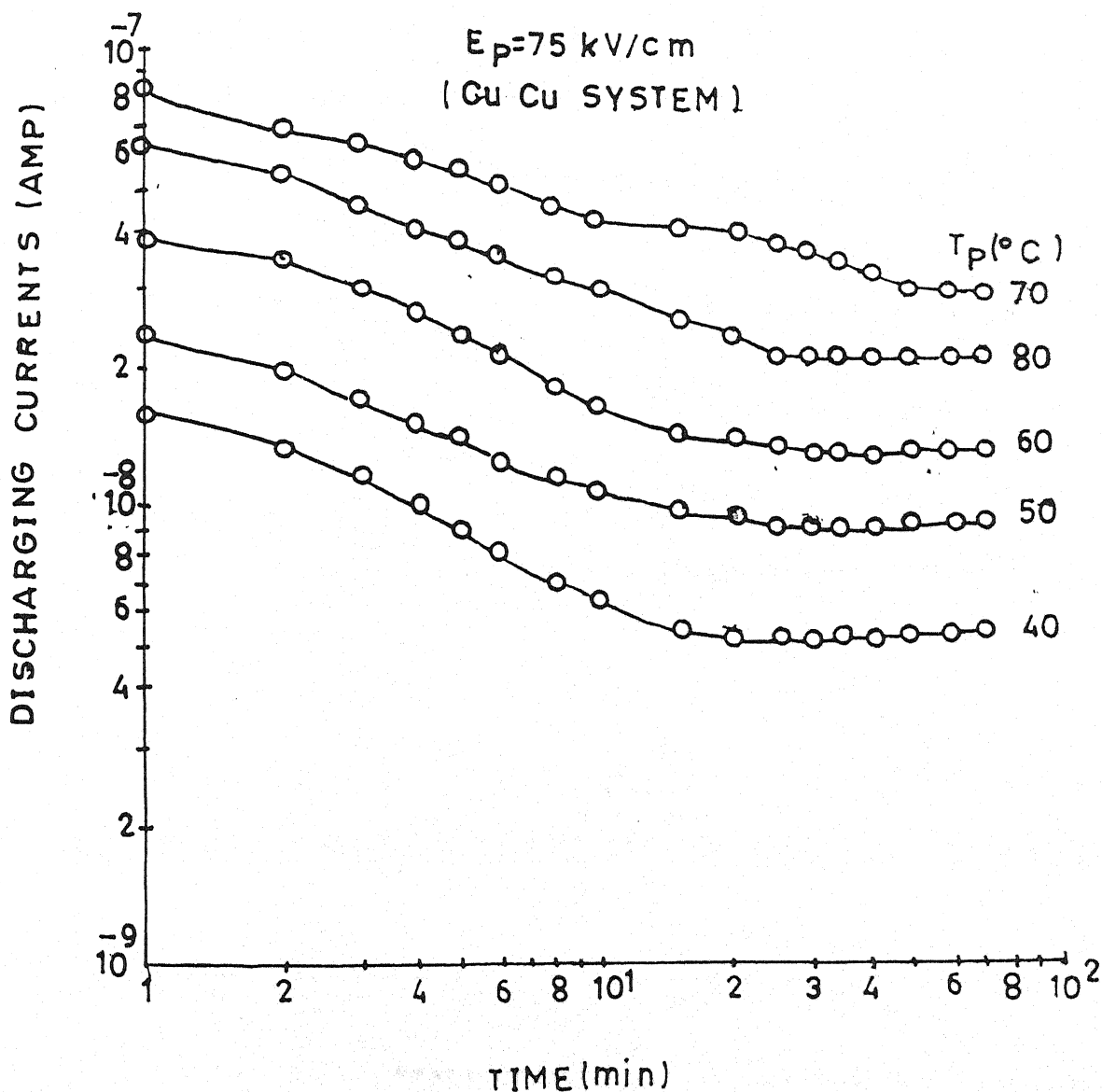


Fig. 5.9

Transient currents in Discharging mode for polyvinylidene fluoride sample ($20 \mu\text{m}$)
 cooled with polarization field 75 kV/cm with different polarization temperature i.e. 40 , 50
 60 , 70 and 80°C for Cu- Cu Electrode system.

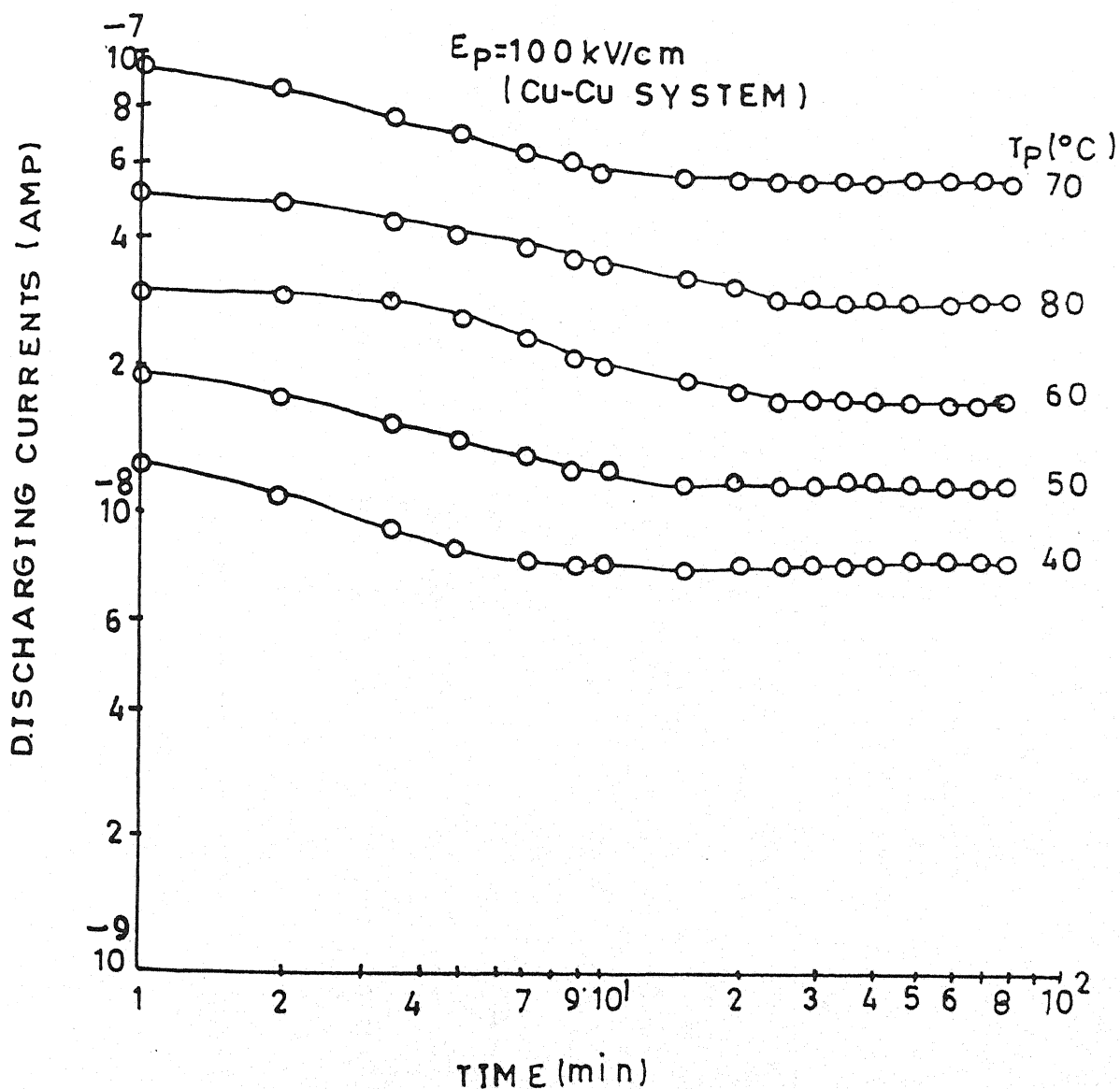


Fig. 5.10

Transient currents in Discharging mode for polyvinylidene fluoride sample ($20 \mu\text{m}$) poled with polarization field 100 kV/cm with different polarization temperature i.e. 40 , 50 , 60 , 70 and 80°C for Cu-Cu Electrode system.

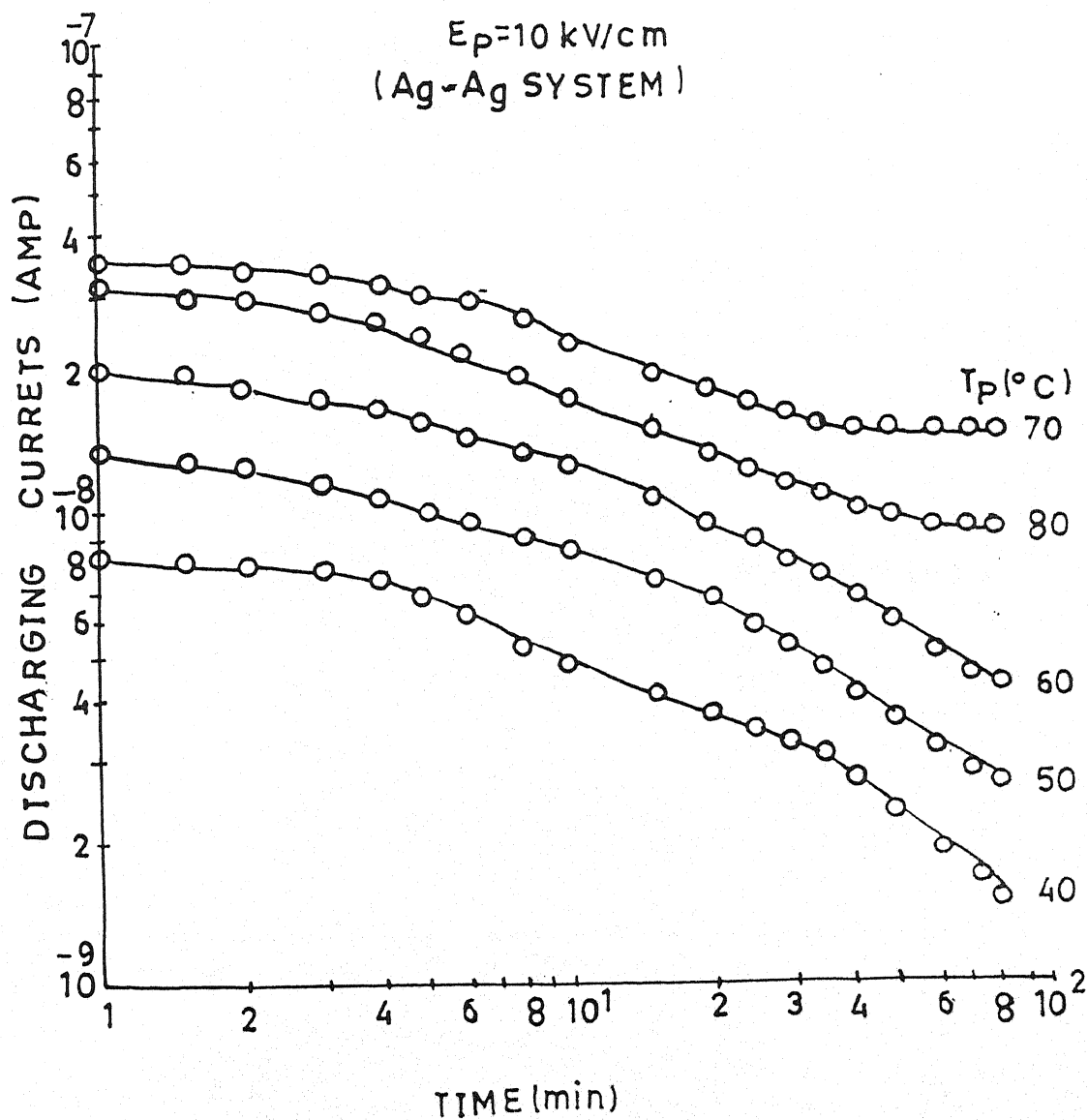


Fig. 5.11

Transient currents in Discharging mode for polyvinylidene fluoride sample ($20 \mu\text{m}$) poled with polarization field 10 kV/cm with different polarization temperature i.e. 40 , 50 , 60 , 70 and 80°C for Ag-Ag Electrode system.

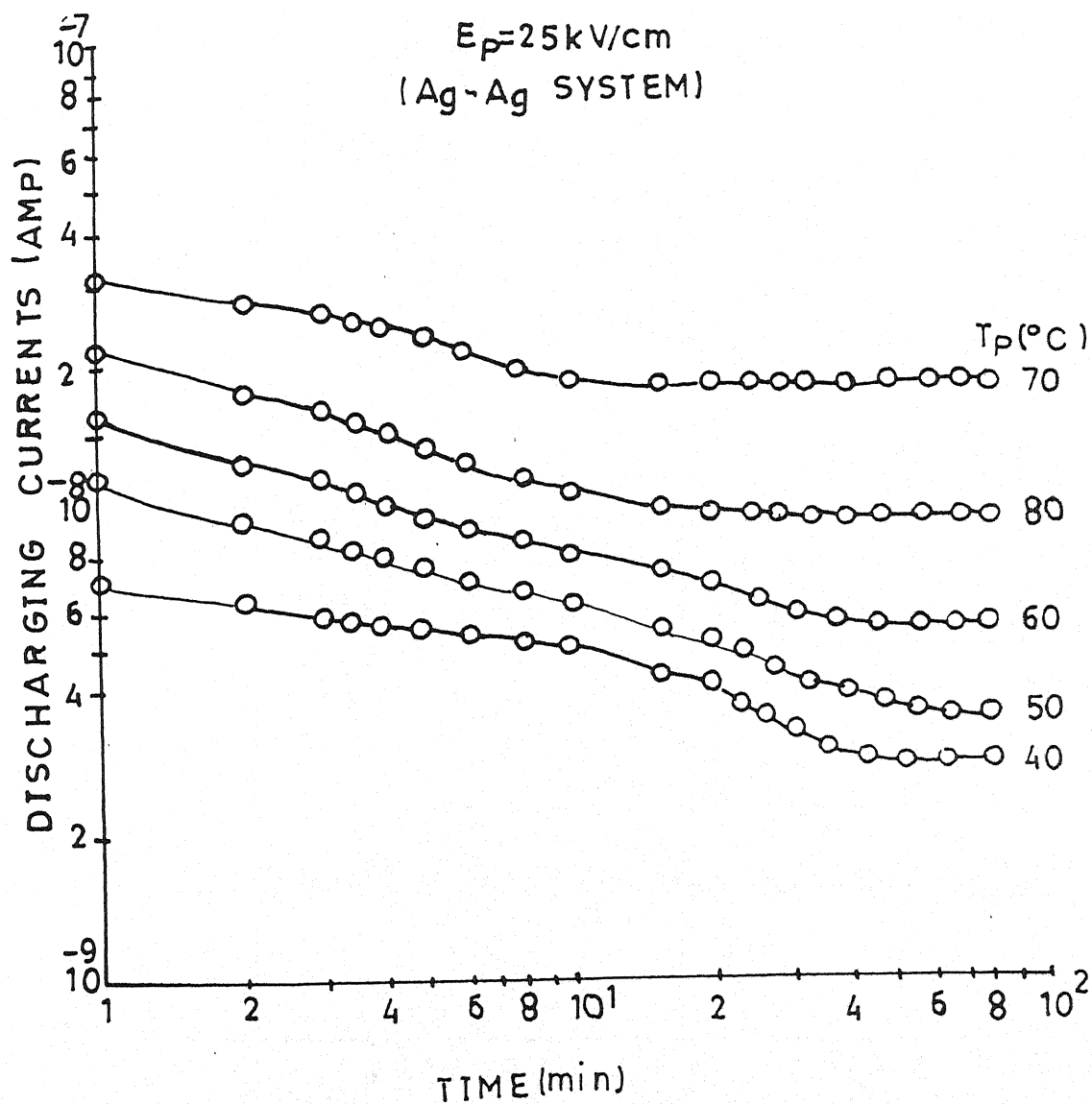


Fig. 5.12

Transient currents in Discharging mode for polyvinylidene fluoride sample ($20 \mu\text{m}$) poled with polarization field 25 kV/cm with different polarization temperature i.e. 40 , 50 , 60 , 70 and 80°C for Ag-Ag Electrode system.

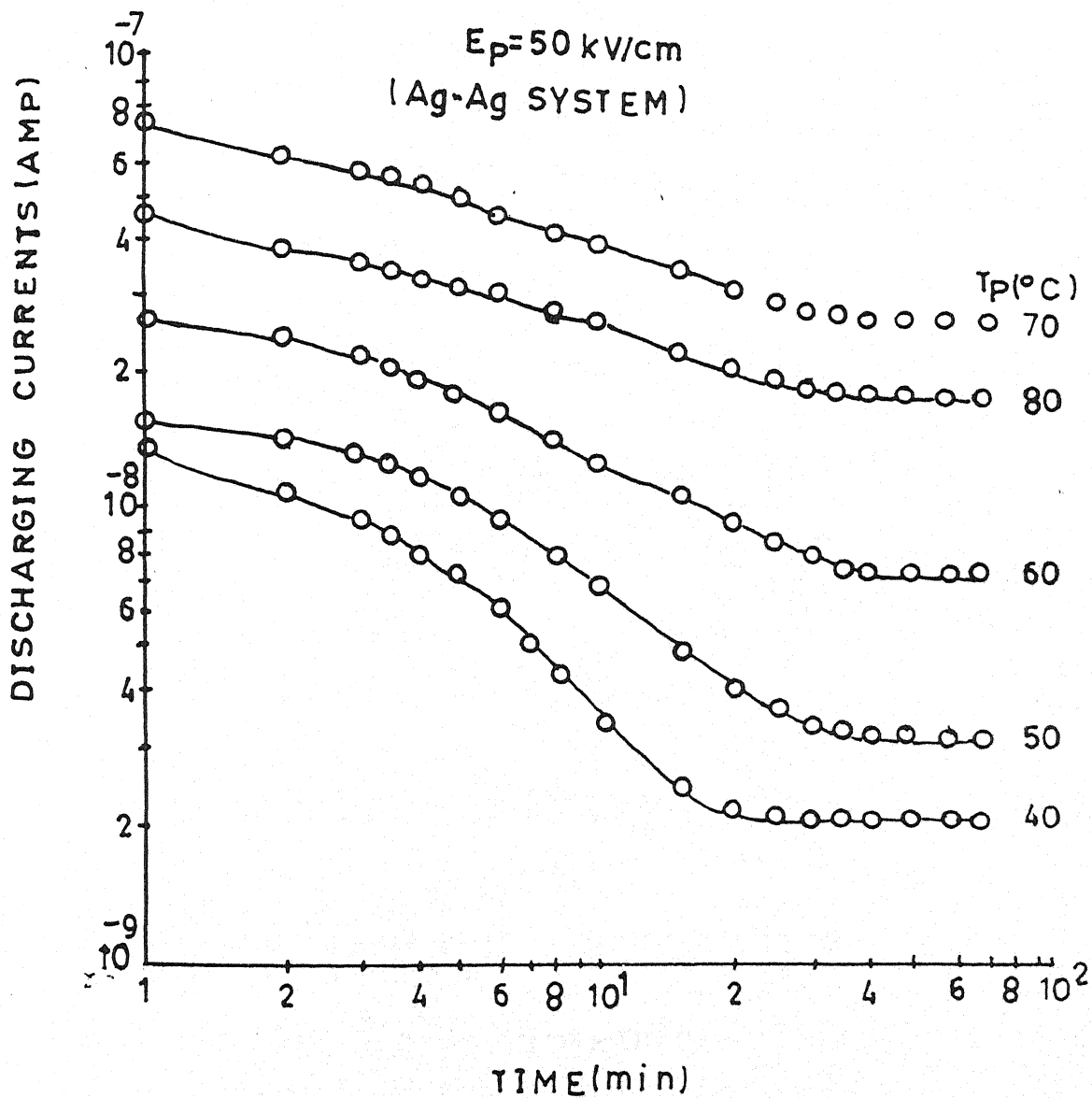


Fig. 5.13

Transient currents in Discharging mode for polyvinylidene fluoride sample ($20 \mu\text{m}$) poled with polarization field 50 kV/cm with different polarization temperature i.e. $40, 50, 60, 70$ and 80°C for Ag-Ag Electrode system.

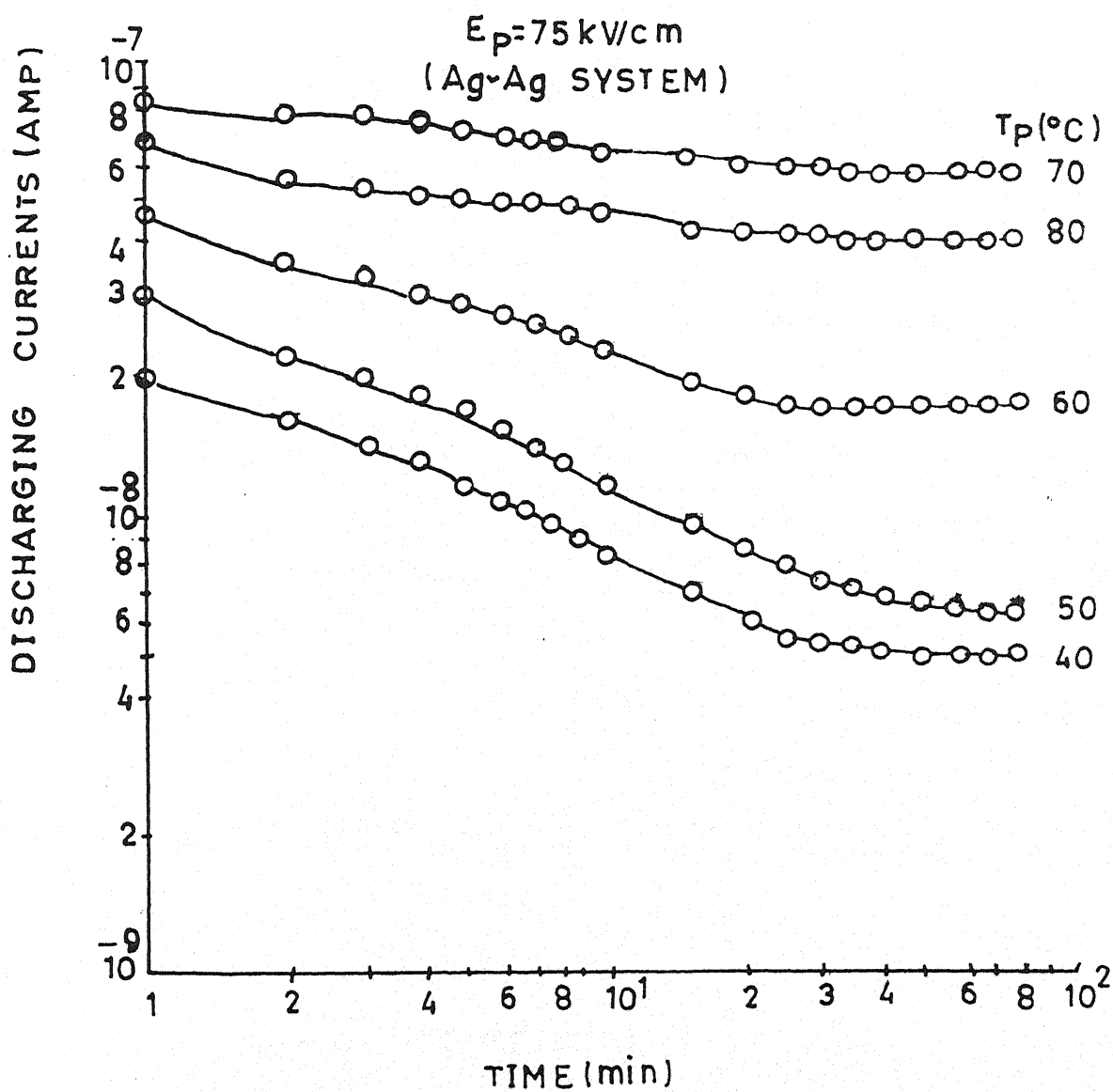


Fig. 5.14

Transient currents in Discharging mode for polyvinylidene fluoride sample ($20 \mu\text{m}$) poled with polarization field 75 kV/cm with different polarization temperature i.e. 40 , 50 , 60 , 70 and 80°C for Ag-Ag Electrode system.

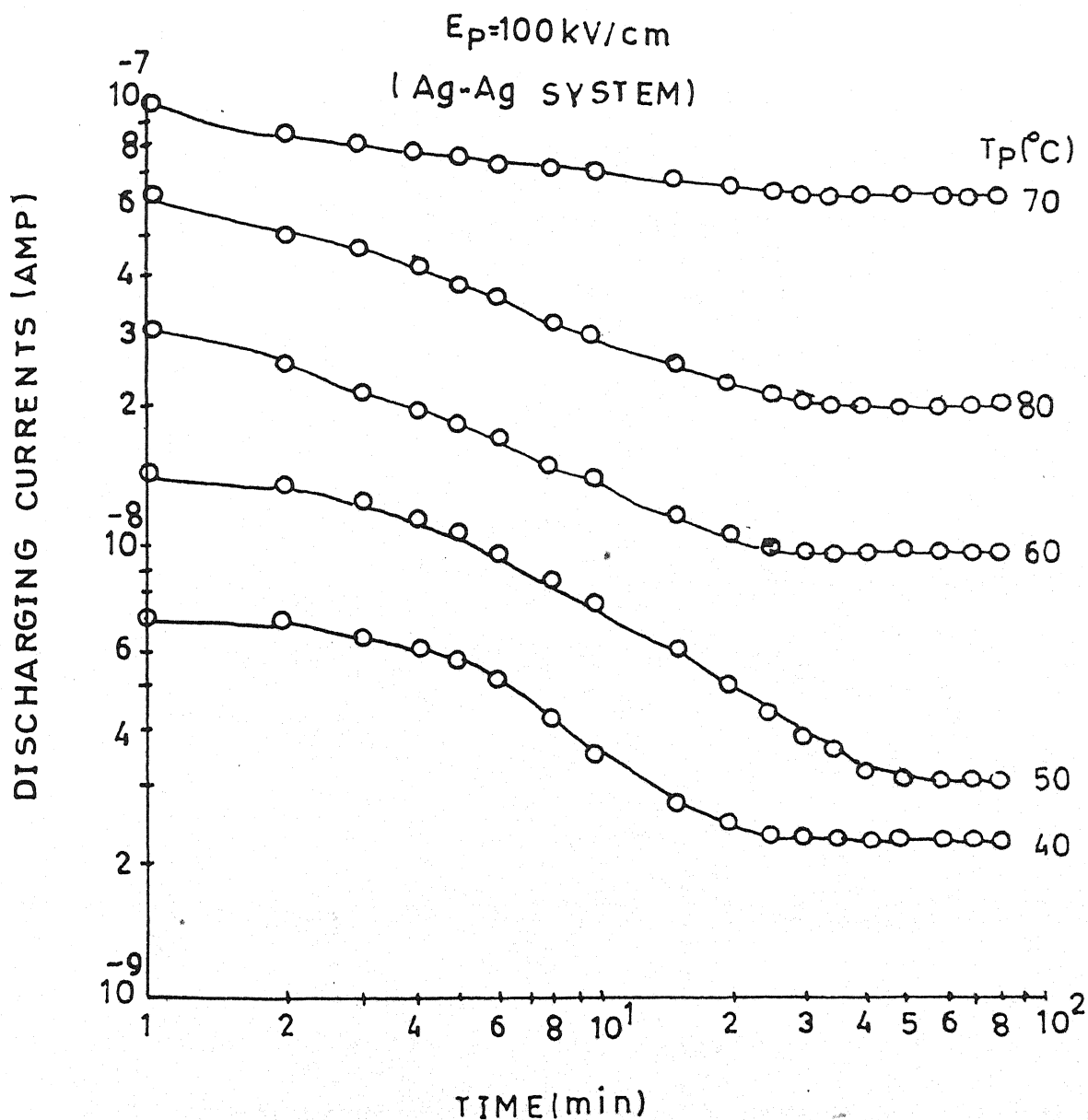


Fig. 5.15

Transient currents in Discharging mode for polyvinylidene fluoride sample ($20 \mu\text{m}$) poled with polarization field 100 kV/cm with different polarization temperature i.e. 40 , 50 , 60 , 70 and 80°C for Ag-Ag Electrode system.

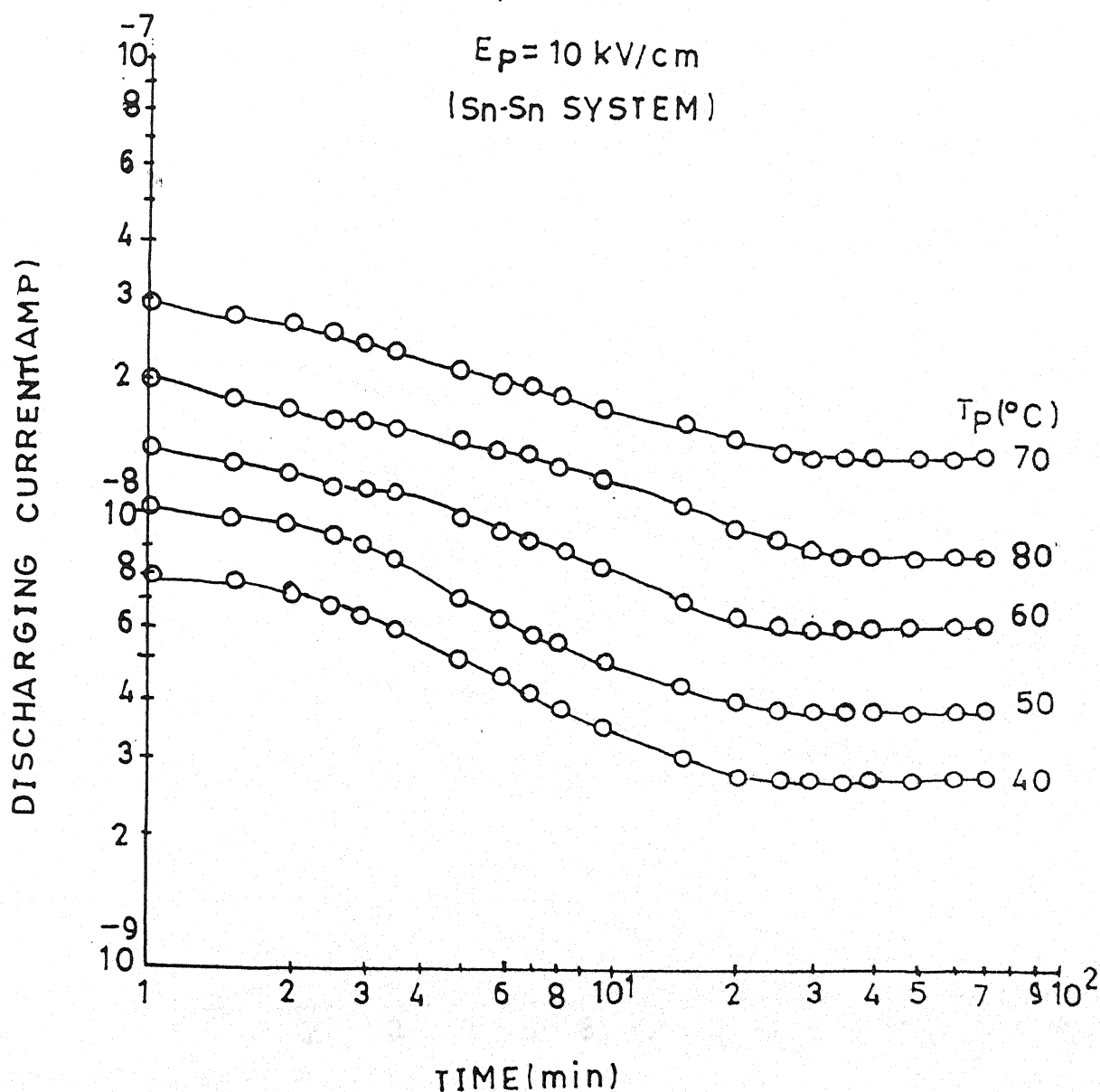


Fig. 5.16

Transient currents in Discharging mode for polyvinylidene fluoride sample ($20 \mu\text{m}$) poled with polarization field 10 kV/cm with different polarization temperature i.e. 40 , 50 , 60 , 70 and 80°C for Sn-Sn Electrode system.

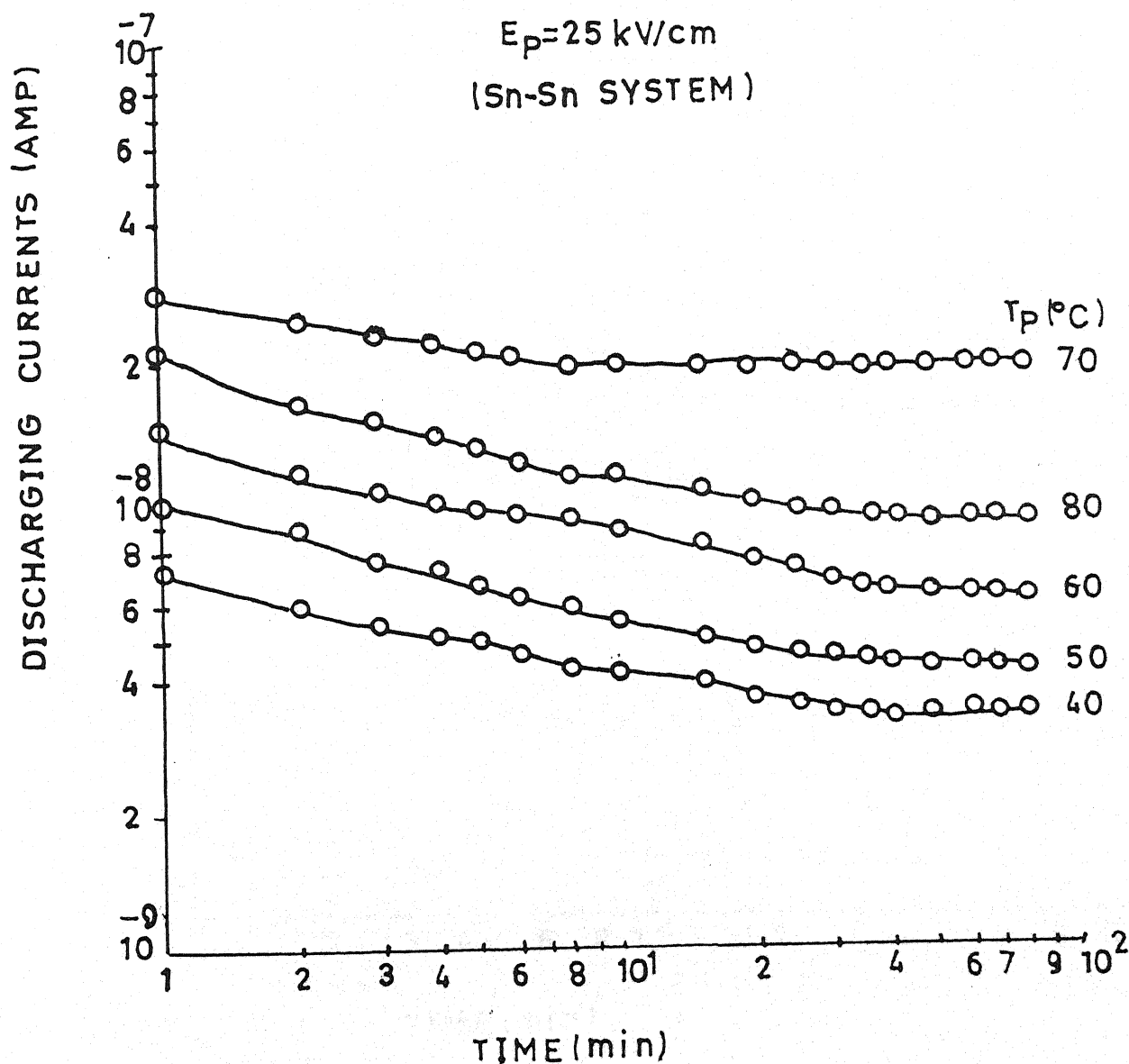


Fig. 5.17

Transient currents in Discharging mode for polyvinylidene fluoride sample ($20 \mu\text{m}$) poled with polarization field 25 kV/cm with different polarization temperature i.e. $40, 50$

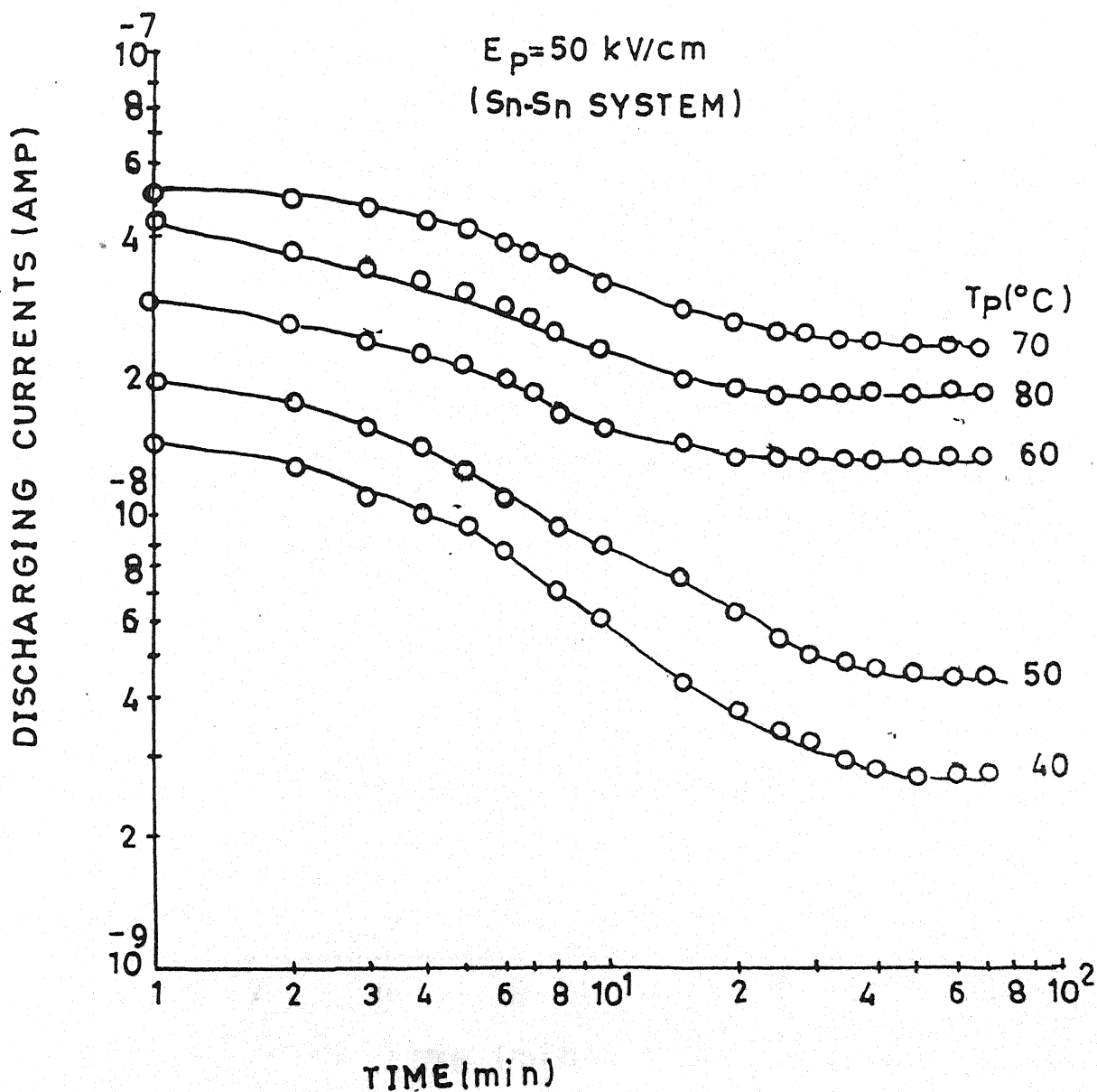


Fig. 5.18

Transient currents in Discharging mode for polyvinylidene fluoride sample (20 μm) poled with polarization field 50 kV/cm with different polarization temperature i.e. 40, 50, 60, 70 and 80°C for Sn-Sn Electrode system.

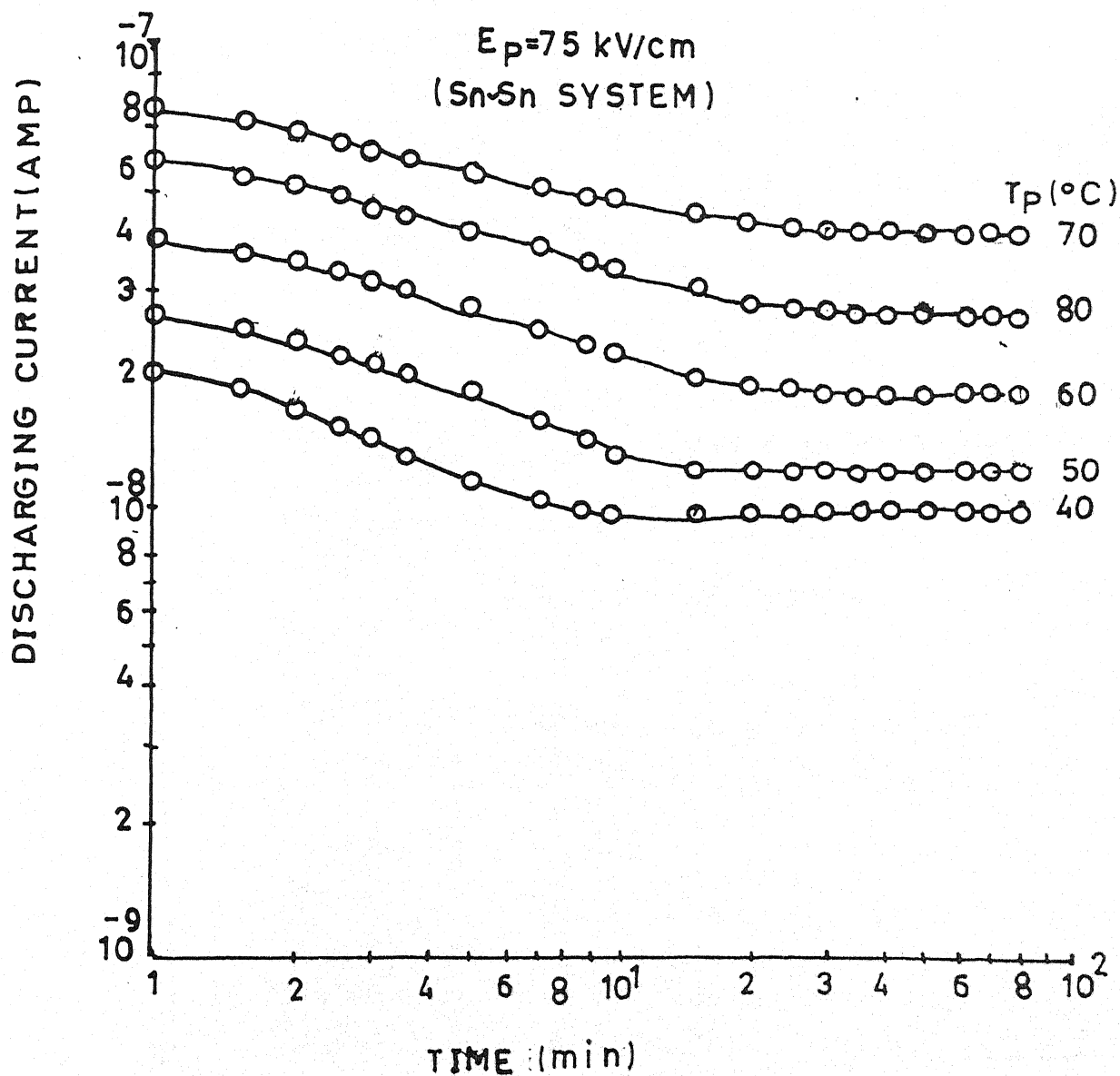


Fig. 5.19
Transient currents in Discharging mode for polyvinylidene fluoride sample ($20 \mu\text{m}$) poled with polarization field 75 kV/cm with different polarization temperature i.e. 40, 50, 60, 70 and 80°C for Sn-Sn Electrode system.

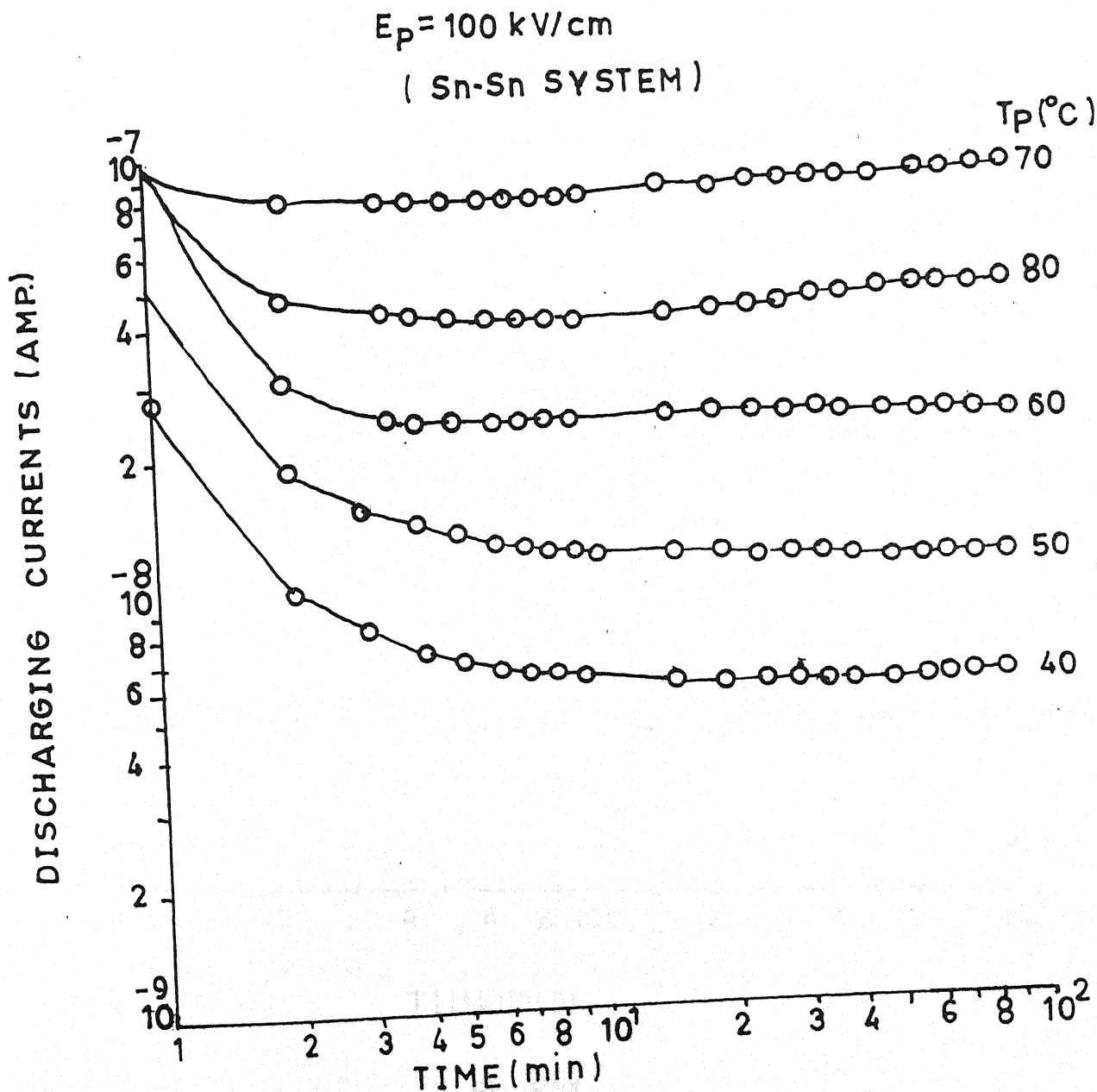


Fig. 5.20

Transient currents in Discharging mode for polyvinylidene fluoride sample ($20 \mu\text{m}$) poled with polarization field 100 kV/cm with different polarization temperature i.e. 40, 50, 60, 70 and 80°C for Sn-Sn Electrode system.

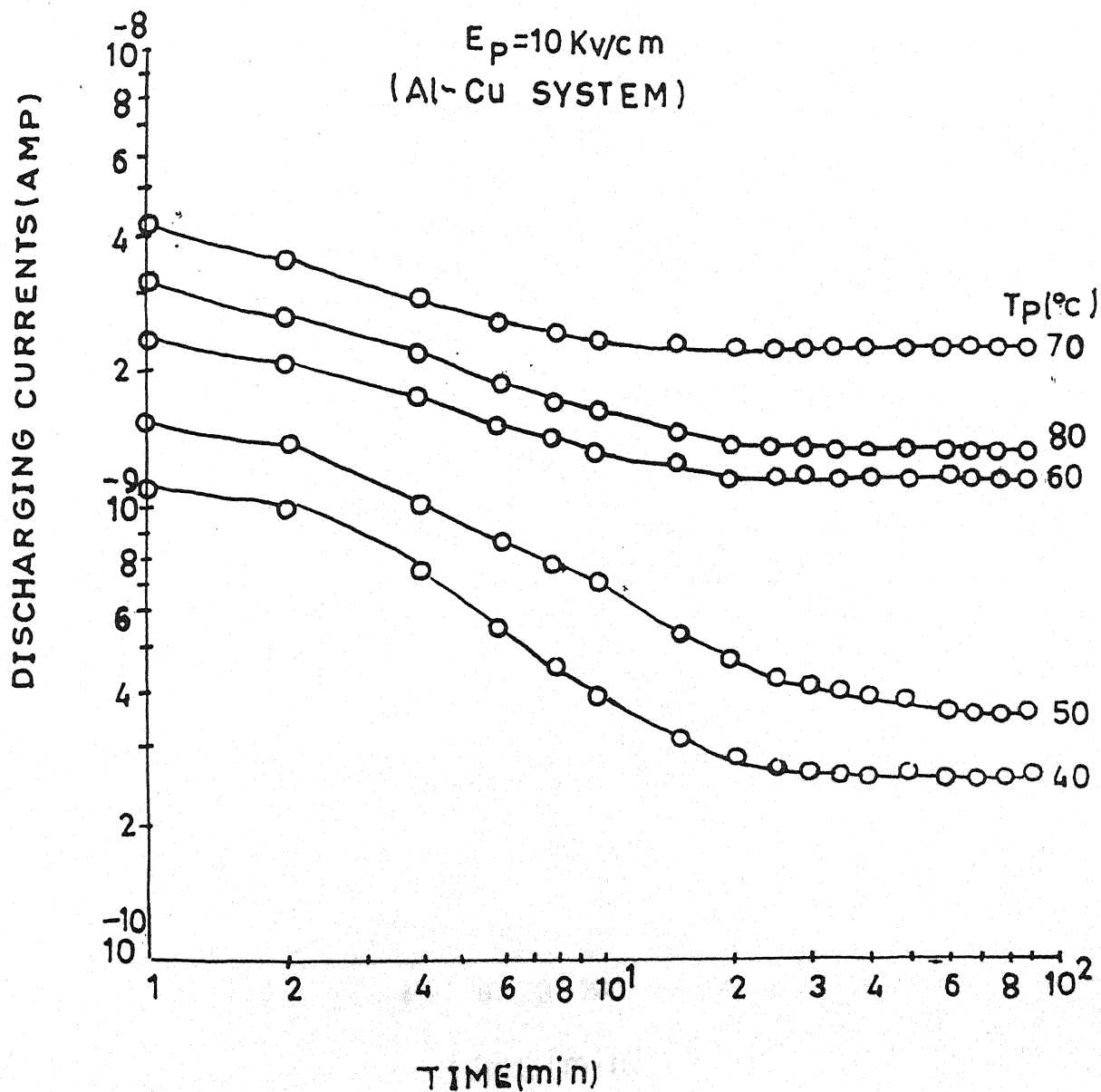


Fig. 5.21

Transient currents in Discharging mode for polyvinylidene fluoride sample ($20 \mu\text{m}$) poled with polarization field 10 kV/cm with different polarization temperature i.e. 40 , 50 , 60 , 70 and 80°C for Al-Cu Electrode system.

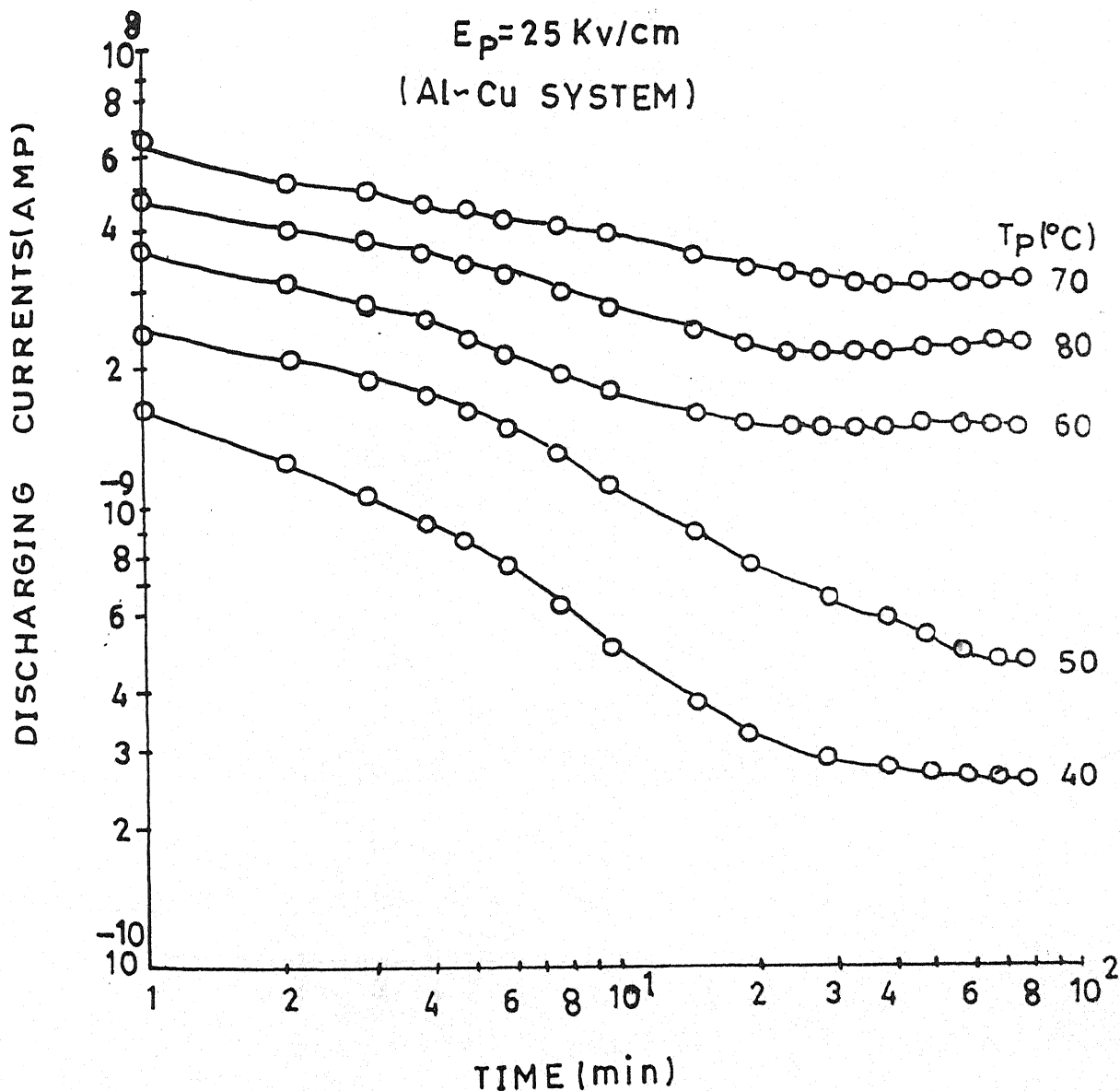


Fig. 5.2.2

Transient currents in Discharging mode for polyvinylidene fluoride sample ($20 \mu\text{m}$) poled with polarization field 25 kV/cm with different polarization temperature i.e. 40 , 50 , 60 , 70 and 80°C for Al-Cu Electrode system.

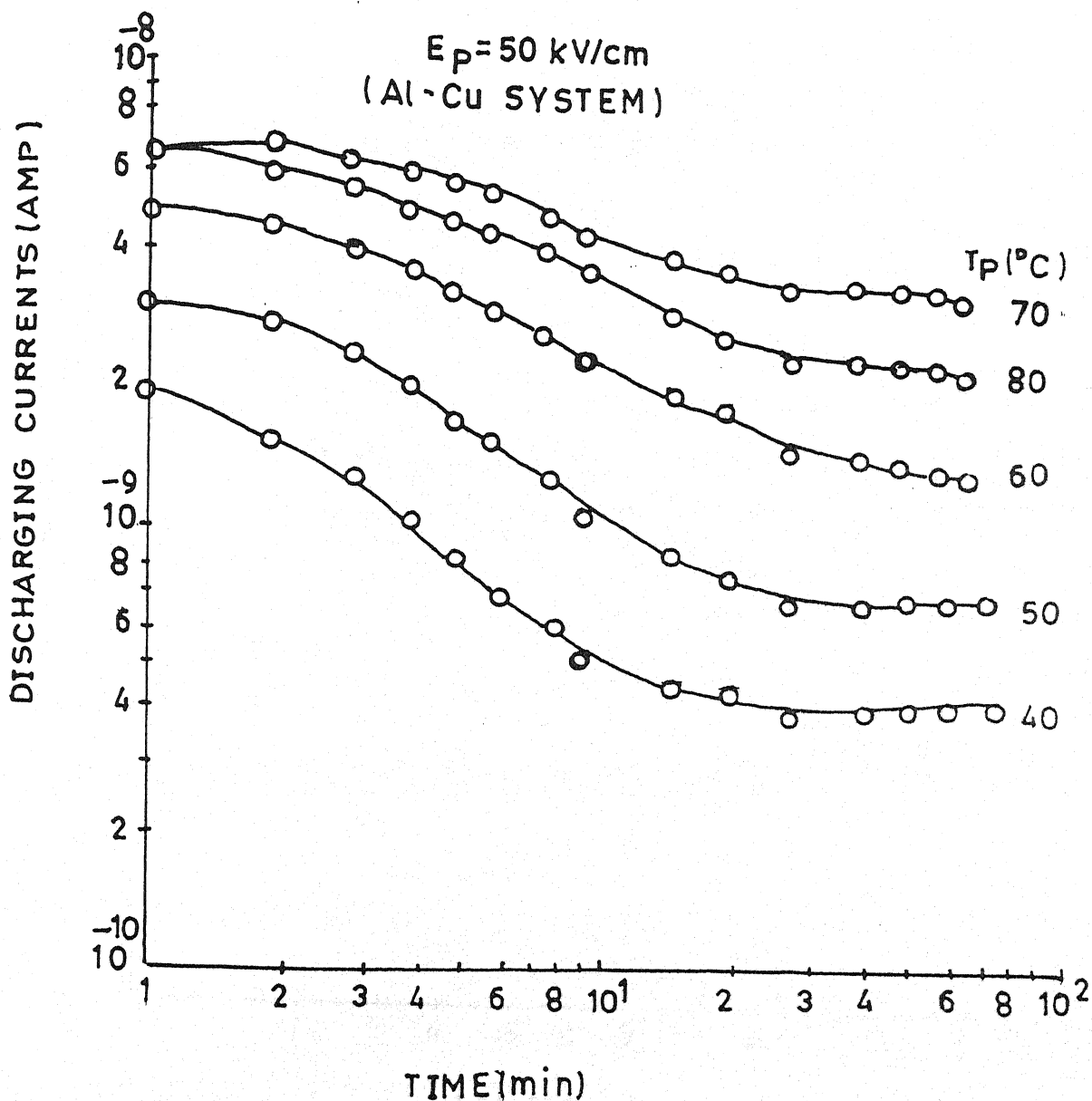


Fig. 5.23

Transient currents in Discharging mode for polyvinylidene fluoride sample ($20 \mu\text{m}$) poled with polarization field 50 kV/cm with different polarization temperature i.e. $40, 50, 60, 70$ and 80°C for Al-Cu Electrode system.

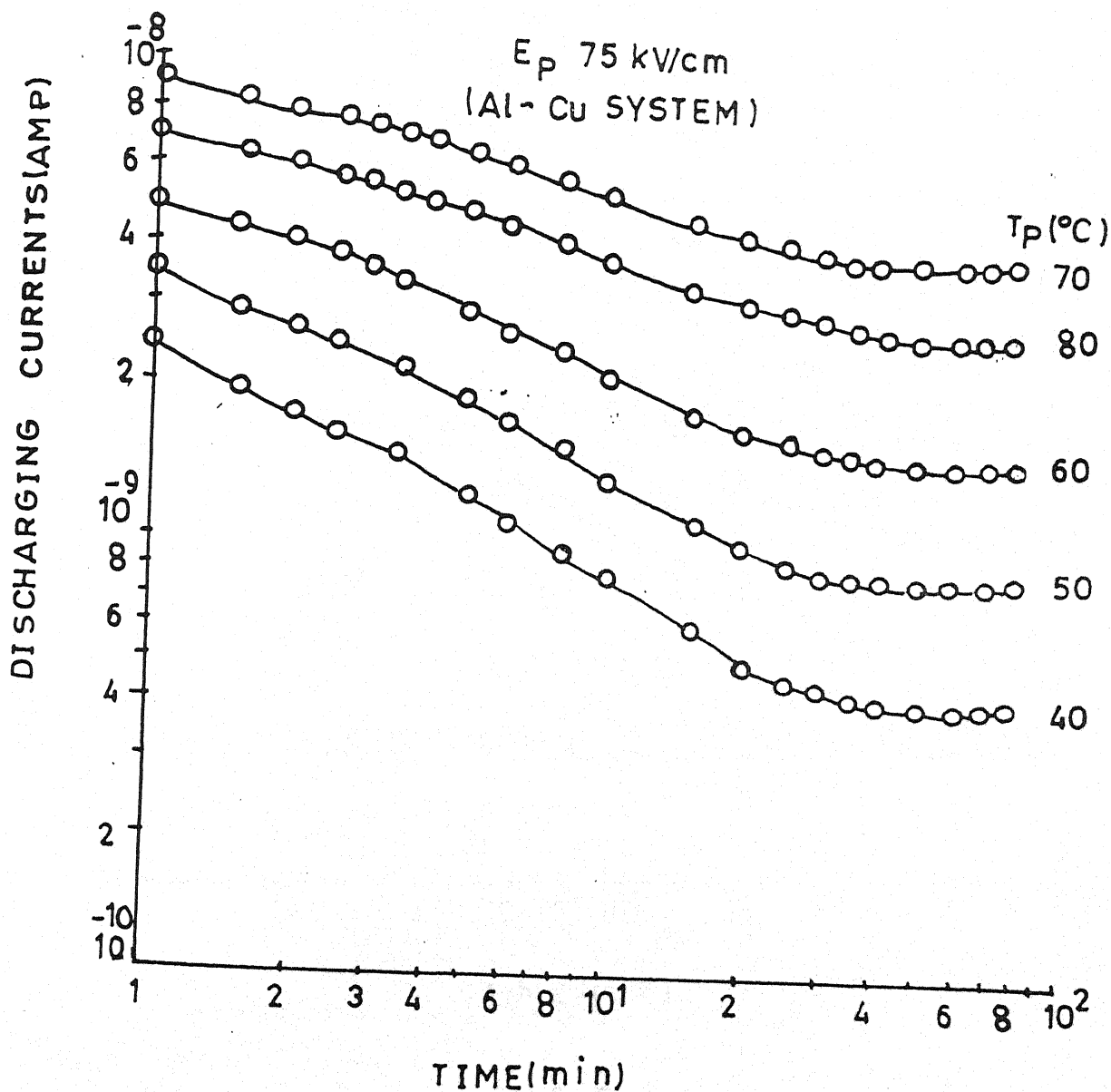


Fig. 5.24
 Transient currents in Discharging mode for polyvinylidene fluoride sample (20 μm)
 poled with polarization field 75 kV/cm with different polarization temperature i.e. 40 , 50
 , 60 , 70 and 80°C.

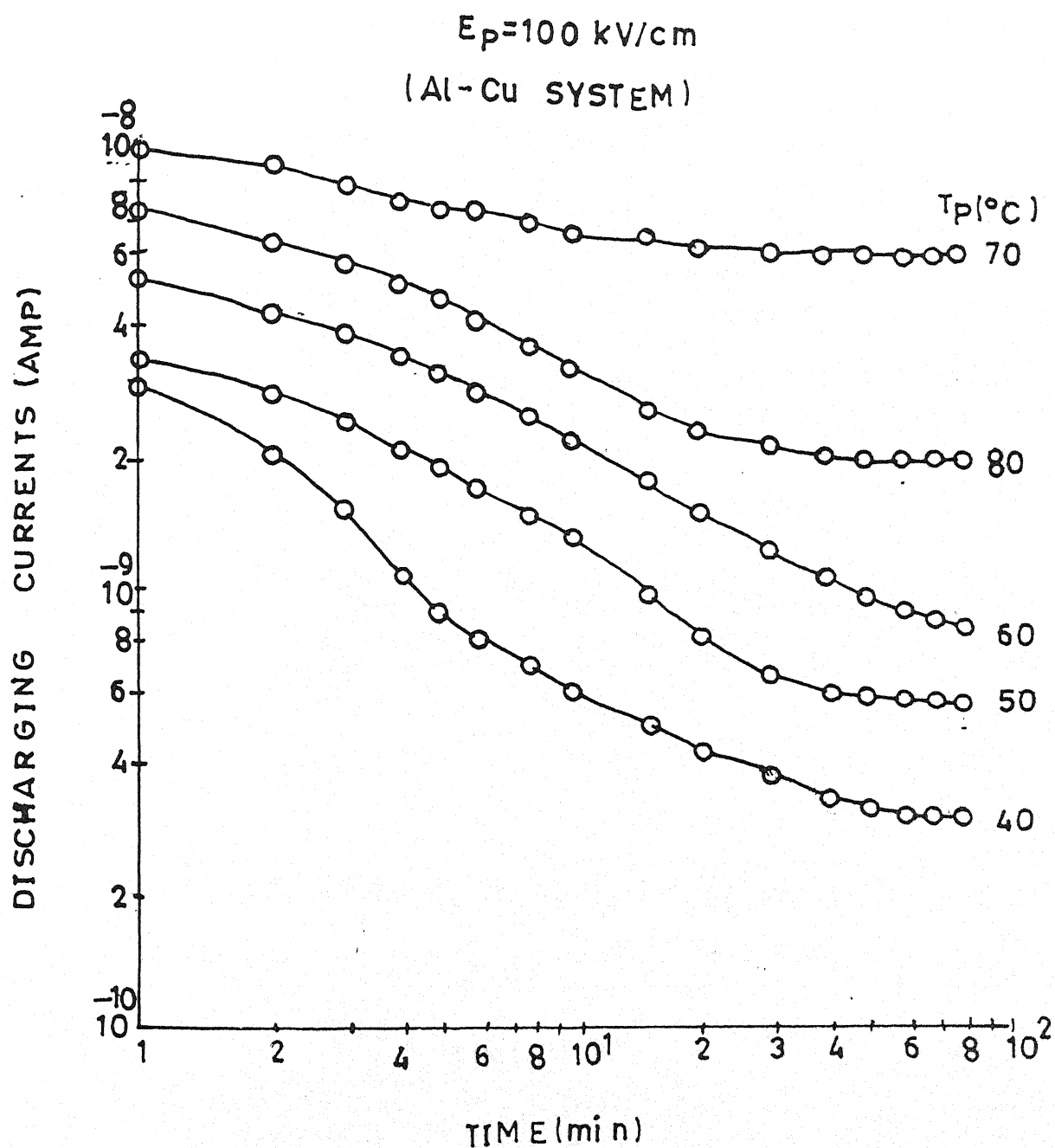


Fig. 5.25
Transient currents in Discharging mode for polyvinylidene fluoride sample ($20 \mu\text{m}$) poled with polarization field 100 kV/cm with different polarization temperature i.e. 40°C , 50°C , 60°C , 70°C and 80°C for Al-Cu Electrode system.

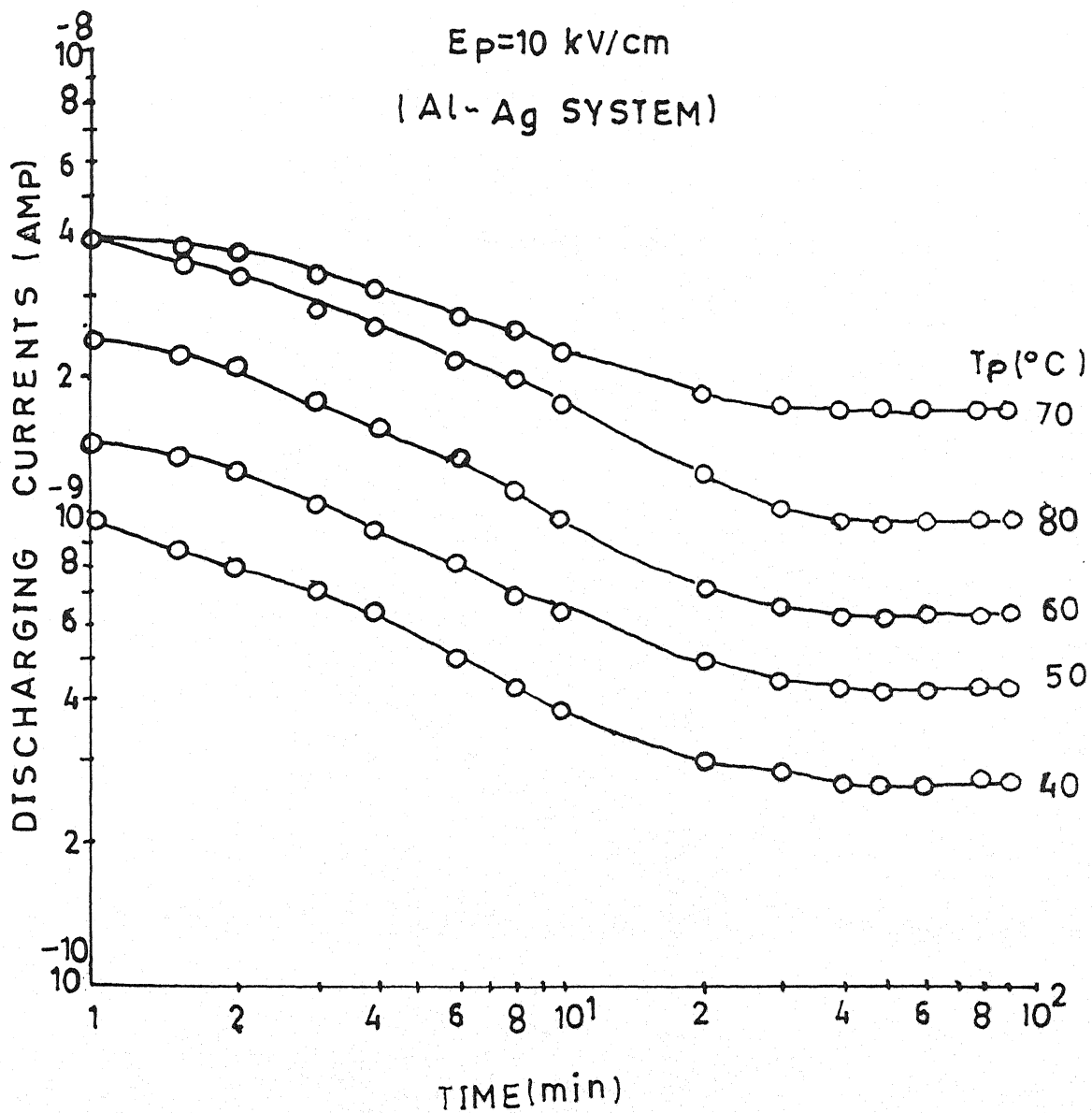


Fig. 5.26

Transient currents in Discharging mode for polyvinylidene fluoride sample ($20 \mu\text{m}$) poled with polarization field 10 kV/cm with different polarization temperature i.e. $40, 50, 60, 70$ and 80°C for Al-Ag Electrode system.

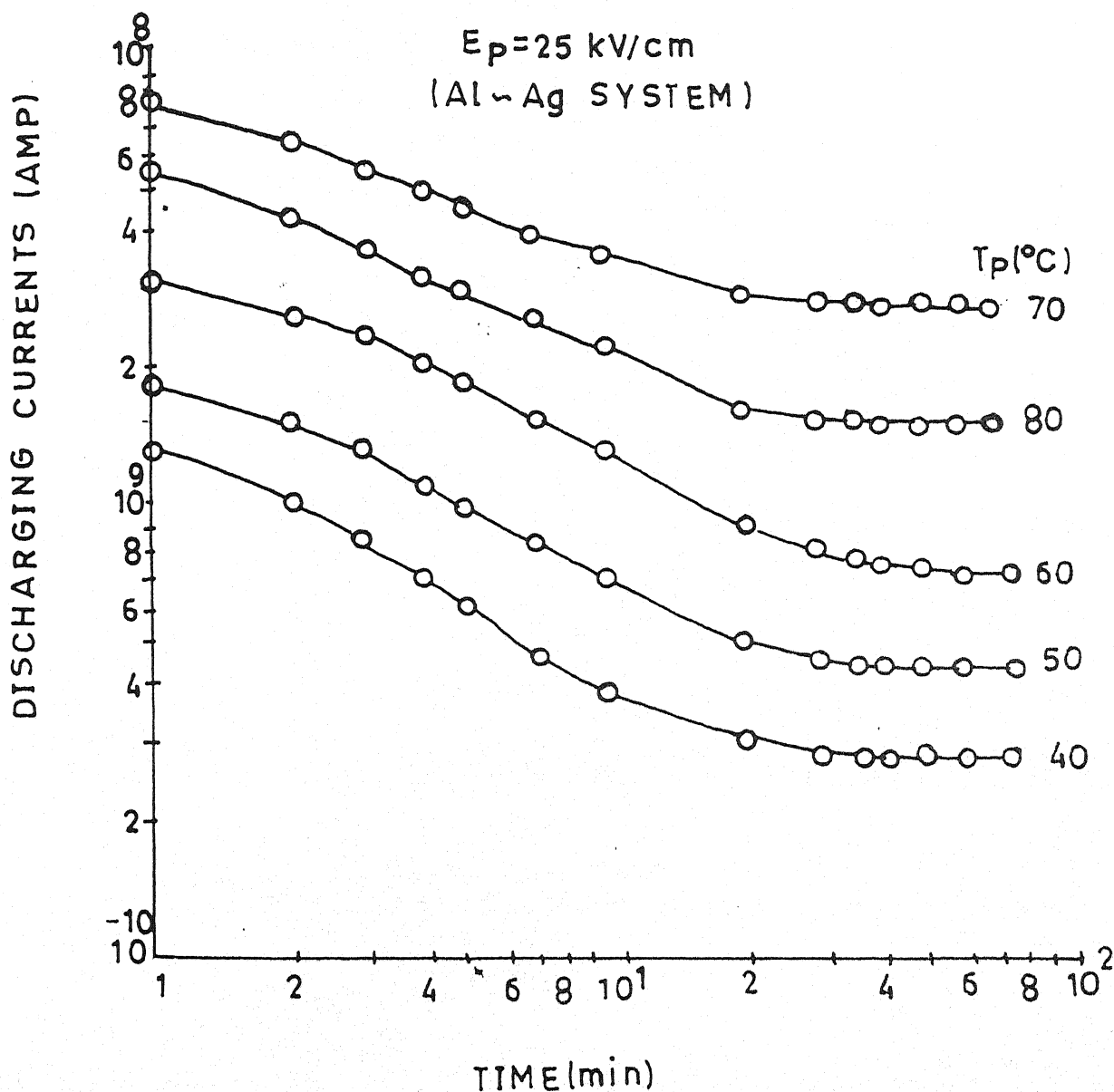


Fig. 5.27

Transient currents in Discharging mode for polyvinylidene fluoride sample ($20 \mu\text{m}$) poled with polarization field 25 kV/cm with different polarization temperature i.e. $40, 50, 60, 70$ and 80°C for Al- Ag Electrode system .

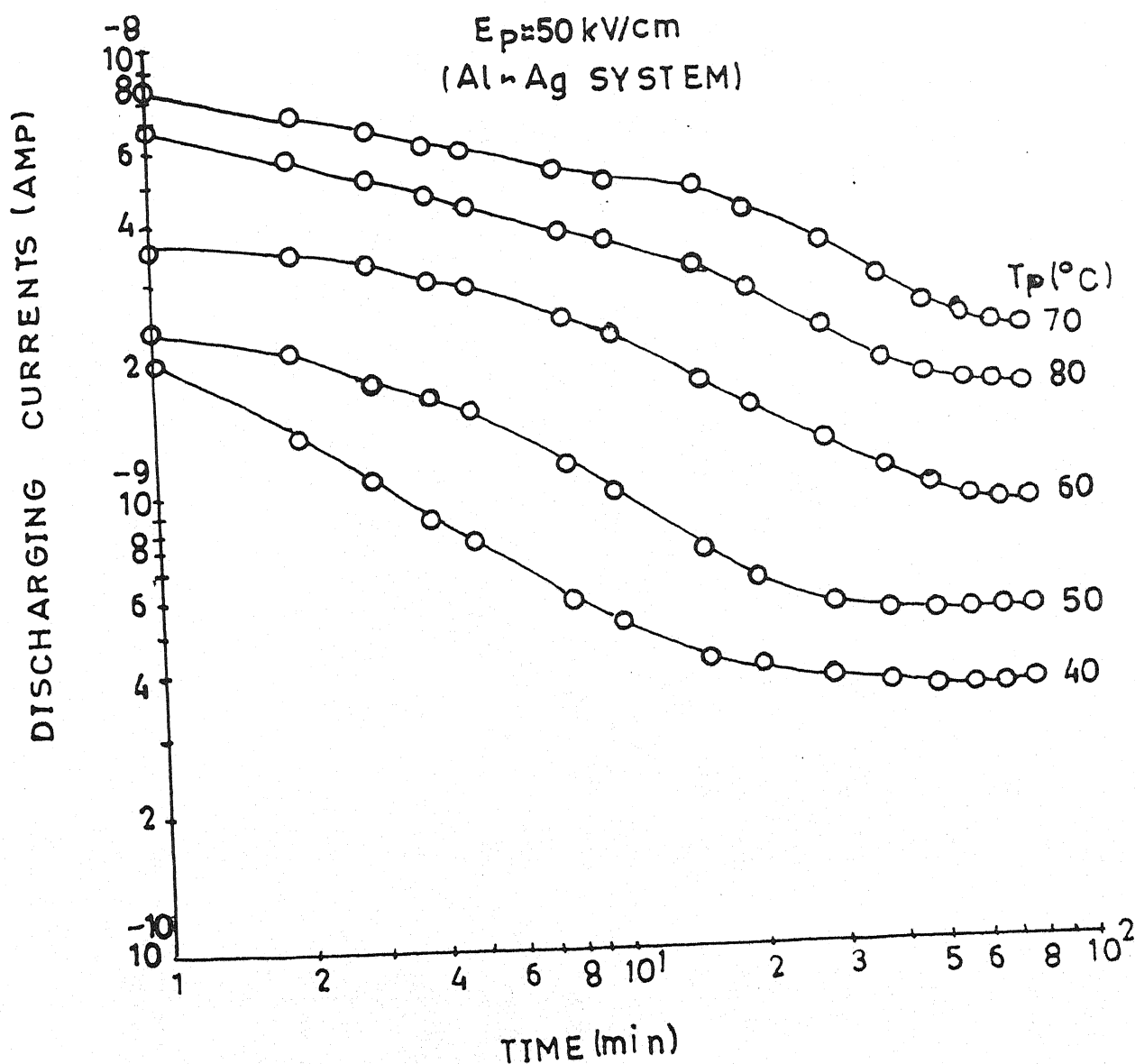


Fig. 5.28
Transient currents in Discharging mode for polyvinylidene fluoride sample ($20 \mu\text{m}$) poled with polarization field 50 kV/cm with different polarization temperature i.e. $40, 50, 60, 70$ and 80°C for Al-Ag Electrode system.

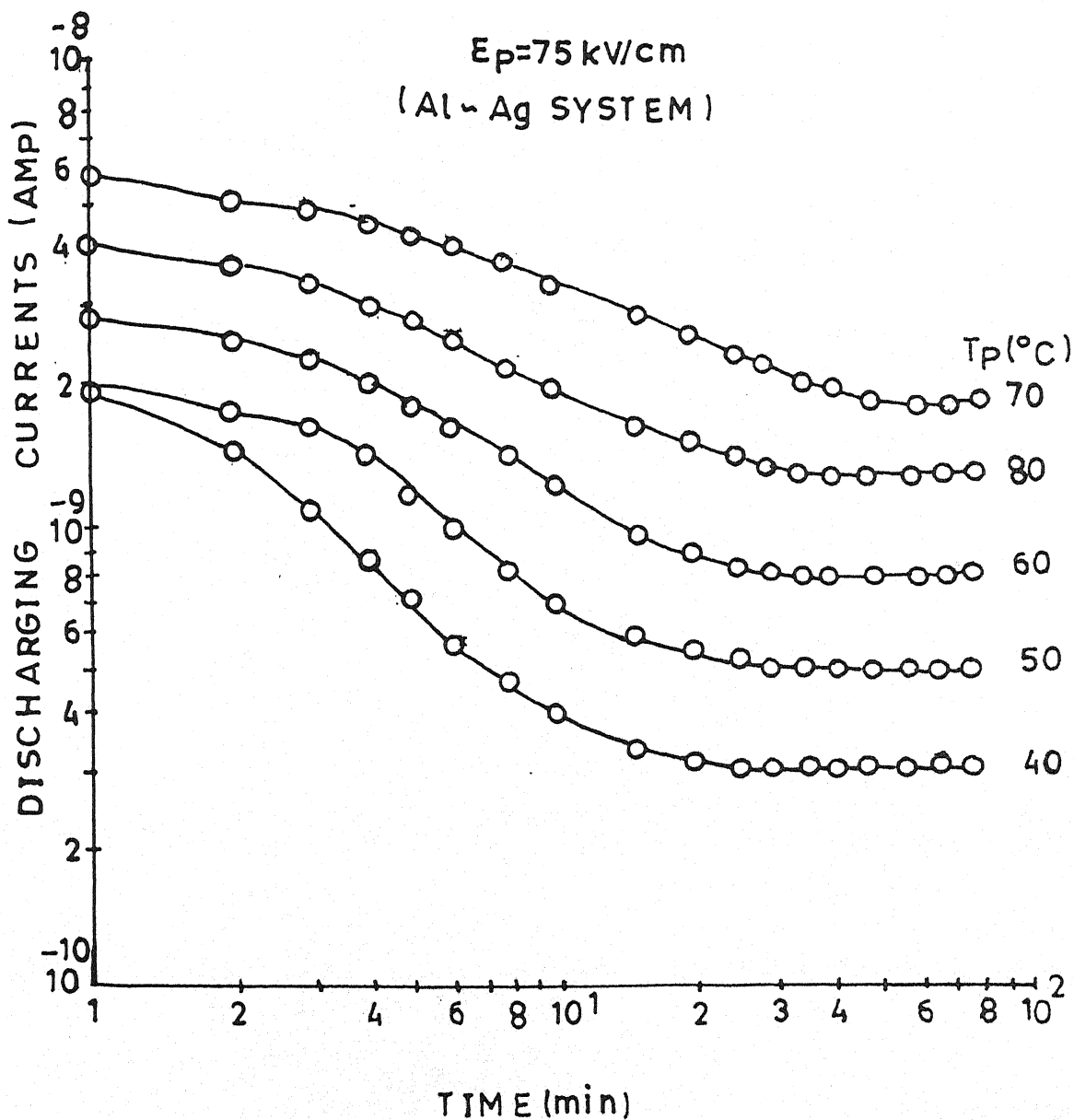


Fig. 5.29

Transient currents in Discharging mode for polyvinylidene fluoride sample ($20 \mu\text{m}$) poled with polarization field 75 kV/cm with different polarization temperature i.e. 40 , 50 , 60 , 70 and 80°C for Al- Ag Electrode system.

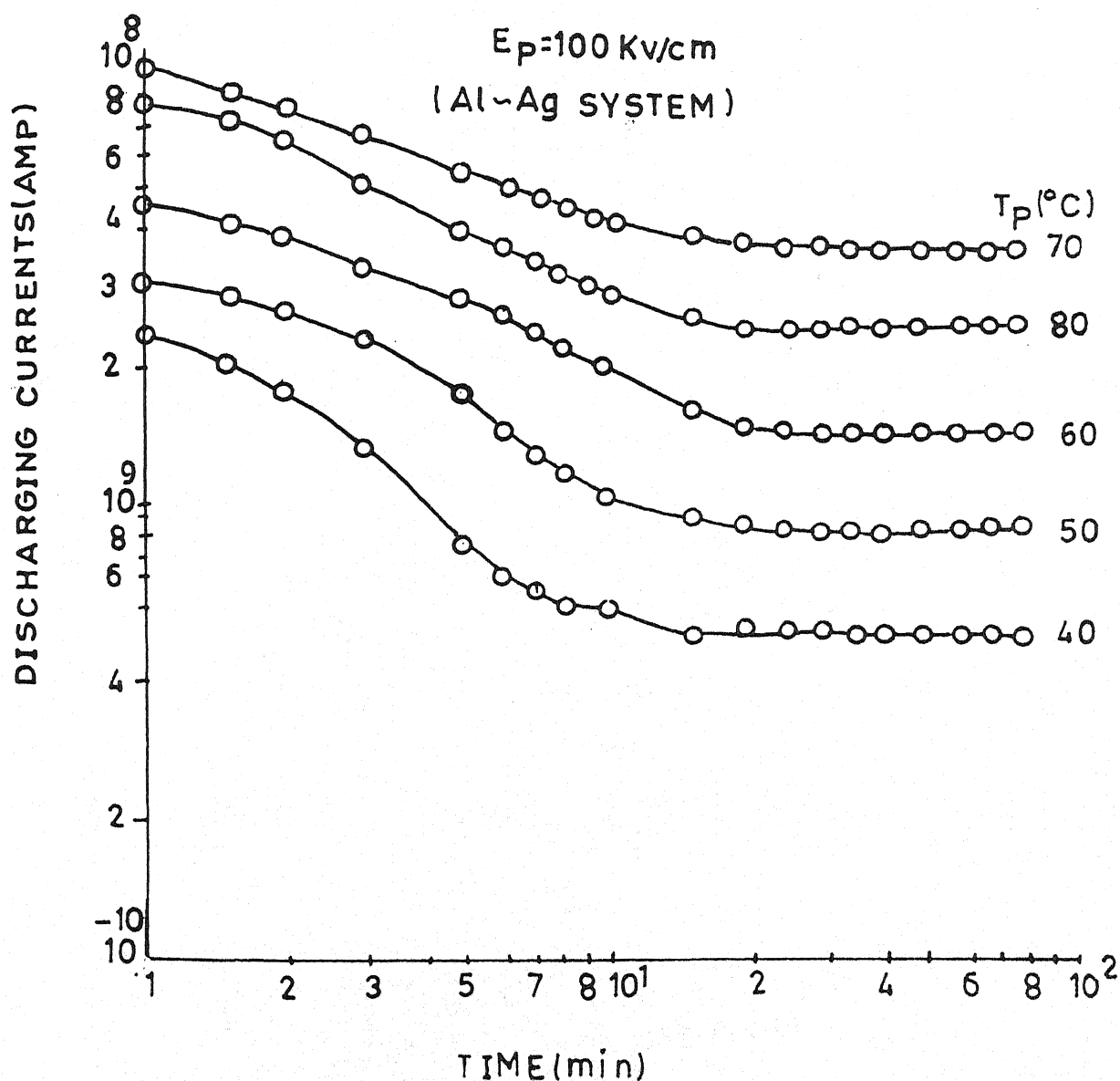


Fig. 5.30

Transient currents in Discharging mode for polyvinylidene fluoride sample ($20 \mu\text{m}$) poled with polarization field 100 kV/cm with different polarization temperature i.e. 40 , 50 , 60 , 70 and 80°C for Al- Ag Electrode system .

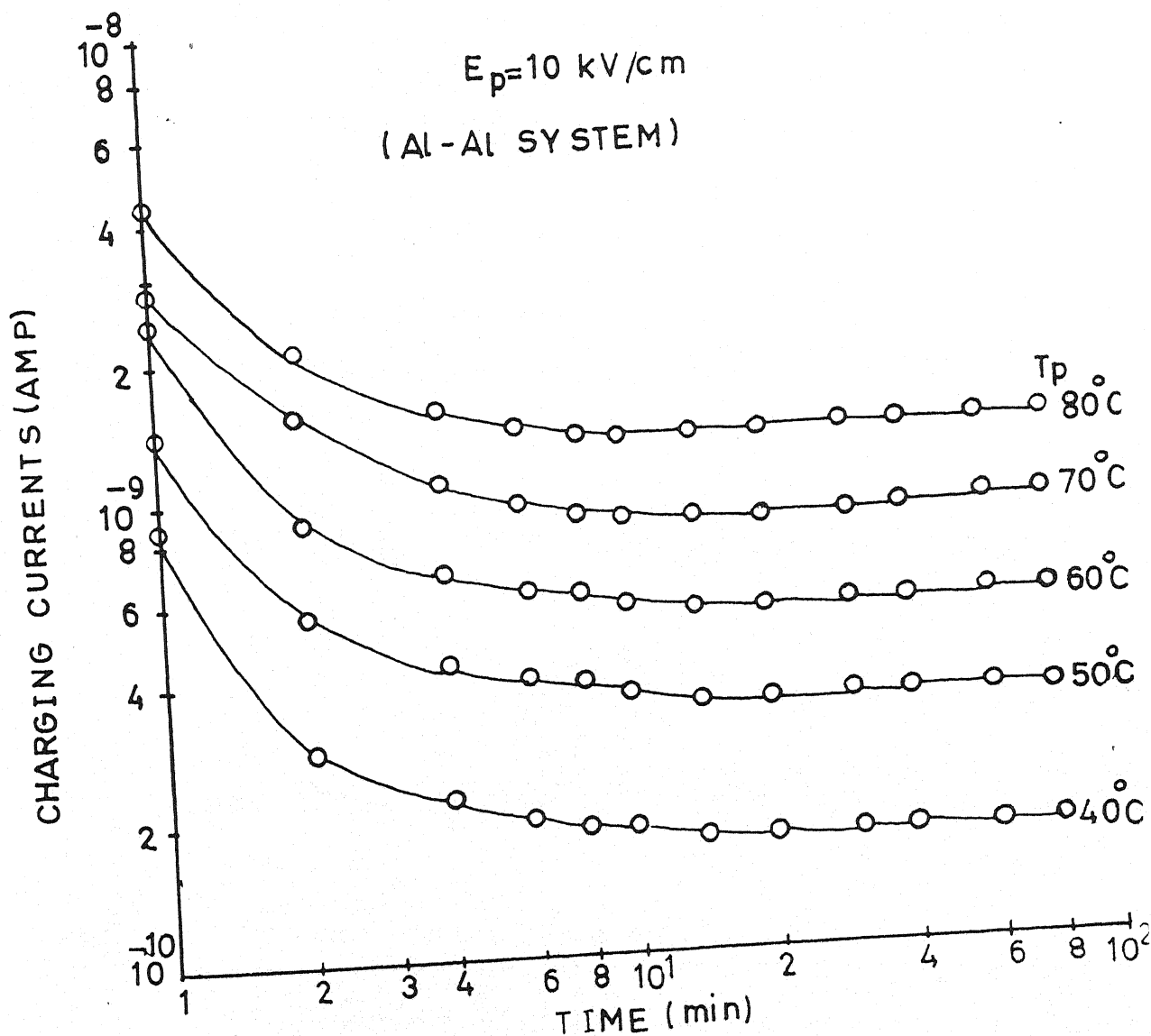


Fig. 5.31
Transient currents in Charging mode for polyvinylidene fluoride sample (20 μm) poled with polarization field 10 kV/cm with different polarization temperature i.e. 40, 50, 60, 70 and 80°C for Al-Al Electrode system.

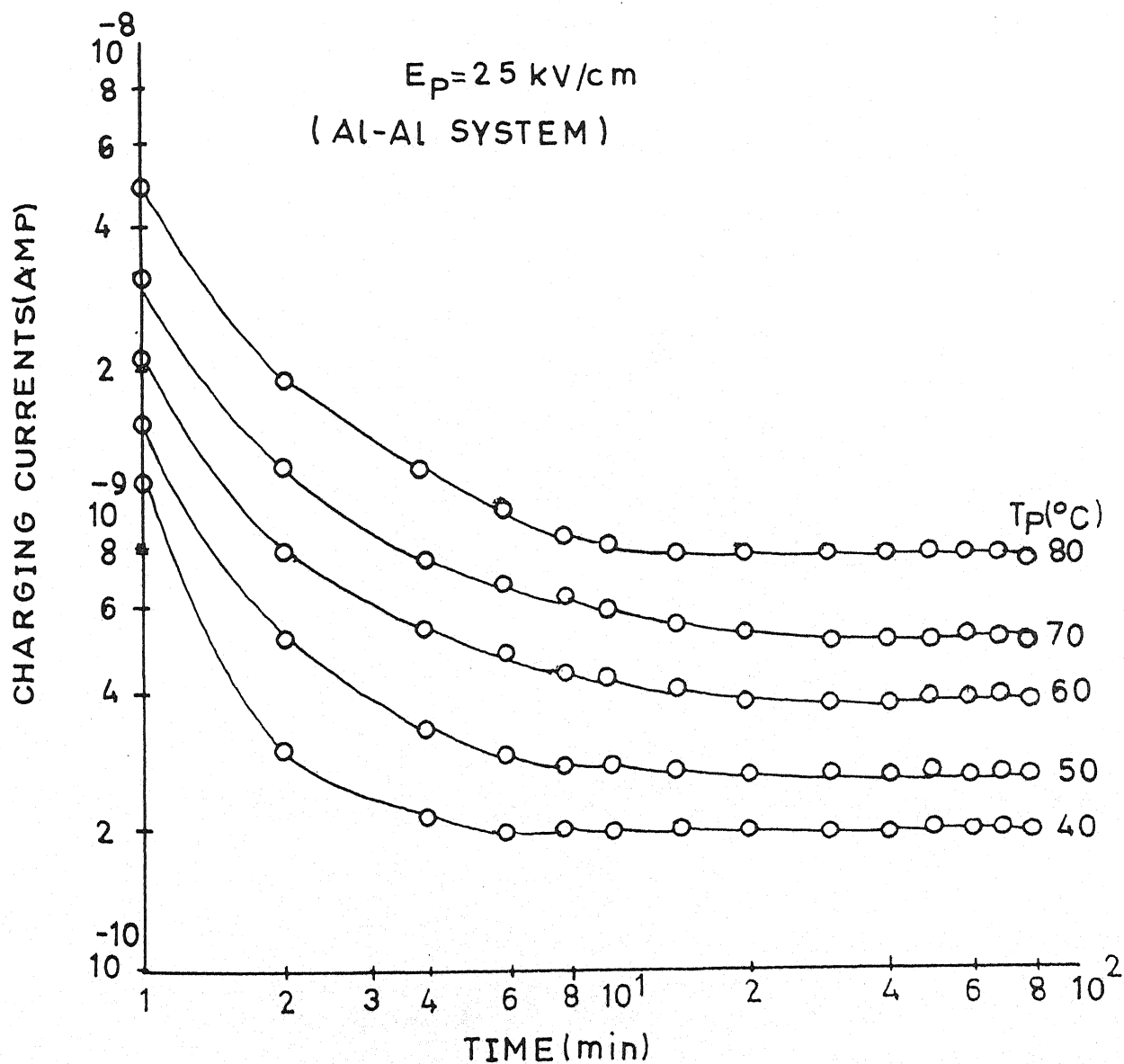


Fig. 5.32

Transient currents in Charging mode for polyvinylidene fluoride sample ($20 \mu\text{m}$) poled with polarization field 25 kV/cm with different polarization temperature i.e. 40 , 50 , 60 , 70 and 80°C for Al- Al Electrode system .

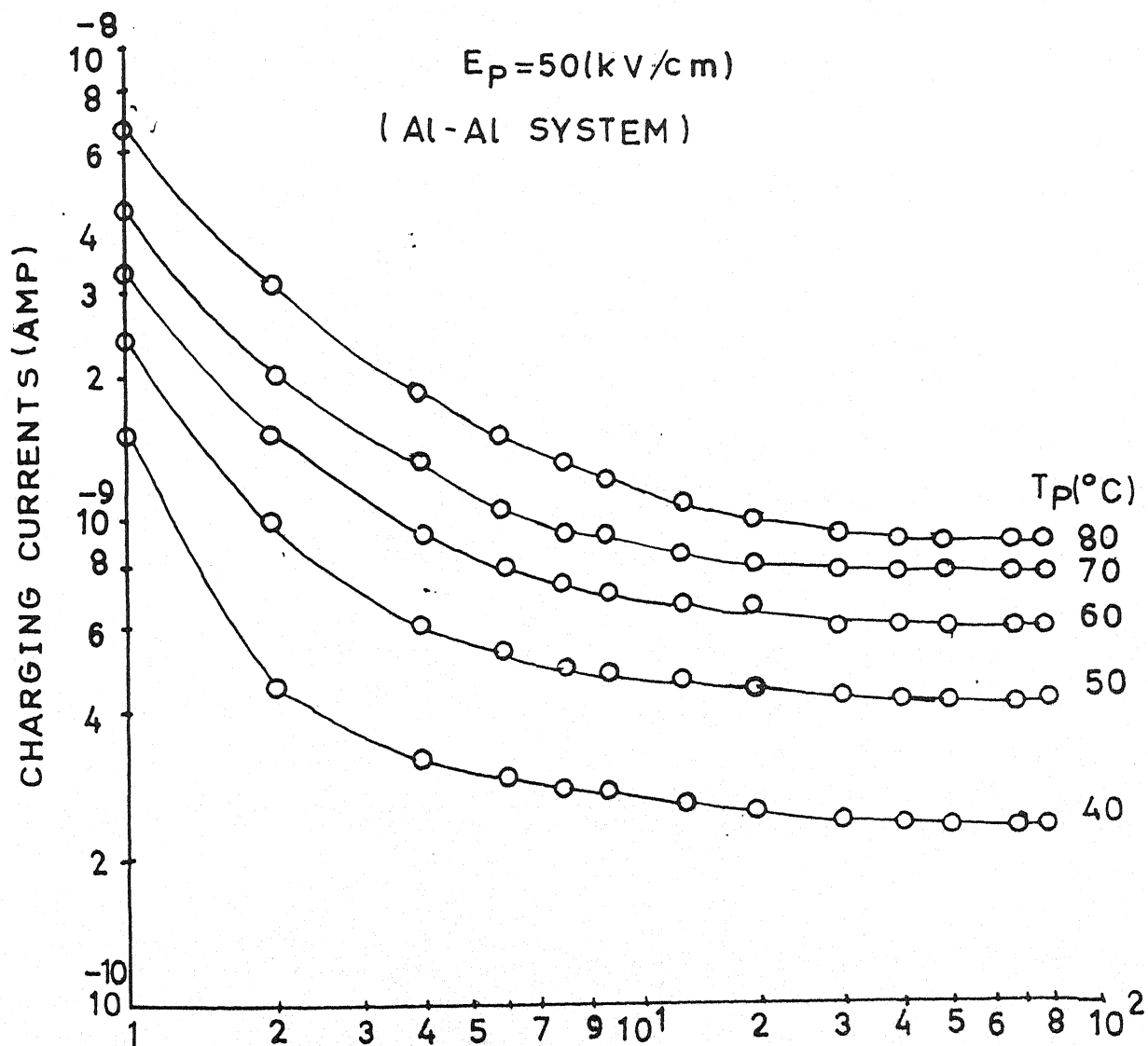


Fig. 5.33

Transient currents in Charging mode for polyvinylidene fluoride sample ($20 \mu\text{m}$) poled with polarization field 50 kV/cm with different polarization temperature i.e. $40, 50, 60, 70$ and 80°C for Al-Al Electrode system.

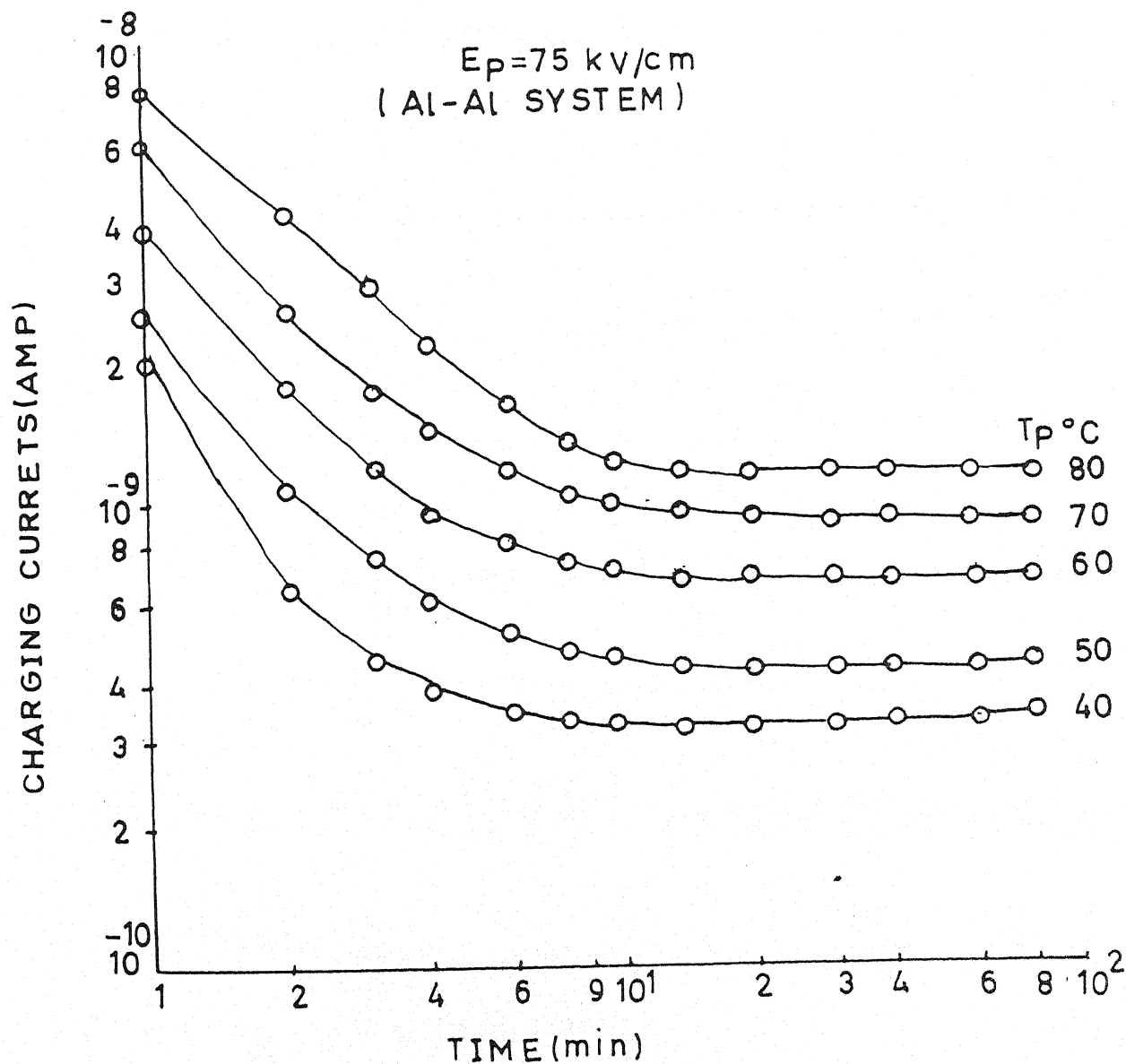


Fig. 5.34

Transient currents in Charging mode for polyvinylidene fluoride sample ($20 \mu\text{m}$) poled with polarization field 75 kV/cm with different polarization temperature i.e. 40 , 50 , 60 , 70 and 80°C for Al-Al Electrode system.

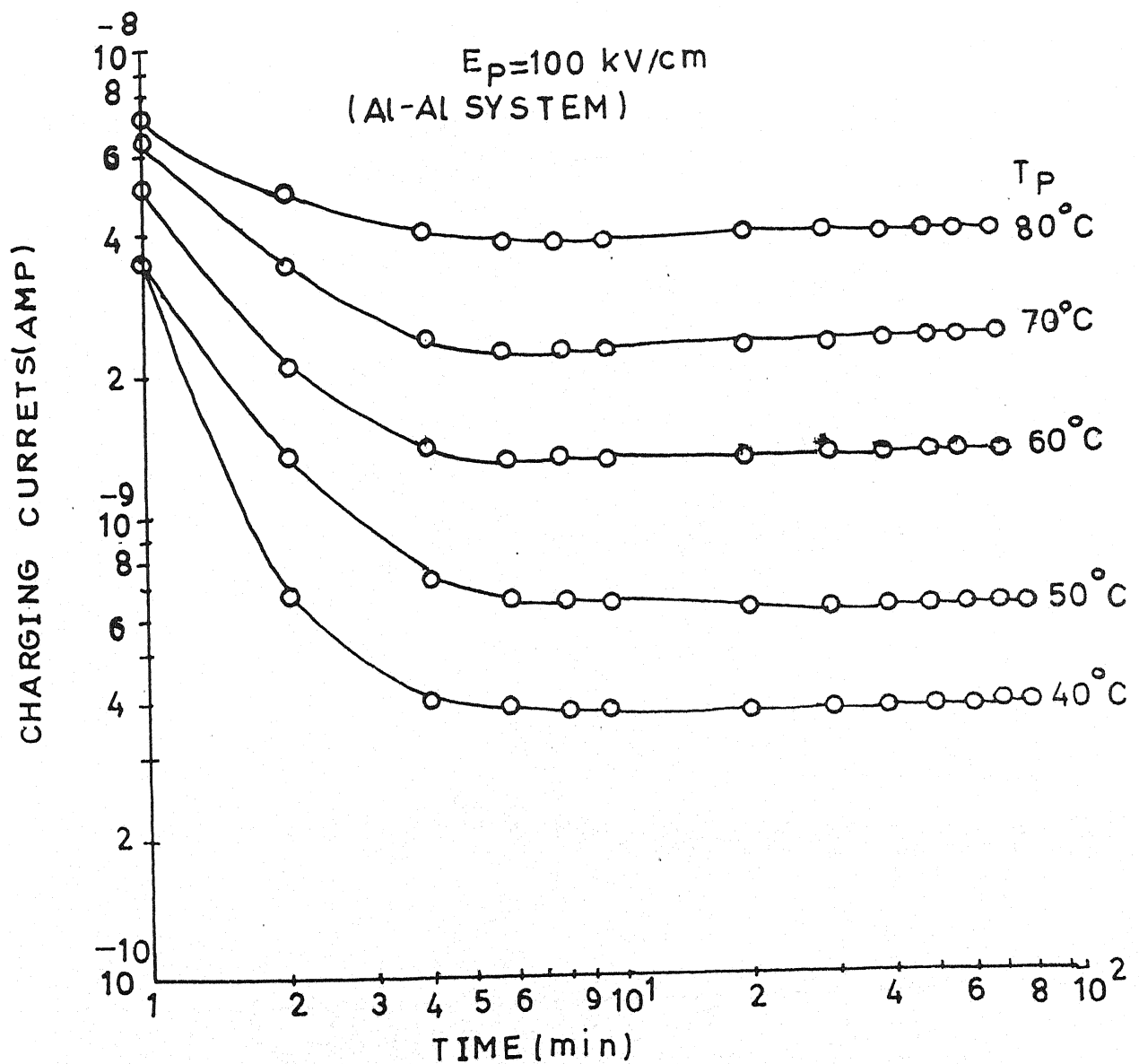


Fig. 5.35
Transient currents in Charging mode for polyvinylidene fluoride sample ($20 \mu\text{m}$) poled with polarization field 100 kV/cm with different polarization temperature i.e. 40°C , 50°C , 60°C , 70°C and 80°C for Al-Al Electrode system.

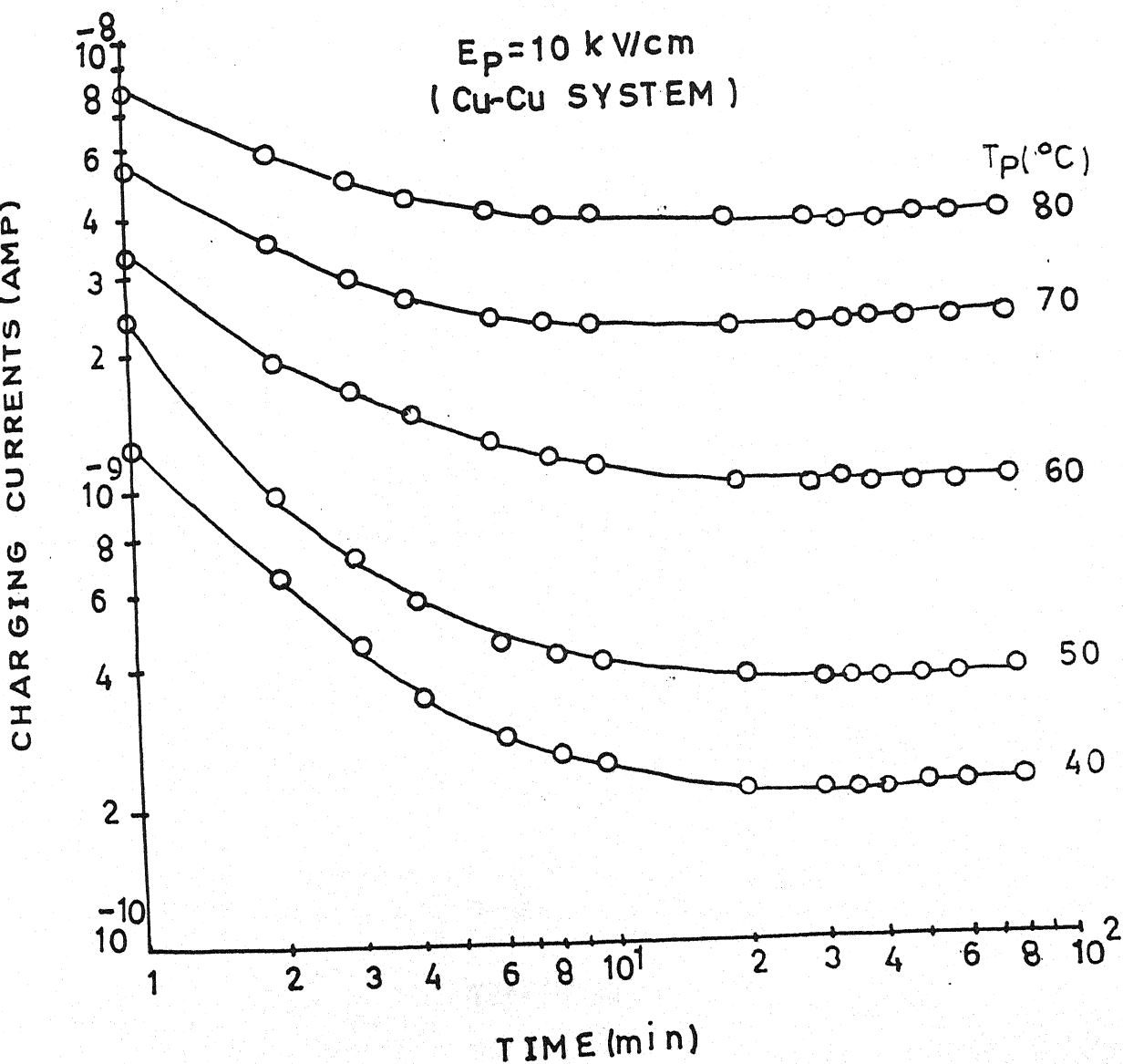


Fig. 5.36.

Transient currents in Charging mode for polyvinylidene fluoride sample ($20 \mu\text{m}$) poled with polarization field 10 kV/cm with different polarization temperature i.e. 40 , 50 , 60 , 70 and 80°C for Cu- Cu Electrode system.

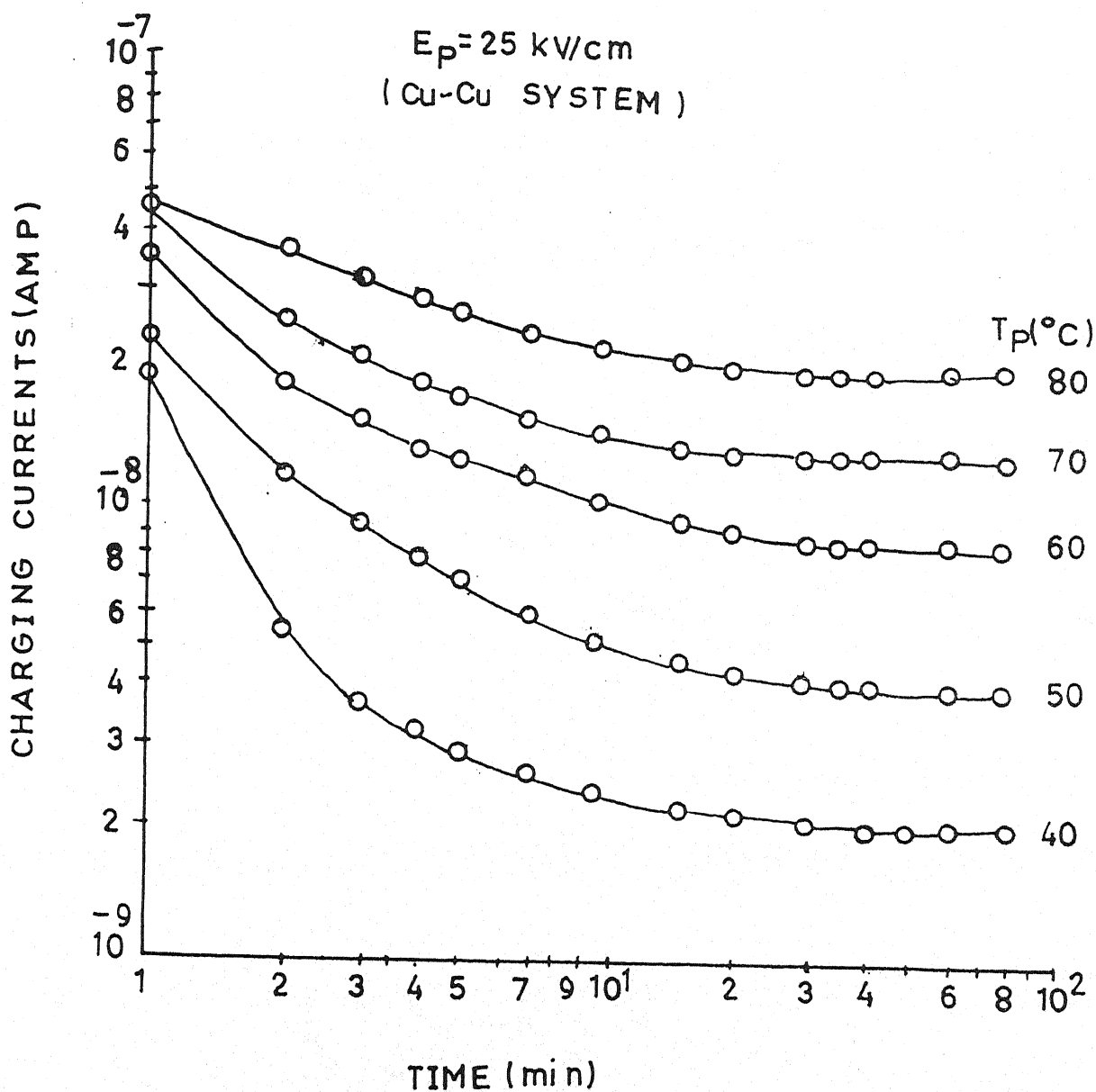


Fig. 5.37

Transient currents in Charging mode for polyvinylidene fluoride sample ($20 \mu\text{m}$) poled with polarization field 25 kV/cm with different polarization temperature i.e. 40°C , 50°C , 60°C , 70°C and 80°C for Cu-Cu Electrode system.

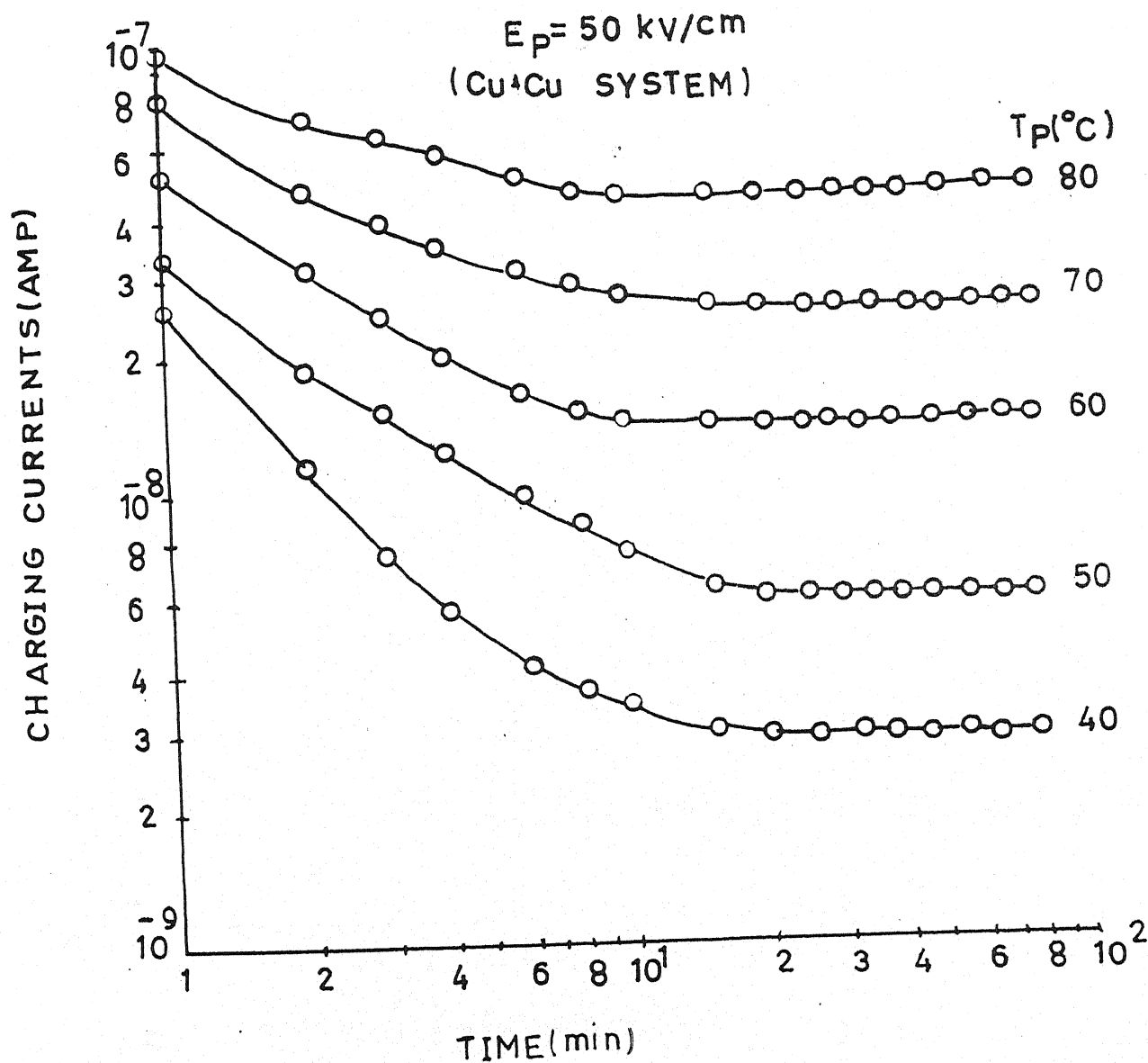


Fig. 5.38

Transient currents in Charging mode for polyvinylidene fluoride sample ($20 \mu\text{m}$) poled with polarization field 50 kV/cm with different polarization temperature i.e. 40 , 50 , 60 , 70 and 80°C for Cu- Cu Electrode system.

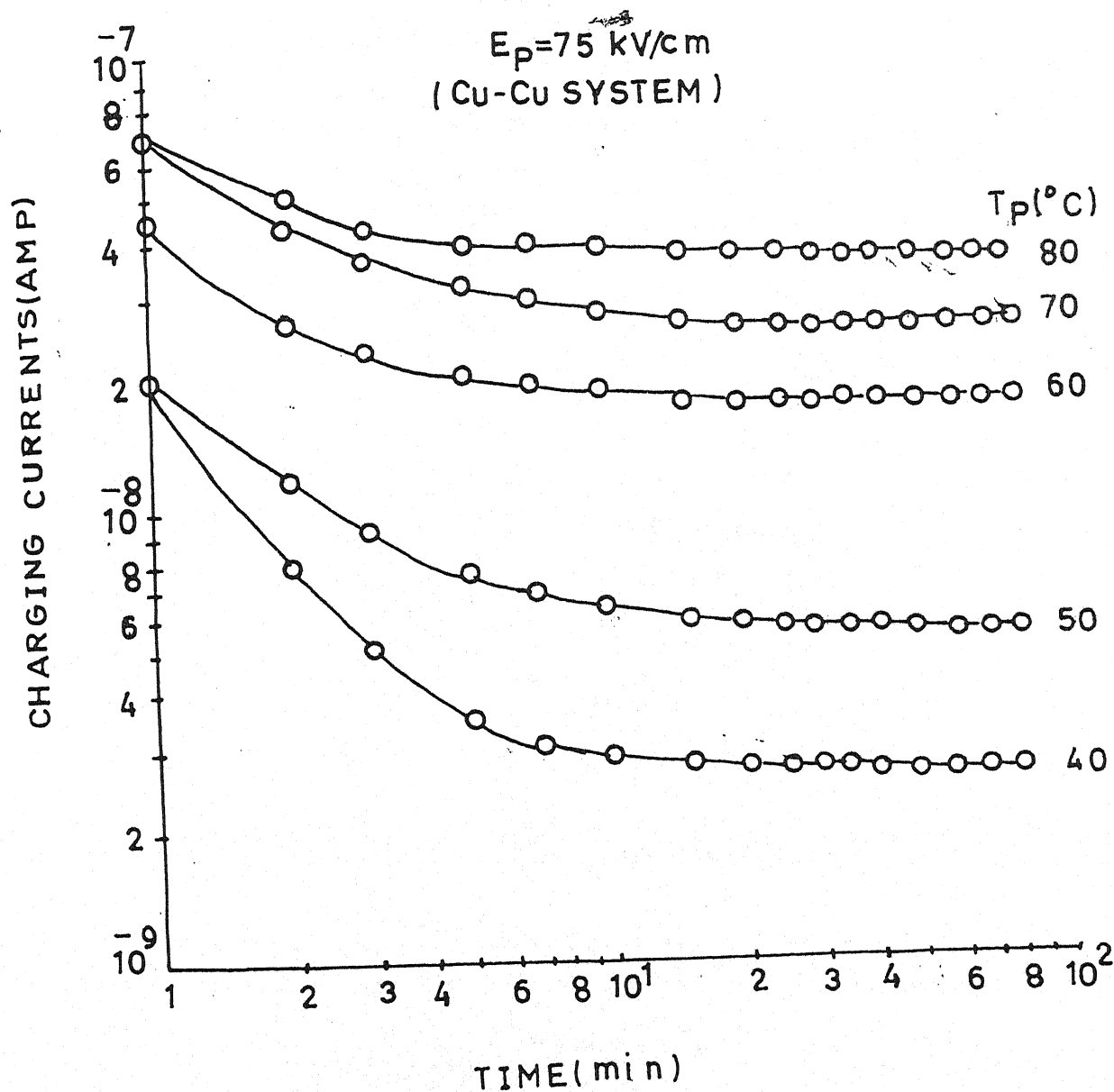


Fig. 5.39

Transient currents in Charging mode for polyvinylidene fluoride sample ($20 \mu\text{m}$) poled with polarization field 75 kV/cm with different polarization temperature i.e. 40 , 50 , 60 , 70 and 80°C for Cu- Cu Electrode system .

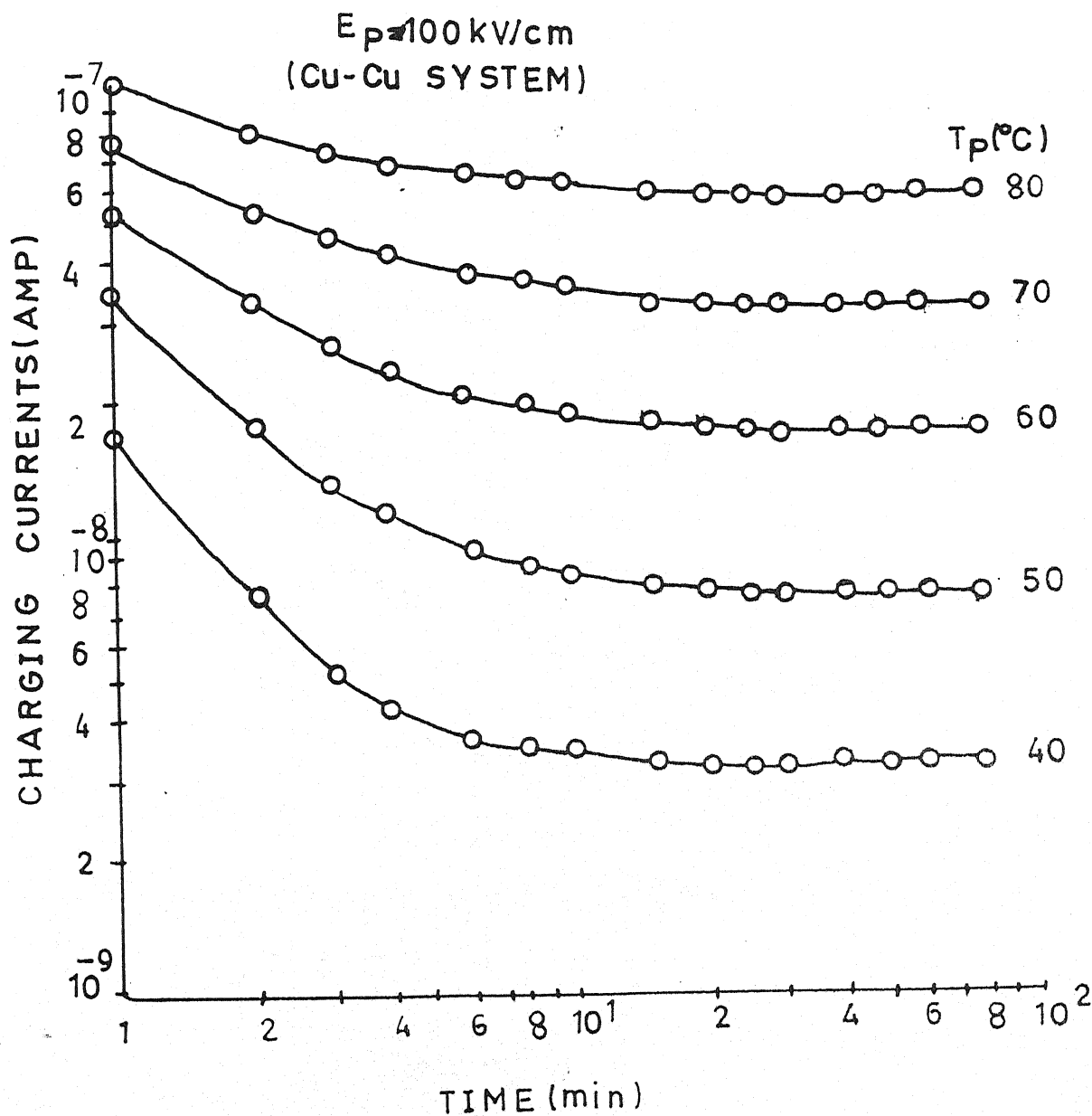


Fig. 5.40

Transient currents in Charging mode for polyvinylidene fluoride sample ($20 \mu\text{m}$) poled with polarization field 100 kV/cm with different polarization temperature i.e. 40 , 50 , 60 , 70 and 80°C for Cu- Cu Electrode system.

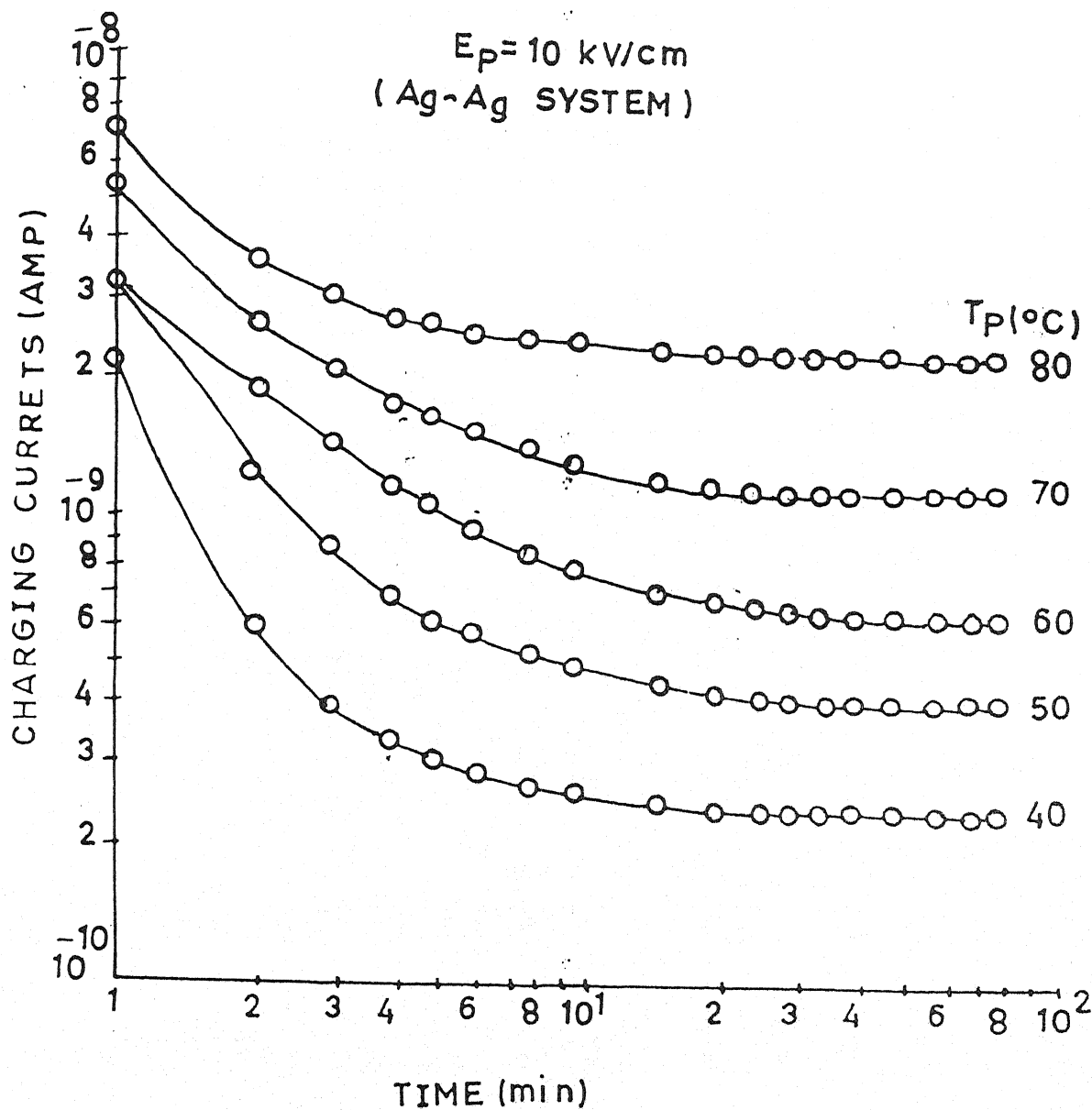


Fig. 5.41i

Transient currents in Charging mode for polyvinylidene fluoride sample ($20 \mu\text{m}$) poled with polarization field 10 kV/cm with different polarization temperature i.e. 40 , 50 , 60 , 70 and 80°C for Ag-Ag Electrode system.

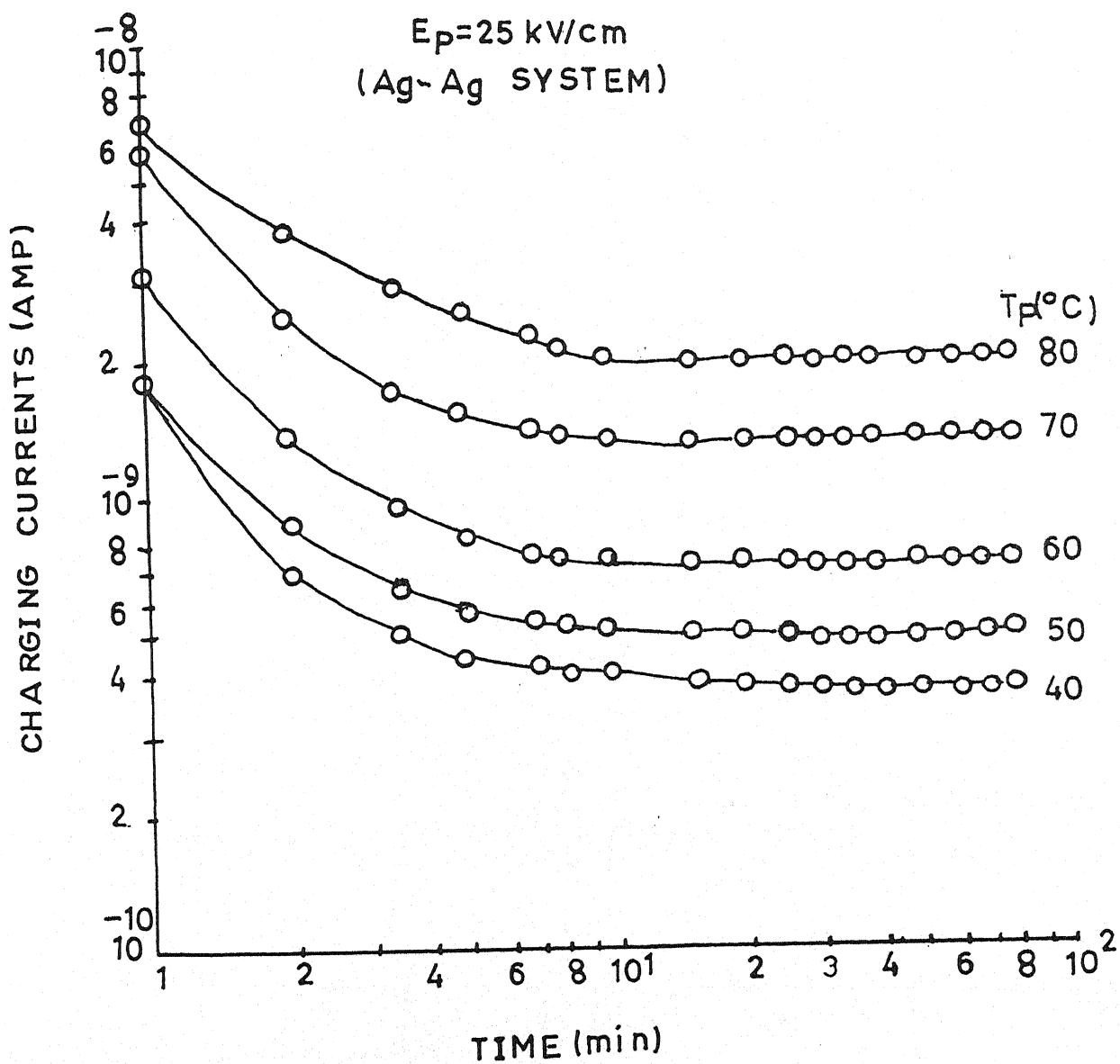


Fig. 5.42

Transient currents in Charging mode for polyvinylidene fluoride sample ($20 \mu\text{m}$) poled with polarization field 25 kV/cm with different polarization temperature i.e. 40 , 50 , 60 , 70 and 80°C for Ag-Ag Electrode system.

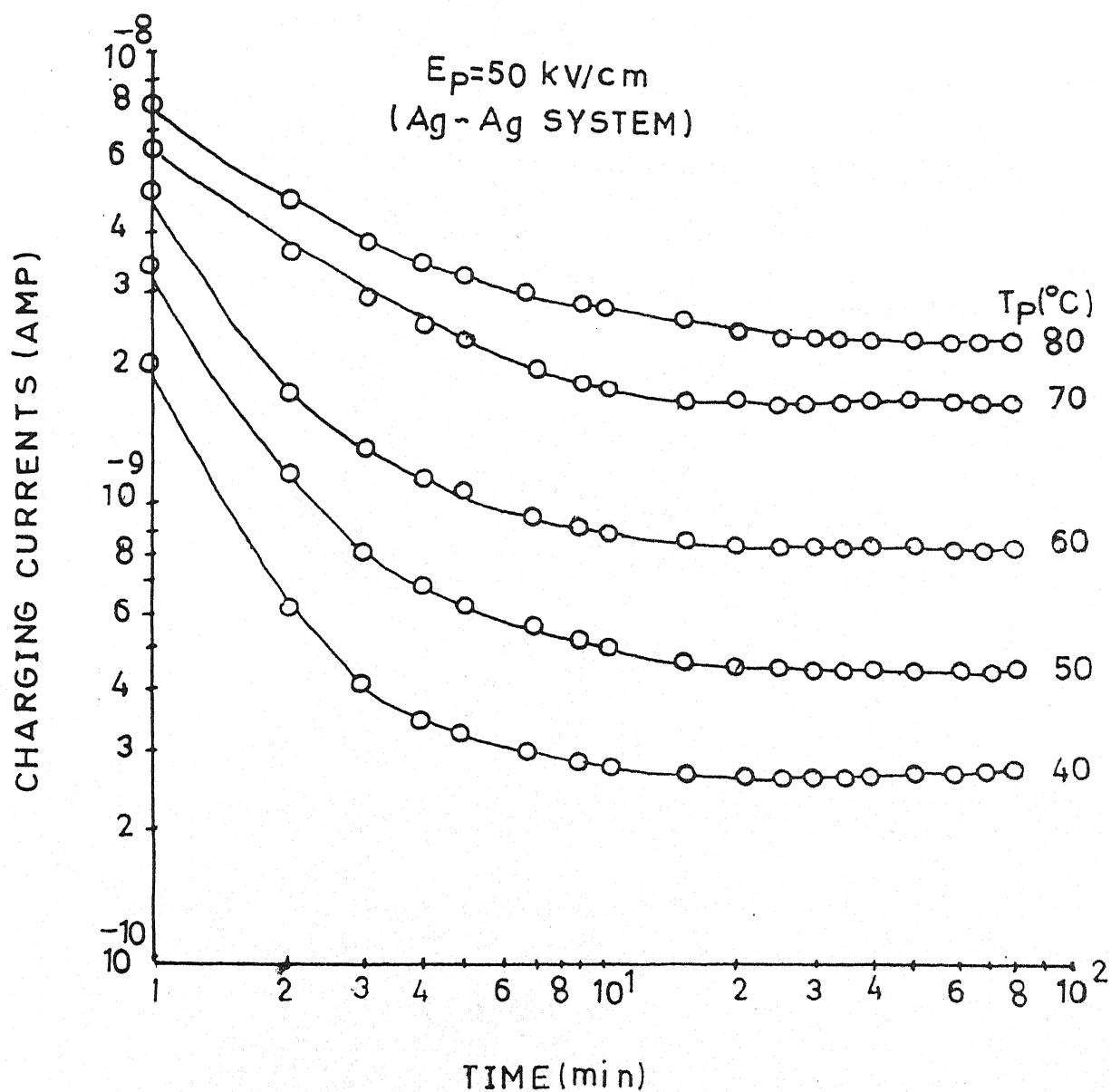


Fig. 5.43

Transient currents in Charging mode for polyvinylidene fluoride sample ($20 \mu\text{m}$) poled with polarization field 50 kV/cm with different polarization temperature i.e. 40 , 50 , 60 , 70 and 80°C for Ag - Ag Electrode system .

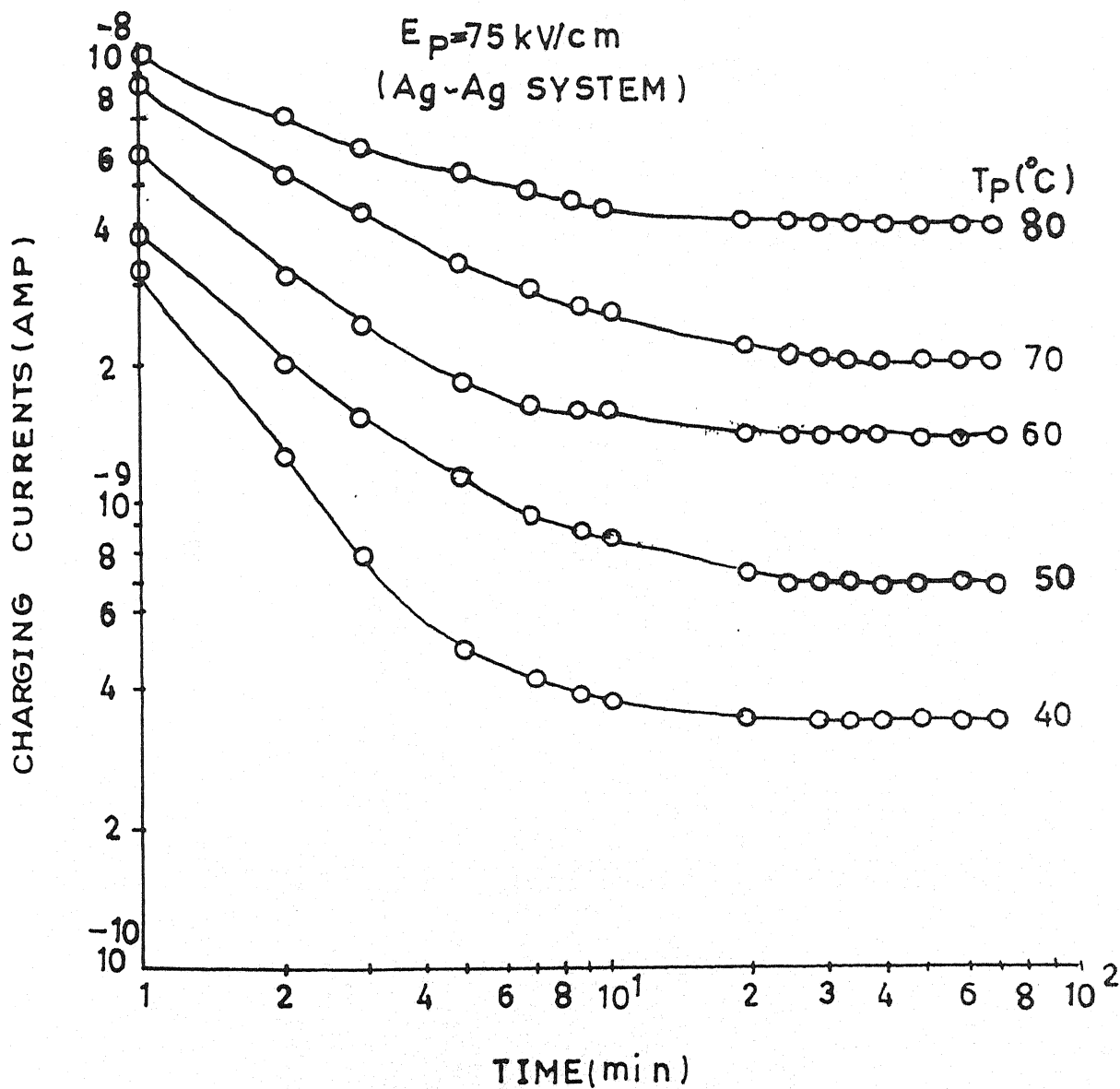


Fig. 5.44

Transient currents in Charging mode for polyvinylidene fluoride sample ($20 \mu\text{m}$) poled with polarization field 75 kV/cm with different polarization temperature i.e. 40 , 50 , 60 , 70 and 80°C for Ag-Ag Electrode system.

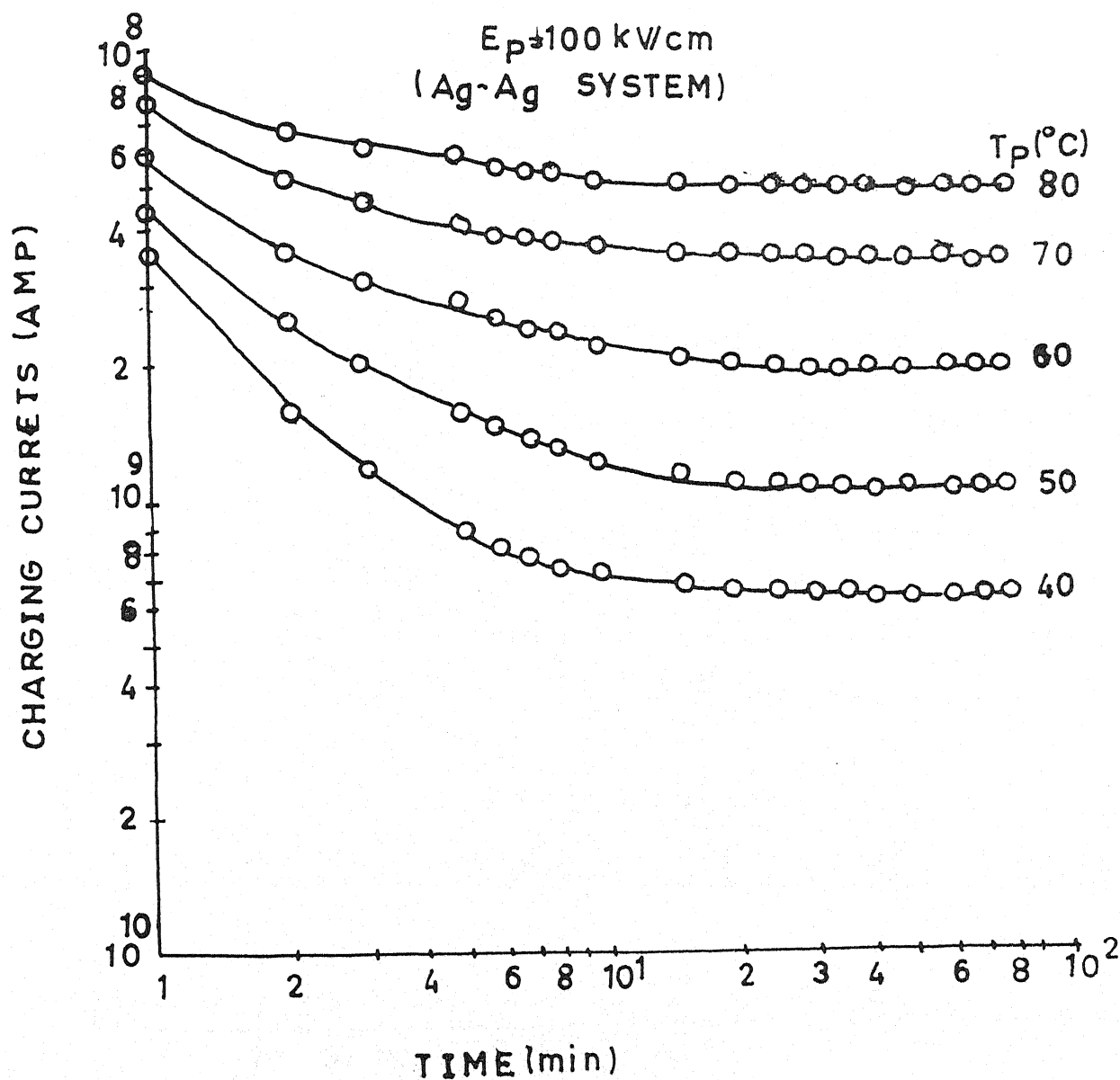


Fig. 5.45 .

Transient currents in Charging mode for polyvinylidene fluoride sample ($20 \mu\text{m}$) poled with polarization field 100 kV/cm with different polarization temperature i.e. 40 , 50 , 60 , 70 and 80°C for Ag-Ag Electrode system .

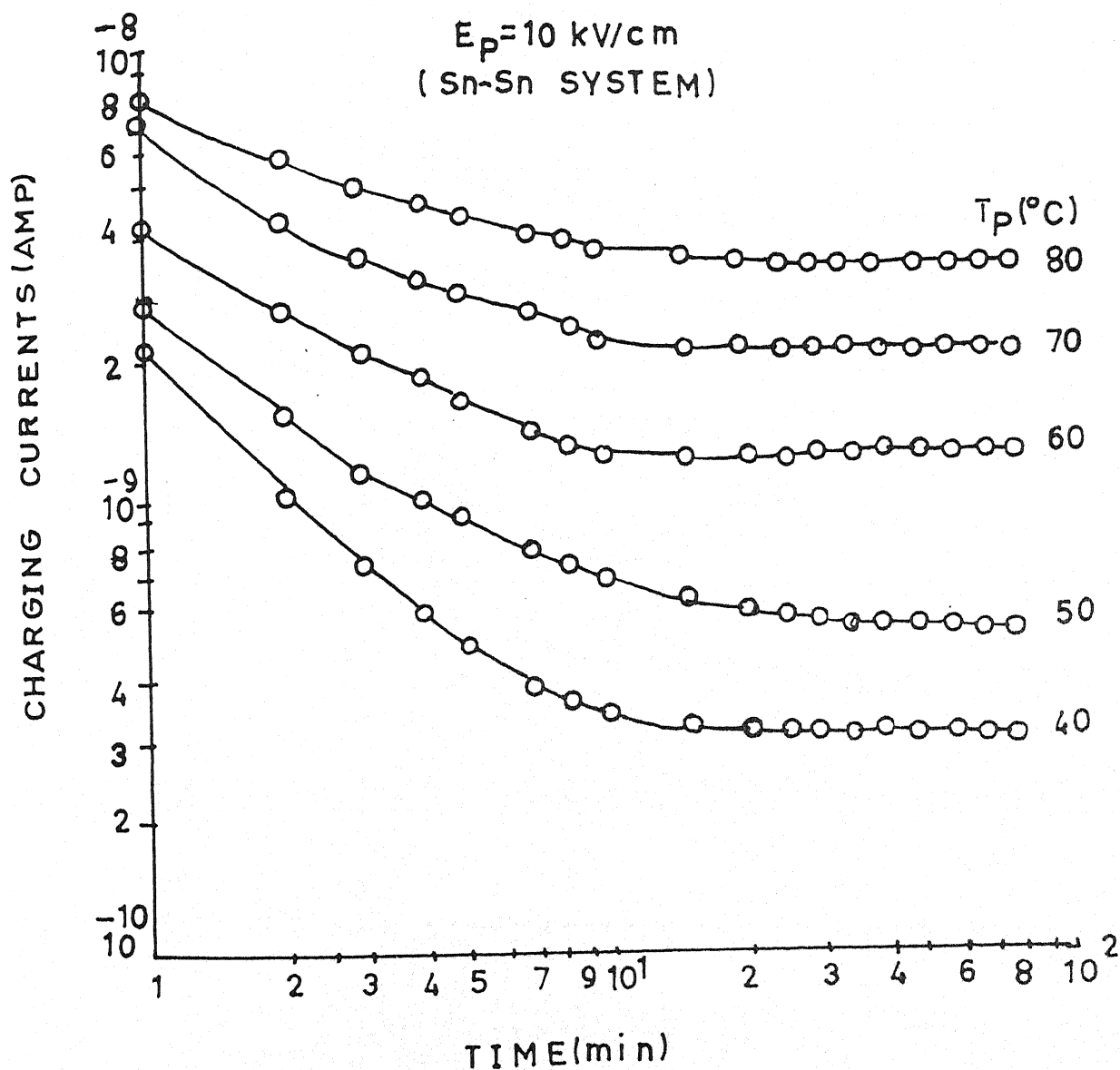


Fig. 5.46
Transient currents in Charging mode for polyvinylidene fluoride sample (20 μm) poled with polarization field 10 kV/cm with different polarization temperature i.e. 40, 50, 60, 70 and 80 $^{\circ}\text{C}$ for Sn-Sn Electrode system.

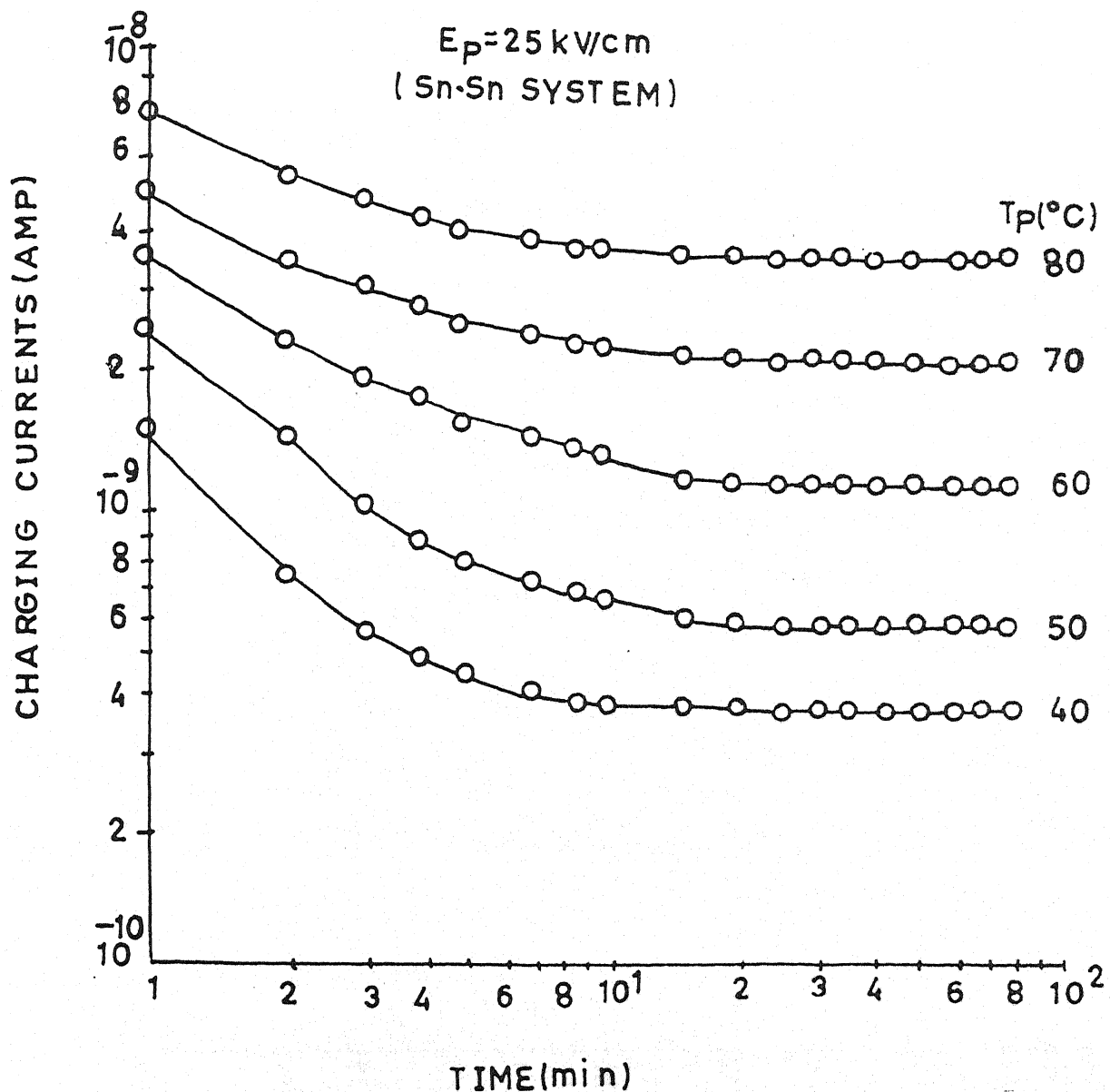


Fig. 5.47

Transient currents in Charging mode for polyvinylidene fluoride sample (20 μm) poled with polarization field 25 kV/cm with different polarization temperature i.e. 40, 50, 60, 70 and 80°C for Sn-Sn Electrode system.

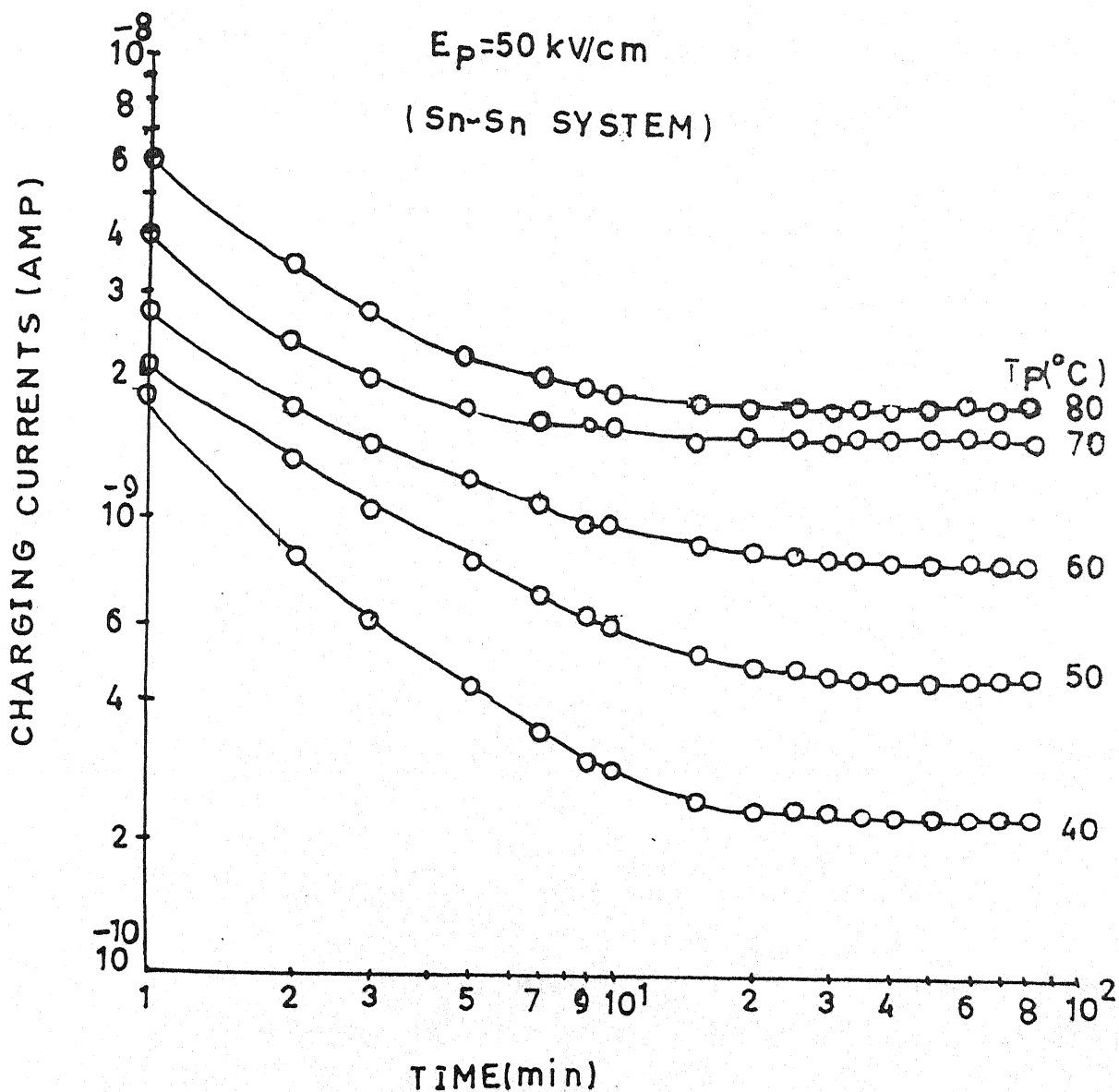


Fig. 5.48:

Transient currents in Charging mode for polyvinylidene fluoride sample ($20 \mu\text{m}$) poled with polarization field 50 kV/cm with different polarization temperature i.e. 40 , 50 , 60 , 70 and 80°C for Sn-Sn Electrode system.

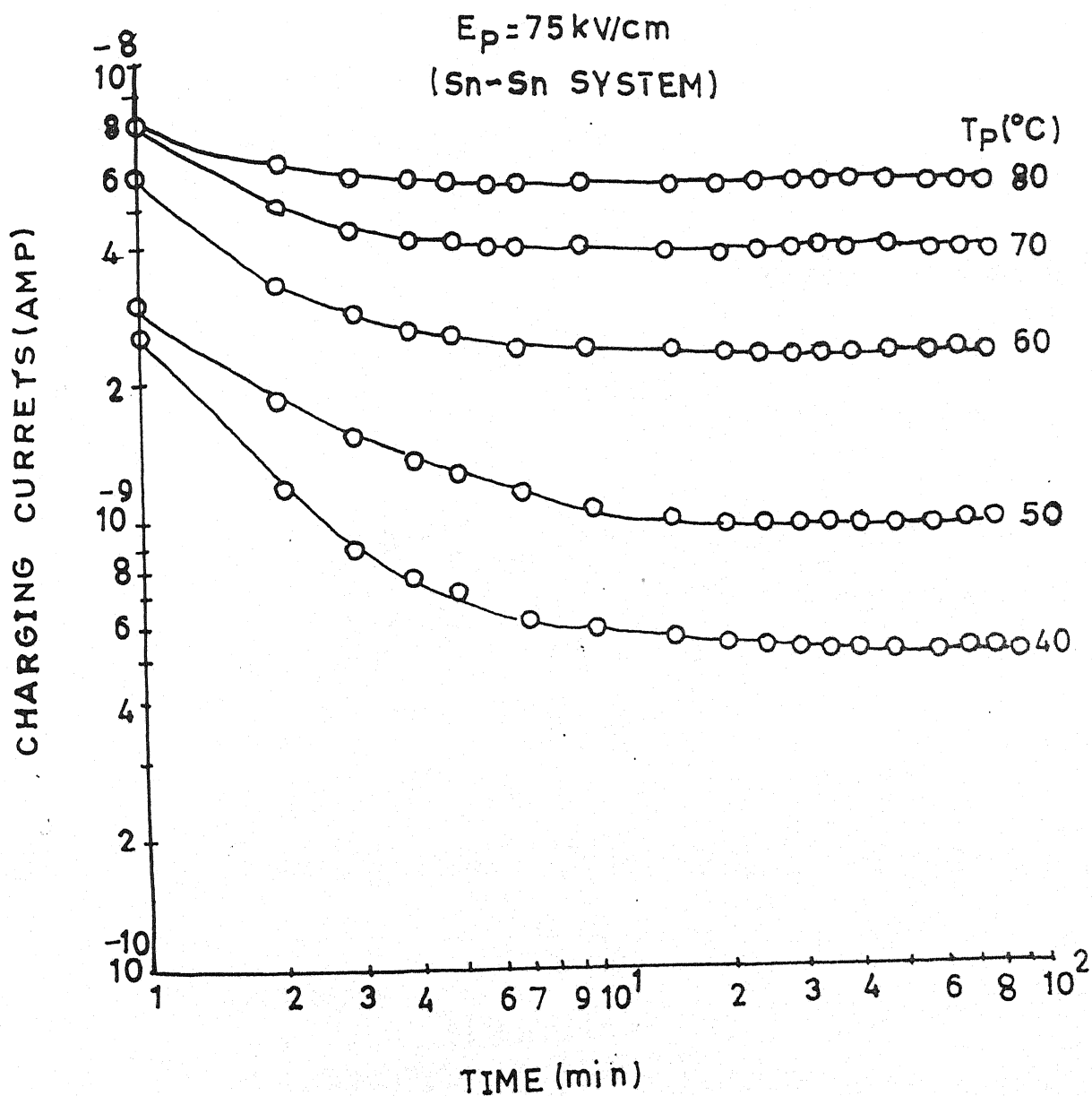


Fig. 5.49

Transient currents in Charging mode for polyvinylidene fluoride sample ($20 \mu\text{m}$) poled with polarization field 75 kV/cm with different polarization temperature i.e. 40 , 50 , 60 , 70 and 80°C for Sn-Sn Electrode system.

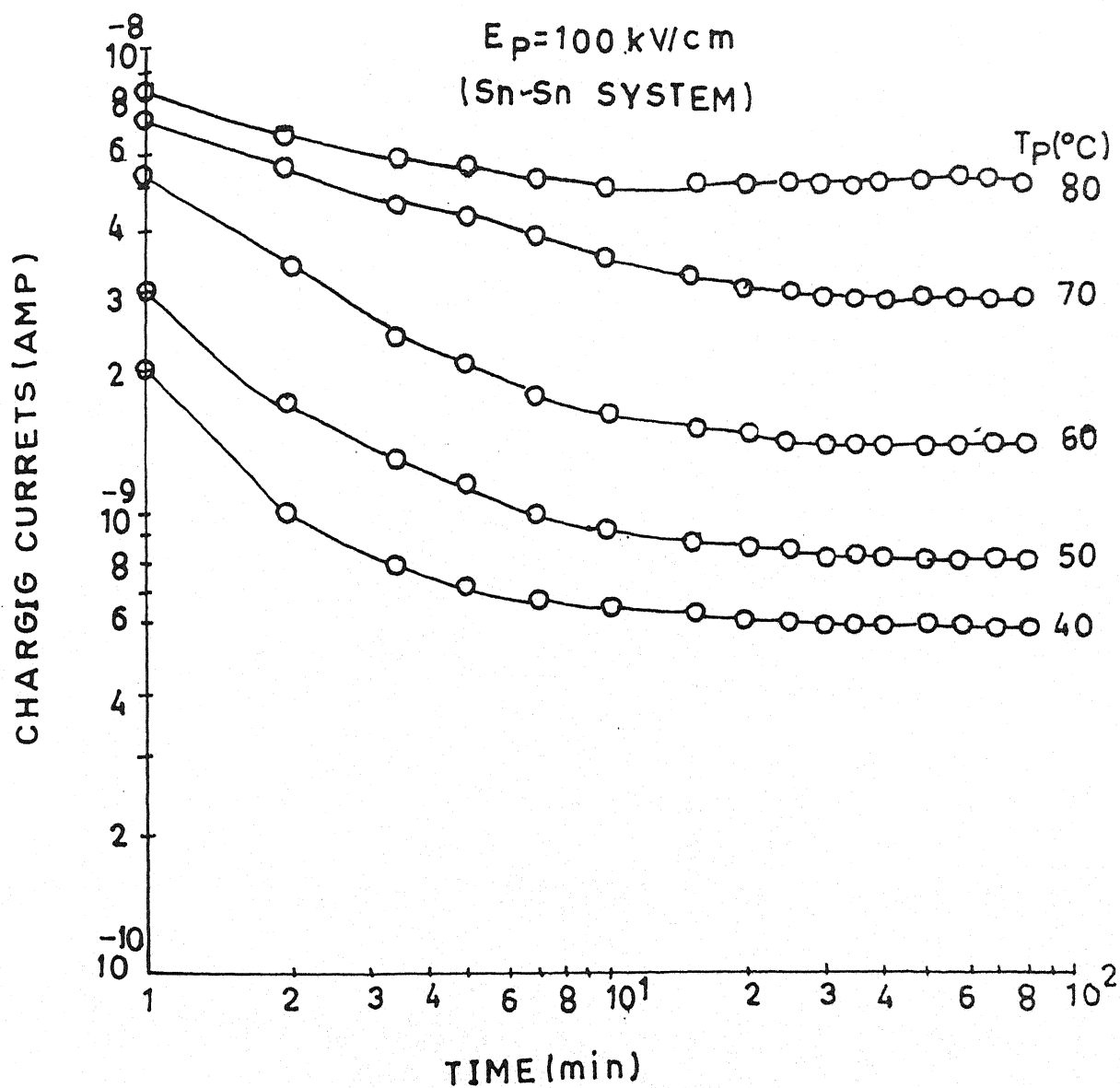


Fig. 5.50

Transient currents in Charging mode for polyvinylidene fluoride sample ($20 \mu\text{m}$) poled with polarization field 100 kV/cm with different polarization temperature i.e. 40 , 50 , 60 , 70 and 80°C for Sn-Sn Electrode system.

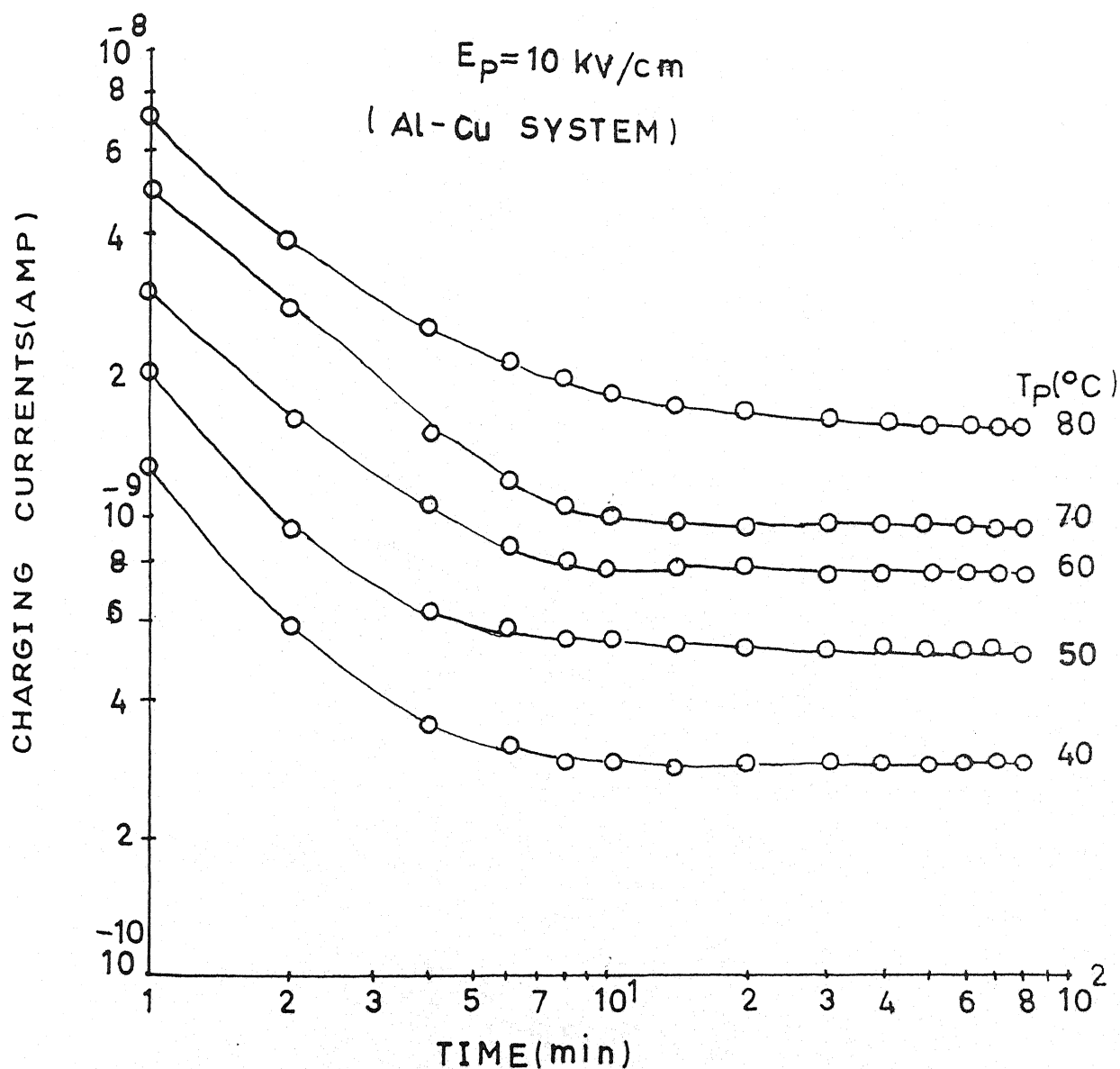


Fig. 5.51

Transient currents in Charging mode for polyvinylidene fluoride sample ($20 \mu\text{m}$) poled with polarization field 10 kV/cm with different polarization temperature i.e. 40 , 50 , 60 , 70 and 80°C for Al-Cu Electrode system.

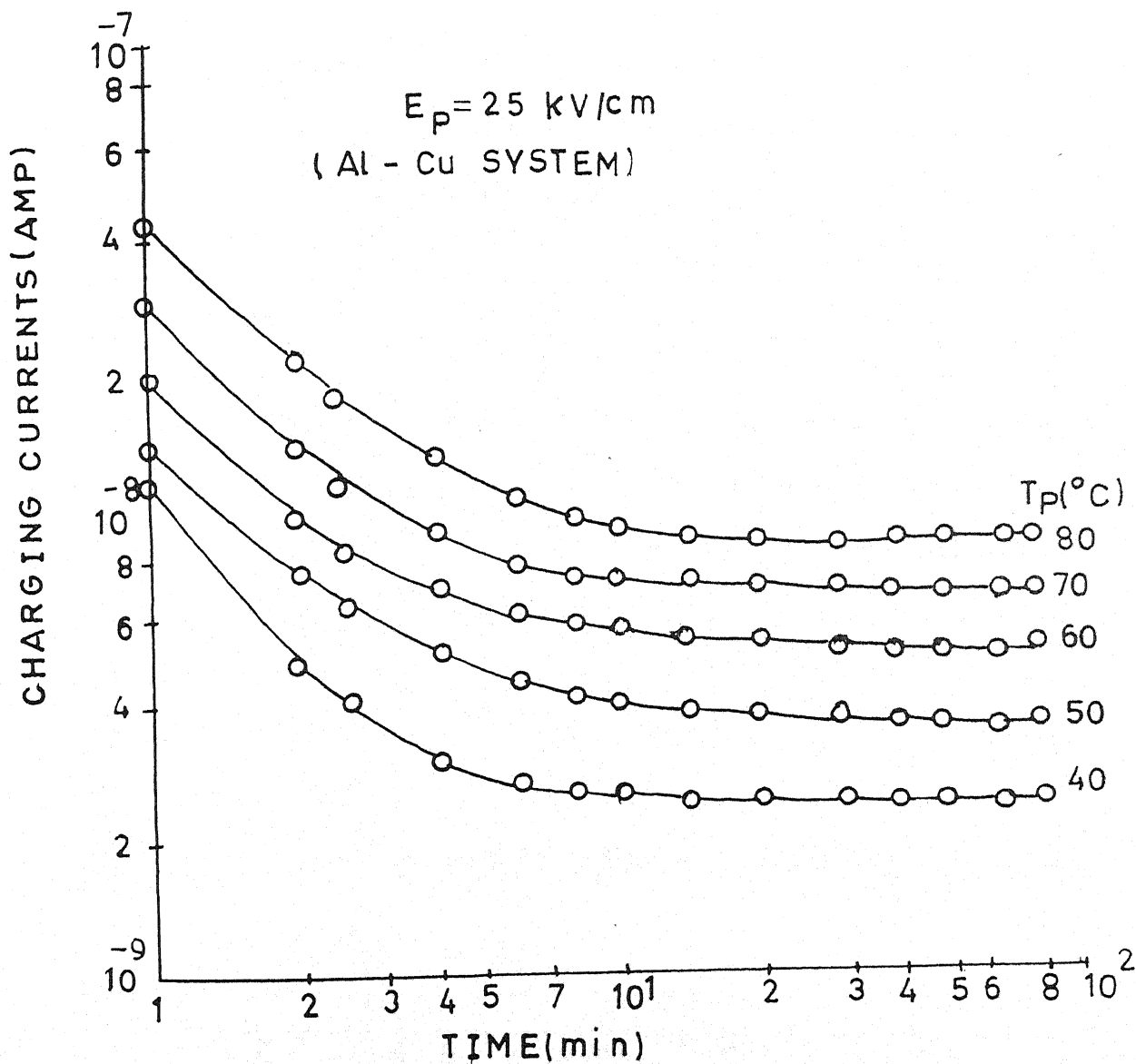


Fig. 5.52

Transient currents in Charging mode for polyvinylidene fluoride sample ($20 \mu\text{m}$) poled with polarization field 25 kV/cm with different polarization temperature i.e. $40, 50, 60, 70$ and 80°C for Al - Cu Electrode system.

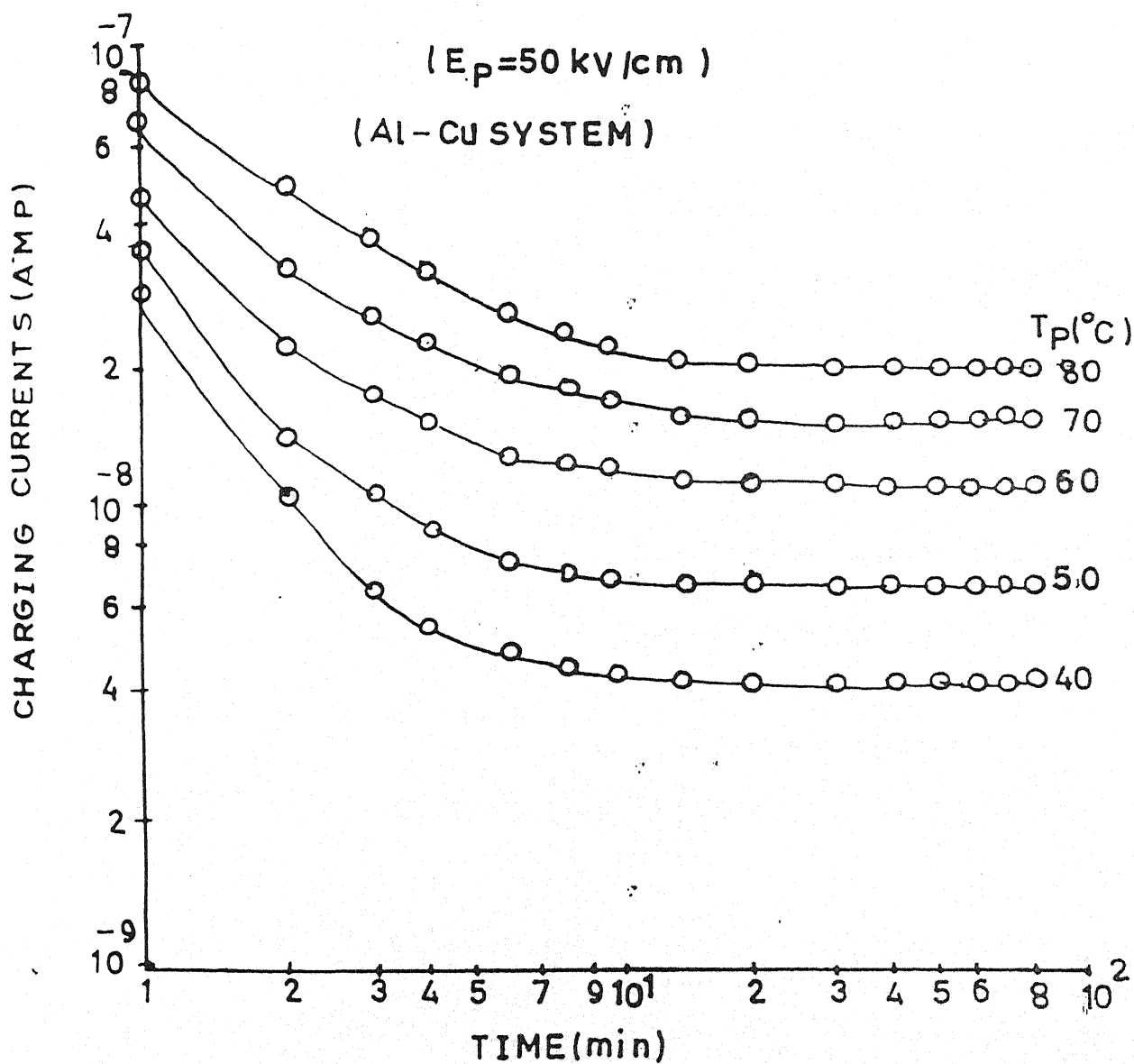


Fig. 5.53

Transient currents in Charging mode for polyvinylidene fluoride sample ($20 \mu\text{m}$) poled with polarization field 50 kV/cm with different polarization temperature i.e. 40 , 50 , 60 , 70 and 80°C for Al - Cu Electrode system.

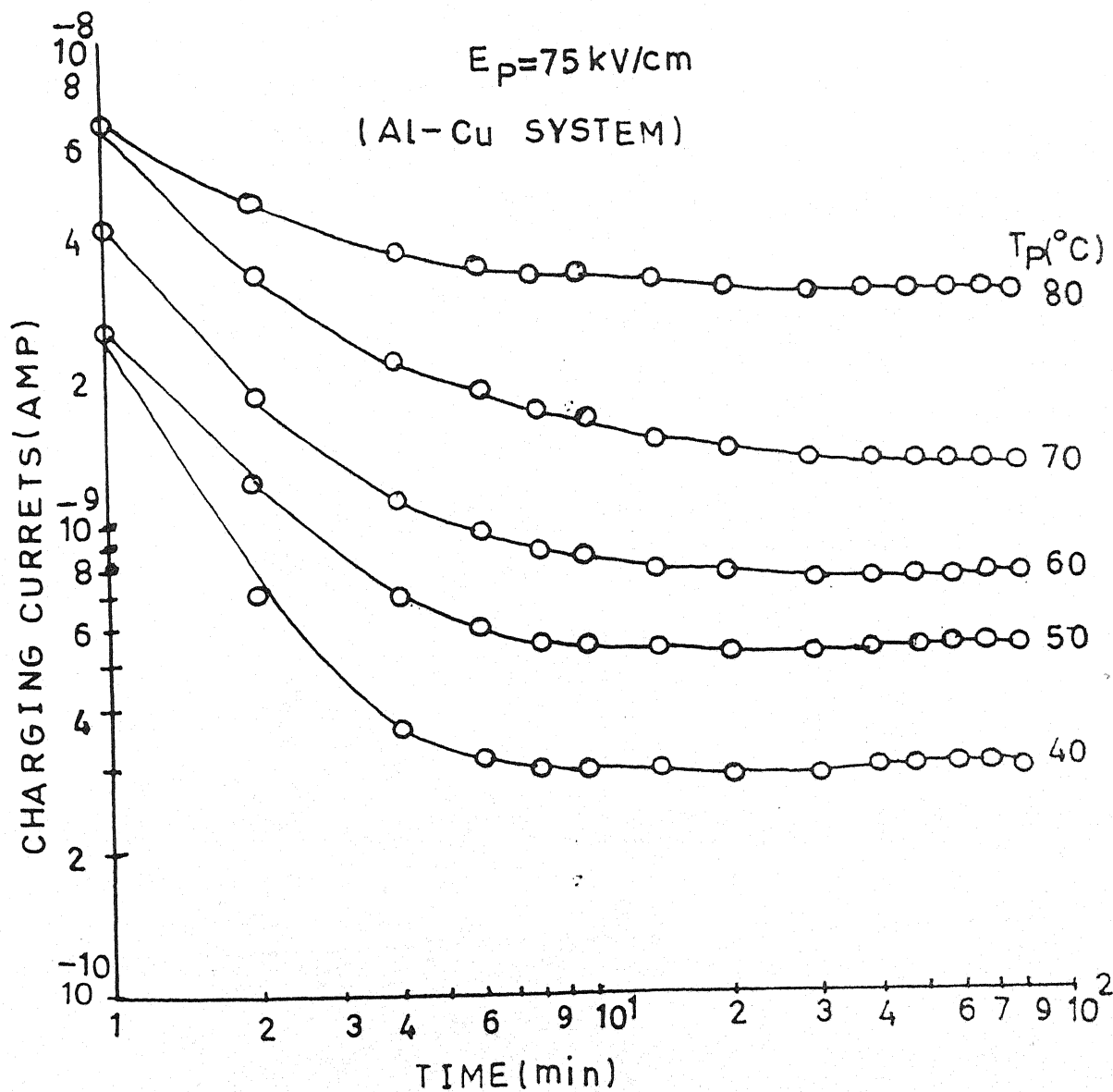


Fig. 5.54.
Transient currents in Charging mode for polyvinylidene fluoride sample ($20 \mu\text{m}$) poled with polarization field 75 kV/cm with different polarization temperature i.e. 40 , 50 , 60 , 70 and 80°C for Al-Cu Electrode system.

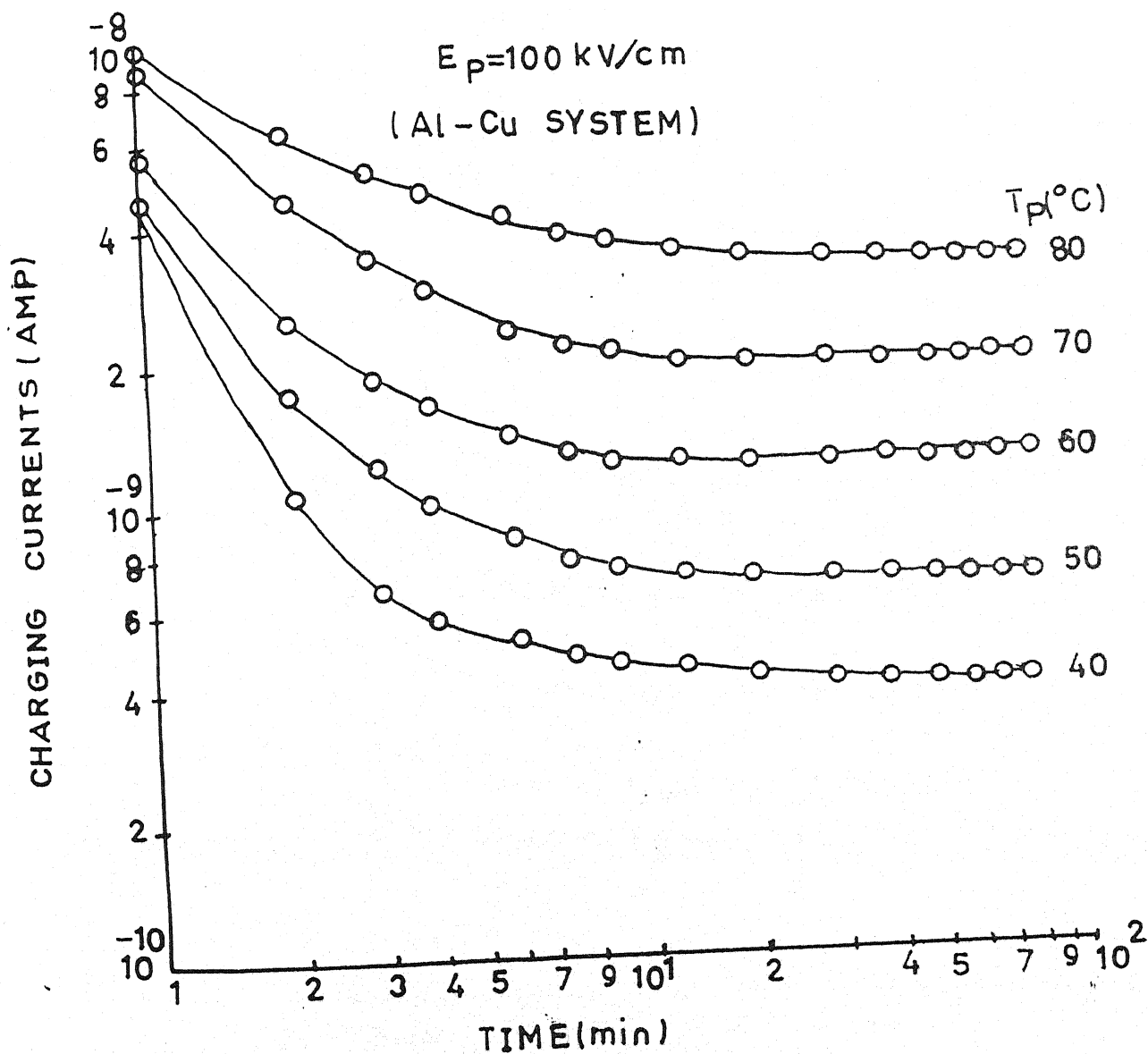


Fig. 5.55

Transient currents in Charging mode for polyvinylidene fluoride sample ($20 \mu\text{m}$) poled with polarization field 100 kV/cm with different polarization temperature i.e. 40 , 50 , 60 , 70 and 80°C for Al-Cu Electrode system.

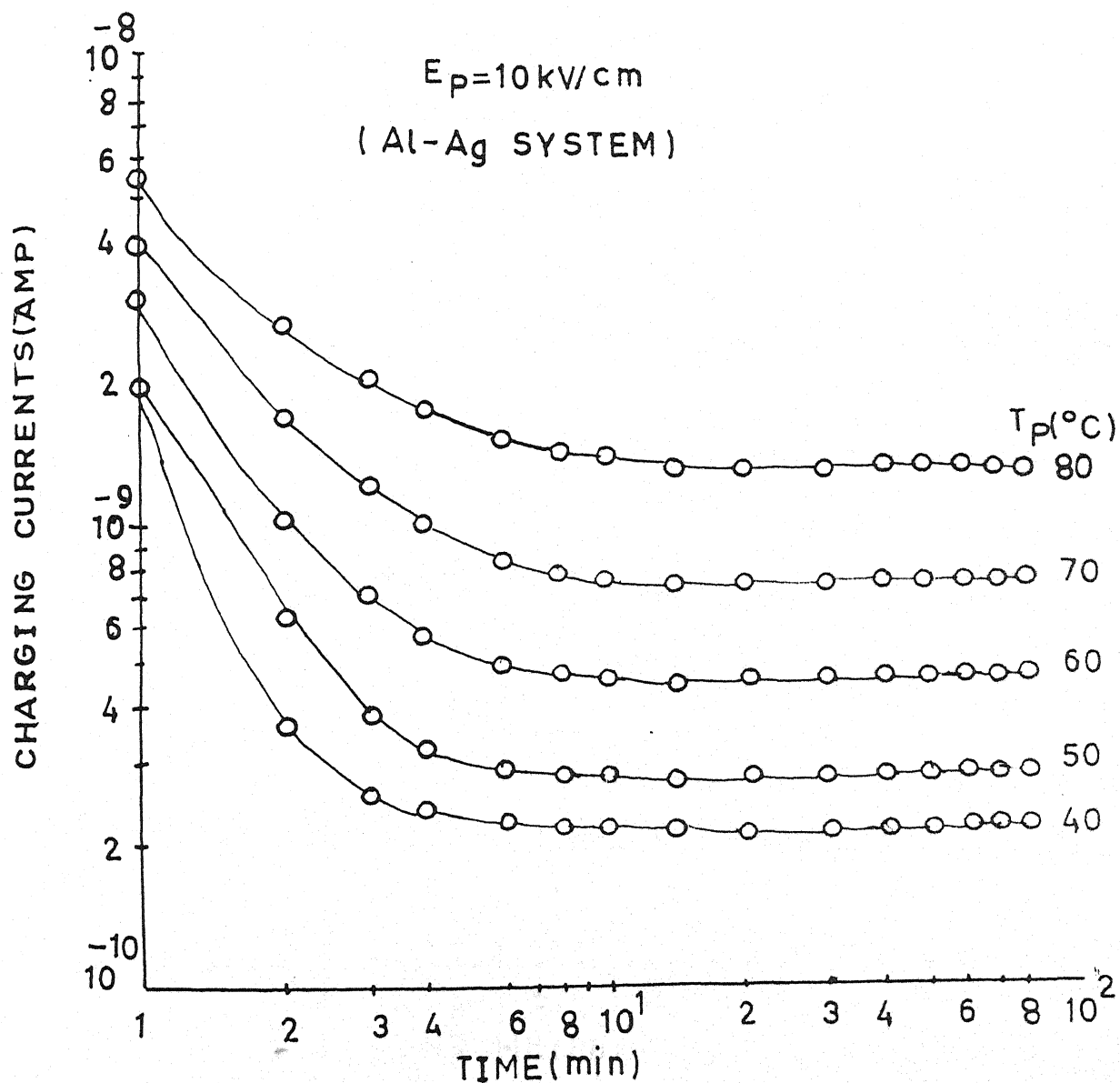


Fig. 5.56
Transient currents in Charging mode for polyvinylidene fluoride sample ($20 \mu\text{m}$) poled with polarization field 10 kV/cm with different polarization temperature i.e. 40 , 50 , 60 , 70 and 80°C for Al- Cu Electrode system.

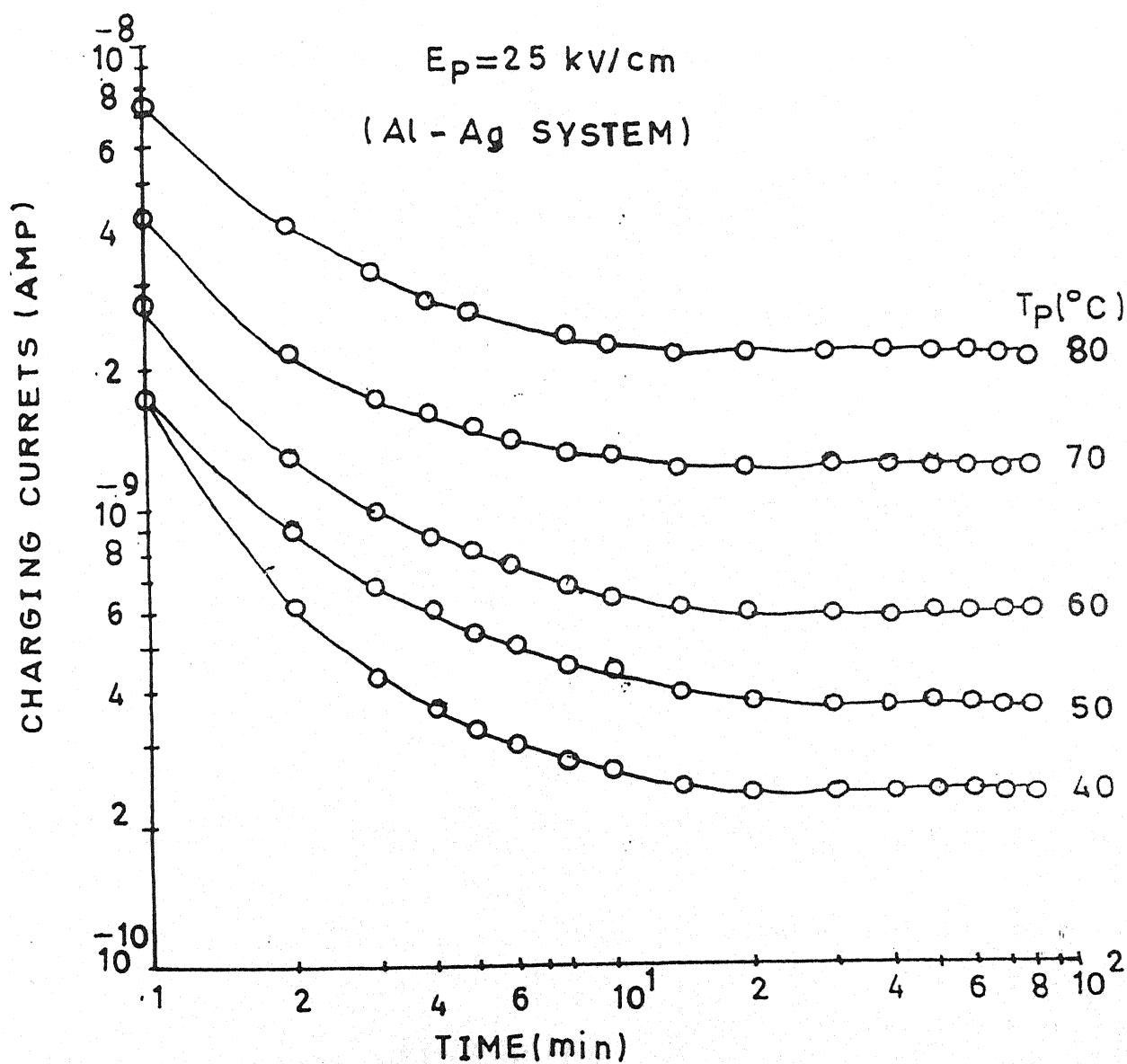


Fig. 5.57

Transient currents in Charging mode for polyvinylidene fluoride sample ($20 \mu\text{m}$) poled with polarization field 25 kV/cm with different polarization temperature i.e. 40°C , 50°C , 60°C , 70°C and 80°C for Al-Ag Electrode system.

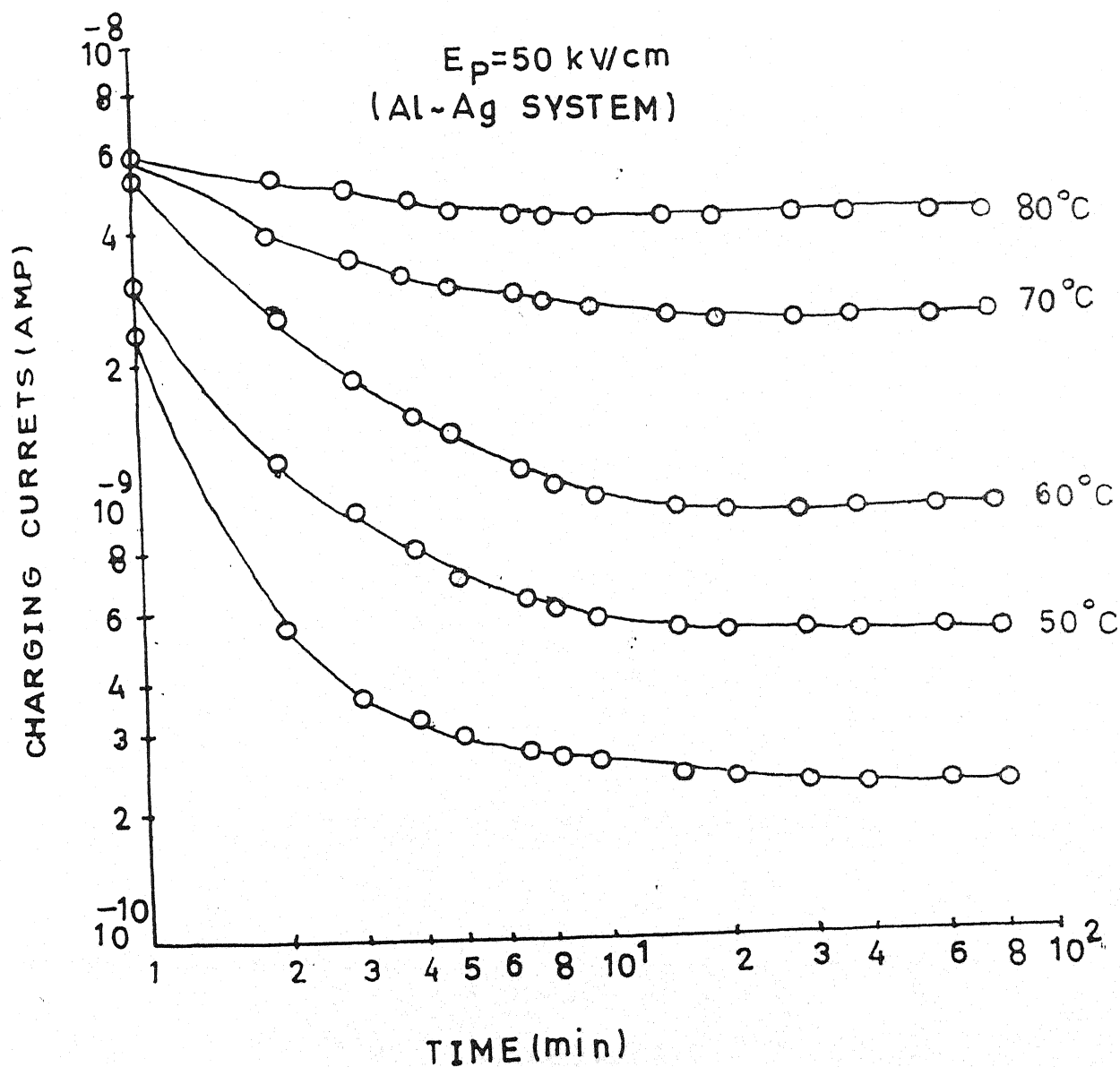


Fig. 5.58

Transient currents in Charging mode for polyvinylidene fluoride sample ($20 \mu\text{m}$) poled with polarization field 50 kV/cm with different polarization temperature i.e. 40°C , 50°C , 60°C , 70°C and 80°C for Al-Ag Electrode system.

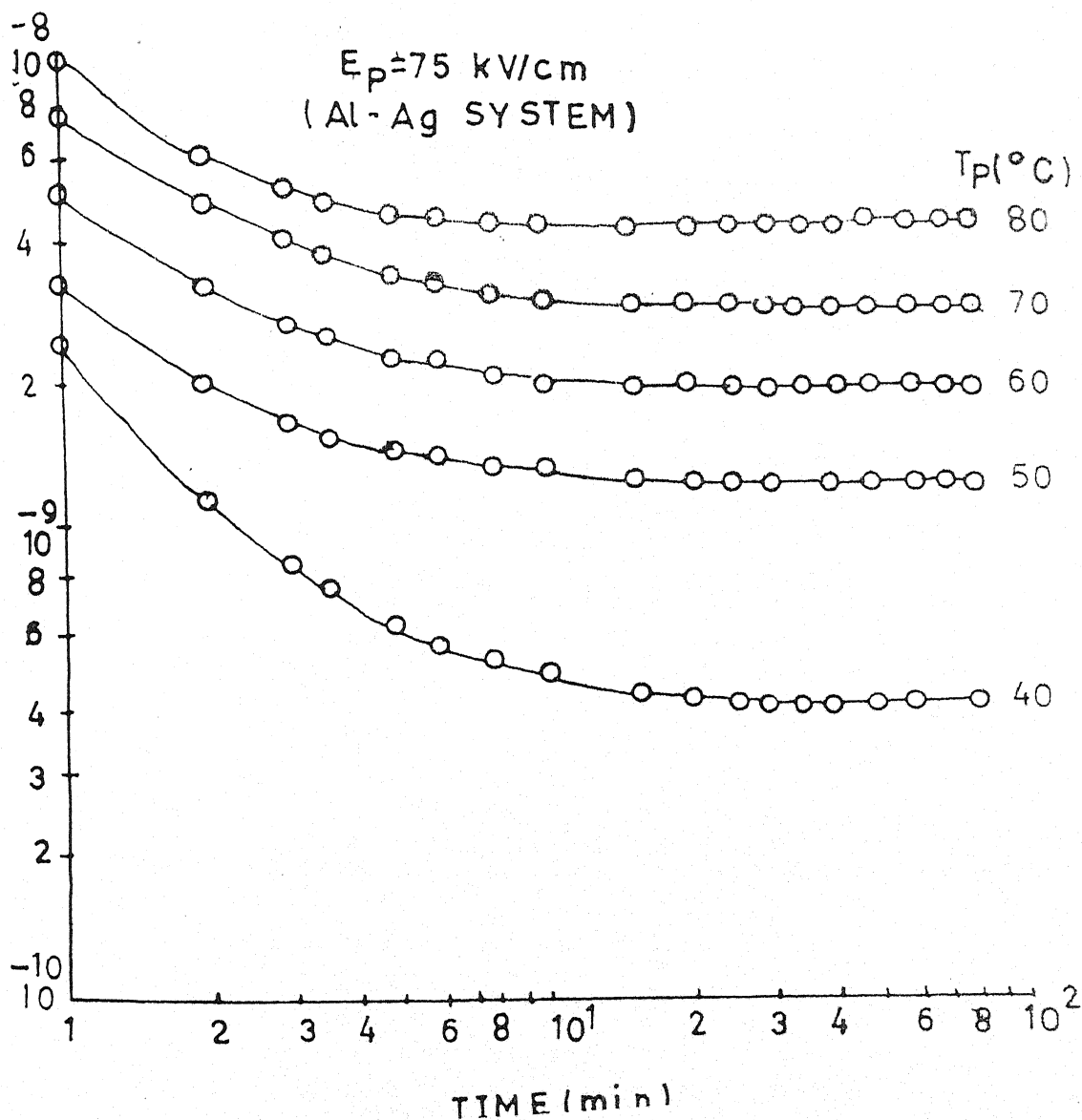


Fig. 5.59

Transient currents in Charging mode for polyvinylidene fluoride sample ($20 \mu\text{m}$) poled with polarization field 75 kV/cm with different polarization temperature i.e. 40 , 50 , 60 , 70 and 80°C for Al-Ag Electrode system.

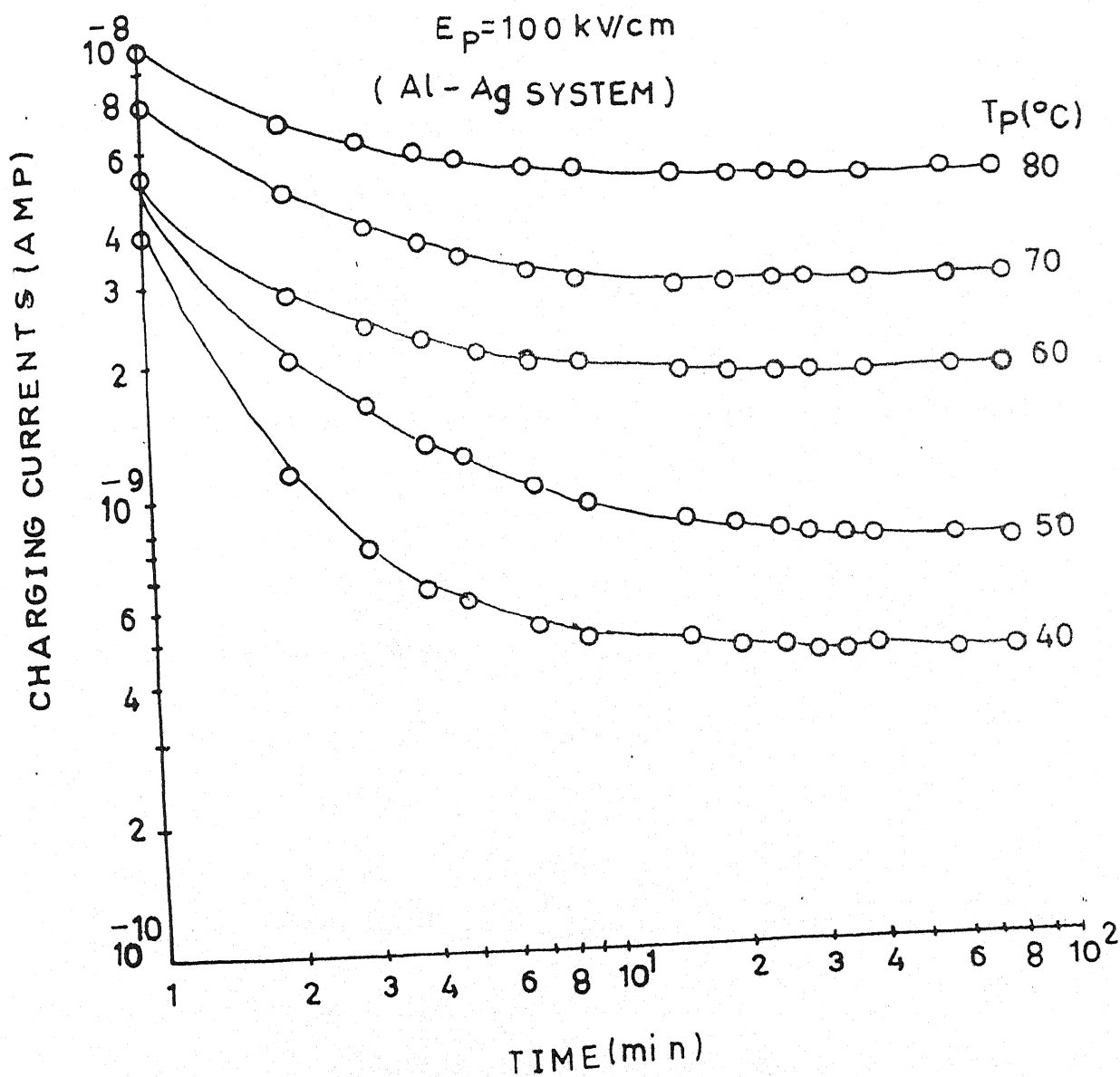


Fig. 5.60-
Transient currents in Charging mode for polyvinylidene fluoride sample ($20 \mu\text{m}$) poled with polarization field 100 kV/cm with different polarization temperature i.e. $40, 50, 60, 70$ and 80°C for Al - Ag Electrode system.

and the other mechanism is operative in the range of long-time with a decay constant of different value.

The temperature dependence of the transient currents in discharging modes are shown more clearly when the current measured at a constant time (isochronals) is plotted against temperature. Such isochronals for charging and discharging mode have been constructed for 2, 6, 10, 20, 40 and 70 min are shown in Figs. 5.61 to 5.90. From these plots, it may be concluded that the currents show thermal dependence. Such isochronals are characterized by a maxima around $70 \pm 5^{\circ}\text{C}$.

Figures 5.91 to 5.120 gives the $\log I$ vs $1000/T$ (where T is the absolute temperature) plots (constructed from linear portion of isochronal current and temperature plots). The value of activation energy is calculated from the slope of these characteristics.

The observed results can be discussed in the light of the existing models of transient currents.

The Curie-von Schweidler type of time dependence has been observed for many polymers with the index close to unity. A number of mechanisms may be used to explain such time dependence. It is, therefore, not possible to specify the origin of transient currents from the analysis of time dependence alone. At temperatures much lower than the glass transition temperature and for the low to moderate fields used, several of the concepts previously postulated to account for the transient

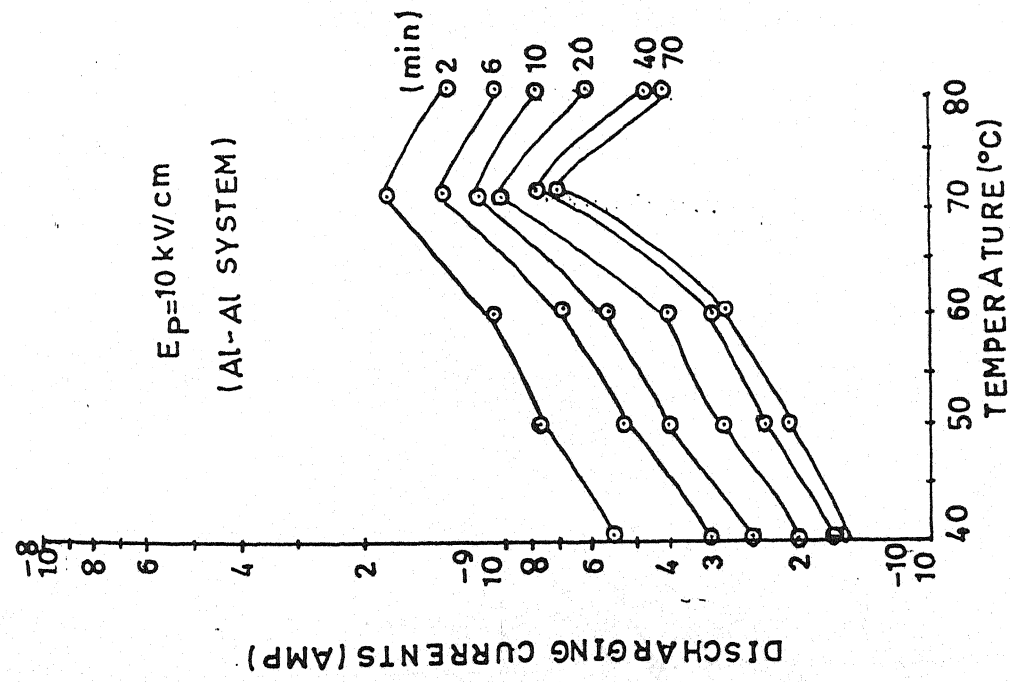


Fig. No. - 5.61
Isochronal Characteristics curves of
figures No. 5.1

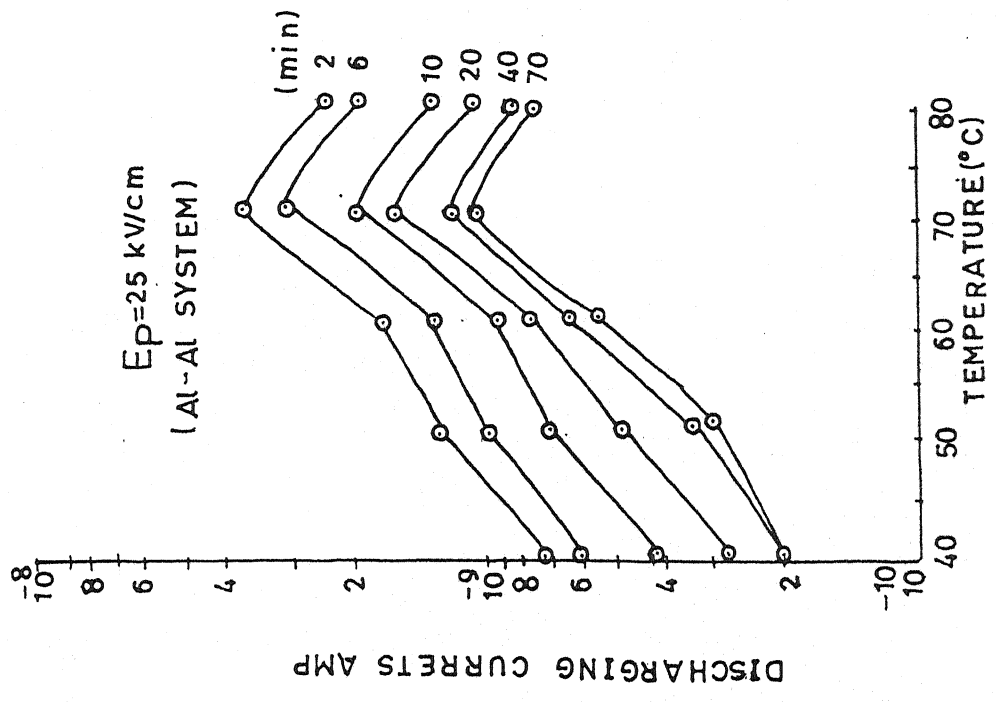


Fig. No. - 5.62
Isochronal Characteristics curves of
figures No. 5.2

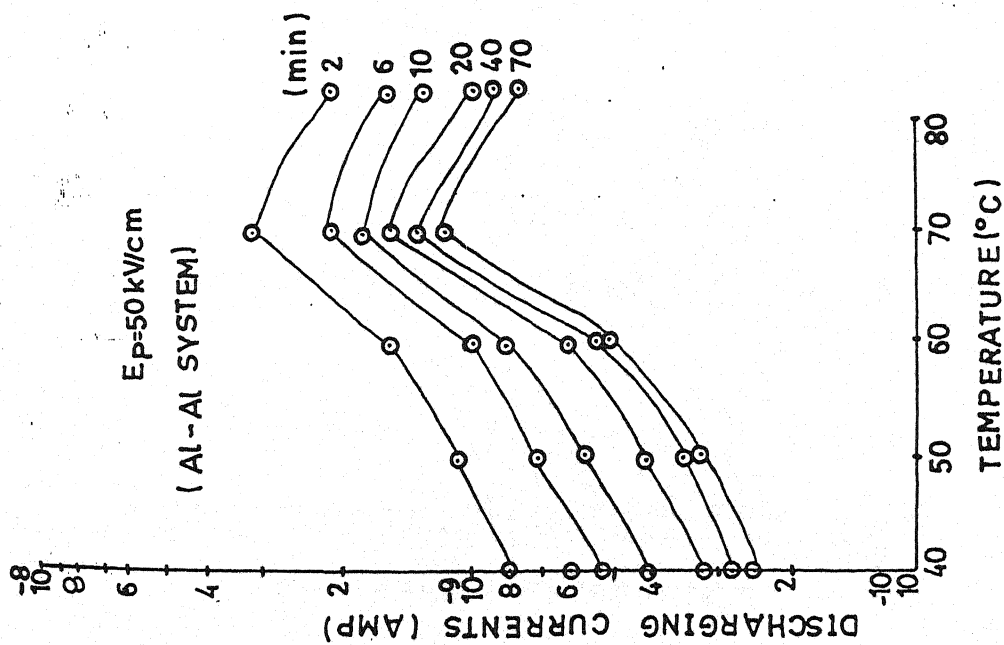


Fig. No. - 5.63
Isochronal Characteristics curves of
figures No. 5.3

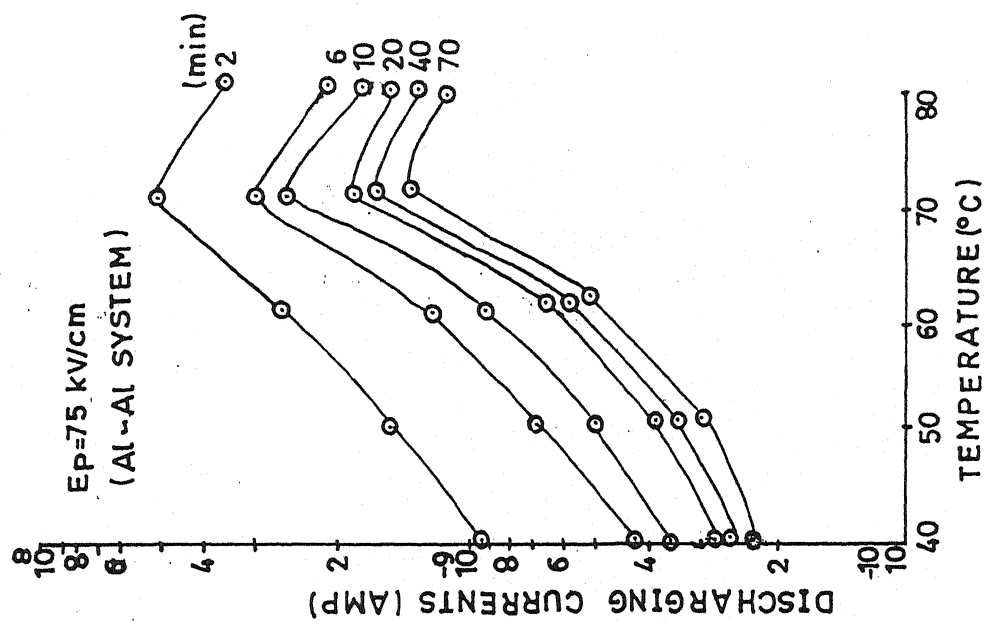


Fig. No. - 5.64
Isochronal Characteristics curves of
figures No. 5.4

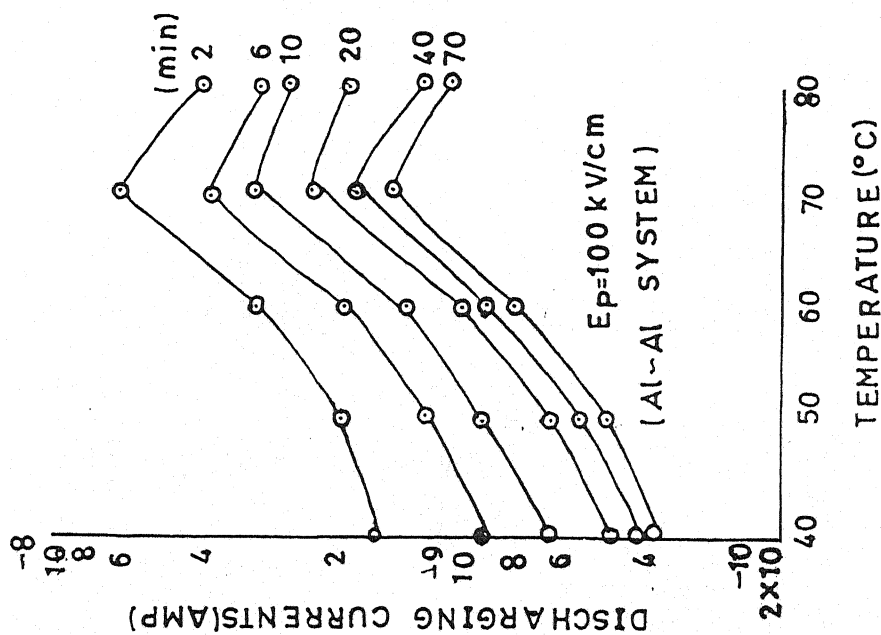


Fig. No. - 5.65
Isochronal Characteristics curves of
figures No. 5.5

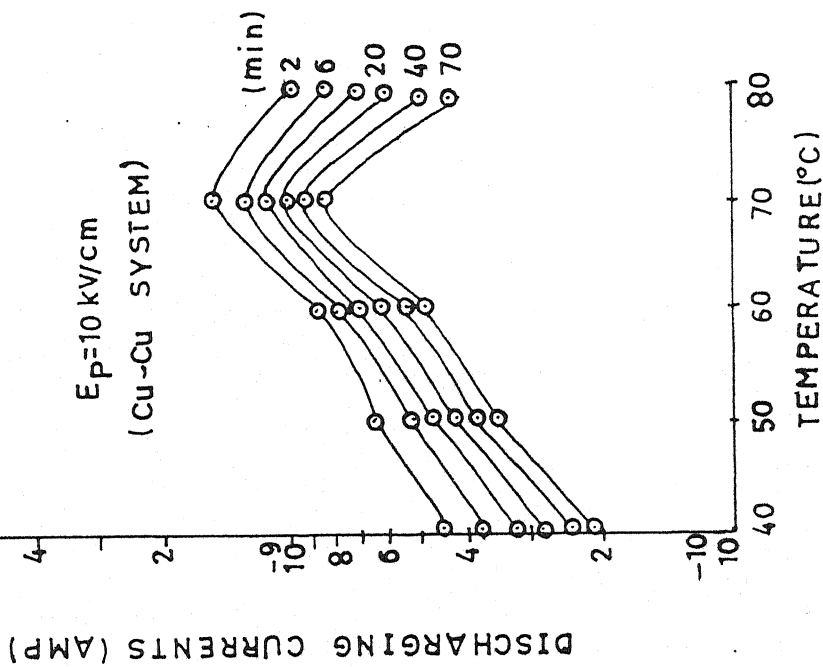


Fig. No. - 5.66
Isochronal Characteristics curves of
figures No. 5.6

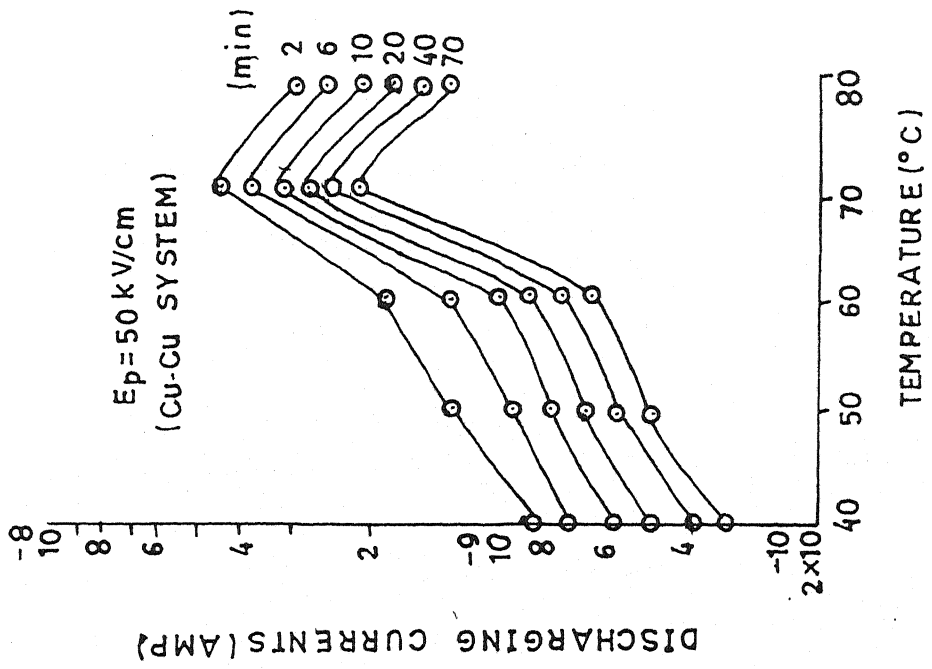


Fig. No. - 5.68
Isochronal Characteristics curves of
figures No. 5.8

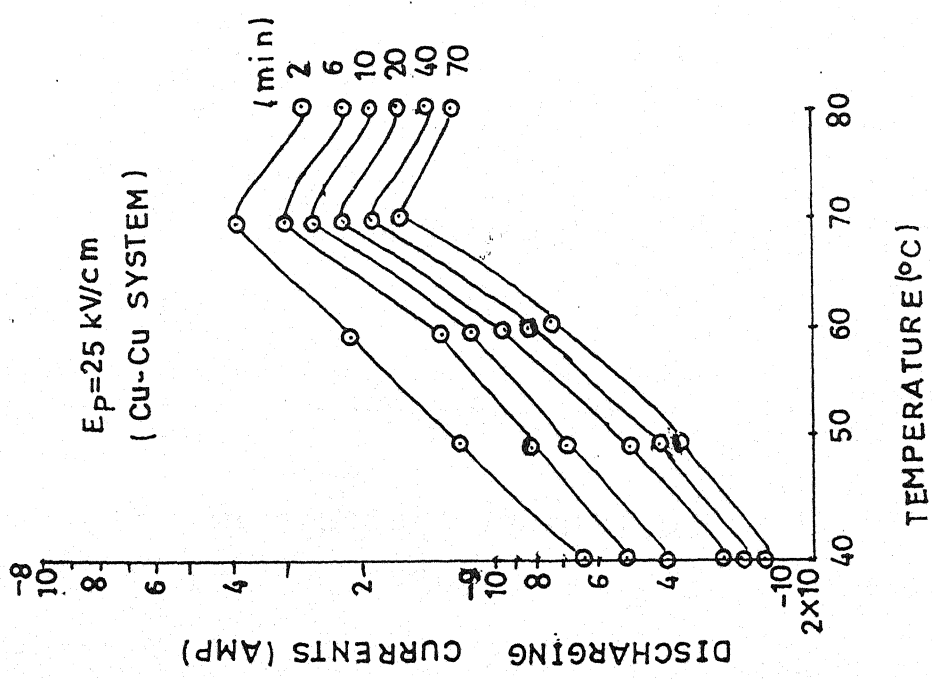


Fig. No. - 5.67
Isochronal Characteristics curves of
figures No. 5.7

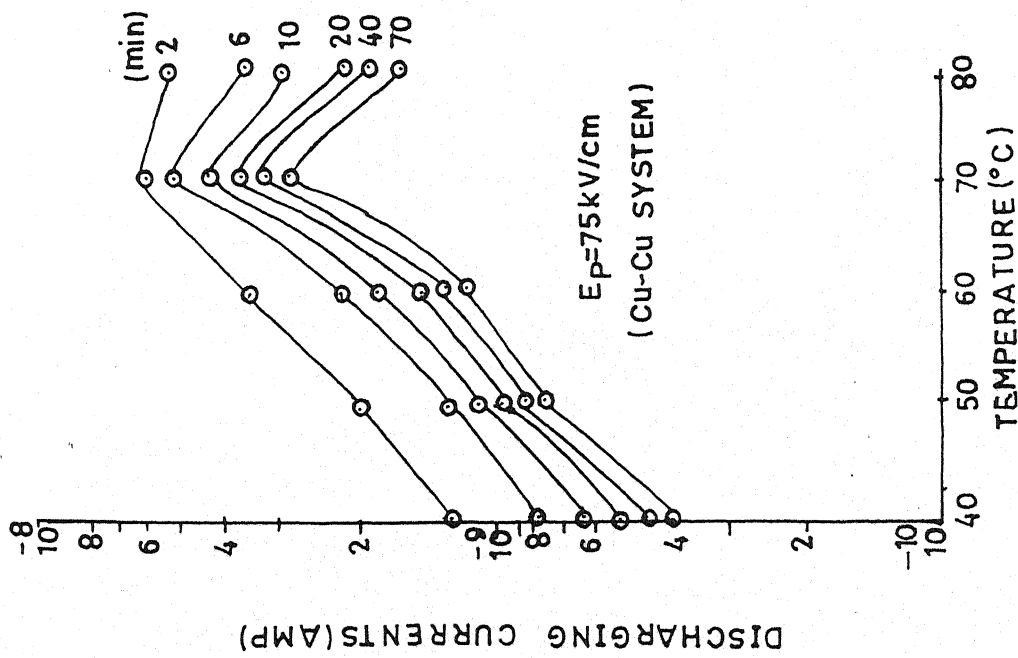


Fig. No. - 5.69

Isochronal Characteristics curves of

figures No. 5.9

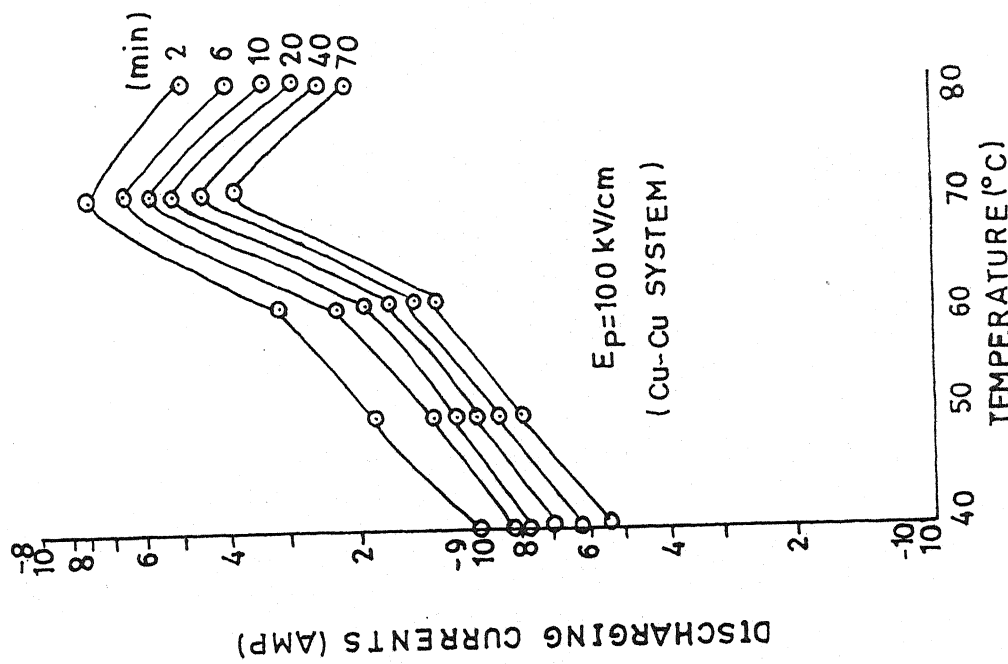


Fig. No. - 5.70

Isochronal Characteristics curves of

figures No. 5.10

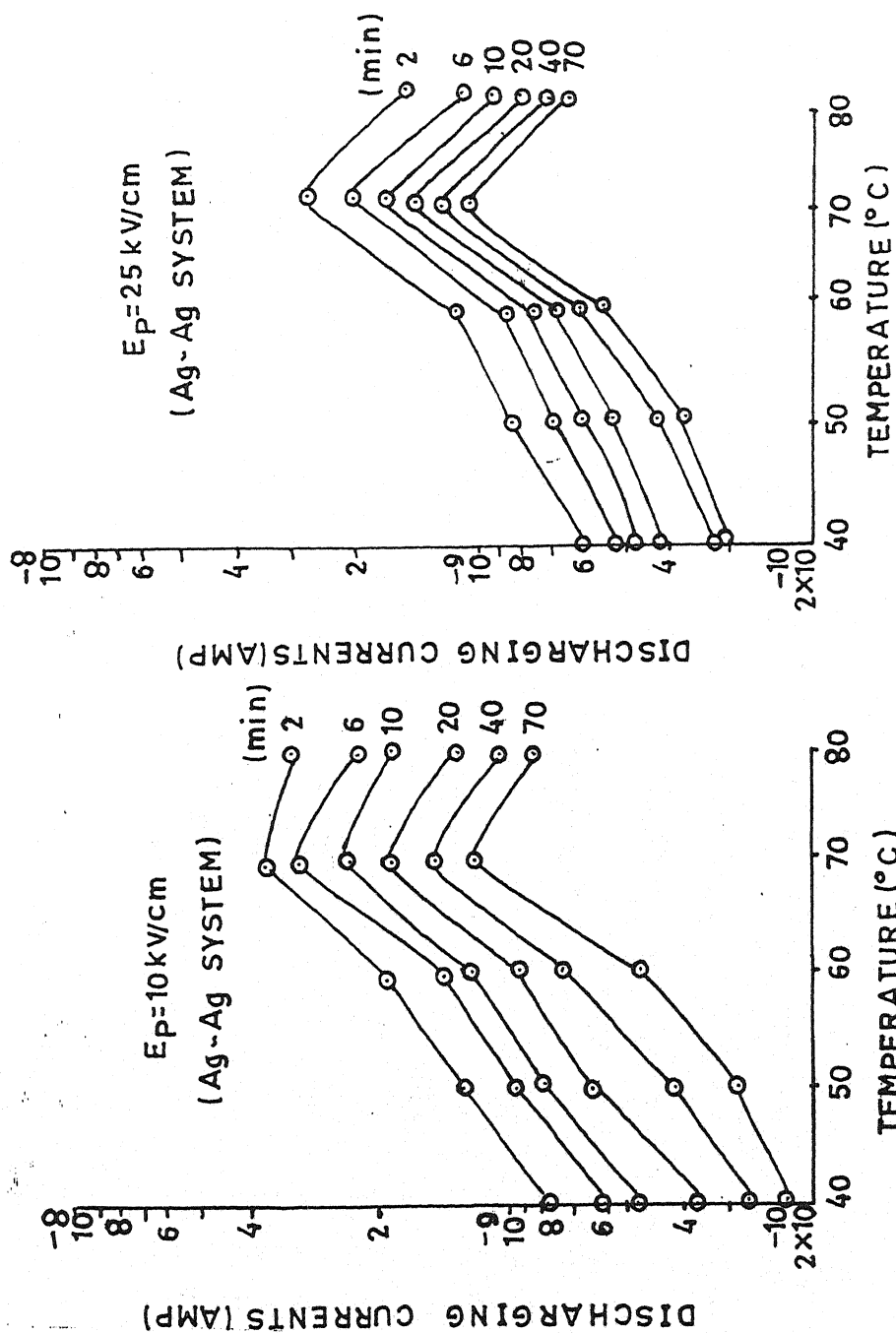


Fig. No. - 5.71

Isochronal Characteristics curves of
figures No. 5.11

Fig. No. - 5.72

Isochronal Characteristics curves of
figures No. 5.12

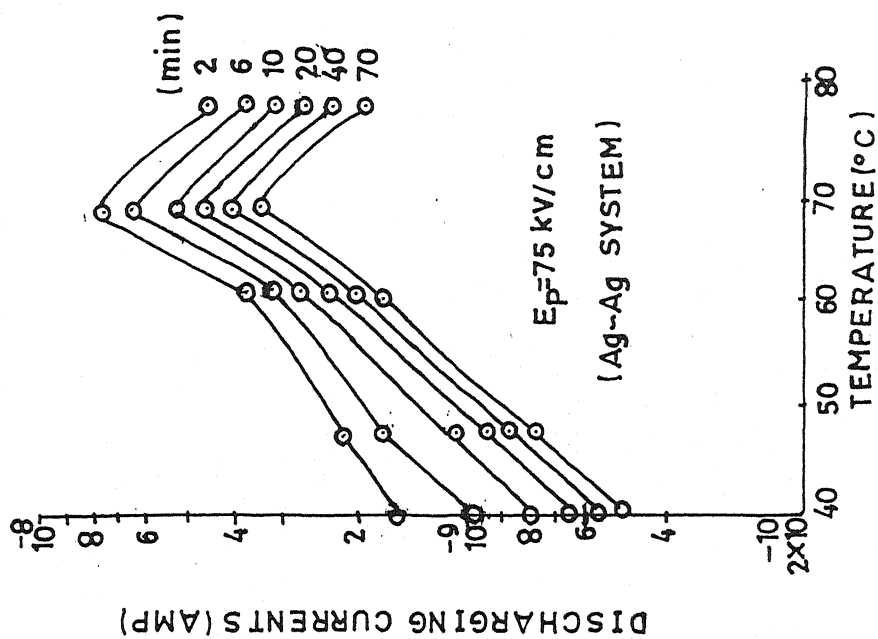


Fig. No. - 5.74
Isochronal Characteristics curves of
figures No. 5.14

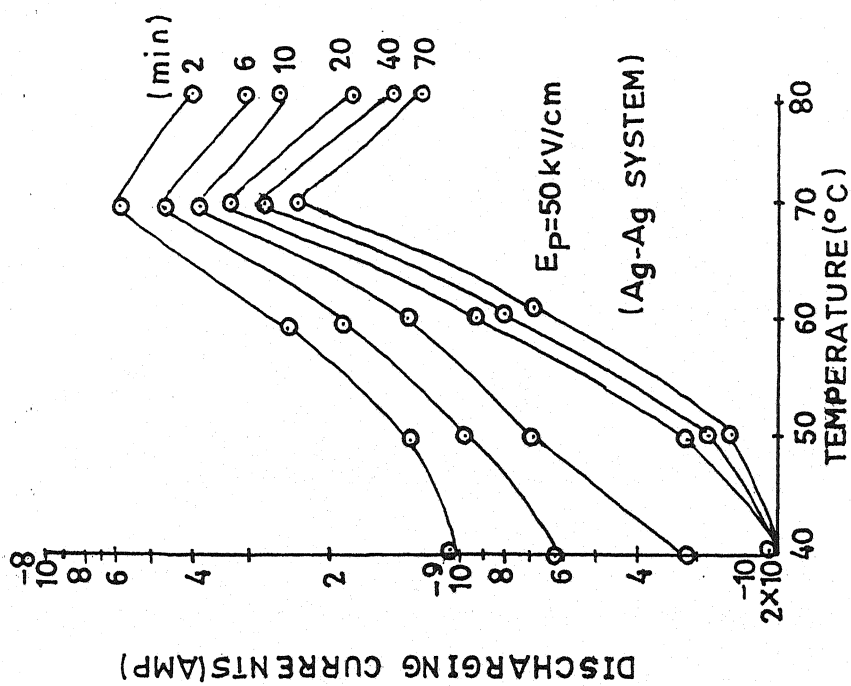


Fig. No. - 5.73
Isochronal Characteristics curves of
figures No. 5.13

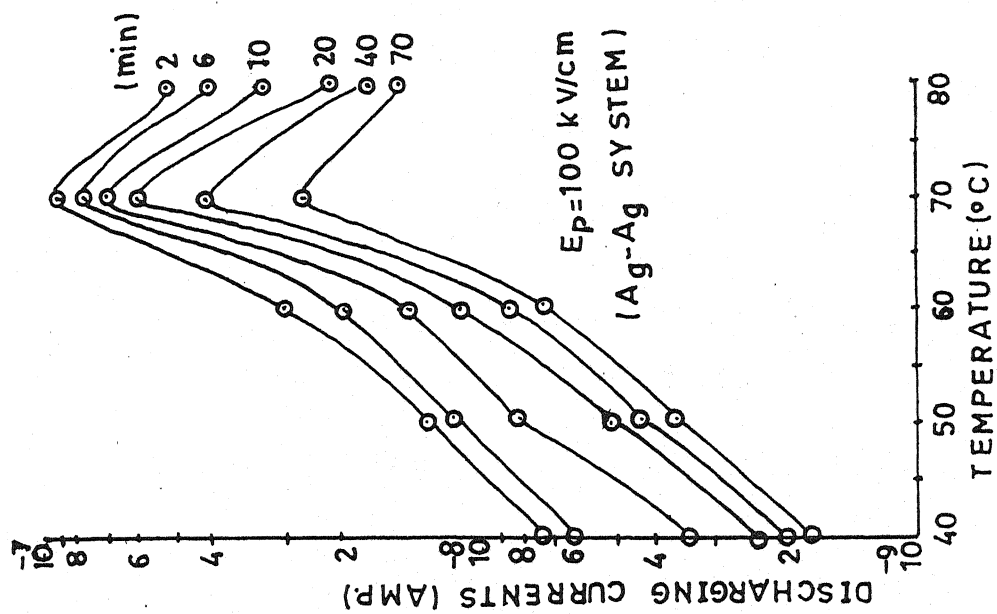
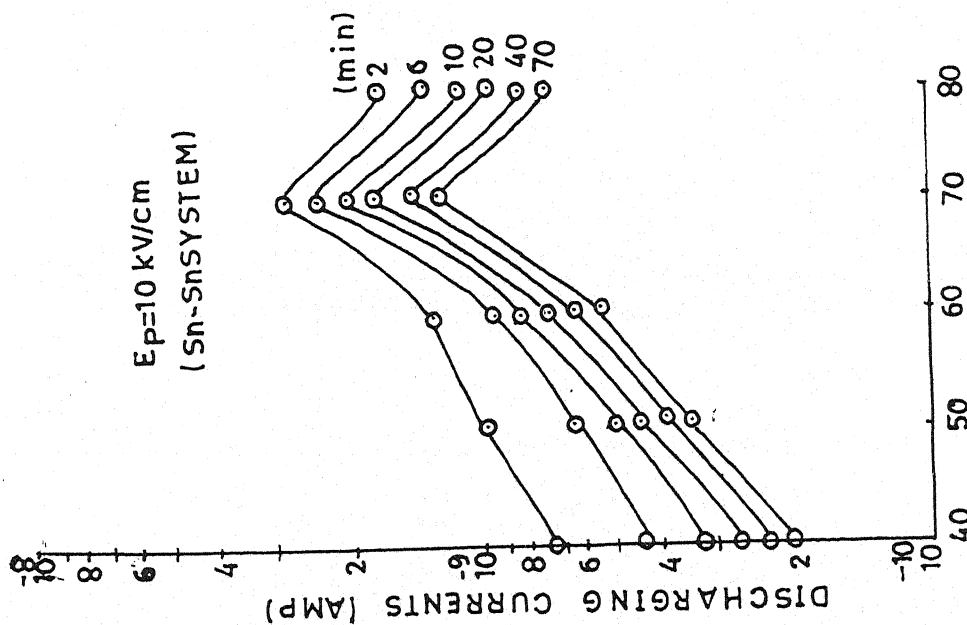
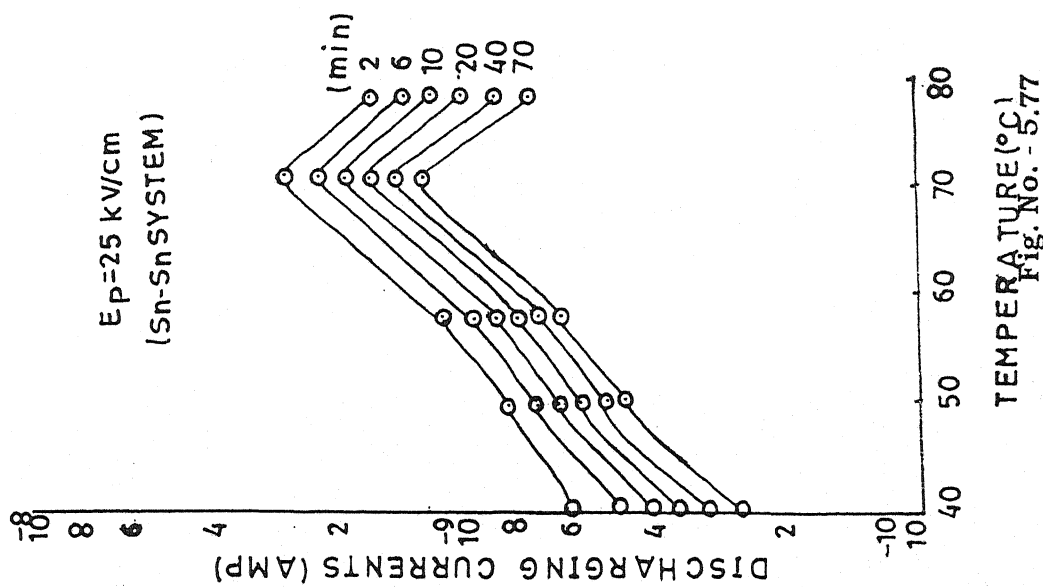


Fig. No. - 5.75
Isochronal Characteristics curves of
figures No. 5.15



Isochronal Characteristics curves of
Fig. No. - 5.76
figures No. 5.16



Isochronal Characteristics curves of
Fig. No. - 5.77
figures No. 5.17

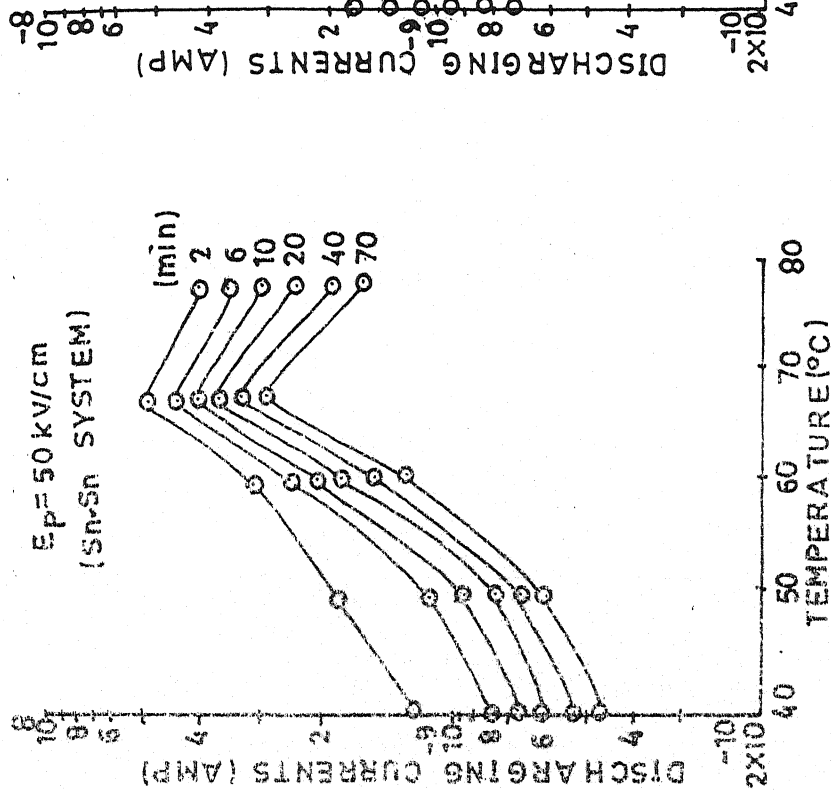


Fig. No. - 5.78
Isochronal Characteristics curves of
figures No. 5.18

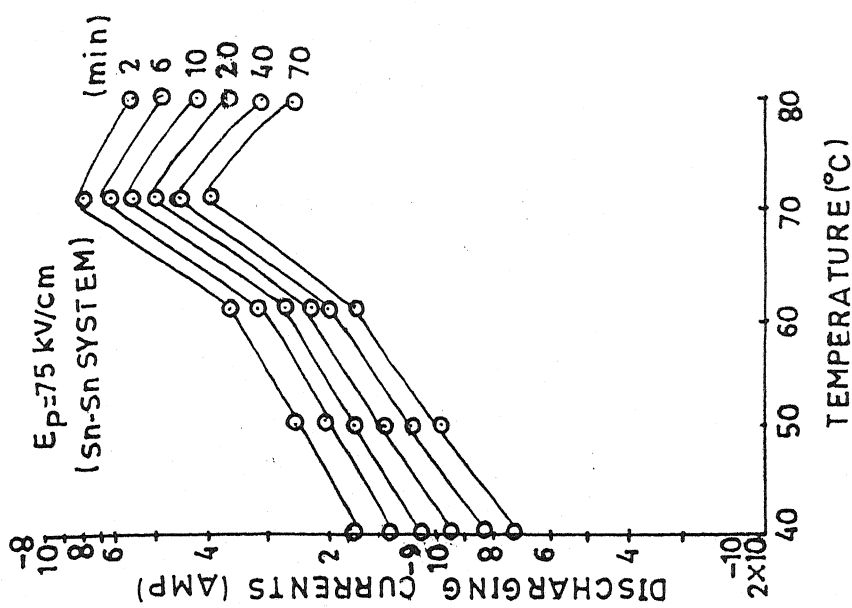


Fig. No. - 5.79
Isochronal Characteristics curves of
figures No. 5.19

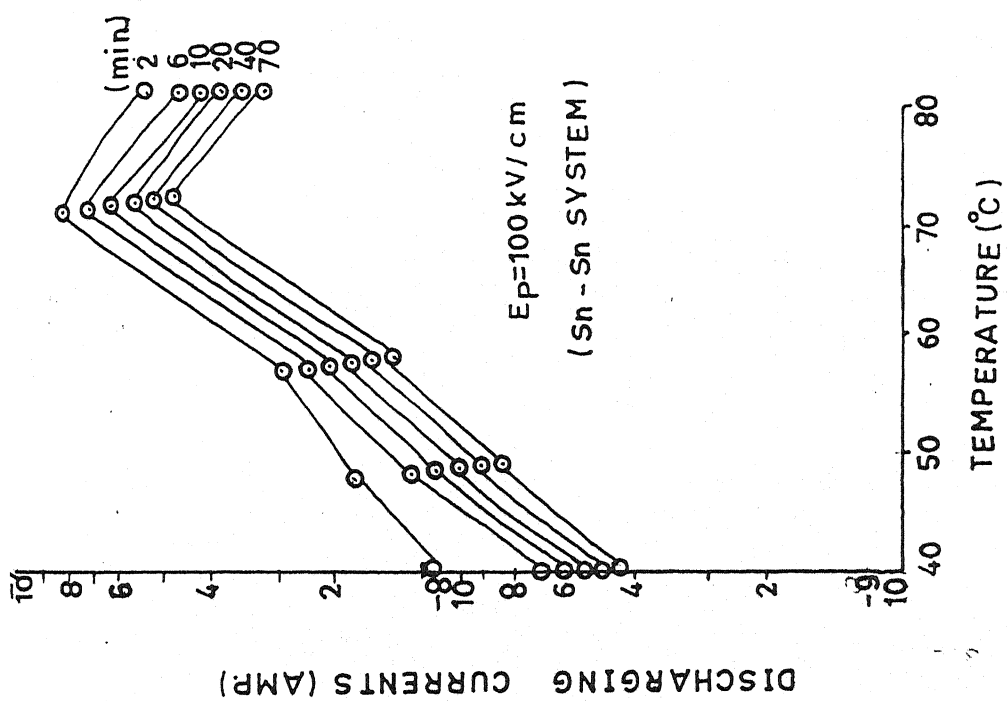


Fig. No. - 5.80

Isochronal Characteristics curves of
figures No. 5.20

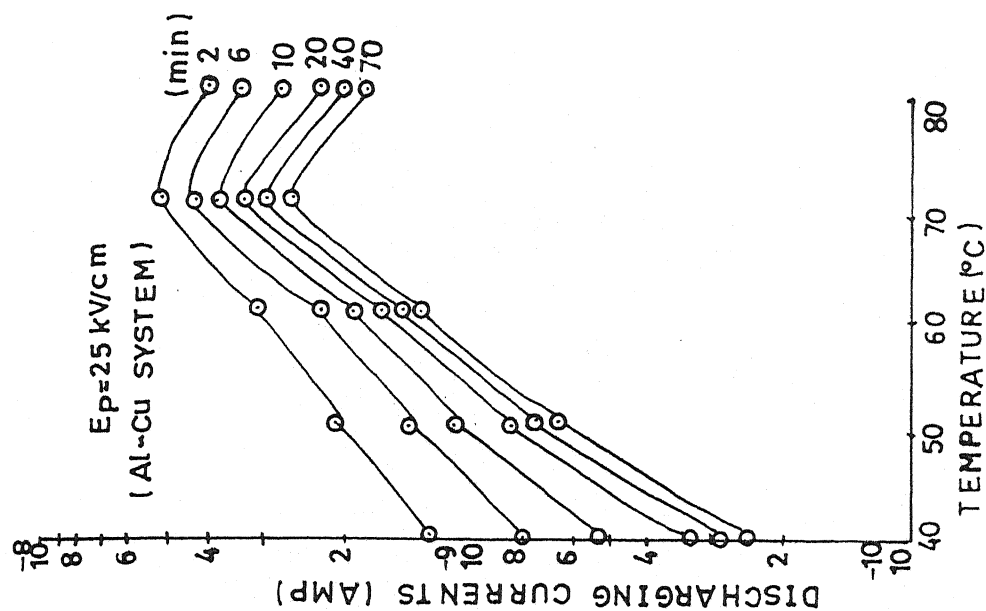


Fig. No. - 5.82
Isochronal Characteristics curves of
figures No. 5.22

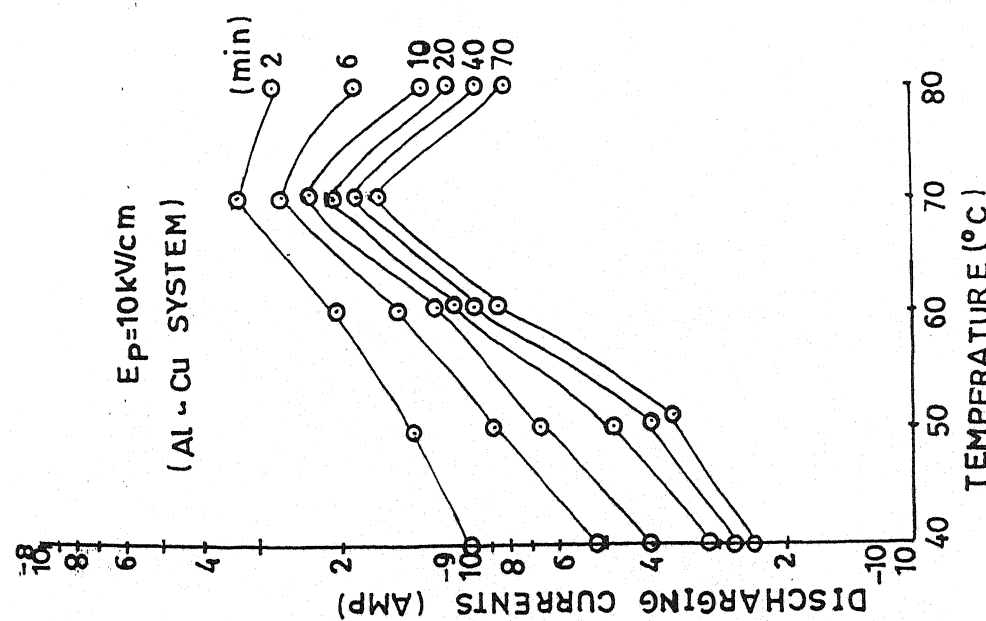


Fig. No. - 5.81
Isochronal Characteristics curves of
figures No. 5.21

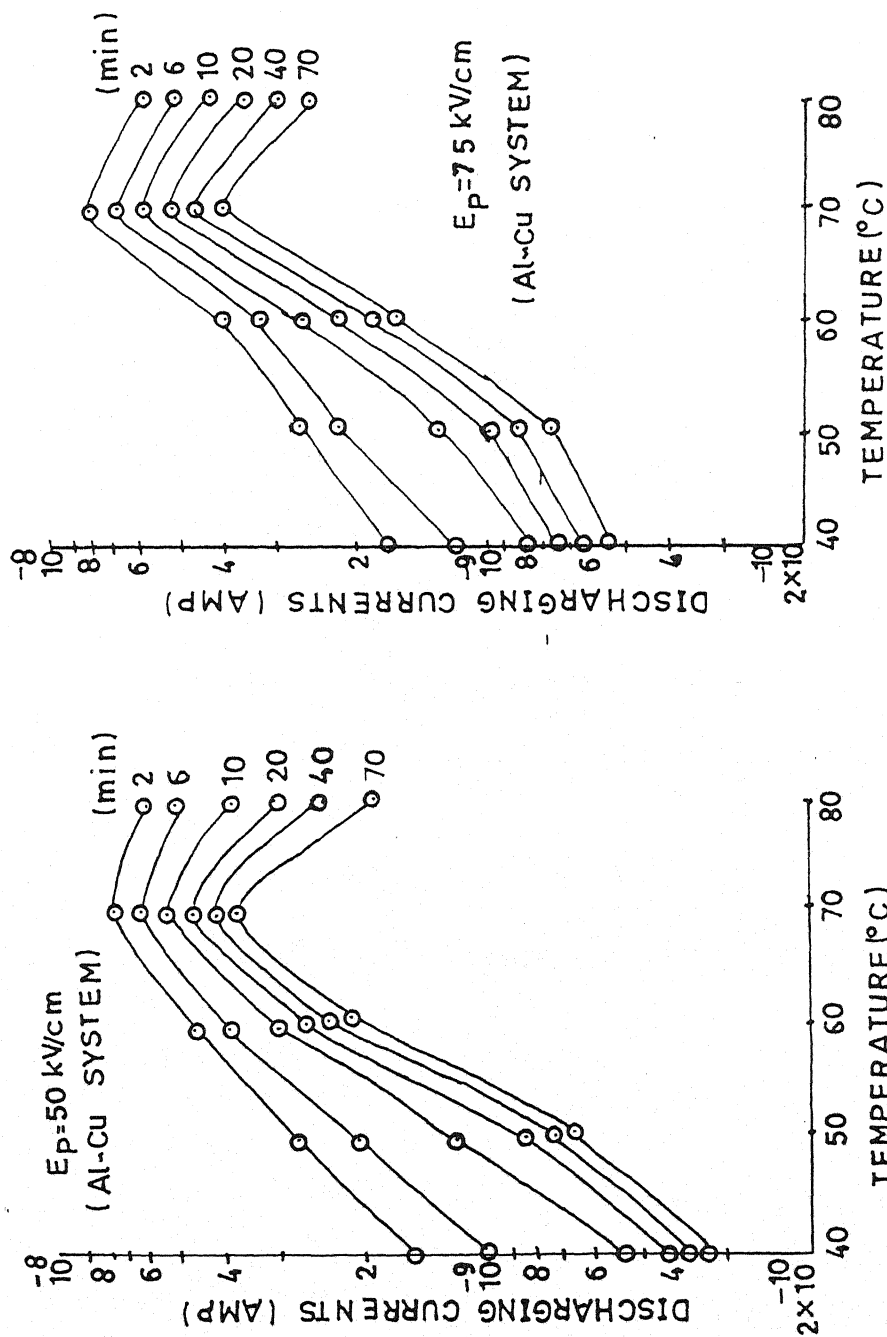
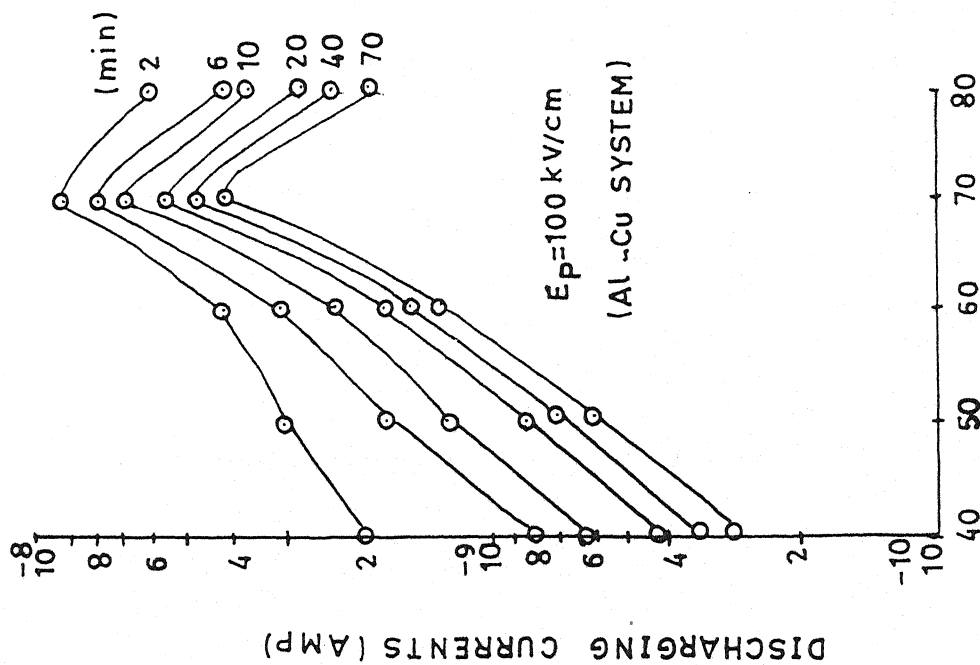


Fig. No. - 5.83

Isochronal Characteristics curves of
figures No. 5.23

Fig. No. - 5.84

Isochronal Characteristics curves of
figures No. 5.24



TEMPERATURE (°C)
Fig. No. - 5.85

Isochronal Characteristics curves of
figures No. 5.25

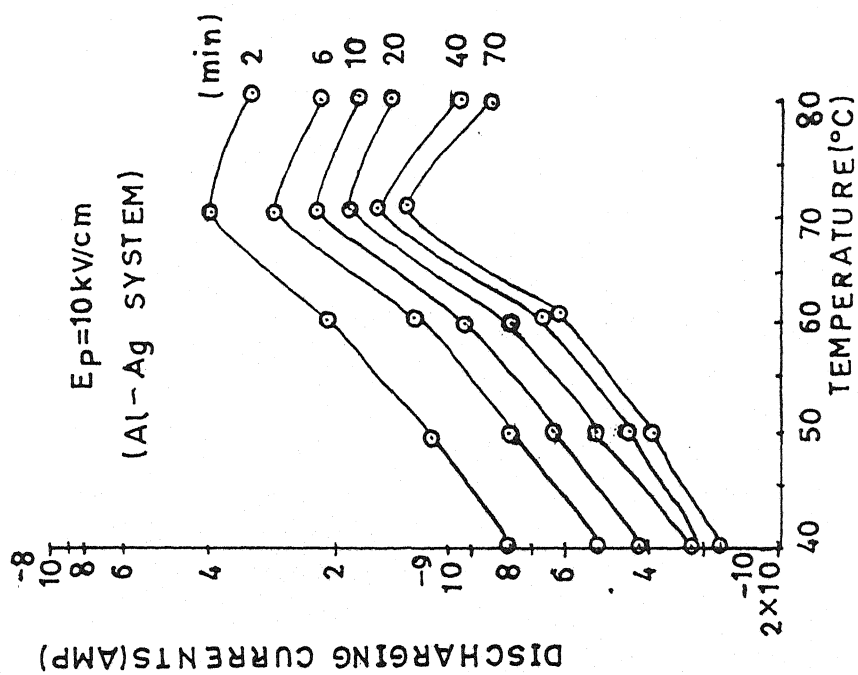


Fig. No. - 5.86

Isochronal Characteristics curves of
figures No. 5.26

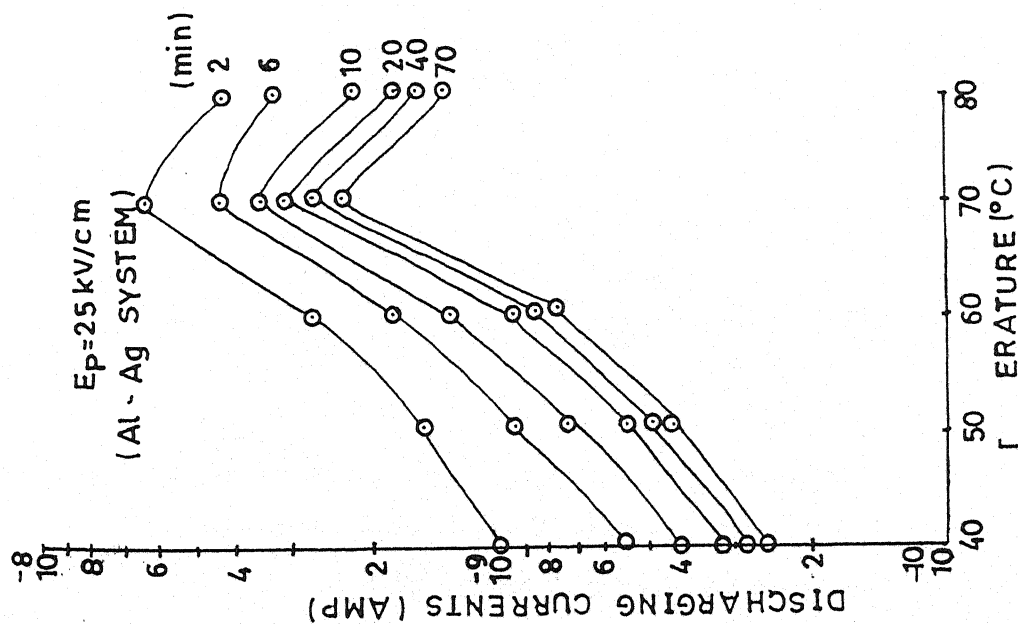


Fig. No. - 5.87

Isochronal Characteristics curves of
figures No. 5.27

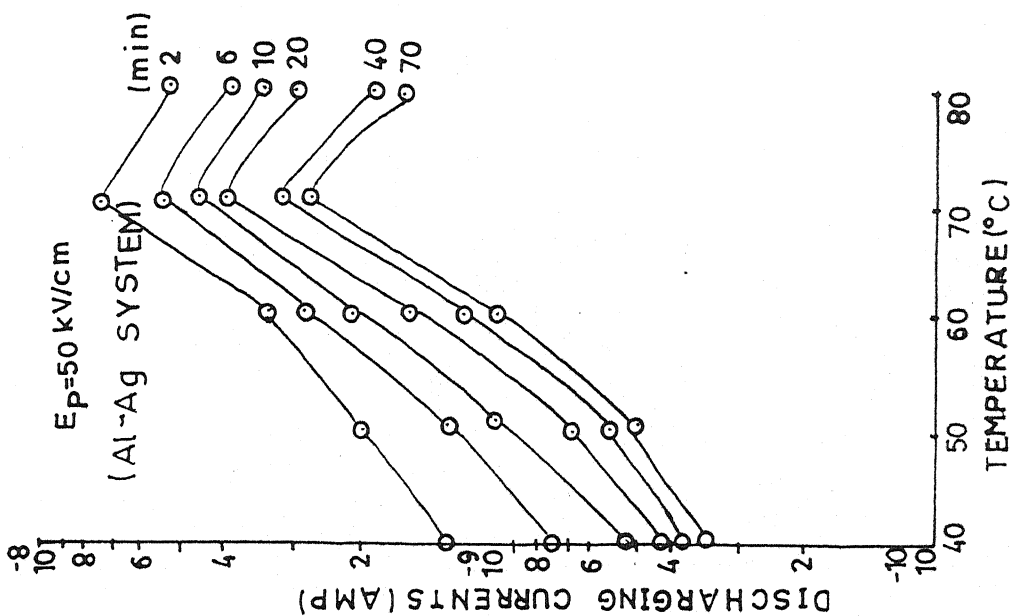


Fig. No. - 5.88

Isochronal Characteristics curves of
figures No. 5.28

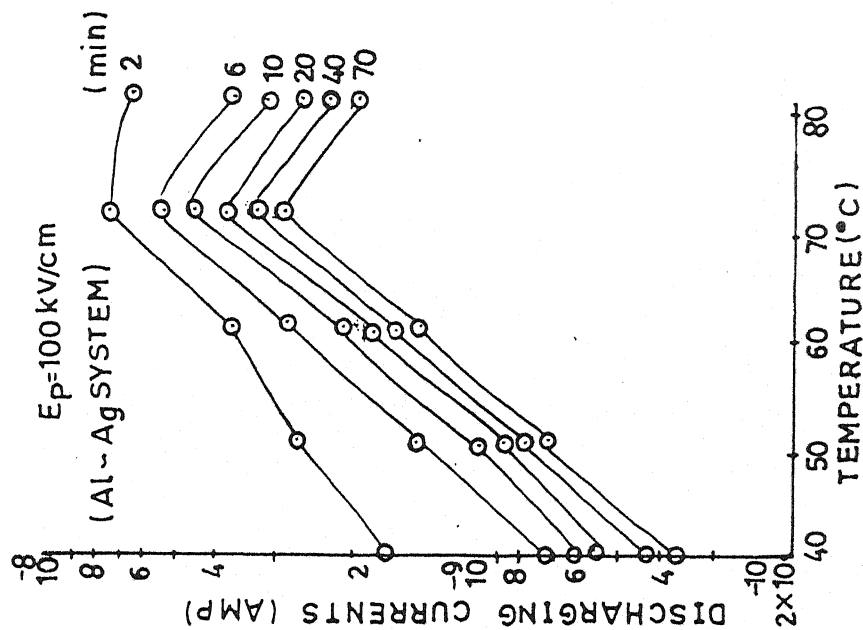


Fig. No. - 5.90
Isochronal Characteristics curves of
figures No. 5.30

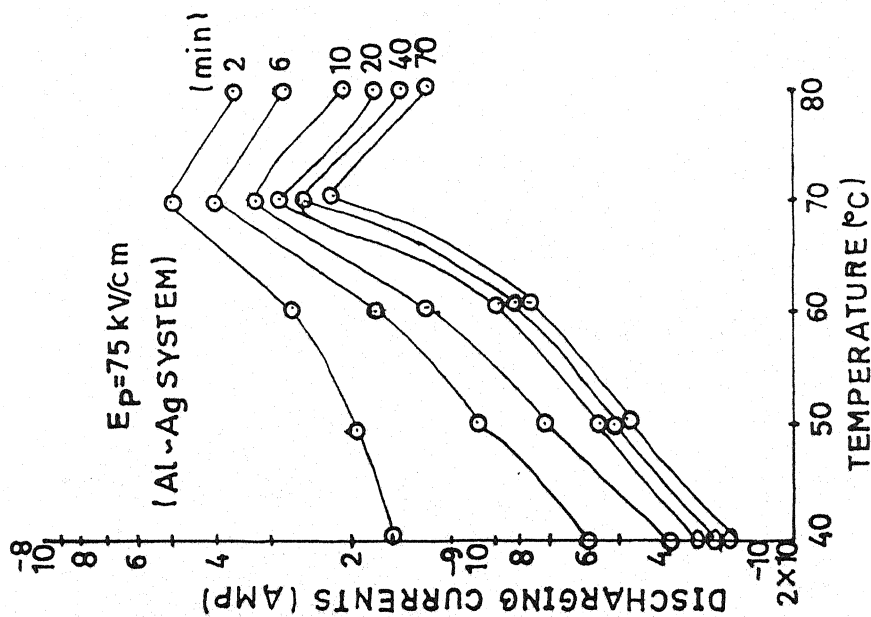


Fig. No. - 5.89
Isochronal Characteristics curves of
figures No. 5.29

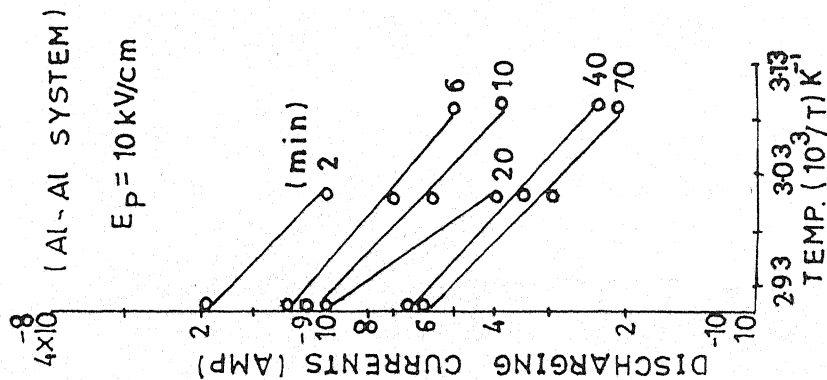


Fig. No. 5.91
Initial rise plots of Fig. No. 5.61

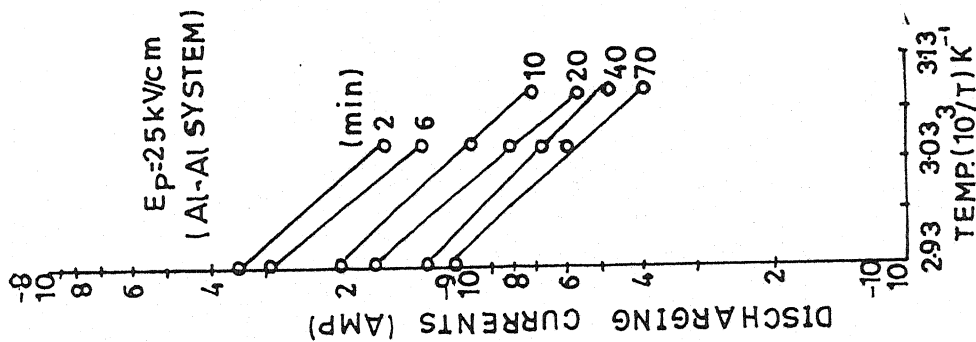


Fig. No. 5.92
Initial rise plots of Fig. No. 5.62

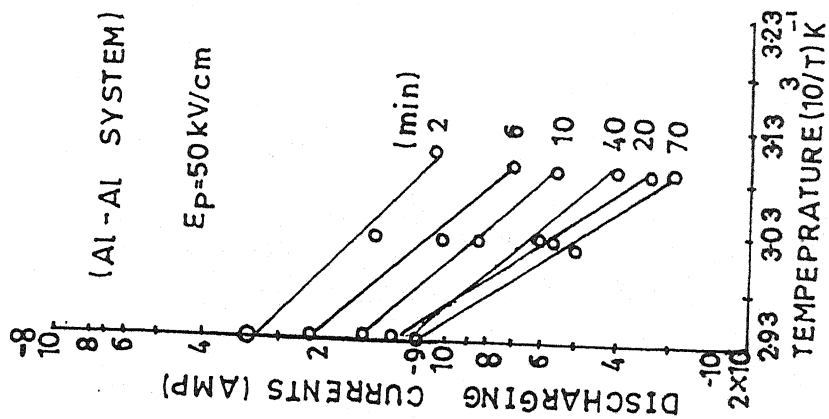


Fig. No. 5.93
Initial rise plots of Fig. No. 5.63

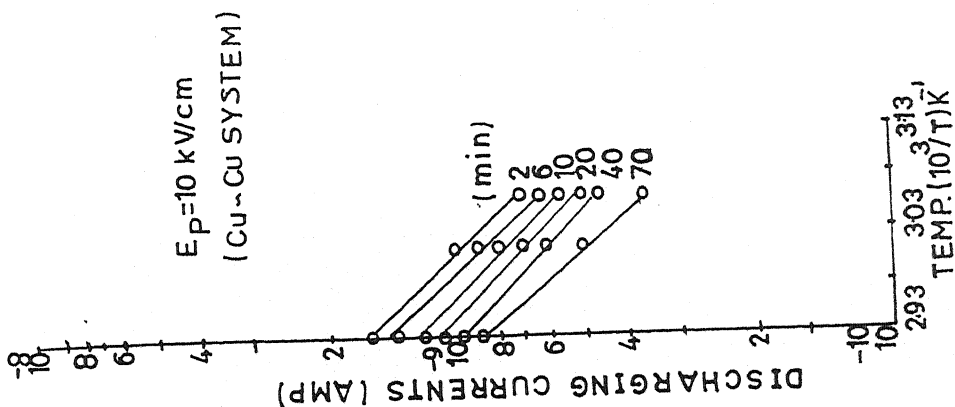


Fig. No. 5.96
Initial rise plots of Fig. No. 5.66

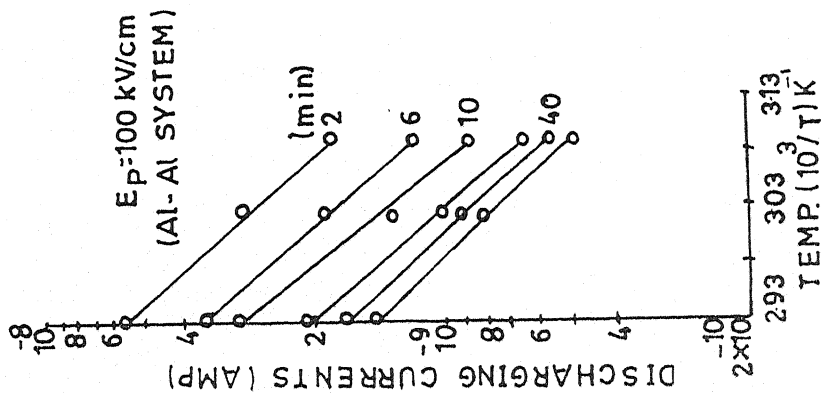


Fig. No. 5.95
Initial rise plots of Fig. No. 5.65

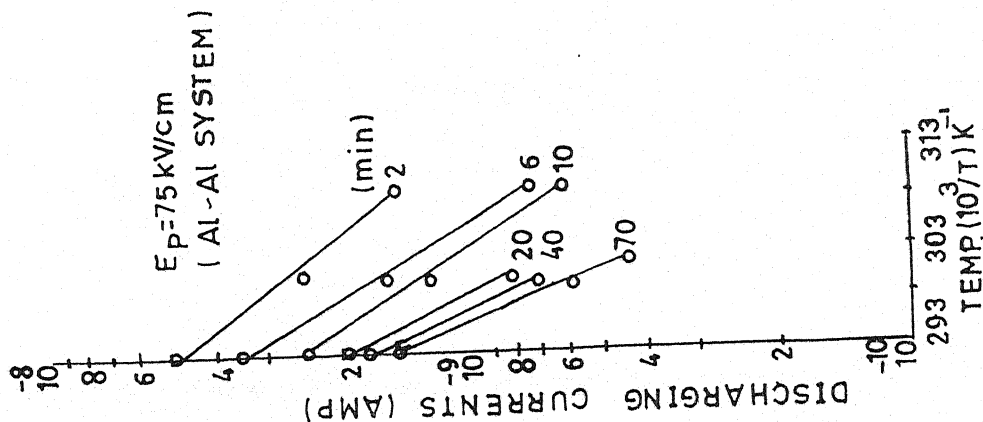


Fig. No. 5.94
Initial rise plots of Fig. No. 5.64

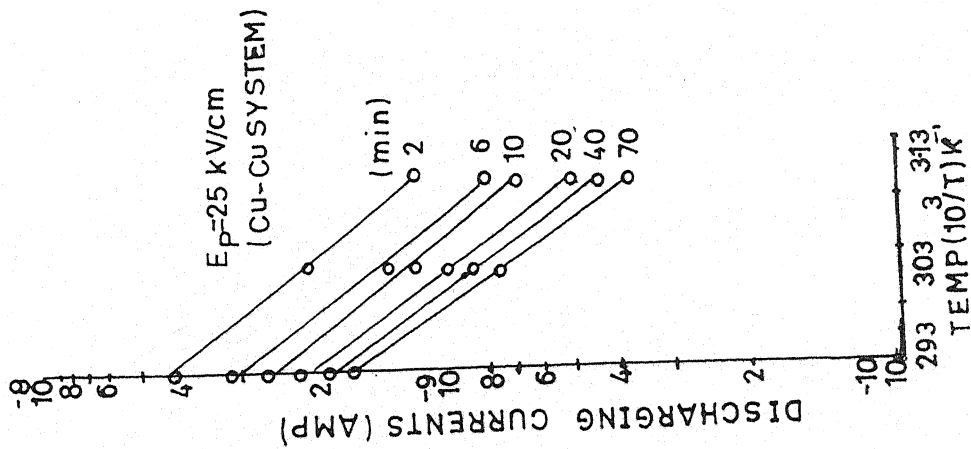


Fig. No. 5.97
Initial rise plots of Fig. No. 5.67

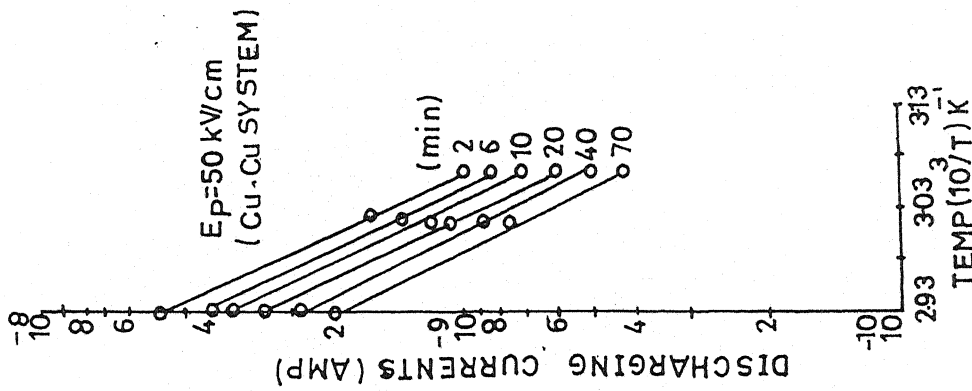


Fig. No. 5.98
Initial rise plots of Fig. No. 5.68

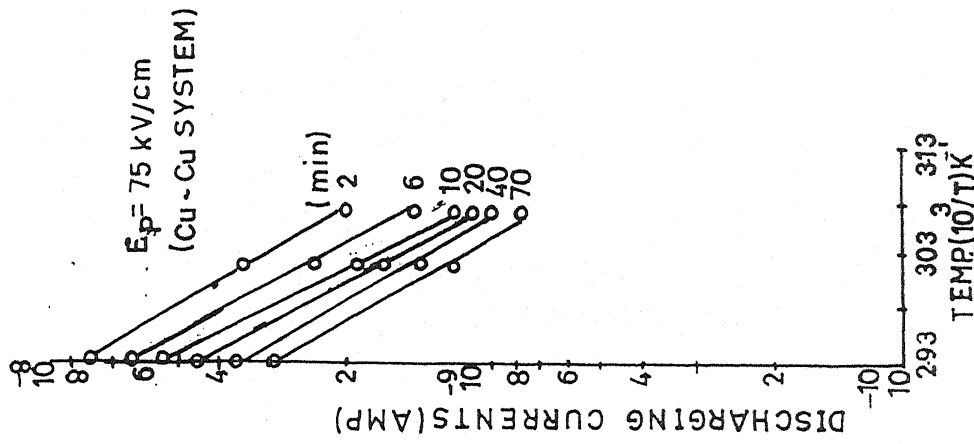


Fig. No. 5.99
Initial rise plots of Fig. No. 5.69

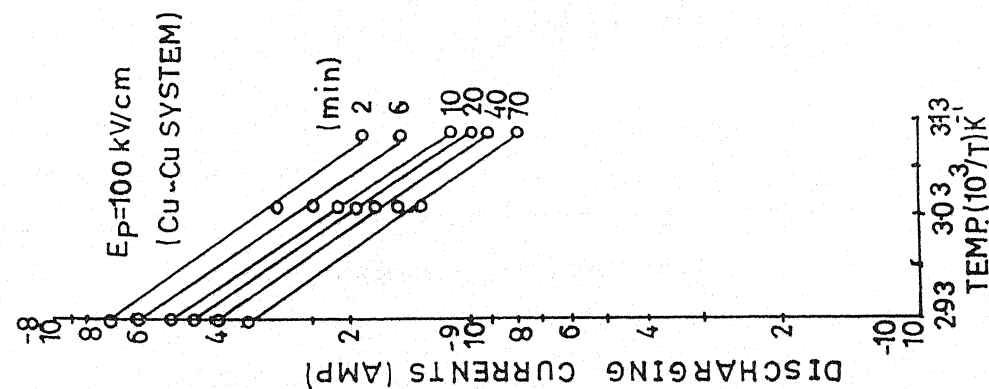


Fig. No. 5.100

Initial rise plots of Fig. No. 5.70

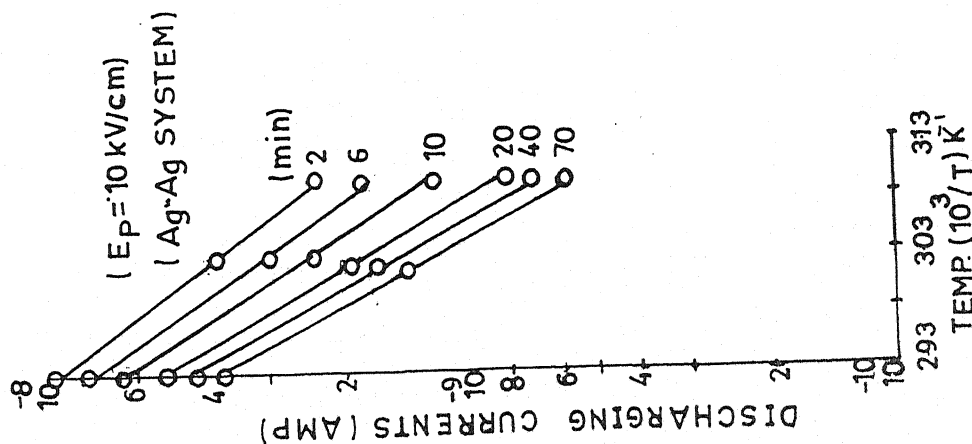


Fig. No. 5.101

Initial rise plots of Fig. No. 5.71

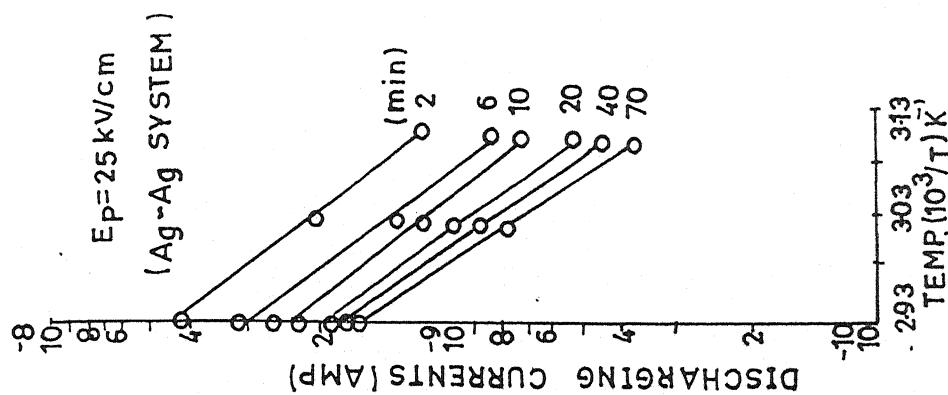


Fig. No. 5.102

Initial rise plots of Fig. No. 5.72

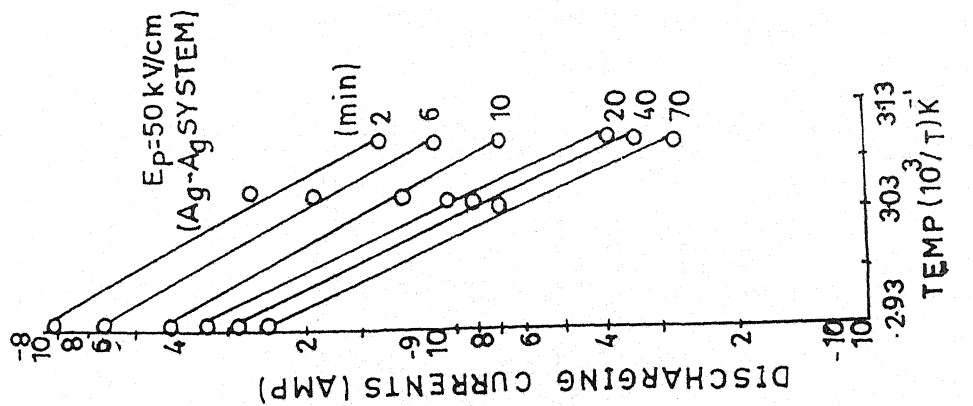


Fig. No. 5.103

Initial rise plots of Fig. No. 5.73

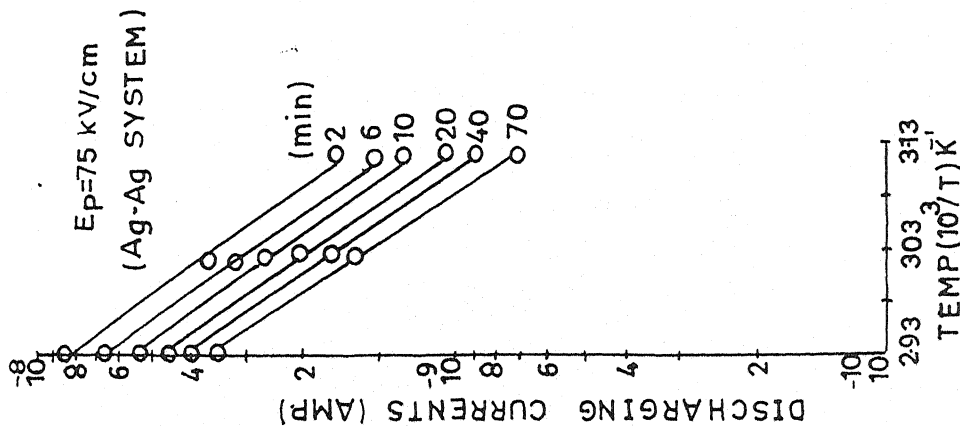


Fig. No. 5.104

Initial rise plots of Fig. No. 5.74

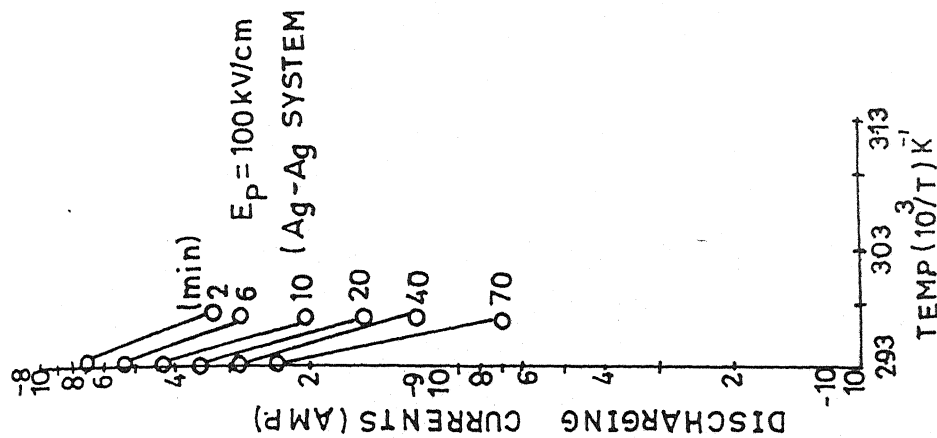


Fig. No. 5.105

Initial rise plots of Fig. No. 5.75

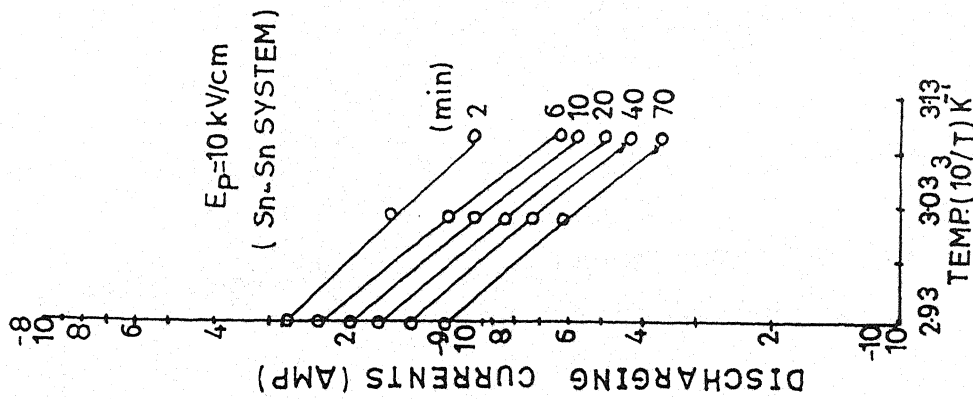


Fig. No. 5.106

Initial rise plots of Fig. No. 5.76

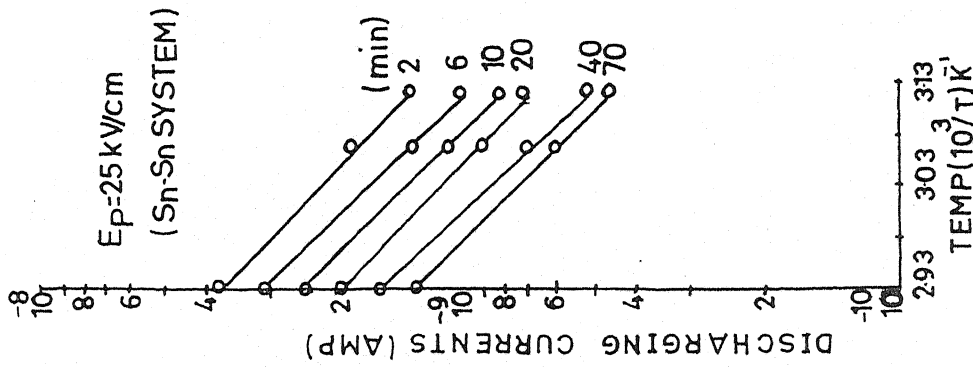


Fig. No. 5.107

Initial rise plots of Fig. No. 5.77

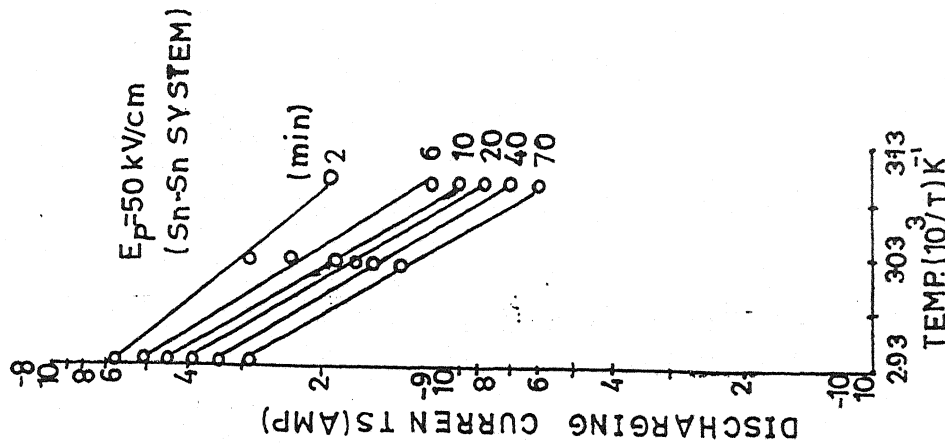


Fig. No. 5.108

Initial rise plots of Fig. No. 5.78

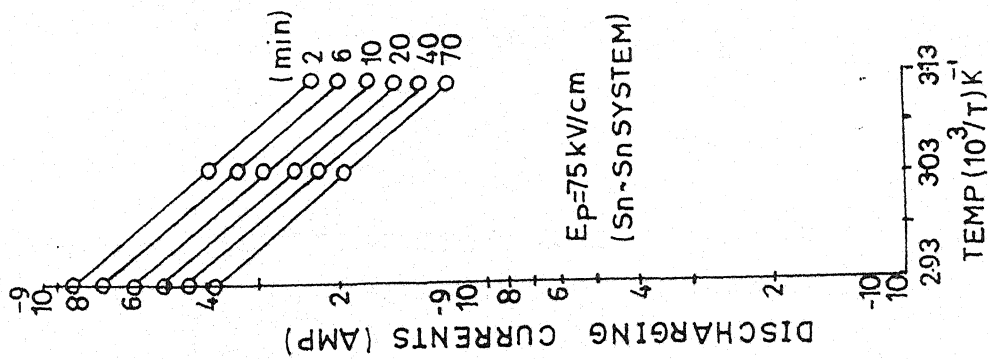


Fig. No. 5.109

Initial rise plots of Fig. No. 5.79

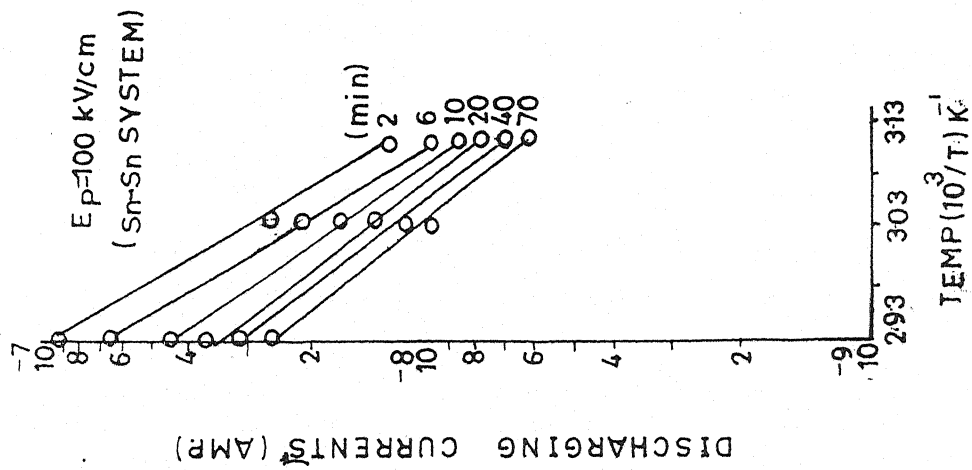


Fig. No. 5.110

Initial rise plots of Fig. No. 5.80

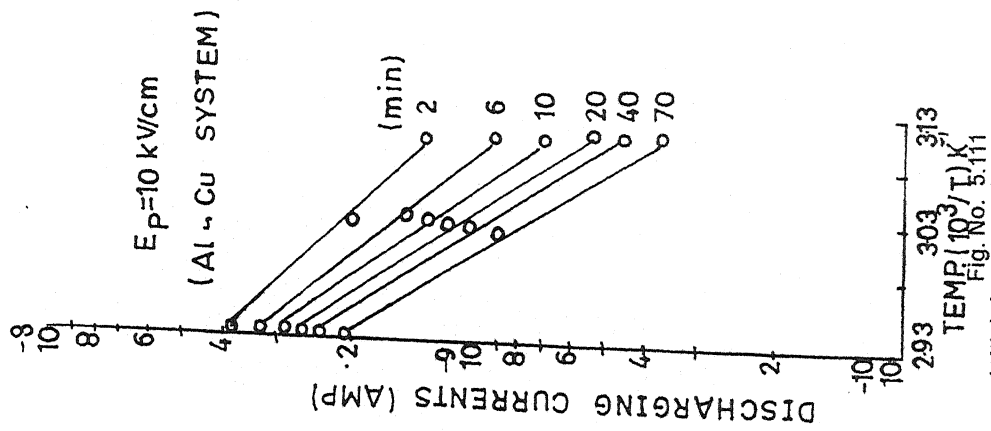
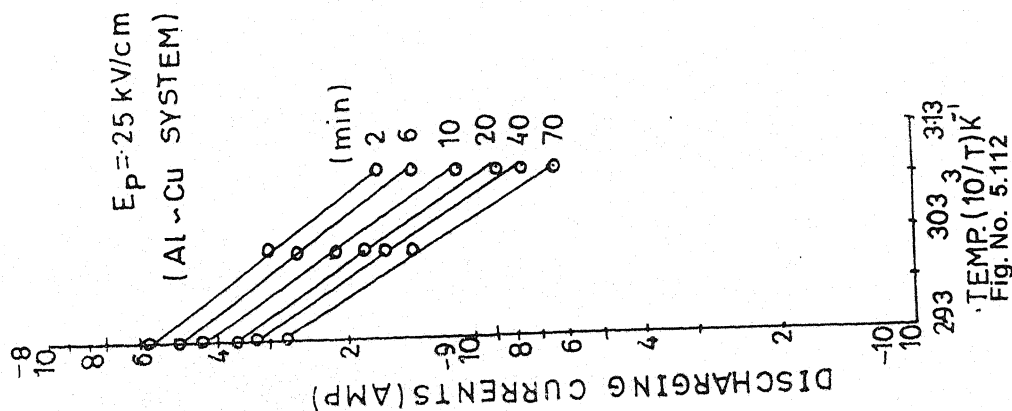
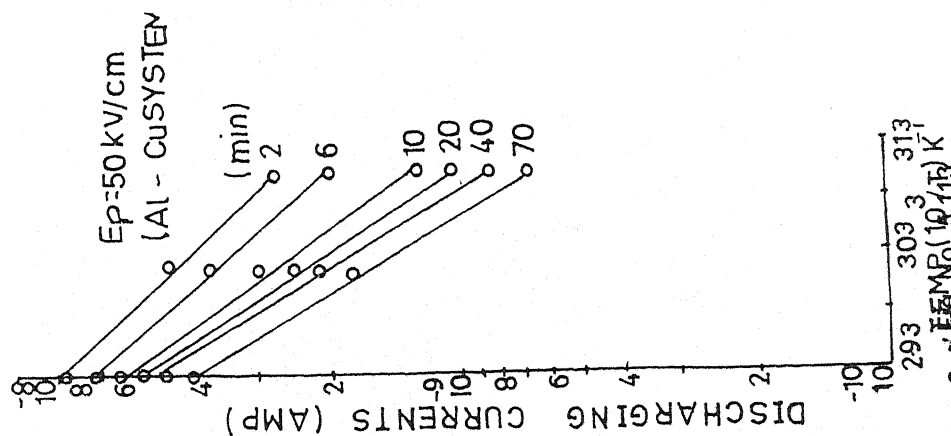


Fig. No. 5.111

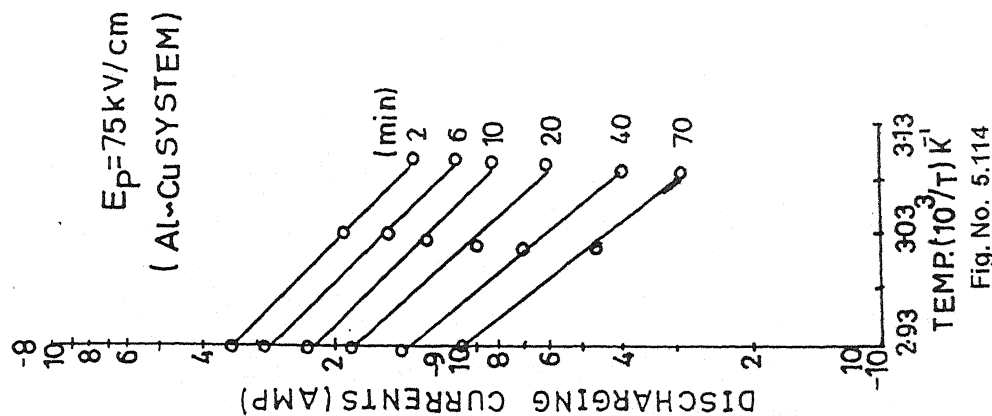
Initial rise plots of Fig. No. 5.81



Initial rise plots of Fig. No. 5.82



Initial rise plots of Fig. No. 5.83



Initial rise plots of Fig. No. 5.84

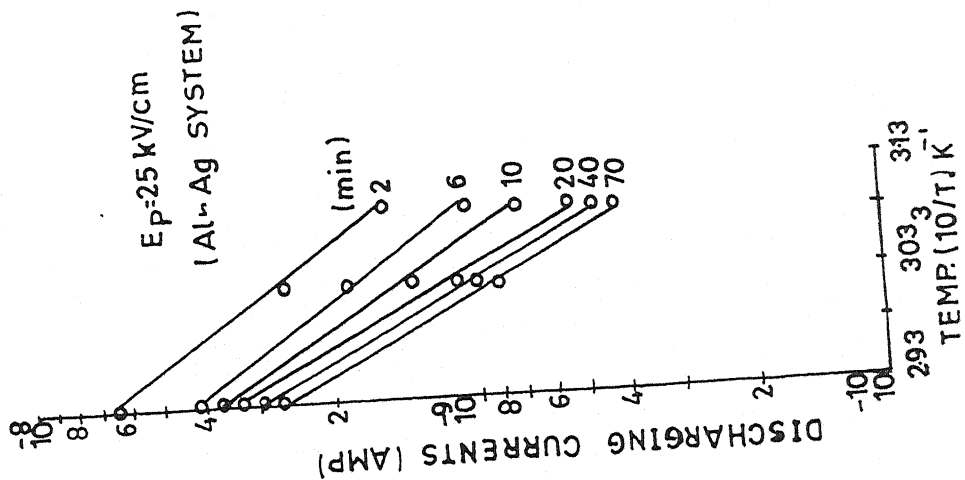


Fig. No. 5.117
Initial rise plots of Fig. No. 5.87

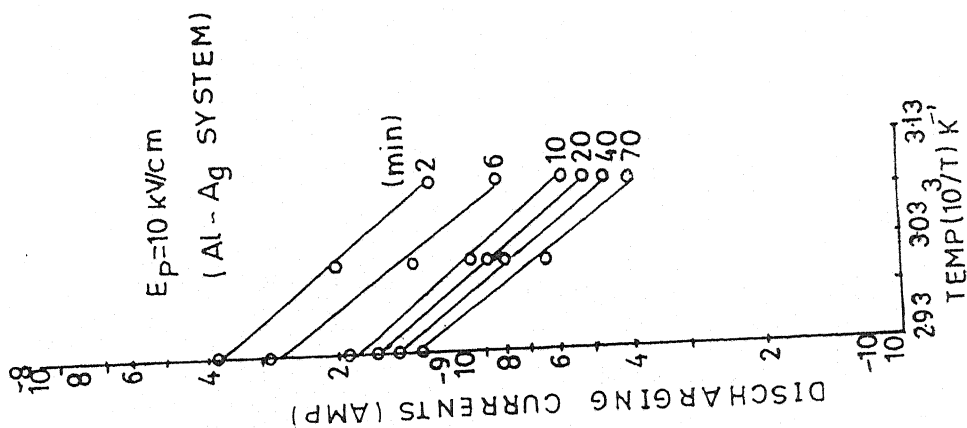


Fig. No. 5.116
Initial rise plots of Fig. No. 5.86

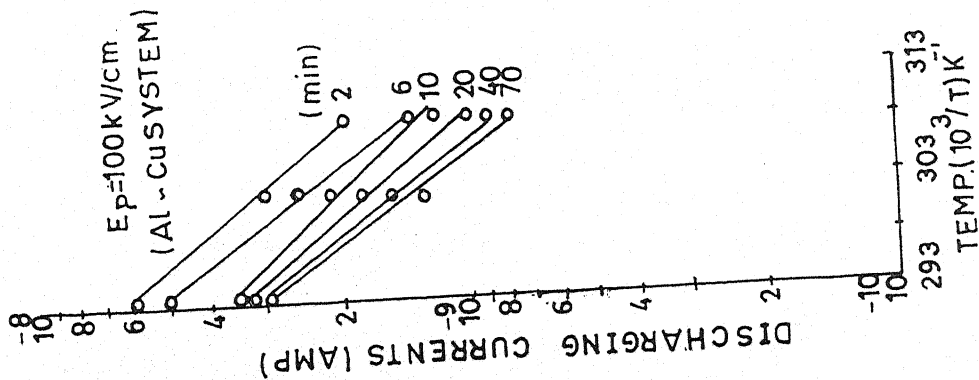


Fig. No. 5.115
Initial rise plots of Fig. No. 5.85

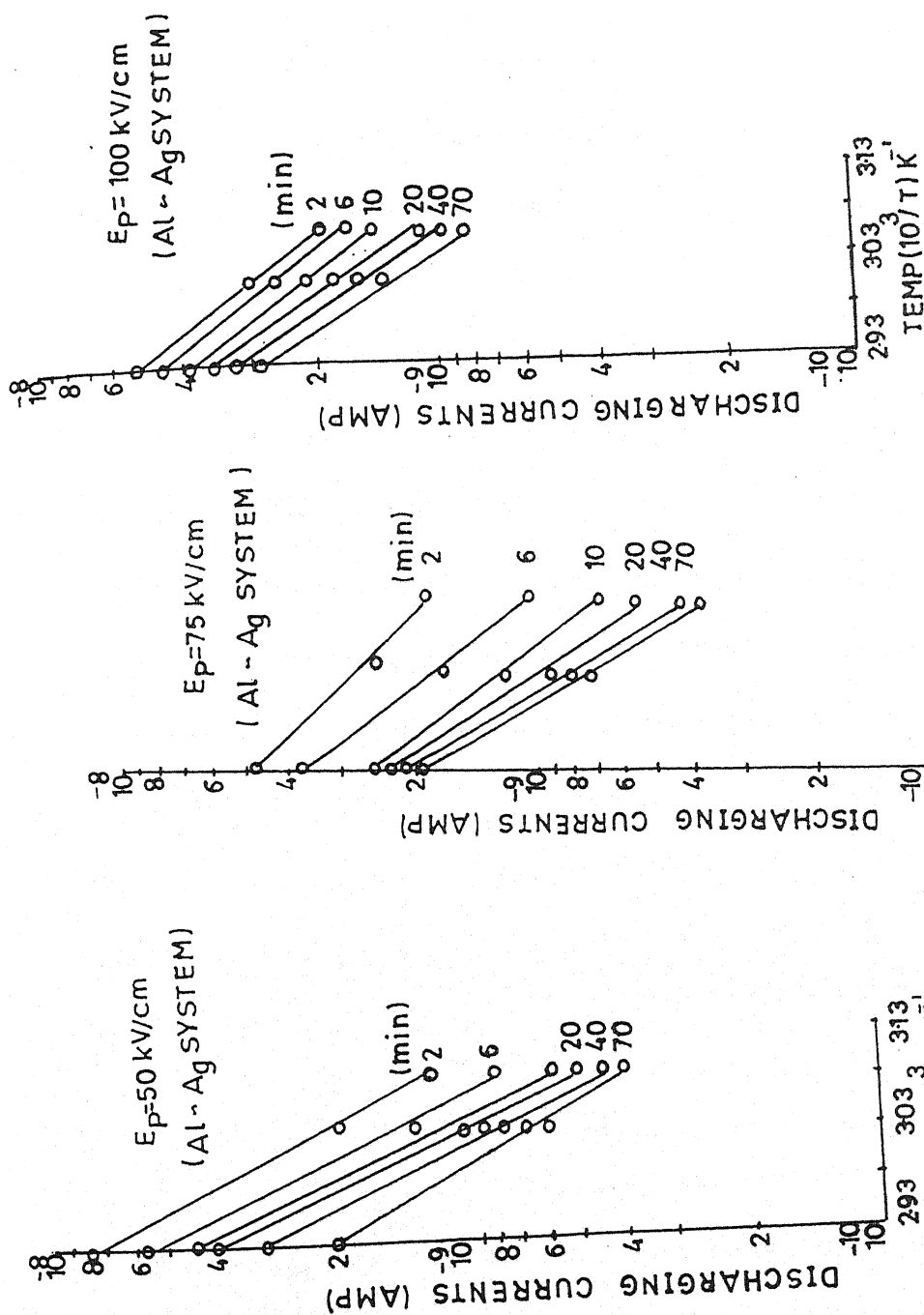


Fig. No. 5.118
Initial rise plots of Fig. No. 5.88

Fig. No. 5.119
Initial rise plots of Fig. No. 5.89

Fig. No. 5.120
Initial rise plots of Fig. No. 5.90

conduction phenomenon can be ruled out on the basis of the experimental facts. The various results summarized here may help to distinguish between various processes. The polarization of polymeric materials may be due to dipolar orientation, space charge formation, trapping in the bulk, tunneling of charges from the electrodes to empty traps, or hopping of charge carriers from one localized state to another. The most probable mechanism responsible for the observed currents in the dielectric can in principle be determined by considering the variation of such currents with temperature, time, fields and electrode materials, etc.

In fact, the charging and discharging currents observed in most of the polymers investigated show the expected behaviour of a dipolar relaxation mechanism in all aspects, i.e., linear dependence on field strength and independence of thickness, field polarity, electrode material, method of sample preparation and additives, non-interfering with the macromolecular motions. The observed time dependence is also compatible with such a dipolar process since the relaxation phenomena in polymers are generally characterized by a distribution in relaxation times leading in the usual formation of Cole and Cole [25] to a t^{-n} transient current.

So far as the nature of the trapping sites are concerned, there is, and has been much speculation on this topic, but at present, it is generally concluded that charge trapping is primarily due to the basic polymer

structure consisting of various traps. This, one can envisage physical traps in cavities due to defects and free volume in the bulk polymer structure, in bonding energy resulting from a polarization of the surrounding molecules. Another type of trap or hopping site may be due to chemical heterogeneities in the polymer structure, such as C=O groups may represent at least a major fraction of the localized centres by which the transport of the injected electrons takes place. The above consideration indicates that the observed discharging current in the present case may be partially be due to dipole orientation and partially due to space charge mechanism.

The current in the time domain for the short time region is characterized by the relation

$$I(t) \propto t^{-n}, \quad 0 < n < 1; \quad t \ll 1/W_p \quad \dots (5.1)$$

i.e. the frequencies which are larger than the loss peak frequency W_p , and for the long time region

$$I(t) \propto t^{-1-p}, \quad 0 < n < 1; \quad t \gg 1 > 1/W_p \quad \dots (5.2)$$

with logarithmic slope steeper than unity. The two power laws determine the time domain response of dipolar system in which a loss peak is seen in the frequency domain. Similarly, behaviour is observed in carrier dominated systems, however, low frequency dispersion below a frequency W_c , which corresponds to long time region is described by the above power laws with small value of n .

Let $n = 1-p$, with p close to unity for low frequency dispersion region.

The long time response of charge carrier system will then be denoted by

$$I(t) \propto t^{-1-p}, \quad p = 1; \quad t \gg 1/W_p \quad \dots (5.3)$$

which corresponds to a very slow time varying current.

The complete representation of the universal dielectric response in the time domain covering both dipolar loss peaks and strong low frequency dispersion associated with the charge carrier dominated system may be represented by

$$I(t) \propto t^{-n}, \quad 0 < n < 2 \quad \dots (5.4)$$

with the exponent n taking value in different ranges at long and short time respectively [26]. There appears a process of thermal activation over the whole range of temperature. It is evident from Figs. 6.11 to 6.18 that both charging and discharging currents obey the well known expression.

$$I_a(t) = A(t) t^{-n} \quad \dots (5.5)$$

where I_a is the absorption current, t the time after application or removal of the external field and $A(t)$ a temperature-dependent factor. It is found that discharging current has been characterized with logarithmic slope smaller in magnitude than 1 ($n < 1$) during the range of short times, and then goes to the longer time region (where the slope is steeper, with n lying between 1 and 2). Similar to discharging, the charging current has also been found to

be characterized with $n < 1$, in short time region, however, at longer times this current tends to approach the steady state conduction current.

In the present case, n values for shorter time region were observed to vary from 0.5–0.8 and for long time region these values are observed to vary from 1.53–1.78. Also, discharging currents vary linearly with the field strength characteristic of dipolar mechanism. These findings indicate that the dipolar polarization is operative in the present case. The nature of current in the observed temperature range may attribute a dipole process involving structural units with a small dipole moment and a broad distribution of relaxation times, this predominates over any hopping mechanism. The partial dipolar nature of sample is expected to manifest itself in the form of a peak in the isochronals. The isochronals constructed from current-time characteristics are found to be characterized with a peak located around 75°C .

Although the dielectric response is commonly associated with orientation of permanent dipoles, it is undesirable that hopping charges of either electronic or ionic nature may give rise to a very similar dielectric behaviour. The important distinction lies in the degree of localization of these carriers. An electron or an ion confined to hopping between two preferred positions is indistinguishable from a dipole, while a distinctly different situation arises where the carrier is free to execute hops over finite paths, some of which may eventually extend all the way from one electrode

to the other. We have to consider four components of the current in such a system, (a) the current controlled by various polarization mechanisms, (b) the current controlled by the charging of the capacitor through a resistance, R , (c) the conduction current, which a hundredth of a second. The third component is due to formation of space charge. The residual former current is referred to as bulk current, which may be ionic, electronic or both. Struik [27] showed that solid like polymers are not in thermodynamic equilibrium at temperatures below their glass transition. For such materials, free volume enthalpy and entropy are greater than they would be in equilibrium state. The gradual approach to equilibrium affects many properties, for example, the free volume of the polymer may be decreased. The decrease in free volume lowers the mobility of chain segments and also charge carriers. The decrease in mobility may be expected to reduce DC conductivity. At higher electric fields, the change in mobility may take place faster than at lower fields and recombination of charge carrier may be more.

The electrode polarization predicts the strong dependence of the electrode material on the decay of transient currents [28]. Moreover, uniform and electrode polarization require the charging and discharging currents at a particular instant to vary linearly with charging field [29-31]. Furthermore, the superposition principle according to which the charging and discharging currents should be equal but opposite at equivalent instants is supposed to be valid in such type of polarization. However, in

the case of space charge polarization the superposition principle is not obeyed and the charging and discharging currents depend more strongly on the applied field [32]. The convincing criterion of the validity of the superposition principle can be provided by the discharging and charging currents ratio of various times, where the charging current value is obtained by subtracting the steady state component [33,34]. A value of unity throughout the transients would indicate the origin of the transients due to uniform or electrode polarization. In the present case, the charging current continued to decay although slowly, even at the end of charging process. Under such circumstances, accurate estimation of steady state current was not possible and hence the reliable evaluation of discharging/charging ratio could be made. However, the charging and discharging at various times after the application or termination of charging field are found to follow the power law dependence on field.

The charging and discharging currents observed in PVDF are also expected to show the behaviour of dipolar relaxation mechanism. In the case of transients governed by space charge, the peak in the current time curve should occur at a time

$$t_m = \frac{0.786 d}{\mu E} \quad \dots (5.6)$$

where E is the applied field, d is the sample thickness and μ the carrier mobility. To have a rough estimate of the time at which this peak should occur, we used the values d , E and μ to be $20 \mu\text{m}$, 100 kV/cm and

$10^{-11} \text{ cm}^2/\text{V}$. It was found that t_m is approximately equal to $3.782 \times 10^3 \text{ s}$.

Thus, there is possibility of space charge relaxation occurring at sufficiently longer times. The above considerations indicate that the observed currents in the present case may partially be due to dipolar orientation and partially due to space charge mechanism.

Discharging current measured at various prescribed times versus temperature plots are shown in Figs. 5.10 to 5.30. It is clearly seen that the various isochronals are characterized by a single peak located at $\sim 75^\circ\text{C}$. However, no shift is observed in the peak temperature with time of observation. It is observed that the peak temperature decreases with increasing time and is a characteristic of relaxation process. Similar qualitative behaviour is observed in the other samples. The isochronal peak is broad and probably it contains several minor processes, one of which may be associated with the glass transition of the polymer and the other may be due to thermal release of trapped carriers.

It is rather difficult to specify the origin of charging/discharging currents unambiguously from the time dependence alone. However, the various facts including the weak polar structure of polyvinylidene fluoride, observed values of n , and thermal activation of current over a certain temperature range as observed in the present case indicate that the space charge due to accumulation of charge carriers near the electrodes and trapping in the bulk may be supported to account for the observed current.

The decay of current in the long time region for different samples indicate the existence of energetically distributed localized trap levels in the sample. It seems that at shorter times only shallow traps get emptied contributing to stronger current. However, at longer times, deeper traps with long detrapping times release their charges and the current decays at longer times. As temperature increases, mobility of carriers also increases, hence, all the deeper traps are filled. Release of a large number of charge carriers from the traps during the process may then result in high return rate of carriers leading to blocking of electrode causing a decrease in current. The charge injection from electrodes with subsequent trapping of injected charges in near surface region gives rise to homospace charge and the thermal release of charge carriers from the traps. Before the trapped space charge injected at higher fields is thermally released, a space charge barrier is presented to the electrode which suppresses the entrance of charge carriers into the sample. Thus, the observed current remains smaller than its corresponding value.

The polymer films are known to be a mixture of amorphous and crystalline regions. The presence of localized states may lead to the localization of injected charge carriers giving rise to the accumulation of trapped space charge [35]. The hopping mechanism is considered to lead to the increase in activation energy. However, in the present case, the activation energy is observed to decrease with increase in time. Such

behaviour suggests that hopping of charge carrier is not expected in the present case.

As PVDF is a polar polymer, the probability that charge carriers are present in it, the only charges could come from those injected through the electrodes. The injected charges are trapped at different trapping sites leading to a space charge which fundamentally influences all the transport phenomena and the effects at the electrode space-charge-limited currents may also determine the transient behaviour, such as a large burst of current immediately after the application of voltage followed by a steady decline in current on standing. In the present study, the large currents obtained just after the application of voltage subsided to much smaller steady values after a certain length of time. When a metal, the work function of which is lower than that of dielectric, is brought into contact with it, a layer of electrons accumulates on the dielectric surface together with a positive charge on the electrode, giving rise to a space charge near the electrode. The space-charge layer accumulated will depend upon the relative difference between the work function of metal electrodes and the dielectric. The space-charge layers may further be modified because of surface states. On application of an electric field at a fixed temperature, the current was found to increase and then decrease with time, and finally attain a steady value [36].

Similarly, during the discharging cycle, at shorter time an instantaneous strong internal field will act on the sample giving a

discharging current which decays at a faster rate. On the other hand, at longer times, when most of the absorbed charge has already decayed, the internal field becomes weak, giving a discharge current which decays at a slower rate [37].

The activation energy values for such isochronal peak are found to vary from 0.57 to 0.69 eV. The activation energy are found to decrease with time of observation. The value of activation energies agrees well with the activation energy obtained for TSDC peaks in the present case (Chapter 4).

/ ***** /

REFERENCES

1. Dayies, D.K., J. Phys., **D6**, 1017 (1973).
2. Wintle, H.J., J. Non Cryst. Solids, **15**, 471 (1974).
3. Das Gupta, D.K. and Joyner, K., J. Phys. D. Appl. Phys., **9**, 829 (1976).
4. Thielen, A. *et al.* (I) and (II), J. Appl. Phys., **75**, 8 (1994).
5. Vanderschueren, J. and Linkens, A., J. Appl. Phys., **49**, 7 (1978).
6. Maiman, S. and Schacham, S.E., J. Appl. Phys., **75**, 4 (1994).
7. Murata, Y. and Koizumi, N., IEEE, Trans. Elect. Insul., **24**, 3, 449 (1989).
8. Ikeda, S. *et al.*, J. Appl. Phys., **64**, 4, 2026 (1988).
9. Nagashima, H.N. and Farai, R.M., J. Appl. Phys., **75**, 5 (1994).
10. Leal Ferreira, G.F. and Morena, R.A., J. Appl. Phys., **75**, 1 (1991).
11. Golden Blum, A. *et al.*, J. Appl. Phys., **75**, 10 (1994).
12. Cole, K.S. and Cole, R.H., J. Chem. Phys., **90**, 341 (1941).
13. Seanor, D.A., J. Polym. Sci., **A-2**, 6, 463 (1968).
14. Wintle, H.J., J. Non-cryst. Solids, **15**, 471 (1974).
15. Das Gupta, D.K. and Joyner, K., J. Phys. D. Appl. Phys., **9**, 829 (1976).
16. Lewis, T.J., Conf. on Electrical Properties of Organic Solid, Inst. Phys. Chem., Warclaw Tech. Univ., Poland Ser. No. 7.
17. Jonscher, A.K., J. Non-cryst. Solids, **8-10**, 293 (1972).

18. Ferreira, Leal, G.F. and Morena, R.A., J. Appl. Phys., **75**, 1 (1994).
19. Adamec, V., Kolloid, **249**, 1085 (1971).
20. Aras, L. and Baysal, B.M., J. Poly. Sci. Poly. Phys., **22**, 1453 (1984).
21. Nagashima, H.N. and Faria, R.M., J. Appl. Phys., **75**, 5 (1994).
22. Golden Blum, A., J. Appl. Phys., **75**, 10 (1994).
23. Maiman, S. and Schacham, S.E., J. Appl. Phys., **75**, 4 (1994).
24. Takeishi, S. and Mashimo, S., Rev. Sci. Instrum., **53**, 115 (1982).
25. Cole, K.S. and Cole, R.H., J. Chem. Phys., **10**, 98 (1974).
26. Jonscher, A.K., Universal Relaxation Law, Chelsea (Dielectric Press, London, 1991).
27. Struik, L.C.E., Physical aging in amorphous polymers and other materials (Elsevier, Amsterdam, 1978).
28. Daniel, V.V., Dielectric relaxations (Academic Press, London, 1967).
29. Flemming, R.J. and Pender, L.F., in Electrets charge storage and transport in dielectrics. The Electrochemical Society, edited by M.M.Pearlman (Princeton, New Jersey, 1973) 474.
30. Walden, R.H., J. Appl. Phys., **43**, 1178 (1972).
31. Turnhout, J. Van, Thermally stimulated discharge of polymer electrets (Elsevier, Amsterdam, 1975).
32. Khare, P.K. and Chandok, R.S., Polym. Int., **36**, 35-40 (1994).
33. Khare, P.K., Chandok, R.S. and Srivastava, A.P., Pramana, J. Phys., **44**, 9-18 (1995).
34. Gaur, M.S., Singh Reeta, Khare, P.K. and Singh, R., Polym. Int., **36**, 33-39 (1995).

35. Sinha, H.C. and Srivastava, A.P., Indian J. Pure Appl. Phys., **17**, 726 (1979).
36. Khare, P.K. and Chandok, R.S., Polym. Int., **38**, 153 (1995).
37. Khare, P.K. and Chandok, R.S., J. Polym. Mater., **12**, 23-29 (1995).

/ ***** /

CHAPTER VI

DARK CONDUCTION CURRENT MEASUREMENT

6.1 INTRODUCTION

Most of the polymers are considered to be insulators because they show low conductivity, low dielectric loss and high breakdown strength [1]. However, recent research in the field of polymers has led to the development of special types of high molecular weight materials which exhibit a conductance high enough to class them as semiconductors (specific conductivity = 10^{-12} to $10^2 \text{ ohm}^{-1} \text{ cm}^{-1}$) or even in some cases as conductors [2].

In past several years, a good amount of work has been reported on electrical conduction in polymeric materials [3-8] and various mechanisms such as ionic conduction [9-11], Schottky emission [12-14], space charge limited conduction [15,16], tunnelling [17], Poole-Frenkel mechanism [18], charge hopping [19] and small polaron mechanism [20] have been proposed to explain the experimental results.

Electric current is an ordered (i.e., having a definite direction) motion of electric charges in space. Current appears in matter under the effect of applied voltage, the charged material particles of the matter being brought into the state of ordered motion by the forces of an electric field. Thus, any matter will be conductive if it contains free charge carriers. When ions move in an electric field, electrolysis takes place. Dielectrics with ionic conduction are also subject to electrolysis but it is not so pronounced due to their high resistivity. A large quantity of electricity can be passed through

them only during a long period of time if a rather high voltage is applied. Electrolysis in dielectrics is more prominent at increased temperatures when the resistivity of matter is reduced. The molecule of most of the organic polymers cannot be ionized but ionic conduction still takes place due to presence of impurities. Nonohmic conduction at high fields in ionic model is explained by diffusion over field perturbed potential barriers, by internal heating and by polymer structure modification by the field. The exponential temperature dependence and disproportionality between current and voltage are usually explained on the basis of temperature and field dependence of mobility. In that case, current-voltage curves follows a hyperbolic sine-function. But it is not a definite proof of ionic conduction [2]. In polymers with halogens in their molecular structure, electrical conductivity is qualitatively proved to be ionic [10].

The fact that electronic conduction plays a role in polymers was established experimentally by Seanor [21]. To discuss electronic conduction, it is necessary to investigate the generation of free carriers and their transport through the material. Several books and reviews [22-26] deal with the problem of carrier generation. Contact limited emission was first studied for the metal-vacuum interface. In this case three mechanisms of current flow may be distinguished. Thermionic emission [27] (Schottky emission) occurs in the low-field high-temperature limit. Field emission [28,29] (Fowler-Nordheim tunnelling) occurs in the high-field low-temperature limit and is the direct quantum mechanical tunnelling of

electrons from allowed states below the fermi level in a metal into allowed states in vacuum. Thermal-field emission [30-32] occurs when the dominant contribution to the observed currents arises from the tunnelling of thermally excited electrons through the narrow upper region of the image-force-lowered work-function barrier. Murphy and Good [33] showed that each of these mechanisms is a limiting approximation observed under appropriate conditions of applied field and temperature.

In polymers at or below room temperature, the density of free charge carriers is extremely low and with an electric field, non-equilibrium conditions can be achieved, which can be easily enhanced by injecting a charge through an ohmic contact. If the contact is equivalent to sufficiently large reserve of free charges, the current-voltage characteristic does not depend on the manner in which the charges are generated but is strictly connected with the charge transport mechanism. Current-voltage curve is generally nonlinear on account of two basic causes. At high fields the charges are accumulated between the electrodes [34]. The presence of traps within the forbidden gap reduces the free charge density and produces a localized charge density within the polymer. The density, energy distribution and nature of the traps have a determining influence on current-voltage characteristic which also depends on the type of charges involved in the conduction process. Space charge limited current theory of Rose [35] has been modified by Lampert [36].

Trapping sites exert a strong influence on the current flow, i.e. the concentration of free carriers and their mobility. Mobility values in polymers are very low suggesting strong trapping. Phenyl rings and aliphatic or aromatic groups may be active traps. The trapping ability of unsaturation sites in the chains and at the chain ends of pure polymers is confirmed. Similar conclusions are obtained by Perlman and Unger [37] in the studies of electron traps in irradiated polyethylene and teflon. Mobility values of polyethylene satisfy the relation for carrier hopping between localized sites. If the activation value of hopping are low 0.2-0.3 eV, hopping is connected with charge jumps brought about by motions of chain elements and the process is related to so called chain hopping mechanism while of greater values (0.5 eV) the so called trap hopping mechanism is involved. Martin and Hirsch [38] proposed energy traps 0.2-0.75 eV for polystyrene and 0.2-0.3 eV for polyethylene terephthalate, showing that both mechanisms play a significant part. Lifetime of carriers in traps depends on the field. Thus, band model with traps of various depths explains experimental results reasonably. However, the nature of charge carriers and trapping sites has not yet been settled conclusively.

In the case of polymers where H-atoms in the backbone chains are replaced by large aromatic groups with π -electrons, the highest filled and the lowest empty molecular orbits are formed from the substituents and the charge transfer occur within the pendant groups where charge carrier density is higher due to higher affinity to electrons or holes. The role of

backbone chain is less important. Taking into consideration that the overlapping of π -systems is small, the band width must be narrow. The bandwidth depends on the method used but does not exceed 0.1 eV. This narrow band width is responsible for the fact that the electrons are for quite a long time connected with the particular π -system which exceeds the vibrational and the high frequency dielectric relaxation time. This results in deformation of electron density in the π -system and in induced polarization of the neighbouring π -systems. The bonding energy of an electron to the potential well can be calculated. Thermal energy (phonons) can be transferred to electrons, inducing thermally assisted hopping. This mechanism is called small polaron mechanism [39]. In polymers, conduction can be explained in terms of small polaron mechanism and in some cases as intrinsic phenomenon.

The trapping capability of a polymer can be greatly modified by doping it with certain impurities. Carrier mobility in polymeric materials is increased by small molecules such as iodine [40]. Recently, Srivastava and coworkers [41-43] doped polystyrene with several impurities and found that the conductivity of the polymer is greatly enhanced due to doping of the matrix with iodine [44]. The enhanced conductivity of the polymer has been interpreted in terms of charge-transfer complexes.

An understanding of the charge-transport mechanism in insulating solids has important practical significance in fields such as electret

production, electrostatic recording [45-48] and electrical insulation. Most of the polymers are considered to be insulators [47,49] as they have low conductivity and low dielectric loss.

Application of an electric field caused polarization of polymers. The electric field may induce an electric moment in the molecules. In the case of molecules with permanent dipole moments, an external electric field brings about their orientation and consequent polarization of the sample. The displacement of polar groups requires some time and is thus dependent on frequency and temperature, which lead to different dispersion phenomena according to segmental motion of the chain or orientation of pendant dipoles. Owing to this variety of electrical properties, the theories of dielectric polarization or conduction elaborated for organic low molecular weight materials cannot be applied to high molecular weight substances without critical consideration.

The large number of reviews and books dealing with the electrical conductivity of polymers [50-54] which have appeared in recent years, indicate that properties of semiconducting polymers hold considerable interest for many investigators. It appears that there are still some serious difficulties in establishing a realistic quantitative theoretical description of semiconduction in macromolecular systems, but important progress has already been made regarding the new possibilities opened up by the general theory of amorphous semiconductors [55]. There are, however, many interesting topics that require further theoretical and experimental work.

The density of thermally generated charge carriers in polymers at room temperature is negligible and the band gap, if the band theory is applicable, is larger than 1.5 eV. For this reason, it was assumed that the conductivity of polymers is due to ionic impurities or to the presence of ionizable groups. Ions may change the order introducing disorder and may enter the amorphous regions producing local order. Ionic theory [56-58] have been modified by taking into account trapping of ions in fixed sites which changes the ionic mobility values and the diffusion currents. The deviation from ohmic conduction at high fields is explained by diffusion over field perturbed potential barriers, by internal heating, and by polymer structure modification by the field. The exponential temperature dependence and disproportionality between current and voltage are explained on the basis of temperature and field dependence of mobility. In various polymers, particularly with halogens in their molecular structure, e.g. polyvinylchloride (PVC), polyvinylidenechloride, polytrifluoroethylene and polyvinylfluoride (PVF), electrical conduction has been qualitatively proved to be ionic [59,60]. In PVC the real motion of Cl^- ions is partially satisfying Faraday's electrolysis law [61]. An electrode reaction qualitatively supports F^- ion migration in PVF [62].

It might be mentioned that the number of papers where the observed conductivity is explained in terms of the ionic mechanism is decreasing. This decrease does not, of course, include the studies where ionic impurities are introduced on purpose. On the other hand, publications in

which the electronic part of conductivity is considered, are becoming more frequent.

In wide gap insulators such as hydrocarbon polymers and in many polymers with π -electrons, intrinsic carrier generation is not possible because of the large band gap. Thus, in a study of electronic conductivity, it is necessary to investigate the following areas :

- (i) the generation of the carriers and in particular
 - (a) the method of generation of charge carriers, taking into consideration the chemical and physical structure as well as the morphology of the investigated substances, the role of electrodes and related effects, e.g. impurities, surface states etc.
 - (b) the nature of free charge carriers (electrons or holes).
- (ii) the transport of charge carriers
 - (a) the nature of charge transport mechanism
 - (b) the nature and energy of traps
 - (c) the influence of chemical and physical factors on traps and other parameters characterizing the charge carrier transport.

Though much work on electronic conduction in polymers has been reported in past several years, yet clear ideas concerning the transport mechanism have not been reached. Various mechanisms such as Schottky

emission [63-66], space charge limited conduction [67-69], tunnelling [70,11], charge hoping [72-74], Poole-Frenkel mechanism [75,76] or small polaron mechanism [77-79] have generally been invoked to interpret the experimental results on polymeric films.

In calculations of band structure for polymers [80-82], it is assumed that the chains are fully extended, rigid, and of infinite length. Electrons are free to move along these chains with a frequency which depends on band width. In actual macromolecular chains, one must consider many types of disorder which influence movement. The same role is played by photons. Both of these factors give rise to the presence of localized states. When electron-phonon coupling is weak, the band structure is retained and the phonons control the life times of these states. An electron moving along a chain is described by a wave function whose amplitude and phase is affected by the local potentials of $-\text{CH}_2-$ groups. If the chain periodicity is interrupted due to disorder, then these wave functions decay. As all types of defects, e.g., impurities and groups, and the finite length of chains, influence the decay of electron wave functions and because of the fact that these effects are not sufficiently understood, it remains difficult to get a satisfactory agreement between theoretical calculations and experimental results.

In most of the polymers intrinsic thermal carrier generation in the dark is not possible. In that situation, it seems that the injection of charge

carriers is of principal importance for any explanation of the origin of carriers and other effects related to dc conductivity in polymeric materials. The different values of conductivity and activation energy for the same material may serve as an argument for the occurrence of the injection mechanism. The importance of the carrier injection phenomenon for the explanation of electrical properties of organic low molecular weight solids was recognized many years ago [50]. Less attention has been given to the application of this concept to the elucidation of electrical conductivity of polymers. Charge transfer between two solids is known, but there is nevertheless a controversy about the cause or causes which determines the polarity as well as the amount of charge transferred under given conditions. These problems stem from a scarcity of theoretical works and a large number of experimental studies where the conclusions do not seem to be fully justified.

The injected charges are trapped in different trapping sites leading to a space charge which influences basically all the transport phenomena and the effects at the electrode. The application of the space charge limited current (SCLC) theory is a very useful concept in studies of electronic conduction in polymers. A very important part is played by surface trapping states in carrier injection. In the case of amorphous and partially crystalline polymers, the nature of surface states is practically unknown. From the surface state the injected carrier will diffuse in its own field or in the external field into the bulk of material where it is again trapped in the volume traps

which reveal different energetical depths. Thus, trapping sites exert a strong influence on current flow, i.e., concentration of free carriers and their mobility. The field dependent mobility appears to be reasonably consistent with the Poole-Frenkel model of conductivity but it may be mentioned that this model can be strictly applicable only when the existence of bands may be supposed, which in the case of amorphous polymers is unlikely (even for crystalline high molecular materials). Thus, one must modify this model or discuss these effects in other terms. However, in many cases where this assumption was not fulfilled, this model was successfully applied for partially crystalline materials or even amorphous ones (with some modifications).

This chapter reports a thorough study of conduction mechanism in PVDF films.

6.2 EXPERIMENTAL

In the present investigation samples were thermally poled with fields 10 to 100 kV/cm at various temperatures (ranging from 40-80°C). The polarization was carried out by connecting a dc power supply (EC-HV 4800 D) in series with an electrometer which was carefully shielded and grounded to avoid ground loops and extraneous electrical noise.

After making proper electrical connections, the sandwiched sample mounted on electrode assembly was placed inside the thermostat and allowed to attain required temperature. The temperature of the cell was

controlled with an accuracy of ± 1 K by adjusting the input voltage from the variac for which the calibration has been made. It took about 1.5 hrs. When the sample attained the desired temperature, a dc voltage was applied. A sudden burst of current observed in the beginning decreases with time. Its initial as well as steady value was recorded. At lower voltages and temperatures, it took longer period to reach the steady state while at higher voltages and temperatures, steady state was obtained in considerable low period. The effect of voltage variation in current was noted by increasing the voltage at fixed temperatures while temperature variation was measured keeping voltage constant and increasing the temperature. A fresh sample is used for each set of observation.

6.3 RESULTS AND DISCUSSION

Figure 6.1-6.7 shows the current-voltage (I-V) characteristics of PVDF films at temperatures ranging from 40-80°C for similar (Al-Al, Cu-Cu, Ag-Ag and Sn-Sn) and dissimilar electrodes (Al-Cu, Al-Ag and Al-Sn) combinations. Also, at constant temperature 40°C, 60°C and 80°C current-field characteristics are observed for Al-Al, Al-Cu, Al-Ag, Al-Sn and Cu-Cu electrode configurations (Figures 6.8-6.10). The observed increment in the current was approximately the same throughout the studied range of temperature. For all the temperatures, the thermograms, though non-linear, were similar.

The steady state conduction-current-temperature characteristics with different poling fields (i.e., 10, 25, 50, 75 and 100 kV/cm) for similar

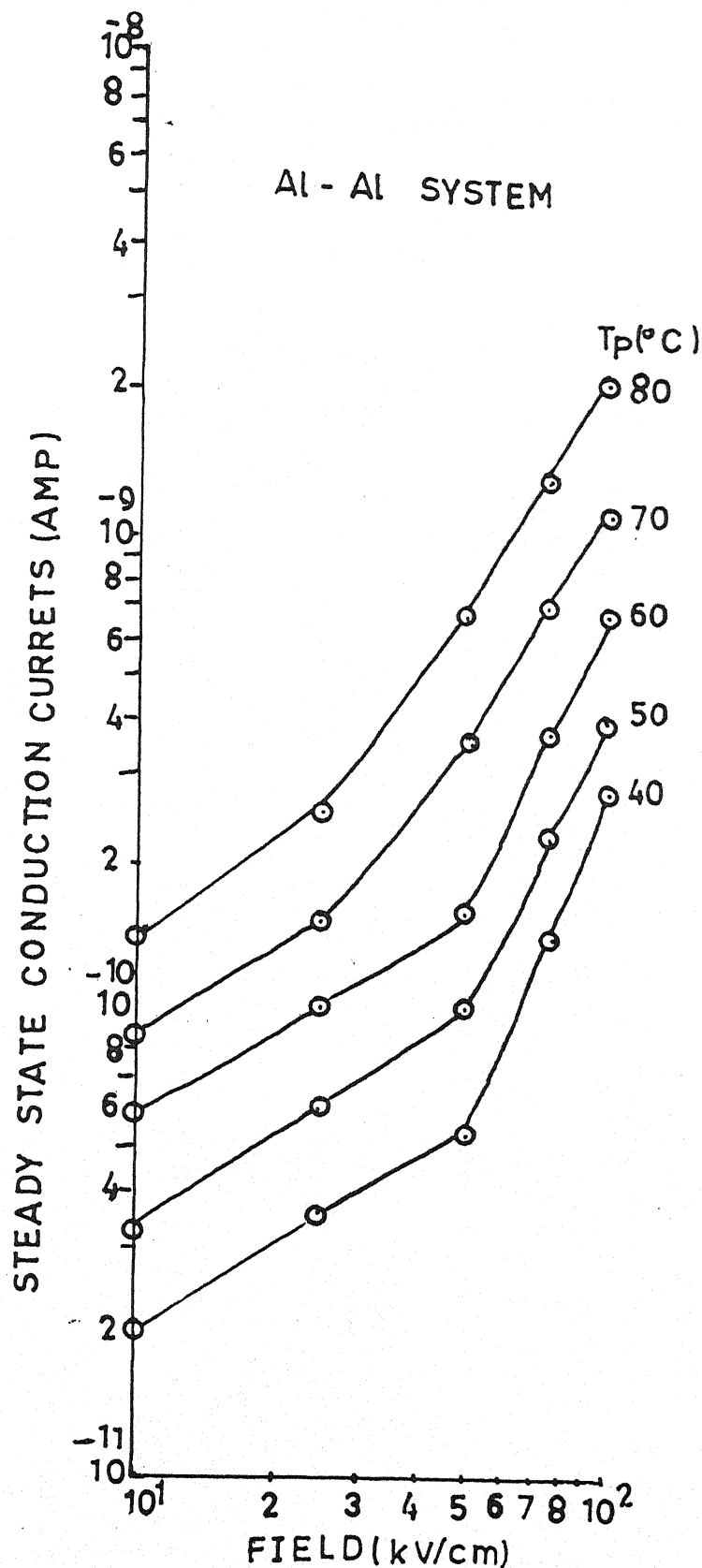


Fig. No. - 6.1

Log I versus field curve for polyvinylidene fluoride samples at different Temperatures (i.e. 40, 50, 60, 70 and 80 °C) for Al - Al system.

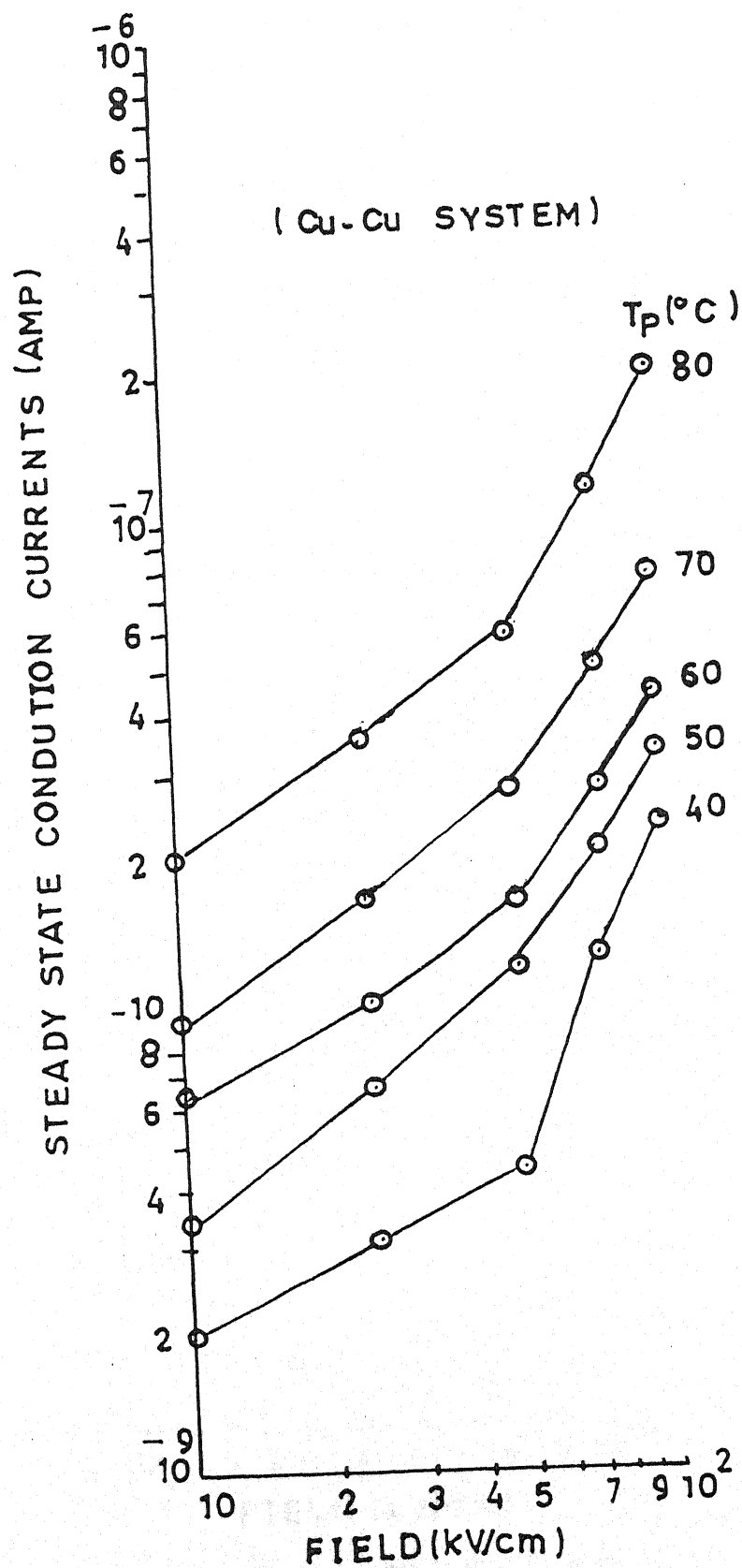


Fig. No. - 6.2

Log I versus field curve for polyvinylidene fluoride samples at different Temperatures (i.e. 40, 50, 60, 70 and 80 °C) for Cu - Cu system.

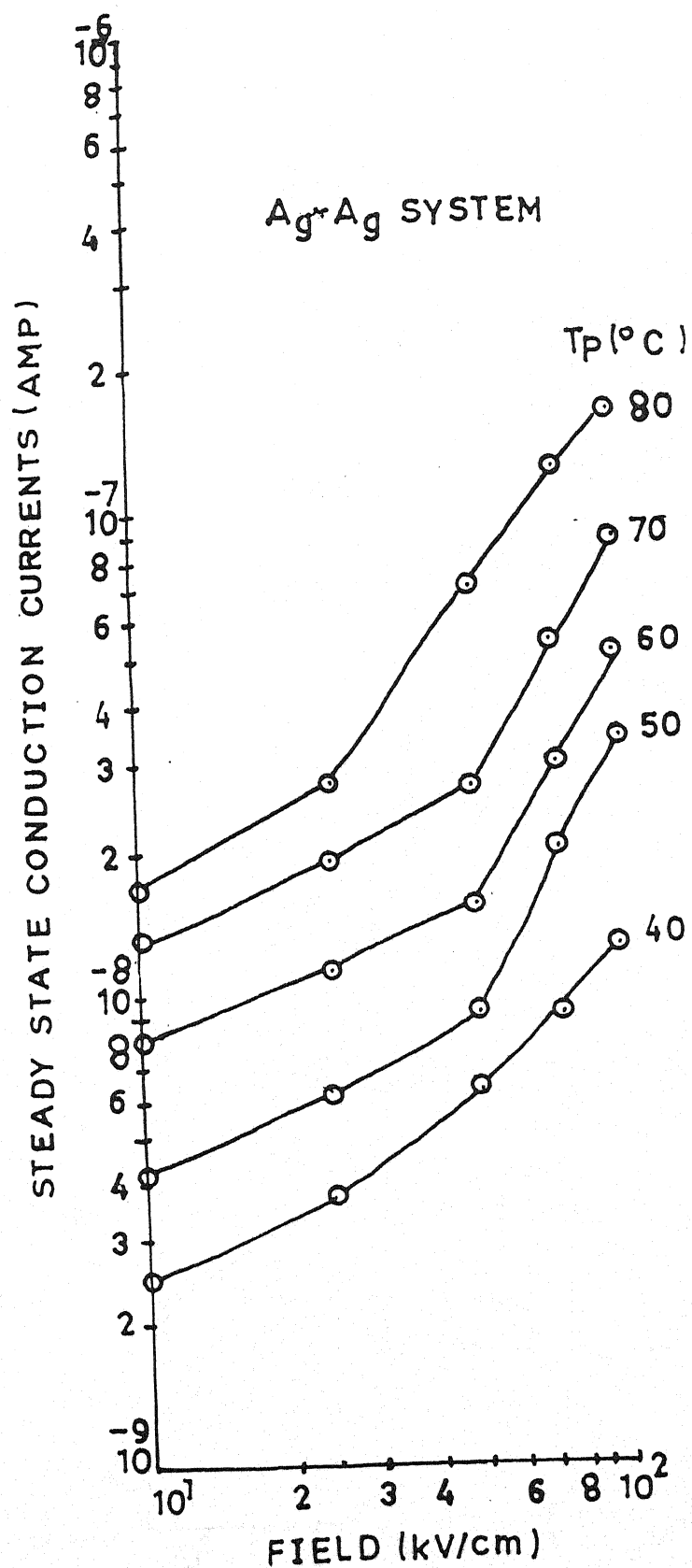


Fig. No. - 6.3

Log I versus field curve for polyvinylidene fluoride samples at different Temperatures (i.e. 40, 50, 60, 70 and 80 °C) for Ag - Ag system.

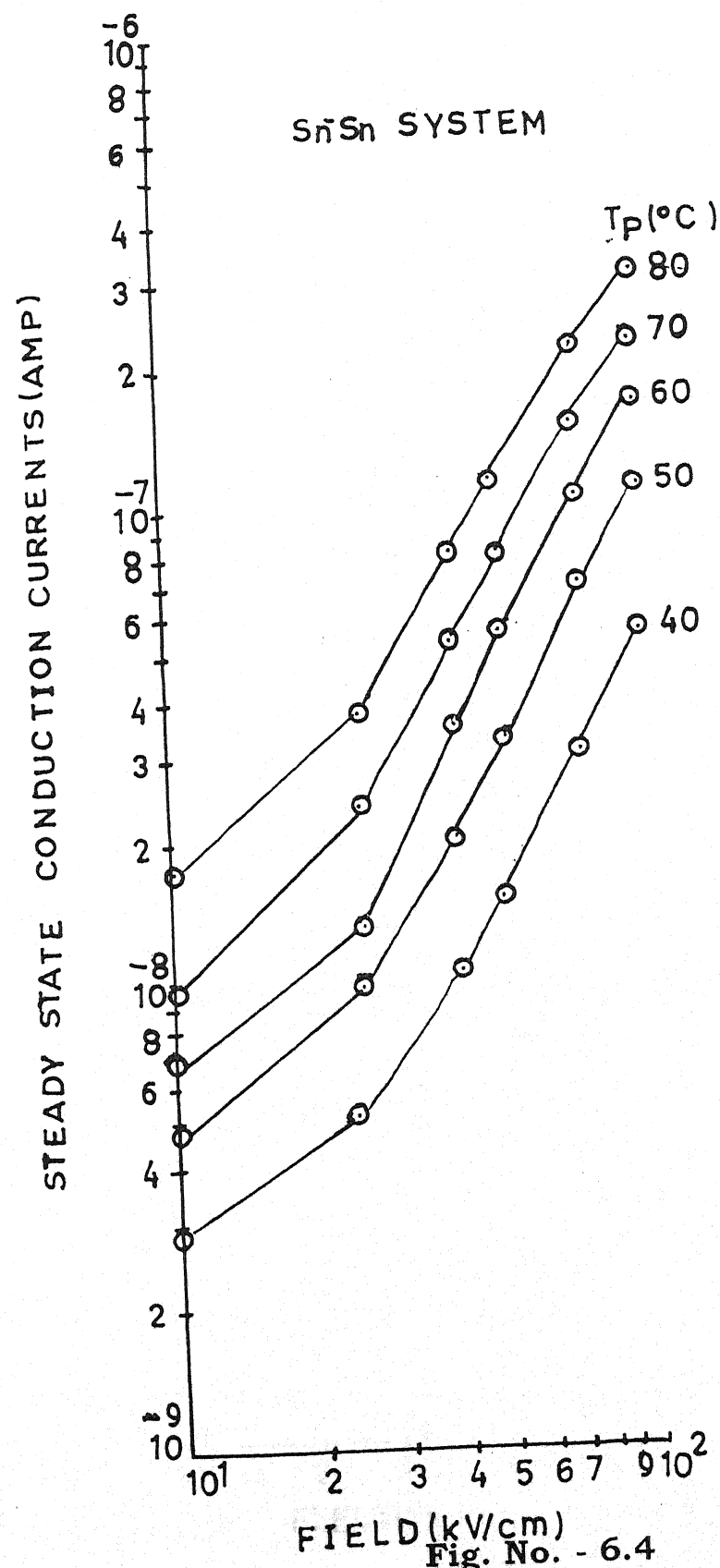


Fig. No. - 6.4

Log I versus field curve for polyvinylidene fluoride samples at different Temperatures (i.e. 40, 50, 60, 70 and 80 $^{\circ}\text{C}$) for Sn - Sn system.

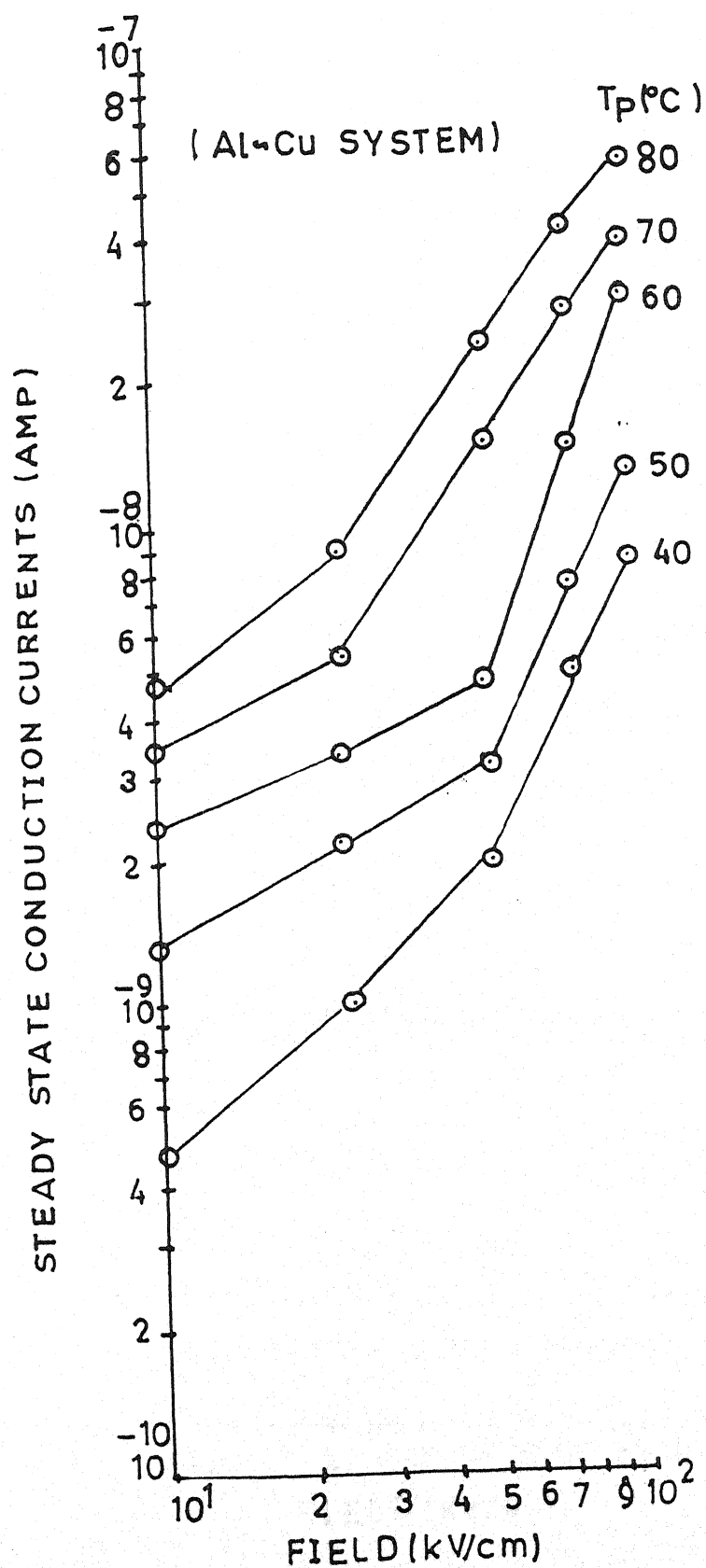


Fig. No. - 6.5

Log I versus field curve for polyvinylidene fluoride samples at different Temperatures (i.e. 40, 50, 60, 70 and 80 °C) for Al - Cu system.

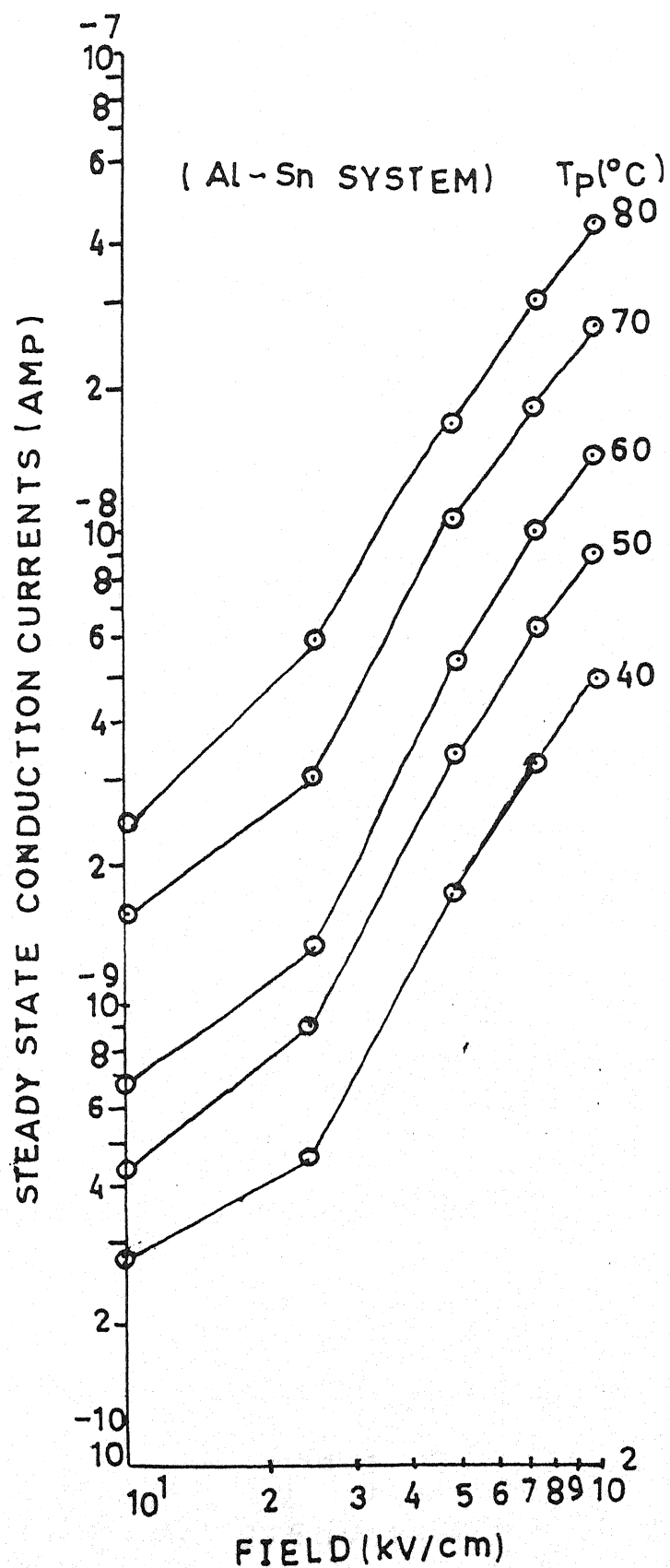


Fig. No. - 6.6

Log I versus field curve for polyvinylidene fluoride samples at different Temperatures (i.e. 40, 50, 60, 70 and 80 °C) for Al - Sn system.

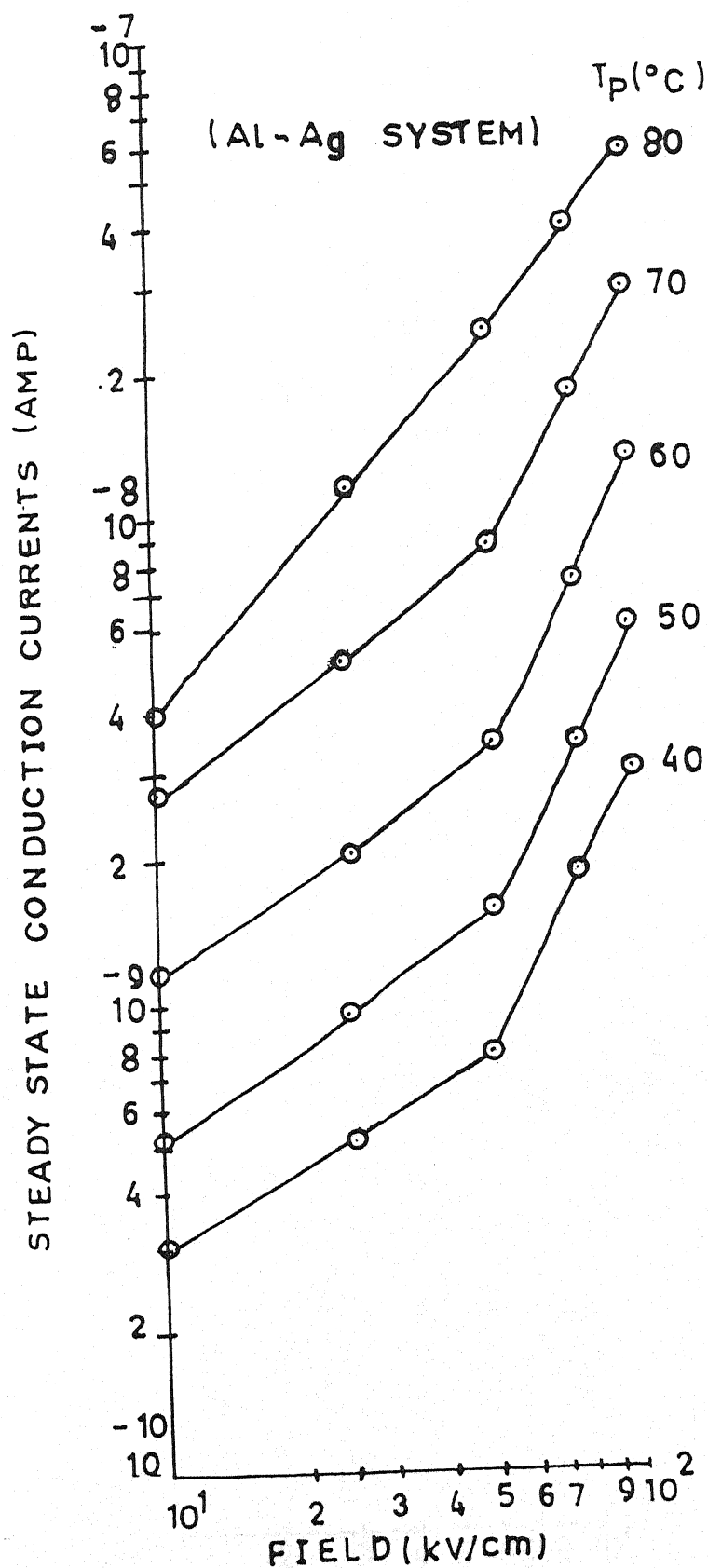


Fig. No. - 6.7

Log I versus field curve for polyvinylidene fluoride samples at different Temperatures (i.e. 40, 50, 60, 70 and 80 °C) for Al - Ag system.

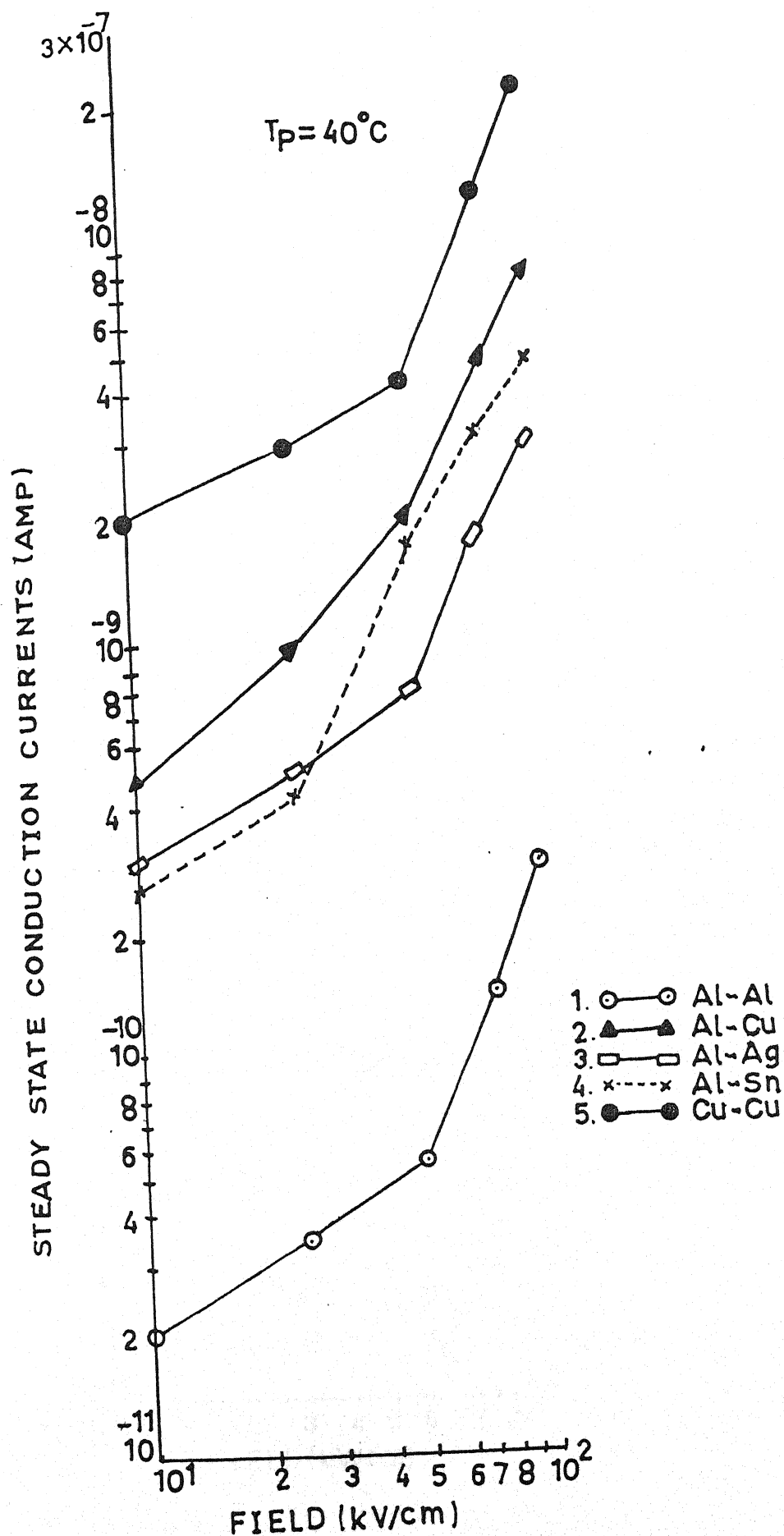


Fig. No. - 6.8

Log I versus field curves for polyvinylidene fluoride samples at $T_p = 40^\circ\text{C}$ for dissimilar Electrode (i.e. Al-Al, Al-Cu, Al-Ag, Al-Sn, Cu-Cu) Configuration.

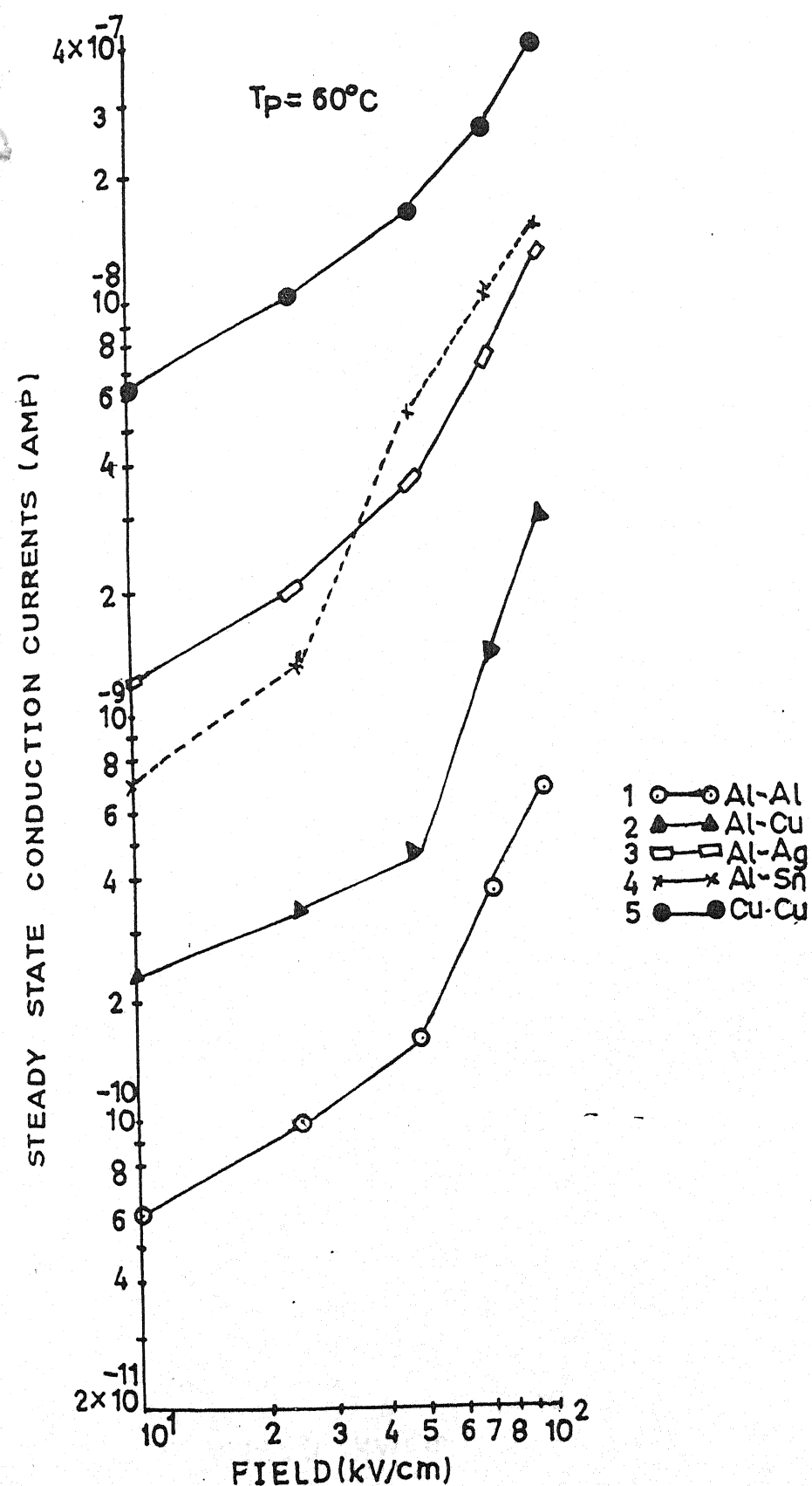


Fig. No. - 6.9

Log I versus field curves for polyvinylidene fluoride samples at $T_p = 60^\circ\text{C}$ for dissimilar Electrode (i.e. Al-Al, Al-Cu, Al-Ag, Al-Sn, Cu-Cu) Configuration.

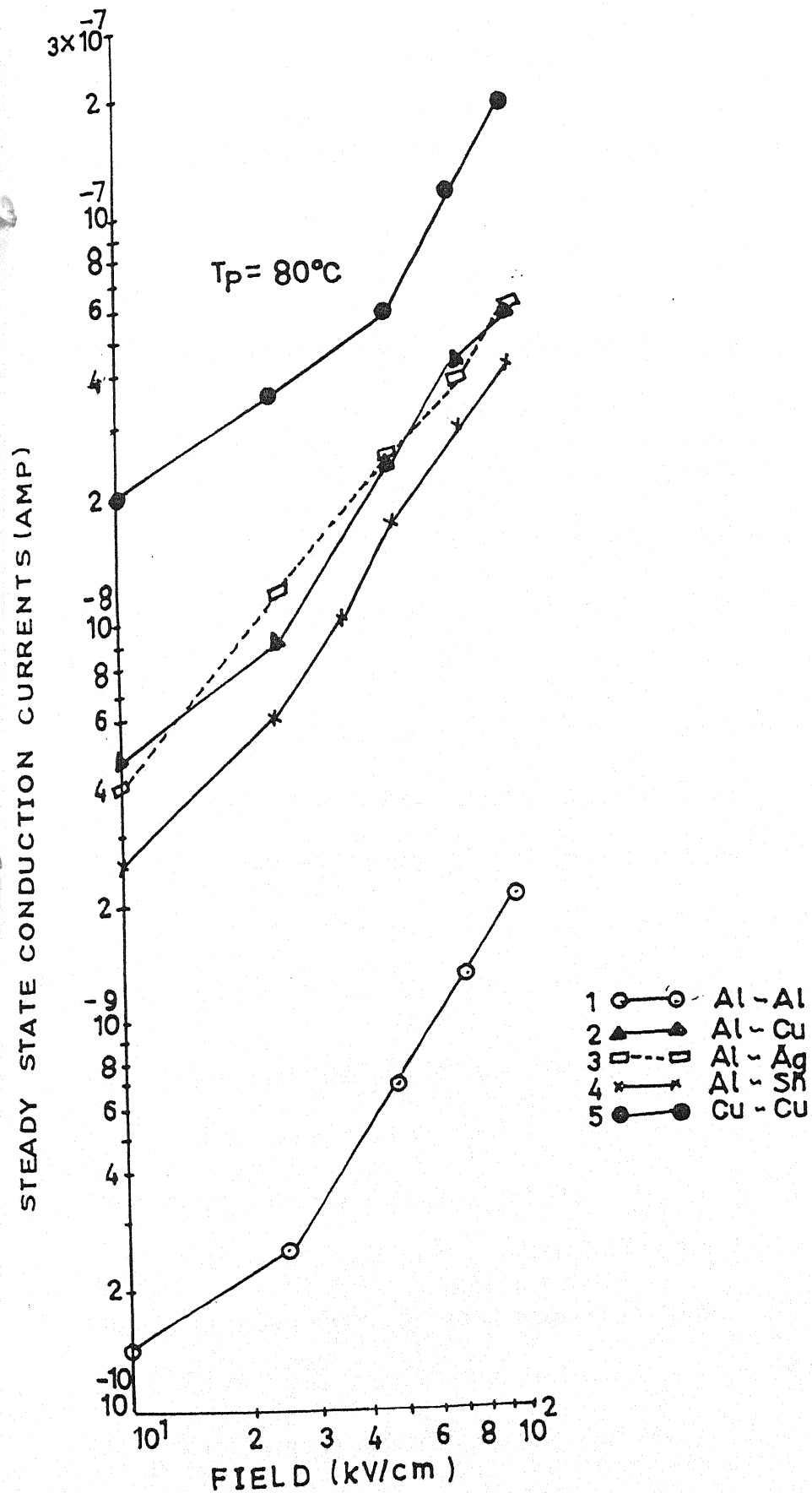


Fig. No. - 6.10

Log I versus field curves for polyvinylidene fluoride samples at $T_p = 80^\circ\text{C}$ for dissimilar Electrode (i.e. Al-Al, Al-Cu, Al-Ag, Al-Sn, Cu-Cu) Configuration.

(i.e. Al-Al, Cu-Cu, Ag-Ag and Sn-Sn) and dissimilar electrode combination (i.e. Al-Cu, Al-Ag and Al-Sn) are shown in Figures 6.11, 6.13, 6.14, 6.15 and 6.12, 6.16, 6.17) respectively.

The Schottky plots ($\log I$ vs \sqrt{E}) for PVDF samples with similar (Al-Al, Cu-Cu, Ag-Ag and Sn-Sn) and dissimilar electrode (Al-Cu, Al-Ag and Al-Sn) combinations are shown in Figures 6.18, 6.20, 6.21, 6.22 and 6.19, 6.23 and 6.25 respectively. The plots exhibit two regions at the lower and higher fields. The isothermal reveals almost ohmic behaviour initially, which gradually becomes non-ohmic. The slope values in the lower field region lie between 1.2 to 1.5 and slope of 1.97 to 2.00 are observed at higher field strength (Table 6.1). It is evident from the Figures that order of conduction currents varies with electrode materials. The activation energy values calculated from the slopes of $\log I$ versus $1000/T$ plots (Figures 6.25 to 6.31) and found to be independent of applied field (Table 6.3).

The Curie-Von Schweidler type of time dependence has been observed for many polymers with the index n close to shallow trapping, although the possibility for the presence of deep traps in the present case, cannot be excluded. The $\log I$ - V plots showed the slope in the lower field region, upto 50 kV/cm, as 1. In contrast, in the higher field region, the value of slopes was greater than 1, but not exceeding 2. The slope value of 1, in the low-field region indicates that the electrical conduction in this region obeys Ohm's law. However, since the complete I - V characteristics were

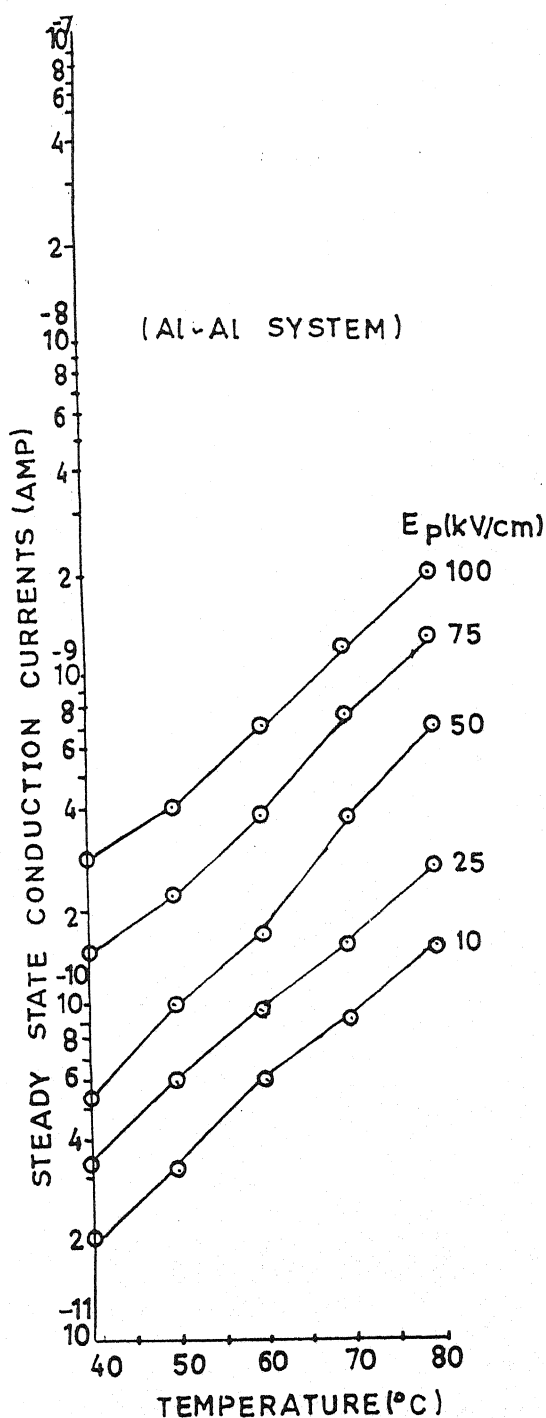


Fig. No. - 6.11
Log I versus Temperature curves for polyvinylidene fluoride samples with various poling field (i.e. 10, 25, 50 75 and 100 kV/cm.) for Al-Al system

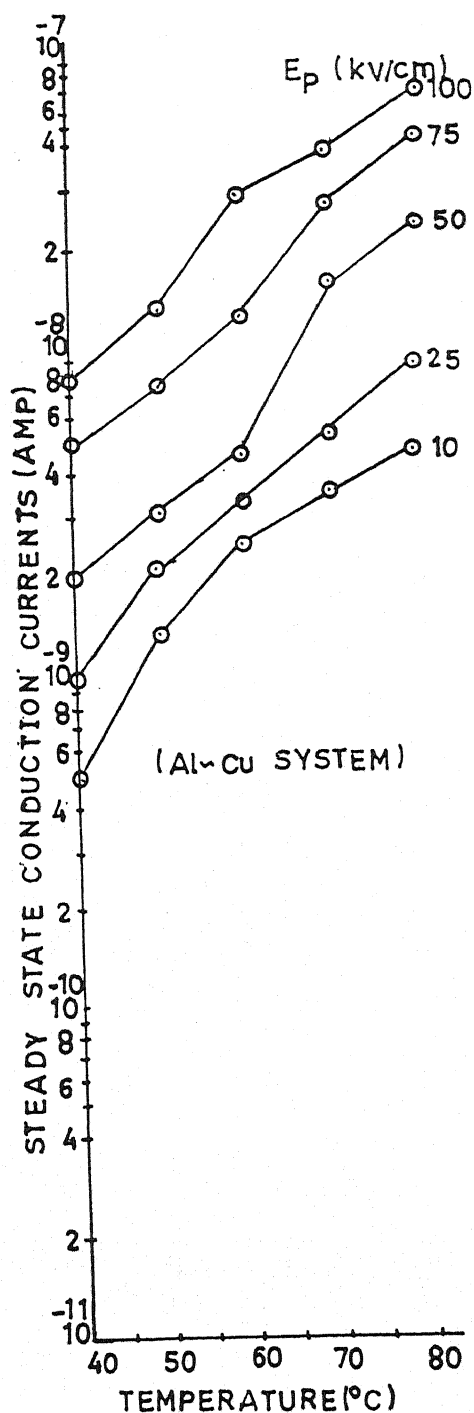


Fig. No. - 6.12
Log I versus Temperature curves for polyvinylidene fluoride samples with various poling field (i.e. 10, 25, 50 75 and 100 kV/cm.) for Al-Cu system

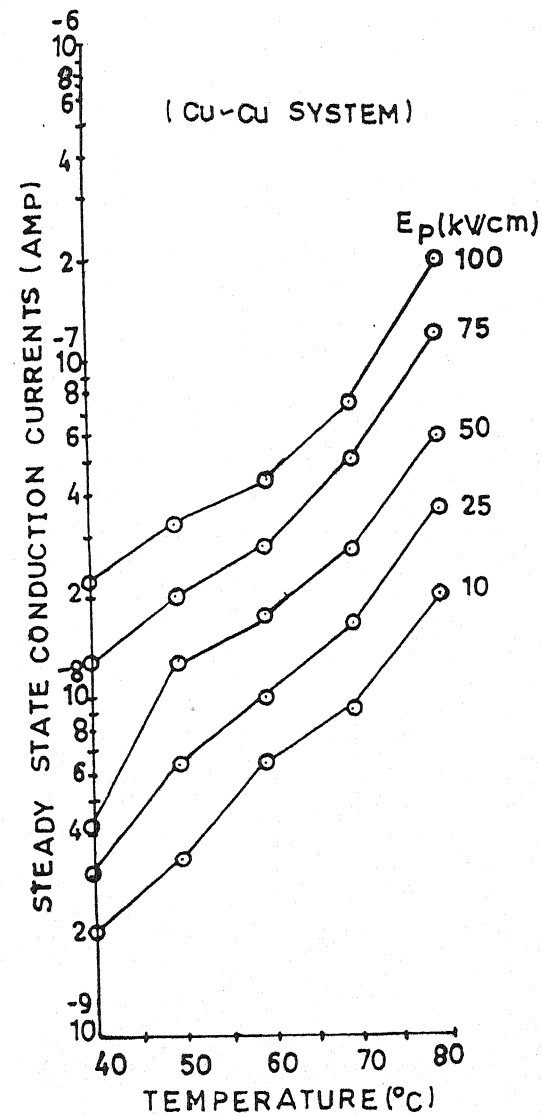


Fig. No. - 6.13
Log I versus Temperature
curves for polyvinylidene
fluoride samples with various
poling field (i.e. 10, 25, 50 75
and 100 kV/cm.) for Cu-Cu
system

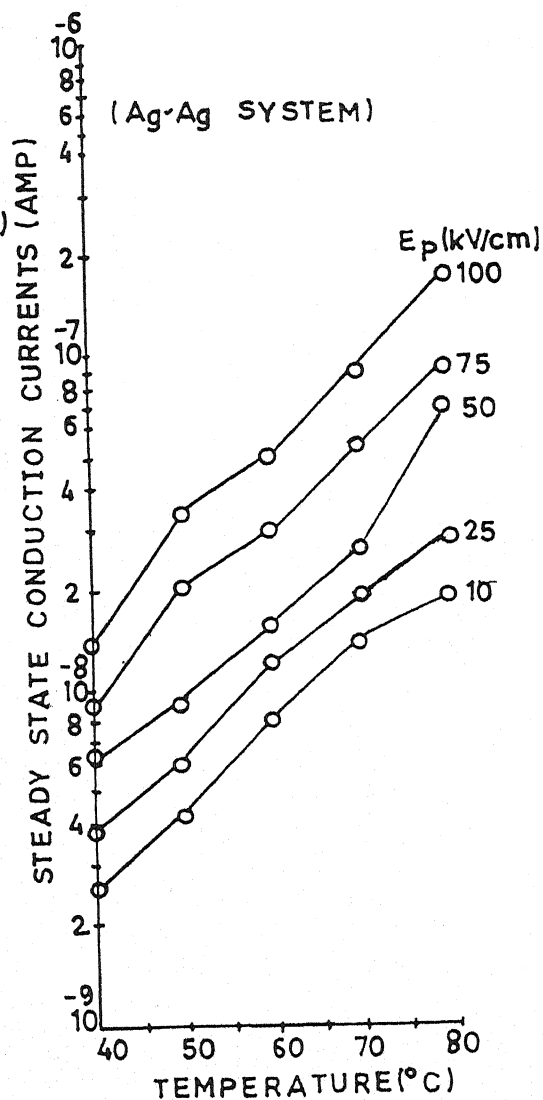


Fig. No. - 6.14
Log I versus Temperature
curves for polyvinylidene
fluoride samples with various
poling field (i.e. 10, 25, 50 75
and 100 kV/cm.) for Ag-Ag
system

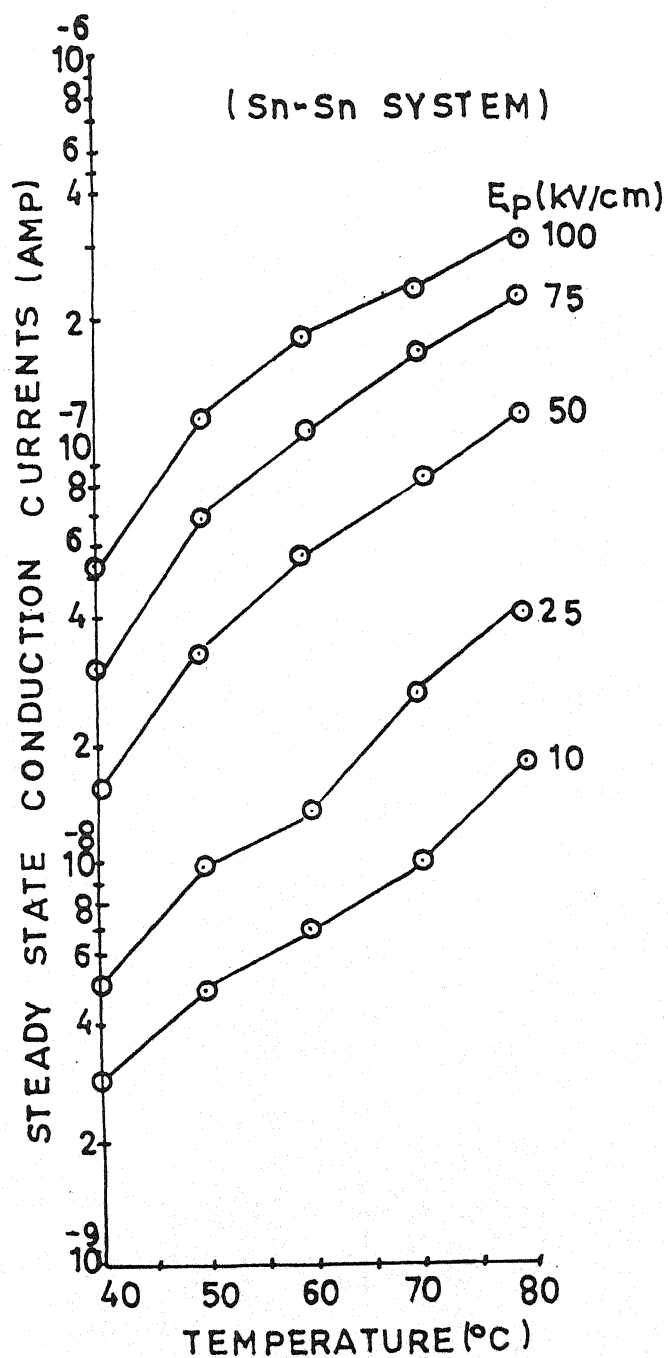


Fig. No. - 6.15

Log I versus Temperature curves for polyvinylidene fluoride samples with various poling field (i.e. 10, 25, 50 75 and 100 kV/cm.) for Sn - Sn system

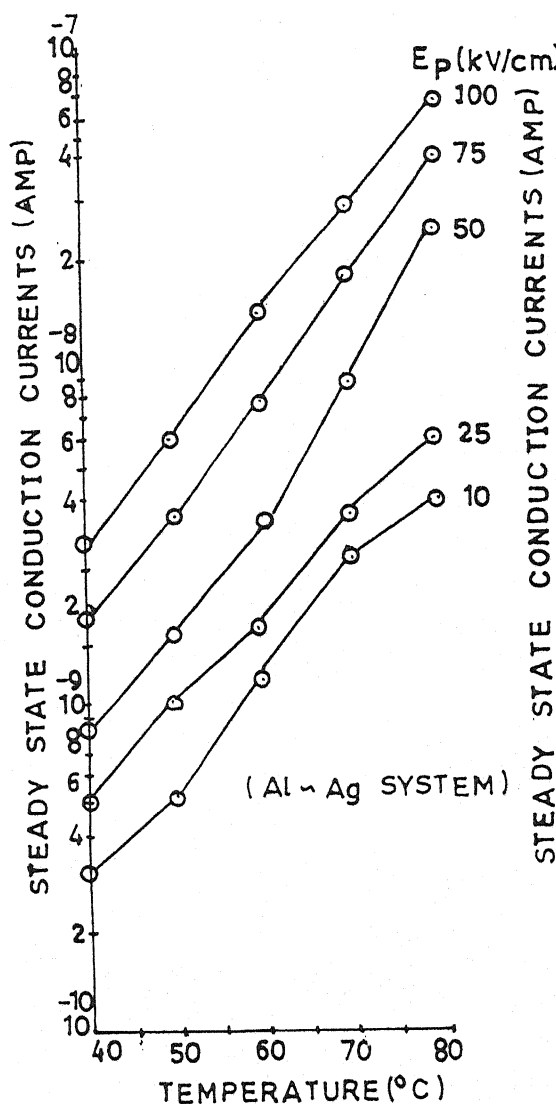


Fig. No. - 6.16
Log I versus Temperature curves for polyvinylidene fluoride samples with various poling field (i.e. 10, 25, 50 75 and 100 kV/cm.) for Al - Ag system

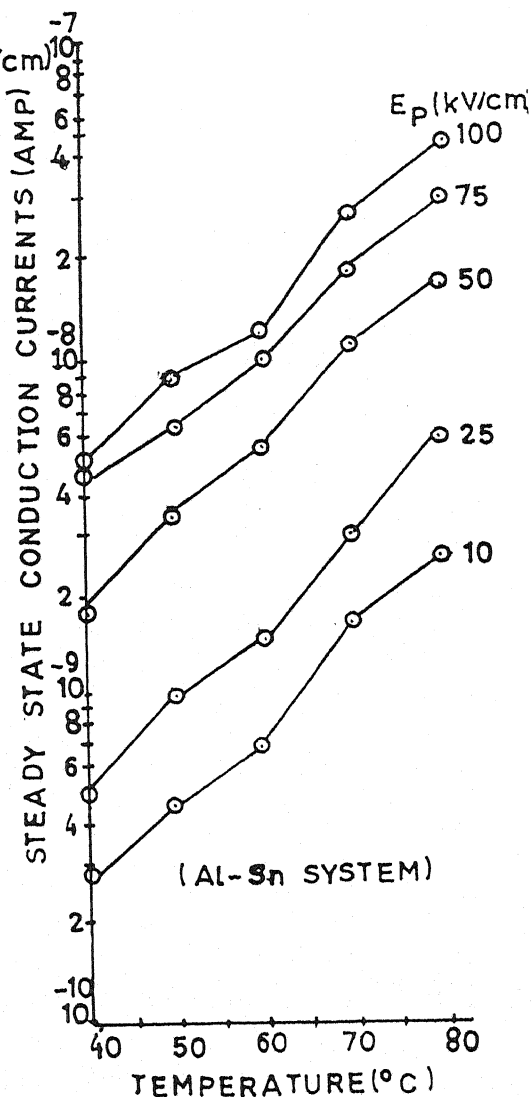


Fig. No. - 6.17
Log I versus Temperature curves for polyvinylidene fluoride samples with various poling field (i.e. 10, 25, 50 75 and 100 kV/cm.) for Al - Sn system

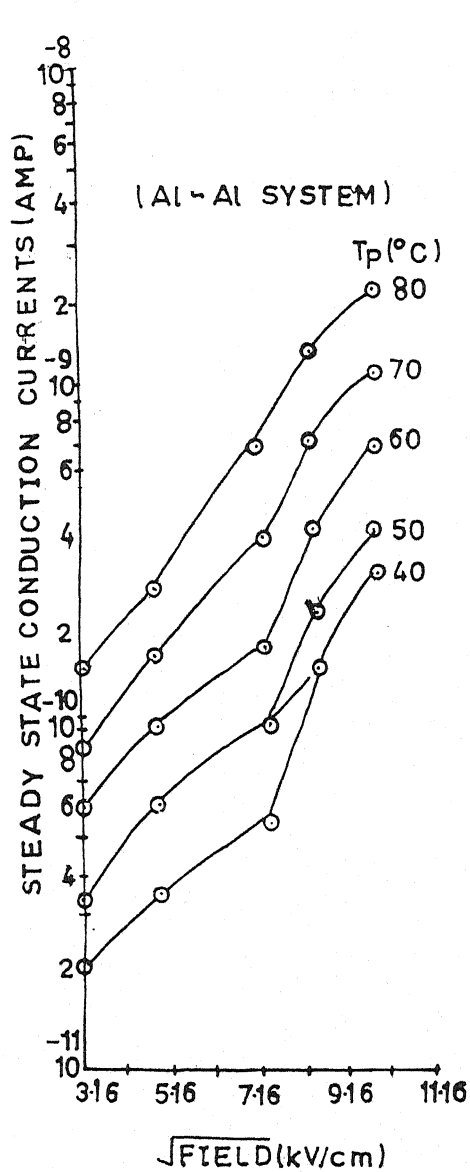


Fig. No. - 6.18

Log I versus $\sqrt{\text{field}}$ curves for polyvinylidene fluoride samples at different Temperature (i.e. 40, 50, 60 70 and 80 $^{\circ}\text{C}$) for Al - Al system

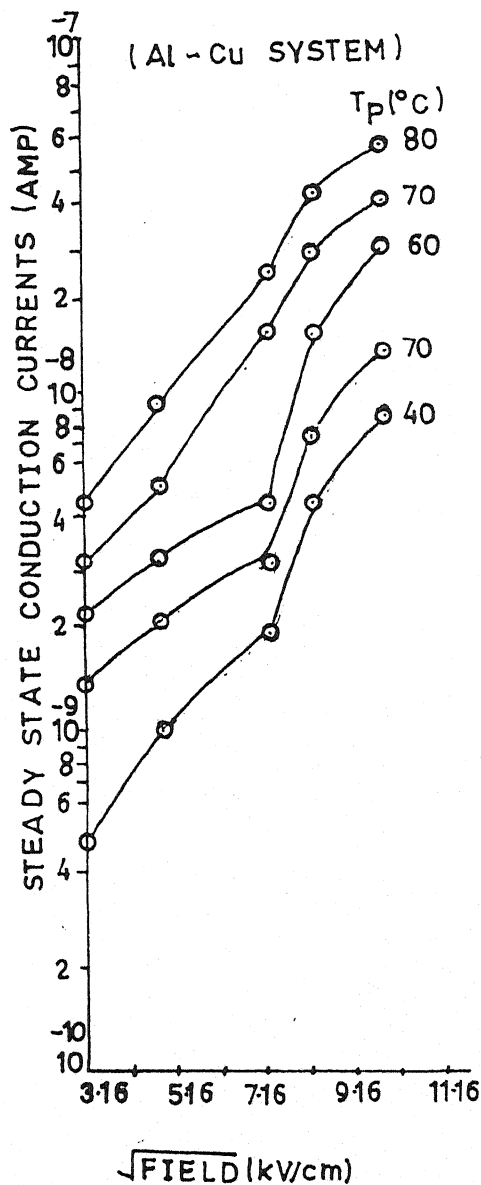


Fig. No. - 6.19

Log I versus $\sqrt{\text{field}}$ curves for polyvinylidene fluoride samples at different Temperature (i.e. 40, 50, 60 70 and 80 $^{\circ}\text{C}$) for Al - Cu system

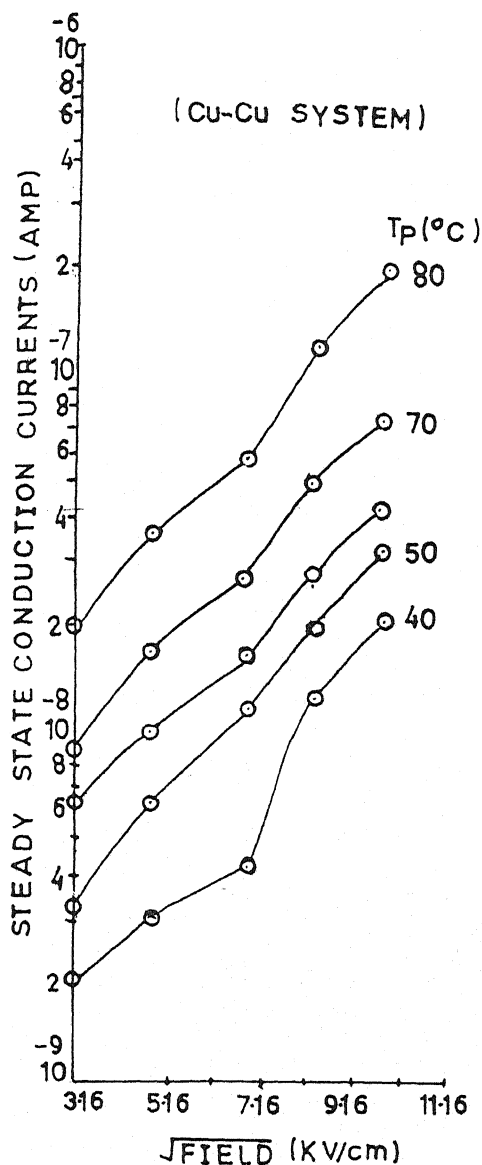


Fig. No. - 6.20

Log I versus $\sqrt{\text{field}}$ curves for polyvinylidene fluoride samples at different Temperature (i.e. 40, 50, 60 70 and 80 $^{\circ}\text{C}$) for Cu - Cu system

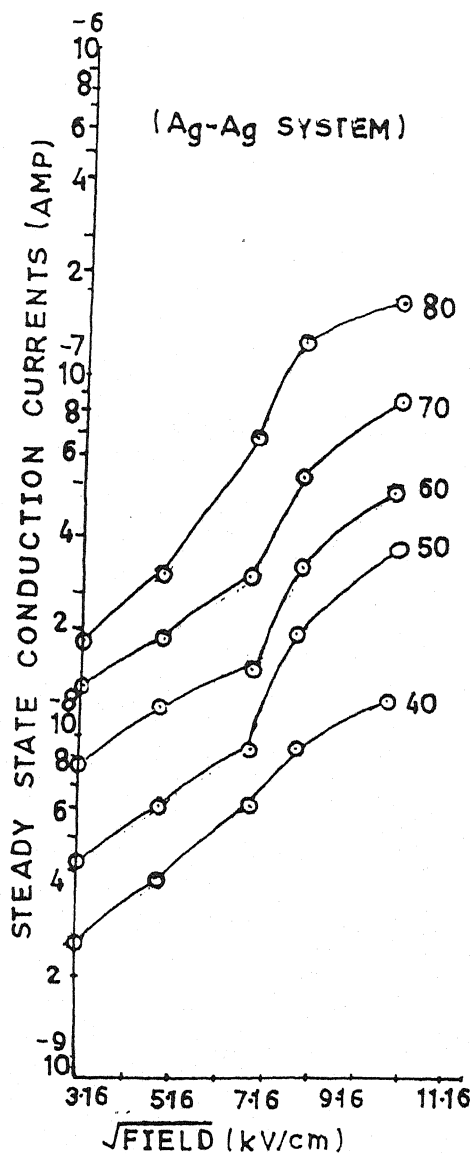


Fig. No. - 6.21

Log I versus $\sqrt{\text{field}}$ curves for polyvinylidene fluoride samples at different Temperature (i.e. 40, 50, 60 70 and 80 $^{\circ}\text{C}$) for Ag - Ag system

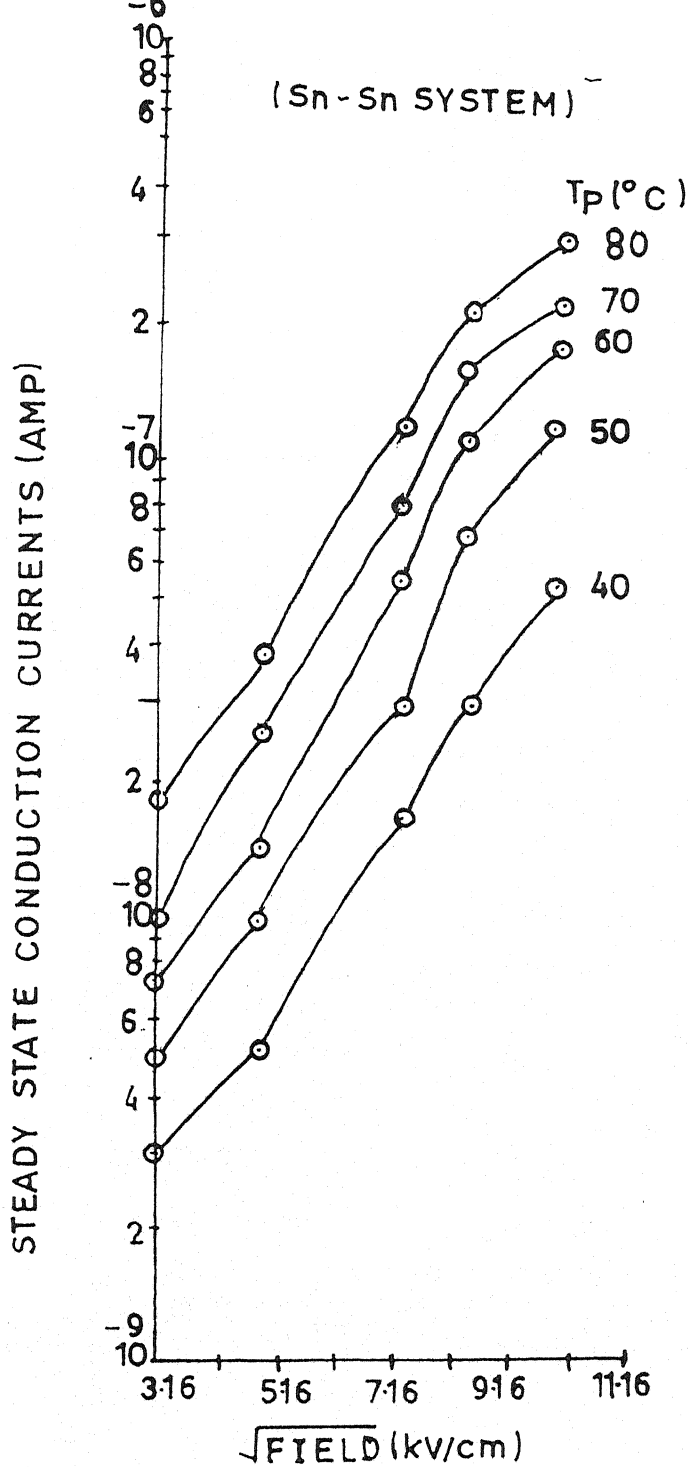


Fig. No. - 6.22

Log I versus $\sqrt{\text{field}}$ curves
for polyvinylidene fluoride
samples at different
Temperature (i.e. 40, 50, 60
70 and 80 °C) for Sn - Sn
system

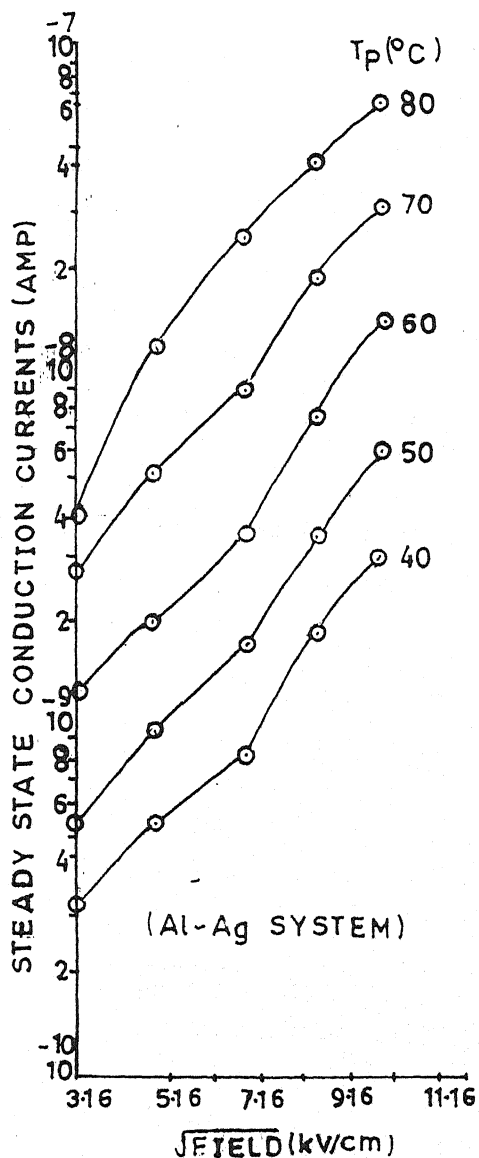


Fig. No. - 6.23

Log I versus $\sqrt{\text{field}}$ curves for polyvinylidene fluoride samples at different Temperature (i.e. 40, 50, 60 70 and 80 °C) for Al-Ag system

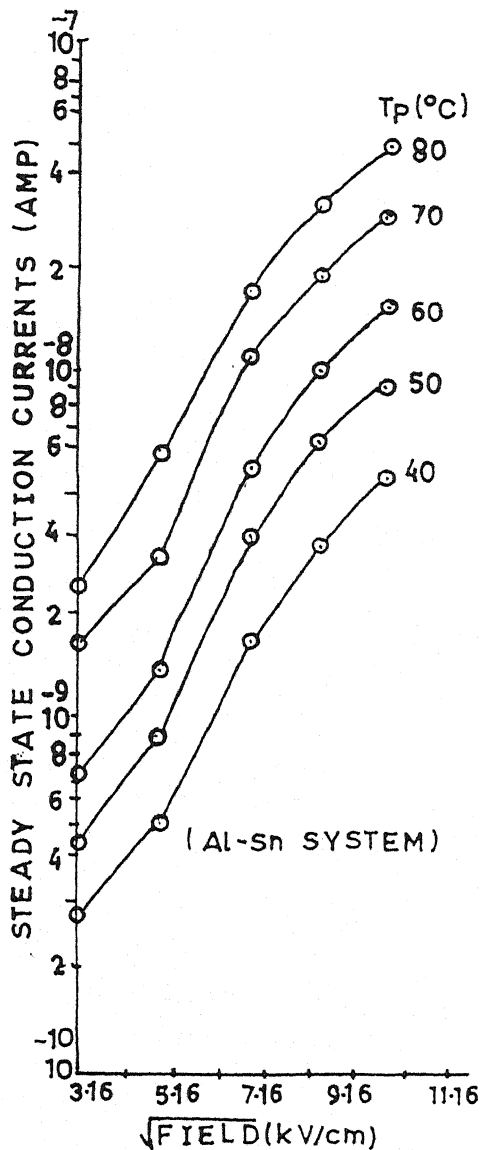


Fig. No. - 6.24

Log I versus $\sqrt{\text{field}}$ curves for polyvinylidene fluoride samples at different Temperature (i.e. 40, 50, 60 70 and 80 °C) for Al-Sn system

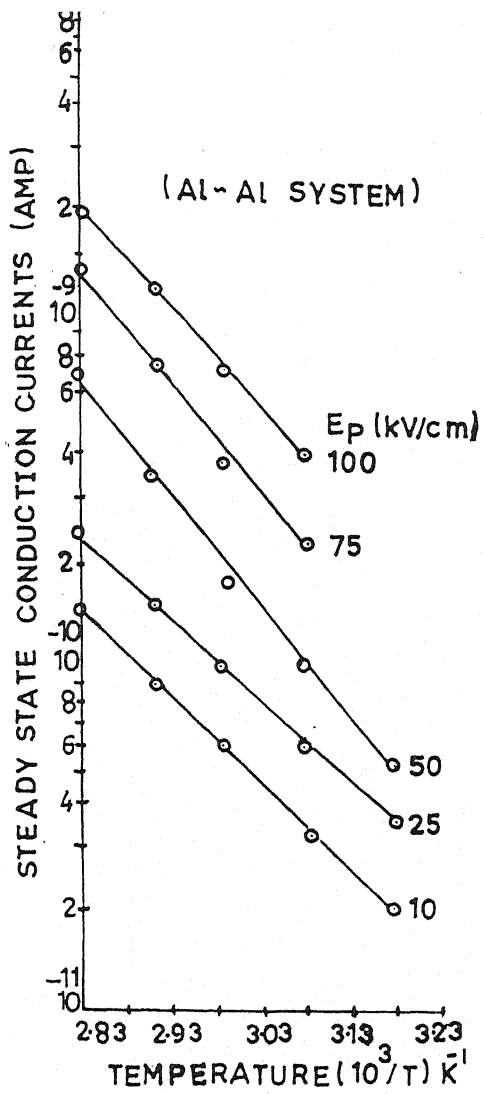


Fig. No. - 6.25

Initial Rise Plotes of Figure
No. 6.11

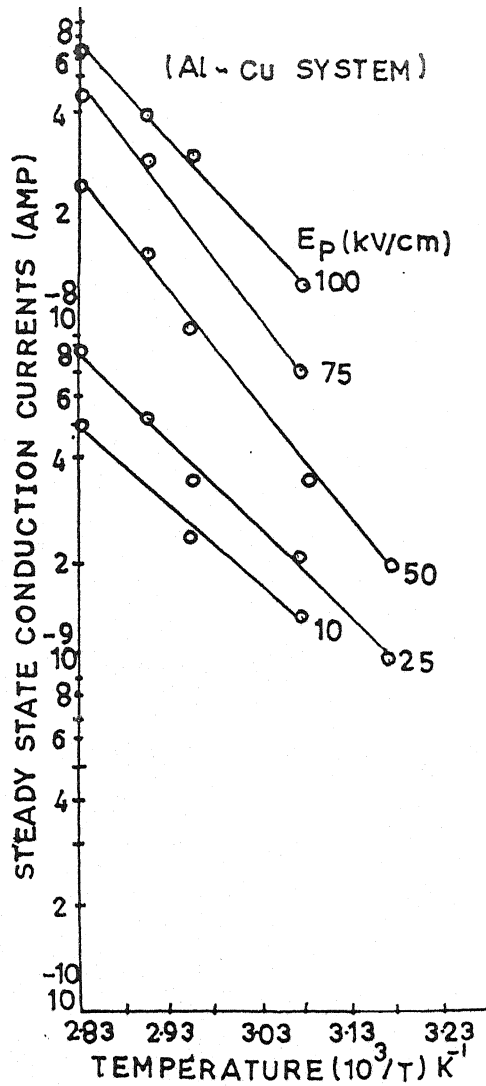


Fig. No. - 6.26

Initial Rise Plotes of Figure
No. 6.12

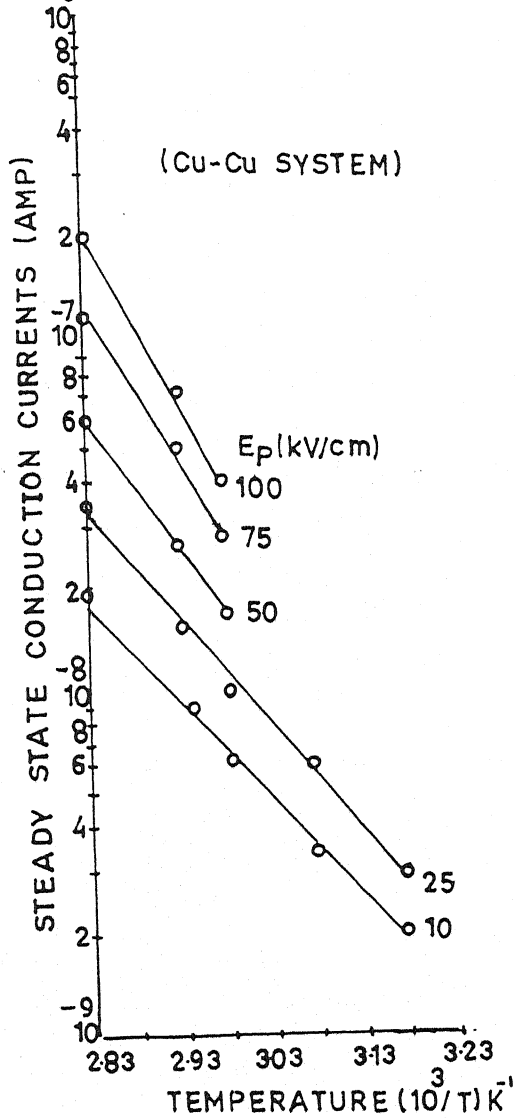


Fig. No. - 6.27

Initial Rise Plotes of Figure
No. 6.13

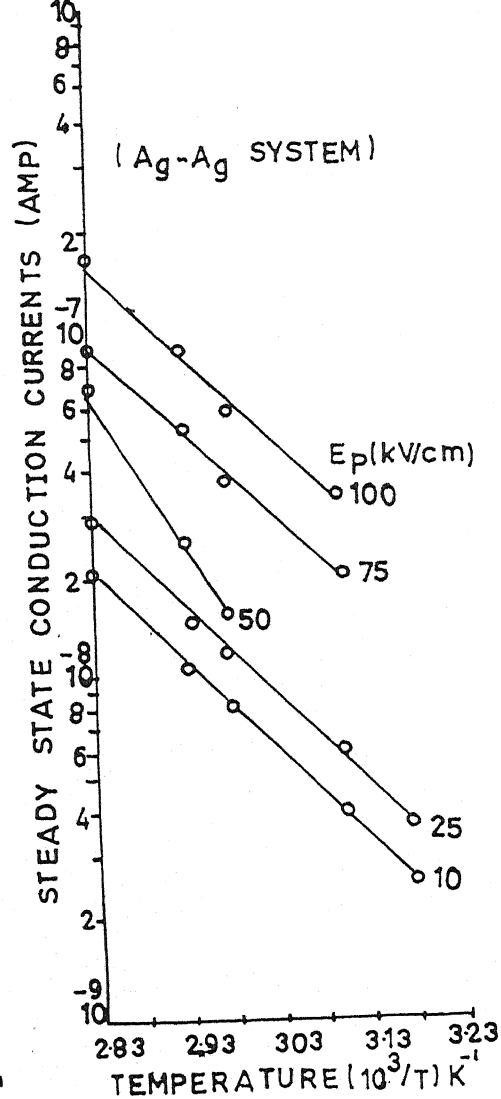


Fig. No. - 6.28

Initial Rise Plotes of Figure
No. 6.14

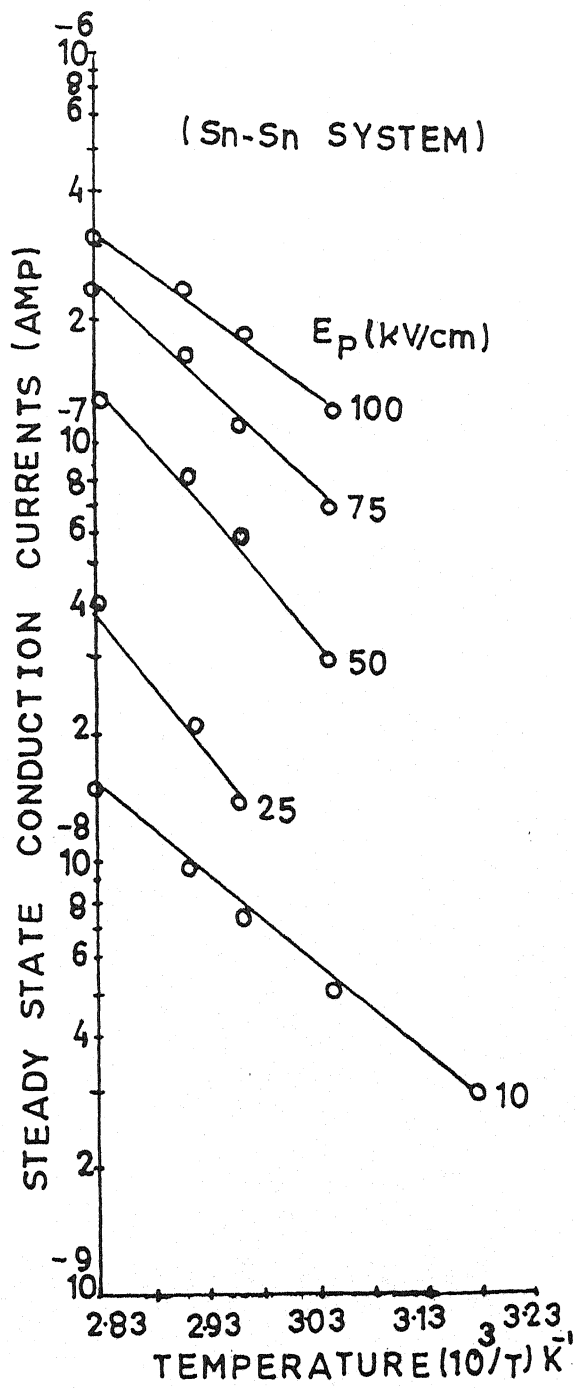


Fig. No. - 6.29

Initial Rise Plotes of Figure
No. 6.15

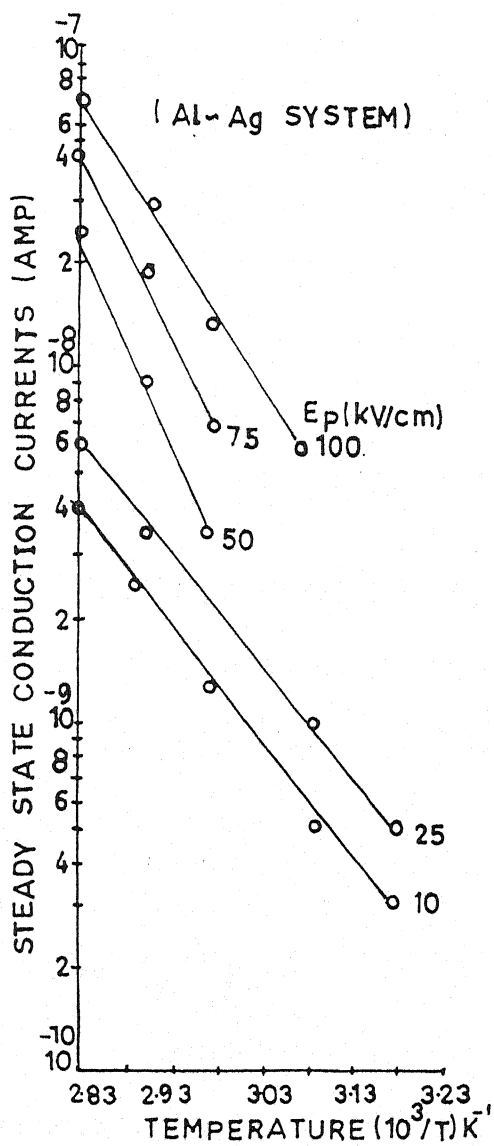


Fig. No. - 6.30

Initial Rise Plotes of Figure
No. 6.16

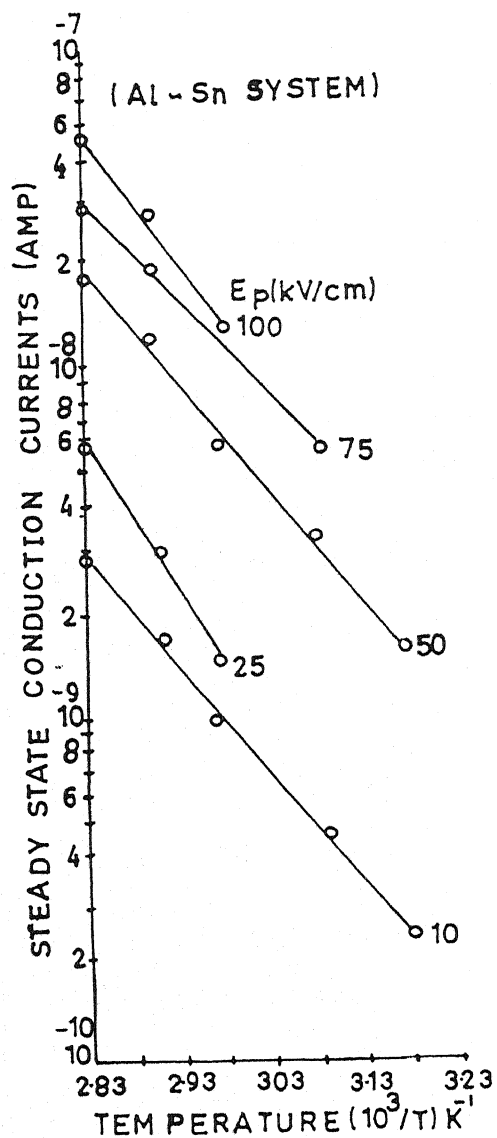


Fig. No. - 6.31

Initial Rise Plotes of Figure
No. 6.17

nonlinear, they indicate the presence of other modes of electrical conduction as well. The observed non-linearity could be due to build up of a space charge resulting in nonuniformity of field distribution between the electrodes. Moreover, the linearity of I-V curves in the high-field region indicates that either of the mechanisms, Schottky-Richardson or Poole-Frenkel, may be operative. However, the slope value (~ 2) also indicates that space charge limited currents may also take part in this region.

On the basis of the various factors governing the variation of current with temperature, i.e. (i) nature of trap distribution in the sample, (ii) presence of impurity in the sample, and (iii) production of defects due to thermal excitation, O'Dwyer [83] suggested the presence of numerous isolated shallow traps covering an energy range ΔW below the continuum of free electron levels. Presence of deep traps, whose energy W is between the conduction and valency levels, is also a possibility. While at sufficient low temperature (absolute zero), all the trapped electrons would be in deep traps, at a finite temperature, and the presence of an applied field, some of these electrons can be excited into the shallower traps (or conduction levels), either thermally or due to action of the applied field. Under the influence of the applied field, these electrons participate in electrical conduction.

Our results indicate that with increasing temperature, the probability of thermal ionization of the trapping centres also increases, resulting

thereby in a shift in the quasi Fermi level. This shift lowers the barrier across which electrons are transported, and the electrical conduction is ohmic. At low energy fields, fewer carriers are injected from the electrodes, and therefore, the initial current is governed by the intrinsic free carriers in the materials. At higher-energy fields, the change of slope is suggestive of deviation from Ohm's law based conduction to the space charge limited conduction. This mode of electrical conduction continues until the injected free carrier density. However, at sufficiently higher energy fields, the current is dominated by space-charge limited conduction and the conduction is mainly due to injected space charge [84]. The departure from Ohm's law in high-energy fields is due to perturbation of active barrier even in the absence of thermal and chemical effects. Since, for our studies, the film thickness was very high (20 μm), the conduction mechanism by tunnelling is ruled out, which requires the film thickness to be very small.

The observed relation between the current and voltage points to a conduction mechanism in which the charge carriers are released by thermal activation over a Coulombic potential barrier that decreases with the applied electric field. The physical nature of such a potential barrier can be interpreted in two basic ways : (i) barrier between the electrodes and dielectric taking the classic image force into consideration (Schottky emission), and (ii) barriers due to trapping centres in the dielectric Poole-Frenkel (P-F) effect.

While the expression for the current density in Schottky emission is

$$J_{SR} = A^* T^2 \exp(-\phi/kT) \exp \left[\frac{e}{kT} \left(\frac{eE}{4\pi\epsilon} \right)^{1/2} \right] \quad \dots (6.1)$$

where C is the constant independent of field and temperature and ϕ is the barrier height.

To determine the actual conduction mechanism, the value of β -factor, at different temperatures, calculated from the slope of the plots of $\log I$ versus \sqrt{E} , were compared with the theoretically calculated value of β , based on the assumption that one of the mechanisms was operating. The experimental value of β (Table 6.2) in the present case, were close to the theoretically observed values of β_{RS} based on the premise that R-S was the particular mechanism that was operating. Jonscher and Ansari [85] pointed out that instead of basing the distinction between the two mechanisms, on the magnitude of β , it should be based on studies taking an asymmetric M-I-M structure with two electrodes of different work functions. The current in the case of Schottky effect will be asymmetrical when polarities are reversed. On the other hand, it will remain practically unchanged in the case of P-F effect. Since it does not depend on potential barrier at the interfaces, i.e. the basic difference between them is : one is electrode-dependent and the other is not. This can be further substantiated by a study of thermally stimulated discharge currents as a function of polarizing field strength, to determine the actual conduction mechanism.

But in the present investigation, the P-F model of conduction, in its conventional model assumes a field assisted thermal excitation of electrons from traps situated in the conduction band of insulators. Once the electron has acquired sufficient energy for reaching the conduction band, it is free to move unhindered and unobstructed. But Mott and Davis [86] pointed out that a drift mobility, less than about $1 \text{ cm}^2 \text{ V}^{-1} \text{ s}^{-1}$, cannot correspond to this unhindered free-hand conduction. Taking this into account, a modified model for conduction was, therefore, proposed by Jonscher and Ansari for substances of low mobility. This model involves the use of a large number of localized trap states, randomly distributed in space and energy. Mott and Davis [86] too conjectured the presence of traps states in disordered structures. In polymers, these traps may be a result of regular chain folding, their (chain) termination, the presence of crystalline-amorphous interfaces, chain entanglements, etc.

The value of activation energy ($< 1 \text{ eV}$) indicates the predominance of electronic conduction in the present case. The activation energy values found to be independent of the applied field suggesting that the potential barriers are highered due to the applied field. This suggests that the applied field interacts with the field of the ionizable centre so that the energy required for an electron to escape in a direction opposite to the field direction (i.e. in the field-assisted or 'forward' direction) is reduced by an amount [87,88]. As the activation energy values obtained in the present

case are high, therefore, the possibility of charge carrier species inside the polymer bulk ionic in nature cannot be ruled out.

The new model furthermore suggests that the process of field-assisted ionization of donor-like carriers, which is the basis of P-F mechanism, does not produce free carrier in a conduction band, as is normally considered to be the case, but merely causes hopping like movements of localized carriers in the trap levels. This process of hopping is assisted by the presence of an external field which reduce 'hop behaviour' by $vE^{1/2}$, where $v = (e^3/\pi\epsilon\epsilon_0)^{1/2}$, as given in the conventional P-F model. The revised expression can thus be written as :

$$I = I_0 \exp E (W_0 - vE^{1/2}) / kT \quad \dots (6.2)$$

where W_0 is the average barrier height of 'hops', I_0 the pre-exponential coefficient that may be defined as the current at an infinite temperature, e the electronic charge, ϵ the high-frequency dielectric constant and ϵ_0 the permittivity of space charge [89]. The space charge limited currents may also determine the transient behaviour such as a large burst of current immediately after the application of field followed by a steady decline in current on standing. In the present case large currents obtained just after the application of voltage subsided to much smaller steady values after a certain length of time. The possible application of voltage causes a cloud of carriers, that is, a space charge, to be injected, from the contact into the sample. This free charge give rise to a large burst of current. If the space

charge remained untrapped, the peak value of the transient current would continue as a steady current.

In the present case, the slope of I-V curves are seen not to exceed the value 2. Usually a slope of 2 indicates shallow trapping but this does not seem to exclude the possibility of deep traps in the present case. Also, in the lower field region, ohmic conduction prevails; space charge build up at high field may be associating factor for the conduction current and a two fold mechanism explains the high field conduction. Besides space charges injected from electrodes Richardson-Schottky emission is the dominant process, responsible process for the transport of the charge carriers.

/ ***** /

Table 6.1
"m" values

Temp. (°C)	Lower Field				Higher Field Onwards			
	Al-Al	Cu-Cu	Ag-Ag	Sn-Sn	Al-Al	Cu-Cu	Ag-Ag	Sn-Sn
40	1.1	1.2	1.3	1.4	2.00	2.00	1.98	1.99
50	1.2	1.4	1.2	1.3	1.97	1.98	1.97	1.96
60	1.4	1.3	1.5	1.2	1.99	2.00	1.95	2.00
70	1.5	1.2	1.1	1.5	1.96	1.97	2.00	1.98
80	1.3	1.5	1.4	1.1	1.98	1.99	1.96	1.97

Table 6.2
Theoretical and experimental values of β_{RS} and β_{PF}

Temp. (°C)	β_{RS} (Theo.) ... x 10 ⁻⁴	β_{RS} (Expt.) ... x 10 ⁻⁴	β_{PF} (Theo.) ... x 10 ⁻⁴	β_{PF} (Expt.)	ϵ_{PF}	ϵ_{RS}	ϵ Stand.
40	8.46	9.87	16.92	8.79×10^{-5}	15.70	3.48	3.18
50	8.17	9.67	16.34	7.66×10^{-5}	18.34	3.51	3.18
60	7.85	8.95	15.7	6.82×10^{-5}	19.64	3.59	3.18
70	7.68	8.93	15.36	5.99×10^{-5}	20.72	3.42	3.18
80	7.32	8.11	14.64	5.24×10^{-5}	21.44	3.49	3.18

Table 6.3
Variation of activation energy with field

Field (kV/cm)	Activation Energy (eV)			
	Al-Al	Cu-Cu	Ag-Ag	Sn-Sn
10	0.61	0.63	0.62	0.64
25	0.63	0.65	0.64	0.63
50	0.64	0.68	0.65	0.66
75	0.65	0.68	0.67	0.68
100	0.66	0.69	0.68	0.67

REFERENCES

1. Kryszewski, M., *Polymeric Semiconductor*, PWN, Warsaw (1968) (in Polish).
2. Chiang, C.K., Park, Y.W., Heeger, A.J., Shirakawa, H., Louis, E.J. and Mac Diarmid, A.G., *J. Chem. Phys.*, **69**, 5098 (1978).
3. Michel, R.E. and Chapman, F.W., *J. Polym. Sci. A-2*, **8**, 1159 (1970).
4. Mayne, J.E.O. and Scantlebury, J.D., *Brit. Polym. J.*, **2**, 240 (1970).
5. Cowan, D.O., Park, J., Pittman, C.U. Jr., Sasaki, Y., Mukherjee, T.K. and Diamond, N.A., *J. Am. Chem. Soc.*, **94**, 5110 (1972).
6. Sasabe, H. and Saito, S., *J. Polym. Sci. A-2*, **6**, 1401 (1968).
7. Oster, A., *Z. Angew. Phys.*, **23**, 120 (1967).
8. Kosaki, M., Ohshima, H. and Ieda, M., *J. Phys. Soc. Japan*, **4**, 1012 (1970).
9. Lengyel, G., *J. Appl. Phys.*, **37**, 807 (1966).
10. Mann, H., *J. Appl. Phys.*, **35**, 2173 (1964).
11. Vodenicharov, H., Vodenicharov, M. and Shopov, I., *C. R. Acad Bulg. Sci.*, **24**, 1939 (1971).
12. Caserta, G., Rispoli, B. and Serva, A., *Phys. Stat. Sol.*, **35**, 237 (1969).
13. Patora, J., Piotrowski, J., Kryszewski, M. and Szymanski, A., *J. Polym. Sci. Polym. Lett.*, **10**, 23 (1972).
14. Connell, R.A. and Gregor, L.V., *J. Electrochem. Soc.*, **112**, 1198 (1965).

15. Kulshrestha, Y.K. and Srivastava, A.P., Thin Solid Films, **69**, 269 (1980).
16. Pearson, J.A., Am. Chem. Soc. Polym. Prepr., **12**, 68 (1971).
17. Williams, D.J., Am. Chem. Soc. Polym. Prepr., **14**, 83 (1973).
18. Seanor, D.A., J. Polym. Sci. A-2, **6**, 463 (1968).
19. Gross, B., Charge Storage in Solid Dielectrics, Elsevier, Amsterdam (1964).
20. Scher, H., Photoconductivity and Related Phenomena, Am. Elsevier, New York (1976).
21. Gill, W.D., Amorphous and Liquid Semiconductors, Taylor and Francis, London (1974).
22. Enck, R. and Pfister, G., Photoconductivity and Related Phenomena, Am. Elsevier, New York (1976).
23. Burnett, G.M., North, A.M. and Sherwood, J.N., Transfer and Storage of Energy by Molecules, John Wiley, New York (1974).
24. Schottky, W., Z. Physik., **15**, 872 (1914).
25. Nordheim, L.W., Proc. Roy. Soc., **A121**, 626 (1928).
26. Fowler, R.H. and Nordheim, L.W., Proc. Roy. Soc., **A119**, 173 (1928).
27. Sommerfeld, A. and Bethe, H., Handbuch Der Physik, Springer, Berlin (1933).
28. Guth, E. and Mullin, J.C., Phys. Rev., **61**, 339 (1942).
29. Dolan, W.W. and Dyke, W.P., Phys. Rev., **95**, 327 (1954).
30. Murphy, E.L. and Good, R.H., Phys. Rev., **102**, 1464 (1956).

31. Pulfray, D.L., J. Phys., **D5**, 647 (1972).
32. Martin, E.H. and Hirsch, J., J. Non Cryst. Solids, **4**, 133 (1970).
33. Bhargava, B. and Srivastava, A.P., Ind. J. Phy. Part 53, 47 (1979).
34. Pillai, P.K.C. and Rashmi, J. Polym. Sci. Polym. Phys. Ed., **17**, 1731 (1979).
35. Rose, A., Phys. Rev., **6**, 1538 (1955).
36. Lampert, M.A., Phys. Rev., **6**, 1648 (1956).
37. Perlman, M.M. and Unger, S., Electrets Charge Storage and Transport in Dielectrics, Electrochem. Soc. Inc. Princeton, New Jersey (1973).
38. Martin, E.H. and Hirsch, J., Solid State Commun., **7**, 738 (1969).
39. Rose, A., Concepts in Photoconduction and Allied Problems, Interscience, New York (1963).
40. Herman, A.M. and Rembaum, A., J. Polym. Sci., **C17**, 107 (1967).
41. Sinha, H.C. and Srivastava, A.P., Ind. J. Pure Appl. Phys., **17**, 726 (1979).
42. Kulshrestha, Y.K. and Srivastava, A.P., Polym. J. Japan, **12**, 771 (1980).
43. Shrivastava, S.K. and Srivastava, A.P., Polymer, England, **22**, 765 (1980).
44. Tiwari, A.R., Shrivastava, S.K., Saraf, K.K. and Srivastava, A.P., Thin Solid Films, **70**, 191 (1980).
45. Moncrieff, A.J. - Yeates, U. S. Patent No. 2, **904**, 431 (1959).
46. Walkup, L.E., U. S. Patent No. 2, **897**, 660 (1961).

47. Williams, R., U. S. Patent No. 3, **579**, 332 (1971).
48. Engelbrecht, R.S., J. Appl. Phys., **45**, 3421 (1974).
49. Caserta, G., Bispoli, B. and Serra, A., Phys. Stat. Sol. **35**, 237 (1969).
50. Gutman, F. and Lyons, L.E., Organic Semiconductors, Wiley, New York (1967).
51. Pohl, H.A. in Progress in Solid State Chemistry, Vol.I, Ed., H. Reiss, Pergamon Press, New York (1964).
52. Lupinski, J.H., Ann. N. Y. Acad. Sci., **155**, 561 (1969).
53. Electrical Conduction in Organic Solids, Discuss. Faraday Soc., 51 (1971).
54. Dutt, S.C., J. Sci. Ind. Res., **28**, 5 (1969).
55. Mott, N.F. and Davis, E.A., Electronic Processes in Noncrystalline Materials, Clarendon Press, Oxford (1971).
56. Yu, L.T., J. Phys. Medium, **34**, 330 (1963).
57. Beker, W.O., J. Polym. Sci., **C4**, 633 (1964).
58. Sashin, B.J., Electrical Properties of Polymers, Izd. Chimie, Leningrad (1970).
59. Sasaba, H. and Saito, S., J. Polym. Sci., **A2**, 6, 1401 (1968).
60. Oster, A., Z. Angew. Phys., **23**, 120 (1967).
61. Takamatsu, T., Proc. of the Second Symp. on Atomic Energy B-7, Tokyo (1958).
62. Kosaki, M., Oshima, H. and Ieda, M., J. Phys. Soc. Japan, **29**, 1012 (1970).

63. Lengyal, M.A., J. Appl. Phys., **37**, 807 (1966).
64. Clilly, A. and McDowell, J.R., J. Appl. Phys., **39**, 141 (1968).
65. Rastogi, A.C. and Chopra, K.L., Thin Solid Films, **26**, 61 (1975).
66. Mahendru, P.C., Pathak, N.L., Singh, S. and Mahendru, P., Phys. Stat. Sol. **A36**, 355 (1976).
67. Vodencherova, C., Phys. Stat. Sol. **A41**, 487 (1977).
68. Bradwell, A., Cooper, R. and Verlow, B., Proc. IEE, **118**, 247 (1971).
69. Shatzkes, M., J. Appl. Phys., **49**, 4868 (1978).
70. Christy, M.M., J. Appl. Phys., **36**, 1805 (1965).
71. Connell, R.A. and Gregor, L.V., J. Electrochem. Soc., **112**, 1198 (1965).
72. Lovell, R., J. Phys. D. : Appl. Phys., **7**, 1518 (1974).
73. Pillai, P.K.C., Agrawal, S.K. and Neir, P.K., **15**, 379 (1977).
74. Brehmer, L. and Pinnow, M., Phys. Stat. Sol., **A50**, 239 (1978)
75. Jonscher, A.K., Thin Solid Films, **1**, 213 (1967).
76. Ieda, M., Sawa, G. and Kato, L., J. Appl. Phys., **42**, 3737 (1971).
77. Tanaka, T., J. Appl. Phys., **44**, 2430 (1973).
78. Rose, A., Concepts in Photoconductivity and Allied Problems, Interscience, New York (1963).
79. Pearson, J.M., Amer. Chem. Soc. Polym. Prepr., **12**, 68 (1971).
80. Williams, D.J., Amer. Chem. Soc. Polym. Prepr., **14**, 83 (1973).
81. McCubbin, W.C. and Munno, R., Chem. Phys. Lett., **2**, 230 (1968).
82. Fleming, R.J., Trans. Faraday Soc., **66**, 3090 (1970).

83. O'Dwer, J.J., J. Appl. Phys., **37**, 599 (1966).
84. Khare, P.K., Keller, J.M., Gaur, M.S., Singh Ranjeet and Datt, S.C., Polym. Int., **35**, 337 (1994).
85. Jonscher, A.K. and Ansari, A.A., Philos. Mag., **23**, 205 (1971).
86. Mott, N.F. and Davis, E.A., Electronic processes in non crystalline materials (Oxford : Clarendon Press) (1971).
87. Srivastava, A.P. and Agrawal, S.R., Phys. Lett., 322 (1974).
88. Tripathi, A.K. and Srivastava, A.P., Indian J. Pure & Appl. Phys., **20**, 863 (1982).
89. Turnhout, J. Van, Thermally stimulated discharge of polymer electrets (New York) (1975).

CHAPTER VII

DIELECTRIC MEASUREMENT

7.1 DIELECTRIC BEHAVIOUR

The dielectric constant and dissipation factor are the crucial quantities in the design of devices. The study of these parameters as a function of temperature and frequency reveal much information on the chemical and physical state of a polymer [1]. A knowledge of the dielectric loss behaviour of thin films is very important because of their possible technical application for insulation, isolation and passivation in microelectronic circuits. Some of the work reported in the literature is reviewed briefly below. Excellent reviews on dielectric properties appeared in the literature [2-5].

Tanaka [6] investigated dielectric relaxation in high polymers. It was shown that the dielectric properties can be interpreted phenomenologically in terms of a generalized Frohlich's response absorption. Dielectric α and β dispersions in polyvinyl butyral was studied by Takashi [7]. The higher temperature dispersion labelled as α and the low temperature dispersion was labelled β , dielectric relaxation of polyvinylidene fluoride was studied by Koizumi *et al.* [8]. The α -relaxation was related to molecular motions in crystalline regions and the β to the microbrownian motion in amorphous regions. Dielectric properties of impurity doped polyethylene was studied by Kosaki and Ieda [9]. Two peaks of dielectric absorption were observed. Dielectric relaxation of high polymers in the solid state was studied by Ishida [10]. Sasabe *et al.* [11] investigated the dielectric relaxations in PVF₂. Three distinct absorption peaks α_c , α_b and β were observed.

Dielectric characteristics of styrene formed by glow discharge was studied by Valentin and Carchano [12]. The results were explained in terms of dipolar and hopping process. Bahri and Singh [13] studied A.C. electrical properties of solution grown thin polyvinyl chloride films. Two high temperature loss peaks were observed and these were explained on the basis of a cluster model proposed by Ubbelohde. Gupta *et al.* [14] studied anisotropy of dielectric relaxation in polyethylene terephthalate fibres. Considerable directional anisotropy was observed in the β relaxation process, which was independent of frequency. Gowrikrishna *et al.* [15] studied the dielectric behaviour of isocyanate terminated polymers. Activation energies were calculated. Maxwell-Wagner sillars interfacial polarization was proposed as the probable mechanism. Ribelles and Calleja [16] studied the β dielectric relaxation in some methacrylate polymers. Apparent activation energies and relaxation strengths were calculated.

Dielectric properties of bioriented polypropylene films were studied by Umemura *et al.* [17]. Ramu *et al.* [18] studied the dielectric properties of plasma polymerized hexamethyl disiloxane films. The observed dielectric properties were correlated with film structure and morphology. Basha *et al.* [19] studied the dielectric properties of pure and doped PVA films and the observed dielectric relaxation was attributed to the glass transition. Variation of dielectric loss of polyethylene terephthalate film with different parameters was reported by Prasad and Gupta [20].

The dielectric loss $\tan \delta$, and the capacitance C of plasma polymerized styrene films were measured between room temperature and 250°C at 1 kHz by Deok-Chool Lee and Kyoung-Si Jin [21]. The effects of the oxidation, heating and plasma treatment on $\tan \delta$ and C were investigated. Contour maps of complex relative permittivity in the range -170°C to $+175^{\circ}\text{C}$ and 0.1 Hz to 3 MHz were presented for commercial polybutylene terephthate by Pratt and Smith [22].

Effect of temperature on the dielectric constant of vinylidene fluoride trifluoroethylene was studied by Eatah and Tawlik [23]. There was a marked change in dielectric constant (ϵ') at 70°C . The maximum value of (ϵ') at 70°C was attributed to the phase transition. The poling field reduced ϵ' and shifted ϵ'_{max} towards higher temperature. Dielectric properties of a one dimensional polymer PTS were measured along the chain direction in the temperature range 77-273 K by Ruan Yao Zhong *et al.* [24]. A second order phase transition from a high temperature nonpolar state to a low temperature polar state accompanied by an anomaly in dielectric constant was observed at 195 K. Two peaks in the dielectric loss were found at 150 and 100 K. These results were explained by a model which involves modes of side group motion. The variation of dielectric constant (ϵ') of polyethylene terephthalate (PET) film was studied as a function of temperature and frequency ranging from 0.3 to 15.0 MHz, by Prasad *et al.* [25]. The study of ϵ vs T plots showed a transient temperature at 349 K, independent of frequency. Thus, below the transition temperature the

sample behaved as ferro-electric and above it as paraelectric. The plot $1/\epsilon'$ vs T also confirmed the transition and the Curie temperature T_C . From the positive slopes of this curve, calculated value of Curie constant was found to be nearly 1.4×10^2 .

A.C. conductivity $\sigma(\omega)_m$ and the dielectric constant ϵ' of vinyl chloride vinyl acetate (VC:VAc) copolymers having 3, 10 and 17% VAc content (by weight) was measured in the temperature range 77-410 K and in the frequency range 50-100 kHz by Mahendru *et al.* [26]. At temperatures up to 250 K the dielectric constant showed a very weak frequency and temperature dependence, whereas at temperatures above 300 K, showed a strong frequency dispersion. The mechanism of conduction in low and high temperature regions was discussed in the light of an existing theoretical model.

Composites of PZT with polymethyl methacrylate (PZT/PMMA); polystyrene (PZT/PS); polyvinyl chloride (PZT/PVC); and PZT/PVDF in the weight ratio 90:10 were prepared by the solvent cast technique and their dielectric properties were studied by Sinha and Pillai [27]. From these results it was concluded that the absolute value of the dielectric constant of the composite depends on the dielectric constant of the polymer phase.

The dielectric permittivity and loss of bisphenol-A polycarbonate (PC) was measured over the frequency range 100 Hz to 200 kHz and temperature 77-383 K by Pathmanathan *et al.* [28]. One sub-T_g relaxation

peak was observed which rapidly broadened with decrease in temperature. This was attributed to a progressive separation of the γ and β peaks, which at high temperatures merged to form one peak of high strength.

Measurements of the complex permittivity of cross linked polyurethanes at different temperatures in the frequency range $1-10^5$ Hz were studied by Schlosser and Schonhals [29]. Using a new model, the shape parameters were related to small and large scale interaction.

High frequency dielectric measurements in the range 10 MHz to 10 GHz were performed on poly(ethylene oxide) PEO and its complexes with lithium percholate using time domain spectroscopy by Gray and Vincent [30]. Measurements were made over a wide polymer to salt composition and in the temperature range $50-75^\circ\text{C}$. All the samples were amorphous. A relaxation was observed for PEO and its complexes with LiClO_4 in the GHz region and was attributed to the (β) relaxation arising from long range segmental motion of the polymer or the ion polymer complex.

Plasticization of poly(ethyl methacrylate) (PEMA) by CO_2 was investigated by Kamiya *et al.* [31] by dielectric relaxation spectroscopy. The dissipation factor was measured as a function of frequency (1-10000 kHz) and CO_2 pressure (-60 atm) over the temperature range $35-115^\circ\text{C}$. A maximum in the frequency dependence of the dissipation factor was

attributed to the relaxation of PEMA, which shifted to higher frequency with increasing temperature, pressure or concentration.

7.2 BASIC THEORY

Debye [32] gave the classical picture of relaxation of polarization with a single relaxation time. In this model he considered a set of non interacting dipoles free to rotate against some viscous resistance in a fluid like medium.

Equation for complex permittivity given by Debye is

$$\epsilon^* = \epsilon_{\infty} + \frac{\epsilon_0 - \epsilon_{\infty}}{1 + i\omega\tau} \quad \dots (7.1)$$

- where ϵ_0 - dielectric constant at low frequency
- ϵ_{∞} - dielectric constant at high frequency
- ω - angular frequency
- τ - relaxation time.

Frohlich modified Debye theory. According to him real and imaginary part of the dielectric constants are given by -

$$\epsilon' = \epsilon_{\infty} + \frac{\epsilon_0 + \epsilon_{\infty}}{1 + \omega^2\tau^2} \quad \dots (7.2)$$

$$\epsilon'' = \left(\frac{\epsilon_0 - \epsilon_{\infty}}{1 + \omega^2\tau^2} \right) \omega\tau \quad \dots (7.3)$$

The maximum value of ϵ' and ϵ'' is

$$\epsilon' = \frac{\epsilon_0 + \epsilon_{\infty}}{2} \quad \dots (7.4)$$

$$\epsilon'' = \frac{\epsilon_0 - \epsilon_\infty}{2} \quad \dots (7.5)$$

The magnitude of dielectric dispersion is given by -

$$\epsilon_0 - \epsilon_\infty = \left(\frac{3 \epsilon_0}{2 \epsilon_0 + \epsilon_\infty} \right) \left(\frac{\epsilon_0 + 2}{3} \right) \frac{4}{3} \cdot \frac{\pi n g \mu^2}{kT} \quad \dots (7.6)$$

where n = number of dipoles
 μ = dipole moment
 g = parameter related to dipole interaction
 T = temperature

Polymers rarely follow the Debye theory and they show much broader dispersion and low loss as compared to single relaxation process.

Cole [33] pointed out that this anomaly arises due to the fact that the long chain molecular compounds do not have a single relaxation time. On the contrary their relaxation times are distributed within certain minimum and maximum limits.

Every molecular dipole in a given chain is coupled to neighbouring dipoles of the same chain by primary valence bands so that the motion of any dipole affects the motion of its neighbours and they in turn influence its response to a torque. Furthermore, in various configurations which a chain molecule can assume, we can find one or another segment of chain acting effectively as a co-operative electrical unit and these segments will of course vary in length between the improbable extremes of a single monomeric unit and the whole extended chain. Such a state of affair leads to distribution of relaxation time.

On eliminating the parameter $\omega\tau$ between the two equations and rearranging the two parameters (ϵ' and ϵ'') we get -

$$\left[\epsilon' - \frac{\epsilon_0 + \epsilon_\infty}{2} \right]^2 + \epsilon''^2 = \left[\frac{\epsilon_0 - \epsilon_\infty}{2} \right]^2 \quad \dots (7.7)$$

The above equation represents a circle with center $[(\epsilon_0 + \epsilon_\infty)/2, 0]$ and radius $(\epsilon_0 - \epsilon_\infty)/2$. Only the semicircle over which ϵ'' is positive has physical significance. Materials with single relaxation time yield a semicircle in ϵ' and ϵ'' plane. Polymers do not yield such a semi circle and the ϵ' - ϵ'' plane falls within the Debye semicircle (Fig. 7.1). Cole Cole [33] modified the Debye equation by an empirical equation for the complex permittivity

$$\epsilon^* - \epsilon_\infty = \frac{\epsilon_0 - \epsilon_\infty}{1 + (i\omega T)^{1-\alpha}} \quad \dots (7.8)$$

where α is an empirical parameter. It lies between 0 and 1 and it denotes the angle of tilt of the circular arc from the real axis.

Though the modified expression measures the small deviation from the ideal Debye behaviour, but there are materials which deviate very much from the Debye behaviour.

Havriliak and Negami [34] gave an expression which is of the form -

$$\epsilon^* - \epsilon_\infty = \frac{\epsilon_0 - \epsilon_\infty}{\left[1 + (j\omega T)^{1-\alpha} \right]^{1-\beta}} \quad \dots (7.9)$$

where β is an empirical parameters which lies between 0 and 1 and represents the angle of tilt.

7.3 EXPERIMENTAL

Dielectric studies were carried out on all the sample to study dielectric constant and dielectric loss. The instrument used was HP 4192A impedance analyzer which gives a direct display of capacitance and $\tan \delta$ in the frequency range 10 Hz to 13 MHz.

The sample of polyvinylidene fluoride was placed inside the temperature controlled measurement cell and the test leads of the impedance analyzer were connected to it. The sample capacitance and dielectric loss tangent of the samples were measured at fixed temperature and the frequency was varied from 500 Hz to 1000 kHz in steps. These observations were repeated for different temperatures ranging from 40 to 70°C. A fixed voltage of 1 V was applied to the sample.

The dielectric constant and losses were calculated from C and $\tan \delta$ using the equation valid for parallel plate capacitor.

$$\epsilon' = \frac{C_x d}{\epsilon_0 A} \text{ and } \epsilon'' = \epsilon' \tan \delta \quad \dots (7.10)$$

where C_x is the sample capacitance in Farad, A is the area of the sample, d is the thickness of the sample and ϵ_0 is a constant representing permittivity of free space.

7.4 RESULTS AND DISCUSSION

The dielectric constant and dielectric losses of polyvinylidene fluoride samples are observed in the temperature 40-70°C and frequency (500 Hz to 1000 kHz) range. The result are interpreted in terms of existing theories.

(A) Dielectric Constant

(i) Effect of Temperatures

To observe an effect of temperature on dielectric constant, its variation as a function of temperatures is plotted at different frequencies (i.e. 500 Hz, 2, 10, 100, 500 and 1000 kHz) are shown in the Figs. 7.1-7.7 for similar (Al-Al, Cu-Cu, Ag-Ag and Sn-Sn) and dissimilar electrode (Al-Cu, Al-Ag and Al-Sn) combinations. It is clear from the figures that the value of dielectric constant decreases with increasing frequencies. For higher frequencies (i.e. 500 kHz and 100 kHz) the value of dielectric constant increases attaining a maxima at 70°C and then decreasing. This nature is not observed for other frequencies.

(ii) Effect of Frequencies

The frequency dependence of dielectric constant of the sample at different temperatures (i.e. 40, 50, 60 and 70°C) are shown in Figs. 7.8-7.14 for similar (Al-Al, Cu-Cu, Ag-Ag and Sn-Sn) electrode system and dissimilar electrodes (Al-Cu, Al-Ag and Al-Sn) combinations. It is found that with increasing temperature dielectric constant increases. As per nature of the curve is concern, it is clear that the value of dielectric constant decreases up to 10^4 Hz and beyond this it increases. The rate of decrease and increase of dielectric constant is sharp.

(B) Dielectric Losses

(i) Effect of Temperatures

The effect of temperatures on PVDF samples of 20 μ m thickness for similar (Al-Al, Cu-Cu, Ag-Ag and Sn-Sn) and dissimilar (Al-Cu, Al-Ag and

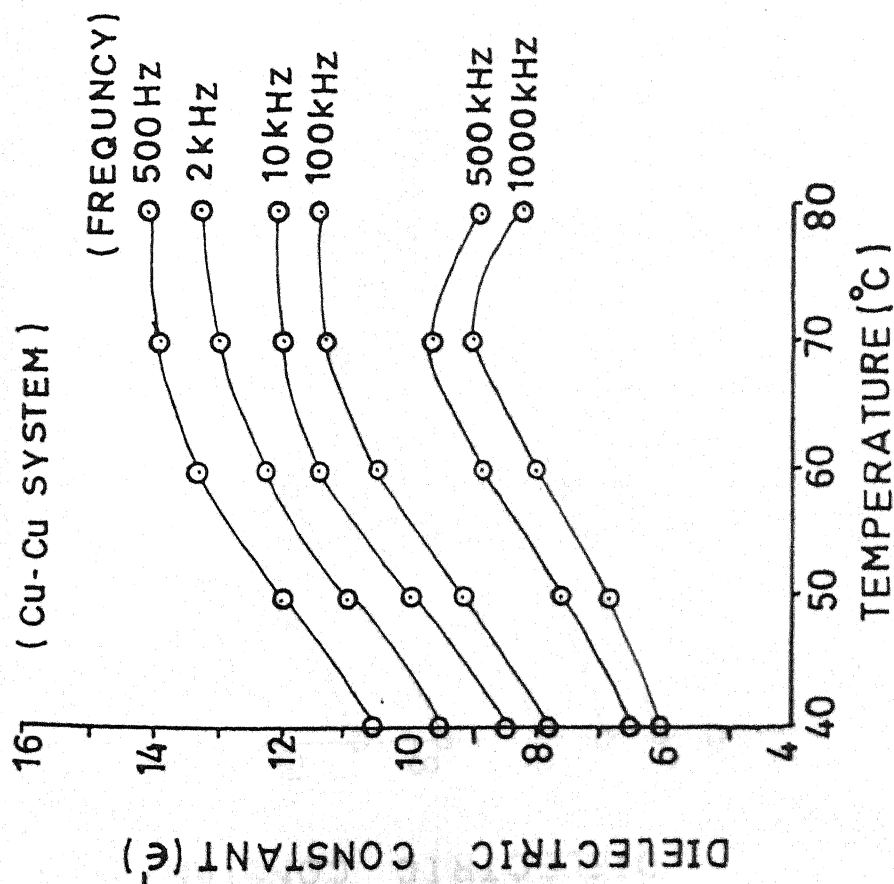


Fig. No. - 7.3

Dielectric constant versus Temperature for polyvinylidene fluoride samples with various frequency (i.e. 500 Hz, 2 kHz, 10 kHz, 100 kHz, 500 kHz and 1000 kHz) for Cu - Cu system

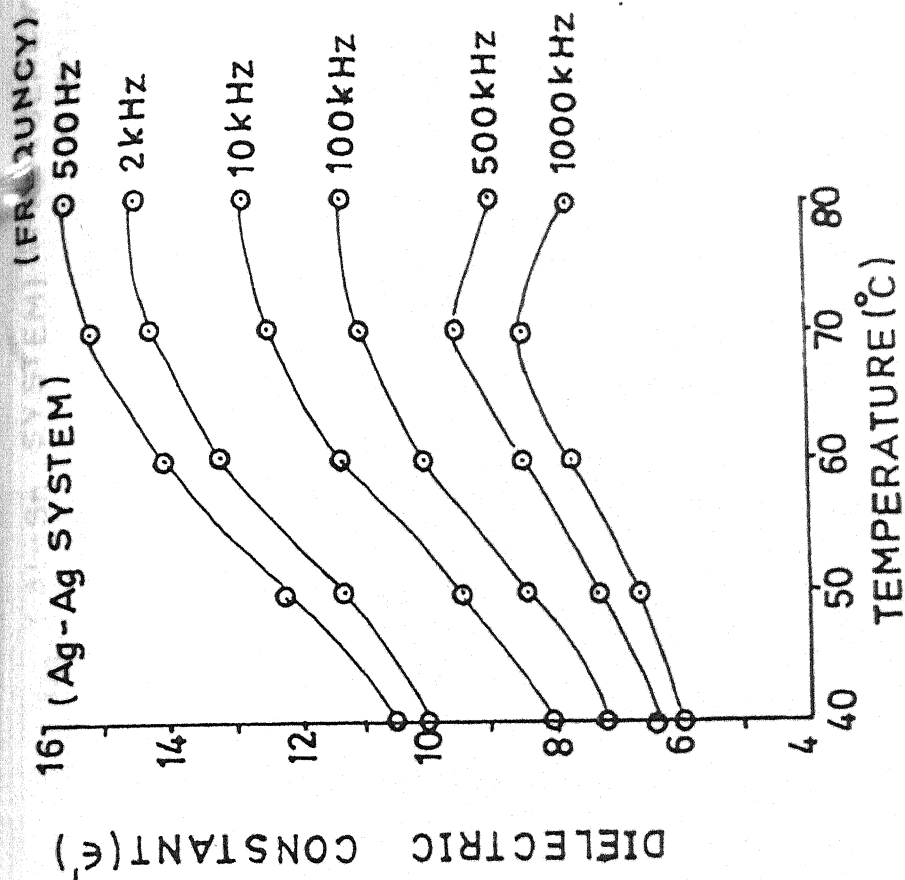


Fig. No. - 7.4

Dielectric constant versus Temperature for polyvinylidene fluoride samples with various frequency (i.e. 500 Hz, 2 kHz, 10 kHz, 100 kHz, 500 kHz and 1000 kHz) for Ag - Ag system

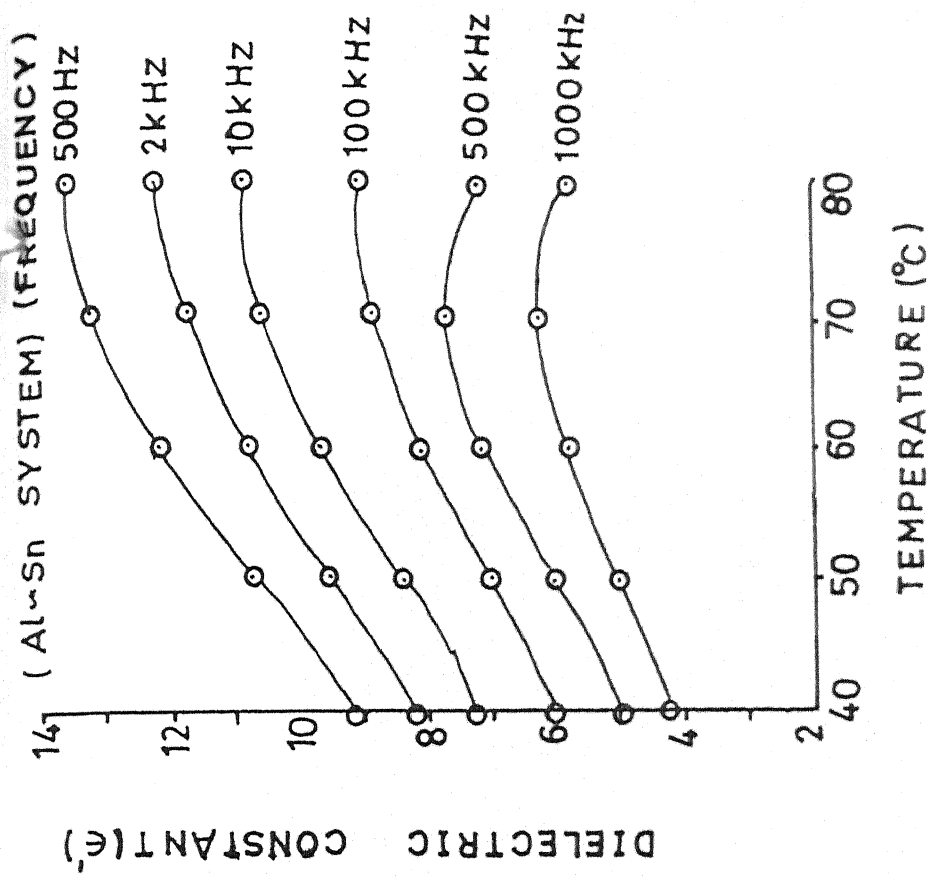


Fig. No. - 7.6

Dielectric constant versus Temperature for polyvinylidene fluoride samples with various frequency (i.e. 500 Hz, 2 kHz, 10 kHz, 100 kHz, 500 kHz and 1000 kHz) for Al - Sn system

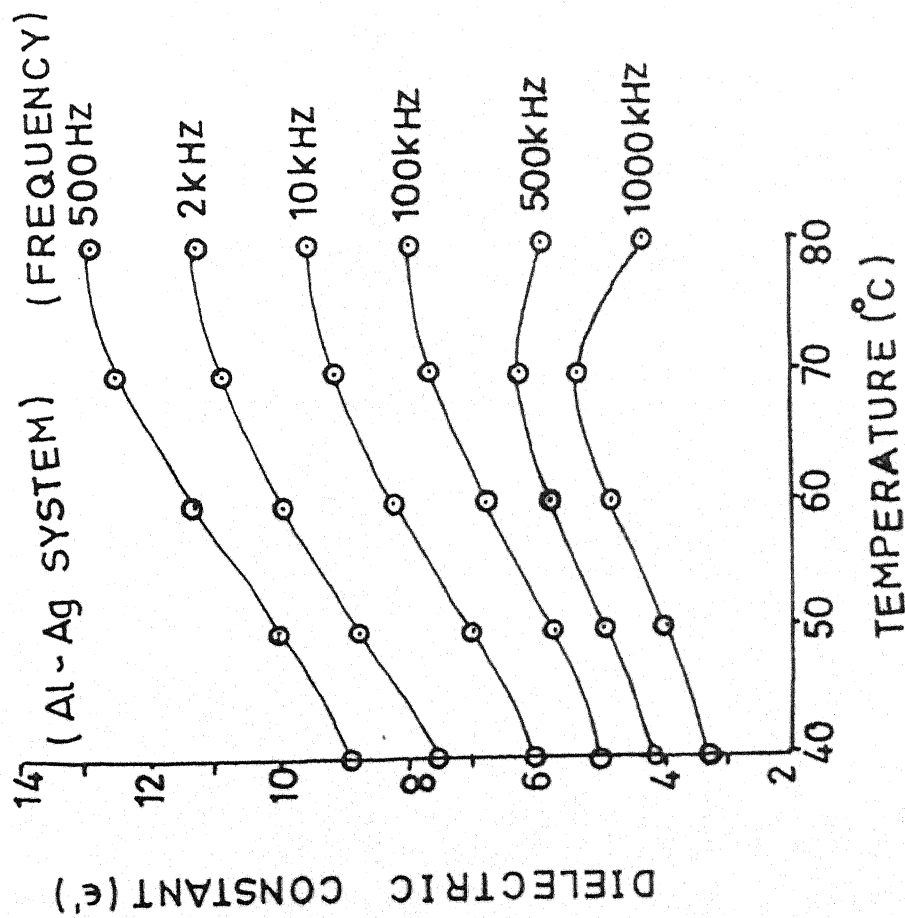


Fig. No. - 7.5

Dielectric constant versus Temperature for polyvinylidene fluoride samples with various frequency (i.e. 500 Hz, 2 kHz, 10 kHz, 100 kHz, 500 kHz and 1000 kHz) for Al - Ag system

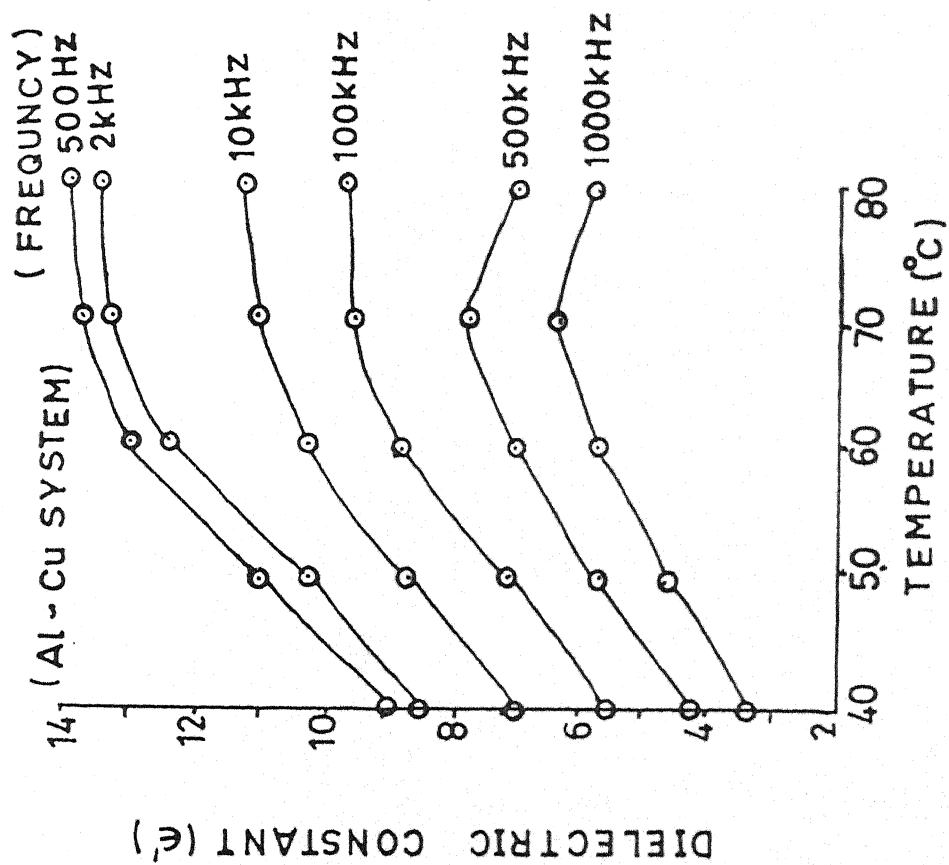


Fig. No. - 7.7

Dielectric losses versus Temperature for polyvinylidene fluoride samples with various frequency (i.e. 500 Hz, 2 KHz, 10 KHz, 100 KHz, 500 KHz and 1000 KHz) for Al - Cu system

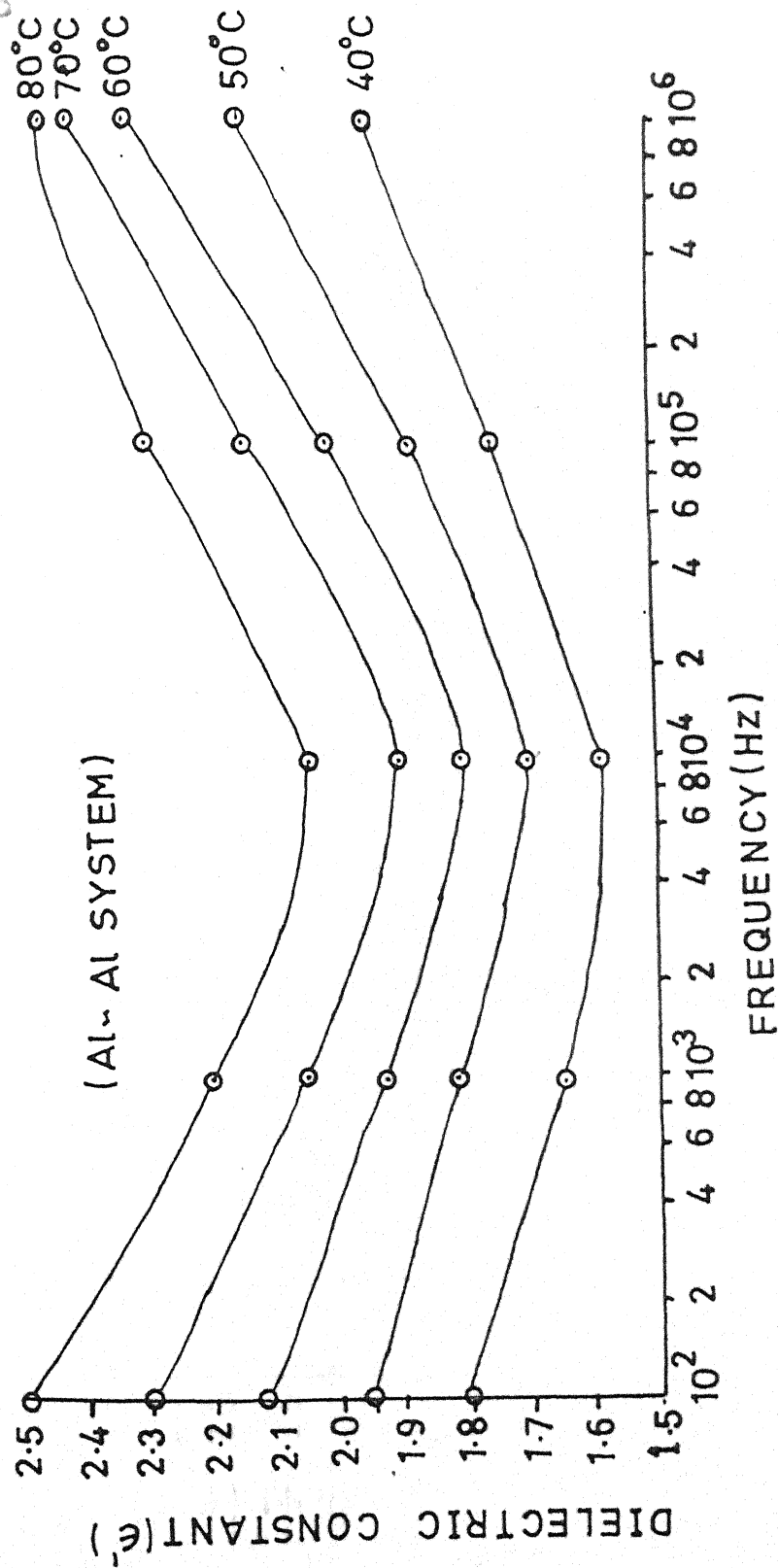


Fig. No. - 7 .8

Dielectric constant versus frequency for polyvinylidene fluoride samples at different Temperature (i.e. 40, 50, 60, 70 and 80 °C) for Al - Al system.

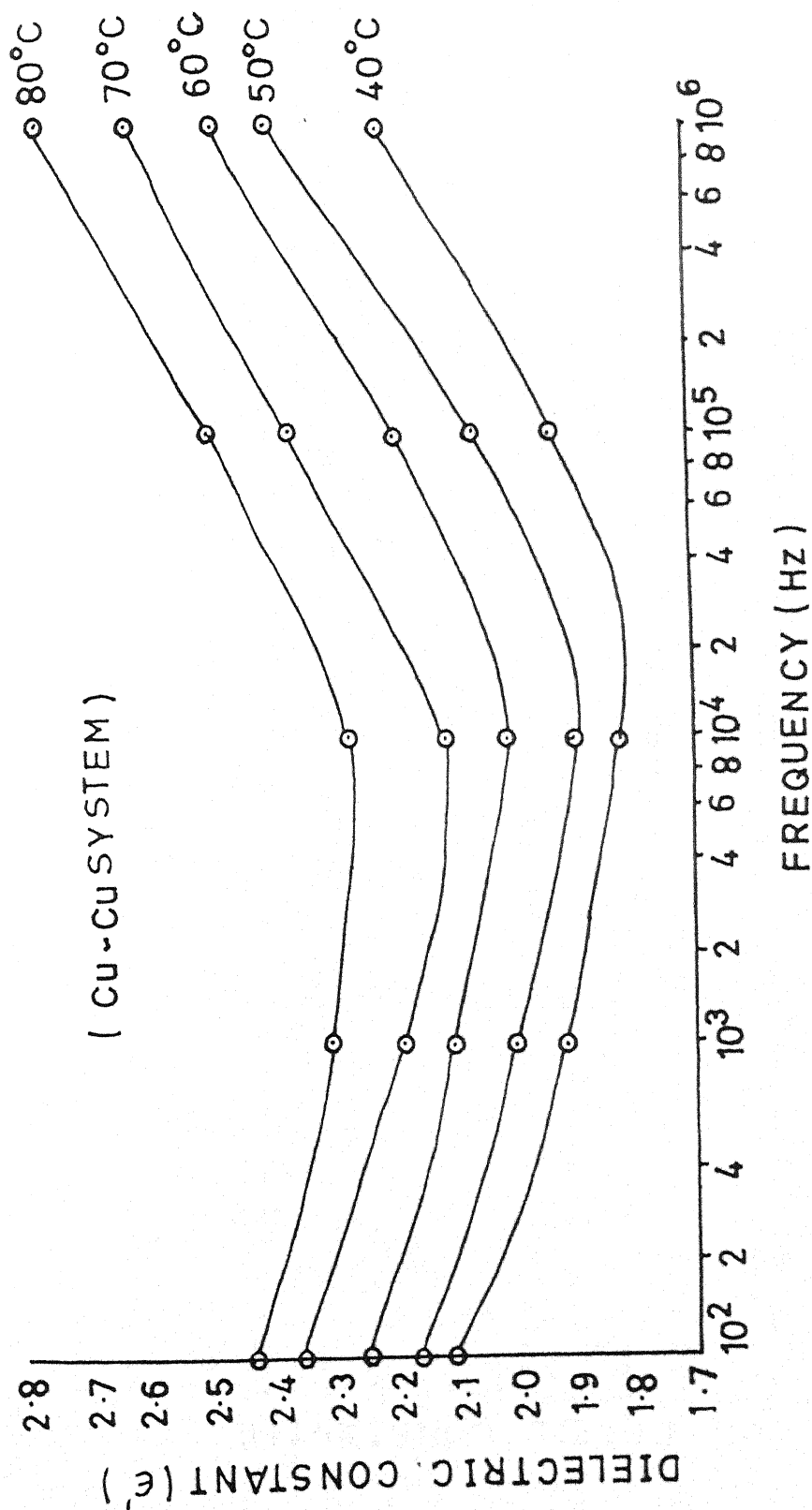


Fig. No. - 7.9

Dielectric constant versus frequency for polyvinylidene fluoride samples at different Temperature (i.e. 40, 50, 60, 70 and 80 °C) for Cu - Cu system.

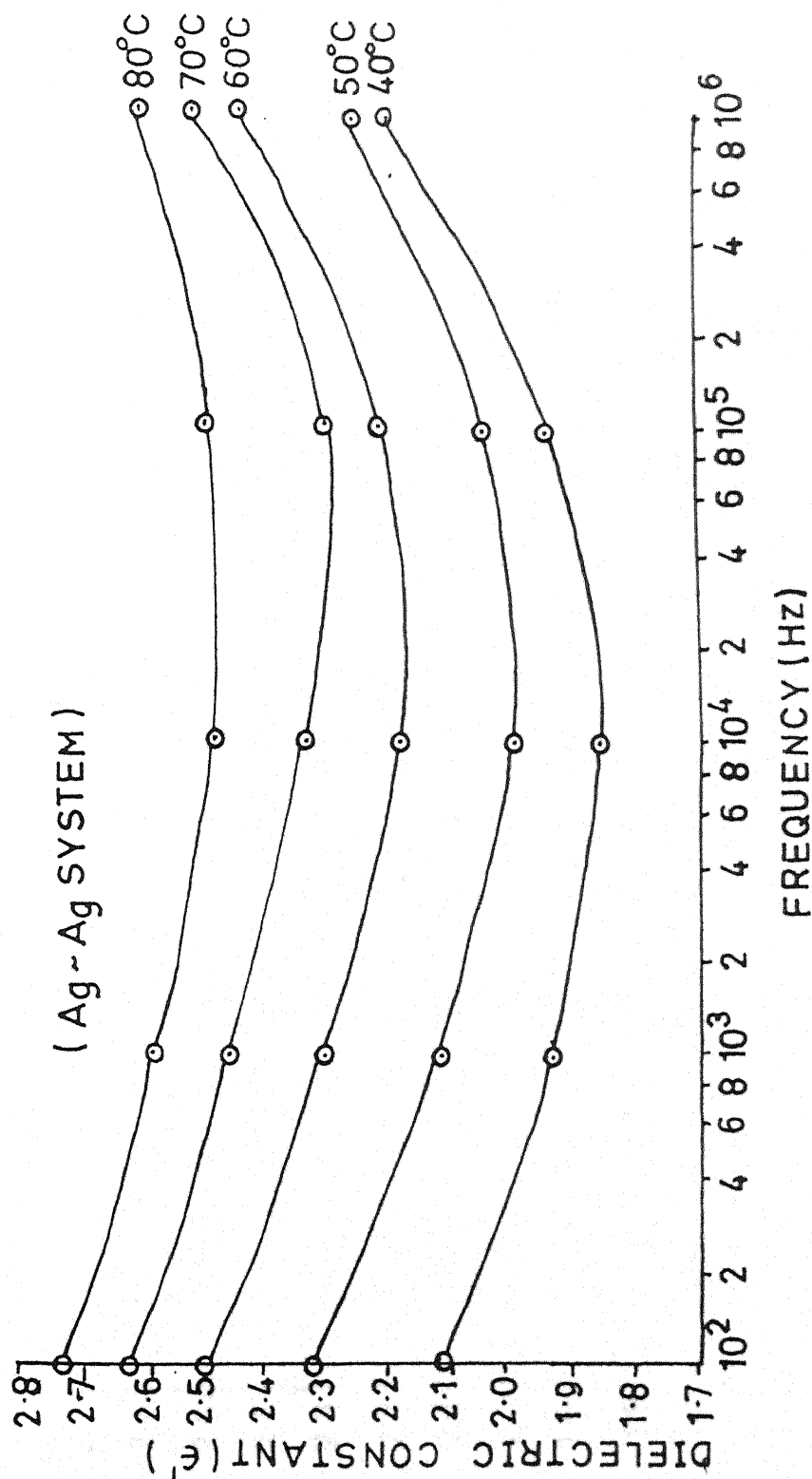


Fig. No. - 7.10

Dielectric constant versus frequency for polyvinylidene fluoride samples at different Temperature (i.e. 40, 50, 60, 70 and 80 °C) for Ag - Ag system.

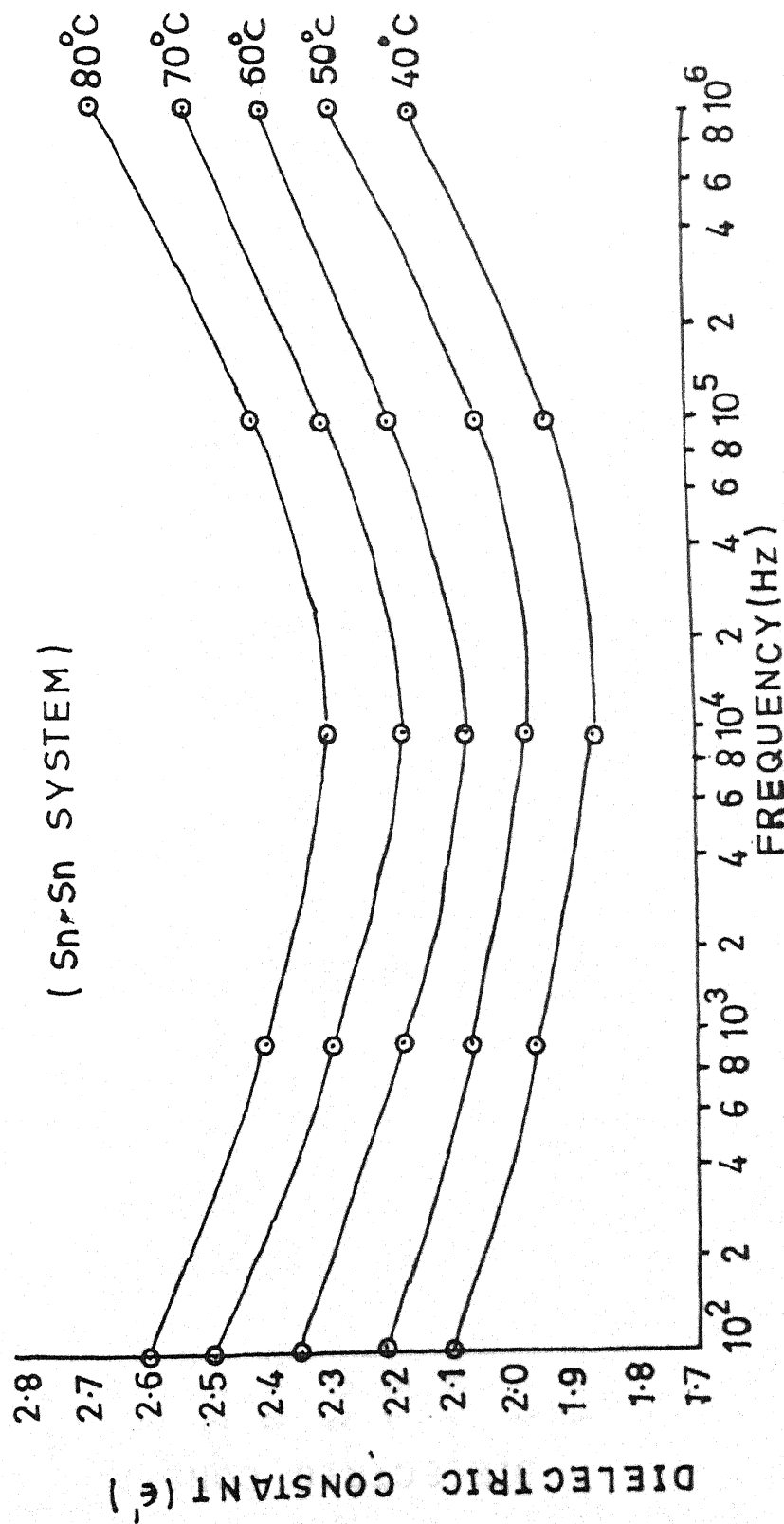


Fig. No. - 7.11

Dielectric constant versus frequency for polyvinylidene fluoride samples at different Temperature (i.e. 40, 50, 60, 70 and 80 °C) for Sn - Sn system.

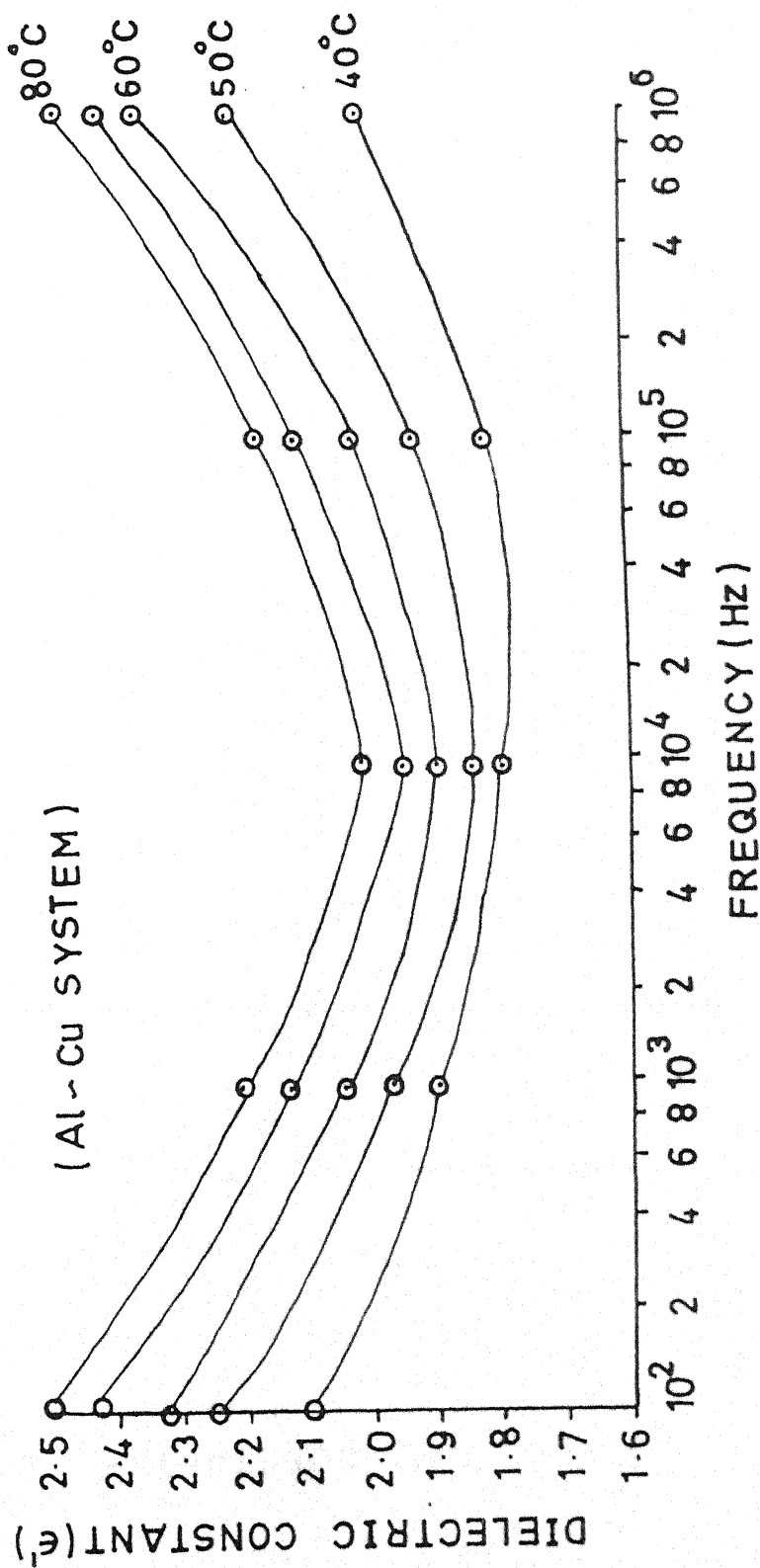


Fig. No. - 7.12

Dielectric constant versus frequency for polyvinylidene fluoride samples at different Temperature (i.e. 40, 50, 60, 70 and 80 °C) for Al - Cu system.

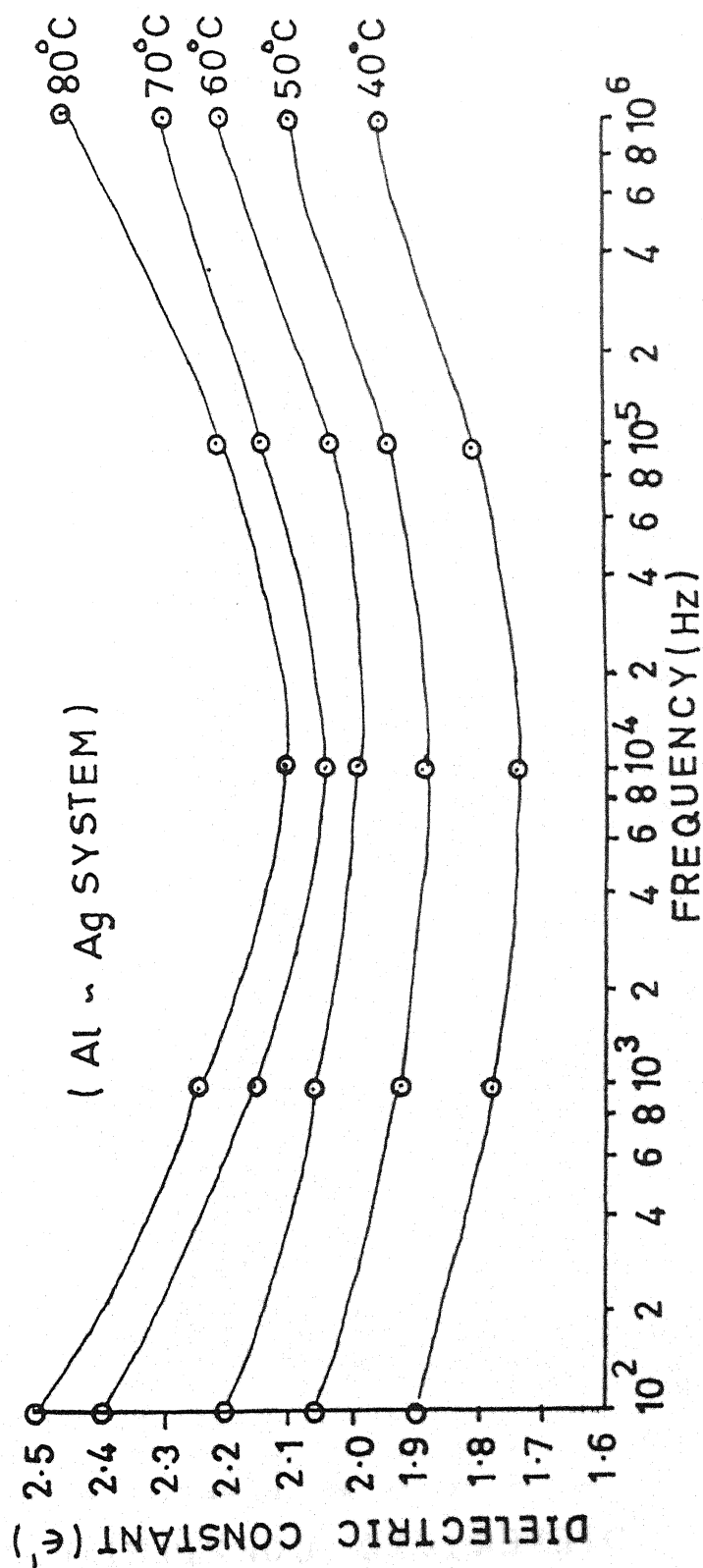


Fig. No. - 7.13

Dielectric constant versus frequency for polyvinylidene fluoride samples at different Temperature (i.e. 40, 50, 60, 70 and 80 °C) for Al - Ag system.

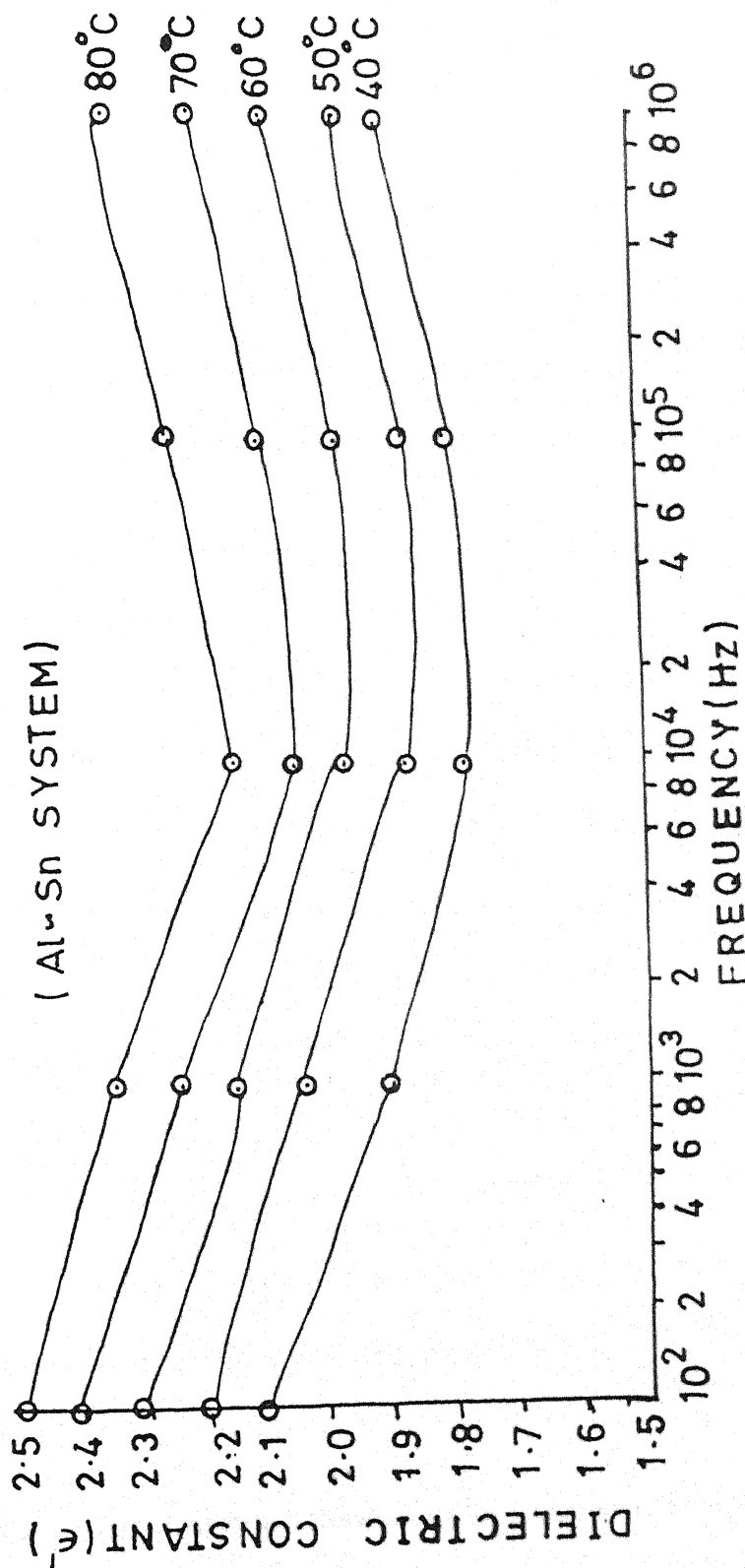


Fig. No. - 7.14

Dielectric constant versus frequency for polyvinylidene fluoride samples at different Temperature (i.e. 40, 50, 60, 70 and 80 °C) for Al - Sn system.

Al-Sn) are shown in Figs. 7.15 to 7.21. It is clear from dielectric loss versus frequency curves that dielectric loss value sharply decays attaining a minima and again it sharply increases. It is very interesting to note that with increasing temperature (i) the value of dielectric losses are less for higher temperature in the first half and after attaining a minimum value, dielectric losses are more for higher temperatures, and (ii) the minima position shifts towards lower frequency range. The nature of all the curves are similar.

(ii) Effect of Frequencies

Figures 7.22 to 7.28 represent the dielectric losses versus temperature curves at constant frequencies (i.e. 500 Hz, 2, 10, 100, 500 and 1000 kHz) for similar (Al-Al, Cu-Cu, Ag-Ag and Sn-Sn) and dissimilar (Al-Cu, Al-Ag and Al-Sn) electrode combinations. The nature of the curves are approximately similar. In general, losses decreases with increase in frequency. In certain cases the curve show slight decrease in the value of dielectric losses and then continuous increasing character is found. The value of losses are found higher, when Al-Al electrode system are replaced by Cu-Cu and Ag-Ag electrode combination.

We have observed a pronounced effect of electrode materials on dielectric constant as well as dielectric losses of the sample when dielectric parameters, i.e. temperature and frequency are changed.

The dielectric behaviour of the polymer is determined by the charge distribution and also by statistical thermal motion of its polar groups. The

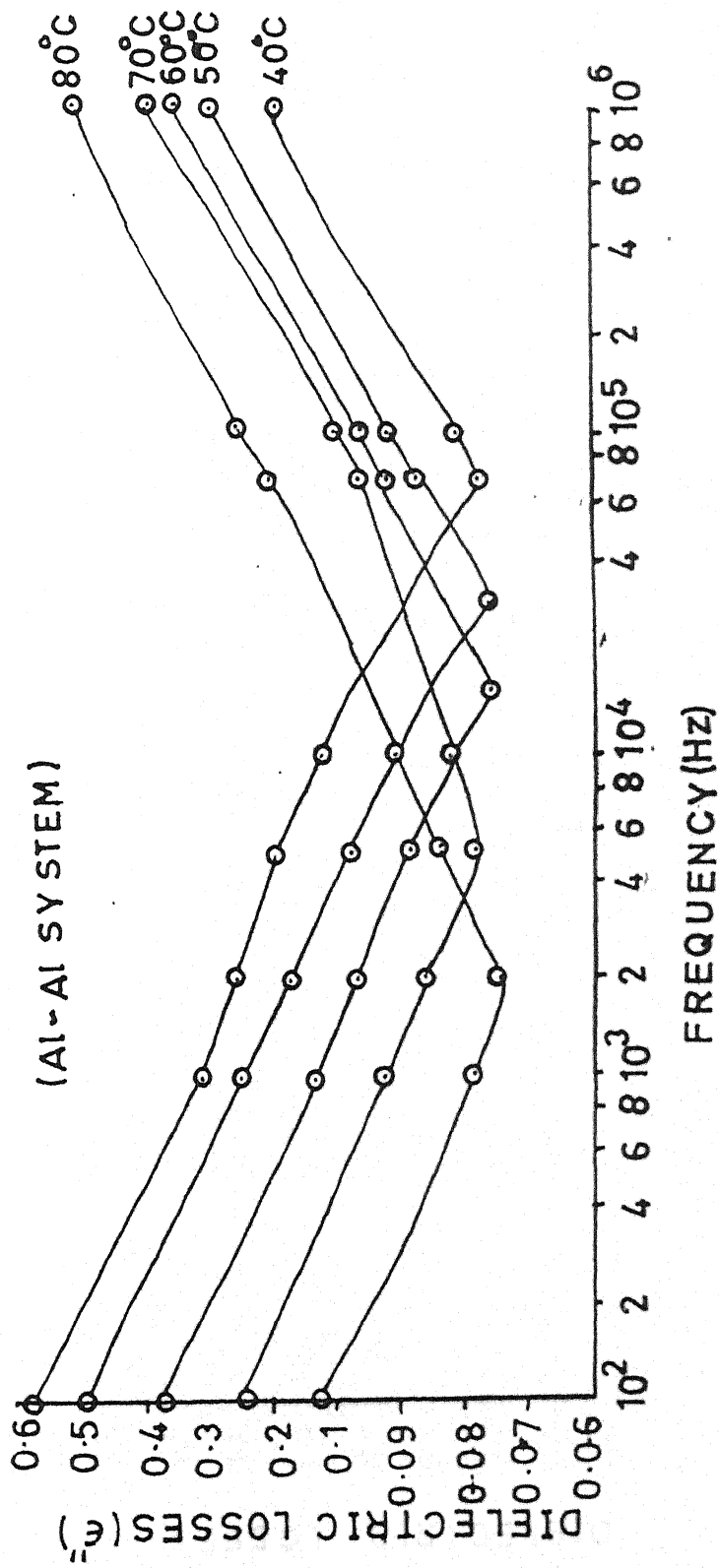


Fig. No. - 7.15

Dielectric losses versus frequency for polyvinylidene fluoride samples at different Temperature (i.e. 40, 50, 60, 70 and 80 °C) for Al - Al system.

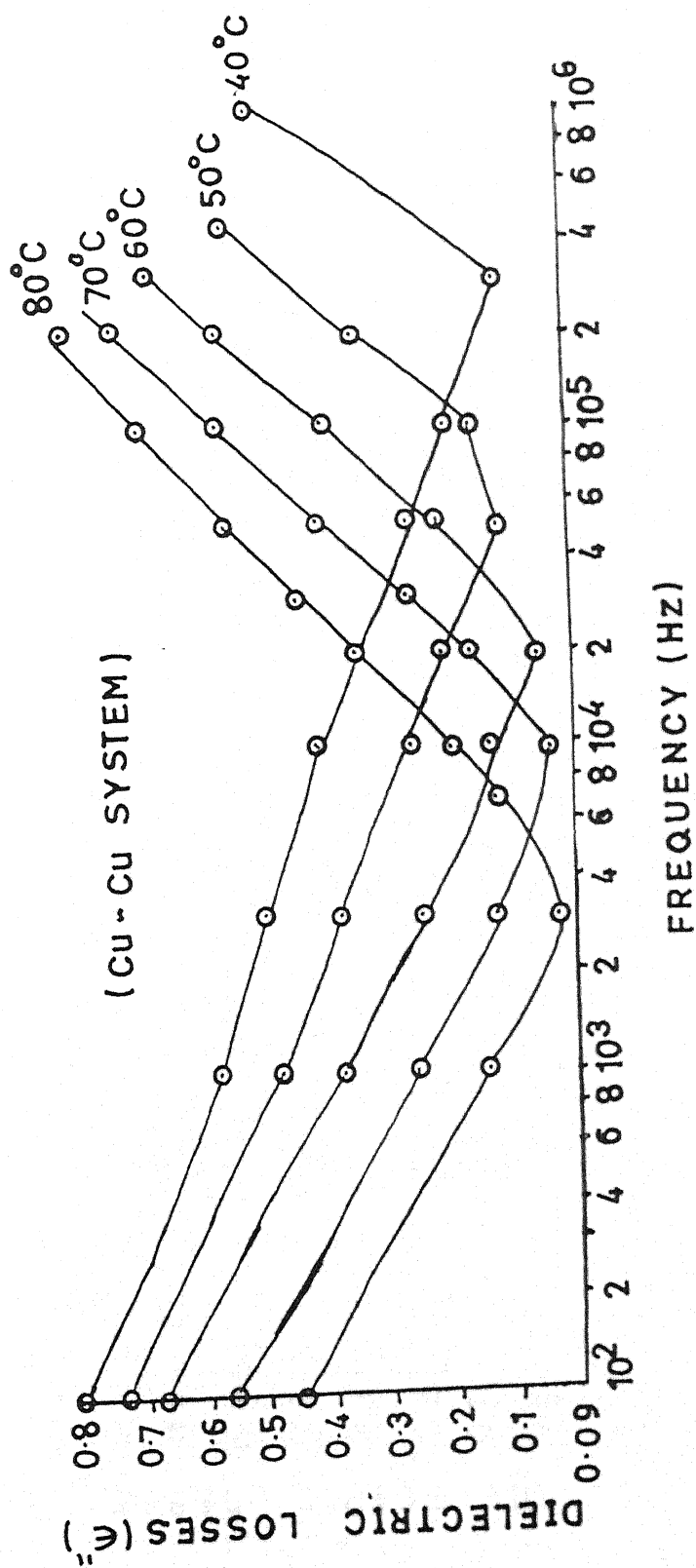


Fig. No. - 7.16

Dielectric losses versus frequency for polyvinylidene fluoride samples at different Temperature (i.e. 40, 50, 60, 70 and 80 °C) for Cu - Cu system.

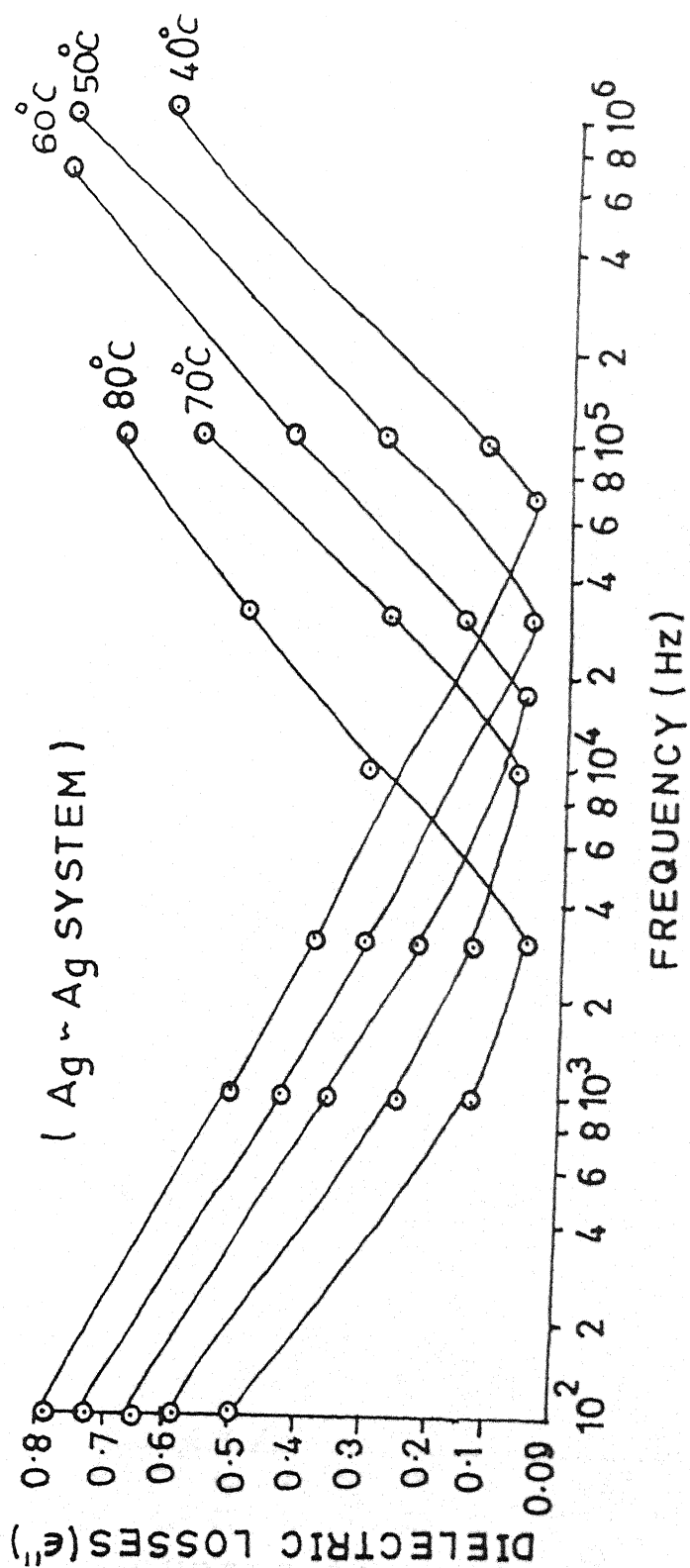


Fig. No. - 7.17

Dielectric losses versus frequency for polyvinylidene fluoride samples at different Temperature (i.e. 40, 50, 60, 70 and 80 °C) for Ag - Ag system.

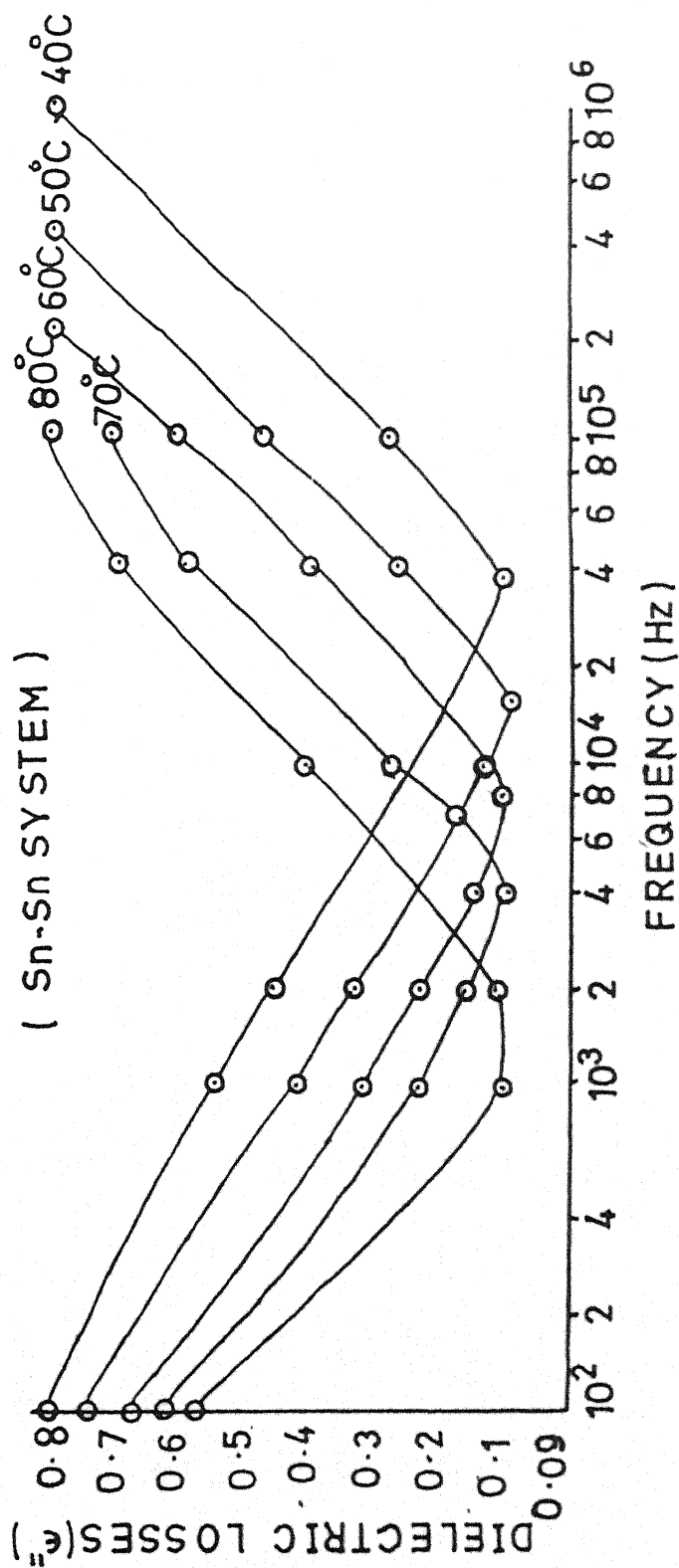


Fig. No. - 7.18

Dielectric losses versus frequency for polyvinylidene fluoride samples at different Temperature (i.e. 40, 50, 60, 70 and 80 °C) for Sn - Sn system.

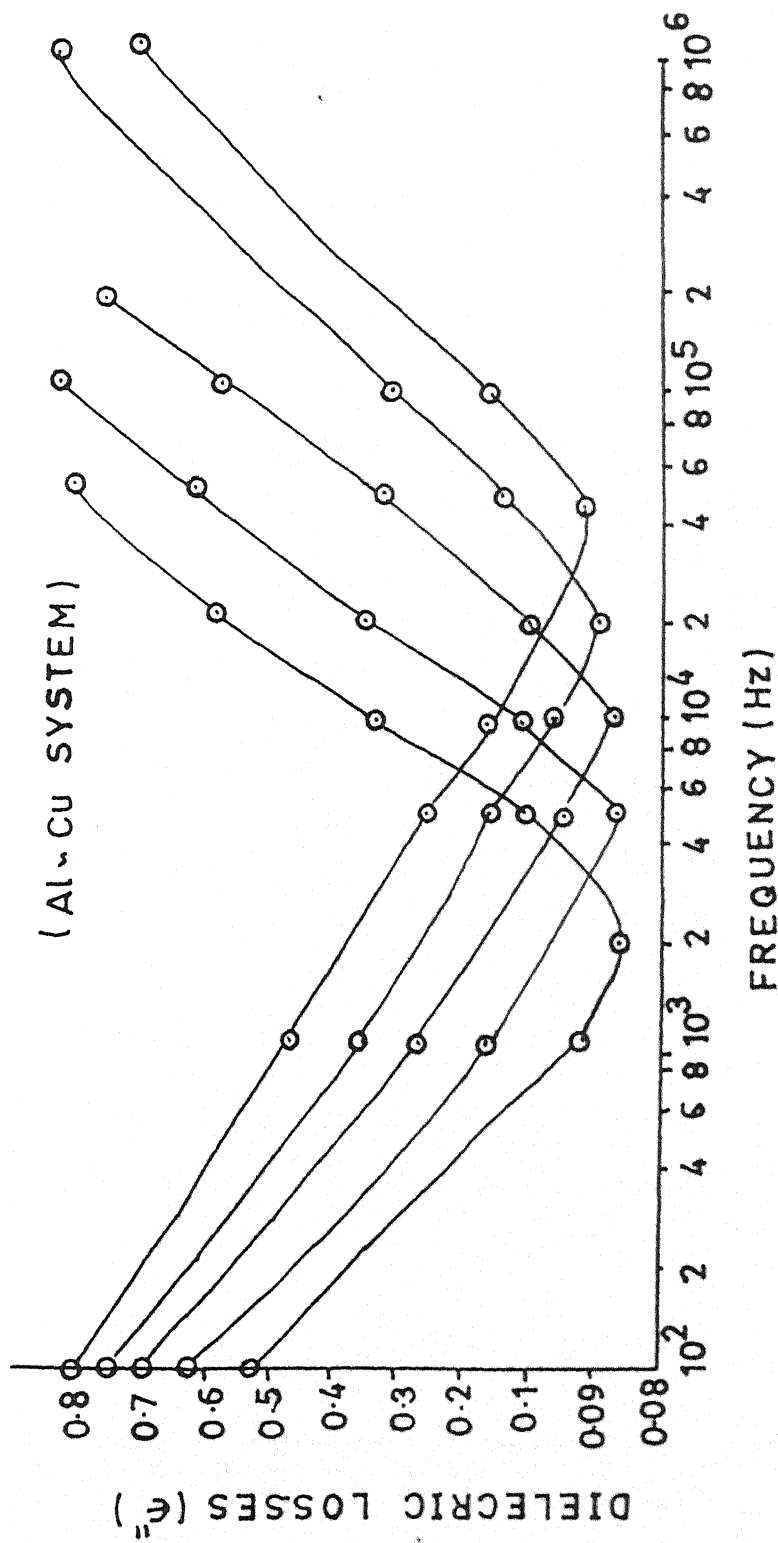


Fig. No. - 7.19

Dielectric losses versus frequency for polyvinylidene fluoride samples at different Temperature (i.e. 40, 50, 60, 70 and 80 °C) for Al - Cu system.

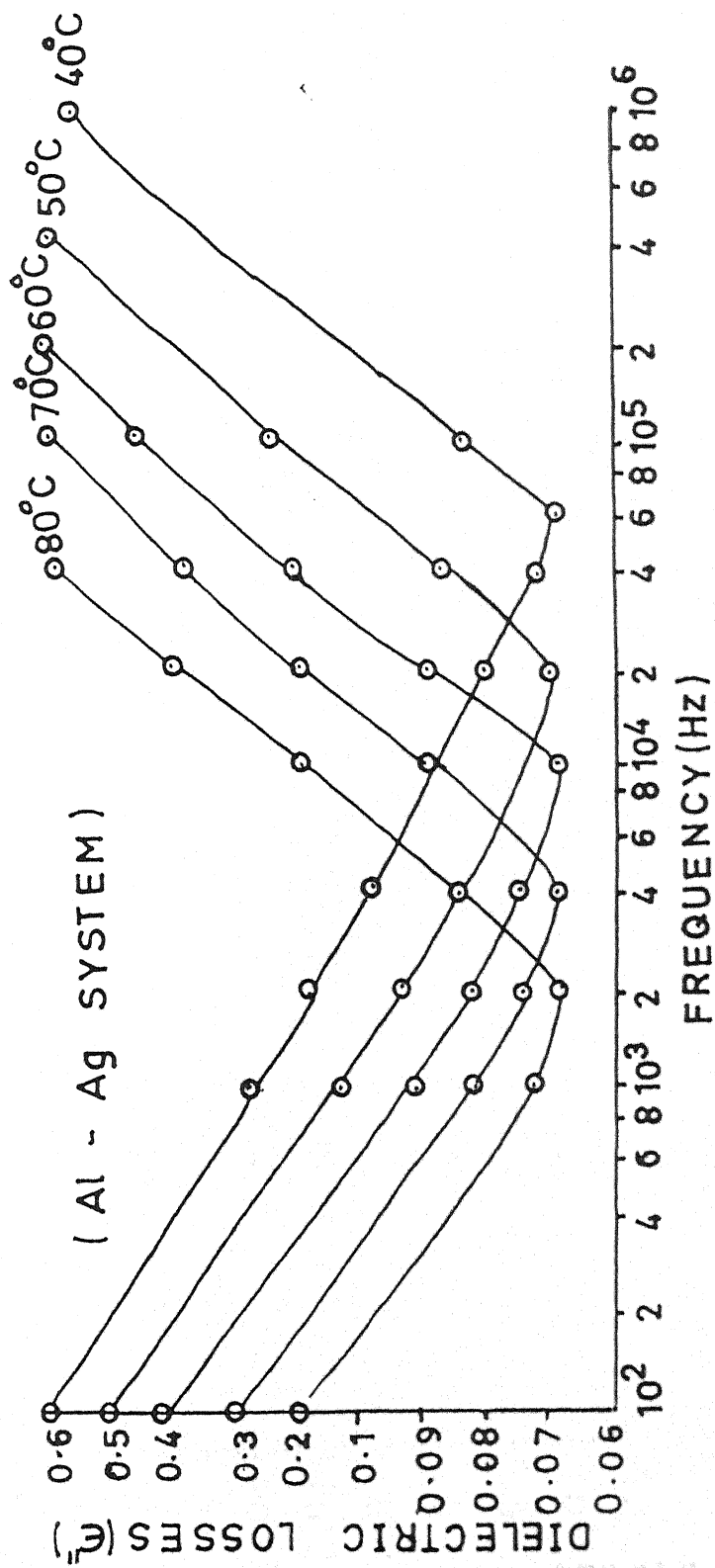


Fig. No. - 7.20

Dielectric losses versus frequency for polyvinylidene fluoride samples at different Temperature (i.e. 40, 50, 60, 70 and 80 °C) for Al - Ag system.

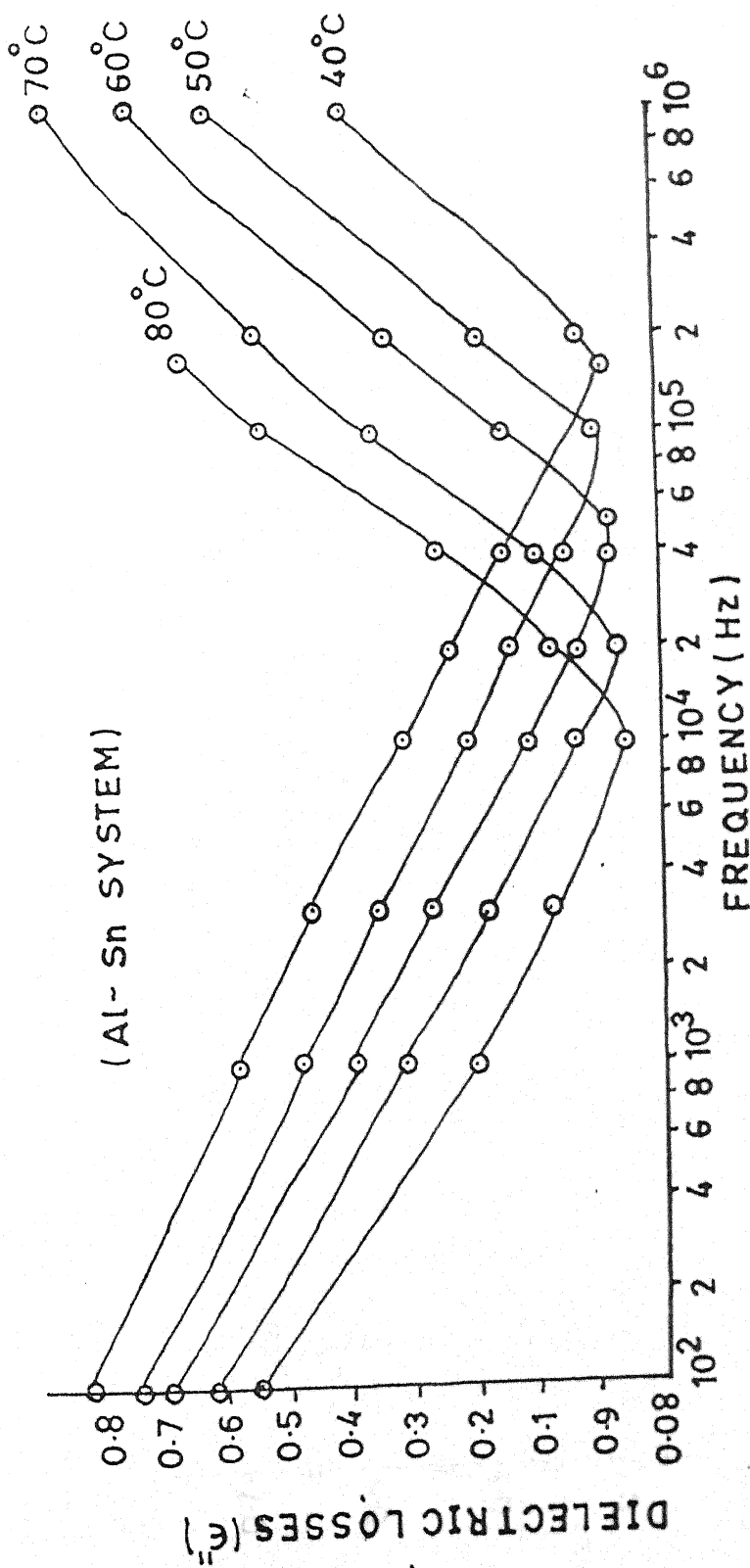


Fig. No. 7-21

Dielectric constant versus frequency for polyvinylidene fluoride samples at different Temperature (i.e. 40, 50, 60, 70 and 80 °C) for Al - Sn system.

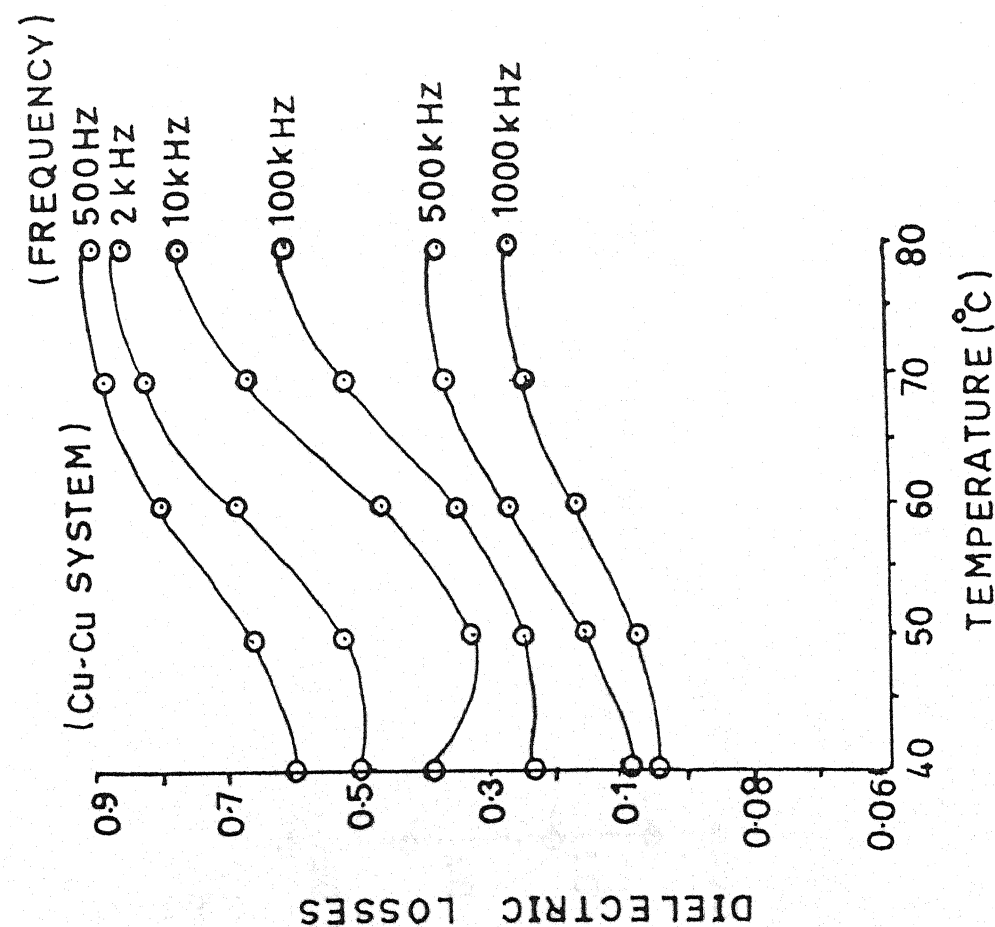


Fig. No. - 7.23

Dielectric losses versus Temperature for polyvinylidene fluoride samples with various frequency (i.e. 500 Hz, 2 kHz, 10 kHz, 100 kHz, 500 kHz and 1000 kHz) for Cu - Cu system

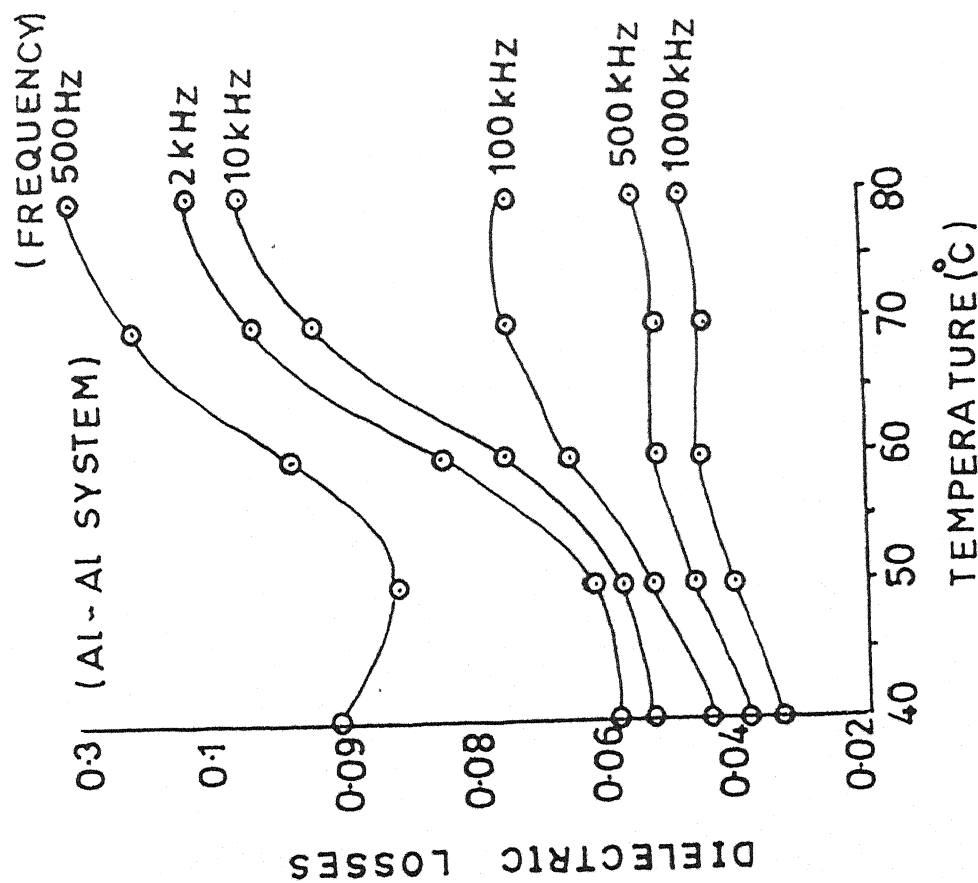


Fig. No. - 7.22

Dielectric losses versus Temperature for polyvinylidene fluoride samples with various frequency (i.e. 500 Hz, 2 kHz, 10 kHz, 100 kHz, 500 kHz and 1000 kHz) for Al - Al system

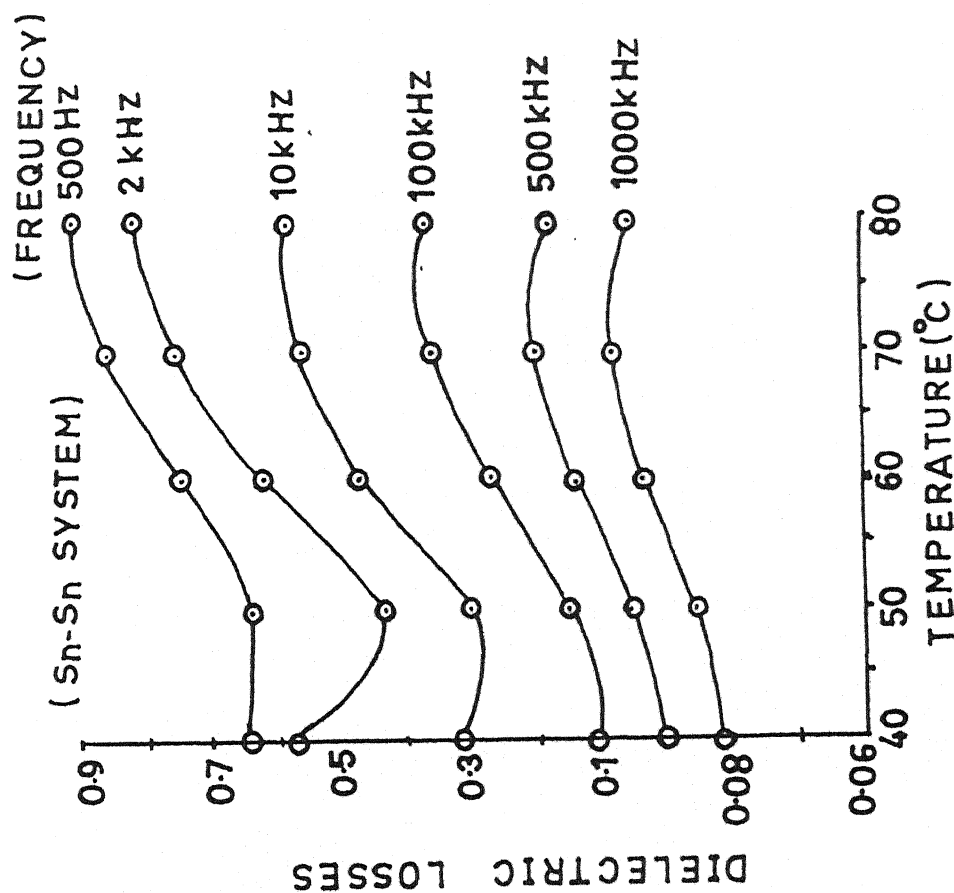


Fig. No. - 7.25

Dielectric losses versus Temperature for polyvinylidene fluoride samples with various frequency (i.e. 500 Hz, 2 kHz, 10 kHz, 100 kHz, 500 kHz and 1000 kHz) for Sn - Sn system

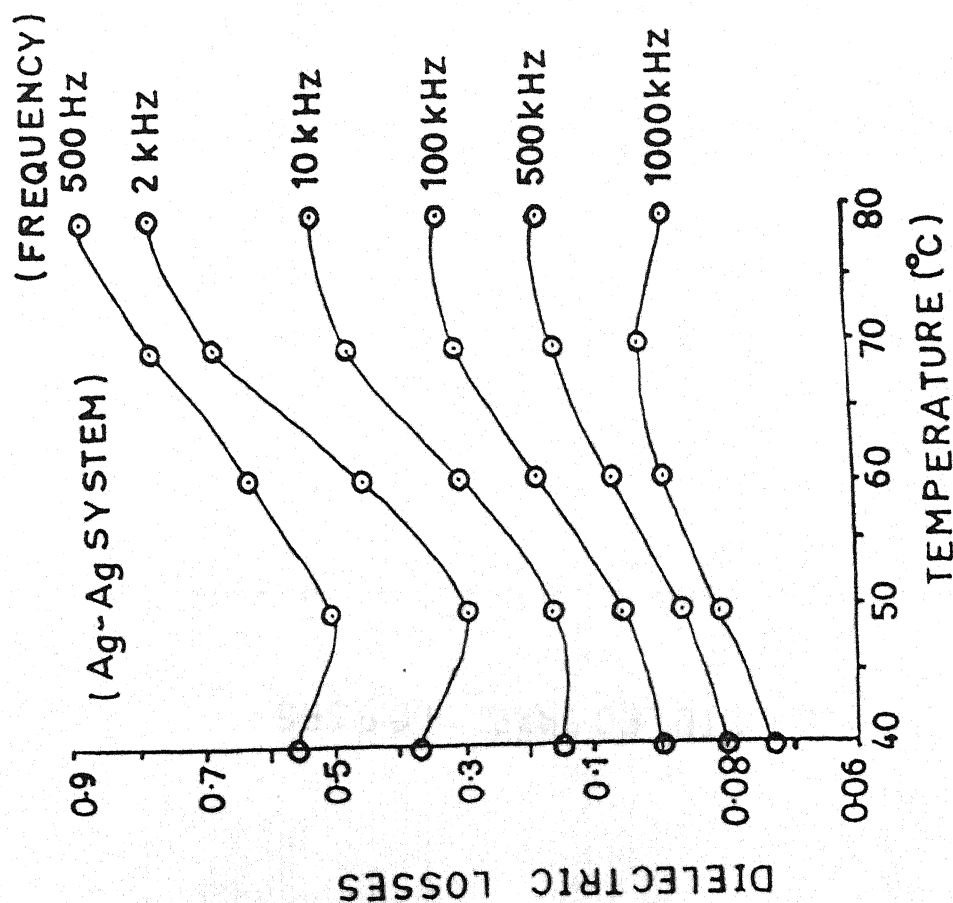


Fig. No. - 7.24

Dielectric losses versus Temperature for polyvinylidene fluoride samples with various frequency (i.e. 500 Hz, 2 kHz, 10 kHz, 100 kHz, 500 kHz and 1000 kHz) for Ag - Ag system

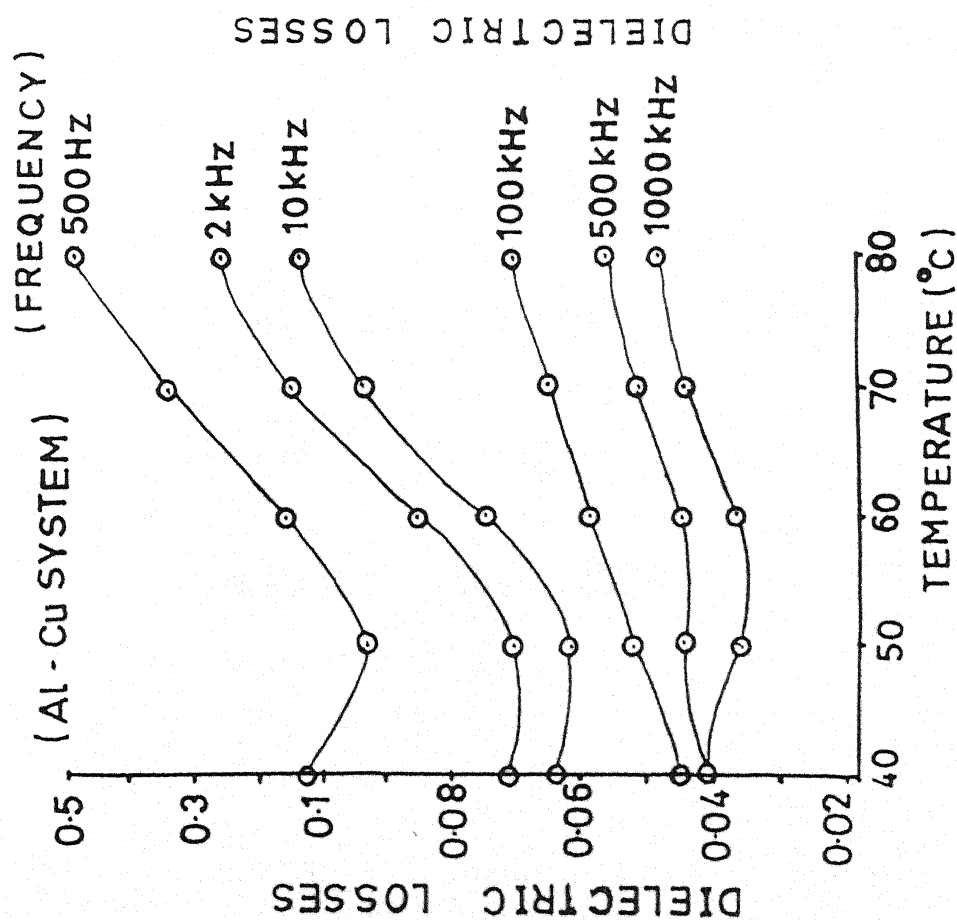


Fig. No. - 7.26

Dielectric losses versus Temperature for polyvinylidene fluoride samples with various frequency (i.e. 500 Hz, 2 kHz, 10 kHz, 100 kHz, 500 kHz and 1000 kHz) for Al - Cu system

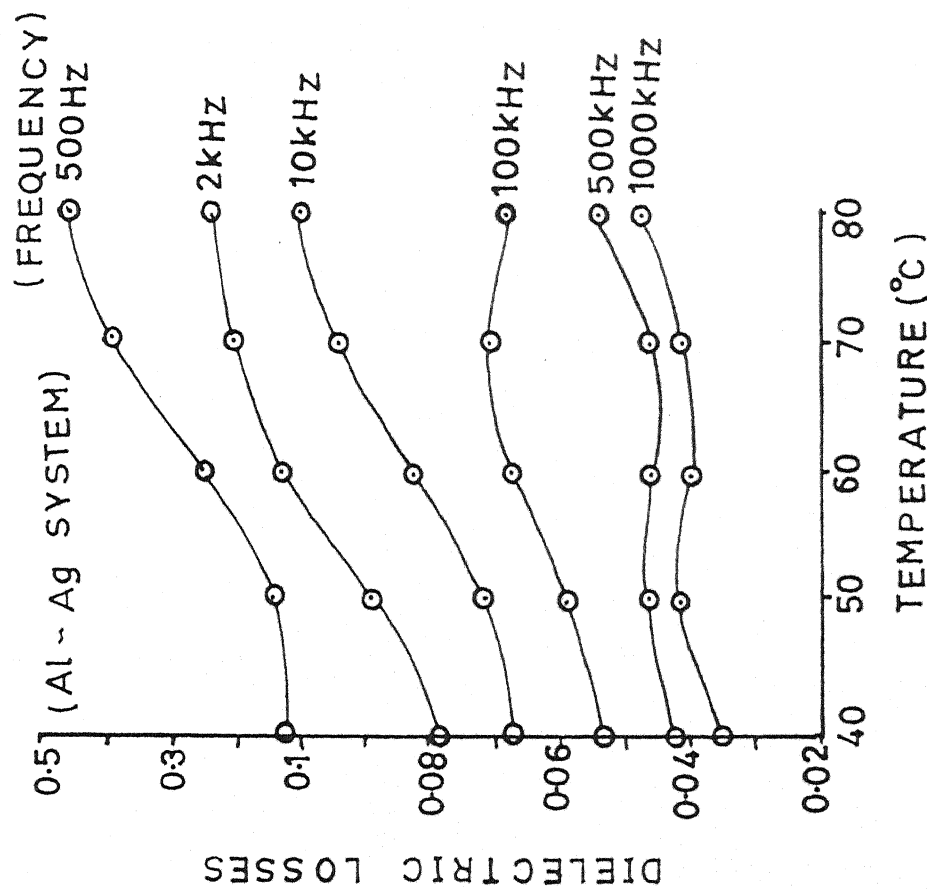


Fig. No. - 7.27

Dielectric losses versus Temperature for polyvinylidene fluoride samples with various frequency (i.e. 500 Hz, 2 kHz, 10 kHz, 100 kHz, 500 kHz and 1000 kHz) for Al - Ag system

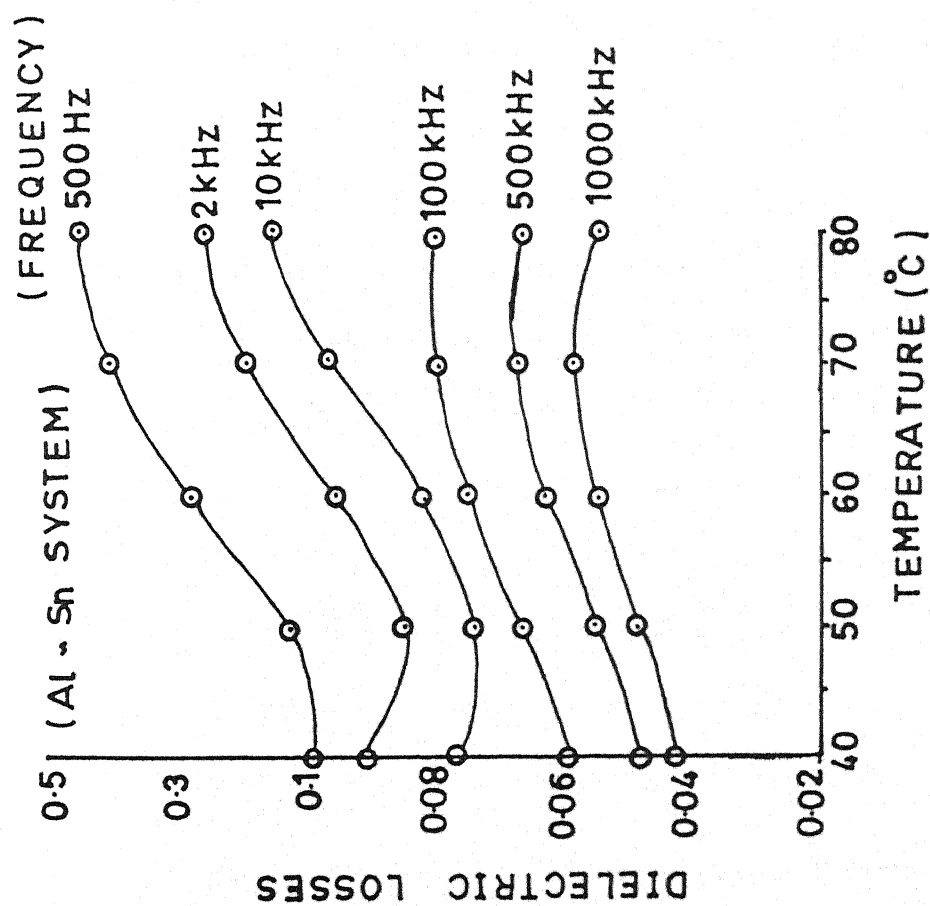


Fig. No. - 7.28

Dielectric losses versus Temperature for polyvinylidene fluoride samples with various frequency (i.e. 500 Hz, 2 kHz, 10 kHz, 100 kHz, 500 kHz and 1000 kHz) for Al - Sn system

polarization of a dielectric is contributed by the ionic, electronic and dipole polarization. The electronic polarization occurs during a very short interval of time (of the order of 10^{-15} sec), but longer than for electronic polarization, i.e. 10^{-13} – 10^{-12} sec required for the process of ionic polarization to set in. Dipole polarization requires a relatively long time compared with that of practically almost inertialess phenomena of deformational polarization so dielectric constant of non-polar polymer remains invariable with frequency. In case of polar polymers, the dielectric constant begins to drop at a certain critical frequency. The dipole molecules cannot orient themselves in the lower temperature region. However, owing to thermal expansion, the ratio of the number of molecules to the effective length of the dielectric decreases when the temperature increases. As the temperature increases, the orientation of dipoles is facilitated and this increase the dielectric constant. This behaviour is apparent from the upward trend of the slopes of dielectric constant curves in the neighbourhood of glass transition temperature (T_g). As the temperature increases further, the chaotic thermal oscillations of molecules are intensified and the degree of order of orientation is diminished.

The dielectric dispersion appearing at high temperature is generally admitted to be due to the rotatory diffusional motion of the molecules from one quasi-stable position to another around the skeletal bond involving large-scale conformational rearrangement of the main chain, and is known as primary dispersion region or the α -relaxation. The low temperature

dielectric dispersion is attributed to the dielectric response of the side groups which are considered to be more mobile or the small displacement of the dipoles near the frozen-in position and known as the secondary dispersion region or β -relaxation.

Thin polymer films are known to be a mixture of amorphous and crystalline regions. The amorphous regions are the areas in which the chains are irregular and entangled, whereas, in crystalline regions the chains are regularly folded or orderly arranged. In the crystalline areas, because of the presence of hindering structural units (due to greater density of these regions) the polymeric chains move with a greater difficulty than in the amorphous regions. The hinderance can be assumed to possess a certain potential energy. When the polymer is heated the movements of the main chain sets in, becoming maximum at T_g , at which maximum losses occur corresponding to the α -relaxation peak. This relaxation peak, corresponding to T_g , may also be understood by the free volume theory [35] according to which the molecular mobility (and consequently the relaxation time) near T_g depends mainly on the free volume. In the glassy state below T_g , the free volume will be frozen in and will remain fixed. As the temperature increases, the glassy state will expand due to normal expansion of all the molecules, which results from the changing vibrational amplitudes of bond distances [36]. As T_g is reached, in addition to the normal expansion process, there will be an expansion of free volume itself, which results in a larger expansion of the

free volume itself, which results in a larger expansion of the rubber-like polymer. This yields room for rotational or translational motion of the molecules to occur at T_g , accounting for the maximum dielectric loss at T_g [37].

The presence of dipolar molecules may also contribute in the process. The dipoles associated with the backbone of a segment of polymer chain will orient with a certain frequency governed by the elastic restoring force which binds the dipoles to their equilibrium positions and the rotational frictional forces exerted by the neighbouring dipoles [38]. In the crystalline or ordered polymers, the forces which hold the structural unit together are of a homopolar chemical binding nature and are much stronger than the vander Wall's forces between the molecules in the amorphous phase which vary from region to region. Moreover, the dipolar molecules in the crystalline phase will make discontinuous jumps from one equilibrium position to another and hence contribute to the absorption at the same temperature or frequency, whereas, in the amorphous phase, dipolar molecules should be able to orient from one equilibrium position to another relatively more easily and will contribute to the absorption over a wide frequency or temperature range since each dipole in the later case would have slightly different environments and hence would have different intermolecular interaction.

The variation in dielectric constant and loss tangent, suggests the net effect of some internal field within the polymer alongwith the external ac field. The dipole-dipole interactions between the different groups or many body interactions suggest the lower losses with higher frequency range. The dependence of the dielectric constant on frequency can be determined from the equation

$$C = C_g + \frac{S \tau}{1 + \tau^2 \omega^2} \quad \dots (7.11)$$

where C_g is the geometrical capacitance, S the conductance corresponding to the absorption current, τ the dipole relaxation time and ω the angular frequency. Above equation show that C should diminish with increasing frequency. The increase in losses at low frequency could be associated with the polarization of the trapped charge carriers. With the increase in frequency, polarization decreases and becomes vanishingly small at high frequencies. The decrease in losses with frequency also seems to show the decrease in the number of charges and delay in settling of dipoles due to availability of very short time in one half cycle of alternating voltage. The general expression for dielectric loss is given by the equation -

$$\tan \delta = \frac{\omega^2 \tau^2 (G_{in} + S) + G_{in}}{\omega \{S \tau + C_g (\omega^2 \tau^2 + 1)\}} \quad \dots (7.12)$$

where G_{in} is the conductance for the residual current. Obviously, from eqn. (7.12),

$$\omega \xrightarrow{\lim} 0 \quad \tan \delta = \infty \quad \dots (7.13)$$

$$\omega \xrightarrow{\lim} \infty \quad \tan \delta = 0 \quad \dots (7.14)$$

Differentiating eqn. (7.12) with respect to ω and equating the derivative to zero, it is possible to obtain the value of ω' of the frequency, corresponding to maximum loss.

Figures 7.1-7.28 exhibit the variation of dielectric constant and losses versus temperature and frequency curves for different electrode materials. Values of dielectric constant and losses seems to be controlled by the effective work function of metal-insulator-metal interfaces, i.e. the difference in energy between the Fermi level in metal and the bottom of the conduction band in the insulator. The difference between the work function of metal (1) and metal (2) will control the magnitude of loss but for similar electrode system the characteristic of the polymer may prevail as the net contribution of charges injected from the electrode would then be zero [39]. The various thermograms represent the distributed relaxation. The reason for distributed relaxations may be due to the combined effect of space charge injected from electrodes and dipolar relaxations in the polymer. In these results, we suggest that the internal field of polymer may get modified by the difference in the work function of various electrode metals [40].

/ ***** /

REFERENCES

1. Scott, A.H., Scheiber, D.J., Curtis, A.L., Lauritzen, J. P. and Hoffman, J.D., J. Res. Natl. Bur. Stand. Sect A., **66**, 269 (1962).
2. Physics of Thin Films, Vol. II, Universal Dielectric Respnse by A.K.Jonscher (Academic Press, New York).
3. McCrum, N.G., Read, B.E. and Williams, G., Anelastic and Dielectric Effects in Polymeric Solids, John Wiley and Sons, 1967.
4. Hedvig Peter, Dielectric Spectroscopy of Polymers, Adam Hilger Ltd., Bristol Printed in Hungary, 1977.
5. Ku, C. and Liepins Raimond, Electrical Properties of Polymers, Hanser Publishers, 1987.
6. Tanaka, T., Suppl. Progr. Theor. Phys., 121 (1959).
7. Takashi, J. Phys. Soc. (Japan), **16**, 1024 (1961).
8. Koizumi, N., Yano, S. and Tsunashima, K., J. Polym. Sci. Pt. B. Poly, Lett., **7**, 59 (1969).
9. Kosaki, M. and Ieda, M., J. Phys. Soc. Jap., **27**, 1604 (1969).
10. Ishida, Y., J. Polym. Sci., Part A-2, **7**, 1835 (1969).
11. Sasabe, H., Saito, S., Asahina, M. and Kakutani, H., J. Polym. Sci., **7**, 1405 (1969).
12. Valentin, M. and Carchano ETAl Bni, H., Thin Solid Films, **30**, 351 (1975).
13. Bahri, R. and Singh, H.P., Thin Solid Films, **62**, 291 (1979).
14. Gupta, A.K., Chand, N. and Mansing, A., Polymer, **20** 875 (1979).

15. Gowrikrishna, J., Josyulu, O.S., Sobhanadri, J. and Subramaniam, R., J. Phys. D. Appl. Phys., **15**, 2315 (1982).
16. Gomez Ribelles, J.L. and Calleja Diaz, R., J. Polym. Sci. Polym. Phys. Educ., **23**, 1297 (1985).
17. Umemura, T., Akiyama, K. and Coudere, D., IEEE, Trans. Elect. Insul., **EI-21**, 137 (1985).
18. Ramu, T.S., Wertheimer, M.R. and Klemberg, T., Sapiena, IEEE Trans. Electr. Insul., **EI-21**, 549 (1986).
19. Basha, A.F., Amin, M., Darwish, K.A. and Samad Abdel, H.A., J. Polym. Mate., **5**, 115 (1988).
20. Prasad, M. and Gupta, D., Ind. J. Pure and Appl. Phys., **26**, 384 (1988).
21. Lee Deok-Chooi and Jin, Kyoung-Si, Trans. Korean Inst. Electr. Eng. (South Korea), **36**, **4**, 273 (1988).
22. Pratt, G.J. and Smith, M.J.A., In International Conference "Electrical, Optical and Acoustic Properties of Polymers", Canterbury, U.K., 5-7 Sept. (1988).
23. Eatah, A.I. and Tawfik, A., Indian J. Phys., A. India, **62A**, **8**, 88 (1988).
24. Zhong, Ruan Yao, Li-Ping Li, You-Jun Chen and He Ping Sheng Chin, Phys. (U.S.A.), **8**, **4**, 937 (1988).
25. Prasad, M., Karimi, N.A. and Gupta, D., Ind. J. Pure and Appl. P hys., **26**, **12**, 729 (1988).
26. Mahendru, P.C., Singh, R., Panwar, V.S. and Gupta, N.P., VI International Symposium on Electrets (ISE 6) Proceedings (IEEE

Cat No. 88, CH 2593-2), Oxford U.K., 1-3 Sept. 1988 (New York, N.Y. U.S.A., I.E.E.E. 1988), p. 627-31.

27. Sinha, D. and Pillai, P.K.C., J. Mater. Sci. Letter (UK) **8**, 6, 673 (1989).
28. Pathmanathan, K., Cavaille, J.Y. and Johari, G.P., J. Polym. Sci. B. Polym. Phys. (U.S.A.), **27**, 7, 1519 (1989).
29. Schlosser, E. and Schonhals, A., Colloid Polym. Sci. (West Germany), **267**, 2, 133 (1989).
30. Gray, F.M. and Vincent, C.A., J. Polym. Sci. B. Polym. Phys. (USA), **27**, 10, 2011 (1989).
31. Kamiya, Y., Mizo-guchi, K. and Naito, Y., J. Polym. Sci. B. Polym. Phys. (USA), **28**, 1, 1955 (1990).
32. Debye, P., "Polar Molecules", Chemical Catalogue Co., N.Y. (1929).
33. Cole, K.S. and Cole, R.H., J. Chem. Phys., **9**, 341 (1941).
34. Havirilik, S. and Negami, H., Polymer, **8**, 161 (1967).
35. Fox, T.G. and Flory, P.J., J. Am. Chem. Soc., **70**, 12384 (1950).
36. Roberts, G.E. and White E.F.T., The Phys. of Glossy Polymers (ed.) R.M. Howard (London, 1979), (1973).
37. Talwar, I.M., Sinha, H.C. and Srivastava, A.P., J. Mater. Sci., **L-4**, 448 (1985).
38. Khare, P.K., Keller, J.M., Gaur, M.S., Singh, Ranjeet and Datt, S.C., Polym. Int., **35**, 337 (1994).
39. Khare, P.K. and Srivastava, A.P., Indian J. Pure & Appl. Phys., **30**, 131 (1992).
40. Khare, P.K., Surinder, P. and Srivastava, A.P., Indian J. Pure & Appl. Phys., **30**, 165 (1992).

CHAPTER VIII

REVIEW OF THE RESULTS AND CORRELATION

REVIEW OF THE RESULTS AND CORRELATION

Study of polymers is one of the most promising and exciting branch of modern science. Today, these are extensively used in construction, textile, transport, electronics, computers, military hardware, aeronautics, space research, etc. Earlier polymers were mainly used as electric insulators but modern researches have given a new dimension to its applications and enhanced its versatility. Polymers offer a high resistance to the passage of electric current on application of an electric field. These materials behave as insulators and store electric charge for long periods as against the conducting materials. Such charge storage has been found to be very useful in many engineering and industrial fields, medical and biosciences, solid state physics and material sciences and environmental studies. Due to their good charge storage properties in electrets coupled with excellent mechanical properties, polymers have emerged as invaluable material in a large number of applications.

Charge storage, charge transport, its distribution, relaxation and discharge phenomena of different polymers are studied with a view to achieve better performance and reduce the degradation. Polymers offer enormous scope for modification by way of copolymerization, mixing and blending of different polymers which modify or alter the electrical properties to suit our specific requirement.

Polymer science is one of the most promising and exciting branch of modern science. Polymers, natural or synthetic, are in use throughout the world in construction, communication, textile, transport, etc. Space and aeronautics technology is widely using the polymers for solving the different problems associated with the design, time factor and the variation in temperature at different stages. Based on the above mentioned applications, polymeric materials are subjected to various types of environments like thermal, chemical, high energy radiations, etc. The change in the structure and physical properties are, therefore, essential aspect of the study in the development of these materials.

The electrical behaviour and exhibition of electret effect by the polymeric materials in pure, doped and blended form has been clearly identified and has been studied deeply over the past few decades. The studies on mixed polymeric systems such as blends and doped polymers and copolymers are of fundamental importance, for understanding the complexity of inherent electrical behaviour in the light of existing knowledge of field, and to explore the possibilities of synthesizing tailored systems with predetermined properties to suit special applications. For example, rapidly and economically it can generate desired set of properties : mechanical, chemical, electrical, etc.

Polymer thin films are being used in a number of exploratory electronic technologies such as thin film triodes, thin film memory circuits,

cryotron logic and associating storage circuits, etc. apart from their use as insulators. Also, these are finding many technological applications such as electret microphones, electrostatic voltage generators, air filters, IR detectors and transducers. The physical properties of all polymers are not alike. The polymer properties depend on average molecular weight and molecular weight distribution of the polymer. But even these two parameters do not fully characterize a polymer. Two polymer samples can have the same chemical structure and almost similar molecular weight distributions, but may have different properties due to difference in structure. All properties depend on intermolecular and intramolecular interactions of polymer chains in the aggregated state. Such interactions are caused by forces, such as dispersion force, induction force, dipole interaction and hydrogen bonding, acting within various parts of the same molecule as well as between the neighbouring molecules. Studies of the structure of the polymer, its physical and chemical properties and electrical properties will characterize the polymer and give an insight into the various mechanisms responsible for the different properties exhibited by it. The characterization of a polymer using different technique is essential to understand its physical behaviour and to explore its potential for device applications. The wide industrial applications of polymers have made them an interesting subject of study. The possibility of electronic conduction and persistent internal polarization in them have opened a new field of application. Recent years have witnessed an interesting progress in the

theory and experiments describing the charge storage and transport phenomena in solid polymers. Polymers have found application in almost all spheres of life. In addition to their conventional use of electrical insulators, they now feature as sensitive elements (sensitive to temperature, radiation and electrical stress). The foremost commercial incentive for the use of these polymer film electrets is the redundancy of an external power supply with consequent simplification and saving in cost, size and weight. Unfortunately still there are available no complete theories of charge storage and transport mechanism because, firstly very little in depth studies revealing the nature of microscopic mechanisms responsible for charge storage and transport have been carried out and, secondly, the capability of various techniques for resolving the different undergoing processes have not been fully exploited. The complexity and considerable variety of physical and chemical structure of numerous polymers of long chain and high molecular weight make it difficult to consider the behaviour of a generalized transport theory.

The research on charge storage and transport phenomenon in electrets of various class of solids is in a very active phase since last decade. Work has been performed on a large number of organic substances, biomaterials and on inorganic materials such as ionic crystals or metal oxides. However, the main interest has been concentrated on polymer electrets since they are available as flexible thin films. Choice of polymeric dielectric for concrete use depends on its dielectric and other

physical properties over a wide range of temperature and electric field frequencies. Consequently, thin films of polymer are being extensively studied so that they may be used in solid state microelectronic devices. The prospects of practical application of polymeric electrets are extensive at present. With the likely impact of the proposed investigation electret effect in polymers can be produced by orientation of dipoles and/or trapping of charge carriers generated from the electrodes as well as generated in the bulk. Knowledge of the basic electrical properties, generation, storage and transport of charge in polymeric dielectric is extremely important for making stable and useful electrets. The information about these mechanisms can be obtained by employing the methods like transient current measurement under charging and discharging mode, dark conduction current measurement, dielectric measurement and thermally stimulated discharge current measurement. The various studies will help to venture a description of the role played by multiple trapping levels and carrier injection on persistence and transport of charges. In addition to the academic importance, the work summarized is of considerable technical and industrial applications and is a step towards finding the suitable conditions for most suitable and stable electrets. Various measurements, made in the present case, provides a wealth of information on charge storage mechanism of the polymer.

The polymer poly(vinylidene fluoride) has been one of the most studied polymers of the last twenty years for its useful electrical properties.

There is a continuous current interest in the structure and properties of the polymer, especially with regard to understanding mechanisms that are responsible for its piezoelectric properties. Although there have been many detailed analysis of the problem, the situation is still not resolved in a totally satisfactory manner. The present investigation comprising short circuit thermally stimulated discharge current (TSDC) measurements, transient charging and discharging current measurements, was therefore undertaken to provide information about charging polarization, its dependence on structure and morphology and various relaxation occurring in sample.

(A) THERMALLY STIMULATED DISCHARGE CURRENT STUDIES

The experimental conditions under which the thermally stimulated discharge currents were measured are summarised below -

Polarizing field strength	-	10 kV/cm to 100 kV/cm
Polarizing temperature	-	40°C to 80°C
Heating Rates	-	3°C/min
Electrode materials	-	Aluminium, Silver, Copper and Tin

The thermally stimulated discharge current (TSDC) spectra for polyvinylidene fluoride (PVDF) films polarized with 10, 25, 50, 75 and 100 kV/cm at fixed temperatures 40, 50, 60, 70 and 80°C are illustrated in Figs. 4.1 to 4.20 and 4.21 to 4.35 for similar electrodes (i.e. Al-Al, Cu-Cu, Ag-Ag and Sn-Sn) combination and for dissimilar electrodes (Al-Cu, Al-Ag and Al-Sn) combination respectively. Similarly, Figs. 4.36 to 4.55 and 4.56

to 4.70 represent TSDC spectra for PVDF films with constant poling fields, i.e, 10, 25, 50, 75 and 100 kV/cm) at different temperatures, i.e. 40, 50, 60, 70 and 80°C for similar (i.e., Al-Al, Cu-Cu, Ag-Ag and Sn-Sn) and dissimilar electrode configurations (i.e., Al-Cu, Al-Ag and Al-Sn) respectively. For comparison purpose and to observe the electrode effects at constant poling temperature and poling field, TSD spectra are shown in Figs. 4.71-4.75.

The initial rise (i.e., current versus $10^3/T$) curves for constant poling fields (i.e, 10, 50 and 100 kV/cm) at different poling temperature for Cu-Cu, Ag-Ag and Sn-Sn electrode systems and Al-Cu, Al-Ag and Al-Sn electrodes combinations are shown in Figs. 4.76 to 4.93. Also, Figs. 4.94 to 4.102 and 4.103 to 4.111 exhibit the initial rise curves for constant poling temperature (i.e. 40, 60 and 80°C) with various poling fields (i.e., 10, 25, 50, 75 and 100 kV/cm) for Cu-Cu, Ag-Ag, Sn-Sn, Al-Au, Al-Ag and Al-Sn electrode configurations. The values of activation energy are calculated with the help of these curves.

The depolarization kinetic data for polyvinylidene fluoride, samples poled at various temperatures with different polarizing fields are shown in Tables 4.1 to 4.7.

All the TSDC spectra of specimen polarized at different temperatures with different poling fields, consist of only one broad peak. The peak currents increased with increase in field strength. The variation of peak currents as a function of field strength shows a linear behaviour. The

charge released can be computed by integrating the area under the TSDC spectra and are plotted as a function of field strength for electret polarized under different poling temperatures and show a linear relationship with field strength (results not shown). TSDC characteristics of PVDF films have also been recorded as a function of polarizing temperature under identical conditions of polarization. It is evident from the figures that with the variation in electrodes the magnitude of TSD current increases in general. It is also clear from the figures that the peak current increases and the peak shifts towards the higher temperature with increasing polarizing temperatures for a given polarizing field strength.

In the present investigation, TSDC thermograms exhibits a broad peak. This peak gets centered around $80 \pm 10^{\circ}\text{C}$. Broad peak represent presence of multiplicity of relaxation mechanism. The multiplicity of relaxation in PVDF may be because of presence of trapping levels of different depths. In the present case, the appearance of peak in the high temperature region imply that the injection of ions may be significant in this polymer. It is also possible that PVDF contains a high number of impurity molecules prior to field treatment and these molecules are dissociated into various ionic species by a combination of the high internal and external fields. The charge trapping in a polymer takes place at the molecular main chain, the side chain and at the interface of crystalline and amorphous regions of the polymer [1]. The high field applied during electret formation may also produce some additional trapping sites.

The values of activation energies have been observed can only be associated with the ionic and electronic trapping [2]. The superlinear behaviour of peak current versus poling field plot in the higher field region indicates the space charge phenomena. The peak observed in the thermograms is not due to single relaxation but seems to be complex and may arise due to the release of the frozen dipoles by their cooperative motion with adjoining segments of the main polymer chain. The superlinear increase of peak current and release charge versus poling field (not reported) in the higher field region suggests that the peak is contributed both by electronic and ionic processes, arising in the bulk and injected from the electrodes which are subjected to a higher field. It is not a simple process but a complicated one of Maxwell-Wagner type [3].

When the polymer is polarized under identical conditions of polarisation with electrodes (Al, Cu, Ag, Sn) of different work function determined by contact potential method [4], but less than that of PVDF, the metal with higher work function injects a large number of charge carriers than that with lower work function [5]. Since the injection of charge carriers from the electrodes to the polymer results in a reduction of the contribution of the heterocharge (due to the charge carriers present in the bulk of the material) so the charge released to the external circuit and the magnitude of the peak current I_m , should decrease with the work function of the metal. Slight difference in peak positions for different metal-electrode-metal combinations were observed. These results suggest that the liberated

opposite part of ions and carriers may be slightly affected by the work function different of different combinations. In these results, a possibility seems to be present that the internal field of PVDF may get modified by the difference in the work function of different electrodes. Peak value of the current seems to be controlled effectively by the work function for metal-insulator-metal interfaces.

It is clear from the Table 4.1 to 4.17 that the activation energies associated with the process responsible for TSDC and relaxation times are found to vary slightly, with that of the polarizing temperatures. Further, the dependence of TSDC peak on the polarizing temperature also suggest the distribution in relaxation times. Such relaxation process of activation energy and for a fixed rate of heating the position of the peak is independent of polarizing temperature. Hence, it may be concluded that the TSDC spectra may be of dipolar origin with contribution from space charges [6-8].

(B) TRANSIENT CURRENTS IN CHARGING AND DISCHARGING MODES

The time dependence of the charging and discharging transient currents in polyvinylidene fluoride (PVDF) samples have been investigated over a period of time 1-80 min. The Figs. 5.1 to 5.30 show the variation of discharging transient currents with time at different temperatures, i.e. 40, 50, 60, 70 and 80°C with polarizing fields of 10, 25, 50, 75, 100 kV/cm, respectively. It is evident from the figures that the current decays at a faster rate for a few minutes and then the decay rate slows down. Curves

illustrating the time-dependence of transient discharging currents are, in general, characterized with two regions which are designated as the short-time and the long-time regions, respectively.

Figures 5.31 to 5.60 illustrate the charging characteristics of PVDF films at different temperatures, i.e. 40, 50, 60 and 70°C with different polarizing fields (10, 25, 50, 75 and 100 kV/cm). From the above characteristics, it is clear that at least two distinct mechanisms should be responsible for the observed transient currents. One mechanism is operative in the short-time range with a particular value of decay constant and the other mechanism is operative in the range of long-time with a decay constant of different value.

The temperature dependence of the transient currents in discharging modes are shown more clearly when the current measured at a constant time (isochronals) is plotted against temperature. Such isochronals for charging and discharging mode have been constructed for 2, 6, 10, 20, 40 and 70 min are shown in Figs. 5.61 to 5.90. From these plots, it may be concluded that the currents show thermal dependence. Such isochronals are characterized by a maxima around $70 \pm 5^\circ\text{C}$.

Figures 5.91 to 5.120 gives the $\log I$ vs $1000/T$ (where T is the absolute temperature) plots (constructed from linear portion of isochronal current and temperature plots). The value of activation energy is calculated from the slope of these characteristics.

The observed results can be discussed in the light of the existing models of transient currents.

The complete representation of the universal dielectric response in the time domain covering both dipolar loss peaks and strong low frequency dispersion associated with the charge carrier dominated system may be represented by

$$I(t) \propto t^{-n}, \quad 0 < n < 2 \quad \dots (8.1)$$

with the exponent n taking value in different ranges at long and short time respectively. There appears a process of thermal activation over the whole range of temperature. It is evident from Figs. 6.11 to 6.18 that both charging and discharging currents obey the well known expression.

$$I_a(t) = A(t) t^{-n} \quad \dots (8.2)$$

where I_a is the absorption current, t the time after application or removal of the external field and $A(t)$ a temperature-dependent factor. It is found that discharging current has been characterized with logarithmic slope smaller in magnitude than 1 ($n < 1$) during the range of short times, and then goes to the longer time region (where the slope is steeper, with n lying between 1 and 2). Similar to discharging, the charging current has also been found to be characterized with $n < 1$, in short time region, however, at longer times this current tends to approach the steady state conduction current.

In the present case, n values for shorter time region were observed to vary from 0.5–0.8 and for long time region these values are observed to vary from 1.53–1.78. Also, discharging currents vary linearly with the field strength characteristic of dipolar mechanism. These findings indicate that the dipolar polarization is operative in the present case. The nature of current in the observed temperature range may attribute a dipole process involving structural units with a small dipole moment and a broad distribution of relaxation times, this predominates over any hopping mechanism. The partial dipolar nature of sample is expected to manifest itself in the form of a peak in the isochronals. The isochronals constructed from current-time characteristics are found to be characterized with a peak located around 75°C.

The charging and discharging currents observed in PVF are also expected to show the behaviour of dipolar relaxation mechanism. In the case of transients governed by space charge, the peak in the current time curve should occur at a time

$$t_m = \frac{0.786 d}{\mu E} \quad \dots (8.3)$$

where E is the applied field, d is the sample thickness and μ the carrier mobility. To have a rough estimate of the time at which this peak should occur, we used the values d , E and μ to be 20 μm , 100 kV/cm and $10^{-11} \text{ cm}^2/\text{V}$. It was found that t_m is approximately equal to $3.782 \times 10^3 \text{ s}$. Thus, there is possibility of space charge relaxation occurring at sufficiently

longer times. The above considerations indicate that the observed currents in the present case may partially be due to dipolar orientation and partially due to space charge mechanism.

Discharging current measured at various prescribed times versus temperature plots are shown in Figs. 5.10 to 5.30. It is clearly seen that the various isochronals are characterized by a single peak located at $\sim 75^{\circ}\text{C}$. However, no shift is observed in the peak temperature with time of observation. It is observed that the peak temperature decreases with increasing time and is a characteristic of relaxation process. Similar qualitative behaviour is observed in the other samples. The isochronal peak is broad and probably it contains several minor processes, one of which may be associated with the glass transition of the polymer and the other may be due to thermal release of trapped carriers.

It is rather difficult to specify the origin of charging/discharging currents unambiguously from the time dependence alone. However, the various facts including the weak polar structure of polyvinylidene fluoride, observed values of n , and thermal activation of current over a certain temperature range as observed in the present case indicate that the space charge due to accumulation of charge carriers near the electrodes and trapping in the bulk may be supported to account for the observed current. The decay of current in the long time region for different samples indicate the existence of energetically distributed localized trap levels in the sample

[9]. It seems that at shorter times only shallow traps get emptied contributing to stronger current. However, at longer times, deeper traps with long detrapping times release their charges and the current decays at longer times. As temperature increases, mobility of carriers also increases, hence, all the deeper traps are filled. Release of a large number of charge carriers from the traps during the process may then result in high return rate of carriers leading to blocking of electrode causing a decrease in current. The charge injection from electrodes with subsequent trapping of injected charges in near surface region gives rise to homospace charge and the thermal release of charge carriers from the traps. Before the trapped space charge injected at higher fields is thermally released, a space charge barrier is presented to the electrode which suppresses the entrance of charge carriers into the sample. Thus, the observed current remains smaller than its corresponding value.

As PVDF is a polar polymer, the probability that charge carriers are present in it, the only charges could come from those injected through the electrodes. The injected charges are trapped at different trapping sites leading to a space charge which fundamentally influences all the transport phenomena and the effects at the electrode [10]. Space-charge-limited currents may also determine the transient behaviour, such as a large burst of current immediately after the application of voltage followed by a steady decline in current on standing. In the present study, the large currents obtained just after the application of voltage subsided to much smaller

steady values after a certain length of time. When a metal, the work function of which is lower than that of dielectric, is brought into contact with it, a layer of electrons accumulates on the dielectric surface together with a positive charge on the electrode, giving rise to a space charge near the electrode. The space-charge layer accumulated will depend upon the relative difference between the work function of metal electrodes and the dielectric. The space-charge layers may further be modified because of surface states. On application of an electric field at a fixed temperature, the current was found to increase and then decrease with time, and finally attain a steady value [11].

The activation energy values for such isochronal peak are found to vary from 0.57 to 0.69 eV. The activation energy are found to decrease with time of observation. The value of activation energies agrees well with the activation energy obtained for TSDC peaks in the present case (Chapter 4).

(C) STEADY STATE CONDUCTION CURRENTS

Figure 6.1-6.7 shows the steady state conduction current-voltage (I - V) characteristics of PVDF films at temperatures ranging from 40-80°C for similar (Al-Al, Cu-Cu, Ag-Ag and Sn-Sn) and dissimilar electrodes (Al-Cu, Al-Ag and Al-Sn) combinations. Also, at constant temperature 40°C, 60°C and 80°C current-field characteristics are observed for Al-Al, Al-Cu, Al-Ag, Al-Sn and Cu-Cu electrode configurations (Figures 6.8-6.10). The observed increment in the current was approximately the same throughout the

studied range of temperature. For all the temperatures, the thermograms, though non-linear, were similar.

The steady state conduction-current-temperature characteristics with different poling fields (i.e., 10, 25, 50, 75 and 100 kV/cm) for similar (i.e. Al-Al, Cu-Cu, Ag-Ag and Sn-Sn) and dissimilar electrode combination (i.e. Al-Cu, Al-Ag and Al-Sn) are shown in Figures 6.11, 6.13, 6.14, 6.15 and 6.12, 6.16, 6.17 respectively).

The Schottky plots ($\log I$ vs \sqrt{E}) for PVDF samples with similar (Al-Al, Cu-Cu, Ag-Ag and Sn-Sn) and dissimilar electrode (Al-Cu, Al-Ag and Al-Sn) combinations are shown in Figures 6.18, 6.20, 6.21, 6.22 and 6.19, 6.23 and 6.25 respectively. The plots exhibit two regions at the lower and higher fields. The isothermal reveals almost ohmic behaviour initially, which gradually becomes non-ohmic. The slope values in the lower field region lie between 1.2 to 1.5 and slope of 1.97 to 2.00 are observed at higher field strength (Table 6.1). It is evident from the Figures that order of conduction currents varies with electrode materials. The activation energy values calculated from the slopes of $\log I$ versus $1000/T$ plots (Figures 6.25 to 6.31) and found to be independent of applied field (Table 6.3).

The $\log I$ - V plots showed the slope in the lower field region, upto 50 kV/cm, as 1. In contrast, in the higher field region, the value of slopes was greater than 1, but not exceeding 2. The slope value of 1, in the low-field region indicates that the electrical conduction in this region obeys Ohm's

law. However, since the complete I-V characteristics were nonlinear, they indicate the presence of other modes of electrical conduction as well. The observed non-linearity could be due to build up of a space charge resulting in nonuniformity of field distribution between the electrodes. Moreover, the linearity of I-V curves in the high-field region indicates that either of the mechanisms, Schottky-Richardson or Poole-Frenkel, may be operative. However, the slope value (~ 2) also indicates that space charge limited currents may also take part in this region.

Our results indicate that with increasing temperature, the probability of thermal ionization of the trapping centres also increases, resulting thereby in a shift in the quasi Fermi level. This shift lowers the barrier across which electrons are transported, and the electrical conduction is ohmic. At low energy fields, fewer carriers are injected from the electrodes, and therefore, the initial current is governed by the intrinsic free carriers in the materials. At higher-energy fields, the change of slope is suggestive of deviation from Ohm's law based conduction to the space charge limited conduction. This mode of electrical conduction continues until the injected free carrier density. However, at sufficiently higher energy fields, the current is dominated by space-charge limited conduction and the conduction is mainly due to injected space charge [12]. The departure from Ohm's law in high-energy fields is due to perturbation of active barrier even in the absence of thermal and chemical effects. Since, for our studies, the

film thickness was very high (20 μm), the conduction mechanism by tunnelling is ruled out, which requires the film thickness to be very small.

To determine the actual conduction mechanism, the value of β -factor, at different temperatures, calculated from the slope of the plots of $\log I$ versus \sqrt{E} , were compared with the theoretically calculated value of β , based on the assumption that one of the mechanisms was operating. The experimental value of β (Table 6.1) in the present case, were close to the theoretically observed values of β_{RS} based on the premise that R-S was the particular mechanism that was operating.

In the present case, the slope of I-V curves are seen not to exceed the value 2. Usually a slope of 2 indicates shallow trapping but this does not seem to exclude the possibility of deep traps in the present case. Also, in the lower field region, ohmic conduction prevails; space charge build up at high field may be associating factor for the conduction current and a two fold mechanism explains the high field conduction. Besides space charges injected from electrodes Richardson-Schottky emission is the dominant process, responsible process for the transport of the charge carriers.

(D) DIELECTRIC MEASUREMENT

The dielectric constant and dielectric losses of polyvinylidene fluoride samples are observed in the temperature 40-70 $^{\circ}\text{C}$ and frequency (500 Hz to 1000 kHz) range.

(a) Dielectric Constant

(i) Effect of Temperatures

To observe an effect of temperature on dielectric constant, its variation as a function of temperatures is plotted at different frequencies (i.e. 500 Hz, 2, 10, 100, 500 and 1000 kHz) are shown in the Figs. 7.1-7.7 for similar (Al-Al, Cu-Cu, Ag-Ag and Sn-Sn) and dissimilar electrode (Al-Cu, Al-Ag and Al-Sn) combinations. It is clear from the figures that the value of dielectric constant decreases with increasing frequencies. For higher frequencies (i.e. 500 kHz and 100 kHz) the value of dielectric constant increases attaining a maxima at 70°C and then decreasing. This nature is not observed for other frequencies.

(ii) Effect of Frequencies

The frequency dependence of dielectric constant of the sample at different temperatures (i.e. 40, 50, 60 and 70°C) are shown in Figs. 7.8-7.14 for similar (Al-Al, Cu-Cu, Ag-Ag and Sn-Sn) electrode system and dissimilar electrodes (Al-Cu, Al-Ag and Al-Sn) combinations. It is found that with increasing temperature dielectric constant increases. As per nature of the curve is concern, it is clear that the value of dielectric constant decreases up to 10^4 Hz and beyond this it increases. The rate of decrease and increase of dielectric constant is sharp.

(b) Dielectric Losses

(i) Effect of Temperatures

The effect of temperatures on PVDF samples of 20 µm thickness for similar (Al-Al, Cu-Cu, Ag-Ag and Sn-Sn) and dissimilar (Al-Cu, Al-Ag and

Al-Sn) are shown in Figs. 7.15 to 7.21. It is clear from dielectric loss versus frequency curves that dielectric loss value sharply decays attaining a minima and again it sharply increases. It is very interesting to note that with increasing temperature (i) the value of dielectric losses are lower for higher temperature in the first half and after attaining a minima value of dielectric losses are more for higher temperatures, and (ii) the minima position shifts towards lower frequency range. The nature of all the curves are similar.

(ii) Effect of Frequencies

Figures 7.22 to 7.28 represent the dielectric losses versus temperature curves at constant frequencies (i.e. 500 Hz, 2, 10, 100, 500 and 1000 kHz) for similar (Al-Al, Cu-Cu, Ag-Ag and Sn-Sn) and dissimilar (Al-Cu, Al-Ag and Al-Sn) electrode combinations. The nature of the curves are approximately similar. In general, losses decreases with increase in frequency. In certain cases the curve show slight decrease in the value of dielectric losses and then continuous increasing character is found. The value of losses are found higher, when Al-Al electrode system are replaced by Cu-Cu and Ag-Ag electrode combination.

We have observed a pronounced effect of electrode materials on dielectric constant as well as dielectric losses of the sample when dielectric parameters, i.e. temperature and frequency are changed.

The presence of dipolar molecules may contribute in the process. The dipoles associated with the backbone of a segment of polymer chain

will orient with a certain frequency governed by the elastic restoring force which binds the dipoles to their equilibrium positions and the rotational frictional forces exerted by the neighbouring dipoles [13]. In the crystalline or ordered polymers, the forces which hold the structural unit together are of a homopolar chemical binding nature and are much stronger than the vander Wall's forces between the molecules in the amorphous phase which vary from region to region. Moreover, the dipolar molecules in the crystalline phase will make discontinuous jumps from one equilibrium position to another and hence contribute to the absorption at the same temperature or frequency, whereas, in the amorphous phase, dipolar molecules should be able to orient from one equilibrium position to another relatively more easily and will contribute to the absorption over a wide frequency or temperature range since each dipole in the later case would have slightly different environments and hence would have different intermolecular interaction.

The variation in dielectric constant and loss tangent, suggests the net effect of some internal field within the polymer alongwith the external ac field. The dipole-dipole interactions between the different groups or many body interactions suggest the lower losses with higher frequency range. The dependence of the dielectric constant on frequency can be determined from the equation

$$C = C_g + \frac{S \tau}{1 + \tau^2 \omega^2} \quad \dots (8.4)$$

where C_g is the geometrical capacitance, S the conductance corresponding to the absorption current, τ the dipole relaxation time and ω the angular frequency. Above equation show that C should diminish with increasing frequency. The increase in losses at low frequency could be associated with the polarization of the trapped charge carriers. With the increase in frequency, polarization decreases and becomes vanishingly small at high frequencies. The decrease in losses with frequency also seems to show the decrease in the number of charges and delay in settling of dipoles due to availability of very short time in one half cycle of alternating voltage. The general expression for dielectric loss is given by the equation -

$$\tan \delta = \frac{\omega^2 \tau^2 (G_{in} + S) + G_{in}}{\omega \{S \tau + C_g (\omega^2 \tau^2 + 1)\}} \quad \dots (8.5)$$

where G_{in} is the conductance for the residual current. Obviously, from eqn. (8.5),

$$\omega \xrightarrow{\lim} 0 \quad \tan \delta = \infty \quad \dots (8.6)$$

$$\omega \xrightarrow{\lim} \infty \quad \tan \delta = 0 \quad \dots (8.7)$$

Differentiating eqn. (8.5) with respect to ω and equating the derivative to zero, it is possible to obtain the value of ω' of the frequency, corresponding to maximum loss.

Figures 7.1-7.28 exhibit the variation of dielectric constant and losses versus temperature and frequency curves for different electrode materials. Values of dielectric constant and losses seems to be controlled

by the effective work function of metal-insulator-metal interfaces, i.e. the difference in energy between the Fermi level in metal and the bottom of the conduction band in the insulator. The difference between the work function of metal (1) and metal (2) will control the magnitude of loss but for similar electrode system the characteristic of the polymer may prevail as the net contribution of charges injected from the electrode would then be zero [14]. The various thermograms represent the distributed relaxation. The reason for distributed relaxations may be due to the combined effect of space charge injected from electrodes and dipolar relaxations in the polymer. In these results, we suggest that the internal field of polymer may get modified by the difference in the work function of various electrode metals [8,15].

In addition to dipolar relaxation space charge has been found to make considerable contribution to Thermally stimulated discharge currents (TSDC) and also to time dependent transient currents in the present case. Such charges may be attributed to the localization of bulk generated and also to injected charge carriers into various traps indicating the existence of trapping levels of various origins, which may be distributed both energetically and spatially [16]. Trap depths of such levels obtained, in the present case from transient as well as TSDC are of the same order indicating that in both cases the same group of traps is operative [11,17]. The energetic trap structure may consist of surface and bulk traps. The bulk traps can be caused by a number of intrinsic structural defects, such as branching chain entanglements, chain ends, pendent groups [18-20],

etc. On the other hand, the surface traps may exist due to chemical impurities, surface oxidation, adsorbed molecules, etc. [21,22]. With such a trap structure present in the polymer, the detrapping of electronic carriers and their microscopic transport can be described by the Mott-Davis model [23] which distinguishes between transport over (a) extended state, (b) localized band-tail states, (c) localized state near the Fermi level. The extended states and the localized band-tail states are separated by the critical energy. Pfister and Scher [24] have suggested a model which combines hopping and the trap controlled transport picturing to a model named "trap controlled hopping". In this model, the carriers move by hopping over energetic deeper traps, such deeper traps are responsible for the observed activation energies.

Identification of the hopping through energetic shallow band-tail states as motion in a quasi-conduction band allows to use the conventional "trap controlled" transport model [25]. According to this model, the effective velocity of charges slows down due to presence of traps in the material. The release time of charge out of traps is thermally activated, and so with rising temperature the measured current increases because the number of available carriers in the quasi-controlled band increases. This leads to an initially exponential increase in the current, the current maximum appears because the free carriers (in the quasi-conduction band) either leave the sample or captured in traps with a longer release time and so immobile [26].

Another acceptable approach, for charge transport can be considered to be that proposed by Lewis [27]. According to this approach electron localisation and weak wave-function overlap in molecular organic solids inherently leading to insulating properties which can be exploited in electret situations. Electron and hole transport proceeds by tunnelling which is localized and vectorial in two separate donor (E_D) and acceptor (E_A) bands of states of molecular solids, the broadness of which is determined by local structure and polarization of the matrix. The localized nature of the trap states encourages charge storage and a low effective mobility for charge transport, the latter will consist of a series of hops from occupied E_D and E_A states to adjacent empty ones. Electrons will be able to tunnel between sites at rates which depend sensitively on the potential barriers and on the degree of wavefunction overlap. The transfer rate also depends on the likelihood of an adjacent occupied, empty, pair and only frequency of attempt to tunnel. The transfer rate has been depended implicitly on temperature [28]. The residence time in any local state has been shown to be inverse of transfer rate (t) [29] and it is shown that the residence time is very strongly dependent on the energy of t . The deeper states in the E_D and E_A bands have been shown to be characterized with long residence times, while shallow states have been considered not to be occupied for longer than microsecond. With these considerations the charge transfer has been envisaged as a sequence of hole between states

with long residence times interspersed with sequence of short times or even passage through a delocalized state of a polymer.

In the present work various techniques have been employed to investigate the polarization processes along with the estimation of various parameters. Anticipating the difficulty to analyse the experimental data in such complex situations when in one and the same temperature range the various decay mechanism may compete, the different techniques are used to interpret the experimental results. The various results obtained in the present investigation have been discussed in the light of the available literature.

Transient charging and discharging currents were investigated over a period of time 01 to 80 min. The currents were found to follow Curie-Von Schweidler law with two different slopes having index value n_1 at shorter times being smaller than index value n_2 at longer times. The systematic analysis of the various results from such study has indicated that the time dependent transient currents in this polymer may combinedly be due to dipole reorientation and space charge dissipation [30]. Thermal activation of isochronal current in a specific temperature range followed by a peak centered at about $70 \pm 5^\circ\text{C}$ and peak appearing in TSDC thermograms has indicated the close correlation of transient currents with TSD described in Chapter IV. Careful analysis of the observed characteristics of various TSD have led to the conclusion that the peak located around 90°C can be

attributed to α -relaxation. This relaxation in the present case is supposed to arise due to dipolar relaxation. The dependence of TSDC spectra on the electrode materials suggests that there may be charges which may be injected into the dielectric from the electrode. These may be trapped subsequently and form a pair of opposite charges, which act as dipoles oriented by the applied field. Thus, simultaneous mechanism of movement of charges through microscopic distance coupled with dipolar orientation may be responsible for the observed results. The broadness of the peak may be considered to be a manifestation of dipolar relaxation process with a wide distribution in relaxation time. The other feature of this peak further led to the conclusion that this peak is also contributed by space charge polarization produced due to macroscopic displacement of the bulk generated charge carriers as well as due to injection of charges into the bulk of the sample with subsequent trapping during polarization. The peak obtained with the combined effect of dipolar relaxation and space charge formation is observed to grow with increase in polarizing temperature. During TSDC cycle trapped excess charge carriers are subjected to space charge limited drift under their own field, diffusion or neutralization by thermally generated free carriers [31]. Further, partial blocking of electrodes and diffusion of charge carriers may occur but to an insignificant extent and ohmic conduction of free charge carriers mainly account for the observed of positive discharge current under certain conditions of polarizing field and temperature [32]. The peak may partially originate from those space

charges that first took part in conduction and were accumulated in the polymer close to the electrodes during the formation.

The steady state conductivity in the present case was in general found to increase with increase in temperature. The effect of electrodes of different work functions on the current-voltage characteristics was found to be very effective. The observed conduction mechanism was explained in terms of Richardson-Schottky effect alongwith space charge mechanism. The observed electrode dependence on current-voltage characteristics suggests that charges may be injected from the electrodes. The charges may be trapped at the trapping sites and subsequently excited. Pronounced departure at higher temperature and fields has been considered as an indication of the possibility of space charge effect [10,33].

The various results described above have indicated that electret state in the present case is due to dipole polarization and space charge polarization. The space charge polarization has been considered to be due to injection of carriers followed by their localization in various traps distributed spatially and energetically in the sample. Various features of transient currents, dark conduction current, short circuit thermally stimulated currents and dielectric measurements together with the different parameters derived from such measurements have been found to be in agreement with the dipolar polarization as well as space charge polarization.

REFERENCES

1. Perlman, M.M. and Cresswell, R.A., J. Appl. Phys., **42**, 531 (1971).
2. Jonscher, A.K., Thin Solid Films, **1**, 213 (1967).
3. Pillai, P.K.C., Gupta, B.K. and Goel, Matti, J. Polym. Sci. Phys., **19**, 1461 (1981).
4. American Institute of Physics Handbook, New York, McGraw Hills Book Co., 9 (1965).
5. Gupta, N.P., Jain, K. and Mahendru, P.C., Thin Solid Films, **61**, 297 (1979).
6. Gill, J.L., Zabrano, T. and Juhasz, J.C., J. Phys. Appl. Phys., **15**, 119 (1982).
7. Wintle, H.J., J. Appl. Phys., **43**, 2927 (1972).
8. Khare, P.K. and Srivastava, A.P., Indian J. Phys., **68A**, 291 (1994).
9. Narsimha Rao, V.V.R., Mahinder, T. and Subba Rao, B., J. Noncryst. Solids, **104**, 224 (1988).
10. Khare, P.K. and Chandok, R.S., J. Polym. Mater., **12**, 23 (1995).
11. Khare, P.K. and Chandok, R.S., Polym. Int., **38**, 153 (1995).
12. Khare, P.K., Keller, J.M., Gaur, M.S., Singh, Ranjeet and Datt, S.C., Polym. Int., **35**, 337 (1994).
13. Talwar, I.M., Sinha, H.C. and Srivastava, A.P., J. Mater. Sci., **L-4**, 448 (1985).
14. Khare, P.K. and Srivastava, A.P., Indian J. Pure and Appl. Phys., **30**, 131 (1992).

15. Khare, P.K., Surinder, P. and Srivastava, A.P., Indian J. Pure Appl. Phys., **30**, 165 (1992).
16. Khare, P.K., Keller, J.M., Gaur, M.S., Ranjeet Singh and Datt, S.C., Polymer International, **39**, 303 (1996).
17. Khare, P.K., Pramana - J. of Phys., **46**, 109 (1996).
18. Seggern, H. Von, J. Appl. Phys., **36**, 1039 (1979).
19. Bauser, H., Kunststoffe, **62**, 192 (1972).
20. Fuhrmann, J., J. Electrostat., **4**, 109 (1977).
21. Hays, D.A., J. Chem. Phys., **61**, 1455 (1974).
22. Creswell, B.A., Gribbon, B.I., Kabayama, M.A. and Perlman, Telesis, **2**, 21 (1971).
23. Mott, N.F. and Davis, E.A., Electronic Processes in Noncrystalline Materials (Clarendon, Oxford 1979).
24. Pfister, G. and Scher, H., Phys. Rev., **B15**, 2062 (1977).
25. Noolandi, J., Phys. Rev., **B16**, 4466 (1977).
26. Gaur, M.S., Reeta Singh, Khare, P.K. and Ranjeet Singh, Polymer International, **37**, 33 (1995).
27. Lewis, T.J., Inst. Phys. Cont. SER, **66**, 183 (1983).
28. Redi, M. and Hopfield, J.J., J. Chem. Phys., **72**, 6651 (1980).
29. Khare, P.K., Keller, J.M., Gaur, M.S., Ranjeet Singh and Datt, S.C., Polymer International, **39**, 303 (1996).
30. Khare, P.K., Jain, P.L. and Pandey, R.K., Bull. Mater. Sci., **24**, 401 (2001).

31. Khare, P.K., Jain, P.L. and Pandey, R.K., Bull. Mater. Sci., **23**, 529 (2000).
32. Khare, P.K. and Jain Sandeep, Polymer International, **49**, 265 (2000).
33. Khare, P.K., Pandey, R.K. and Jain, P.L., Polymer International, **22**, 1003 (1999).

/ ***** /

LIST OF RESEARCH PAPERS SUBMITTED

1. Thermally Stimulated Discharge Currents (TSDC) Studies of Poly Vinylidene Fluoride Foils - Bulletin of Materials Science, Bangalore.
2. The Evaluation of Dielectric Properties of Polyvinyl Pyrrolidone Films in Indian Journal of Physics, Calcutta (Accepted for publication).
3. Transient Current in Charging and Discharging Mode in Pure Polyvinyl Pyrrolidone Films in Japanese Journal of Applied Physics (Communicated).
4. Electrical Transport in Solution-Grown Thin Films of Polyvinyl Pyrrolidone in Indian Journal of Physics, Calcutta (Communicated).